

This electronic thesis or dissertation has been downloaded from the King's Research Portal at <https://kclpure.kcl.ac.uk/portal/>



Studies on the performance of open fronted and 'ultra-clean' ventilation systems.

Nicholson, Graham Philip

The copyright of this thesis rests with the author and no quotation from it or information derived from it may be published without proper acknowledgement.

END USER LICENCE AGREEMENT



Unless another licence is stated on the immediately following page this work is licensed

under a Creative Commons Attribution-NonCommercial-NoDerivatives 4.0 International

licence. <https://creativecommons.org/licenses/by-nc-nd/4.0/>

You are free to copy, distribute and transmit the work

Under the following conditions:

- Attribution: You must attribute the work in the manner specified by the author (but not in any way that suggests that they endorse you or your use of the work).
- Non Commercial: You may not use this work for commercial purposes.
- No Derivative Works - You may not alter, transform, or build upon this work.

Any of these conditions can be waived if you receive permission from the author. Your fair dealings and other rights are in no way affected by the above.

Take down policy

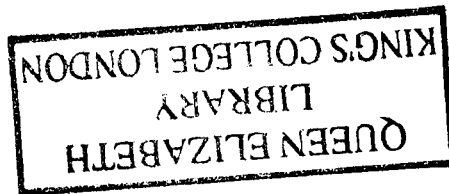
If you believe that this document breaches copyright please contact librarypure@kcl.ac.uk providing details, and we will remove access to the work immediately and investigate your claim.

20 0359147 X



UMDS

Studies on the Performance of Open Fronted Containment and 'Ultra-Clean' Ventilation Systems



**A thesis presented in part fulfilment of the requirements for
the degree of Doctor of Philosophy of the University of London**

**Graham Philip Nicholson
Thermal Biology Research Unit
Division of Biomedical Sciences
King's College
University of London**

1997

PAGE
NUMBERING
AS ORIGINAL

Abstract

The damaging effects of contamination can be critical in industry, research and healthcare delivery. Accordingly, reliable contamination control systems are a necessity in these areas. This study focused on assessment strategies and methods for Open Fronted Containment (OFC) and Ultra Clean Ventilation (UCV) systems.

A simple assessment strategy (flow visualisation and face velocity) was used to rank the performance of 221 fume cupboards in a college and to eliminate those considered unsatisfactory among them. It was concluded that flow visualisation using a water fog generator was a better indicator of performance than the other tests.

Theoretical and practical attempts were made to correlate a gas tracer containment test method (BS 7258 : 1994 Part 4) and a particulate method (BS 5726 : 1992 : Part 1) for testing OFC systems. This was found to be impracticable due to differences in tracer generation, sampling methods and distribution of equipment. For the overall assessment of OFC systems a 3 stage strategy (flow visualisation, face velocity measurement and quantitative tracer testing) was found to be most suitable. This 3 stage strategy was expanded and used successfully to evaluate an UCV system in a hospital burns unit.

The technique of Computational Fluid Dynamics (CFD) was used to simulate airflow and tracer dispersal within OFC and UCV systems. CFD demonstrated systematically, for the first time, a number of advantages over physical measurements. One advantage of CFD was that it visualised and quantified the complete flow field in any plane. Although CFD simulations could be used in predicting how a design could function, it did not necessarily indicate how it would function when built. Physical tests are still necessary for validation and commissioning.

Both CFD and physical measurements were found to be useful for solving many problems but the combination of these techniques highlighted how some design changes could introduce new and unexpected problems.

Acknowledgements

JOHN & KAY CLARKE (FUMAIR Ltd.) for their sponsorship of this work and the use of their test room facilities.

DR. RAY CLARK, MERVYN L. de CALCINA-GOFF and DR. DAVID KENNEDY for their supervision, support and encouragement.

DR. BILL NEWSOM and PEGGY SHAW for the use of the laboratory facilities at the Simms Woodhead Memorial Laboratory, Papworth Hospital and to Peggy for her work in assessing microbiological safety cabinet performance using the microbiological method.

MR. IAN MUIR, DR. COLIN MARTIN and FIONA COULL at the Aberdeen Royal Infirmary, for their help and support in the evaluation of the burns unit and for allowing the use of the results in this thesis.

FRED GROVER for his help and advice on the practical work.

DR. ROGER SLADE for the loan of the MIRAN infra-red gas analyser.

DAVID POLLINGTON (CONTAINMENT TECHNOLOGY Ltd.) for the loan of the KI-Discus equipment.

MARK SEYMOUR (FLOMERICS Ltd.) for providing the computational fluid dynamic software package, Flovent.

DIANE WARREN for the use of the facilities at NIBSC for testing safety cabinets.

GEOFFREY and JOAN NICHOLSON, BEVERLEY and SINJ ASPREY for their unselfish help and support.

MY FRIENDS too numerous to mention for being ready to talk at the right times.

Contents

Abstract	ii
Acknowledgements	iii
Contents	iv
Chapter 1 General Introduction	
1.1 Airborne contamination control problems in some workplaces	1
1.1.1 Electronics industry - protection of the product	1
1.1.2 Scientific laboratories - protection of the product and the worker	1
1.1.3 Healthcare - protection of the patient	2
1.1.4 Food industry - protection of the product	2
1.1.5 Pharmaceutical industry - protection of the product and the worker	2
1.2 Airborne contamination control strategies and equipment	2
1.3 Performance assessment strategies for contamination control equipment	4
1.4 Key interim conclusions	8
Chapter 2 Review of performance assessment strategies for open fronted containment systems	
2.1 System function and performance assessment strategies	9
2.2 Fume cupboards	10
2.2.1 Historical	10
2.2.2 Review of test methods	12
2.2.3 What strategy and methods for inclusion into BS 7258 : 1994?	16
2.3 Microbiological safety cabinets (class I and class II)	24
2.3.1 Historical	24
2.3.2 Review of test methods	26
2.4 The state of open fronted containment systems - Field survey of fume cupboards in terms of type, condition and performance	32
2.5 Key interim conclusions	34
Chapter 3 A study of the British Standard, BS 7258 : 1994 performance tests for general purpose laboratory fume cupboards	
3.1 Introduction	35
3.2 Test fume cupboard	35
3.3 Test room	36
3.4 Position of input and extract ducting systems in test room and factory	36
3.5 Flow rate of air supplied to and extracted from the test room	37
3.6 Distribution of airflow into the test room through the perforated supply wall	38
3.7 Estimation of the ventilation rate of the test room	38
3.8 BS 7258 : 1994 : Part 1. Determination of "specification for safety and performance"	39
3.8.1 Method	39
3.8.1.1 Anemometers	39
3.8.1.2 Calibration of anemometers	40
3.8.1.3 Position of anemometer	40
3.8.1.4 Measurements	41
3.8.1.5 Expression of results	43
3.8.2 Results	43
3.8.2.1 Effect of anemometer orientation with respect to direction of airflow	43
3.8.2.2 Time taken for rotating vane anemometer to reach steady readings from zero	44
3.8.2.3 "Type test"	45
3.8.2.4 "Commissioning test"	45
3.8.2.5 "Routine maintenance test"	45
3.9 BS 7258 : 1994 : Part 4. Use of a "method for determination of the containment value of a laboratory fume cupboard".	45
3.9.1 Method	45
3.9.1.1 Tracer gas	45
3.9.1.2 Gas injector device and positioning	49
3.9.1.3 Measurement of flow rate of gas through injector device	49
3.9.1.4 Sampling probes and positioning	50
3.9.1.5 Gas collection	50
3.9.1.6 Gas analyser and calibration for use with gas tracer	51
3.9.1.7 Test procedure	53
3.9.1.8 Expression of results	54
3.9.2 Results and discussion	54
3.9.2.1 Set-up problems	54

3.9.2.2	Gas analyser instrument noise	54
3.9.2.3	Background	55
2.9.2.4	Response time of the sampling system to changes in SF ₆ concentration	56
2.9.2.5	Test results	57
3.9.3	Tracer flow from funnel	60
3.9.4	Effect of funnel position and mixing	60
3.9.5	Effect of face velocity on containment	63
3.9.6	Effect of design features on containment	63
3.10	Discussion of BS 7258 : 1994 : Parts 1 and 4 and other national standards testing methodologies used for assessing the performance of a general purpose laboratory fume cupboard	68
3.11	Key interim conclusions	70
Chapter 4 A study of the British Standard BS 5726 : 1992 performance tests for microbiological safety cabinets		
4.1	Introduction	71
4.2	Methods	71
4.2.1	Flow visualisation	71
4.2.2	Face velocity measurements	71
4.2.3	Quantitative assessment of the performance of class I and class II microbiological safety cabinets: Determination of a protection factor	71
4.2.4	Quantitative assessment of external contamination for class II microbiological safety cabinets	72
4.2.5	Quantitative assessment of cross contamination for class II microbiological safety cabinets	72
4.2.6	Expression of results for type test, commissioning and routine maintenance	73
4.2.6.1	Flow visualisation	73
4.2.6.2	Airflows	73
4.2.6.2.1	Airflow (Class I cabinet)	73
4.2.6.2.2	Airflow (class II cabinet)	73
4.2.6.3	Assessment of operator protection factor	74
4.2.6.3.1	Calculation of the protection factor from using the microbiological method	74
4.2.6.3.2	Calculation of the protection factor from using the KI method	74
4.2.6.4	Assessment of external and cross contamination	75
4.3	Test results	75
4.3.1	Class I microbiological safety cabinets	75
4.3.2	Class II microbiological safety cabinets	76
4.4	Results and discussion	76
4.4.1	Class I and II microbiological safety cabinets results	76
4.4.2	Particle/droplet velocity	77
4.4.2.1	Theory	77
4.4.2.2	Experimental	81
4.4.3	Phoretic forces	82
4.4.4	Operator protection	83
4.4.5	Cross contamination	83
4.4.6	Particle deposition in the containment test	84
4.4.7	Contamination during the test	85
4.4.8	Microbiological safety cabinet performance during environmental disturbance	87
4.5	Key interim conclusions	90
Chapter 5 The application of the potassium iodide tracer method (KI-Discus) for assessing the containment efficiency of fume cupboards and comparison with the method described in BS 7258 : 1994 : Part 4		
5.1	Introduction	91
5.2	Qualitative comparison of air flow through fume cupboards and safety cabinets	93
5.3	The potential use of a particle tracer for assessing the performance of fume cupboards	93
5.4	The application of the KI containment test method for the assessment of microbiological safety cabinet performance (BS 5726 : 1992 : Part 1) to the assessment of fume cupboard performance	94
5.4.1	Aerodynamic fume cupboard performance in a test room	94
5.4.2	Field survey of fume cupboard performance	95
5.5	Correlation of the KI containment test method (BS 5726 : 1992 : Part 1) with the grading scheme used for assessing fume cupboard performance in the field survey	95
5.6	Theoretical comparison and correlation of the KI test method (BS 5726 : 1992 : Part 1) with the gas test method for fume cupboards (BS 7258 :1994 : Part 4)	98
5.7	Use of a nitrogen gas jet to induce leakage from the fume cupboard aperture into the test room for subsequent assessment of both methods	101

5.8	Use of the induced leakage to assess the applicability of the KI containment test method (BS 5726 : 1992 : Part 1) for use with the aerodynamic fume cupboard	103
5.9	Comparison of the relative position of tracer source and samplers recommended in BS 7258 for use with the KI test equipment	103
5.10	Use of the induced leakage to establish the relative position of the KI source and samplers for further assessment of fume cupboard performance	105
5.11	Comparison of the BS 7258 test method and the modified KI test method results at different fume cupboard face velocities	108
5.12	Comparison of BS 7258 test method and the modified KI test method results with deterioration in fume cupboard performance by design modifications	109
5.13	Comparison of sampling methods for SF ₆ and KI particles with common source (Collison nebuliser)	110
5.13.1	Discharge of SF ₆ from Collison nebulizer	111
5.13.2	Concentration of SF ₆ sampled in front of the Collison nebuliser with increasing distance	112
5.13.3	Number of KI particles sampled, when released from the Collison nebuliser, with increasing distance	112
5.13.4	Sampling of SF ₆ in series with the KI test system	113
5.14	Comparison of sampling procedures during building re-entrainment	116
5.15	Discussion and conclusions	116
5.16	Key interim conclusions	119
Chapter 6 The application of computational fluid dynamics (CFD) for assessing open fronted containment facilities		
6.1	Introduction	120
6.1.1	What is CFD and how is it used?	120
6.1.2	What are the fundamentals behind CFD?	121
6.1.3	What are the limitations and developments?	123
6.2	Two dimensional visualisation and analysis of airflows in fume cupboards	125
6.2.1	Problem set up of an aerodynamic fume cupboard	125
6.2.2	Effect of turbulence specification and grid refinement	126
6.2.3	Comparison of simulation to physical measurements	137
6.2.4	Airflow around individual design features and comparison with whole flow field	140
6.2.4.1	Front steps	140
6.2.4.2	Lipfoils	144
6.2.4.3	Sash handles	146
6.2.5	Comparison of fume cupboard type and the effect of fume cupboard design on the overall flow field	146
6.2.6	Modelling the dispersal of a contaminant	150
6.2.7	Fume cupboard type compared in terms of contaminant profile	156
6.2.8	Discussion and conclusions	156
6.3	The use of a 3 dimensional model to describe and predict the effect of blockage, poor design and disturbance of airflows on the performance of open fronted containment systems (steady state)	157
6.3.1	Three dimensional model set-up	157
6.3.2	Description of air flow and comparison with 2 dimensional simulation and physical measurements	158
6.3.3	Effect of fume cupboard design features on the overall flow field	162
6.3.4	Effect of a mannequin/operator and blockage on simulated airflow and contaminant dispersal	162
6.3.4.1	Set up	162
6.3.4.2	'Aerodynamic' fume cupboard	166
6.3.4.3	'Aerodynamic' fume cupboard with rear baffle and lipfoil removed	166
6.3.4.4	Conclusions	175
6.3.5	Effect of environmental disturbance on simulated airflow and contaminant dispersal	175
6.3.5.1	Set up	175
6.3.5.2	'Aerodynamic' fume cupboard	175
6.3.5.3	'Aerodynamic' fume cupboard with rear baffle and lipfoil removed	178
6.3.5.4	Conclusions	178
6.4	Simulation of the distribution of a contaminant with relevance to British, German and American Standard methods for the assessment of fume cupboard containment	178
6.4.1	Introduction	178
6.4.2	BS 7258 1994 : Part 4	183
6.4.2.1	Set up	183
6.4.2.2	Simulations	184
6.4.3	ASHRAE 110 : 1993	184

6.4.3.1	Set up	184
6.4.3.2	Simulations	190
6.4.4	DIN 12 924 : 1991	190
6.4.4.1	Set up	190
6.4.4.2	Simulations	195
6.4.5	Effect of sash handle on test results (BS 7258)	195
6.4.6	Discussion and comparison of test methods	200
6.5	Two - dimensional visualisation and analysis of airflows in microbiological safety cabinets	200
6.5.1	Problem setup	200
6.5.2	Class I cabinets: Simulation of air flow	202
6.5.3	Class II cabinets: Effect of design and balance on overall flow patterns	202
6.6	Key interim conclusions	205
Chapter 7 Aerobiological performance assessment of a burns unit		
7.1	Introduction	207
7.2	Historical	207
7.3	Review of test methods	210
7.4	The burns unit and ultraclean ventilation system	211
7.5	Materials, equipment and methods	214
7.5.1	Pressure	214
7.5.2	Velocity	214
7.5.3	Temperature	214
7.5.4	Humidity	214
7.5.5	Potassium iodide tracer method	214
7.5.6	Gas tracer method	214
7.5.7	Particle measurement	215
7.5.8	Smoke visualisation	215
7.5.9	Airborne bacterial sampling	215
7.5.10	Computational fluid dynamics (CFD)	215
7.6	Results and discussion of the physical measurements made in the burns unit	215
7.6.1	Air pressures and air flows (as visualised with smoke) within the unit	215
7.6.2	Air temperature and relative humidity distribution	218
7.6.3	Nitrous oxide and potassium iodide tracer measurements	218
7.6.4	Particle counts	221
7.6.5	Airborne bacteria	222
7.7	Results and discussion of the physical measurements made in the intensive care room and viewing area	224
7.7.1	Ventilation and air flows (as visualised with smoke)	224
7.7.2	Velocity measurements beneath the UCV	226
7.7.3	Air temperature and relative humidity	226
7.7.4	Nitrous oxide and potassium iodide tracers measurements	229
7.7.5	Particle counts	230
7.7.6	Start-up conditions under the UCV	232
7.8	Conclusions from using physical measurements	233
7.8.1	Burns unit	233
7.8.2	Intensive care room	233
7.8.3	Entrainment of contamination from staff etc. onto the bed surface in the intensive care room	234
7.8.3.1	No movement of people in the room	234
7.8.3.2	People present and moving within room	234
7.9	Results and discussion of the intensive care room using computational fluid dynamics (CFD) based on physical measurements and design data	234
7.9.1	3 dimensional problem set-up using measured data	234
7.9.2	“Visualisation” of airflows	236
7.9.3	Velocity data below UCV	242
7.9.4	Air temperature distribution	242
7.9.5	Air temperature data below UCV	243
7.9.6	Distribution of a contaminant	243
7.9.7	Simulation using design data	245
7.10	Conclusions from CFD simulations	246
7.11	Use of CFD and physical measurements for analysing design changes	246
7.11.1	Problems identified within intensive care room affecting contamination control performance	246
7.11.2	Proposed design changes	246
7.11.3	Effect of room ventilation supply and extracts on UCV performance (2 dimensional CFD simulations)	246

7.11.3.1	Simulation set up	246
7.11.3.2	Change in UCV performance with supply velocity / temperature (open boundaries)	247
7.11.3.3	Change in UCV performance with supply velocity / temperature (high and low level extracts and open boundaries)	250
7.11.4	Drafts stopped by “brushes” fitted to drawers/cupboards/doors	254
7.11.5	Effect of diffusing air entry into room through doors (CFD)	254
7.11.6	Effect of repositioning viewing area door (CFD)	258
7.11.7	Canopy extended	258
7.11.8	Extended canopy (foot end only)	265
7.11.9	Low Air Loss Bed (LALB) switched on/off, canopy extended/not extended	265
7.12	Conclusions from analysing design changes	267
7.13	Discussion of CFD and Physical measurements as containment testing strategies applied to a complex ventilated environment	267
7.13.1	Physical measurements	267
7.13.2	Comparison of CFD simulation with physical measurements and use for performance assessment	271
7.14	Key interim conclusions	276
7.14.1	Physical measurements	276
7.14.2	Comparison of CFD simulation with physical measurements and use for performance assessment	277
Chapter 8 General discussion and conclusions		
8.1	Contamination control equipment and assessment strategies	278
8.2	Open fronted containment systems	278
8.3	Burns unit and ‘Ultra Clean’ Ventilation (UCV) Systems	286
8.4	Computational Fluid Dynamics (CFD)	289
Bibliography		293
Appendix 1 A summary of the physical properties, methods of generation, dispersal and deposition of potential airborne contaminants		Ai
A1.1	Definitions	Ai
A1.1.1	Gases and vapours	Ai
A1.1.2	Dusts	Ai
A1.1.3	Smoke and fumes	Ai
A1.1.4	Mists	Ai
A1.1.5	Aerosols	Ai
A1.2	Generation	Aii
A1.3	Transport	Aii
A1.3.1	Gases and vapours	Aii
A1.3.2	Droplets/Particles	Aii
A1.4	Summary of size distribution	Aiii
Appendix 2 Qualitative assessment methods		Av
Appendix 3 Quantitative assessment methods		Avi
Appendix 4 Fume cupboard survey at King’s College London		Aviii
A4.1	Methods used in performance evaluation	Aviii
A4.1.1	Air flow visualisation	Aviii
A4.1.2	Face velocity	Aviii
A4.2	Number and type of fume cupboards tested at King’s College London	Aix
A4.3	Fume cupboard exterior material types	Ax
A4.4	Subjective assessment of fume cupboard cleanliness	Ax
A4.5	Subjective assessment of fume cupboard condition	Ax
A4.6	Subjective assessment of fume cupboard performance	Axi
A4.7	Fume cupboard performance	Axi
A4.7.1	Mean face velocity	Axi
A4.7.2	Variation of velocity across the plane of the working aperture	Axii
A4.7.3	Visualisation/Fog score	Axvi
A4.7.4	Grading of scores	Axx
List of Figures		
Fig. 1.1	Systems used for controlling the contamination of people, products and/or work processes.	4
Fig. 2.1	Box type fume cupboard and airflows	10
Fig. 2.2	‘Modern’ features of an aerodynamic fume cupboard and airflows	11
Fig. 2.3	Arrangement of equipment for the USA fume cupboard containment test (ASHRAE 110).	15
Fig. 2.4	Arrangement of equipment for the German fume cupboard containment test (DIN 12 924).	15
Fig. 2.5	Arrangement of equipment for the British fume cupboard containment test (BS 7258 1994).	15

Fig. 2.6	Class I microbiological safety cabinet and airflows	25
Fig. 2.7	Class II microbiological safety cabinet and airflows	26
Fig. 2.8	Arrangement of equipment for the USA (NSF 49 : 1983), German (DIN 12 950 : 1991) and Japanese (JAS : 1981) class II cabinet microbiological containment tests.	29
Fig. 2.9	Arrangement of equipment for the British class I cabinet microbiological containment tests (BS 5726 : 1992)	29
Fig. 2.10	Arrangement of equipment for the British class II cabinet microbiological containment tests (BS 5726 : 1992).	29
Fig. 2.11	Arrangement of equipment for the British class I cabinet KI containment tests (BS 5726 : 1992)	30
Fig. 2.12	Arrangement of equipment for the British class II cabinet KI containment tests (BS 5726 : 1992).	30
Fig. 3.1	Aerodynamic fume cupboard used in this investigation (Fumair Ltd., Hertford).	35
Fig. 3.2	Dimensions of test room (Fumair Ltd, Hertford).	36
Fig. 3.3	Ventilation ducting to the test room.	36
Fig. 3.4	Position of test room in the factory, showing supply and discharge points.	37
Fig. 3.5	Change in face velocity, calculated volume flow rate and calibrated volume flow rate through the supply duct with Wilson flow grid differential pressure	37
Fig. 3.6	Supply and extract duct pressures when the test room is balanced with the factory.	38
Fig. 3.7	Change in gas concentration in the test room during continuous release, and its decay.	39
Fig. 3.8	Average face velocity measurements using the methods described in BS 7258 : 1994 : Part 1	40
Fig. 3.9	Measurement positions specified in BS 7258 : 1994 : Part 1 for type testing of face velocity.	41
Fig. 3.10	Measurement positions specified in BS 7258 : 1994 : Part 1 for commissioning of face velocity.	42
Fig. 3.11	Measurement positions recommended in BS 7258 : 1994 : Part 1 for maintenance of face velocity.	42
Fig. 3.12	Orientation of a thermistor anemometer.	43
Fig. 3.13	Orientation of a rotating vane anemometer.	44
Fig. 3.14	Effect of anemometer orientation on velocity measurements in the aperture plane.	44
Fig. 3.15	Response time of a rotating vane anemometer to reach steady readings from zero.	44
Fig. 3.16	Injection positions for test gas. All dimensions in mm.	49
Fig. 3.17	Sampling positions. All dimensions in mm.	50
Fig. 3.18	Sampling system manifold.	50
Fig. 3.19	Infra-red spectrum of ambient air.	51
Fig. 3.20	Infra-red spectrum of ambient air with 10 % SF ₆ / 90 % N ₂ .	52
Fig. 3.21	Infra-red spectrum of 10 % SF ₆ / 90 % N ₂ .	52
Fig. 3.22	Calibration curve for SF ₆	53
Fig. 3.23	Instrument noise at a response time of 1 second.	55
Fig. 3.24	Instrument noise at a response time 10 seconds.	55
Fig. 3.25	Background concentrations of SF ₆ due to re-entrainment of air into the test room.	56
Fig. 3.26	Response time of the infra-red gas analyser at different sampling flow rates. A 5µl sample was injected into the central probe of the BS 7258 : 1994 : Part 4 grid.	57
Fig. 3.27a	Containment test results.	58
Fig. 3.27b	Containment test results.	59
Fig. 3.28	Containment test results at different face velocities.	62
Fig. 3.29	Effect of face velocity on the concentration of SF ₆ measured in the plane of the sash.	63
Fig. 3.30	Containment test results (modified cupboard).	65
Fig. 3.31	Rearrangement of sampling probes to measure potential leakage in the corner of the aperture.	66
Fig. 3.32	Infra-red traces showing the effect of moving a sampling probe into the positions shown in Fig. 3.31.	67
Fig. 4.1	Arrangement of equipment for KI external contamination tests	72
Fig. 4.2	Arrangement of equipment for KI cross contamination tests	73
Fig. 4.3	Theoretical change in the velocity and horizontal distance travelled by a 40 µm KI droplet when propelled from a spinning disc in still air.	79
Fig. 4.4	Theoretical change in the velocity and horizontal distance travelled by a 7 µm KI particle when propelled from a spinning disc in still air.	79
Fig. 4.5	Theoretical path of a 7 µm particle as it is propelled from the edge of a spinning disc in still air.	80
Fig. 4.6	Theoretical path of a 40 µm droplet as it is propelled from the edge of a spinning disc in still air.	80
Fig. 4.7	Theoretical paths of a 7 µm and 40 µm droplet/particle propelled from the edge of a	

	spinning disc in still air and the decrease in capture velocity from a centripetal sampler.	81
Fig. 4.8	Arrangement of air samplers for environmental disturbance tests.	88
Fig. 4.9	Effect on the operator protection factor for class I and class II cabinets when there is no environmental challenge and when challenged.	90
Fig. 5.1	Arrangement of the KI equipment (using the method specified in BS 5726 : 1992 : Part 1 for class I safety cabinets) for testing containment of fume cupboards.	94
Fig. 5.2	Change in operator protection factor with grade.	97
Fig. 5.3	Change in the number of KI particles sampled with grade.	97
Fig. 5.4	Change in operator protection factor with velocity.	97
Fig. 5.5	Arrangement of the KI equipment as specified in BS 5726 : 1992 : Part1 for class I cabinets and a nitrogen jet for assessing the applicability of the method.	103
Fig. 5.6	Arrangement of the KI equipment for comparison with the position of source and samplers in BS 7258 : 1994 : Part 4.	104
Fig. 5.7	Arrangement of the KI equipment and a nitrogen jet for the assessment of leakages from cupboards.	105
Fig. 5.8	Change in operator protection factor for a pre-BS 5726 class I cabinet, a BS 5726 class I cabinet with a flared inlet and the aerodynamic fume cupboard with mean face velocity.	109
Fig. 5.9	Change in operator protection factor for a pre-BS 5726 class I cabinet, a BS 5726 class I cabinet with a flared inlet with mean face velocity and change in operator protection factor for the aerodynamic fume cupboard with face velocity measured in the aperture plane opposite the source.	109
Fig. 5.10	Arrangement of the KI equipment and with additional sampler for measuring background.	110
Fig. 5.11	Position of a Collison nebuliser in the fume cupboard.	111
Fig. 5.12	The release of SF ₆ from a Collison nebuliser, placed in the fume cupboard, at 3 l/min (discharge velocity 0.85 m/s) 100 mm from the aperture plane, and measured at increasing distance from the plane using a single sampling probe (BS 7258 : 1994) in line with the Collison jet. Cupboard face velocity 0.25 m/s.	112
Fig. 5.13	Arrangement of the equipment for sampling SF ₆ in the KI-Discus sampling system	113
Fig. 5.14	Measurement of SF ₆ concentration in air sampled by centripetal samplers (100 l/min) 100 mm from the aperture plane. SF ₆ released from a Collison nebuliser 100 mm from the plane at 3 l/min (discharge velocity 0.8 m/s). Cupboard face velocity ~0.25 m/s.	114
Fig. 5.15	Measurement of SF ₆ concentration in air sampled by centripetal samplers (100 l/min) 50 mm from the aperture plane. SF ₆ released from a Collison nebuliser 100 mm from the plane at 3 l/min (discharge velocity 0.8 m/s) as a carrier gas for KI nebulisation. Cupboard face velocity ~0.25 m/s.	114
Fig. 5.16	Measurement of SF ₆ concentration in air sampled by centripetal samplers (100 l/min) 100 mm from the aperture plane. SF ₆ released from a Collison nebuliser 100 mm from the plane at 3 l/min (discharge velocity 0.8 m/s) as a carrier gas for KI nebulisation. Cupboard face velocity ~0.25 m/s.	114
Fig. 5.17	Measurement of SF ₆ concentration in air sampled by centripetal samplers (100 l/min) 150 mm from the aperture plane. SF ₆ released from a Collison nebuliser 100 mm from the plane at 3 l/min (discharge velocity 0.8 m/s) as a carrier gas for KI nebulisation. Cupboard face velocity ~0.25 m/s.	115
Fig. 5.18	Measurement of SF ₆ concentration in air sampled through a single probe (BS 7258 : 1994) at 6.8 l/min (5.77 m/s) 100 mm from the aperture plane. SF ₆ released from a Collison nebuliser 100 mm from the plane at 3 l/min (discharge velocity 0.8 m/s) as a carrier gas for KI nebulisation. Cupboard face velocity 0.25 m/s.	115
Fig. 6.1	Aerodynamic fume cupboard and the 2 Dimensional (2 D) computational model domain (xy view).	125
Fig. 6.2	2 D Solution grid.	126
Fig. 6.3	Effect of the turbulence model on the airflow vectors (2 D).	128
Fig. 6.4	Effect of the turbulence model on the airflow speed value contours (2 D).	129
Fig. 6.5	Effect of the turbulence model on the airflow turbulent viscosity contours (2 D).	130
Fig. 6.6	Effect of the turbulence model on vertical x velocity and speed profiles in the aperture plane (2 D).	131
Fig. 6.7	Density and refinement of 2 D solution grids.	132
Fig. 6.8	Effect of grid density and refinement on airflow vectors (2. D, k-ε turbulence model).	133
Fig. 6.9	Effect of grid density and refinement on airflow speed contours (2 D, k-ε turbulence model).	134
Fig. 6.10	Effect of grid density and refinement on airflow turbulent viscosity contours (2 D, k-ε turbulence model).	135
Fig. 6.11	Effect of grid density and refinement on x velocity and speed profiles in the aperture plane (2 D).	136
Fig. 6.12	Comparison of airflows within an aerodynamic cupboard as visualised using smoke and by 2 D CFD simulation.	138

Fig. 6.13	Comparison of x velocity and speed profiles in the aperture plane of an aerodynamic fume cupboard using CFD with physical measurements (2 D).	139
Fig. 6.14	Effect of the turbulence model on the airflow around a front step (2 D).	141
Fig. 6.15	Airflow around a front step with a coarser grid (fixed turbulence revised model 0.005 m ² /s (2 D)).	142
Fig. 6.16	Airflow around a front step, twice as thick (fixed turbulence revised model 0.005 m ² /s (2 D)).	142
Fig. 6.17	Effect of step shape on airflows (2 D).	143
Fig. 6.18	Effect of lipfoil design on airflows past a front step (2 D).	145
Fig. 6.19	Effect of sash handle design on airflows past a sash (2 D).	147
Fig. 6.20	Effect on the airflows within an aerodynamic fume cupboard when the rear baffle and the lipfoil are removed (2 D).	148
Fig. 6.21	Effect on x velocity and speed profiles in the aperture plane of an aerodynamic fume cupboard when the rear baffle and the lipfoil are removed (2 D).	149
Fig. 6.22	Effect on the airflows, x velocity and speed profiles in the aperture plane of an aerodynamic fume cupboard when the lower and upper slots of the rear baffle are closed (2 D).	151
Fig. 6.23	Evolution of a modern day aerodynamic fume cupboard visualised using airflow vectors (2 D).	152
Fig. 6.24	Effect of the turbulence model on concentration profiles in the aperture plane of an aerodynamic fume cupboard (2 D).	153
Fig. 6.25	Effect of grid density and refinement on concentration profiles in the aperture plane of an aerodynamic fume cupboard (2 D).	153
Fig. 6.26	Effect of further grid refinement on concentration profiles in the aperture plane of an aerodynamic fume cupboard (2 D).	155
Fig. 6.27	Effect of the turbulence model on contaminant dispersal in a straight tube.	154
Fig. 6.28	Effect of geometric features on concentration profiles in the aperture plane of an aerodynamic fume cupboard (2 D).	156
Fig. 6.29	3 Dimensional (3 D) model of an aerodynamic fume cupboard.	157
Fig. 6.30	3 D solution grid.	158
Fig. 6.31	Airflow vectors within an aerodynamic fume cupboard (3 D).	159
Fig. 6.32	Comparison of x velocity, speed and concentration profiles in the horizontal centreline of the aperture plane of the 3 D aerodynamic fume cupboard model with the 2 D model.	160
Fig. 6.33	x velocity, speed and concentration profiles across the aperture plane, z direction, near to the work surface and at mid aperture height of an aerodynamic fume cupboard (3 D).	161
Fig. 6.34	Comparison of x velocity and speed profiles in the horizontal centreline of the aperture plane of an aerodynamic cupboard with physical measurements (3 D).	163
Fig. 6.35	Effect on the airflow vectors in the xy plane, centreline of the aperture width, and in the xz plane within an aerodynamic fume cupboard, near to the work surface and at mid aperture height, when the rear baffle and lipfoil are removed (3 D).	164
Fig. 6.36	Effect on the x velocity, speed and concentration profiles across the aperture plane, z direction, of an aerodynamic fume cupboard when the rear baffle and lipfoil are removed (3 D).	165
Fig. 6.37	xy view of blockage in front of an aerodynamic fume cupboard (3 D).	162
Fig. 6.38	xy view of blockage in front of an aerodynamic fume cupboard with the rear baffle and lipfoil removed (3 D).	166
Fig. 6.39	Effect of blockage on the airflow vectors in the xy plane, centreline of the aperture width, and in the xz plane within an aerodynamic fume cupboard, near to the work surface and at mid aperture height (3 D).	167
Fig. 6.40	Effect of blockage on the x velocity, speed and concentration profiles in the horizontal centreline of the aperture plane of an aerodynamic fume cupboard (3 D).	168
Fig. 6.41	Effect of blockage on the x velocity, speed and concentration profiles across the aperture plane, z direction, of an aerodynamic fume cupboard near to the work surface (3 D).	169
Fig. 6.42	Effect of blockage on the x velocity, speed and concentration profiles across the aperture plane, z direction, of an aerodynamic fume cupboard at mid aperture height (3 D).	170
Fig. 6.43	Effect of blockage on the airflow vectors in the xy plane, centreline of the aperture width, and in the xz plane within an aerodynamic fume cupboard, near to the work surface and at mid aperture height with the rear baffle and lipfoil removed (3 D).	171
Fig. 6.44	Effect of blockage on the x velocity, speed and concentration profiles in the horizontal centreline of the aperture plane of an aerodynamic fume cupboard with the rear baffle and lipfoil removed (3 D).	172
Fig. 6.45	Effect of blockage on the x velocity, speed and concentration profiles across the aperture plane, z direction, of an aerodynamic fume cupboard near to the work surface with the rear baffle and lipfoil removed (3 D).	173
Fig. 6.46	Effect of blockage on the x velocity, speed and concentration profiles across the aperture plane, z direction, of an aerodynamic fume cupboard at mid aperture height with the rear baffle and lipfoil removed (3 D).	174
Fig. 6.47	Effect of a cross flow of air (1 m/s) past the aperture of an aerodynamic cupboard on the airflow	

	vectors in the xz plane within the cupboard, near to the work surface and at mid aperture height (3 D).	176
Fig. 6.48	Effect of a cross flow of air (1 m/s) past the aperture of an aerodynamic fume cupboard on the x velocity, speed and concentration profiles across the aperture plane, z direction, near to the work surface and at mid aperture height (3 D).	177
Fig. 6.49	Effect of a cross flow of air (1 m/s) past the aperture of an aerodynamic fume cupboard, with the rear baffle and lipfoil removed, on the airflow vectors in the xz plane within the cupboard, near to the work surface and at mid aperture height (3 D).	179
Fig. 6.50	Effect of a cross flow of air (1 m/s) past the aperture of an aerodynamic fume cupboard, with the rear baffle and lipfoil removed, on the x velocity, speed and concentration profiles across the aperture plane, z direction, near to the work surface and at mid aperture height (3 D).	180
Fig. 6.51	Effect of a cross flow of air (1 m/s) past the aperture of an aerodynamic fume cupboard, with the rear baffle and lipfoil removed and with square edges, on the airflow vectors in the xz plane within the cupboard, near to the work surface and at mid aperture height (3 D).	181
Fig. 6.52	Effect of a cross flow of air (1 m/s) past the aperture of an aerodynamic fume cupboard, with the rear baffle and lipfoil removed and with square edges, on the x velocity, speed and concentration profiles across the aperture plane, z direction, near to the work surface and at mid aperture height (3 D).	182
Fig. 6.53	Position of BS 7258 source in an aerodynamic fume cupboard and solution grid (3 D).	185
Fig. 6.54	xy contour of tracer distribution, in the centreline of the source, when released from source position P1 (BS 7258 : 1994 : Part 4) within the working volume of an aerodynamic fume cupboard (3 D).	185
Fig. 6.55	xz contours of tracer distribution inside the cupboard near to the work surface, at mid aperture height and near to the sash when released from source position P1 (BS 7258 : 1994 : Part 4) in an aerodynamic fume cupboard (3 D).	186
Fig. 6.56	xy contour, centreline of the source, and xz contours, near to the work surface, at mid aperture height and near to the sash, of tracer distribution when released from source positions P2 and P5 (BS 7258 : 1994 : Part 4) within an aerodynamic fume cupboard (3 D).	187
Fig. 6.57	Effect of removing the rear baffle and lipfoil on xy and xz tracer contours when released from source positions P2 and P5 (BS 7258 : 1994 : Part 4) within an aerodynamic fume cupboard (3 D).	188
Fig. 6.58	Effect of removing the rear baffle and lipfoil on tracer concentration profiles in the aperture plane, centreline of the source, and across the aperture plane, z direction, when released from source positions P2 and P5 (BS 7258 : 1994 : Part 4) within an aerodynamic fume cupboard (3 D).	189
Fig. 6.59	Position of ASHRAE 110 injector and solution grid, and airflow vectors in the xy plane, centreline of the source, in an aerodynamic fume cupboard (3 D).	191
Fig. 6.60	xy contour, centre line of source, and xz contours, near to the work surface, at mid aperture height and near to the sash, of tracer distribution when released from the central source positions (ASHRAE 110) within an aerodynamic fume cupboard (3 D).	192
Fig. 6.61	Effect of removing the rear baffle and lipfoil on xy and xz tracer contours when released from the central source positions (ASHRAE 110) within an aerodynamic fume cupboard (3 D).	193
Fig. 6.62	Effect of removing the rear baffle and lipfoil on tracer concentration profiles in the aperture plane, centreline of the source, and across the aperture plane, z direction, when released from the central source position (ASHRAE 110) within an aerodynamic fume cupboard (3 D).	194
Fig. 6.63	Position of DIN 12 924 injector and solution grid, and airflow vectors in the xy plane, centreline of the source, in an aerodynamic fume cupboard (3 D).	196
Fig. 6.64	xy contour, centreline of source, and xz contours, near to the work surface, at mid aperture height and near to the sash, of tracer distribution when released from the DIN injector within an aerodynamic fume cupboard (3 D).	197
Fig. 6.65	Effect of removing the rear baffle and lipfoil on xy and xz tracer contours when released from the DIN 12 924 injector within an aerodynamic fume cupboard (3 D).	198
Fig. 6.66	Effect of removing the rear baffle and lipfoil on tracer concentration profiles in the aperture plane, centreline of the source, and across the aperture plane, z direction, when released from the DIN injector within an aerodynamic fume cupboard (3 D).	199
Fig. 6.67	Effect of a sash handle on the tracer concentration profiles in the aperture plane, centreline of the source, and across the aperture plane, z direction, when released from source positions P2 and P5 (BS 7258 : 1994 : Part 4) within an aerodynamic fume cupboard (3 D).	201
Fig. 6.68	Airflow vectors within a class I microbiological safety cabinet with different front lip design (2 D).	203
Fig. 6.69	The effect of inflow and downflow balance on the airflow vectors and horizontal profiles of x velocity and speed within a class II microbiological safety cabinet (2 D).	204
Fig. 6.70	Effect of airflow balance on the distribution of tracer contours within a class II microbiological safety cabinet when released with the downflow supply and when released outside the cabinet 2D	206

Fig. 7.1	The burns unit as designed.	212
Fig. 7.2	Cross section of the ultra clean ventilation (UCV) system fitted in the ceiling of the intensive care room showing ducting from UCV extracts to the fan chamber. Fan make up air direction and expected velocity profile over the bed surface are also shown.	213
Fig. 7.3	Plan view of the ultra clean ventilation (UCV) system fitted in the ceiling of the intensive care room showing ducting from UCV extracts to the fan chamber, fan make up air and room extracts.	213
Fig. 7.4	The burns unit as used (door positions as commonly found in use).	216
Fig. 7.5	Measurement positions for temperature and humidity within the burns unit.	218
Fig. 7.6	Variation in temperature and % rh within the unit	218
Fig. 7.7	Tracer (T) release and sample (S) positions within the burns unit. Tracer was released ~200 mm from floor level. Air was sampled 200 mm from floor level, midway and 200 mm from the ceiling.	219
Fig. 7.8	Particle counts ($>5 \mu\text{m}$) at various places within the unit	222
Fig. 7.9	Comparison of bacterial counts and total particle counts at various places in the unit and ward	223
Fig. 7.10	Change in mean downflow velocity with height beneath the UCV canopy, and variation in downflow velocity beneath UCV (quadrant 3) with changing supply flow rate and temperature.	226
Fig. 7.11	Plan view of the intensive care room showing the measurement positions for temperature and humidity at three heights; 200 mm from the floor, midway between the floor and the ceiling and 200 mm from the ceiling.	227
Fig. 7.12	Variation in temperature and % rh within the intensive care room	227
Fig. 7.13	Mean temperature and % rh beneath the UCV	228
Fig. 7.14	Variation of temperature with height beneath the UCV with changing supply ventilation and temperature (measured under quadrant 3)	229
Fig. 7.15	Particle counts at various positions within the intensive care room	230
Fig. 7.16	Particle size distribution sampled at various points in the intensive care room and under differing conditions	231
Fig. 7.17	Change in particle counts at the bed surface, in the middle (S2), with time during ventilation start up from standby to normal.	232
Fig. 7.18	Change in temperature with time beneath the UCV (quadrant 3) during ventilation start up from standby to normal.	232
Fig. 7.19	Change in N_2O gas tracer measured at the bed surface, in the middle (S2), with time (gas released into UCV extract Ba)	233
Fig. 7.20	Computational 3 - Dimensional view of the intensive care room	234
Fig. 7.21	End view (top), plan view (middle) and side view (bottom) of intensive care room showing CFD solution grid.	235
Fig. 7.22	Airflow vectors in the xz plane near to floor level of the intensive care room.	237
Fig. 7.23	Airflow vectors in the xz plane midway (near bed surface height) of the intensive care room.	238
Fig. 7.24	Airflow vectors in the xz plane near to ceiling of the intensive care room.	239
Fig. 7.25	Airflow vectors in the xy plane centreline of the UCV.	240
Fig. 7.26	Airflow vectors in the yz plane centreline of the UCV.	241
Fig. 7.27	Mean y velocity and speed profiles with height beneath the UCV canopy.	242
Fig. 7.28	Mean y velocity and speed profiles with height beneath the UCV over the bed area only.	242
Fig. 7.29	Air temperature distribution within the intensive care room	243
Fig. 7.30	xz tracer concentration profiles midway (near bed surface height) in the intensive care room when released in the airflows beneath the doors.	244
Fig. 7.31	Tracer concentration profile along the centreline of the bed surface from the head to the foot end when released in the airflows beneath the intensive care room doors.	245
Fig. 7.32	2 Dimensional domain of UCV canopy, supplies and extracts. Open boundaries.	248
Fig. 7.33	2 D domain of UCV canopy, supplies and extracts. High and low open boundaries and ventilation extracts.	248
Fig. 7.34	Solution grid over 2 D domain.	248
Fig. 7.35	2 D simulation of airflows from the UCV canopy at a supply temperature 20°C and velocity 0.38 m/s . Open boundary walls and ambient 20°C .	249
Fig. 7.36	2 D simulation of airflows from the UCV canopy at a supply temperature 40°C and velocity 0.51 m/s . Open boundary walls and ambient 20°C .	249
Fig. 7.37	Effect of supply temperature on 2 D y velocity profiles with height in the middle of the bed. Ambient 20°C .	250
Fig. 7.38	Effect of supply temperature on tracer concentration in the xz plane near to the bed surface (when released from the open boundaries in the walls). Ambient 20°C .	250
Fig. 7.39	2 D simulation of airflows from the UCV canopy at a supply temperature of 20°C and	

	velocity 0.38 m/s. Low level extracts and high level openings on boundary walls. Ambient 20 °C.	251
Fig. 7.40	2 D simulation of airflows from the UCV canopy at a supply temperature 20°C and velocity 0.38 m/s. Low level openings and high level extracts on boundary walls. Ambient 20 °C.	251
Fig. 7.41	2 D simulation of airflows from the UCV canopy at a supply temperature 40°C and velocity 0.51 m/s. Low level openings and high level extracts on boundary walls. Ambient 20 °C.	252
Fig. 7.42	2 D simulation of airflows from the UCV canopy at a supply temperature 40°C and velocity 0.51 m/s. Low level extracts and high level openings on boundary walls. Ambient 20 °C.	252
Fig. 7.43	Effect of opening and extract position on 2 D y velocity profiles with height in the middle of the bed at a supply temperature of 40 °C. Ambient 20°C.	253
Fig. 7.44	Effect of opening and extract position on 2 D concentration profiles across the bed, in a plane near to the surface, when released from the open boundaries at the walls. Supply temperature 40 °C and ambient 20°C.	253
Fig. 7.45	Effect of door diffusers on xz airflow vectors near to floor level of the intensive care room.	255
Fig. 7.46	Effect of door diffusers on yz airflow vectors in the centreline of the UCV.	256
Fig. 7.47	Effect of door diffusers on xz concentration contours midheight (near bed surface height) of the intensive care room.	257
Fig. 7.48	Effect of moving viewing area door on zx airflow vectors near to floor level of the intensive care room.	259
Fig. 7.49	Variation in downward velocity beneath the UCV, quadrant 3, with changing supply flow rate/temperature.	258
Fig. 7.50	Effect of extending the canopy on xz airflow vectors midheight (near bed surface height) of the intensive care room.	261
Fig. 7.51	Effect of extending the canopy on yz airflow vectors in the centreline of UCV.	262
Fig. 7.52	Effect of extending the canopy on xy airflow vectors in the centreline of UCV.	263
Fig. 7.53	Tracer concentration profiles along the centreline of the bed from head to foot end at heights near to the bed surface (top) and at the canopy edge (bottom) when released within the intensive care room.	264
Fig. 7.54	2 dimensional simulation of airflow from the UCV canopy (extended) at supply temperature 40°C and velocity 0.51 m/s. Open boundary walls and ambient 20 °C.	266
Fig. 7.55	2 dimensional simulation of concentration profile under the UCV canopy (extended) at bed height. Supply temperature 40°C and velocity 0.51 m/s. Open boundary walls and ambient 20 °C.	266
Fig. 7.56	2 dimensional simulation of airflow from the UCV canopy at supply temperature 20°C and velocity 0.38 m/s and concentration contours of a contaminant seeded at the open boundary walls. Ambient 20 °C.	268
Fig. 7.57	2 dimensional simulation of airflow from the UCV canopy at supply temperature 40°C and velocity 0.51 m/s and concentration contours of a contaminant seeded at the open boundary walls. Ambient 20 °C.	268
Fig. 7.58	2 dimensional simulation of airflow from the UCV canopy (extended) at supply temperature 40°C and velocity 0.51 m/s and concentration contours of a contaminant seeded at the open boundary walls. Ambient 20 °C.	268
Fig. 7.59	Plot of regression lines of transfer index for gas and particle tracers with room position. Gas mid height, KI mid height, gas floor height, KI floor level, gas ceiling, KI ceiling.	271
Fig. 7.60	CFD y velocity, speed values and measured velocities beneath each quadrant of the UCV and over the bed surface	273
Fig. 7.61	CFD calculated and measured temperatures within the intensive care room.	275

List of figures in appendices

Fig. A1.1	Particle deposition efficiency as a function of particle size (Hesketh, 1974)	Aiii
Fig. A4.1	Position of rotating vane anemometer head in the plane of the sash for an 'aerodynamic' fume cupboard	Aix
Fig. A4.2	Comparison of the mean face velocity measured at a working aperture (500 mm) of an aerodynamic fume cupboard with differing number of sample positions.	Aix
Fig. A4.3	Velocity measurements at a working aperture height 250 mm	Axiii
Fig. A4.4	Velocity measurements at a working aperture height 500 mm	Axiii
Fig. A4.5	Variation in mean velocity measurements at a point from the overall mean face velocity at a working aperture height 250 mm	Axiii
Fig. A4.6	Variation in mean velocity measurements at a point from the overall mean face velocity at a working aperture height 500 mm	Axiii
Fig. A4.7	Comparison of % variation in the mean velocity measured at a point from the overall mean face velocity at working aperture heights of 250 mm and 500 mm for 'aerodynamic' fume cupboards.	Axiv

Fig. A4.8	Comparison of % variation in the mean velocity measured at a point from the overall mean face velocity at working aperture heights of 250 mm and 500 mm for 'conventional' fume cupboards.	
Fig. A4.9	Fog scores at a working aperture of 250 mm	Axiv
Fig. A4.10	Fog scores at a working aperture of 500 mm	Axv
Fig. A4.11	% of all cupboard faces tested at height 250 mm and their scored variables: velocity, variation of velocity, and fog.	Axv
Fig. A4.12	% of all cupboard faces tested at height 500 mm and their scored variables: velocity, variation of velocity, and fog.	Axvii
Fig. A4.13	% of aerodynamic cupboard faces tested at height 250 mm and their scored variables: velocity, variation of velocity, and fog.	Axvii
Fig. A4.14	% of aerodynamic cupboard faces tested at height 500 mm and their scored variables: velocity, variation of velocity, and fog.	Axvii
Fig. A4.15	% of conventional cupboard faces tested at height 250 mm and their scored variables: velocity, variation of velocity, and fog.	Axvii
Fig. A4.16	% of conventional cupboard faces tested at height 500 mm and their scored variables: velocity, variation of velocity, and fog.	Axvii
Fig. A4.17	% of single sash cupboard faces tested at height 250 mm and their scored variables: velocity, variation of velocity, and fog.	Axviii
Fig. A4.18	% of single sash cupboard faces tested at height 500 mm and their scored variables: velocity, variation of velocity, and fog.	Axviii
Fig. A4.19	% of double sash cupboard faces tested at height 250 mm and their scored variables: velocity, variation of velocity, and fog.	Axviii
Fig. A4.20	% of double sash cupboard faces tested at height 500 mm and their scored variables: velocity, variation of velocity, and fog.	Axviii
Fig. A4.21	% of triple sash cupboard faces tested at height 250 mm and their scored variables: velocity, variation of velocity, and fog.	Axviii
Fig. A4.22	% of triple sash cupboard faces tested at height 500 mm and their scored variables: velocity, variation of velocity, and fog.	Axviii
Fig. A4.23	% of double sided cupboard faces tested at height 250 mm and their scored variables: velocity, variation of velocity, and fog.	Axix
Fig. A4.24	% of double sided cupboard faces tested at height 500 mm and their scored variables: velocity, variation of velocity, and fog.	Axix
Fig. A4.25	Fume cupboard grading scores	Axx
Fig. A4.26	The grading of fume cupboard type at a working aperture height of 250 mm. Aerodynamic, single sash box type, double sash box type, triple sash box type, and double sided box type.	Axxii
Fig. A4.27	The grading of fume cupboard type at a working aperture height of 500 mm. Aerodynamic, single sash box type, double sash box type, triple sash box type, and double sided box type.	Axxii
Fig. A4.28	The grading of fume cupboard type at a working aperture height of 250 mm. Aerodynamic, grouped conventional type.	Axxiii
Fig. A4.29	The grading of fume cupboard type at a working aperture height of 500 mm. Aerodynamic, grouped conventional type.	Axxiii
Fig. A4.30	The grading of fume cupboard type at a working aperture height of 250 mm. conventional cupboards without retro fitted lipfoils, conventional cupboards with retro fitted lipfoils.	Axxiv
Fig. A4.31	The grading of fume cupboard type at a working aperture height of 500 mm. conventional cupboards without retro fitted lipfoils, conventional cupboards with retro fitted lipfoils.	Axxiv

List of plates

Plate 3.1	Gas off/ cupboard off, Tracer gas on/ cupboard off, Tracer gas on/ cupboard on	60
Plate 3.2	Release of smoke in BS 7258 source position P ₂ . Cupboard face velocity 0.5 m/s.	61
Plate 3.3	Release of smoke in BS 7258 source position P ₅ . Cupboard face velocity 0.5 m/s.	61
Plate 7.1	Smoke movement over a patient lying on a Low Air Loss Bed (LALB).	225
Plate 7.2	Air/smoke flow from under the UCV.	225
Plate 7.3	Movement of air/smoke from head to foot end of the bed	225
Plate 7.4 & 7.5	Movement of smoke in the intensive care room overlaid with results of CFD simulations; from beneath the canopy to the windows and towards the viewing area, respectively.	272

List of Tables

Table 1.1	Capture efficiency indexes.	5
Table 1.2	Fume cupboard containment efficiency indices.	6
Table 1.3	Microbiological safety cabinet containment efficiency indices.	7
Table 1.4	Cleanroom and clean area containment efficiency indices.	7

Table 1.5	Performance factors and risk assessment.	7
Table 2.1	Methods for measuring the performance and efficiency of laboratory fume cupboards in terms of operator protection.	13
Table 2.2	Recommended values for BS 7258 : 1994 : Part 4 (Bicen AF, 1993).	22
Table 2.3	Permitted values for DIN 12 924.	22
Table 2.4	Methods for measuring the performance and efficiency of microbiological safety cabinets in terms of operator protection.	31
Table 3.1	Flow rate of air through the test room.	39
Table 3.2	Comparison of anemometer types.	40
Table 3.3	Distribution of average velocities across the aperture when measured in the plane of the sash, using the grid as specified for type testing in BS 7258 : 1994 : Part 1.	46
Table 3.4	Distribution of average velocities across the aperture when measured in the plane of the sash, using the grid as specified for commissioning in BS 7258 : 1994 : Part 1.	47
Table 3.5	Distribution of average velocities across the aperture when measured in the plane of the sash, using the grid as recommended for maintenance in BS 7258 : 1994 : Part 1.	48
Table 3.6	Calibration of the A/D input.	53
Table 3.7	Instrument noise at a response time of 1 and 10 seconds.	54
Table 3.8	Average response times of the infra red gas analyser at different sampling flow rates.	57
Table 3.9	Tracer gas concentration (ppm) measured in the aperture plane recorded by chart recorder.	57
Table 3.10	Tracer gas concentration (ppm) measured in the aperture plane recorded by datalogger.	60
Table 3.11	Tracer gas concentration (ppm) measured in the aperture plane at increased source flow rate, and distribution of tracer inside the cupboard working volume.	61
Table 3.12	Distribution of average velocities across the aperture when measured in the plane of the sash (modified cupboard), using the grid as specified for maintenance in BS 7258 : 1994 : Part 1.	64
Table 4.1	Class I microbiological safety cabinets (Maintenance tested unless specified + which is type tested).	75
Table 4.2	Class II microbiological safety cabinets (Type tested unless specified * which is maintenance).	76
Table 4.3	Time and distance for a droplet/particle to reach its terminal settling velocity.	80
Table 4.4	Change in vertical scatter of KI particles released from a spinning disc with distance.	82
Table 4.5	Contamination during a typical KI test.	85
Table 4.6	Contamination during a typical KI test.	86
Table 4.7	Effect on the operator protection factor for class I and class II cabinets when there is no environmental challenge, when challenged by protocol i, protocol ii, protocol iii and protocol iv.	89
Table 5.1	Operator protection factors for an aerodynamic fume cupboard in a test room using the equipment arranged in Fig. 5.1.	95
Table 5.2	The performance and Operator Protection Factors (OPF) of fume cupboards tested at King's College London.	96
Table 5.3	Sensitivity and efficiency of tracer gas, microbiological and KI tracer methods. *The recommended limits can alter depending on the challenge dose.	99
Table 5.4	Operator protection factors achievable using the gas, microbiological and KI tracer methods. *The OPF may vary as the challenge dose is not fixed.	100
Table 5.5	Determination of leakage using SF ₆ and the BS 7258 : 1994 containment test method	102
Table 5.6	Number of KI particles sampled in front of an aerodynamic fume cupboard with induced leakage using the BS 5726 : 1992 : Part 1 method.	103
Table 5.7	Number of KI particles sampled in front of the cupboard with the equipment arranged as in protocol 5.8 a, b and c.	104
Table 5.8	Number of KI particles sampled in front of the cupboard with the equipment arranged as in protocol 5.9 a, b and c.	106
Table 5.9	Number of particles sampled in front of the cupboard with the KI equipment arranged as in protocol 5.9 d.	106
Table 5.10	Number of KI particles sampled in front of the cupboard with the equipment arranged as in protocol 5.9 e.	107
Table 5.11	Number of KI particles sampled in front of the cupboard with the equipment arranged as in protocol 5.9 e but with the jet directed at the edge of the disc rather than the centre.	107
Table 5.12	Change in operator protection factor with face velocity	108
Table 5.13	Velocity profile of discharge from a Collison nebuliser nozzle with the fume cupboard turned off (velocity along central axis of nozzle and maximum velocity measured above and below axis).	111
Table 5.14	Number of KI particles sampled at varying distances from the aperture plane when discharged from a Collison nebuliser.	113
Table 5.15	Number of KI particles counted simultaneously with SF ₆	116

Table 7.1	Concentration of KI particles and N ₂ O gas in air sampled at floor level from different positions within the unit when released from position T1.	219
Table 7.2	Concentration of KI particles and N ₂ O gas in air sampled at mid height from different positions within the unit when released from position T1.	220
Table 7.3	Concentration of KI particles and N ₂ O gas in air sampled at ceiling level from different positions within the unit when released from position T1.	220
Table 7.4	Concentration of KI particles and N ₂ O in air sampled outside the room near the corridor door (S3), the dressing room door (S7) and in the viewing area (S6) when released from position T3.	220
Table 7.5	Concentration of KI particles in air sampled inside the room near the corridor door (S5), the dressing room door (S8) and in the viewing area (S9) when released from position T4 and T5.	221
Table 7.6	Concentration of particles and KI in air sampled at midheight position T2 when KI released from T1 (and vice versa).	221
Table 7.7	Concentration of particles and KI in air sampled at midheight position T2 when KI released from T1, adjusted for background (and vice versa).	221
Table 7.8	Number of airborne bacteria (CFU/m ³ air sampled) sampled within the hospital ward and burns unit	223
Table 7.9	Air supplies and extracts (m ³ /s) in the intensive care room.	224
Table 7.10	The concentration of KI particles sampled at the bed surface (KI/m ³ sampled air) with and without disturbance, due to the movement of a person into and out of the 'clean zone' near the centre of the bed.	229
Table 7.11	Effect of removing restriction in one of the UCV extracts on the concentration of KI particle sampled on at bed surface/m ³ of sampled air.	230
Table 7.12	Design air supplies and extracts (m ³ /s) in the intensive care room. * These data are interpolated from the recommended figures at supply temperatures of 20°C and 40°C. They also allow for leaky doors by design which are 0.03 m ³ /s of air flowing through the corridor door, 0.06 m ³ /s of air flowing through the viewing area door and none across the dressing room door.	245
Table 7.13	Effect of extending the canopy on the concentration of KI particles/m ³ of air sampled at the bed the bed surface when released from within the intensive care room.	260
Table 7.14	Transfer indices for gas and KI particle distribution in the unit (Fig. 7.7).	270

List of tables in appendices

Table A1.1	Physical characteristics of particles	Aiv
Table A1.2	Typical sizes of airborne particles and gas dispersoids	Aiv
Table A2.1	Summary of methods used for the visualisation of fluid flow (Merzkirch, 1987)	Av
Table A3.1	Aerosol generation and sampling techniques (Hidy, 1984)	Avii
Table A3.2	Gas tracer generation and sampling techniques (Hidy, 1984)	Avii
Table A4.1	Number and type of fume cupboards tested	Aix
Table A4.2	Fume cupboard exterior material	Ax
Table A4.3	Fume cupboard cleanliness	Ax
Table A4.4	Fume cupboard condition	Ax
Table A4.5	Fume cupboard blockage	Axi
Table A4.6	Comparison of grade with sash height (Student's paired t-test)	Axxi
Table A4.7	Grading of cupboards with sashes fully open, ranging from working apertures at 682 - 826 mm for conventional cupboards and 598 mm for an aerodynamic cupboard.	Axxi
Table A4.8	Velocity measurements at a working sash height of 250 mm	Axxv
Table A4.9	Velocity measurements at a working sash height of 500 mm	Axxv
Table A4.10	% variation of velocity measurements from the mean face velocity at a working sash height of 250 mm	Axxvi
Table A4.11	% variation of velocity measurements from the mean face velocity at a working sash height of 500 mm	Axxvi
Table A4.12	Fog scores at a working sash height of 250 mm	Axxvii
Table A4.13	Fog scores at a working sash height of 500 mm	Axxvii
Table A4.14	Grading of fume cupboards at working aperture of 250 and 500 mm)	Axxviii
Table A4.15	Grading of fume cupboards at working aperture of 250 and 500 mm (% total working cupboards)	Axxviii

Chapter 1 General Introduction

1.1 Airborne contamination control problems in some workplaces

Contamination, defined in the Shorter Oxford Dictionary as ‘the action of making impure or polluting; defilement; infection’ can be a critical factor in industry, scientific research and healthcare. A contaminant may be gaseous or particulate and should meet two conditions; (a) have the physical or chemical properties to cause harm or damage (potential contaminant) and (b) have the ability to migrate to or be in place at a vulnerable location where it may cause harm. There are many more potential than actual contaminants, contamination only resulting as a matter of time for the potential contaminant to reach a vulnerable location. The limiting factors are thus time, place and transport.

1.1.1 Electronics industry - protection of the product

In the micro-electronics and semi-conductor industries, the prime concern is to keep manufactured components free from contamination by any airborne gases or particulates, and this is especially important as component details reach sub-micron levels (Austin, 1970). Particles may damage the surface of a component by the removal of material as a result of erosion or grinding, or by embedding a relatively undistorted particle to the extent that the component surface is plastically deformed. Other particles may be smeared over the surface to produce a coated section, and hence interfere with the operation of the device. Gaseous contaminants may react directly with the component metals and particles generated from such reaction products may be transported into critical areas where subsequent damage may occur.

1.1.2 Scientific laboratories - protection of the product and the worker

In scientific and research laboratories, the handling of chemical and microbiological material poses more potential hazards to health than in most other occupations (Grover 1994, Collins, 1988; Kennedy, 1988). The mechanism and route by which infections may be acquired in the laboratory may not be the same as in the community at large and the number of organisms that may potentially challenge the body and cause disease may be greater. Entry into the body may occur through mucous membranes (e.g. the lining of all those passages in the body which communicate with the exterior parts). A very important route is through the respiratory tract. Entry may also occur through the skin, which normally is a natural barrier to micro-organisms but for infection to occur via this route, there needs to be a break in its continuity. It can occur through numerous anatomical openings such as hair follicles and sweat pores or the skin may be broken through damage or lesion. Certain chemicals or fumes can be absorbed into the body by the above routes and directly through the skin. This can be significant when there is sustained skin contact with organic, lipid soluble liquids. The rate of percutaneous absorption varies and for relatively involatile liquids, ^{that} can pass through the skin easily, this route may be more important than inhalation.

1.1.3 Healthcare - protection of the patient

In many areas of healthcare, the control of cross infection in the ward, between wards and in the operating room during surgery is important (Faircliff, 1984). With recent advances in replacement prosthetic surgery there is the requirement for ultra clean environments to prevent contamination of the wound site which can cause infection and even rejection of a prosthetic implant (Lidwell, 1981, 1982, 1983). Almost any micro-organism inoculated into a suitable site may colonise the site and produce disease. This is especially true of the immunosuppressed patient where the normal flora of the human skin may invade generally sterile areas such as heart valves or hip prostheses leading to total breakdown of the implant.

1.1.4 Food industry - protection of the product

In the food industry, micro-organisms may cause the putrefaction of foods and the prime concern is to exclude potential contaminants from the product during preparation and packaging.

1.1.5 Pharmaceutical industry - protection of the product and the worker

In the pharmaceutical industry, particles may contaminate intravenous drugs and the prime concern is to exclude potential contaminants from the product during preparation and packaging.. In pharmacies and hospitals the dispensing of drugs can give rise to hazards (Kruse et. al., 1991; McDevitt, 1993). Dispensing frequently has to be carried out in a clean environment and during the process aerosols may be generated and be inhaled or otherwise gain access to the body. Some drugs entering the body in this way can be allergenic as well as toxic.

1.2 Airborne contamination control strategies and equipment

There is thus a requirement for the prevention, or at least a reduction, in the contamination of the work process, work personnel and the environment to within acceptable limits. This is determined both by economic considerations and by health and safety legislation. The cost of controlling contamination may prove to be high for a particular process, as for example, in the manufacturing industries where functional reliability, operational safety and operating costs, all affect profitability. Industry is also regulated to a large extent by guidelines such as Good Manufacturing Practice (GMP) to control the quality of the process and product. Equally in healthcare, the prevention of cross infection, which is of prime importance, can be very much influenced by litigation and public demands as available technology advances.

Controlling exposure to a potential contaminant requires the development of a control strategy. The selection of an appropriate strategy requires an assessment of risk to be made from the hazard and exposure to potential contaminants. For this the physical and chemical

properties of the potential contaminants, the method of their generation, how they may migrate to a vulnerable location and how they may cause harm or damage all need to be known (App. 1). A combination of high hazard and high exposure results in high risk which requires a high level of control. A negligible hazard activity involving low exposures presents a low risk for which no control is needed. The appropriate control strategy used will depend on the level of risk and the design of control equipment will depend on the way in which exposure takes place.

Intrinsic methods are used for the primary control of exposure of a vulnerable site with respect to the manner in which the material is handled and the equipment that is used. Extrinsic methods are used for controlling exposure from the activity usually by containment of potential contaminants or their displacement or removal away from a vulnerable site. Totally enclosed process and handling systems isolate the work process and product from the operator offering maximum protection from contamination by direct contact or indirectly via the air. Partial enclosures, with local exhaust ventilation, or simply local exhaust ventilation (LEV) can minimise exposure to contamination via the airborne route.

For partial enclosures protection of the work process or product can be achieved by carrying out manipulations in a contaminant free airflow, directed over the critical work area (e.g. laminar flow work stations and clean rooms). Protection of the operator from the work process can be achieved by drawing ambient air into a containment device from which any contamination escape is minimised, but filtered, diluted or otherwise treated before being discharged (e.g. fume cupboards and microbiological safety cabinets). Protection of both the operator and the product can be achieved by carrying out the work process in an enclosure manipulating the airflow using a combination of both the above principles. As part of the total contamination control system protection of the environment requires methods to treat the effluent discharged from equipment to prevent contamination of areas outside the work place. In addition there are methods used to dilute or displace airborne contamination in the working environment to within safe working limits (e.g. natural ventilation or clean rooms).

Examples of totally enclosed and partial enclosures are shown in Fig. 1.1. The design, function and history of contamination control equipment is covered in many excellent reviews. For containment systems, Barkley, 1972; B.O.H.S., 1976; Everett, 1981; Cook & Hughes, 1986; Newsom, 1976; Hughes, 1980; Collins, 1988; Kennedy, 1988; Clark, 1989; R.S.C., 1990; Kruse et. al., 1991. For cleanrooms, Austin, 1970; Farquharson, 1988; Hall, 1988; Schicht, 1988. For hospital ventilation systems, Faircliff, 1984; Howorth, 1984.

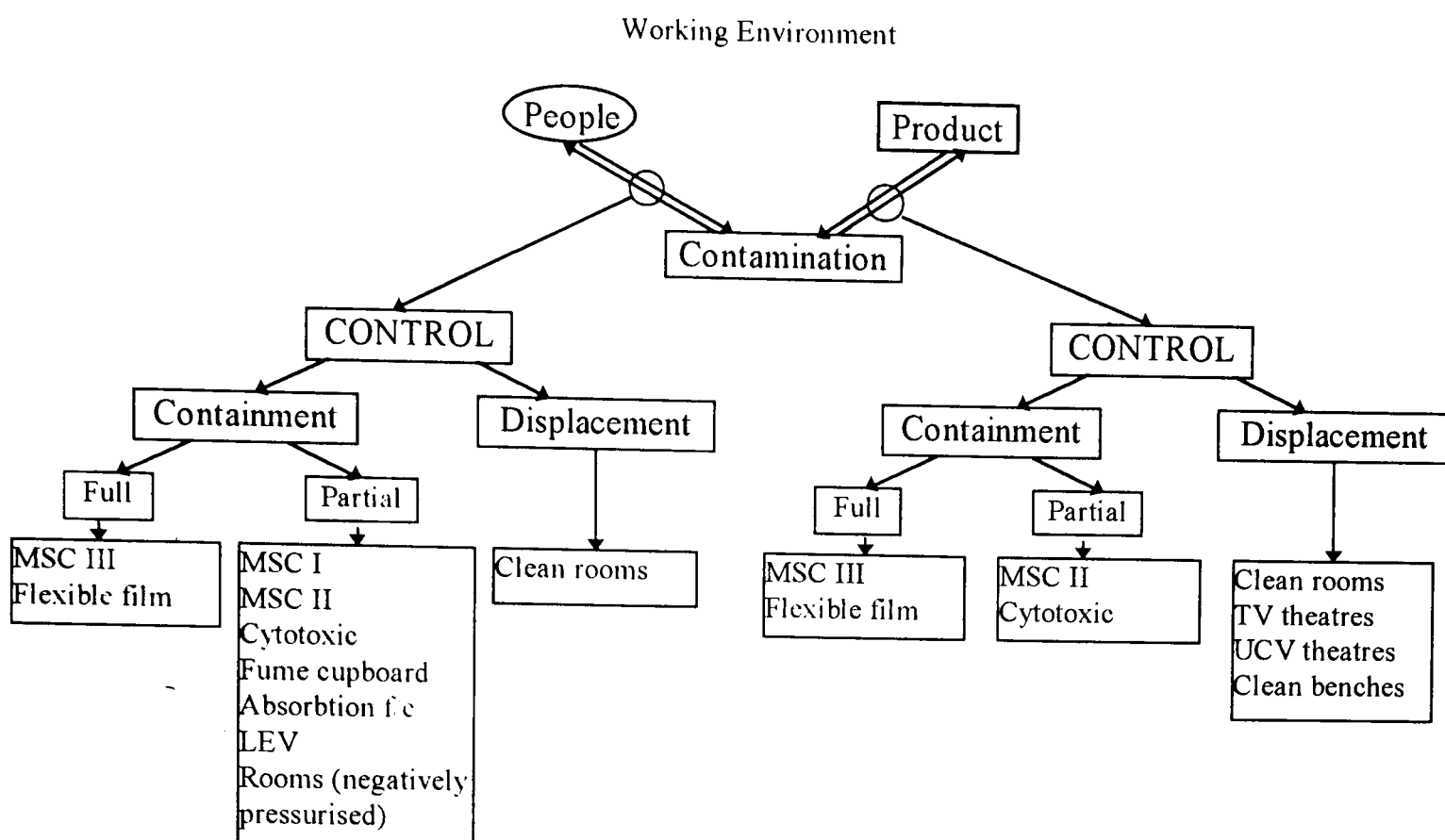


Figure 1.1 Systems used for controlling the contamination of people, products and/or work processes. MSC Microbiological safety cabinet; f/c fume cupboard; LEV is local exhaust ventilation; TV theatre is a turbulently ventilated operating theatre; UCV theatre is an 'Ultra clean ventilation' operating theatre; and LF laminar flow chamber

Once the appropriate control strategy has been selected the next most important step is to ensure that the performance of any control equipment included in this strategy is adequate and that it continues to offer the protection required over its working life.

1.3 Performance assessment strategies for contamination control equipment

Assessing the performance of contamination control equipment as part of the overall contamination control strategy requires a strategy of its own. This depends on the design of the equipment and the form of potential contaminant being protected against. Ideally, assessment will be made by measuring contamination of the work process, operators and product 'in-situ'. However this is often impractical and uneconomical and other methods are used for assessment purposes. These methods include qualitative (App. 2) and quantitative (App. 3) techniques, using tracers that will closely mimic a potential work place contaminant but which are measurable and without any harmful properties. Qualitative assessment methods can give indications of exposure or the function of contamination control devices but only quantitative methods will give information on actual exposure.

As part of the strategy for assessing partial enclosures the test methods commonly used include air flow visualisation, the measurement of air velocity and turbulence, and the quantification of tracer migration. Ideally the air inside or outside an enclosure should be completely seeded with tracer and any breach of control measured. However, this has not proved viable and spot source and sampling methods are used.

There are different methods and strategies available for assessing contamination control equipment. Such differences are in the emphasis on qualitative and quantitative methods used in the strategy and in the protocol and layout of equipment. This makes comparison of results using different methods on the same type of equipment difficult, if not impossible. The results of tests using spot source and sampling methods are influenced by the position of the tracer source, the amount released, the mechanism of release, the position of the samplers, the efficiency of the samplers and the relative disposition of the equipment. Barkley (1972) could not compare the results of many researchers' attempts to quantify the containment of fume cupboards and microbiological safety cabinets because the reports gave performances that may be directly attributable to any one of the above problems.

There are also many alternatives in the interpretation and expression of results. A factor is generally used to indicate equipment performance, calculated from data gathered using tracers, and expressed as either (examples from different authors are listed in tables 1.1 - 1.6):

- 1) The concentration of tracer sampled outside the enclosure with reference to the release rate within it, or vice versa.
- 2) The ratio of the concentration of tracer inside the enclosure to that outside, or vice versa. In this case the volume flow rate of air flowing through the facility has to be taken into account (and perhaps the volume of air sampled, depending on detection method).
- 3) A material balance between the amount of tracer released inside the enclosure to that sampled outside, or vice versa. This requires knowledge of the amount released and the amount of air sampled.

Reference	Capture efficiency index (Eff or η)
(Hampl & Shulman, 1985)	$\text{Eff}\% = \frac{\text{Duct concentration of tracer discharged at a given point}}{\text{Duct concentration of tracer discharged in duct inlet}} \times 100$
(Niemela et. al., 1991)	$\eta = \frac{(C_x - C_b)}{(C_{\text{ref}} - C_b)} \times 100\%$ <p>C_x=tracer concn. in the exhaust duct when tracer released in room. C_{ref}=100% capture efficiency with constant release rate of tracer in capture hood/exhaust flow rate. C_b=background concentration.</p>

Table 1.1 Capture efficiency indexes.

Reference	Fume cupboard containment efficiency indices
(Hampl et. al., 1988)	$\% \text{ leakage} = [1 - (C_a/C)] \times 100$ <p>C_a=SF₆ concentration with air curtain operating. C=SF₆ concentration without air curtain operating.</p>
(Mosovsky, 1995)	$\text{Average leakage} = [1 - (C_o/C_i)] \times 100$ <p>C_o=concentration of tracer gas measured outside the hood. C_i=concentration of tracer released inside the hood based on release</p>

continued

	flow rate and fume cupboard exhaust volume flow rate.
(Diberardinis et. al., 1991)	$\% \text{ leakage} = (C_o/C_i) \times 100$ C_o =outside hood concentration (personal exposure) in ppm. C_i =inside hood concentration in ppm. RR =SF6 release rate (l/min). Q =volume flow rate of hood exhaust (CFM). $C_i = \frac{RR}{28.3Q} \times 10^6$ and $C_o = \frac{\% \text{ leakage}}{100} \times \frac{RR}{28.3Q} \times 10^6$ Protection factor (PF) = 1/ %leakage.
(Caplan & Knutson, 1982)	Rating system=xx AU (or AM) yyy xx=tracer gas release rate AU=As Used test AM=As Manufactured test yyy=concentration of tracer (ppm by volume) measured outside the fume cupboard in the breathing zone
(Peck, 1982)	Factor = $\frac{\text{Breathing zone concentration (mg / m}^3\text{)}}{\text{Ejector release rate (mg / min)}}$ Protection factor (PF) = $-\log_{10} F$
(DD 80, 1980)	$L = \log \frac{r}{C_o} - \log(hwv)$ L =containment index (dimensionless) r =release rate of test gas inside the fume cupboard (ml/s) C_o =concentration of test gas detected in the plane of the sash averaged over space and time (ml/m ³ or ppm). h =the height of the sash opening w =the aperture width v =the average face velocity (m/s) This approximates to $L = \log \frac{C_i}{C_o}$ C_i =the concentration of the test gas inside the fume cupboard
(Bicen, 1993)	Capture efficiency = $\left(1 - \frac{\text{escape level}}{\text{total level to be extracted}}\right) \times 100$
(DS 457, 1986)	$k = (GVg)/(sf)$ k =the maximum permissible escape of tracer gas in the operator's respiration zone (ppm). g =the tracer gas supply during testing (mol/min). f =the expected contamination rate on which the test is based (mol/min). GV =the limit value for the containment as per the Labour Inspectorate's list of limit values (ppm). s =safety factor determined by how close to the contaminant's work hygiene limit value (GV) it is acceptable to be in a given work situation, and by measuring accuracy and harmful effect of the pollutant and the suitability of the measurement for representing long-term and varying work routines.

Table 1.2 Fume cupboard containment efficiency indices.

Reference	Microbiological safety cabinet containment efficiency indices
(BS 5726, 1992)	Performance Factor (PF) = $\frac{N_s}{V_n}$ N =the total number of particles liberated n =the total number of particles sampled/sampler

continued

	<p>s=the sampled volume flow rate (l/min)</p> <p>V=the room ventilation rate (l/min)=a standard 10^4 l/min</p> <p>The PF is the ratio of transfer indices ,T, for release and sampling of tracer without/with the cabinet:</p> <p>without cabinet $T = \frac{l}{V}$ and with cabinet $T = \frac{n}{N_s}$</p>
(Barkley, 1972)	<p>Percent.penetration = $\frac{100RQ}{V_sN}$</p> <p>R=the total number of spores recovered outside the cabinet</p> <p>Q=the total flow rate through the chamber (CFM)</p> <p>Vs=the volume of air sampled (cubic feet)</p> <p>N=the number of spores liberated in the cabinet (no. spores/min)</p>

Table 1.3 Microbiological safety cabinet containment efficiency indices.

Reference	Cleanroom and clean area containment efficiency indices
(Ljungqvist et. al., 1994)	<p>Risk.factor.(RF) = $\frac{\text{particle concentration in critical region}}{\text{particle concentration in ambient air}}$</p>

Table 1.4 Cleanroom and clean area containment efficiency indices.

<p>In all cases the performance factor may be used, for a particular control device, as an assessment of potential exposure:</p> <p>Exposure level of potential or actual contaminant escaping from contamination control equipment:</p> <p>= $[1 - (PF/100)] \times \text{quantity of hazard released (if expressed as percentage)}$</p> <p>= $PF \times \text{quantity of tracer released (if expressed as a fraction)}$</p>
--

Table 1.5 Performance factors and risk assessment.

Attempts have been made to standardise assessment strategies and the methods included in them for similar types of contamination control equipment. These have been developed through manufacturing groups, health and safety legislation and as national and international standards. Where this has not been possible, then it is important that whatever strategy and testing methods are used they should yield comparable results. However, this is not necessarily so and there still remains a great disparity between many strategies that have not been standardised or correlated, and the results of which cannot be compared. The manufacturer of contamination control equipment thus has the expense of testing by all methods for sale in different countries where standards apply.

An example is in the testing of open fronted containment systems such as microbiological safety cabinets and fume cupboards. Assessment methods for microbiological safety cabinets are laid down in British Standard 5726 : 1992 which many other countries have followed. Within this standard there are two quantitative methods described which although use different tracers and methods of generation have been correlated to give comparable results in terms of operator protection. For fume cupboards there is no such standardisation and different strategies and test methods have been written in national standards which have not been correlated. Both fume cupboards and microbiological safety cabinets have strong

similarities in the principle of containment, but the testing methods follow different philosophies.

In this thesis both the fume cupboard and microbiological safety cabinet assessment strategies and methods are reviewed. The British Standard methods BS 7258 : 1994 : Part 4 and BS 5726 : 1992 : Part 1 are studied and their potential use in testing fume cupboards and safety cabinets were investigated. These strategies and methods are used to assess the performance of a burns unit and 'ultra clean' ventilation system. The use of a non physical method of assessment, Computational Fluid Dynamics (CFD), is explored for assessing open fronted containment and UCV systems and compared with physical measurements.

1.4 Key interim conclusions

- Contamination control systems have to be assessed in order to determine whether they function correctly and continue to offer the required level of protection during use.
- Different test strategies are used for assessing the performance of contamination control systems. It is important that whatever strategies for a specific type of system are used, they should yield comparable results. However, this is often not the case.
- Test strategies for assessing open fronted containment systems, such as fume cupboards or microbiological safety cabinets, have potential for testing all types of airborne contamination control systems.

Chapter 2 Review of performance assessment strategies for open fronted containment systems

2.1 System function and performance assessment strategies

In order to develop performance assessment strategies for contamination control facilities it is important to understand their principles of operation. Open fronted containment systems are designed to minimise contamination via the airborne route and this is achieved by controlling the movement of the air itself. The air flow is determined by certain criteria:

- 1) The air flow should be of a magnitude capable of entraining gases and particles and suspending them so they can be transported and discharged safely.
- 2) It should be of a magnitude capable of withstanding environmental disturbances. The general air movement in most work places is of the order of 0.25-0.3 m/s (B.O.H.S., 1988). This movement is brought about by people and workplace machinery (e.g, fans and motors), all of which impart a kinetic energy to the air and cause it to move. This is enough to maintain (sometimes for many hours) the suspension of particles with equivalent diameters $<100\text{ }\mu\text{m}$, having settling velocities less than the general workplace velocity (App. 1). Particles and vapours/gases, with similar densities to the suspending air, once generated will then disperse only because of the motion of the air in which they are located and will move with the airflow. Skin scales $>5\text{ }\mu\text{m}$ have been found to be an important medium by which bacteria may be carried in air currents (Noble et al., 1963; Seal & Clark, 1989). Coarse particles, especially those generated with high velocity, will not be readily diverted from their natural path and will settle onto surfaces. Heavy vapours/gases will tend to sink to the floor.

Air movement may be exaggerated close to contamination control equipment due to the position of room ventilation ducts, doors and thoroughfares. Opening and shutting doors can move large volumes of air at velocities between 0.9 and 2.3 m/s (Saunders, 1993). A person walking at 1 m/s at 100 mm distance from a hot wire anemometer was shown to produce an average peak of 0.53 m/s as air was 'pushed' away from the person and a secondary peak of 0.3 m/s as air was 'pulled' towards the person (Robertson & Bailey, 1980). Higher velocities were obtained when the subject changed direction when adjacent to the probe, initial and secondary peaks up to 1.7 m/s were recorded.

- 3) The airflow should not be so great as to disturb elements of the work process.
- 4) It should not be so great as to displace contaminants from surfaces.
- 5) It should not be so great as to cause substantial unwanted turbulence and turbulent diffusion.
- 6) It should not be so great causing discomfort to workers. Too high an air speed can cause discomfort by disturbing the natural convective boundary layer which insulates the body (Clark, 1973; Clark & Edholm, 1985).

The magnitude of the velocity must be balanced so that none of these factors compromises the ability of the facility to control the movement of potential airborne contamination. However, included in the equation are economic and comfort factors. Some of the above factors can be eliminated by proper design and planning.

2.2 Fume cupboards

2.2.1 Historical

The first fume cupboards or hoods were fireplaces, used by alchemists, in which the hot fumes generated in the burning process were carried up a chimney. In the 19th Century gas burner rings were put in chimney stacks to increase the thermal draft and then with the development of motor driven fans, mechanically ventilated fume cupboards were developed. These were basically a box enclosing the work area, apart from an opening at the front which was adjustable by raising or lowering a sash, and with a hole in the top to which suction was applied (Fig. 2.1).

Airflow visualisation and face velocity were parameters by which the fume cupboard user assessed that the cupboard was working as a safety device. It was clear that with such simple box cupboards considerable eddy formation occurred (as air moved around the sharp edges of the opening) producing vortices which could extend into the fume cupboard, drawing contaminants from inside the cupboard into them but which could easily be expelled from the cupboard by disturbances in the room environment (Cook & Hughes, 1986). There were also large variations of velocity across the face of the aperture and little flow over the work surface. A great many of these "box types" of fume cupboard were produced and remain in use today.

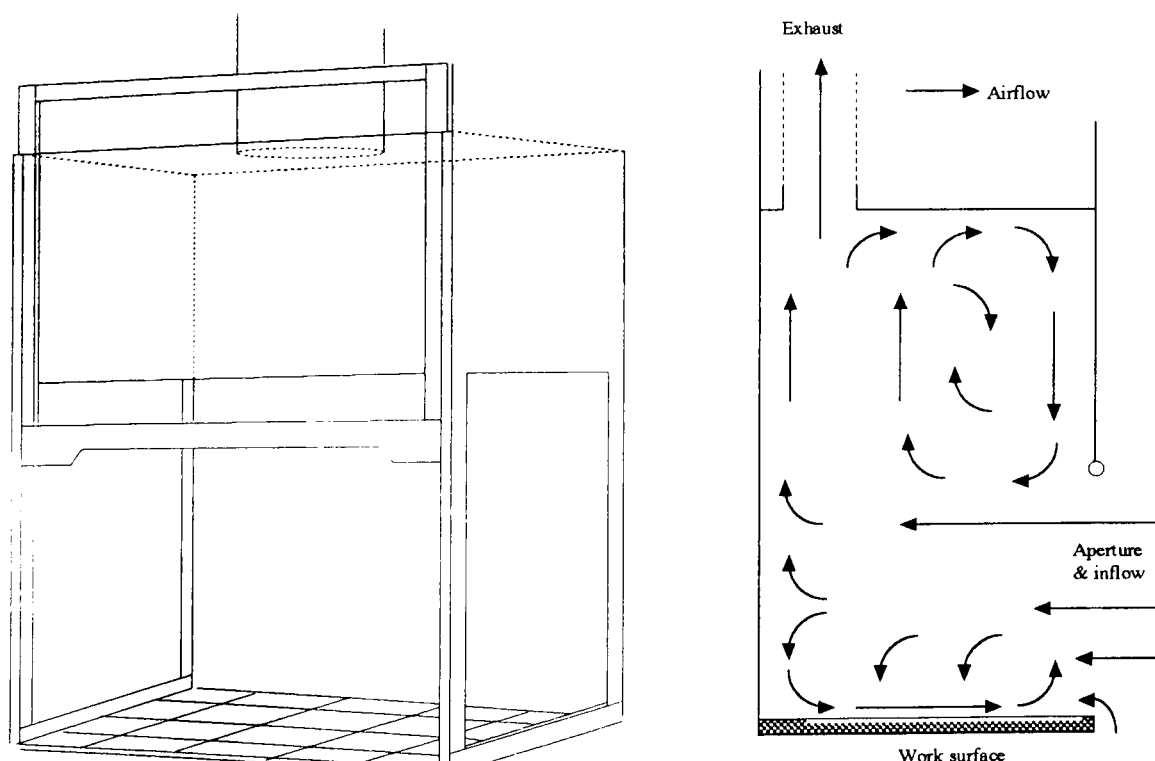


Figure 2.1 Box type fume cupboard and airflows

It was realised that the velocity and quality of distribution of the air entering the openings of fume cupboards had to be such that it would overcome any tendency for contaminated air

inside to escape. Only in the 1940s, when the importance of fume cupboards as practical safety devices was established, developments were made in their design to improve the containment efficiency and resistance to environmental disturbances. Attention was paid to the smoothness of the air flowing into and within the working area in order to reduce turbulent diffusion as a result of boundary layer separation at edges and the aerodynamic fume cupboard was developed (Fig. 2.2).

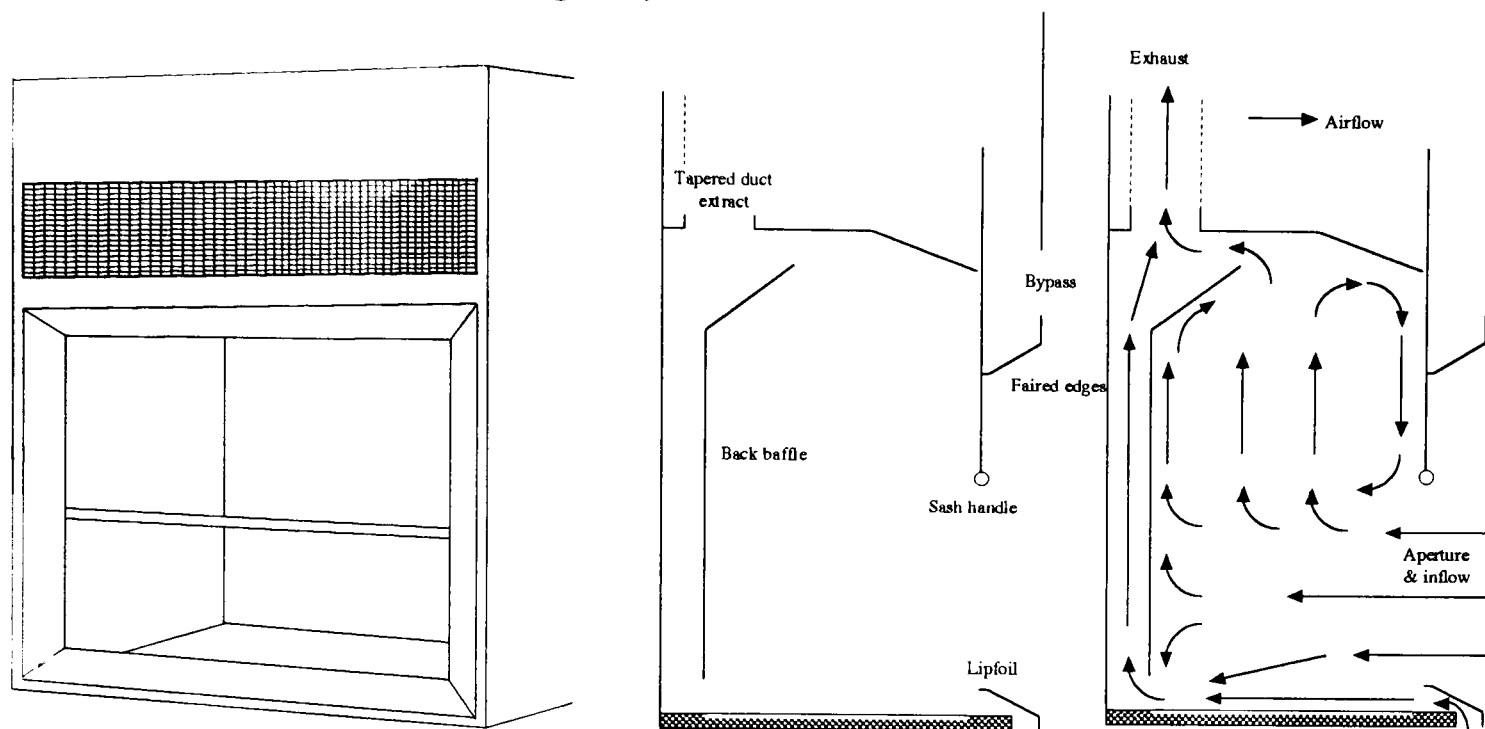


Figure 2.2 'Modern' features of an aerodynamic fume cupboard and airflows

Examples of the features included, a tapered extract duct used to extract air evenly across the width of the cupboard interior so balancing the velocity through the aperture in the horizontal direction: A back baffle was fitted which had slots at the top and bottom to even out the face velocity distribution in the vertical direction, encouraging air to sweep across the work surface purging any heavier gases or vapours; sometimes a middle slot was incorporated. The shape of the baffle and size of the openings were such as to encourage an even flow through the slots and the aperture. A large air recirculating zone behind the sash was formed which helped purge this region of air which could be contaminated from hot thermal gases or discharges from large pieces of equipment. If the flow through the slots was imbalanced then the effects could cause the recirculating region behind the sash to increase and bring air below the sash handle or to reduce the quantity of air passing over the work surface (Smith, 1994).

Faired edges around the aperture were introduced in order to reduce the vortices generated at the edges of the aperture due to boundary layer separation as air flowed past them. Lipfoils were used which had a similar effect to the faired mouldings on the sides and top of the aperture but instead of being flush with the interior were raised with a gap beneath them. When properly designed these ensured that air flowed straight into the cupboard with no recirculation encouraging it to sweep across the work surface and limiting the effect of any obstruction to the airflow by an operator leaning against it (Clark, 1989). Some lipfoils were not designed well and enabled air to leak from the working area. The factors affecting performance were the slope, the height of the gap between the foil and the base, and how

far it protruded into the cupboard, to allow straightening of the airflow (Saunders, 1993). The sash handle could also cause boundary separation at edge of the sash (Robertson & Bailey, 1980). In order to prevent this, the sash handles were faired to allow a smooth flow of air into the work space, eliminating vortex formation.

A bypass was used to allow a variable portion of the room air to flow into the working aperture (sash opening), with the objective of preventing excessively high face velocities at low sash openings and allowing a constant total exhaust air flow irrespective of sash opening. An auxiliary air supply was introduced near to the aperture of the fume cupboard so that the amount of room air exhausted by the fume cupboard was reduced. With variable air volume (VAV) systems the extract volume flow rate from the cupboard varied with the height of the working aperture so that the face velocity remained constant at any sash position. In a semi VAV system the fan speed was set at selected working aperture heights in order to maintain a constant face velocity.

With regards to safety, the larger the size of the opening then the greater the possibility of eddy formation as a result of cross draughts (Cook & Hughes, 1986). The depth of the work space was also considered important with respect to establishing airflow movements through the cupboard. The shallower the work space, then greater was the “bounce back” of air from the back wall and the less space the operator had to work in, forcing them to work near the front.

2.2.2 Review of test methods

An early philosophy was that the higher the velocity at the face of the cupboard and the smoother the flow then the greater the containment (Hughes, 1980). This was especially true when unfavourable environmental conditions existed (Caplan & Knutson, 1982)^b. However it was also shown that turbulent diffusion played a major role and containment could be related more to the volume flow rate than the face velocity (Roach, 1981). It was realised that face velocity measurements were not sensitive or reliable enough for measurement of actual exposure and that quantitative assessment of the containment efficiency of the fume cupboard was required.

The tests which subsequently developed had differing philosophies but ultimately assessed the efficiency of the fume cupboard (regarded as a partial enclosure) to contain fumes. The ideal test was to measure the efficiency of the cupboard to contain those fumes which were directly of concern. However, since the range of chemicals used and procedures carried out in a cupboard were so diverse this was impossible, and did not give the manufacturer or general user enough information on the cupboard design and installation. Further, the tests developed had to be repeatable so that fume cupboard design and installation could be standardised (Table 2.1). Tests carried out on installed cupboards gave absolute measurements of the

Standard	British BS 7258 : 1994	U.S.A. SAMA LF 10 1980 & ASHRAE 110 : 1993	German DIN 12 924 : 1991	Dutch DS 457 : 1986	Australian AS 2243.8 : 1992	French NF X 15 203 & 206 : 1987
Sash position	Normal working sash	Fully open sash. Dynamic sash.	Closed, 1/3 open & fully open sash. 2 dynamic sashes.	As used	Fully open sash	No data given
Flow/velocity	Extract flow or velocity as specified by purchaser. Individual readings >85% of the overall mean face velocity for type test and >80% at commissioning.	Velocity as specified by purchaser. Individual readings $\pm 15\%$ of the overall mean face velocity.	Extract flow as specified by purchaser.	Extract flow as specified by purchaser	Overall average $\geq 0.5\text{m/s}$. Individual measurements within $\pm 20\%$ overall mean. Fluctuations at a point <20% record average, if >20% record max. & min.	Overall average $\leq 0.5\text{m/s}$. Individual measurements within $\pm 20\%$ overall mean.
Velocity test	Hot wire for type and commissioning, rotating vane for maintenance. Complex grid for type and commissioning, 9 point for maintenance in the plane of the sash.	Use SAMA LF 10 1980. Calibrated anemometer. 1 equally spaced measurement/ square foot in the plane of the aperture. Normally 9 readings. Average face velocity.	none	none	Thermal anemometer or rotating vane if used with care. Complex grid or abbreviated test using 5 points in the plane of the sash.	no data given
Smoke/fog test	Suggested for commissioning.	TiCl ₄	no	no	Complex smoke test	no
Equipment loading	no	no	yes	As used	no	no
Manikin	no	yes, with nose in plane of hood front.	yes, ~250mm from sash.	Operator	no	no
Tracer gas/injection rate	10% SF ₆ & 90% N ₂ 2l/min/m sash width.	100 % SF ₆ or R-12 1-4-8l/min fixed	10% SF ₆ & 90% N ₂ 3.33l/min/m sash width.	Any gaseous pollutant not normally present.	no	no
Injector type	30 mm dia. P40 sintered glass funnel Non-entraining/mixing. Positioned at 6 locations at 150mm from sash. typical velocity < 0.1m/s	Entraining/mixing type. Overall 127mm dia. 294mm height. Positioned at 3 locations on work top at 150mm from sash plane. Typical velocity < 0.1m/s.	Entraining/mixing type. 90mm dia. 465mm high. Positioned centrally on work top 200mm from sash. Typical velocity < 0.1m/s.	Not specified	no	no
Sampling	Variable no. of tubes distributed across the plane of the working sash aperture. Grid overall sampling @ 2l/min $\pm 5\%$.	1 sampling probe located close to nose level and in the plane of the hood front. 3 sampling positions local sampling.	20 sampling funnels distributed across a plane parallel to and 100mm away from the fully open sash. Grid overall sampling @ 30l/min.	1 sampling probe located close to the breathing zone of the operator. Local sampling.	no	no
Tracer sampler	Sensitive to 1ppb $\pm 10\%$. Normally by infra-red analysis.	Sensitive to 1ppb $\pm 10\%$. Normally by infra-red analysis.	Infra-red analysis.	Not specified	no	no
Expression of results	6 tests. No specific requirement. Mean escape concentration recommended.	3 tests. Max. of mean escape concentration in ppm.	3 tests repeated for each of 5 conditions. Mean and rms escape concentration.	Not specified		

Table. 2.1 Methods for measuring the performance and efficiency of laboratory fume cupboards in terms of operator protection.

performance in that environment but did not necessarily indicate failings in the cupboard design. Tests carried out in a controlled environment (“type tests”) allowed comparative testing between fume cupboard types and designs and provided a reference for performance of fume cupboards when subsequently tested ‘on site’.

The quantitative assessment of fume cupboard performance^{was} developed in the late 1970’s both in the UK and the USA. The requirement was a test method that could be standardised to give reproducible results. The main emphasis was to assess the effect on fume cupboard performance (mainly of the need, in large institutions, to reduce running costs) by reducing the amount of make-up air from the room being extracted through the fume cupboards. The American Society of Heating, Refrigerating and Air-Conditioning Engineers (ASHRAE) commissioned a study on fume cupboard performance and a test method was published in 1978 as an ASHRAE document RP-70 by Caplan. From this work it was shown that excessive face velocities were not needed and a recommended face velocity of between 0.3 m/s and 0.5 m/s was published in 1982 by the American Conference of Governmental Industrial Hygienists (ACGIH) as providing acceptable and safe operating conditions. The report was proposed as Standard 110-P in 1982 and published in 1985 as ASHRAE 110-1985 and revised in 1993.

The test method described in the report involved the release of a tracer gas, dichlorodifluoromethane (R-12), or sulphur hexafluoride, SF₆, from within the cupboard and sampled in the breathing zone of a manikin positioned erect in front of the fume cupboard (Fig. 2.3). This method could be used on site or as a ‘type test’ in a controlled environment. The test method was near to an absolute test of containment on site and served as a comparative test when type testing, i.e. comparing the performance of one type of cupboard with another or the effect of changing environmental conditions.

The quantitative test method published in the German standard, DIN 12 924, was similar to the ASHRAE standard. Tracer gas (SF₆) was released in the fume cupboard but instead of sampling in the breathing zone of the manikin, samples were taken through a vertical grid of probes in a plane 100 ± 10 mm outside of the plane of the working aperture (Fig. 2.4). A manikin was used to simulate the presence of a worker and standard items of equipment were placed inside the fume cupboard at set positions. This test measured leakage into the room from the aperture and not what entered the breathing zone. This method could be used on site or as a ‘type test’ in a controlled environment.

In 1982 British Standard document BS 3202 for fume cupboards was revised and published as a draft for development, DD 80, which included a proposed method for quantitatively assessing fume cupboard performance. This was later published as BS 7258 : 1990 in which

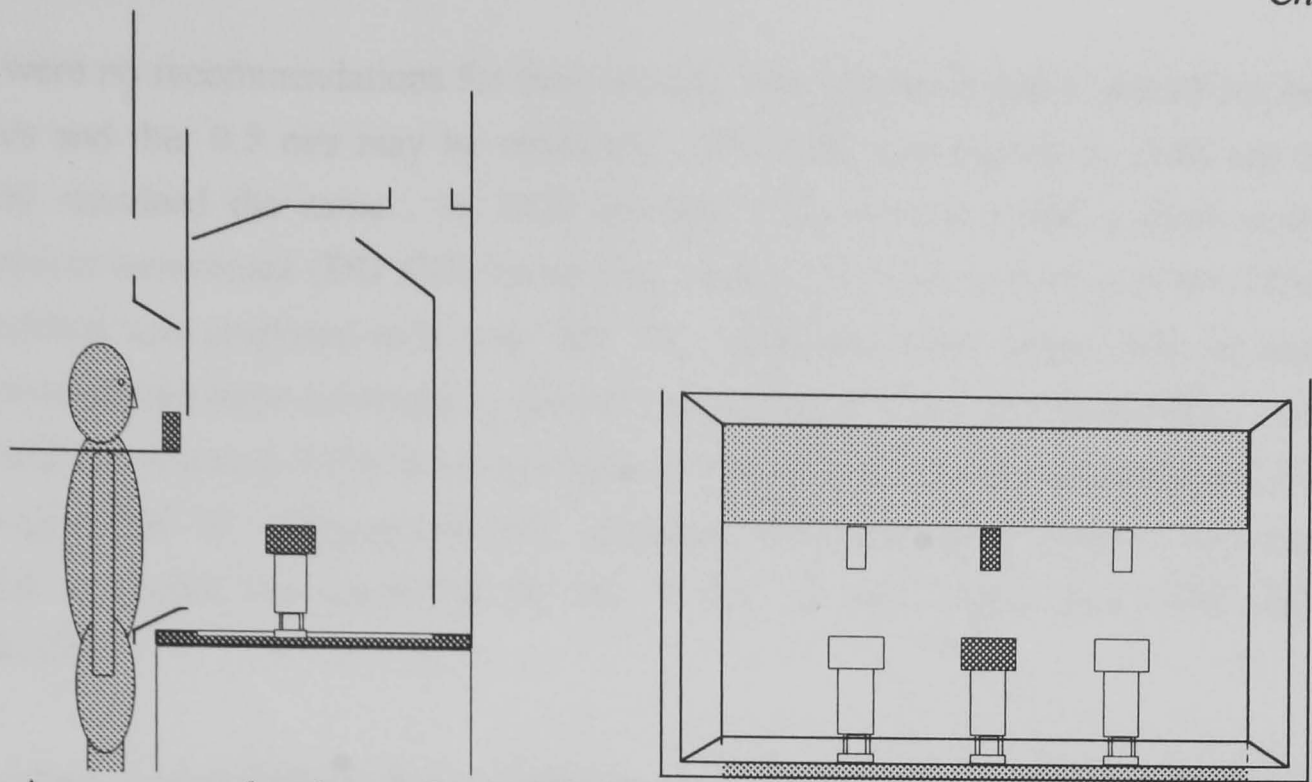


Fig. 2.3 Arrangement of equipment for the USA fume cupboard containment test (ASHRAE 110 : 1993).

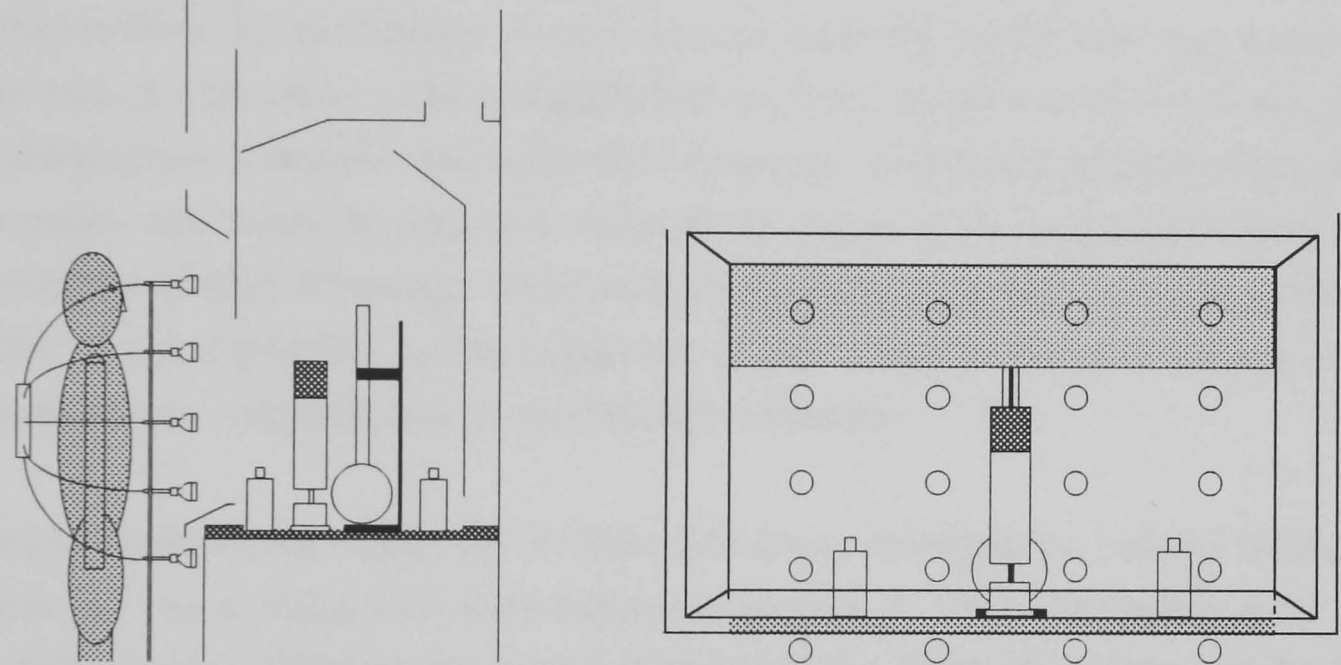


Fig. 2.4 Arrangement of equipment for the German fume cupboard containment test (DIN 12 924 : 1991).

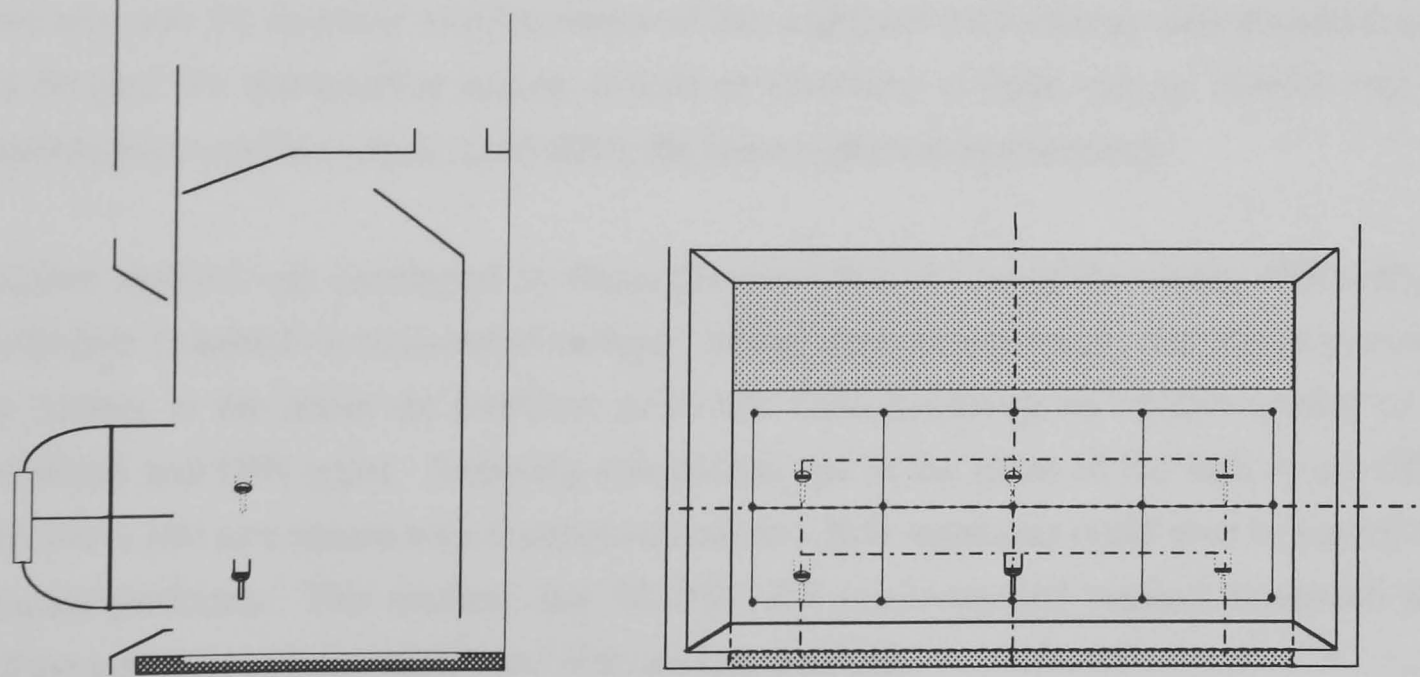


Fig. 2.5 Arrangement of equipment for the British fume cupboard containment test (BS 7258 : 1994).

there were no recommendations for face velocity, only guidance that it should not be below 0.3 m/s and that 0.5 m/s may be necessary. BS 7258 was revised in 1994 but the face velocity remained the same. In 1990 the BS 7258 document had a draft method for quantitative assessment (DD 191) which was adopted in 1994 as Part 4 of BS 7258. This test method was proposed as a 'type test' in a controlled environment with no equipment present inside the fume cupboard or obstructions to the air flow. In this test (Fig. 2.5), tracer gas (SF_6) was released in the fume cupboard and samples taken from a vertical grid of probes in the plane of the working aperture. Because of the sampling position, any tracer gas sampled indicated the **potential** for the facility to leak rather than THE ACTUAL LEAKAGE.

In summary, the ASHRAE 110 quantitative test method gave an estimate of the dose an operator would breathe when working in front of the fume cupboard, the DIN 12 924 gave an estimate of the level of leakage of tracer into the room and the BS 7258 test method gave an estimate of what tracer could potentially leak out from the plane of the working aperture. The philosophies of the tests thus varied from those that relied on the sampling of exposure of the operator and those that tended to estimate the design of the cupboard in terms of the potential and position of leakage. Thus comparison of the results from each test method was difficult, if not impossible, as the magnitude of any actual or potential leakage changed depending on the sampling position and the effect of dilution.

A method similar to the ASHRAE 110 test method was developed for 'on site' testing while the operator was working at the fume cupboard (Ivany et. al. 1989; Diberardinis et. al. 1991). This method used a different gas injector device than the ASHRAE injector and the sample probe was worn by the operator so that any leakage was monitored in the breathing zone. This test was for absolute measurements of the cupboard performance and therefore could not be used for comparative testing of type or condition as there was no control over any confounding variables which could affect the fume cupboard performance.

Another method was developed by Bicen (Invent UK Ltd.) using the testing philosophy of the British Standard recommended method. In this method, gas tracer was discharged inside the cabinet in the same six positions as in BS 7258 but using an injector similar to the ASHRAE and DIN types. Sampling was carried out in the plane of the sash in a localised grid 300 x 300 mm square with 9 samplers and the whole apparatus could then be moved to 6 separate positions. This method, like the BS 7258 recommended method, measured what had the potential to leak rather than what actually did leak.

2.2.3 What strategy for inclusion into BS 7258 : 1994?

There was much protracted discussion between fume cupboard manufacturers, health and safety experts and academics as to the usefulness and complexity of qualitative, semi-

quantitative and quantitative test methods for assessing fume cupboard performance and their inclusion into national standards. Ultimately it was hoped that an internationally recognised standard test method and reporting system for assessing fume cupboard performance would be developed so that results could be compared regardless of their origin and that various test methods could be used, compared and correlated. However, due to the variation in the test methodology between countries, and especially with respect to the British Standard, this left the picture a confused one with no definite test method and an industry still questioning the validity and usefulness of many of the procedures.

Initially, there was opposition and mistrust by manufacturers to the principle and reliability of a quantitative containment test being incorporated into a British Standard, so they continued with the measurement of face velocity and its distribution across the fume cupboard aperture. However, this attitude was changing as more reliable quantitative methods were developed, which showed, time and again, that face velocity did not correlate with the level of containment. Also, there was increasing demand from the purchaser that the fume cupboard should give a performance that could be used in risk assessment as part of COSHH (1988). In the preparation of BS 7258 : 1994 there was research put into the development of testing strategies and the inclusion of a quantitative test for containment. The available national standards were compared in an attempt to use the best parts and also to develop new methods. However, a containment test method could not be entirely agreed which led to a British Standard in which emphasis was still placed on face velocity testing with only the recommendation of a containment test.

Qualitative information such as visualisation of airflow within fume cupboards was said to be of questionable value (Whitelaw, 1993) but nevertheless this, and other semi quantitative tests, could point to areas of poor cupboard performance. Quantitative testing was the focus for identifying specific measures of performance. Airflow visualisation and face velocity measurements could indicate “good” and “better” performance, but did not quantify performance and thus could not indicate what was best. However, in this respect not carrying out a qualitative test and just using quantitative assessment could waste time and be expensive. A large percentage of fume cupboard problems could be solved with basic instruments and devices that every safety or occupational health group should have (Saunders, 1993).

The emphasis on face velocity testing varied between the available national standards and other suggested methods. The British and Australian standards still specified a complex arrangement of measurements positions; the performance of the fume cupboard being assessed by the stability of the airflow. Other standards used a coarser grid for measurement of velocity in order to establish a face velocity and an indication of gross variation across the face. The more velocity measurements made over the aperture then the more accurate would be the result. Single or small numbers of flow measurements were of limited value

(Whitelaw, 1993). However too many points and readings were considered impractical and comparing the commissioning grid with the type test grid showed no significant difference (this thesis), and a reduced grid of 9 points was shown by Bicen (1993)[†] to differ by only 2 - 3 %. The accuracy of the anemometer was expected to be in this region and expected to be no more than 10 % accurate reflecting the instrument, the user and the fluctuation of the room conditions (Saunders, 1993).

In terms of designing, type testing and installing a new cupboard, it was said that the type test lacked spatial resolution near to the boundaries (Bicen, 1992). In this region, depending on the design, greater turbulence would be expected and a higher velocity where the air flowed over 'aerodynamic' features. The type test was suggested to be used only for assessing the quality and distribution of the airflow into the cupboard and not linked to the performance 'on site' using the commissioning test. This should just be used for setting the face velocity and to which further tests results could be compared. The link between type and 'on site' performance should ultimately be made using a quantitative containment test.

It was suggested that a measure of turbulence at the face of the aperture would be more representative of cupboard performance than merely the averaged face velocity and variation across the aperture; turbulence possibly being a means by which leakage may occur (Bicen, 1993)[†]. It certainly seemed from the literature that turbulence did follow leakage. As observed by Fletcher & Johnson (1992)[†] with high turbulence there may be high leakage but it was also shown that leakage could also occur in regions of low turbulence. Draughts were a cause of large fluctuations in the measurement of face velocity but the effect on the mean velocity at that point was weak and did not necessarily show up as variation across the aperture. To this end it was concluded that individual fluctuations should be part of the test and a measure of turbulence made (Bicen, 1992; Saunders, 1993).

This raised the question as to what anemometer should be used. The use of a rotating vane anemometer was derided by a number of people for use with fume cupboards because of its level of insensitivity and inaccuracy at velocities below 0.3 m/s, its slow response time and its bad spatial resolution (Sec. 2.7.1.1). This was exaggerated by the recommendations in BS 7258 : 1990 for routine maintenance in which the potential error and recommended values could lead to low face velocities. The rotating vane anemometer though could be valuable and practical in being used to monitor face velocity with only a few measurements giving an area averaged figure. However for measurements of velocity fluctuations at a point then thermal anemometers were to be used with their better overall characteristics and faster response times.

There was also argument about the type of thermal anemometer used, omni-directional or semi-directional? The BS 7258 : 1990 : Part 1 specified an omni-directional probe. However, with omni directional sensors it was reported as being unclear how well they indicated the

true face velocity of hoods as they were not sensitive to velocity direction (being mainly used for measuring wind and draughts) (Bicen, 1992). It was said that they may be used in the controlled and well defined environment of a test room, but on site, where there may be variations across the face due to environmental disturbances, velocity direction was more important.

Following the discussion of the virtues of face velocity measurements the general observation then was that a containment test should be the main part of performance testing. However, as the procedures previously used in the UK, USA and Germany were substantially different, questions were asked; what should be the type and position of the source and samplers; what flow rates for both challenge and sampling should be used; what tracer should be used; and what measuring instrument should be used?

The tracer substance most commonly specified was sulphur hexafluoride which could be measured to part per billion levels. There were two main methods of its release within the fume cupboard in order to mix it with the cupboard interior. It was shown that for leakage in the lower part of the aperture, an increasing gas density would result in an increase in the measured leakage (Fletcher & Johnson, 1992)^f. The BS used a scintered glass funnel to distribute a gas mixture of 10 % SF₆ in nitrogen so as to reduce its density and release it at a flow rate of ~ 0.1 m/s. The other methods sought to use a device which ejected the gas at high velocity in order to entrain air from the cupboard and then pass it through a diffuser, so producing a near neutral buoyancy. It was observed that gas escaped from the DIN injector as a jet with velocity of 0.5 - 0.8 m/s, extending several diameters above the mesh whilst a smaller, lower speed emission occurred around the top of the mesh side walls (Fletcher & Johnson, 1992)^g.

The tracer gas discharged from the funnel was still slightly heavier than air (s.g. 1.4) and was shown to sink around the BS funnel (Fletcher & Johnson, 1992)^g. The German type injector as used in DIN 12 924 mixed air and the tracer so making it effectively buoyant and dispersing it within the fume cupboard.

Further experience showed that the position and type of the source within the cupboard interior affected its distribution and could have an important effect on leakage. As leakage could be very localised; the closer the source was to the leakage then the greater the leakage (Fletcher & Johnson, 1992)^h. Results from using single probes and the BS injector indicated that gas levels in the plane of the sash were highest at locations close to the injector source (Bicen, 1992). With the BS funnel and the DIN injector at the same position, the DIN type resulted in lower gas concentrations in front of the cupboard and the repeatability of results was claimed to be much better than that of the funnel (Bicen, 1992). It was suggested that the DIN injector gave better mixing inside the cupboard. However in the standard test, the tall German injector was shown to present a more severe challenge in the region of the sash,

because of the relatively high speed ejection of tracer gas, whilst the BS source used in 6 positions around the aperture identified inherently weak spots as far as containment was concerned (Fletcher & Johnson, 1992)^a. It was also commented that leakage using the DIN injector was generally higher than those found with the BS funnel. There was no comment on the ASHRAE injector.

The flow rate of the tracer also had to be considered. It was shown that if a leak was occurring, then increasing the flow rate of tracer gas also increased the measured leakage (Fletcher & Johnson, 1992)^b. Bicen (1991)^b showed that an increase in SF₆ concentrations detected in front of the cupboard increased in an almost linear fashion with the release rate of the test gas. However, if there was no tracer detected then this did not necessarily mean increasing the injection flow rate would result in gas being detected suddenly.

The flow rate selected was normally based on simulated 'in-use' conditions. As a guide, if water boiled on a 500 watt hot plate, the rate of vapour released would be approximately 8 l/min (Saunders, 1993) and the amount of solvent vapour released while pouring acetone, chloroform or toluene from one beaker to another would be approximately 1 l/min. For the ASHRAE test the flow rate was 1, 4 or 8 l/min, for the BS test 2 l/min per m cupboard width and for the DIN test 3.33 l/min per m cupboard width. Fletcher & Johnson (1992)^a thought it more reasonable to assume that leakage from a cupboard would be related to the concentration of tracer in the cupboard and hence, in order to maintain the same test concentration, the influencing factor should be the ratio of the volume of air flowing through the cupboard to the challenge gas flow rate. They proposed to modify the tracer flow rate to 10 Q l/min where Q was the volume flow rate through the cupboard. However, there was no evidence that the working volume of a cupboard became fully mixed with tracer, and in regions of poor scavenging, tracer may concentrate and localised leak would be exaggerated.

As discussed earlier, the concentration of gas measured further from the source reduced if internal mixing was not complete and instantaneous. For a grid as used in DD 191, the probes located further away from the source tended to dilute the sample giving a grid averaged reading over the aperture and a reduction in overall levels. It was proposed that the sampling positions should be localised to the source and a fixed injection flow rate used (Bicen, 1992, 1993)^b. The whole apparatus then being moved over the aperture width, rather than just the source.

The sampling grid was important and the form and positioning was equally as diverse as the type and positioning of the source. As discussed earlier, the BS test sampled in the plane of the sash and measured potential leakage, whereas other methods measured actual leakage at a distance from the sash plane. This was dependent on the philosophy of the test and perhaps was the most fundamental difference between them. It was shown that if tracer gas was detected in the plane of the sash, sampling further away from this plane resulted in a decrease

in the concentrations measured. Bicen (1991, 1992) showed that tracer gas detected using the DD 191 grid was not detected with the DIN 12 924 grid. In some cases, tracer gas could be represented to the plane of the aperture and never escape into the room but be entrained into the air flowing into the cupboard. This would be detected by the BS test and a containment factor applied. The DIN test would measure no actual leakage and another factor applied. Attempts were made to correlate this with exposure for COSHH assessment and to correlate the two test methods based on accepted dilutions of a tracer with distance. However, this could only be worked one way, the assumption that what was measured using the DIN grid would also be sampled by the BS system but giving higher values. The converse was not possible because the detection of gas in the plane of the sash did not automatically mean there was a leak. It could be argued that the BS system was more stringent as it measured not only what would leak out but also what could potentially leak out. Whether this was an advantage or not was questionable.

The type of sampling probe also varied. The ASHRAE method used a single probe in the breathing zone, the DIN method used funnelled probes and the BS method straight probes. The governing factor with the DIN and BS tests was that the sampling flow rate was expected to approach isokinetic sampling and with a suction velocity of the order 0.1 m/s. Fletcher & Johnson (1992) pointed out that as the flow into a sampling probe was in the opposite direction to the general flow, this was somewhat irrelevant and presumably was meant to imply low velocity. The funnelled sampler was suggested in order to maintain a low velocity over the enlarged area removing the need to specify a suction velocity completely (Bicen, 1992).

The instrument used for sampling had to be able to sample to the part per billion level. The main factor which dictated the choice of instrument then was the price and portability of the system. This was narrowed down to infrared analysis and electron capture devices. Both had problems but the infra-red device was preferred because of its selectivity to the tracer gas used whereas the electron capture could be influenced by any electron capture gas. However, the infra-red analyser characteristics had a sudden increase in concentration, followed by a long exponential decay period which was a function of a large measuring cell. The electron capture device was instantaneous with no decay periods. The BS method of sampling would seem to favour collection into a bag and subsequent sampling of the contents at the end of the test period, i.e. single weighted averages. This would give the mean concentration but not max. or min leakage's and real time recordings have been shown to provide more information as to the periodicity of the leakage.

The overall sampling time was also discussed. The DD 191 method required a sampling time of 780 s. The initial 180 s in which no measurements were recorded was the time during which the mixing of the test gas inside the cupboard was allowed to take place. The DIN method required a 500 s test time for the static test and 600 s for the dynamic test. The

ASHRAE test duration was 600 s. Fletcher commented that leakage may take place, not as a continuous process, but in a series of pulse releases. Because of this latter feature, the impression sometimes formed was that the measurements themselves gave rise to non-repeatable results, but in fact environmental disturbances instead were more likely to be the cause of such variability. Bicen (1992) commented that the nature of leakage from the cupboard was characterised with unsteady or intermittent bursts with 300 s or more intervals during which no leakage occurred. In these cases much longer sampling times ($\gg 300$ s) were suggested to achieve statistically meaningful results and to improve repeatability. Increasing sampling time to 900 s or more was proposed to reduce uncertainty and improve the repeatability by 50 % or more. However Saunders (1993) reduced the test duration when using the ASHRAE method to 5 minutes as in his experience he had seen most cupboards to indicate poor performance in the first 3 minutes. A few showed signs of failure in the 4 th or 5th minutes only.

There was much discussion about mechanisms and magnitudes of leakage and detection and what level of performance a fume cupboard should have. In the USA the ACGIH suggested that a hood tested using the ASHRAE method at an injection rate of 4 l/min and ‘as manufactured’ should have a control level not to exceed 0.05 ppm. For hoods tested under ‘as used’ conditions the control level should be 0.10 ppm. In the BS there was no recommended level except that suggested by Bicen (1993)^a, summarised in table 2.2. For the DIN test the permitted values were as shown in table 2.3. Considering that in the ASHRAE and DIN tests measurements were made a distance away from the plane of the aperture and that the DD 191 test measurements were made in the aperture plane, then the recommended BS measurements were very strict.

	Escape concentration	
	C_{mean} highest position	C_{max} highest position
excellent	<0.005 ppm	<0.010 ppm
good	0.005-0.020 ppm	0.010-0.040 ppm
average	0.021-0.100 ppm	0.041-0.200 ppm
below average	0.101-0.200 ppm	0.201-0.400 ppm

Table 2.2 Recommended values for BS 7258 : 1994 : Part 4 (Bicen, 1993)^a

Position	concentration		
	limiting	max	SD
closed	0.2 ppm	0.6 ppm	0.06 ppm
1/3 opened	0.5 ppm	1.5 ppm	0.15 ppm
open (complete)	0.8 ppm	2.4 ppm	0.24 ppm
open 1/3 in 10s	120 s decay time	1.5 ppm	
open fully in 10s	240 s decay time	4.0 ppm	

Table 2.3 Permitted values for DIN 12 924

The face velocity was shown not to correlate with containment, and lower face velocities would be expected to be more sensitive to environmental disturbances. However, it was found that the containment of some cupboards could be influenced by face velocity but in others, reducing the face velocity had no effect or even resulted in improved containment. Fletcher & Johnson (1992)^b showed that a measured leakage did not necessarily decrease with increasing face velocity, even if the cupboard was unobstructed. Very high leakage rates found at low velocities fell quickly with increasing face velocity only to rise again before falling steadily. Thus generally an improvement on containment at all velocities by design would be the preferred solution, and as there was no specified face velocity in the BS then containment testing should be carried out at several face velocities.

Fletcher & Johnson (1992)^b found leakage near to the sash in tests using the DD 191 method on some cupboards, and for distances greater than 20 mm from the sash the concentration fell quickly. The leakage concentration was much steadier closer to the sash than at the distance of 50 mm as specified and the grid was modified so that probes were 15 mm from the edges of the working aperture. It was suggested that leakage would only be found near the periphery of the working aperture and it seemed likely that for an unobstructed cupboard measurements need only be made there.

A frequent comment was that although the type test and the commissioning test showed how a new cupboard could operate, the tests had little bearing on the 'in use' case in which the environment played an important part in stable operation (Caplan & Knutson, 1982)^b. The DIN test approached this by having a dynamic test in which the sash was opened and the containment level measured. There were also blockages caused by equipment inside the cupboard and a manikin outside to obstruct the air flow. Bicen (1991)^b did work using a 2 dimensional blockage and the BS 7258 test method and found that the blockage positioned close to, and in front of the sash, caused significantly increased levels of SF₆ to be sampled in the plane. Moving the blockage away from the sash plane dramatically reduced the SF₆ levels by three orders of magnitude (150, 280 and 400 mm away) ; the position of the manikin (as used in the DIN test at 250 mm away) had a relatively weak influence on containment. In this study by Bicen it was also concluded that the presence of test equipment inside the cupboard, as in the DIN test, would have no significant effect on containment.

However, it was still suggested that some form of challenge was needed in the type and commissioning stages of testing. Saunders (1993) recommended cardboard boxes and paint cans be used to simulate the effect of equipment and that the ASHRAE test be performed with people present and walking past the front of the cupboard and behind the manikin. Robertson and Bailey (1980) concluded, using the DD 191 method, that whilst people walked past, the tracer method was not as effective as the smoke method for indicating the escape of fume because of the difficulty in measuring where leakage occurred.

Further to the suggestions that type tests and commissioning tests should be changed to reflect the 'in-use' situation, there was the routine maintenance test which brought about further complications. Cupboards 'on-site' and 'in-use' often were full of equipment which could not be moved and could not be tested as they were at commissioning - devoid of equipment. Further to this, once a cupboard had been installed and commissioned, it was then left to the purchaser to ensure the routine maintenance and operation. The user may have had little knowledge of the operation of a fume cupboard; their work practices potentially countering containment achieved by the fume cupboard when tested at commissioning or routine maintenance. The 'in-use' case would then include not only equipment blockage and the movement of people around the cupboard, but their work practices as well.

The BS 7258 : 1994 document was eventually published in 4 parts. A containment test method could not be entirely agreed upon and the emphasis in the assessment strategy was still placed on complex face velocity testing with only the recommendation of a containment test included as Part 4 (section 2.2.3). The strategy included a 'type' test and 'commissioning' test, the latter a subset of the 'type' test, and a routine maintenance test. The philosophy of the test was all relative, the commissioning test being comparable to the type test. The routine maintenance test, using the commissioning grid, was referable to the values at installation. There were no absolute performance values specified, only the variation about the mean face velocity as specified by the purchaser and a measure of a decrease in performance. Omni directional anemometers were specified but did not include a measure of turbulence. The routine maintenance test used a rotating vane anemometer. There was no hierarchy of testing and only recommendations for airflow visualisation when commissioning. The cupboards had to be empty, there was no ability to assess already installed cupboards with no type test information and no dynamic tests. The containment test was that described in DD 191 and used the philosophy of sampling in the plane of the sash.

2.3 Microbiological safety cabinets (class I and class II)

2.3.1 Historical

An early version of what is now known as a class I microbiological safety cabinet was like a box type fume cupboard. It was an open fronted cabinet, generally designed for use by one operator (Fig. 2.6), with a fan and filter system fitted to the cabinet roof. Air was continuously exhausted from the working space of the cabinet thereby providing an inflow at the front opening. The inflowing air was derived from the general laboratory air and the rate of entry to the cabinet was designed so that air inside the cabinet's work space couldn't escape back into the laboratory. This type of cabinet was designed specifically to provide operator protection but not to give protection to the work being handled. Present day class I cabinets have not changed significantly. Early class I cabinets had face velocities of 0.25 m/s

(Wedum, 1953) but this was raised to 0.5 m/s (Lind, 1957; Williams and Lidwell, 1957) and then between 0.75 - 1.0 m/s (Newsom, 1979)^a

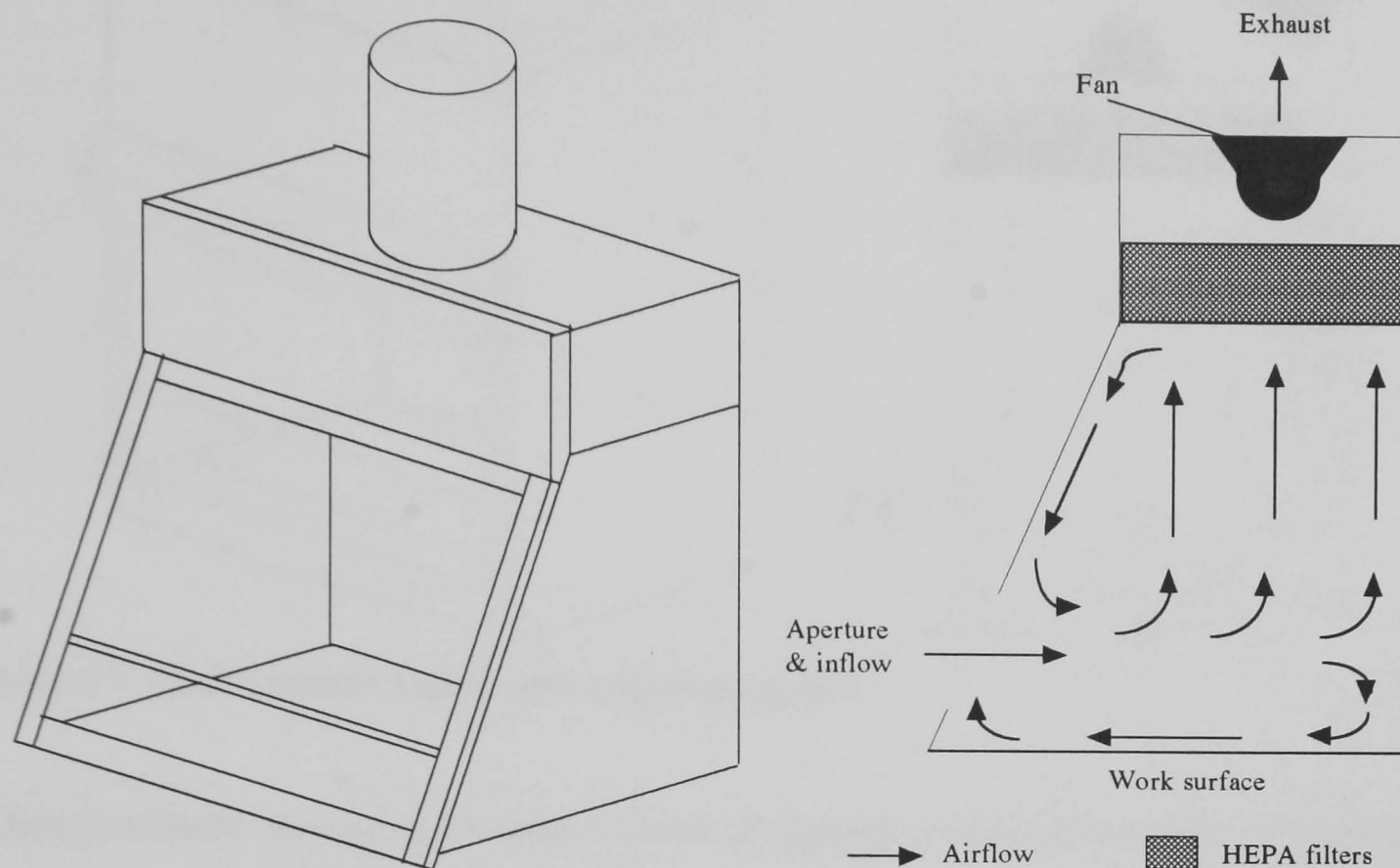


Figure 2.6 Class I microbiological safety cabinet and airflows

The major difference between the class I safety cabinet and the fume cupboard was the size of the opening which was smaller, narrower and fixed. Little was done to smooth out the airflows into the cabinet and there was much turbulence, not dissimilar to early box type cupboards with no rear baffle. There were recirculation zones behind the sash, and reverse flows across the work surface back towards the aperture. Thus potentially contaminated air could be entrained from the work surface towards the aperture. Early cabinets which had vertical apertures with sloping glass viewing panels effectively sat on the bench and invariably leaked as the contaminated air spilt out from the edge of the bench surface in similar circumstances to box type cupboards.

With the development of HEPA filters (Whitfield, 1962) it became possible to produce work areas in which the amount of airborne particulates could be strictly controlled. This technology enabled the development of clean rooms and clean benches. However, in the early days, much emphasis was placed on product protection and little on operator protection. In response to this, cabinets were designed that could protect both. These were called class II cabinets and Fig. 2.7 shows the basic configuration for such a cabinet.

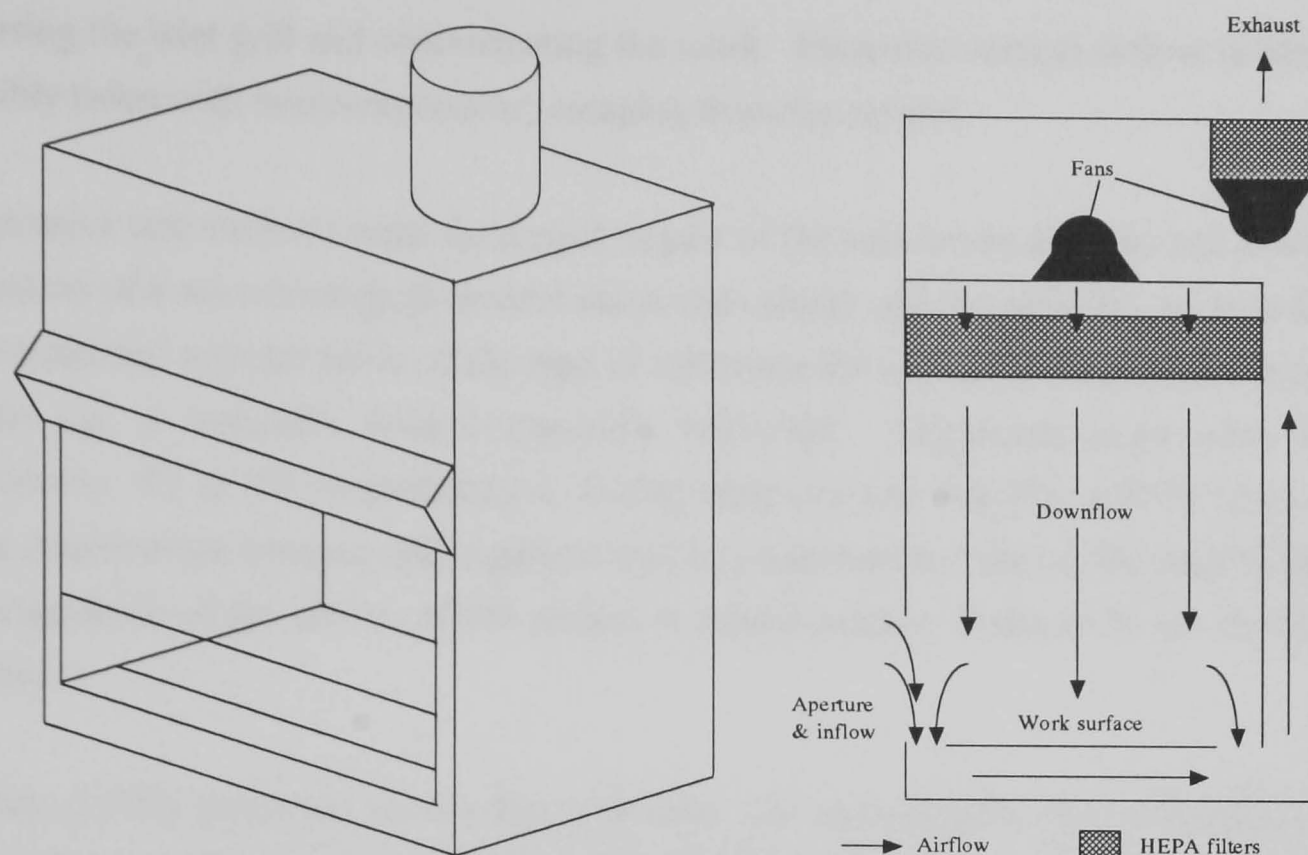


Figure 2.7 Class II microbiological safety cabinet and airflows

Class II cabinets were more complex in terms of engineering and airflow patterns than class I types and were designed to give a high level of product protection as well as operator protection. Within the working area there was a downflow of sterile filtered air which bathed the work area being handled. In addition, air was sucked in at the front opening to provide operator protection against any aerosols generated within the working space. In this design, unlike the class I cabinet, the inflowing air did not pass across the work surface, but deflected downwards through holes in the front part of the base to an air chamber beneath the working surface. The downflow and inflow air-streams came together beneath the working surface and passed to a plenum, generally at the top of the cabinet. Here some 20 - 50 % was exhausted and the rest of the air recirculated again through the working area. The air volume exhausted was equivalent to that taken in at the front opening.

2.3.2 Review of test methods

Microbiological safety cabinets were used to contain aerosols generated while working with pathogenic micro-organisms and to filter and discharge safely the effluent air. If the cabinet leaked into the workplace there was a high risk of exposure and perhaps subsequent infection. Performance assessment was initially carried out using face velocity measurements and smoke visualisation as for fume cupboard testing.

More rigorous testing was prompted by the development of class II cabinets. Many early models were found to have poor performance due to an instability where the downflowing air met the incoming air, sometimes to the extent that air either swept across the work surface or leaked out (Jones et. al., 1990). Excessive incoming airflow resulted in room contaminants

traversing the inlet grill and contaminating the work. Excessive vertical airflow resulted in air (possibly laden with micro-organisms) escaping from the cabinet.

Quantitative test methods were developed as part of the assessment strategy and involved the generation of a microbiological aerosol inside the cabinet and sampling the air outside. This was considered representative of the type of substance for which the cabinet was designed to contain i.e. a respirable hazard especially microbial. Organisms used were *Serratia marcescens*, T1 & T3 bacteriophages, *Escherichia coli* and *Bacillus subtilis* spores. This was a sensitive test because one organism may be recovered and due to bio-amplification and the uniqueness of the colony of the chosen microbial marker, could easily be identified and counted.

Barkley (1972) proposed to develop a reliable and reproducible test method capable of accurately assessing, up to an efficiency of 99.999 % in terms of operator protection, the performance of cabinets. In order to achieve this, the aerosol generated had to be of a high enough concentration of droplets for the escape of 1 organism to indicate the required level of performance, and at a relatively low air flow rate which would not ultimately displace the cabinet air. The aerosols created by normal activity were not in a high enough concentration. The method developed involved the release of bacterial spores using air driven nebulisers within the cabinet and air sampled outside using all glass impingers (AGI) or slit samplers

The viability of the organism during the test procedure was of major importance. In particular, it had to be able to survive aerosolisation and sampling. *Bacillus subtilis* var. *niger* or var. *globigii* spores met the desired criteria. The challenge was aerosolised in the size range 1-5 μm , which would constitute a respirable hazard, which remained viable for the duration of the test and which had easily identifiable orange/brown colonies.

In order to simulate environmental disturbances a typical disturbance was required particularly at the opening of the cabinet which did not compromise the reproducibility of the test. Petersen (1970) concluded that escape of contaminants amongst other factors could be due to the movement of the operators arm, or to the airflow around the arm. Barkley (1972) used a non-mobile arm placed in the opening of the cabinet to represent this. It was shown to cause significant disruption of the airflow parameters at an opening height of 200 mm where the arm was at the position where the downward and inward airflows interacted, the effect decreasing as the opening height was increased. In order to challenge this site where it was considered containment would be most difficult to achieve, the challenge aerosol was positioned 100 mm from the opening plane at a height of 250 mm from the base and directed at the opening such that the aerosol reached this position. All glass impingers were then positioned outside the cabinet around the arm to measure any leakage from the cabinet. This was then considered to represent a severe enough challenge which could be controlled and reproduced, and was an appropriate test method for evaluating performance.

This early work by Barkley (1972) culminated in the production of an American Standard in 1976 from the US National Sanitation Foundation (No. 49) which covered class II cabinets (Fig. 2.8). In 1979 in the U.K. British Standard BS 5726 was published which was similar to the American standard and was developed from work by Newsom (1974 & 1976) covering class I, II and III cabinets (Fig. 2.9 & 2.10). The main difference for assessing class I cabinets was the site considered to be the most vulnerable area where containment would be difficult to achieve. This was considered to be beneath the artificial arm and it was in this position that the challenge aerosol was generated. This document, for the first time, introduced the concept of the operator protection factor (Lidwell, 1960), a method for expressing containment efficiency.

In 1980 an Australia Standard was published (AS 2252) which covered class I and II cabinets. This test used smoke for visualisation and for quantitative assessment, the smoke was released inside the cabinet and air sampled in the plane of the working aperture through a single probe. The French standard, NF X 44 201, published in 1984 also used smoke as a quantitative method similar to the Australian method. Standard test methods for assessing safety cabinet performance and containment were reviewed by Kennedy, 1988 and are summarised in Table 2.4.

It was soon realised that if the test was to be used 'on-site' then in certain laboratories, e.g. tissue culture laboratories, the generation of an aerosol of microbial spores for containment testing would not be tolerated. Furthermore, *Serratia marcescens* was a 'low grade' pathogen and *Bacillus subtilis* spores were believed to be 'allergenic'. The British Standard committee thus sought to develop another test method which did not use spores but would be comparable. Clark & Goff (1982) published a method using potassium iodide (KI) particles as the challenge (Fig. 2.11 & 2.12) and was based on a method for the investigation of cross infection in hospitals by Foord and Lidwell (1972 & 1975)^{ab}. The equipment used was different to the microbiological method but ultimately the philosophy of the test was the same and the relative distribution of the equipment unchanged. From their correlation studies with the microbiological method there was good agreement with the results from both methods (Clark et al., 1982; Matthews, 1985).

The test strategy adopted for BS 7256 : 1992 had a hierarchical structure beginning with flow visualisation, face velocity and the main emphasis was placed on a quantitative containment testing using either microbiological or potassium iodide aerosols. These tests were used for assessing operator protection in class I and II cabinets, and by modifying this method for assessing product protection and cross contamination within class II cabinets. The same strategy was used for both type testing, commissioning and for routine maintenance.

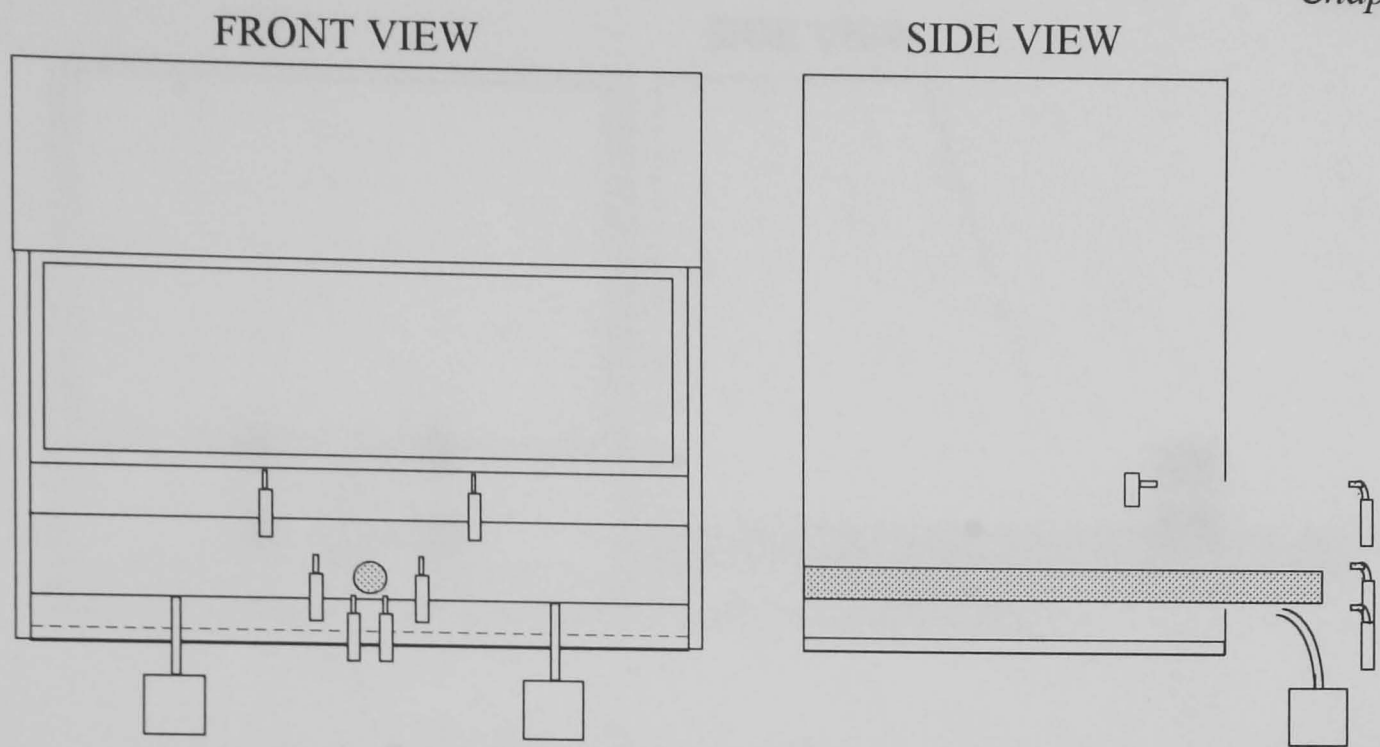


Fig. 2.8 Arrangement of equipment for the USA (NSF 49 : 1983), German (DIN 12 950 : 1991) and Japanese (JIS K 3800 : 1994) class II cabinet microbiological containment tests.

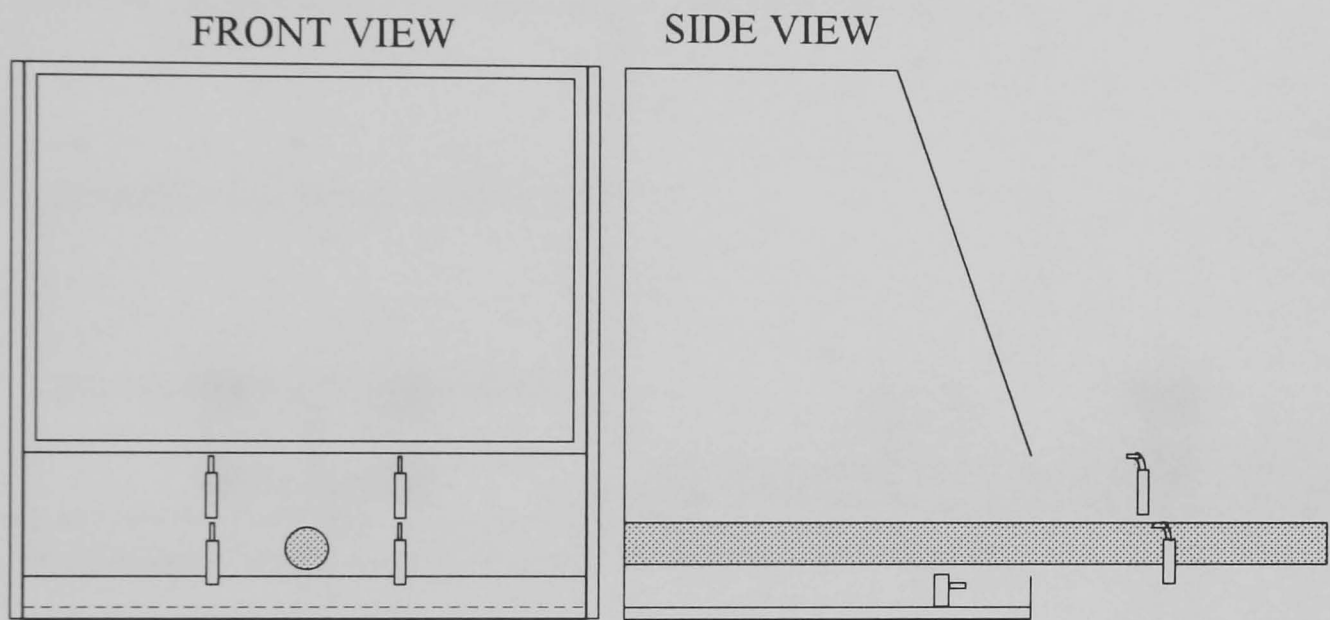


Fig. 2.9 Arrangement of equipment for the British class I cabinet microbiological containment test (BS 5726 : 1992).

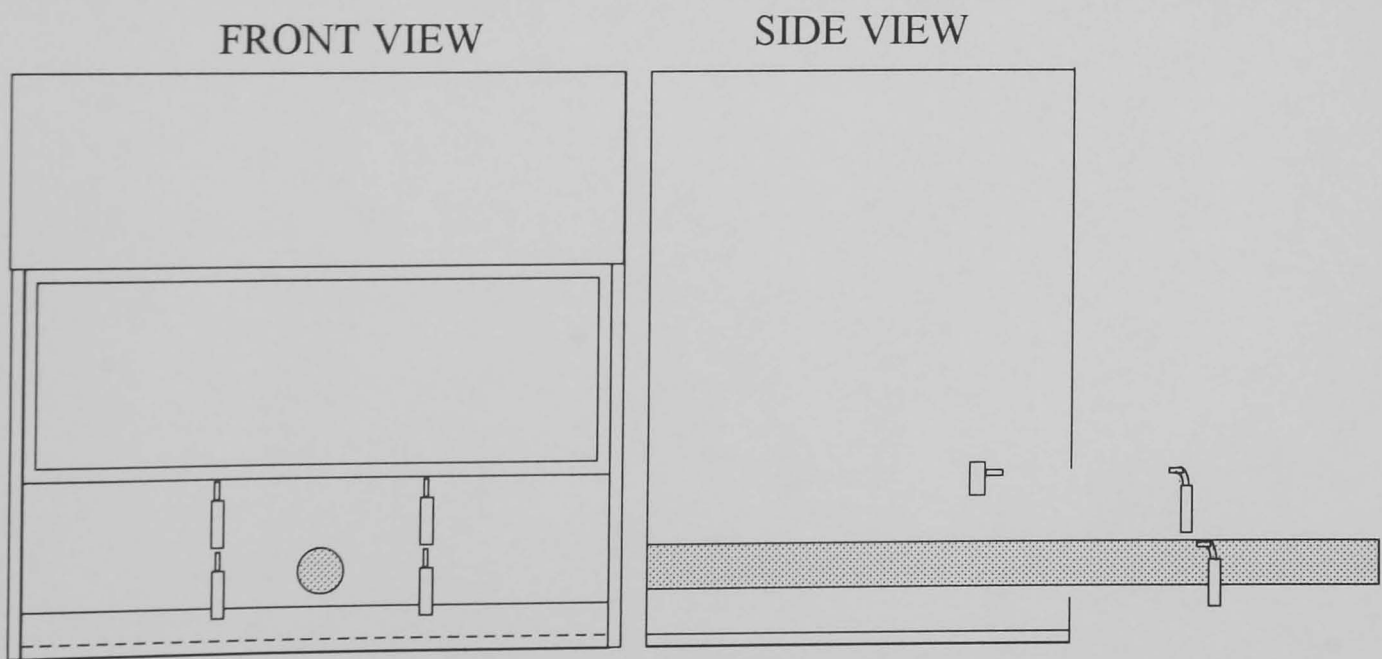


Fig. 2.10 Arrangement of equipment for the British class II cabinet microbiological containment test (BS 5726 : 1992).

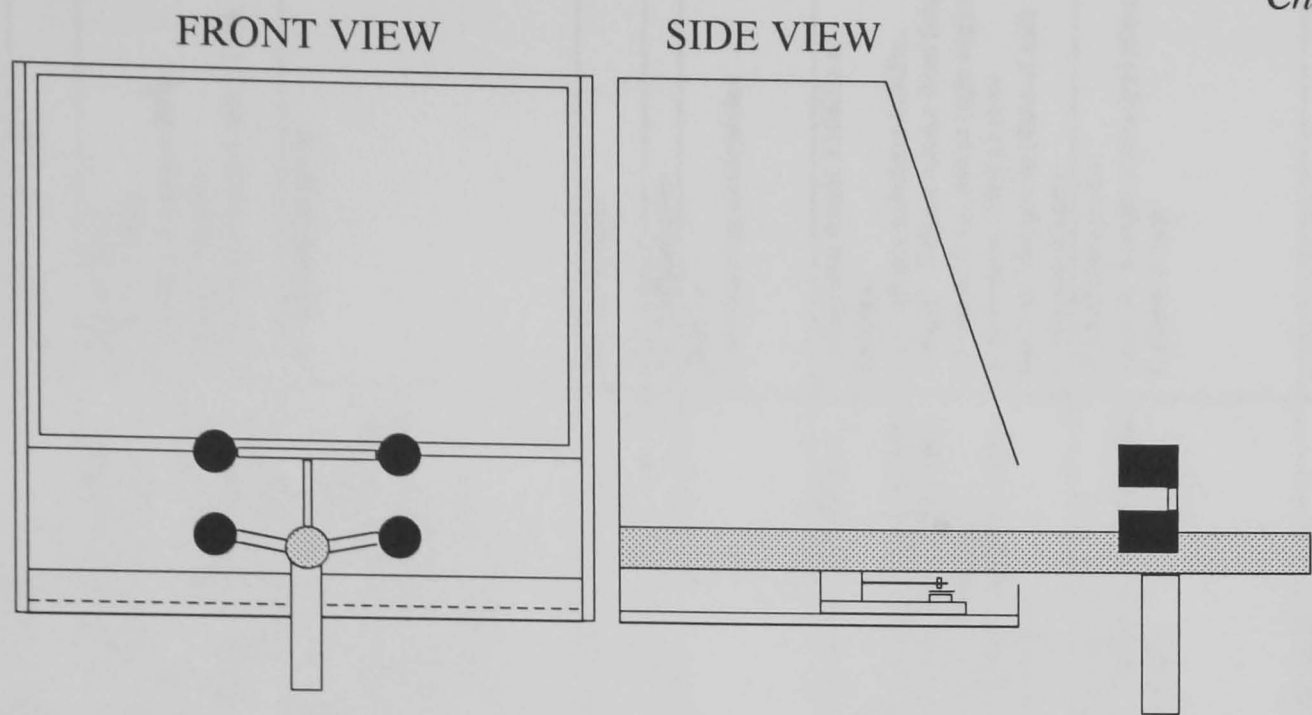


Fig. 2.11 Arrangement of equipment for the British class I cabinet KI containment test (BS 5726 : 1992).

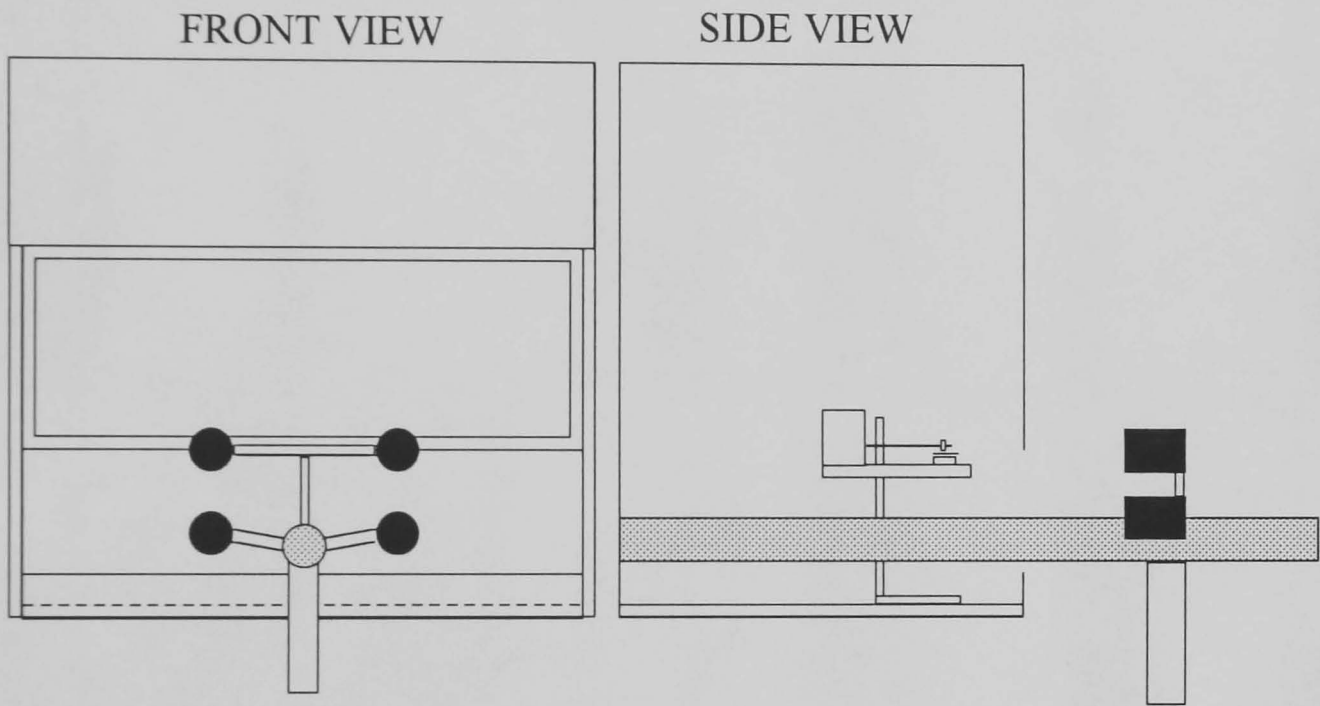


Fig. 2.12 Arrangement of equipment for the British class II cabinet KI containment test (BS 5726 : 1992).

Standard	British BS 5726 1992	U.S.A. NSF 49 1983	Germany DIN 12 950 1991	Japan JAS 1981	Australia AS 2252.1 & AS 2252.2 1992	France NF X 44 201 1984
Cabinet type	Class I, II, III	Class II	Class I, II, III	Class II	Class I, II	Class I, II, III
Sash position	Fixed sash	no information given	no information given	no information given	no information given	500 mm from work surface
Exhaust	Exhausted outside or room (class II)	no information given	no information given	no information given	Exhausted to the room	no information given
Flow/velocity	Inflowing air: Class I. 0.7 - 1.0 m/s \pm 20% Class II \geq 0.4 m/s. Downflowing air: Class II 0.25 - 0.5 m/s \pm 20%	no information given	Inflowing air: Class I. \geq 0.7 m/s \pm 20% Class II \geq 0.4 m/s. Downflowing air: Class II average 0.4 m/s \pm 20%	no information given	Inflow 0.5- 0.8m/s. Individual measurements within \pm 20 % overall mean. Overall mean downflow 0.4 - 0.5 m/s. Individual measurements within \pm 15 % overall mean.	Inflowing air: Class I. \pm 20% Class II \geq 0.4 m/s \pm 20% Downflowing air: Class II average 0.4 m/s \pm 20%
Velocity test	Rotating vane anemometer Inflowing air: Class I 5 points in plane of sash Class II Volume flow rate in exhaust/aperture area Downflowing air: Class II Measure 8 points 100mm above top edge of aperture	no information given	Directional air speed indicator Inflowing air: Class I In plane of sash Class II Volume flow rate in exhaust/aperture area Downflowing air: Class II Measure 50mm above top edge of aperture	no information given	Rotating vane anemometer. For inflow, measure in vertical centre of aperture in plane of sash, 100 mm gap between vane centre across aperture width. For downflow measure 150mm downstream of HEPA.	no information given
Smoke/fog test	Visible aerosol (smoke/fog)	no information given	Visible aerosol (smoke)	no information given	Visible aerosol	Visible aerosol
Obstruction	Artificial arm	no	no	Artificial arm	Artificial arm	2 x artificial arms
Tracer/release rate	<i>Bacillus subtilis</i> var. <i>globigii</i> spores $>10^7$ particles/min. Potassium iodide particles 6×10^8 particles/test.	<i>Bacillus subtilis</i> var. <i>niger</i> spores $>10^8$ particles/min	<i>Bacillus subtilis</i> var. <i>Marburg</i> spores $>10^8$ particles/min	no information given	DOP	DOP or <i>Lactobacillus acidophilus</i>
Source generation type	Microbiological: Reflux blast nebulizer with carrier gas velocity $<$ face velocity 100m from sash plane. Potassium iodide: Spinning disc generator 100 mm from sash plane.	Reflux blast nebulizer particles/min with carrier gas velocity $>$ face velocity	Microbiological: Reflux blast nebulizer with carrier gas velocity $>$ face velocity 100m from sash plane.	Microbiological: Reflux blast nebulizer with carrier gas velocity $>$ face velocity 100m from sash plane.	Laskin type nozzle 140 \pm 5KPa at 30l/min. Class II. Release smoke from tube 25 mm in from, and at right angles to sash plane, 25mm below window. Sample in plane of sash 0.01% penetration.	Laskin type nozzle 110KPa at 28l/min. Low volume nebuliser 61KPa. Class II. Release smoke from tube 25 mm in from, and at right angles to sash plane, 25mm below window. Sample in plane of sash 0.01% penetration.
Sampling	Microbiological: 4 slit samplers (25-30l/min each) or 4 all glass impingers (\geq 12.5l/min) $<$ 200mm from sash plane. Potassium iodide: 4 centripetal samplers 150-160mm from sash plane, 100 l/min.	2 slit samplers and 6 all glass impingers	2 slit samplers (30 \pm 3l/min) or 6 all glass impingers (12.5 \pm 1 l/min) 200mm from sash plane	4 slit samplers or 4 all glass	Aerosol photometer. Class II. Sample across grid plane in plane of sash.	Aerosol photometer. Class II. Sample across grid plane in plane of sash.
Performance	5 repeat tests. Performance factor $>10^5$	$<$ 5 CFU slit samplers $<$ 60 CFU impingers	5 repeat tests. $<$ 5 CFU slit samplers. $<$ 10 CFU/impinger.	no information given	0.01% penetration	0.03% penetration

Table. 2.4 Methods for measuring the performance and efficiency of microbiological safety cabinets in terms of operator protection.

2.4 The state of open fronted containment systems in use - A field survey of fume cupboards in terms of type, condition and performance

For the purposes of this study it was considered necessary in the first instance to evaluate the type, condition and performance of open fronted containment systems. This could be used to assess the awareness of people to the operation of such systems and the impact of containment testing strategies on performance.

An opportunity arose to assess subjectively and objectively the installed and 'in-use' fume cupboard stock at King's College London (1994-1995). Of the 221 fume cupboards surveyed there were aerodynamic and conventional box types, the latter having one, two and three sashes, with some opposing (Table 2.5). 309 apertures were tested.

Number of fume cupboards tested in the survey 221		
Number of tests performed (1 test per sash) 309		
Fume cupboard type	Number in survey	% of total
Aerodynamic	61	27.6 %
Box type with single sash	89	40.3 %
Box type with double sash	46	20.8 %
Box type with triple sash	12	5.4 %
Box type with opposing sashes (x2)	8	3.6 %
Portable type with aerodynamic front	4	1.8 %
Walk-in	1	0.5 %

Table 2.5 Number and type of fume cupboards tested

This work was commissioned as part of a fume cupboard replacement program and required a strategy to yield information on those that were not working at all, those that had poor performance and those that had satisfactory performance. The assessment strategy had to take into account:

1. The need for a quick performance assessment.
2. The large number of cupboards involved and the limited time available.
3. No previous performance figures were available for the majority.
4. The variation in performance was expected to be large.

British Standard BS 7258 : 1994 for general purpose laboratory fume cupboards was not used as this document was written primarily for the design, installation and follow up of new cupboards, and the face velocity method was considered too complex and time consuming. A hierarchical test strategy using flow visualisation and face velocity measurements was chosen (App.4) based on King's College own methods and British Standard BS 5726 : 1992 for microbiological safety cabinets. No test of containment was included at this stage because it was considered not to yield any additional information and was therefore time consuming and not cost effective.

Tests were performed at working sash heights of 250 and 500 mm. This height was measured from the top edge of either the bench or lipfoil (where fitted) to the lower edge of the sash. Where a cupboard had two or three sashes, all sashes were positioned at the same working height during the tests, and each face tested.

Performance tests were carried out for each fume cupboard in the condition in which it was found (viz. with whatever equipment was present at the time). No attempt was made to alter the environmental conditions around the cupboard and people were allowed to enter and leave the laboratory as they wished. This gave an indication of the cupboard performance as installed and in working conditions. At the same time the condition, cleanliness and blockage were subjectively assessed and recorded as average/above average/poor and good/just acceptable/dirty/filthy and cluttered/moderate/minimal/none respectively.

For airflow visualisation water fog generated by an ultrasonic nebuliser (Kennedy, 1987) was used to visualise the direction of air flowing into and within the cupboard. Subjective assessment was made and recorded as satisfactory when there was a clear inward flow of water fog over the entire aperture/questionable when water fog was shown to linger around the lipfoil or sash handle/unsatisfactory when there was substantial leakage of water fog back into the room from the cupboard.

The inflow face velocity was measured with a 100 mm diameter rotating vane anemometer (Airflow Developments Ltd.) at six positions equally spaced in the plane of the aperture for a working height of 500 mm and three positions for a working height of 250 mm. The face velocity was expressed as the overall mean of the average velocity measured at each position. The variation in velocity across the face was expressed as the maximum percentage deviation of the average velocity at that position from the overall mean face velocity.

In order to rank the fume cupboards based on performance the mean face velocity, its variation across the aperture and flow visualisation variables were scored using the following index

Velocity:	score	Velocity variation:	score	Flow:	score
$\geq 0.5\text{m/s}$	1	Variation $\leq 20\%$ & face velocity $\geq 0.5\text{m/s}$	1	Satisfactory	1
$< 0.5 > 0.3\text{m/s}$	2	Variation $\geq 20\%$ & face velocity $\geq 0.5\text{m/s}$	2	Questionable	2
$< 0.3 > 0\text{m/s}$	3	Variation $\leq 20\%$ & face velocity $\leq 0.5\text{m/s}$	3	Unsatisfactory	3
		Variation $\geq 20\%$ & face velocity $\leq 0.5\text{m/s}$	4		

and then these scores were used in the following formula to give each fume cupboard a performance grade:

$$\text{Grade} = \text{Velocity score} \times \text{Variation score} \times (\text{Water Fog visualisation score})^2$$

The lower the grade the better the performance. The water fog score was squared so as to give weight to this parameter as it was considered to be a more indicative factor in the overall assessment of the fume cupboard performance.

The main conclusions from the results of this survey (App.4) were:

- The majority were dirty.
- The majority were average and above average condition.
- Very few were devoid of equipment inside when tested.
- 96.6 % of aerodynamic cupboards had a face velocity > 0.5 m/s at a working aperture height of 250 mm.
- 70.2 % of aerodynamic cupboards had a face velocity > 0.5 m/s at a working aperture height of 500 mm.
- 86.0 % of conventional cupboards had a face velocity > 0.5 m/s at a working aperture height of 250 mm.
- 38.5 % of conventional cupboards had a face velocity > 0.5 m/s at a working aperture height of 500 mm.
- The effect of raising the sash resulted in a significant drop in face velocity.
- 93.2 % of aerodynamic cupboards had a velocity variation < 20 % at a working aperture height of 250 mm.
- 71.6 % of aerodynamic cupboards had a velocity variation < 20 % at a working aperture height of 500 mm.
- 84.9 % of conventional cupboards had a velocity variation < 20 % at a working aperture height of 250 mm.
- 36.9 % of conventional cupboards had a velocity variation < 20 % at a working aperture height of 500 mm.
- There was a significant increase in velocity variation as the sash was raised.
- The correlation between equipment blockage and velocity variation was not possible because of uncontrolled factors (viz. environmental disturbances).
- There was a significant difference in the velocity variation for aerodynamic and conventional cupboards at a working aperture height of 500 mm. However, there was no significant difference between the aerodynamic cupboards and the triple sash box or opposing side box type cupboards.
- 87.0 % of aerodynamic cupboards had a satisfactory flow visualisation at a working aperture height of 250 mm.
- 30.0 % of aerodynamic cupboards had a satisfactory flow visualisation at a working aperture height of 500 mm.
- 34.0 % of conventional cupboards had a satisfactory flow visualisation at a working aperture height of 250 mm.
- 15.0 % of conventional cupboards had a satisfactory flow visualisation at a working aperture height of 500 mm.

- The water fog visualisation test was a better indicator of poor performance than either the velocity or variation tests.
- There was a poor correlation between all three measured variables.
- At a height of 250 mm the majority of the aerodynamic type had a low grade (good performance).
- There was no real difference between the percentage of aerodynamic and conventional cupboards of a particular grade at a working aperture height of 500 mm.
- There was a significant difference in grade as the sash was raised.
- The installation and use had a major influence on cupboard performance whether aerodynamic or conventional.

This survey showed that using a simple strategy and methods could yield important information on the performance of the fume cupboards without using complex face velocity measurements and containment tests. This was due to the large variation in fume cupboard performance encountered. There were those that were switched off and did not work at all (unknown to the user), those in which the variation in face velocity across the aperture was extreme, those with very low or very high face velocities, those which were cluttered with almost total obstruction of the airflow, those in which the airflow was visibly poor due to equipment blockage or to poor siting, and those which were satisfactory.

It was apparent that the majority of fume cupboards in this survey were installed and used in a way that was far removed from the ideal conditions of a type test in a test room and, perhaps, the conditions at commissioning. There appeared to be little understanding by the user of fume cupboard containment, the effects of equipment bulk within it, of personnel movement and of environmental disturbances near to the aperture. There were also problems in the manner in which make up air was introduced into some rooms, which on occasions involved the opening of windows resulting in draughts.

It was concluded that no real performance assessment strategy had previously been applied to the majority of fume cupboards given the diversity of type, condition and performance even though the college had its own strategy and BS 7258 was available. It was also concluded that for performance assessment strategies to work, the user had to know how the facilities functioned and that work discipline was very important. Of those that had been tested by the college or to BS 7258, none had been assessed by containment testing.

This was not necessarily representative of all institutions and in those where strict testing and user awareness was required, better performance would be expected. This did reflect though people's attitude to an unidentifiable risk, not necessarily treating performance seriously. It also reflected the notice given to the available BS 7258 and guidelines which did not specify any minimum performance criteria. From discussions with fume cupboard

users in this survey, it seemed that microbiological safety cabinet testing was much better received and the user had more respect for its use. This was most probably due to an identifiable risk and perhaps to clear performance guidelines.

2.5 Key interim conclusions

- A simple strategy involving airflow visualisation and face velocity measurements was adequate, quick and simple to execute. However, these were not sensitive or reliable enough for the measurement of actual exposure and quantitative containment tests were required.
- For assessing the performance of fume cupboards, there were fundamental differences in the test strategies of the national standards that were considered.
- There was a close similarity between the test strategies of the national standards for microbiological safety cabinets.

Chapter 3 Study of British Standard, BS 7258 : 1994 performance tests for general purpose laboratory fume cupboards

3.1 Introduction

For the purposes of this study all work using the test methods for assessing the performance of a general purpose laboratory fume cupboard, BS 7258 : 1994 : Parts 1 and 4, were carried out in a test room using an aerodynamic fume cupboard. The minimum level of performance of a general purpose fume cupboard (Part 1) is established by a performance ‘type’ test, in which the pattern and quality of air flow into the fume cupboard is assessed by measurement of air velocities in the plane of the aperture carried out in the test room. When the fume cupboard is installed on-site other than in the test room, a commissioning test is specified to establish that the minimum performance in the type test has not deteriorated after installation. Further, a test method is described for the determination of the average face velocity with reduced accuracy for routine maintenance. The main difference between the type test and the commissioning test is the number of points in the plane of the aperture at which measurement of velocity using a thermal anemometer is made. The routine maintenance test differs in the number of points at which velocity measurements are made using a rotating vane anemometer. At installation it is suggested (Part 3) that before commissioning tests flow visualisation may be used to identify environmental disturbances.

For quantitative assessment a method using sulphur hexafluoride (SF_6) gas tracer is recommended in Part 4 of BS 7258 : 1994. This method is designed to yield standardised containment test values and is described as being “dissociated from any direct relationship with occupational exposure or short term exposure limits safety values”.

3.2 Test fume cupboard

The fume cupboard used was made of glass reinforced plastic (GRP) with aerodynamic front facia and rear baffle (Fig. 3.1).

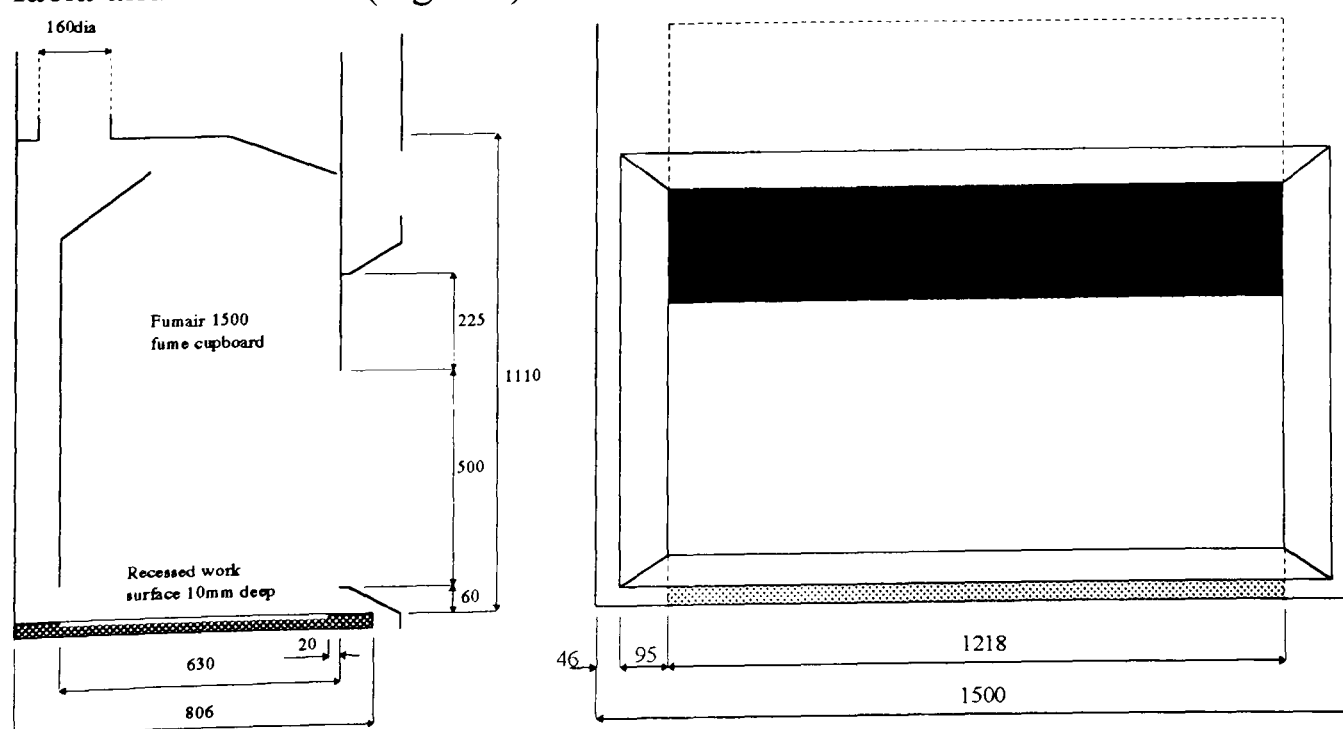


Figure 3.1 Aerodynamic fume cupboard used in this investigation (Fumair Ltd., Hertford).

3.3 Test room

The tests were carried out in a test room built to the specifications of BS 7258 : 1994 : Part 1 : B.1.1. The room (Fig. 3.2) consisted of an enclosure of rectangular shape within a factory environment. The internal width and length were not less than 4.0 x 4.0 m and the ceiling height not less than 2.7 m. The ceiling was level and all internal surfaces were devoid of internal supports or partitions.

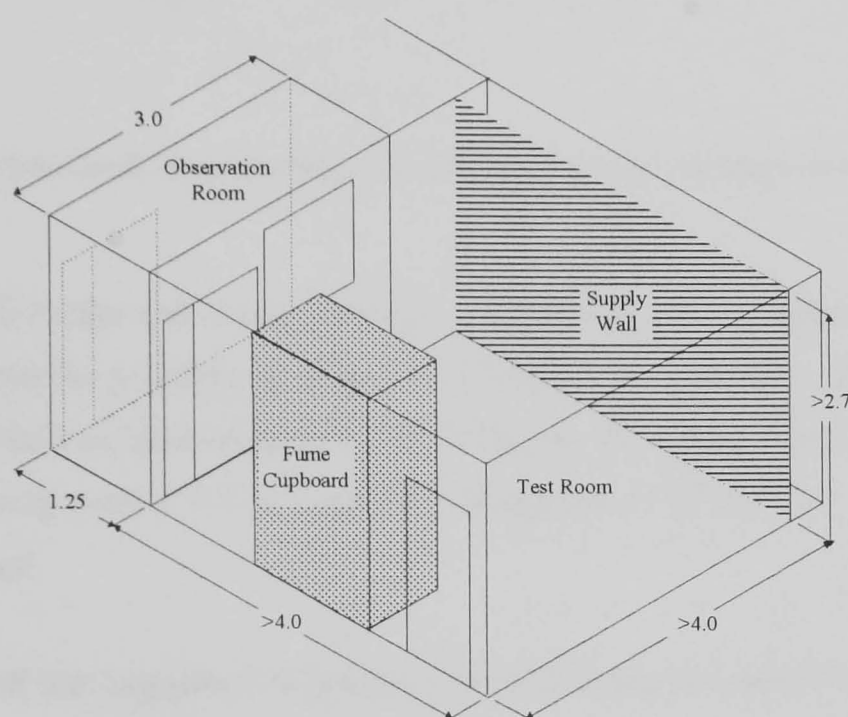


Figure 3.2 Dimensions of test room (Fumair Ltd, Hertford).

3.4 Position of input and extract ducting systems in test room and factory

The supply and extracts to the room are shown in Fig. 3.3. Air was extracted from the test room through the fume cupboard and exhausted outside. Makeup air to the test room was drawn via the factory shop floor through the main door (Fig. 3.4).

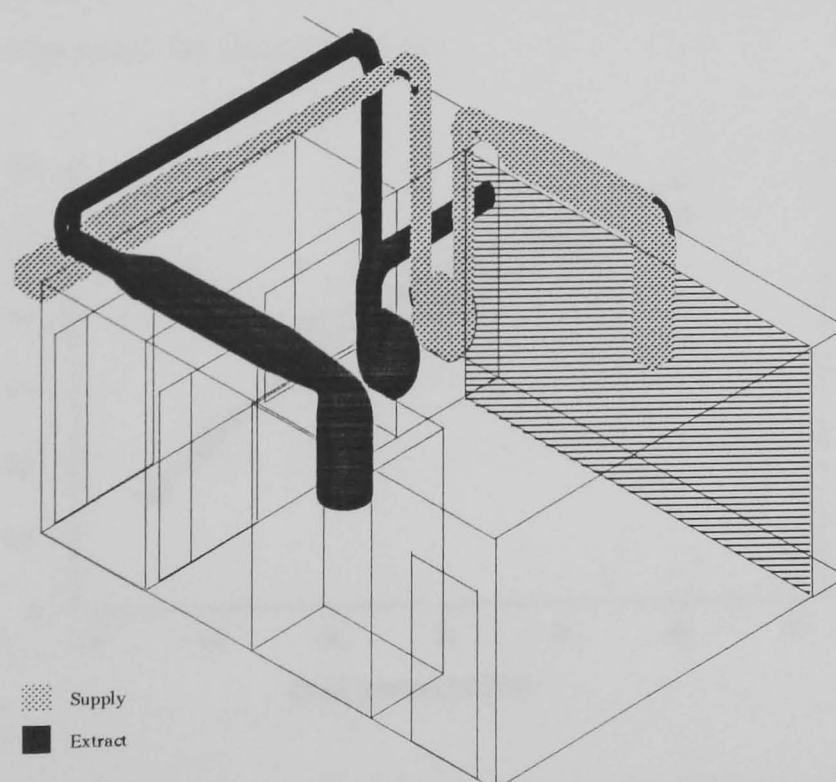


Figure 3.3 Ventilation ducting to the test room.

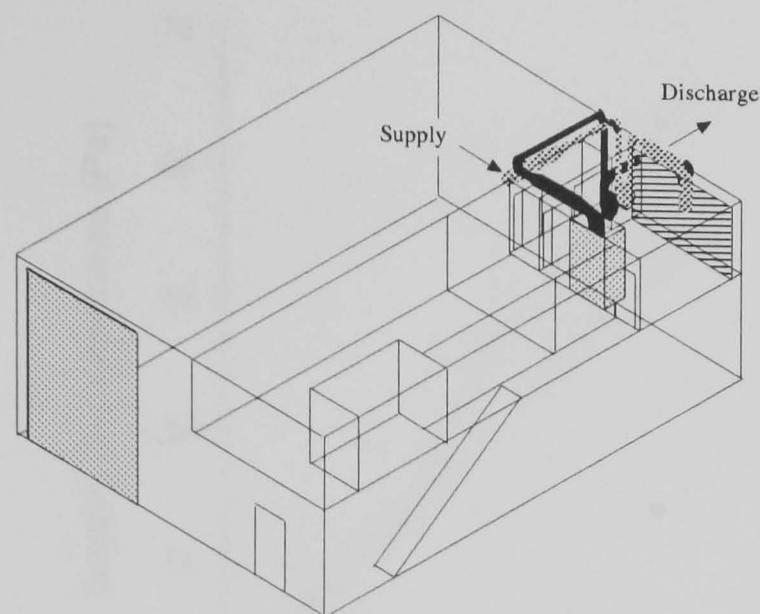


Figure 3.4 Position of test room in the factory, showing supply and discharge points.

The air was supplied to the test room through a perforated wall opposite the fume cupboard in as uniform a manner as possible so as not to influence the operation of the fume cupboard. The perforated wall had an open area of 9.5 % made up of regular 4 mm diameter holes. The air velocity in the room was $< 0.1 \text{ m/s}$ and at a temperature of $20 \text{ }^{\circ}\text{C} \pm 3 \text{ }^{\circ}\text{C}$. The input and extract were balanced.

3.5 Flow rate of air supplied to and extracted from the test room

The flow rate of air into and out of the test room was monitored using Wilson flowgrids (Airflow Developments Ltd.). These were installed in the supply and extract ducting and the volume flow rate across them was calibrated using the method described in BS 848 : 1990 for on-site installations. The velocity pressure was measured by traversing the duct with a pitot static tube and then calculating the volume flow rate from the measured pressures. The test length was a section of square ducting (300 x 300) upstream of the supply fan and the traverse cross-section used was 450 mm upstream of the Wilson flow grid. The calibration from the supply fan was used for the extract fan.

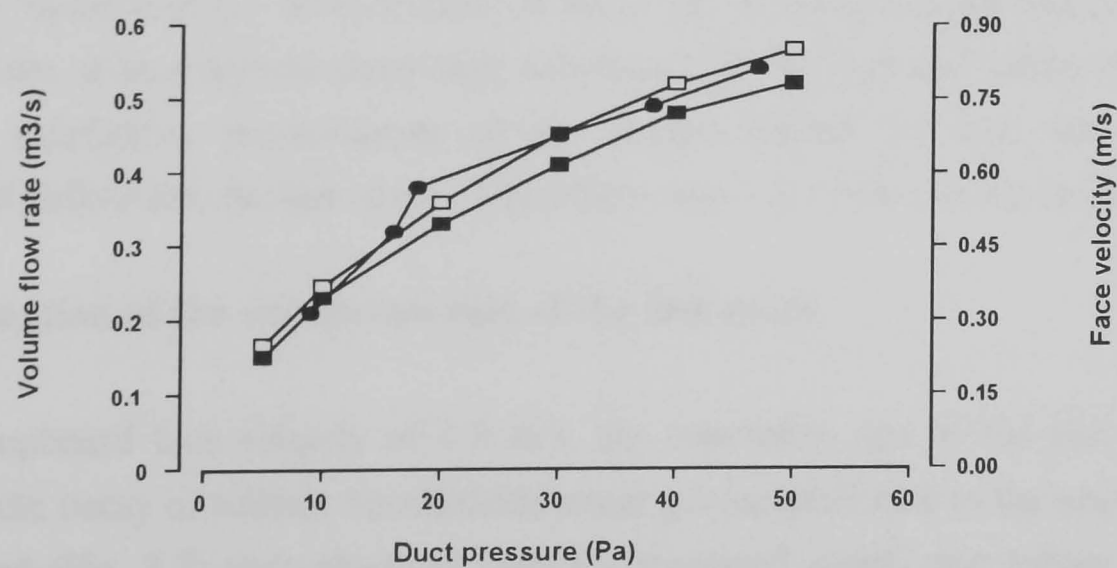


Figure 3.5 Change in face velocity □, calculated volume flow rate ■ and calibrated volume flow rate ● through the supply duct with Wilson flow grid differential pressure.

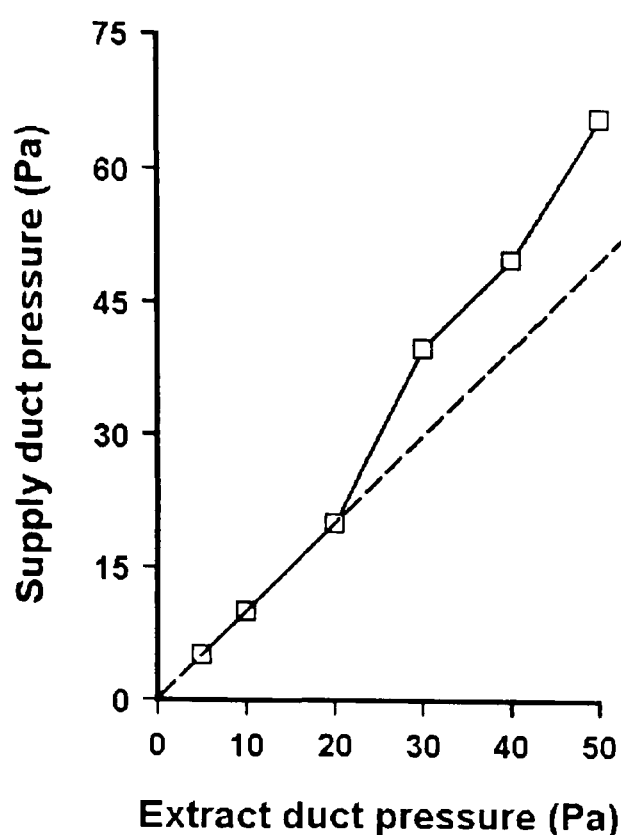


Figure 3.6 Supply and extract duct pressures when the room is balanced with the factory.

The calibration curve for volume flow rate and pressure differential across the Wilson flow grid were in close agreement with the calculated volume flow rate from the face velocity (Fig. 3.5). There were slight differences because the flow rate was calculated using the area of the working aperture, the open area beneath the lipfoil was not taken into account. The air pressure inside the testroom was balanced with the air pressure in the factory by measuring the pressure difference across the entrance door with an inclined manometer (Airflow Developments Ltd.), and adjusting the supply flow rate accordingly (Fig. 3.6).

3.6 Distribution of airflow into the test room through the perforated supply wall

Sulphur hexafluoride tracer gas was injected into the supply ventilation and the distribution over the perforated wall was measured using a Miran IA infra red gas analyser (Foxboro Ltd., U.S.A). The variation in the concentration of tracer gas sampled was between 0.139-0.140 absorbance units at an analytical absorption wavelength of 10.7 μm and pathlength 12.75 m indicating a satisfactory pressurisation of the plenum behind the wall and a uniform distribution of airflow into the test room. The airflow was < 0.1 m/s over the entire wall.

3.7 Estimation of the ventilation rate of the test room

At a fume cupboard face velocity of 0.5 m/s, the ventilation rate in the test room was described by the decay of sulphur hexafluoride tracer gas sampled near to the aperture of the fume cupboard (Fig. 3.7) and calculated from the measured supply and extract flow rates (Table 3.1).

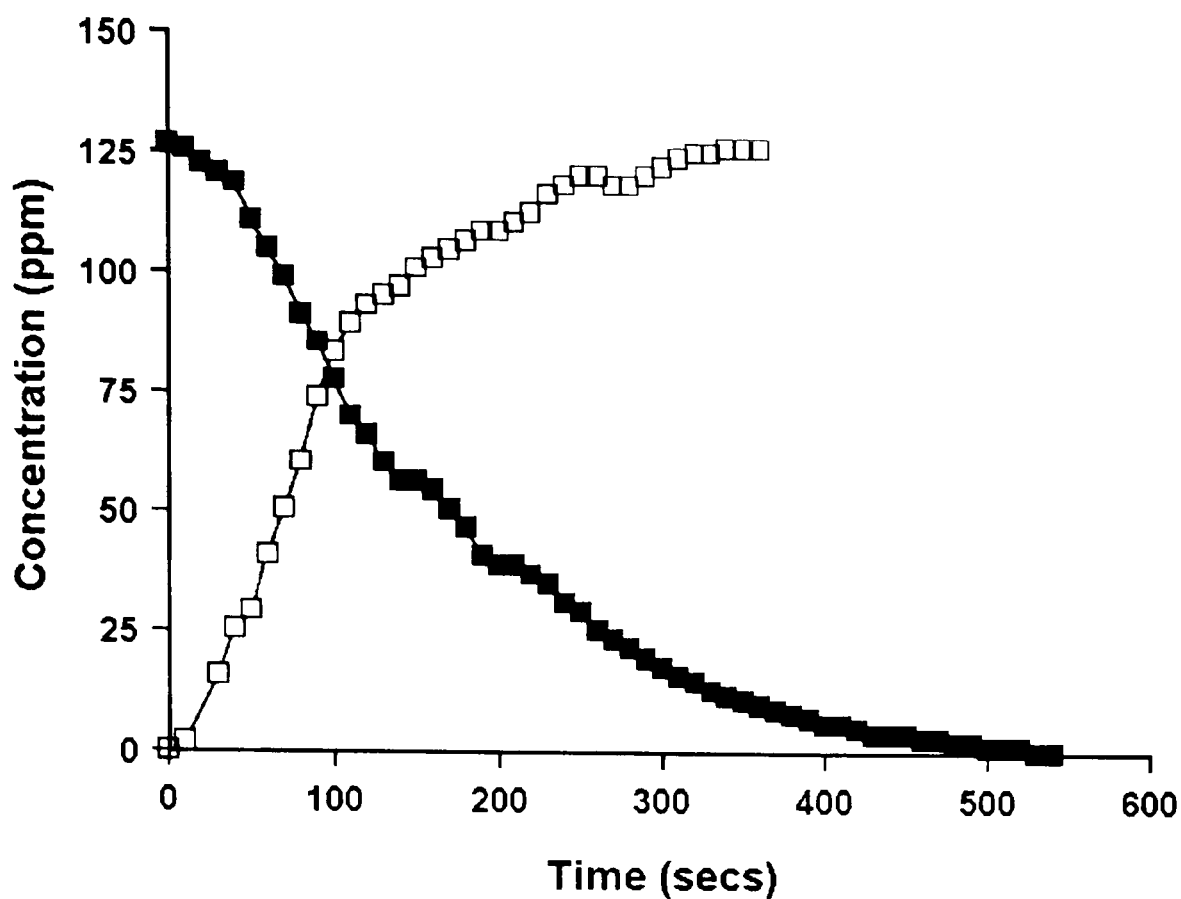


Figure 3.7 Change in gas concentration in the test room during continuous release □, and its decay ■.

Room Volume $V = 45.15 \text{ m}^3$

ΔPa	Volume flow rate $Q \text{ (m}^3/\text{s)}$	Residence time T_R $V/Q \text{ (secs)}$	Dilution rate D $Q/V \text{ (secs}^{-1}\text{)}$	No. air changes /h $3600/T_R \text{ (hr}^{-1}\text{)}$
10	0.21	215	0.005	16.7
20	0.32	141	0.007	25.5
30	0.38	119	0.008	30.3
40	0.41	100	0.001	36.0
50	0.49	92	0.011	39.0
60	0.54	84	0.012	42.9

Table 3.1 Flow rate of air through the test room.

3.8 BS 7258 : 1994 : Part 1. Determination of “specification for safety and performance”

3.8.1 Method

3.8.1.1 Anemometers

The anemometer described for use in type testing and commissioning (B.2.1) was an omni-directional type capable of measuring air velocities between 0.1 m/s and 2.0 m/s with a response time of the sensor not more than 2 seconds. The required accuracy for an individual reading was better than 15 % at air velocities between 0.2 m/s and 1.5 m/s.

A thermistor type anemometer, TA-2-15 from Airflow Developments Ltd was used in this study. It had a shroud covering the sensing head but was considered omni-directional for the test purposes. For routine maintenance purposes the anemometer used was a rotating vane

type with a diameter of 100 mm (Airflow Developments Ltd.). Table 3.2 gives a comparison between the anemometer types.

Type	Rotating vane	Thermistor	Hot wire
Spatial resolution	100 mm diameter	2 - 5 mm	2 - 5 mm
Velocity Range	0.25 - 30 m/s	0 - 30 m/s	0 - 5 m/s
Accuracy (20°C, 1.013 bar)	0.5-30 m/s calibrated better than $\pm 2\%$ of reading	$\pm 2\%$ FSD	
	0.25-4.99 m/s ± 0.1 m/s		
	calibrated better than $\pm 1\% \pm 1$ digit		
Inaccurate @ turbulence	> 10 %	> 30 %	> 30
Response time	> 5 secs	> 1 sec.	< 0.5 sec

Table 3.2 Comparison of anemometer types.

3.8.1.2 Calibration of anemometers

The thermistor anemometer had not been calibrated within 1 year of its use. This was not considered important, as in the performance tests the variation in velocity over the plane of the sash was a performance criterion rather than the mean. The rotating vane anemometer used had also not been calibrated within 1 year of its use but on direct comparison with a calibrated rotating vane anemometer there was no significant difference between the readings. The mean face velocity measured using the thermistor anemometer did not significantly differ from measurements made over the aperture using a rotating vane anemometer (Fig. 3.8).

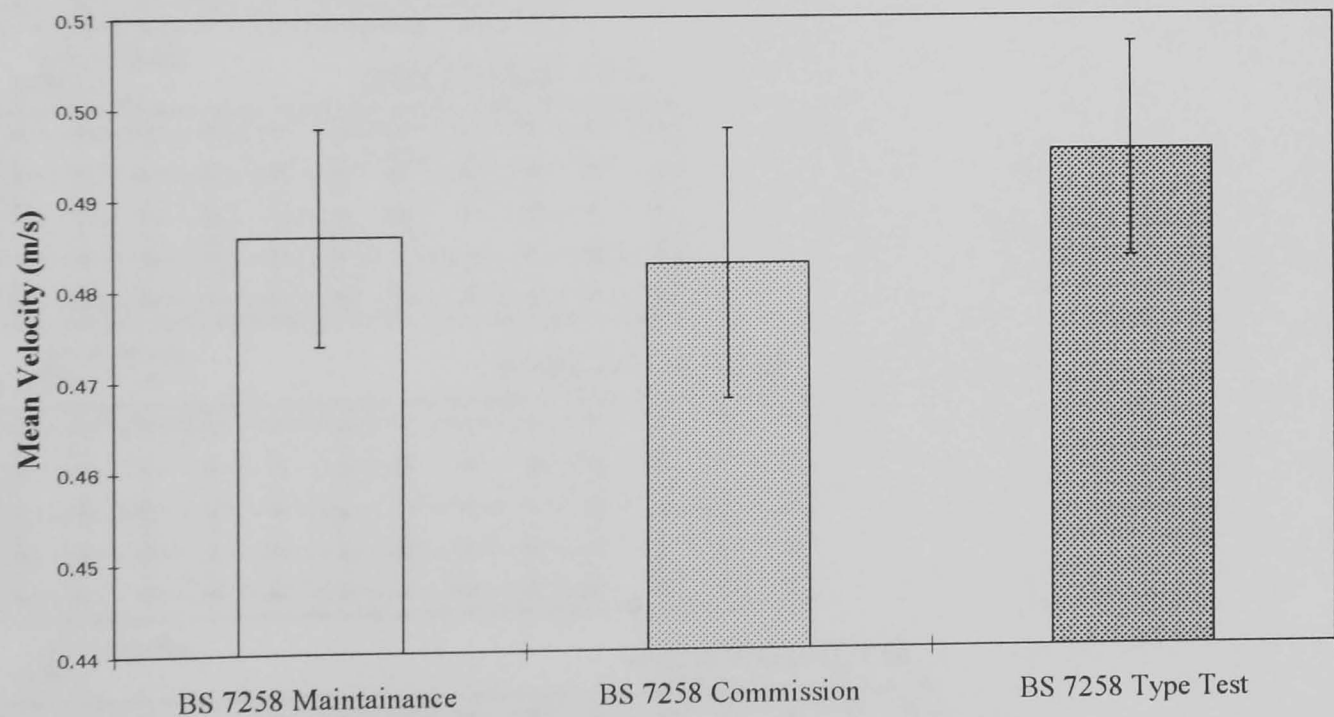


Figure 3.8 Average face velocity measurements using the methods described in BS 7258 : 1994 : Part 1. (Error bars = 1 x standard deviation).

3.8.1.3 Position of anemometer

The anemometer was held in position in the plane of the aperture using a floor standing clamp such that it could be moved across the aperture to the required position as prescribed for type testing (Fig. 3.9), commissioning (Fig. 3.10) and routine maintenance purposes (Fig. 3.11).

3.8.1.4 Measurements

For type testing and commissioning 12 measurements of air velocity were taken, one every 2 seconds at each grid point. The average velocity at each grid point was calculated and then the overall mean face velocity calculated. For the routine maintenance test (which was carried out at the commissioning stage and subsequently at regular intervals) three readings were taken over a period of 30 seconds (i.e. at intervals of 15 seconds). The average velocity at each grid point was calculated and then the overall mean face velocity calculated.

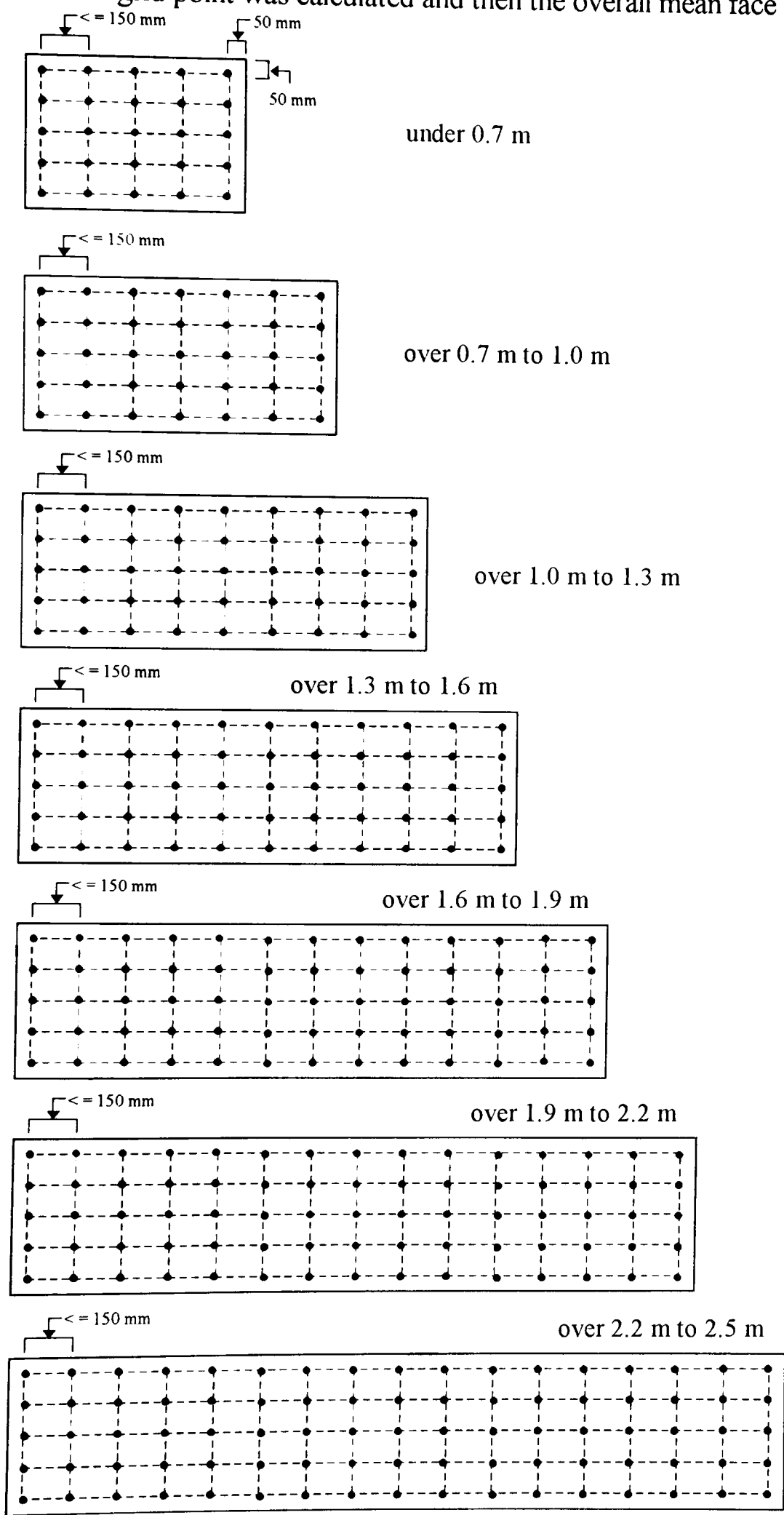


Figure 3.9 Grid positions specified in BS 7258 : 1994 : Part 1 for type testing of face velocity.

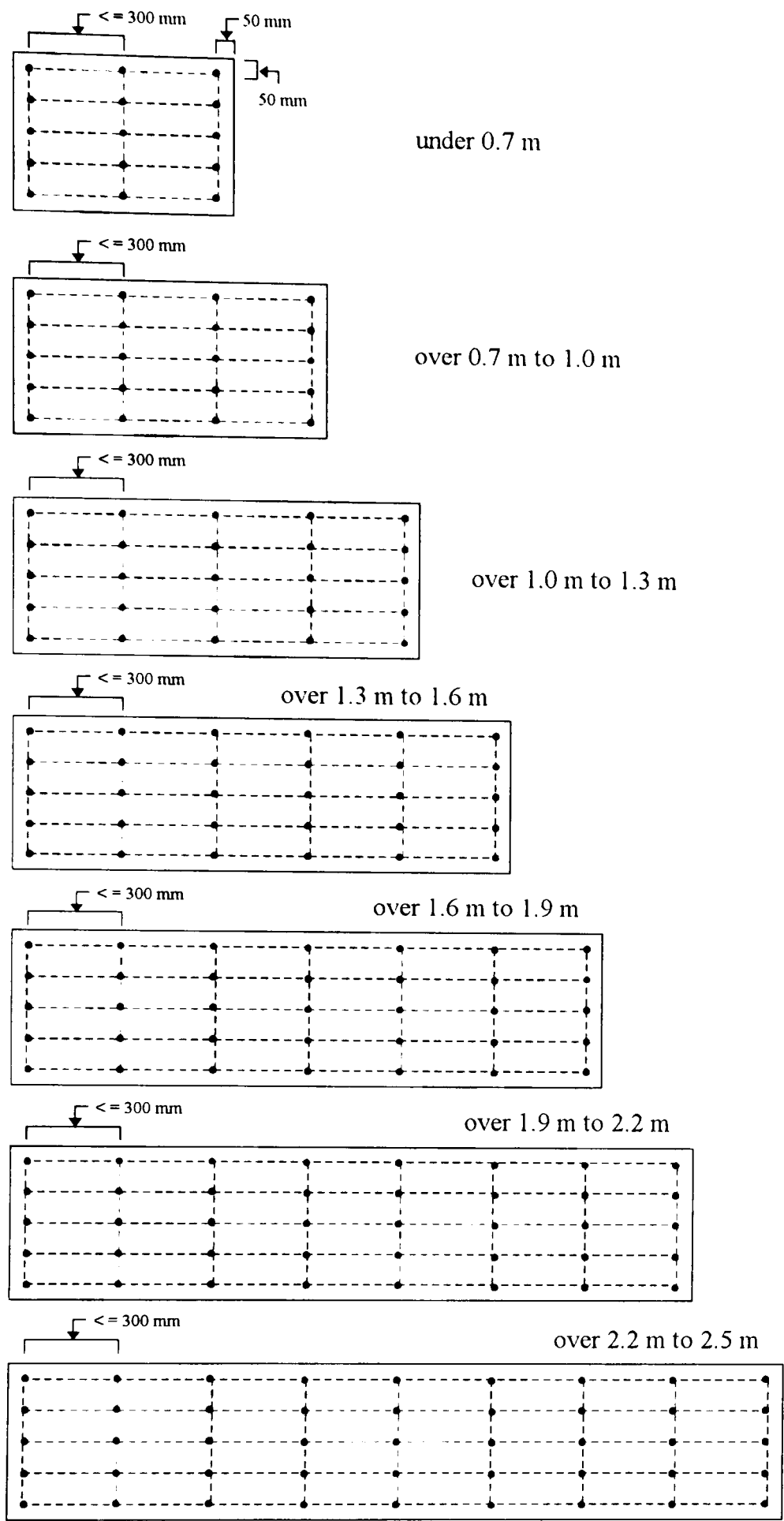


Figure 3.10 Grid positions specified in BS 7258 : 1994 : Part 1 for commissioning of face velocity.

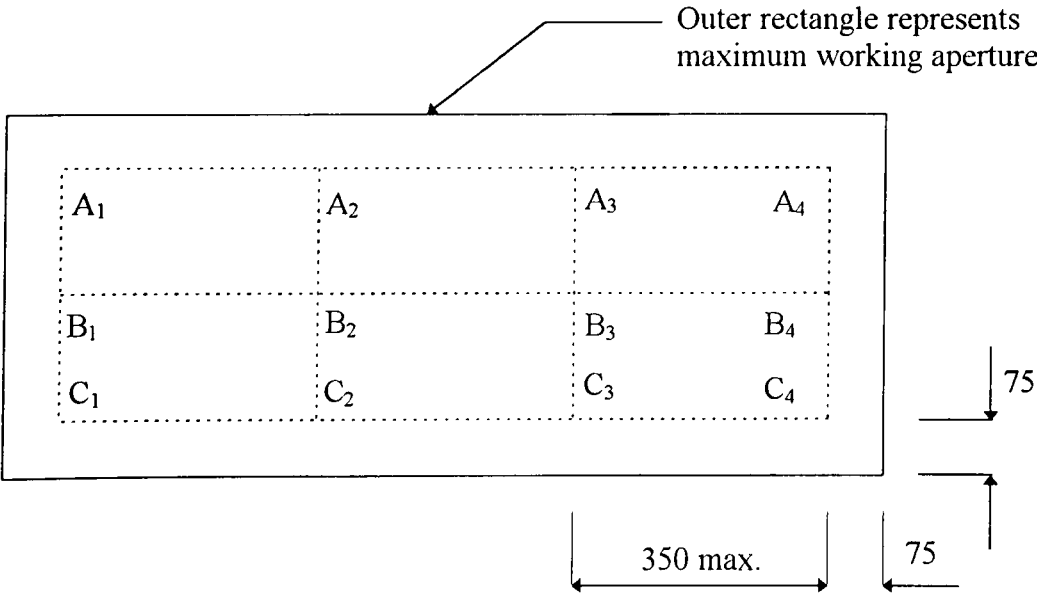


Figure 3.11 Grid positions recommended in BS 7258 : 1994 : Part 1 for maintenance of face velocity.

3.8.1.5 Expression of results

For the type test the criterion for performance was that the average velocity at any grid point was not less than 0.85 times the face velocity. In addition it was specified that the ratio of the larger of the velocities at any pair of corresponding points either side of the centre line of the fume cupboard aperture to the smaller velocity was between 1.3 : 1. A further test specified that the velocity should be measured at 0.8 times the extract volume flow rate used previously and that the grand mean of the corrected local average velocities be divided by 0.8. The value obtained was specified not to differ by more than 10 % from the grand mean of the corresponding velocities determined at the previous face velocity. For commissioning, the criteria for performance was that the average velocity at any grid point was not less than 0.8 times the face velocity. The objective of the routine maintenance test was to compare values measured at regular intervals with those measured at commissioning so that any deterioration in performance could be monitored.

3.8.2 Results

3.8.2.1 Effect of anemometer orientation with respect to direction of airflow

Both the thermistor and rotating vane anemometers were shielded. The effect of this shielding and orientation with respect to the direction of the air flow on measurements was investigated. The thermistor anemometer was rotated about its horizontal axis when positioned parallel to the lipfoil and normal to the air flow direction (Fig. 3.12). Readings were taken in the centreline of the plane of the fume cupboard aperture. It was found that an angle of rotation in the direction shown greater than 30 degrees resulted in a reduction in the readings (Fig. 3.14).

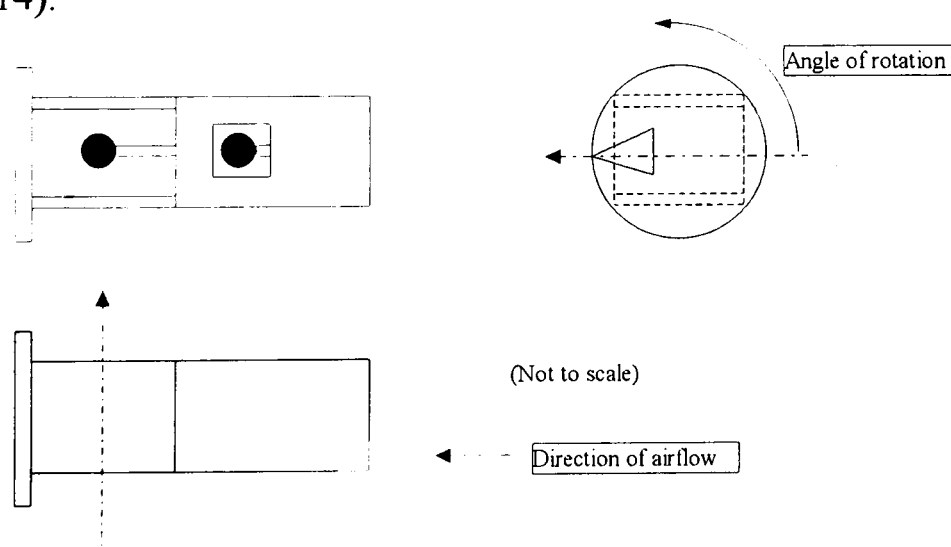


Figure 3.12 Orientation of thermistor anemometer.

The vane anemometer was rotated about its vertical and horizontal axis as shown in Fig. 3.13. It was positioned 70 mm above the horizontal centreline of the plane of the fume cupboard aperture and in the vertical centreline. In this case an angle of rotation greater than 40 degrees resulted in a decrease in measured velocity (Fig. 3.14). When the vane was rotated about its vertical axis there was still some influence even when parallel to the direction of the flow i.e. at 90 degrees to the plane.

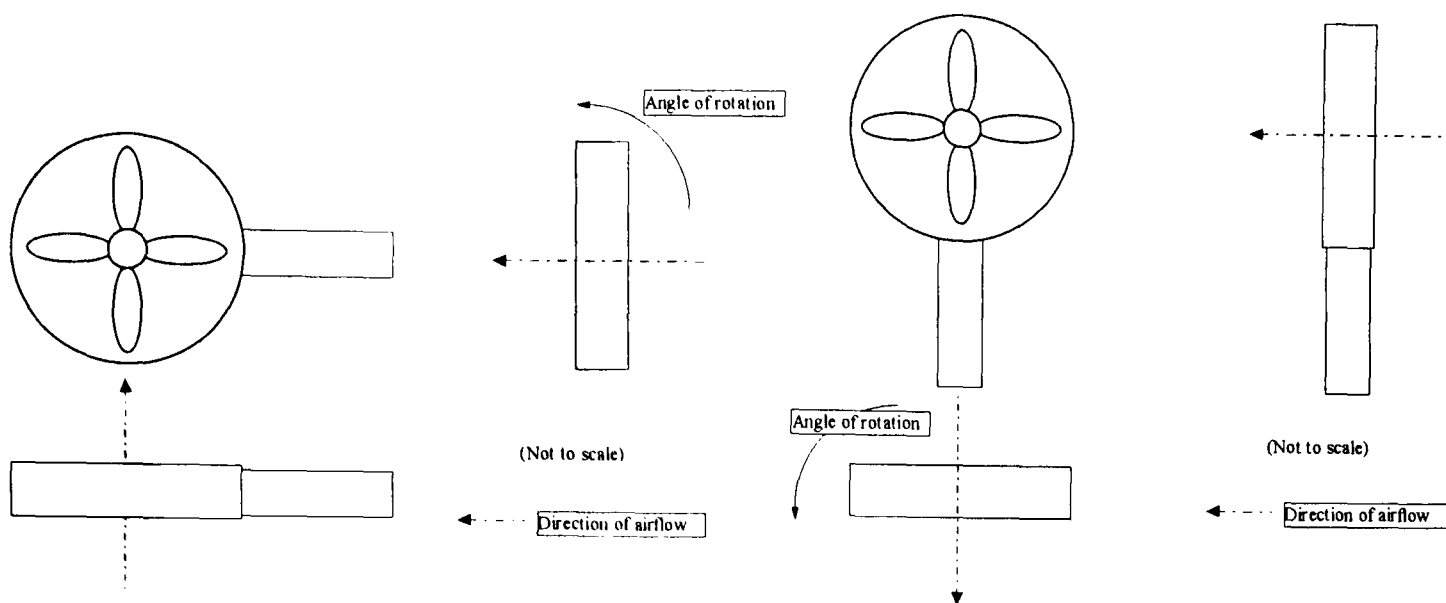


Figure 3.13 Orientation of rotating vane anemometer.

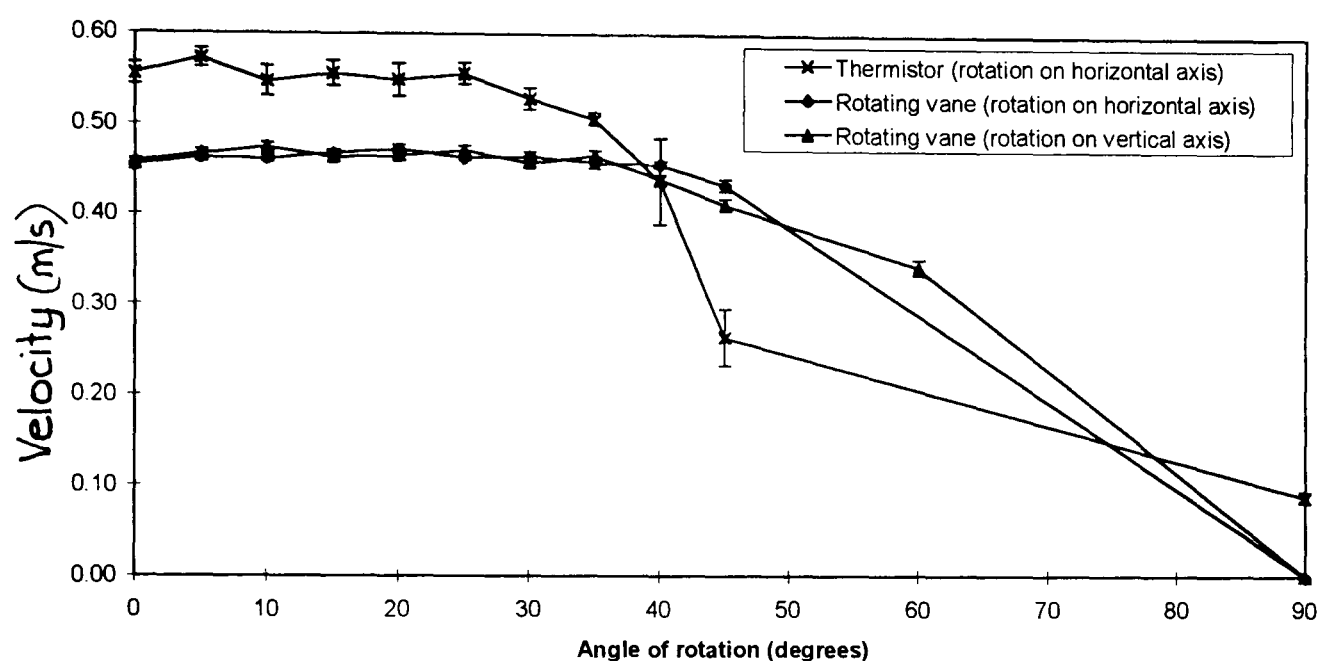


Figure 3.14 Effect of anemometer orientation on velocity measurements in the aperture plane.

3.8.2.2 Time taken for rotating vane anemometer to reach steady readings from zero

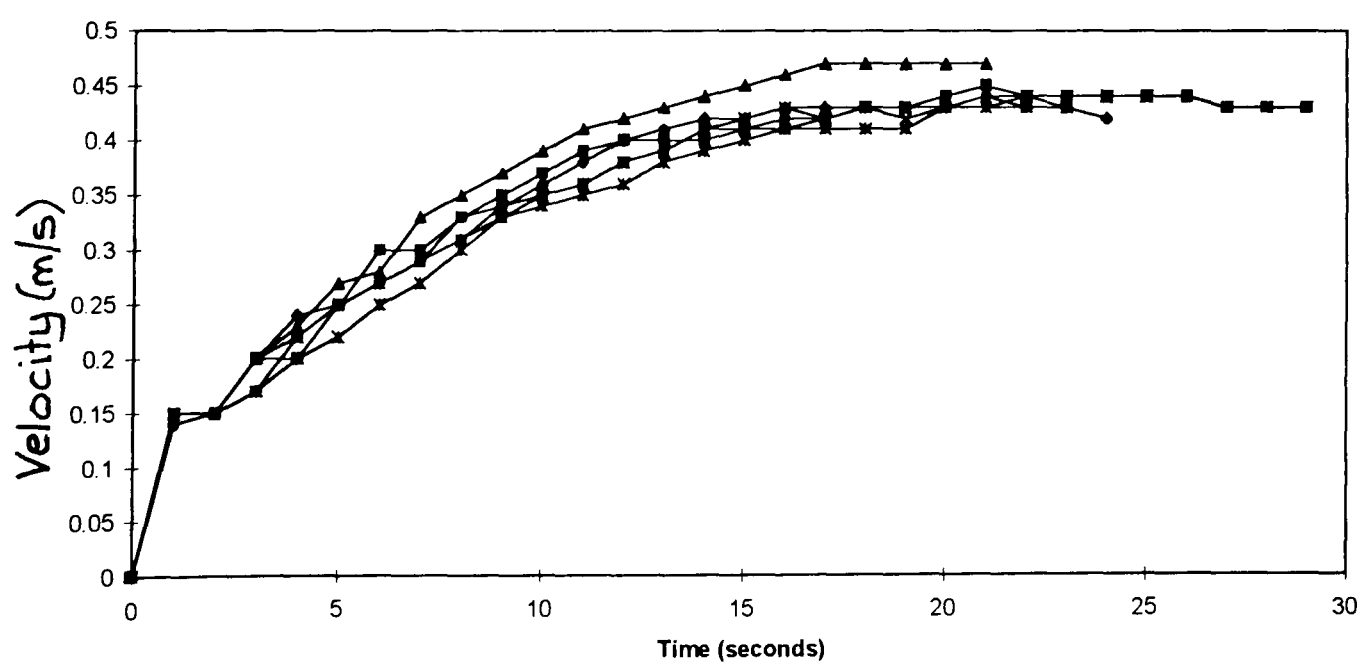


Figure 3.15 Response time of a rotating vane anemometer to reach steady readings from zero.

From zero flow the average time taken for the rotating vane to reach a steady reading of ~ 0.45 m/s as measured in the plane of the fume cupboard aperture was some 15 seconds (Fig.

3.15). The response time to fluctuations in velocity of the air flow therefore would be expected to be somewhat better than this. This indicated an average reading integrated over the whole of the vane.

3.8.2.3 Type test

As shown in Table 3.3, the performance of the aerodynamic fume cupboard tested was within the specifications of BS 7258 : 1994 : Part 1.

3.8.2.4 Commissioning test

As shown in Table 3.4, the performance of the aerodynamic fume cupboard tested was within the specifications of BS 7258 : 1994 : Part 1.

3.8.2.5 Routine maintenance test

The performance of the aerodynamic fume cupboard tested using the routine maintenance test as recommended in BS 7258 : 1994 : Part 1 is shown in Table 3.5.

3.9 BS 7258 : 1994 : Part 4. Use of a “method for determination of the containment value of a laboratory fume cupboard”.

3.9.1 Method

3.9.1.1 Tracer gas

The tracer gas, sulphur hexafluoride (SF_6) has a low solubility in air and water, is colourless, odourless, chemically inert, thermally stable up to 500°C , non-explosive, non-flammable and non-toxic. It can be detected to parts per trillion (ppt) level using gas chromatography with electron capture; the measured background concentration in the atmosphere being around $0.548 \pm 0.014 \times 10^{-12} \text{ mol/l}$ (Watson & Liddicoat, 1988). It is a heavy gas and as recommended in BS 7258 : 1994 : Part 4 was diluted 10 % SF_6 /90 % N_2 to have near neutral buoyancy when released in air.

For air at standard conditions, 101.3 KPa Abs., 21°C :

Specific gravity (sg): $\text{SF}_6 = 5.11$; $\text{N}_2 \approx 1$; 10 % SF_6 /90 % $\text{N}_2 = 1.411$

Estimated density: 10 % SF_6 /90 % N_2 1.7 kg/m^3

10 % SF_6 /90 % N_2 (BOC Special gases)

Cylinder size L (200 bar)

Certified calibration: 9.999%

Cylinder fill capacity $\pm 5 \%$

Stratification of the gases in the cylinder was not expected to occur if stored above 15°C

Table 3.3 Distribution of average velocities across the aperture when measured in the plane of the sash, using the grid as specified type test in BS 7258 : Part 1 : 1994. (2 Tests)

Anemometer - Airflow Developments Ltd. TA-2-15 (thermistor type)

Overall mean face velocity 0.52 m/s (SD 0.04 m/s)

Minimum average velocity at a grid point: 0.44 m/s = 85 % overall mean face velocity

(Figures in small type are standard deviation of 12 measurements from average calculated)

0.47 0.1	0.48 0.06	0.55 0.08	0.52 0.05	0.49 0.06	0.48 0.04	0.47 0.04	0.51 0.06	0.44 0.06
0.48 0.09	0.52 0.05	0.54 0.04	0.49 0.05	0.48 0.05	0.50 0.03	0.50 0.02	0.53 0.02	0.57 0.04
0.57 0.05	0.55 0.04	0.52 0.04	0.50 0.01	0.49 0.01	0.50 0.01	0.50 0.01	0.52 0.01	0.61 0.01
0.56 0.05	0.52 0.04	0.52 0.01	0.50 0.01	0.50 0.01	0.50 0.01	0.51 0.01	0.50 0.01	0.55 0.02
0.58 0.04	0.58 0.03	0.52 0.04	0.52 0.01	0.54 0.03	0.51 0.01	0.51 0.02	0.56 0.03	0.59 0.02

Overall mean face velocity 0.53 m/s (SD 0.04 m/s)

Minimum average velocity at a grid point: 0.47 m/s = 89 % overall mean face velocity

(Figures in small type are standard deviation of 12 measurements from average calculated)

0.50 0.06	0.54 0.04	0.51 0.06	0.53 0.07	0.50 0.06	0.47 0.04	0.48 0.07	0.52 0.07	0.59 0.04
0.59 0.01	0.54 0.03	0.51 0.04	0.49 0.04	0.49 0.04	0.50 0.02	0.51 0.02	0.52 0.03	0.60 0.01
0.59 0.03	0.53 0.03	0.51 0.01	0.51 0.01	0.50 0.01	0.49 0.03	0.50 0.01	0.51 0.01	0.61 0.01
0.58 0.02	0.50 0.01	0.51 0.01	0.50 0.01	0.50 0.01	0.50 0.01	0.50 0.01	0.51 0.01	0.54 0.03
0.61 0.01	0.55 0.03	0.52 0.02	0.52 0.02	0.51 0.01	0.53 0.01	0.52 0.02	0.53 0.03	0.60 0.01

Table 3.4 Distribution of average velocities across the aperture when measured in the plane of the sash, using the grid as specified for commissioning in BS 7258 : Part 1 : 1994. (2 Tests)

Anemometer - Airflow Developments Ltd. TA-2-15 (thermistor type)
Overall mean face velocity 0.52 m/s (SD 0.05 m/s)
Minimum average velocity at a grid point: 0.44 m/s = 85 % overall mean face velocity
(Figures in small type are standard deviation of 12 measurements from average calculated)

0.47	0.55	0.49	0.47	0.44
0.1	0.08	0.06	0.04	0.06
0.57	0.52	0.49	0.50	0.61
0.05	0.03	0.01	0.01	0.01
0.58	0.52	0.54	0.51	0.59
0.04	0.04	0.03	0.02	0.02

Overall mean face velocity 0.54 m/s (SD 0.05 m/s)
Minimum average velocity at a grid point: 0.48 m/s = 89 % overall mean face velocity
(Figures in small type are standard deviation of 12 measurements from average calculated)

0.50	0.51	0.50	0.48	0.59
0.06	0.06	0.06	0.07	0.04
0.58	0.51	0.50	0.50	0.61
0.02	0.01	0.01	0.01	0.01
0.61	0.52	0.51	0.52	0.60
0.01	0.02	0.01	0.02	0.01

Table 3.5 Distribution of average velocities across the aperture when measured in the plane of the sash, using the grid as specified for maintenance in BS 7258 : Part 1 : 1994. (10 Tests)

Anemometer - Airflow Developments Ltd. (rotating vane type)

Overall mean face velocity 0.50 m/s (SD 0.05 m/s)

Minimum average velocity at a grid point: 0.42 m/s = 84 % overall mean face velocity
(Figures in small type are standard deviation of 12 measurements from average calculated)

0.53	0.50	0.53	0.60
0.01	0.01	0.02	0.02
0.5	0.42	0.43	0.49
0.02	0.01	0.01	0.03
0.55	0.48	0.46	0.52
0.01	0.01	0.01	0.01

Overall mean face velocity 0.50 m/s (SD 0.05 m/s)

Minimum average velocity at a grid point: 0.44 m/s = 88 % overall mean face velocity
(Figures in small type are standard deviation of 12 measurements from average calculated)

0.54	0.56	0.52	0.59
0.02	0.01	0.02	0.01
0.52	0.44	0.44	0.49
0.01	0.01	0.01	0.02
0.52	0.47	0.45	0.49
0.01	0.01	0.01	0.02

Overall mean face velocity 0.49 m/s (SD 0.06 m/s)

Minimum average velocity at a grid point: 0.41 m/s = 84 % overall mean face velocity
(Figures in small type are standard deviation of 12 measurements from average calculated)

0.58	0.54	0.52	0.54
0.02	0.01	0.01	0.02
0.50	0.41	0.41	0.50
0.02	0.01	0.01	0.02
0.53	0.44	0.46	0.49
0.01	0.01	0.01	0.01

Overall mean face velocity 0.50 m/s (SD 0.05 m/s)

Minimum average velocity at a grid point: 0.42 m/s = 84 % overall mean face velocity
(Figures in small type are standard deviation of 12 measurements from average calculated)

0.55	0.55	0.54	0.55
0.02	0.02	0.01	0.01
0.53	0.43	0.42	0.50
0.01	0.01	0.01	0.01
0.52	0.44	0.44	0.51
0.01	0.01	0.01	0.02

Overall mean face velocity 0.51 m/s (SD 0.05 m/s)

Minimum average velocity at a grid point: 0.43 m/s = 84 % overall mean face velocity
(Figures in small type are standard deviation of 12 measurements from average calculated)

0.54	0.53	0.55	0.58
0.02	0.01	0.02	0.03
0.53	0.45	0.43	0.48
0.02	0.01	0.02	0.02
0.57	0.46	0.50	0.52
0.01	0.01	0.01	0.01

Overall mean face velocity 0.50 m/s (SD 0.05 m/s)

Minimum average velocity at a grid point: 0.43 m/s = 86 % overall mean face velocity
(Figures in small type are standard deviation of 12 measurements from average calculated)

0.50	0.50	0.53	0.61
0.02	0.01	0.01	0.02
0.48	0.43	0.45	0.50
0.01	0.01	0.01	0.02
0.55	0.47	0.49	0.52
0.02	0.01	0.01	0.01

Overall mean face velocity 0.51 m/s (SD 0.05 m/s)

Minimum average velocity at a grid point: 0.44 m/s = 86 % overall mean face velocity
(Figures in small type are standard deviation of 12 measurements from average calculated)

0.51	0.50	0.55	0.61
0.03	0.02	0.01	0.01
0.50	0.45	0.44	0.49
0.01	0.01	0.02	0.02
0.55	0.48	0.49	0.53
0.01	0.01	0.01	0.01

Overall mean face velocity 0.48 m/s (SD 0.08 m/s)

Minimum average velocity at a grid point: 0.39 m/s = 81 % overall mean face velocity
(Figures in small type are standard deviation of 12 measurements from average calculated)

0.58	0.54	0.60	0.61
0.02	0.03	0.02	0.02
0.47	0.42	0.43	0.45
0.01	0.01	0.01	0.01
0.42	0.39	0.41	0.41
0.01	0.01	0.01	0.01

Overall mean face velocity 0.50 m/s (SD 0.10 m/s)

Minimum average velocity at a grid point: 0.41 m/s = 82 % overall mean face velocity
(Figures in small type are standard deviation of 12 measurements from average calculated)

0.64	0.66	0.64	0.64
0.02	0.02	0.02	0.01
0.47	0.42	0.41	0.44
0.02	0.01	0.03	0.01
0.48	0.42	0.41	0.43
0.01	0.01	0.01	0.01

Overall mean face velocity 0.50 m/s (SD 0.05 m/s)

Minimum average velocity at a grid point: 0.43 m/s = 86 % overall mean face velocity
(Figures in small type are standard deviation of 12 measurements from average calculated)

0.56	0.55	0.55	0.58
0.04	0.01	0.02	0.02
0.46	0.43	0.43	0.50
0.01	0.01	0.01	0.02
0.52	0.46	0.45	0.52
0.01	0.01	0.01	0.01

3.9.1.2 Gas injector device and positioning

The inlet device through which the tracer gas was injected into the cupboard was a cylindrical filter funnel with a scintered glass disc near its base 30 mm in diameter and having a pore rating of P 40 in accordance with BS 1752 : 1983. The distance from the disc and the end of the tube did not exceed 100 mm. The funnel was mounted in a clamp and retort stand so that it could be positioned at 6 points within the fume cupboard as shown in figure 3.16, with its axis parallel to the plane of the sash and open end facing upwards.

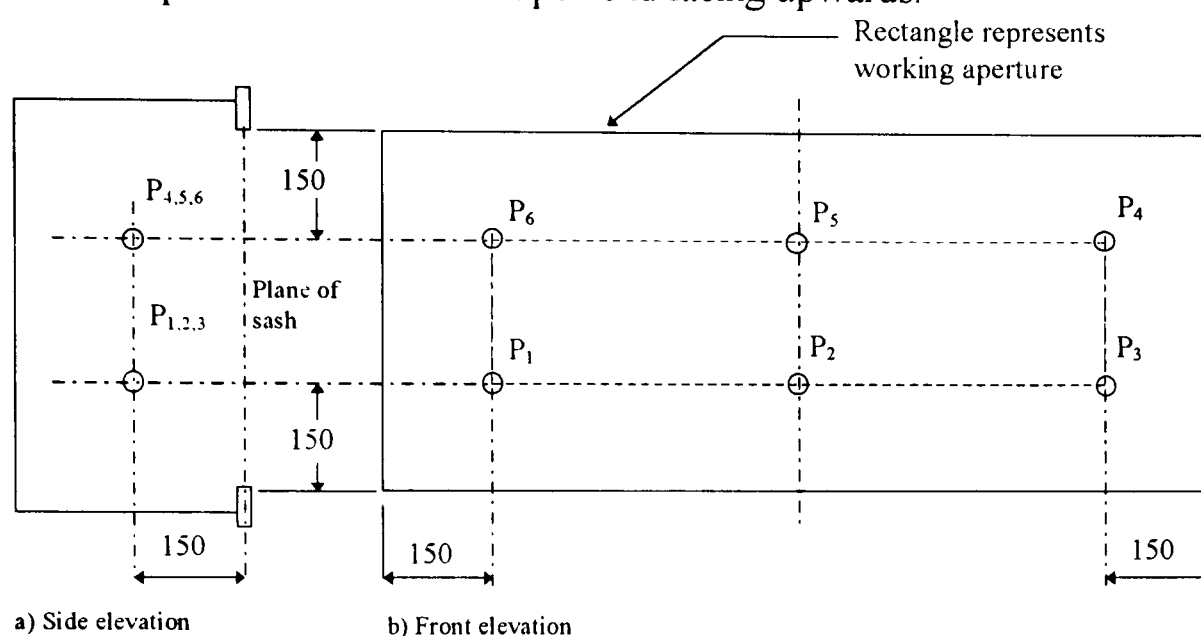


Figure 3.16 Injection positions for test gas. All dimensions in mm.

3.9.1.3 Measurement of flow rate of gas through injector device

In order to measure the flow rate of the tracer gas through the source funnel, a N_2 calibrated rotameter was corrected for its equivalent flow rate in N_2 at standard conditions from the following expression:

$$Q_{(gas1)} = Q_{(gas2)} \times \frac{\sqrt{SG(gas_2)}}{\sqrt{SG(gas_1)}} \times \frac{T(gas_2)}{T(gas_1)} \times \frac{P(gas_1)}{P(gas_2)}$$

Where gas_1 was the calibrated gas of the rotameter
 gas_2 was the specific gas to be used
 Q was the flow rate, m^3/s
 SG was the specific gravity
 T was the absolute temperature of the gas, $^{\circ}K$
 P was the pressure of the gas, KPa .

Assuming perfect gases and omitting factors concerning non-standard temperature, pressure conditions, and viscosity then:

$$Q_{(gas1)} = Q_{(gas2)} \times \frac{\sqrt{SG(gas_2)}}{\sqrt{SG(gas_1)}} \quad Q_{(gas2)} = Q_{(indicated \text{ flow rate on rotameter, } gas1)} \times \frac{\sqrt{SG(gas_1)}}{\sqrt{SG(gas_2)}}$$

Thus on the assumption that gas molecules were in constant motion, for each molecule:

Kinetic energy (K.E.) = $\frac{1}{2} mv^2$

For two gases: $K.E._1 = K.E._2 = \frac{1}{2} m_1 v_1^2 = \frac{1}{2} m_2 v_2^2$

Then: $v_1/v_2 = \sqrt{m_2}/\sqrt{m_1}$

and if s.g. $\propto m$: $v_1 = (\sqrt{sg_2}/\sqrt{sg_1}) \times v_2$

(This could have been expressed per unit time to give volume flow rates).

Assuming the specific gravity of N_2 to be near that of air (1), then the correction factor for the N_2 rotameter to be used for measuring tracer gas flow was $0.84 \times \text{indicated flow rate}_{(gas1)}$.

3.9.1.4 Sampling probes and positioning

Sampling was through stainless steel probes 150 mm long with an internal diameter of 5 mm ± 0.5 mm. These probes were arranged so that the open end was in the plane of the aperture and positioned as in Fig. 3.17, the number and positions of the probes depending on the size of the aperture.

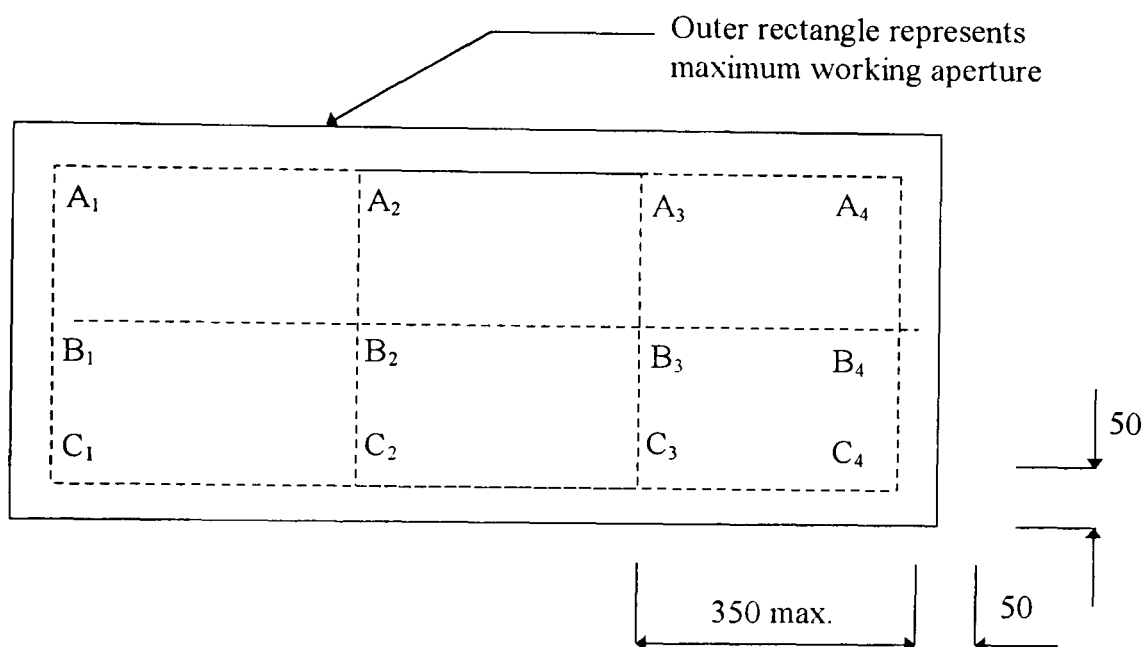


Figure 3.17 Sampling positions. All dimensions in mm.

3.9.1.5 Gas collection

The sampling probes were connected up to a manifold using nylon tubing (Fig. 3.18), each tube 1 m length and internal diameter ~ 0.5 mm. A nylon tube was used to connect the manifold to the gas analyser 3 m in length and internal diameter 10 mm.

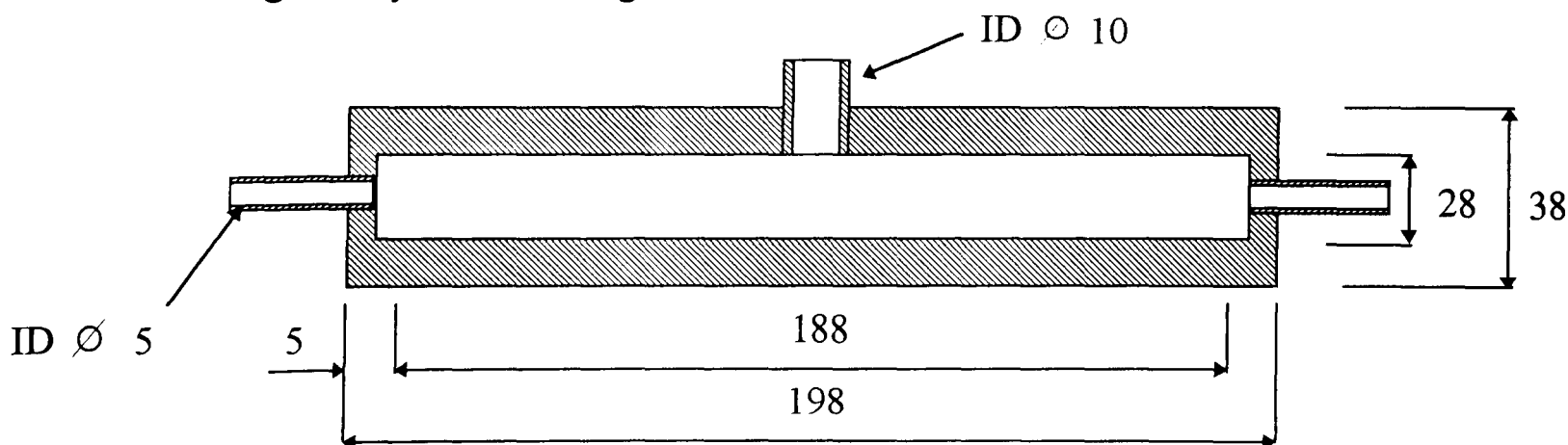


Figure 3.18 Sampling system manifold.

3.9.1.6 Gas analyser and calibration for use with SF₆

The instrument recommended for use had to be “capable of measuring concentrations of SF₆ down to $10^{-9} \pm 10\%$ (V/V)”. For this investigation a Miran Infra-red gas analyser (Foxboro Ltd, USA) was used. This analyser was calibrated for detection of SF₆ using a path length of 20.25 m, response time 1 second, slit size 1 mm and an analytical wavelength of 10.7 μm which was the wavelength at which SF₆ absorbed strongly, free from interference of water and CO₂ (Figs. 3.19 & 3.20) and air (Fig. 3.21).

The output from the Miran was initially recorded by chart recorder but subsequently by computer (PC386SX) through an analogue - digital converter, ADC - 16 (Pico Technology), and the data logged with PICOLOG software (Pico Technology), the results being analysed in Microsoft Excel®.

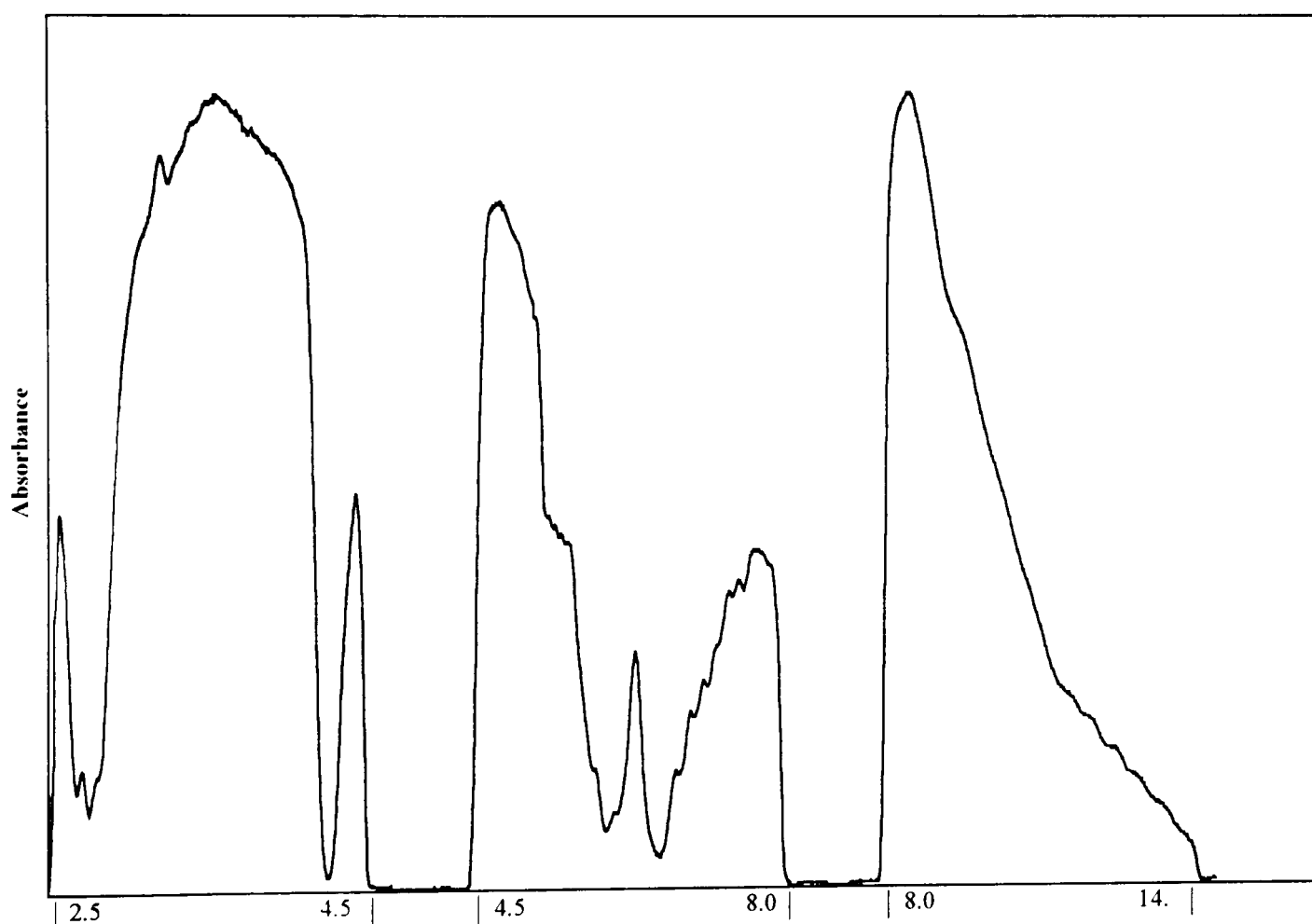


Fig. 3.19 Infra-red spectrum of ambient air (wavelength 2.5 - 14.5 μm)

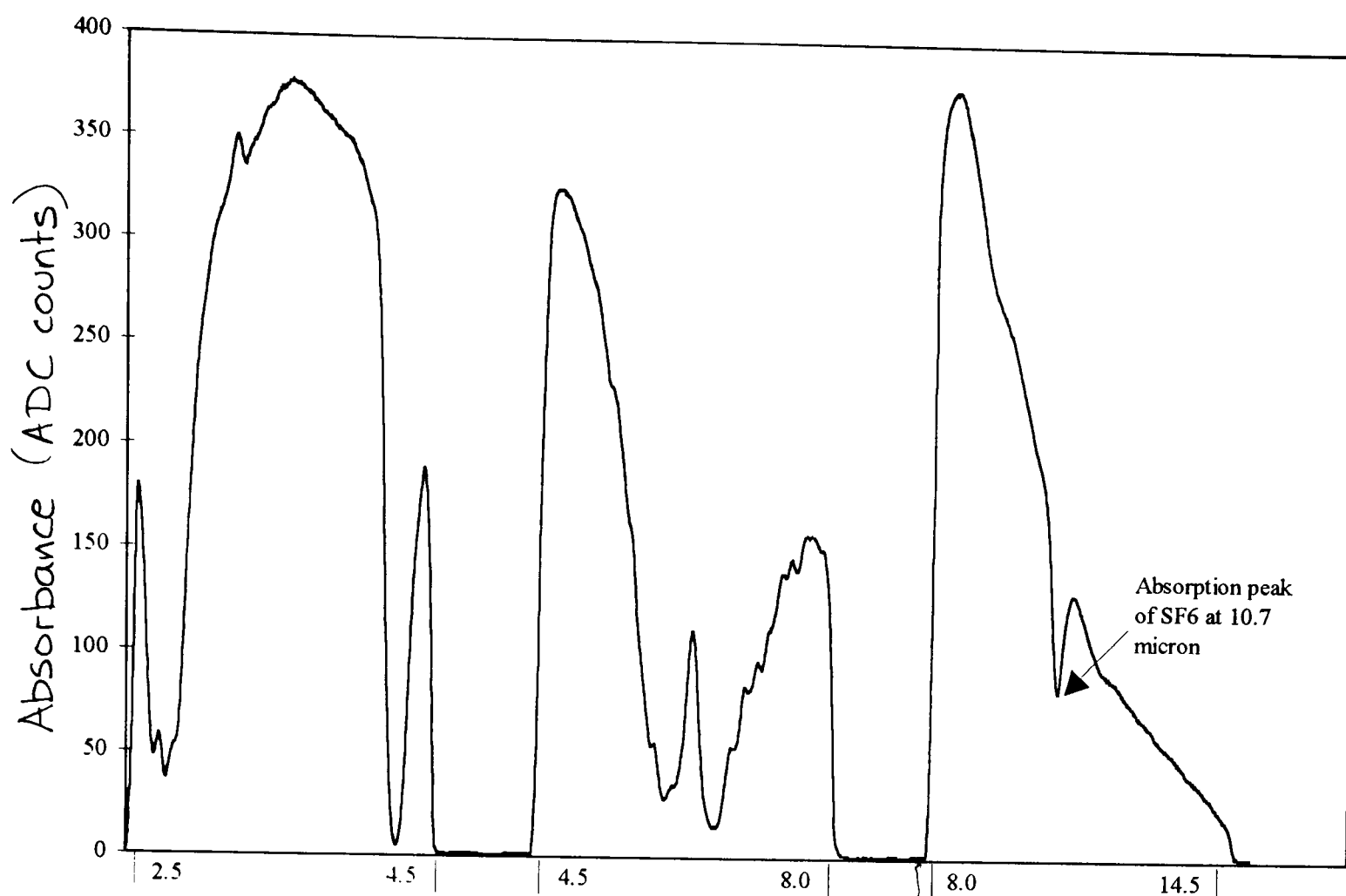


Fig. 3.20 Infra-red spectrum of ambient air with 10 % SF_6 / 90 % N_2 (wavelength 2.5 - 14.5 μm)

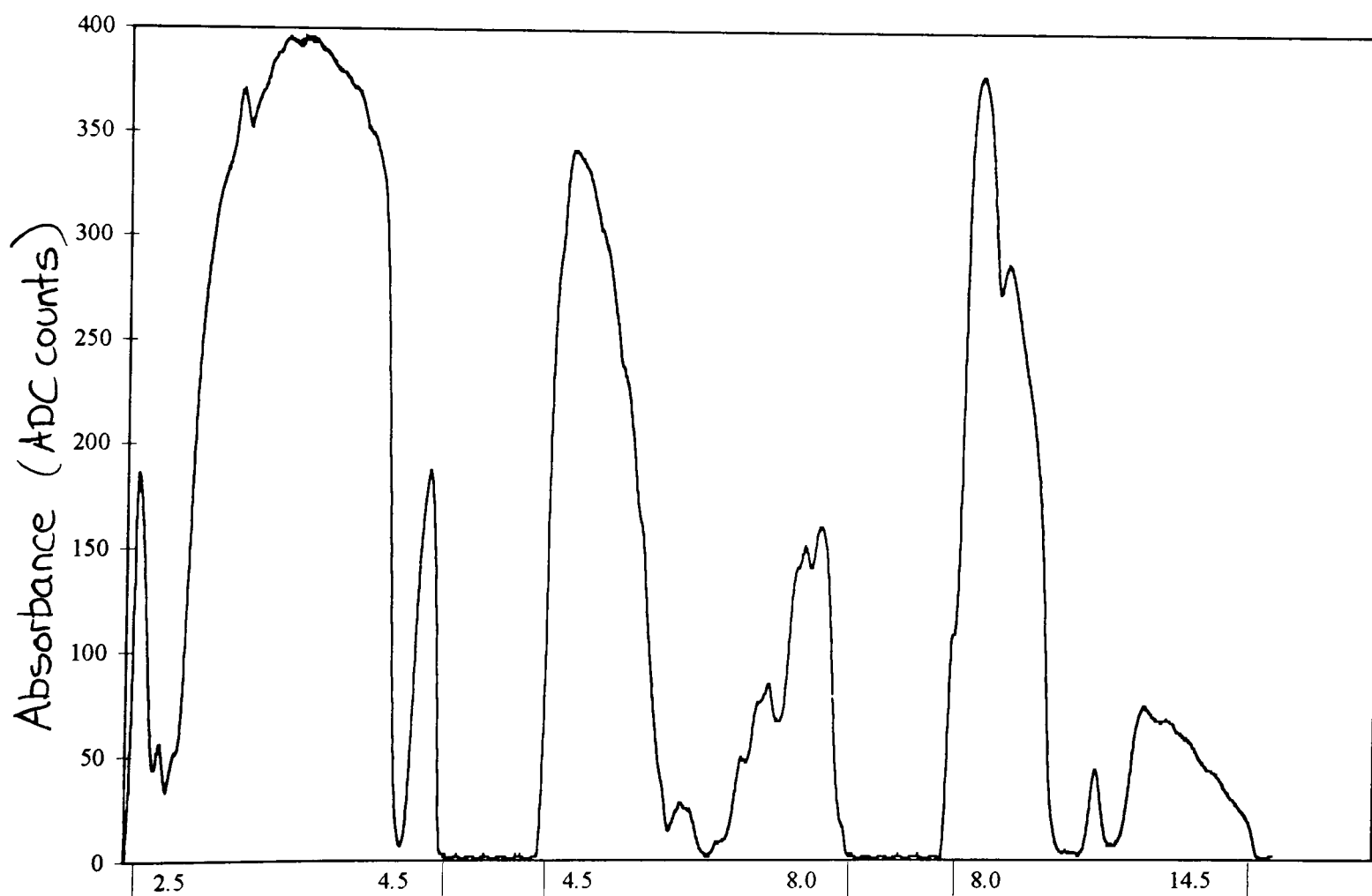


Fig. 3.21 Infra-red spectrum of 10 % SF_6 / 90 % N_2 (wavelength 2.5 - 14.5 μm)

The ADC had an input of 0 - 2.5 volts, which corresponded to logging units of 0 - 1023 (1 logged unit \equiv 0.00244 volts input). The Miran had an output of 0 -1 volts for full scale deflection (FSD) in each absorbance range but it was found that the Miran had an output voltage beyond FSD for external data recording.

The Miran was calibrated at the absorbance ranges of 0 - 0.025 AU and 0 - 0.1 AU. 1 μ l aliquots of gas tracer (0.0177 ppm SF₆) were injected into a closed circuit calibration loop (Foxboro Ltd.) using a gas sealed syringe and a calibration curve constructed (Fig. 3.22).

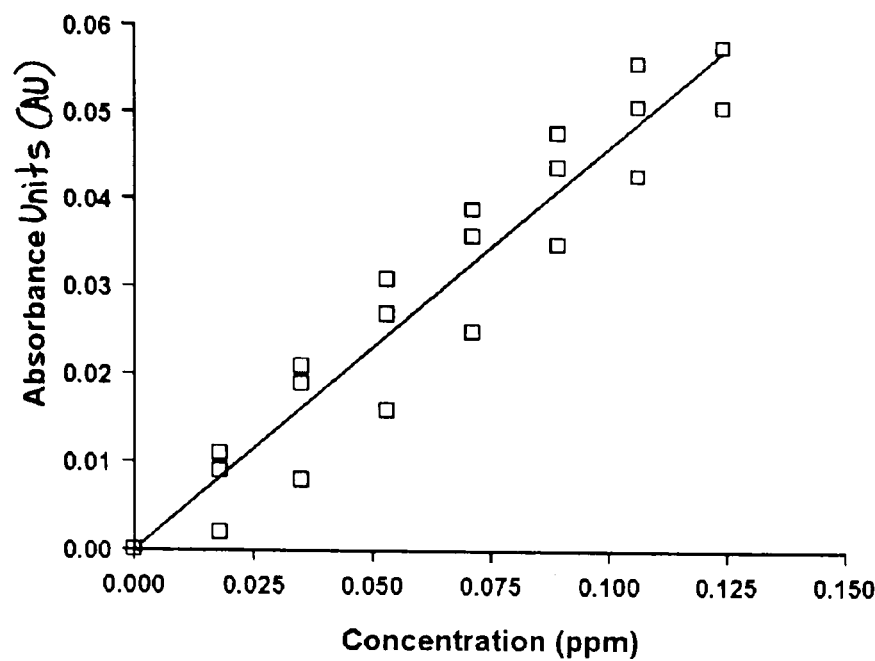


Figure 3.22 Calibration curve for SF₆. 1 μ l aliquots 10 % SF₆/90 % N₂ (0.0177 ppm SF₆)

The linear term concentration (ppm)/Absorbance (AU)) for SF₆ recommended by Foxboro at a wavelength of 10.7 μ m and path length 0.75 m was 974.1. After calibration of the Miran at a path length of 20.25 m and absorbance range 0 - 0.025AU this linear term was 2.14 (Table 3.6).

Absorbance	Input voltage	ADC counts	AU/count	ppm/AU	ppm/count
0 - 0.025AU	0 - 1 Volts	409.2	0.000061	2.14	0.000131

Table 3.6 Calibration of A/D input(Analogue/Digital), AU absorbance units; ADC analogue digital converter

3.9.1.7 Test procedure

The test was performed with the cupboard at a known face velocity and with a working aperture of 500 mm measured from the top of the lipfoil to the underside of the sash handle. The funnel was placed in the position P1 and tracer gas was injected into the fume cupboard through nylon tubing from the gas cylinder at a rate of 2 l/min per metre width of cupboard \pm 5 % as recommended in BS 7258 : Section 5.2. For this cupboard a flow rate of 2.4 l/min was used. The Miran integral pump was switched on and adjusted to a sampling flow rate of 2 l/min \pm 5 % as recommended in BS 7258 : Section 5.7.

In Part 4 it was recommended that the tracer gas be passed through the inlet device (5.2) for 180s \pm 20s and the sampled air allowed to run to waste through the gas analyser. Air was collected for a further period of 600 s \pm 20 s and the concentration of SF₆ in the sample measured. After this period the Miran pump and gas injection systems were turned off. The inlet device was then moved successively to a further five positions and the test procedure repeated at each position.

This method was applicable to grab sampling. However, using the data logger, continuous monitoring was possible and the concentration of SF₆ in the air sampled was recorded over 840 seconds. For the first 60 seconds a zero reading was established and then for the next 780 seconds the data were logged. In - line with BS 7258 : Part 4 only the last 600 seconds were counted as the test period and the results were expressed as the mean of these logged data adjusted for a zero baseline.

3.9.1.8 Expression of results

The highest value from the six values of concentration of SF₆ found for the inlet device positions was selected and the containment value taken was the concentration of SF₆ in p.p.m (V/V) at that position.

3.9.2 Results and discussion

3.9.2.1 Set-up problems

During initial tests, there was a slow drift upwards from the baseline on the chart recording due to instrument zero drift. It appeared to be temperature dependent, a rise in temperature causing a positive drift. This was rectified by an instrument service.

3.9.2.2 Gas analyser instrument noise

The maximum sensitivity of the instrument was theoretically 0.000131 ppm when the output was logged by computer. However, instrument electrical noise was far in excess of this with a standard deviation of 0.0008 ppm; peak to peak being 0.0033 ppm, 4 times the SD (Table. 3.7) at an instrument response time of 1 second (Fig. 3.23). This then produced an error when measurements were made within the limits of the maximum sensitivity. At an instrument response time of 10 seconds (Fig. 3.24) the fluctuations were reduced (Table 3.7), the standard deviation half that at a response time of 1 second.

Baseline mean value 0 ppm	Response time	
	1 second	10 seconds
Standard deviation	0.0008 ppm	0.0004 ppm
Standard error of the mean	0.00008 ppm	0.00004 ppm
Maximum	0.0017 ppm	0.0012 ppm
Range	0.0029 ppm	0.0023 ppm

Table 3.7 Instrument at response time of 1 second

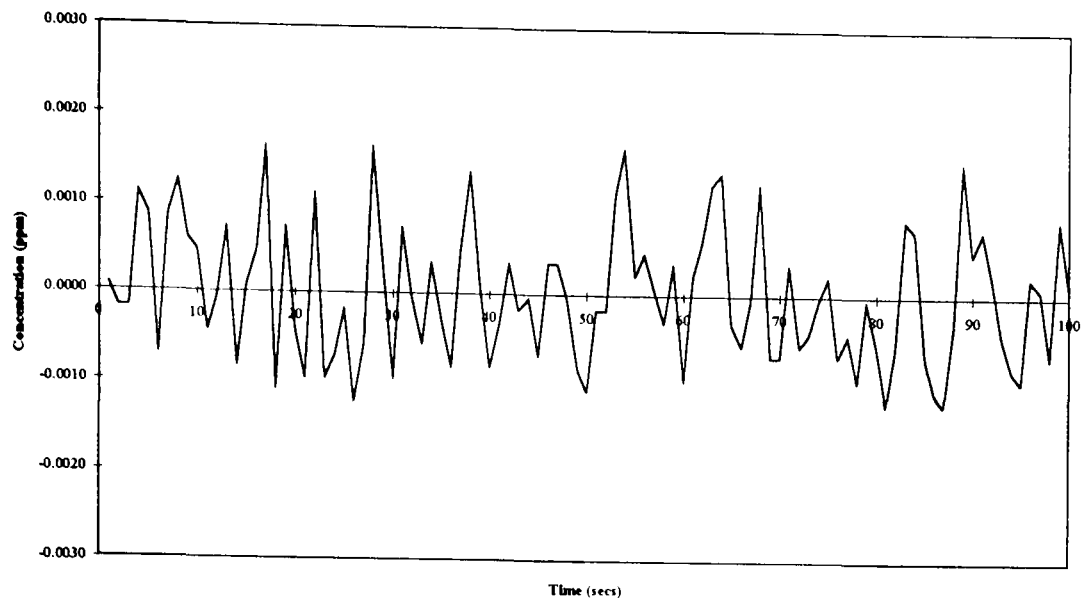


Figure 3.23 Instrument noise at response time of 1 second

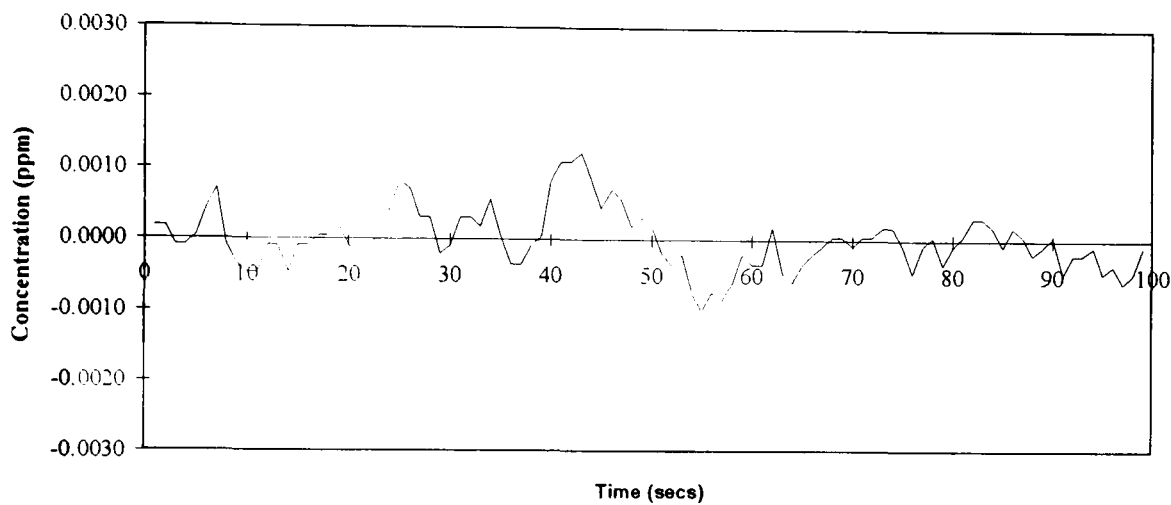


Figure 3.24 Instrument noise at response time 10 seconds

3.9.2.3 Background

During initial tests, there was constant drift on the readings which was too steady to be leakage from the cupboard and the onset was rapid enough to suggest a rise in background contamination. On inspection of the ductwork it was found that on the downstream side of the extract fan which was routed within the building, there was a leak at the joint. This was repaired and sealed.

During further tests there was again a constant drift from baseline which again was too steady to be leakage from the cupboard, yet the onset was not rapid to indicate leaking ductwork. It was surmised the source of the problem was the manner in which the factory air was made up following extraction from the test room. With the factory door open there was no rise in the background levels. However, with the factory door closed there was an eventual drift during a performance test (Fig. 3.25).

It was considered that SF_6 was being drawn into the building from under the eaves near to the point of discharge from the test room. The extract duct was finished flush with the outside wall of the factory and hence was not discharged high enough into atmosphere to prevent it

accumulating in the wash of the building. A high discharge stack was not fitted due to local planning legislation. Knowing this it was also considered that local atmospheric conditions may on occasion result in SF_6 being drawn into the test room whether the factory door was open or closed. All tests were therefore performed with the factory doors open in order to limit as far as possible any reentrainment of discharged test room air back into the factory.

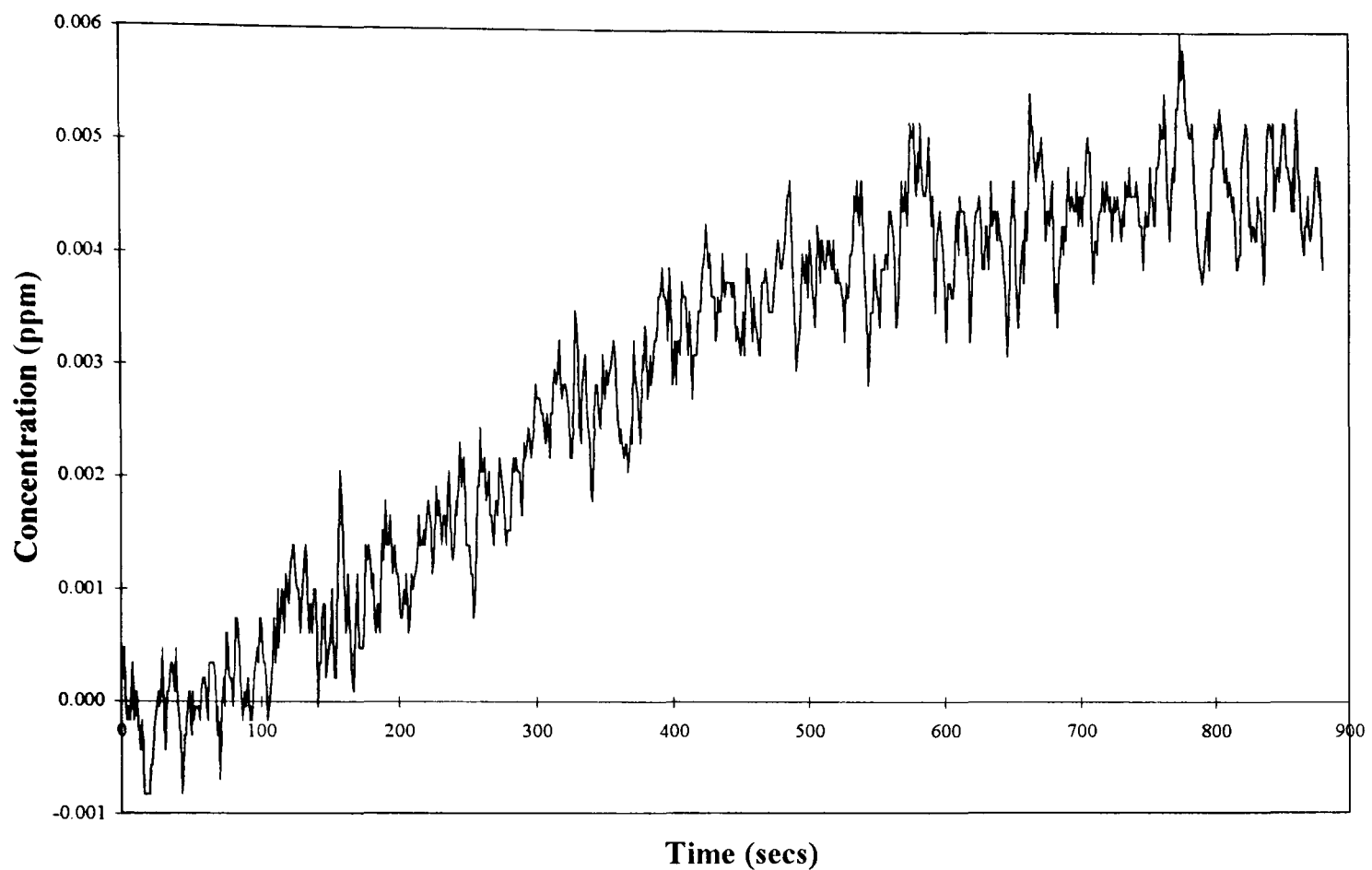


Figure 3.25 Background concentrations of SF_6 due to re-entrainment of air into the test room.

3.9.2.4 Response time of the sampling system to changes in SF_6 concentration

In the BS 7258 : 1994 : Part 4, the sampling flow rate is recommended to be 2 l/min. However, as indicated by Fletcher & Johnson, 1992, this produces a very slow response time of the sampling to changes in detected gas concentration (Fig. 3.26). The biggest problem is the purging of the sampling system and gas cell.

At the recommended sampling flow rate of 2 l/min the dilution rate is long due to the relatively large volume of the system, ~ 6.64 l. This includes the volume of the sampling probes (ID 5 mm x 150 mm long), probe tubing (ID 5 mm x 1 m long), collection manifold, instrument tubing (ID 10 mm x 2 m long) and the gas cell volume of the infra-red gas analyser (5.64 l based on calibration volume). Thus any gas drawn into the gas cell will decay slowly reducing the response time to further small increases in gas concentration (Fig. 3.34, Table 3.8). By increasing the sampling flow rate the detection time and residence time are both decreased. For the experiments, the Miran pump was not restricted and the sampling flow rate through the complete sampling grid was ~ 8 l/min.

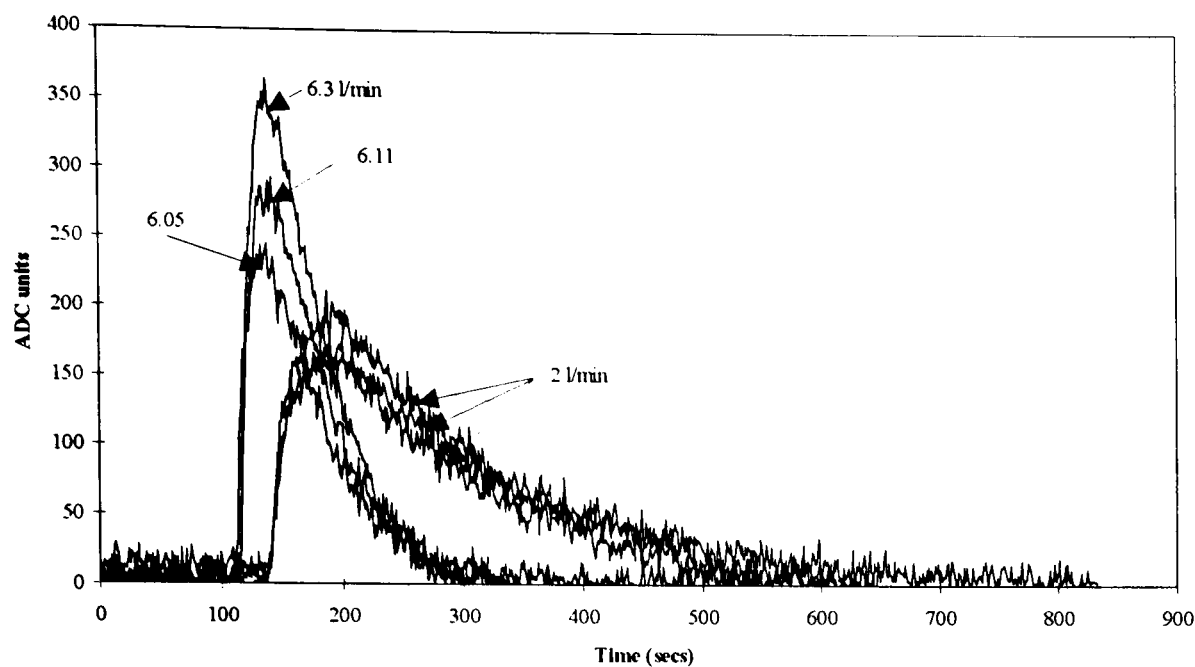


Figure 3.25 Response time of the infra-red gas analyser at different sampling flow rates. A 5µl sample was injected into the central probe of the BS 7258 : 1994 : Part 4 grid.

Sampling flow rate l/min	Time to detection seconds	Time to peak concentration seconds	Initial rate of detection ADC/s	Time to decay seconds	Rate of decay T-half seconds
2	138	200	8	400	101
6	112	138	21	132	48

Table 3.8 Average response times of the infra red gas analyser at different sampling flow rates.

3.9.2.5 Test results

Average face velocity 0.5 m/s. Injection flow rate of tracer gas 2.4 l/min (1.2 m wide aperture @ 2 l/min/m aperture width)

As recorded by chart recorder

(Indicated flow rate of tracer gas 2.4 l/min, actual 2.02 l/min)

Face	Source Position					
Velocity	P ₁	P ₂	P ₃	P ₄	P ₅	P ₆
0.47 m/s	0	0	0	0	0	0

Table 3.9 Tracer gas concentration (ppm) measured in the aperture plane recorded by chart recorder.

From these recordings, Table 3.9, there was no evidence of SF₆ being detected in the plane of the sash.

As recorded by datalogger

(Indicated flow rate of tracer gas 3.4 l/min, actual 2.86 l/min)

From the logged test data, Fig. 3.27a & 3.27b and Table 3.10, there was no difference between the mean of the test data and the mean of the baseline data. At the instrument response time of 1 second there was substantial noise but there also appeared to be an

Fig. 3.27a Containment test results: Infra red traces of air (sampled in the plane of the sash) when SF_6 is released inside the fume cupboard from positions P1 - P3 according to the method described in BS 7258 : 1994 : Part 4

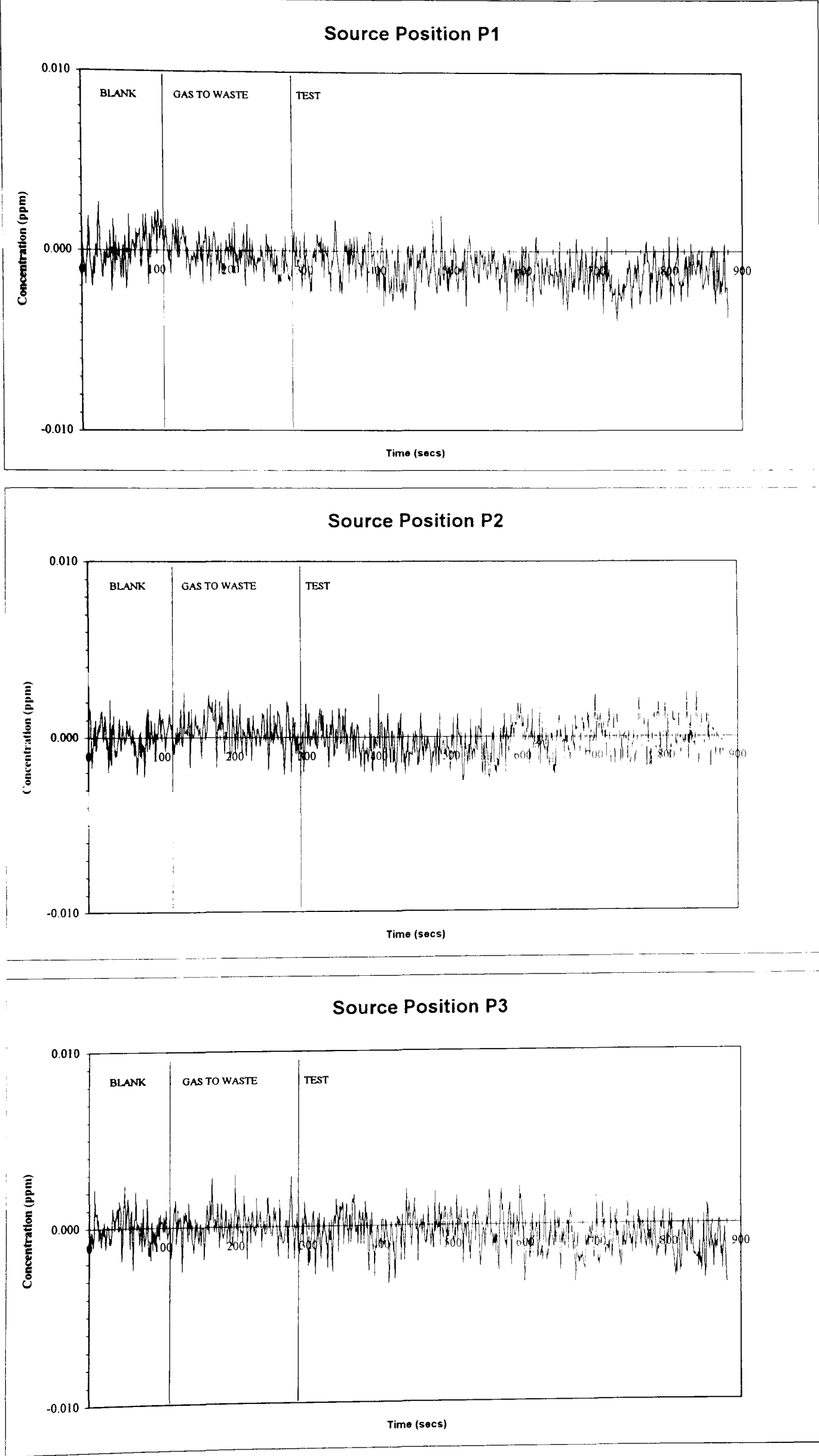
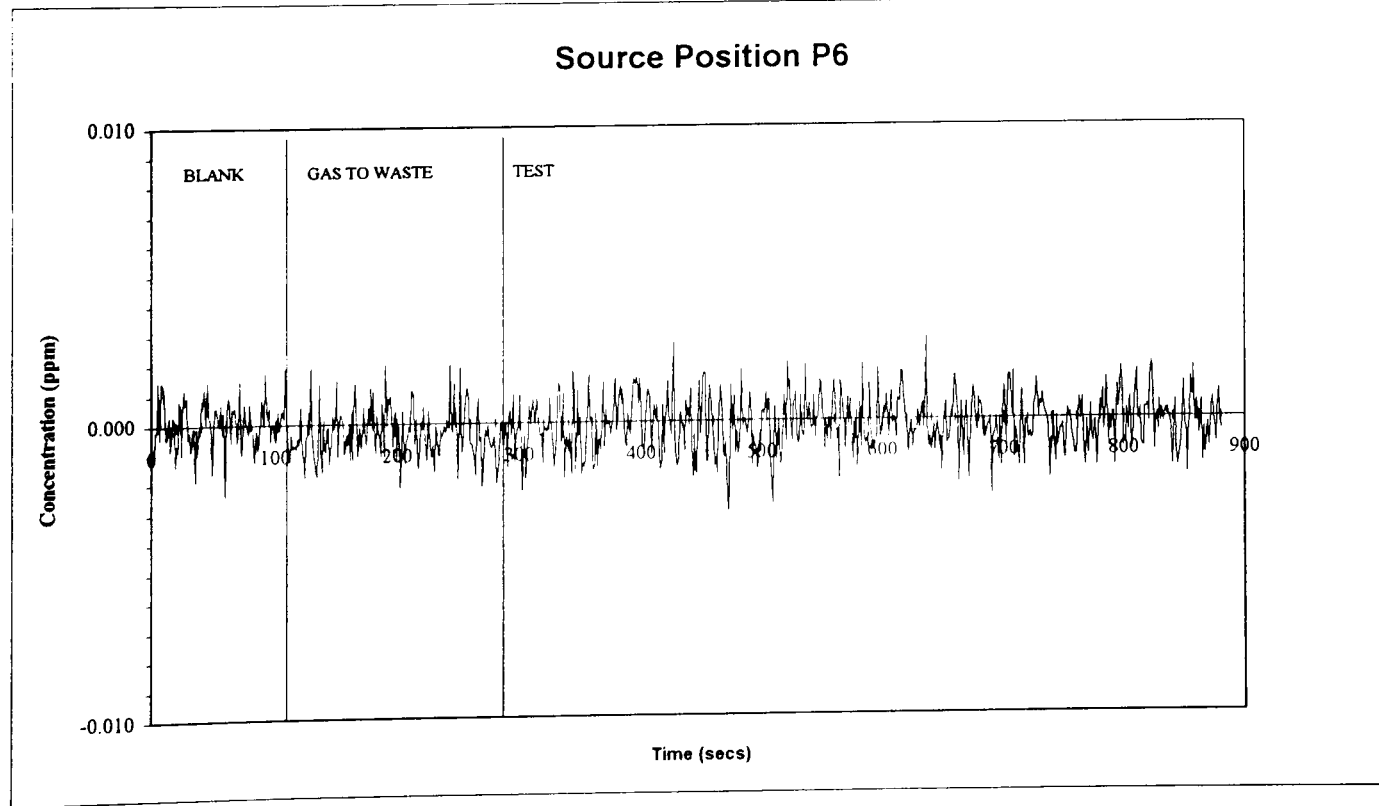
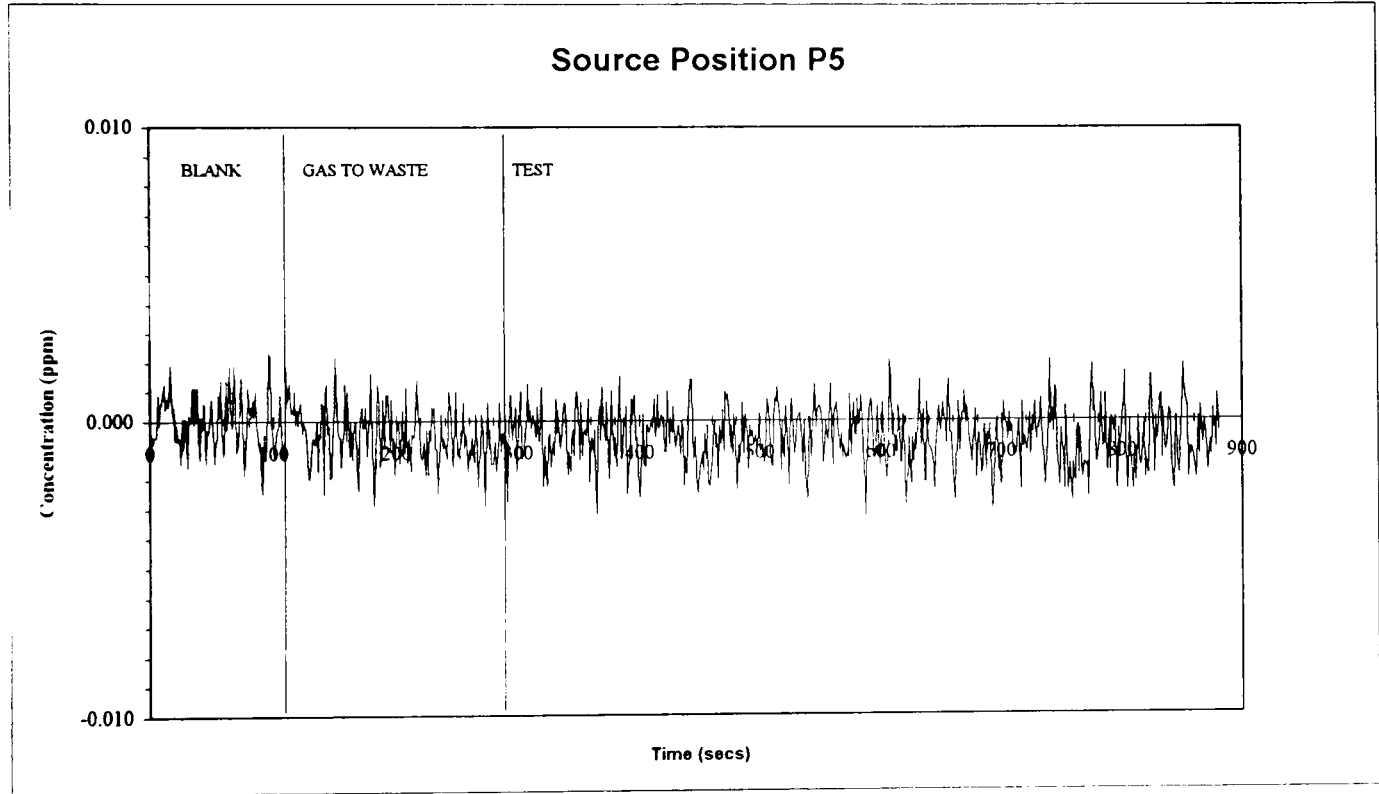
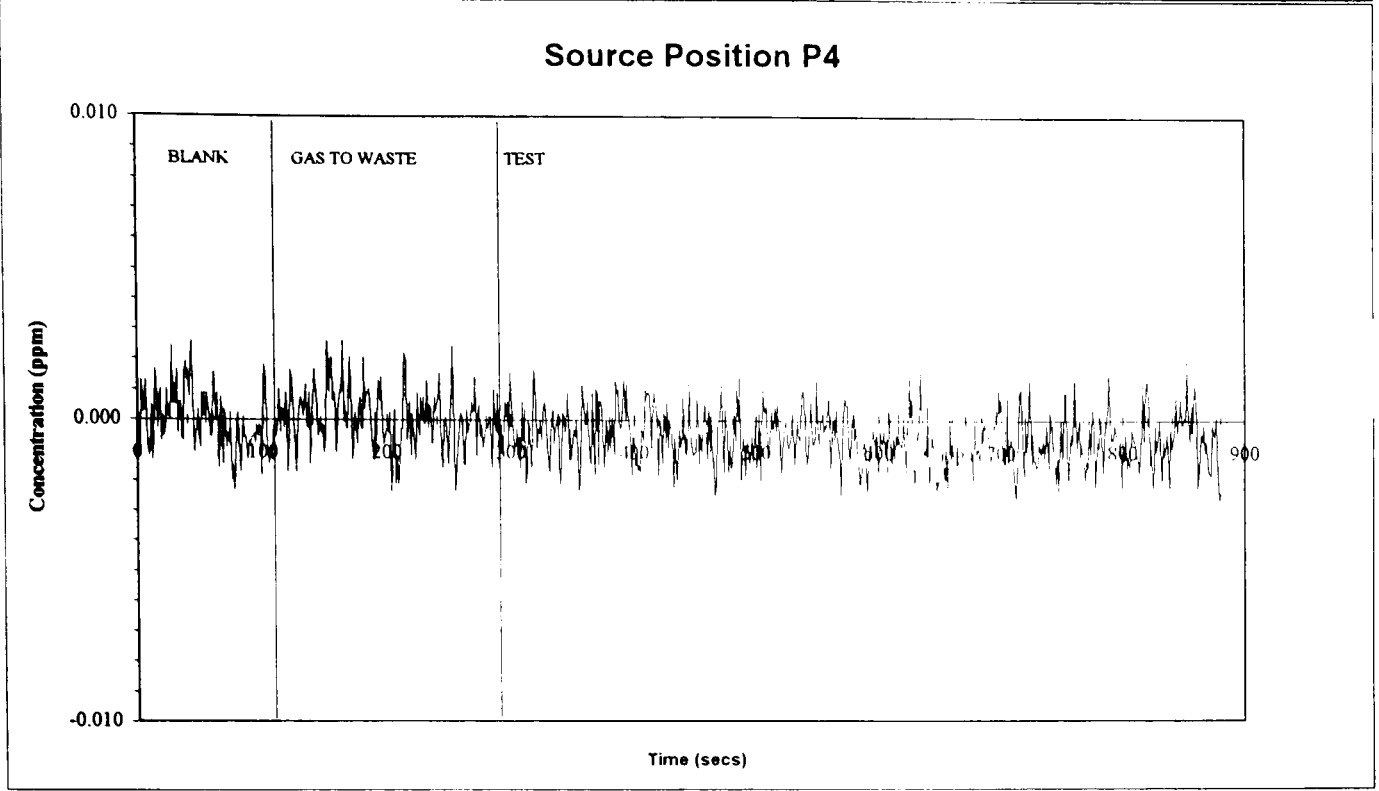


Fig. 3.27b Containment test results: Infra red traces of air (sampled in the plane of the sash) when SF_6 is released inside the fume cupboard from positions P4 - P6 according to the method described in BS 7258 : 1994 : Part 4



underlying unstable trend which was apparent in both the baseline and test data. From this data it was assumed that for the cupboard tested with no environmental disturbance, no SF₆ was detected in the plane of the sash. The only signal being the inherent noise in the instrument.

Source	P ₁	P ₂	P ₃	P ₄	P ₅	P ₆
Blank	0.005	0.003	0.004	0.003	0.004	0.004
Waste	0.005	0.003	0.004	0.003	0.004	0.003
Test	0.004	0.002	0.004	0.002	0.004	0.003
Test-blank	-0.001	0.000	-0.001	-0.001	-0.001	0.000

Table 3.10 Tracer gas concentration (ppm) measured in the aperture plane recorded by data logger.

3.9.3 Tracer flow from funnel

With no environmental disturbance the tracer gas, being denser than air and negatively buoyant, sank to the cupboard floor as it was discharged from the funnel (Fletcher & Johnson, 1990). This was demonstrated in this study using smoke, seeding the tracer gas as it flowed from the funnel (Plate 3.1). With the fume cupboard switched off and no gas flow the smoke was shown to rise under its own thermal buoyancy. The gas flow was turned on and the smoke sank to the work surface. When the fume cupboard was switched on the smoke was immediately swept away being influenced by the air flowing through the working volume. It was assumed that the movement of the smoke reflected the movement of gas tracer and the effect of buoyancy was negligible compared to the influence of the cupboard airflow.

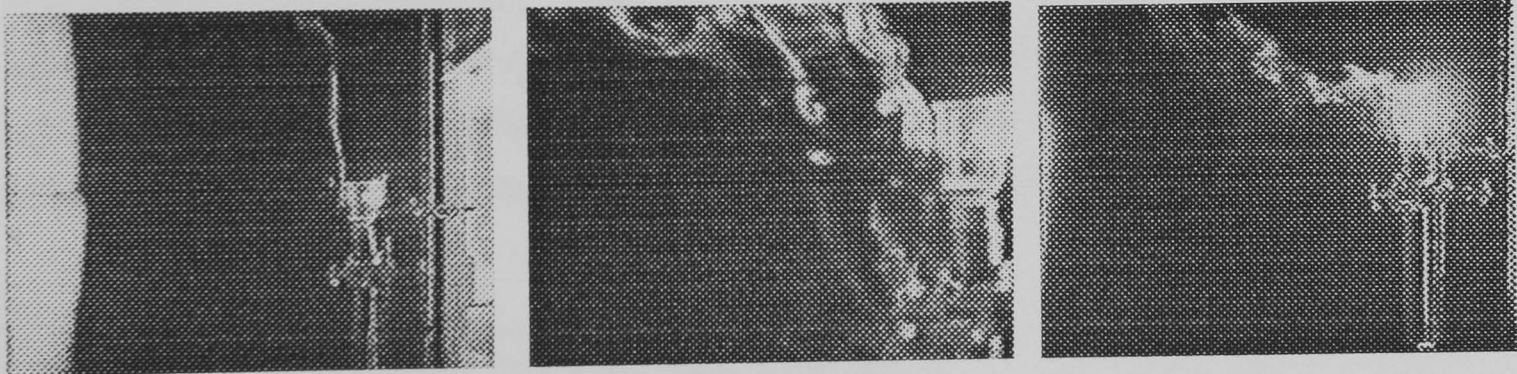


Plate 3.1 Gas off/cupboard off

Tracer gas on/cupboard off

Tracer gas on/cupboard on

3.9.4 Effect of funnel position and mixing

Tracer gas released from each of the six positions P1 - P6 is assumed to be fully mixed within the cupboard working volume for the expression of some performance factors (section 1.2). However, releasing smoke at each of these positions indicated that tracer would not be fully mixed in the working volume either by bulk movement or turbulent diffusion. The effect of aerodynamic features in the cupboard resulted in smoke released at one of the lower positions, P123, being rapidly scavenged through the lower extract slot and for some approaching the rear baffle being carried up towards the top extract slot (Plate 3.2). That released from one of the positions, P456, was carried up towards the top extract slot, where

some was entrained in the recirculating zone of air at the top of the cupboard, which moved down behind the sash to be re-entrained with the inflowing air (Plate 3.3).

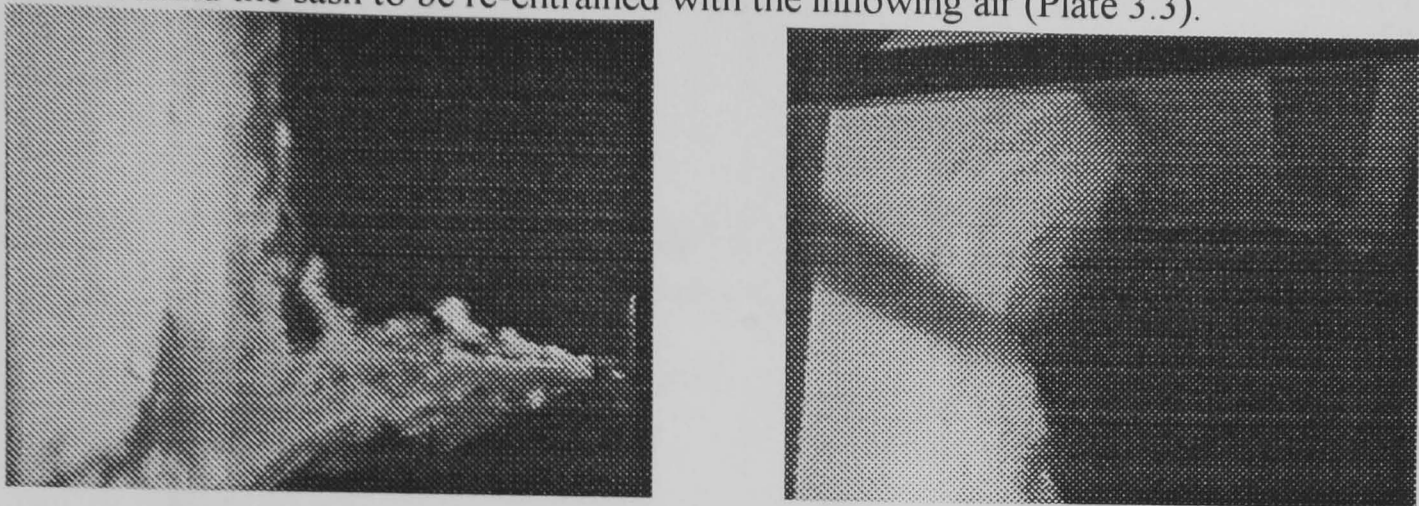


Plate 3.2 Release of smoke in BS 7258 source position P₂. Cupboard face velocity 0.5 m/s.

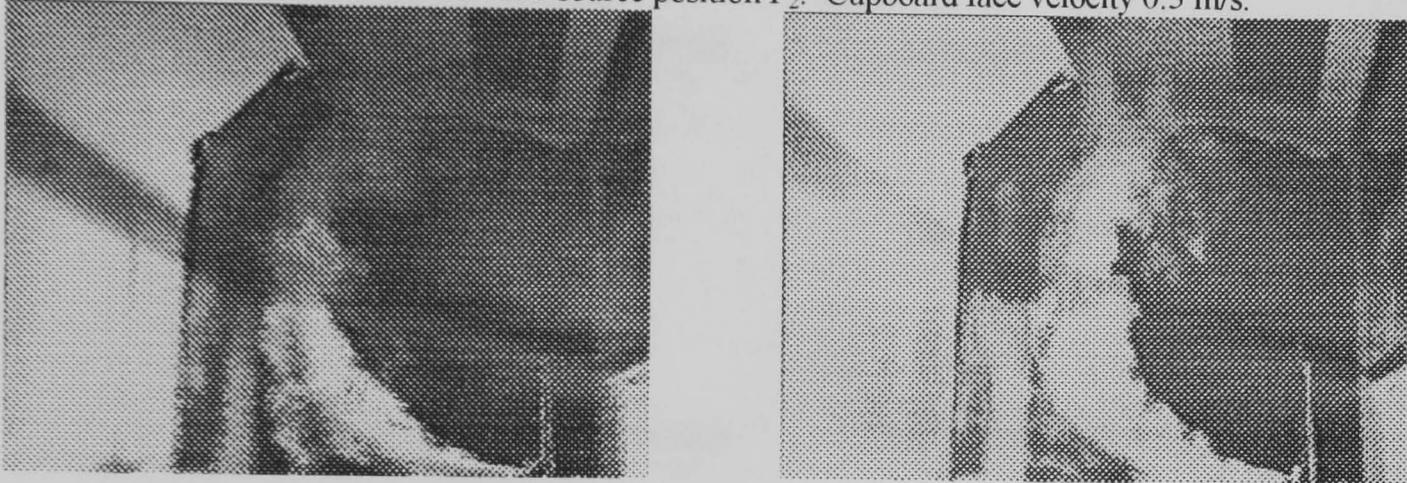


Plate 3.3 Release of smoke in BS 7258 source position P₅. Cupboard face velocity 0.5 m/s.

This was then shown using the BS funnel and tracer gas that the positions of the source across the cupboard width did not result in complete mixing of the internal, air volume. Table 3.11 shows measurements of SF₆ that were made within the interior volume when tracer gas was released from position P₂. There was a peak in concentration measured at the upper centre right position, of 0.07 ppm, supporting smoke visualisation that some tracer may flow up the work side of the baffle and be entrained in the recirculation zone behind the sash. However, no tracer gas was measured in the lower centre right position.

Source	P ₆	P ₂	P ₂ *	P ₂ +
Face vel	0.5 m/s	0.5 m/s	0.5 m/s	0.5 m/s
Injection	6.55 l/min	6.55 l/min	6.55 l/min	6.55 l/min
Blank	0.0032	0.0040	0.0038	0.0038
Waste	0.0031	0.0037		
Test	0.0036	0.0036	0.0044	0.0038
Test-blank	0.0004	0.0004	0.0006	0.0000
Peak	/	/	0.07	/

Table 3.11 Tracer gas concentration (ppm) measured in the aperture plane at increased source flow rate, and distribution of tracer inside the cupboard working volume: P₂* sampled inside cupboard top mid right and P₂+ sampled inside cupboard bottom mid right.

With this test cupboard, increasing the amount of tracer discharged up to 6.55 l/min did not result in any change in the measurement of tracer in the plane of the aperture.

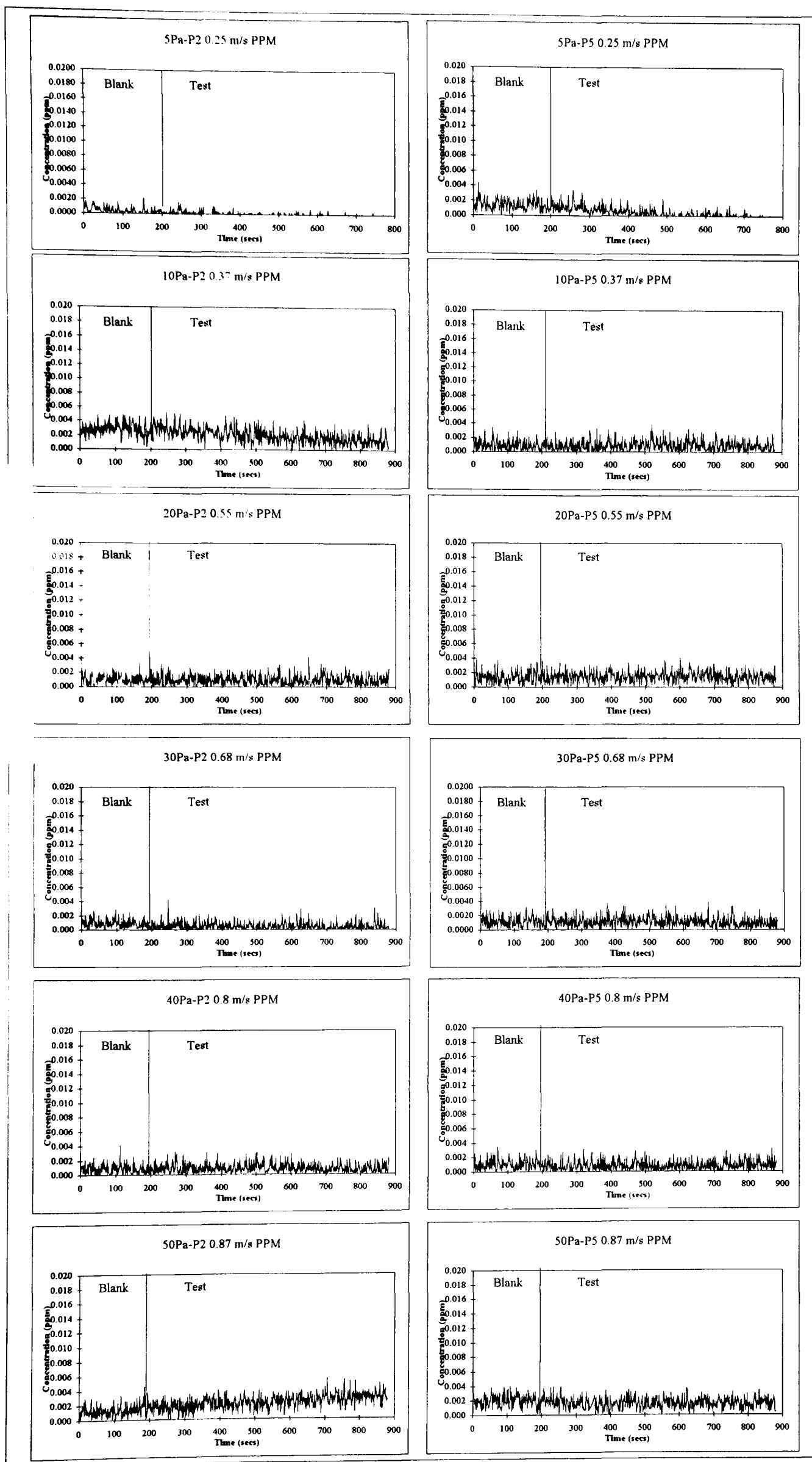


Fig. 3.28 Infra-red traces of air sampled in the plane of the sash at varying face velocity

3.9.5 Effect of face velocity on containment

When using the BS 7258 : 1994 test on this aerodynamic cupboard, no tracer gas was detected in the plane of the aperture within the sensitivity of the method at a face velocity of 0.5 m/s (section 3.9.2.5). The test was then repeated at face velocities 0.25, 0.55, 0.68, 0.80 and 0.87 m/s and source positions P2 and P5. Only at a face velocity of 0.87 m/s was any SF₆ measured in the plane of the sash when tracer was released from position P2 (Fig. 3.28 & 3.29). There was no tracer measured in the plane of the sash at the lower face velocity of 0.25 m/s. This was a condition known to be inadequate in the working environment where general velocities may exceed this.

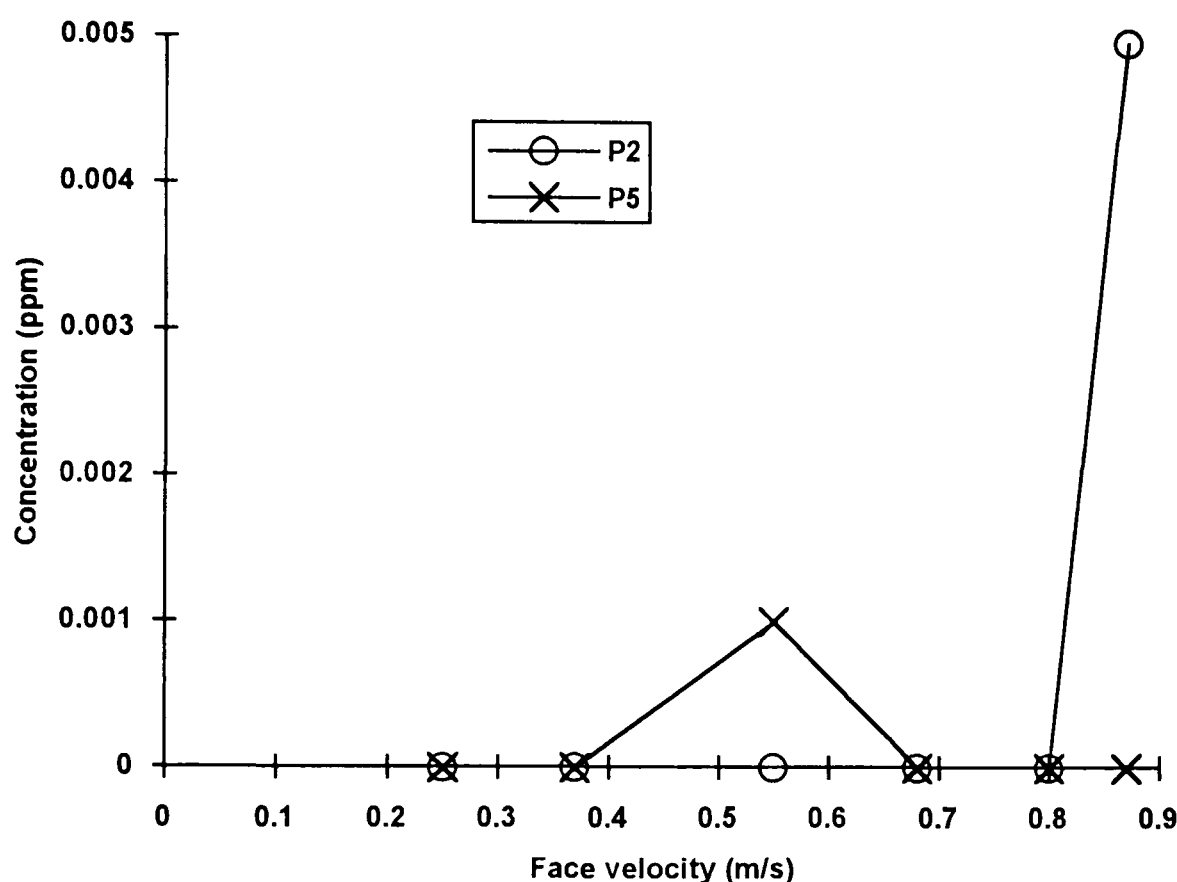


Figure 3.29 Effect of face velocity on the concentration of SF₆ measured in the plane of the sash

3.9.6 Effect of design features on containment

It must be concluded so far, that a well designed fume cupboard operating in a stable environment gave a good performance; that the tests used were repeatable and consistent. The design of the fume cupboard used in this investigation was then changed. The major difference being that the vertical gap between the work surface and the lipfoil was reduced, the work surface shortened so that the lipfoil covered less of it, and the top rear extract slot also reduced in cross section. Type tests were carried out at two face velocities, 0.56 m/s and 0.79 m/s using again the BS 7258 : 1994 : Part 1 (Table 3.12) and a containment test carried out as in Part 4 at the higher velocity (Fig. 3.30). The type test results were comparable to the previous design and within the specifications of the standard, and the containment test only showed traces of gas (0.002 ppm) sampled in the plane of the sash when the source was positioned at P2. At all other source positions no gas was detected.

Table 3.12: Distribution of average velocities across the aperture when measured in the plane of the sash (cupboard Model B1500SS), using the grid as specified in BS 7258 : Part 1 : 1994.

Anemometer - Airflow Developments Ltd. TA-2-15 (thermistor type)

Overall mean face velocity 0.56 m/s

Minimum average velocity at a grid point: 0.51 m/s = 91 % overall mean face velocity

(Figures in small type are standard deviation of 12 measurements from average calculated)

0.58 0.04	0.58 0.04	0.57 0.06	0.56 0.03	0.52 0.06	0.56 0.05	0.57 0.06	0.58 0.04	0.58 0.04
0.54 0.033	0.51 0.05	0.55 0.04	0.52 0.03	0.52 0.01	0.55 0.03	0.55 0.04	0.52 0.02	0.54 0.03
0.57 0.041	0.52 0.04	0.52 0.03	0.51 0.01	0.53 0.02	0.55 0.03	0.55 0.03	0.55 0.02	0.53 0.09
0.6 0.011	0.59 0.02	0.53 0.04	0.56 0.03	0.55 0.02	0.56 0.04	0.57 0.03	0.60 0.01	0.61 0.01
0.58 0.043	0.60 0.04	0.60 0.03	0.59 0.04	0.61 0.01	0.66 0.01	0.63 0.04	0.63 0.04	0.61 0.01

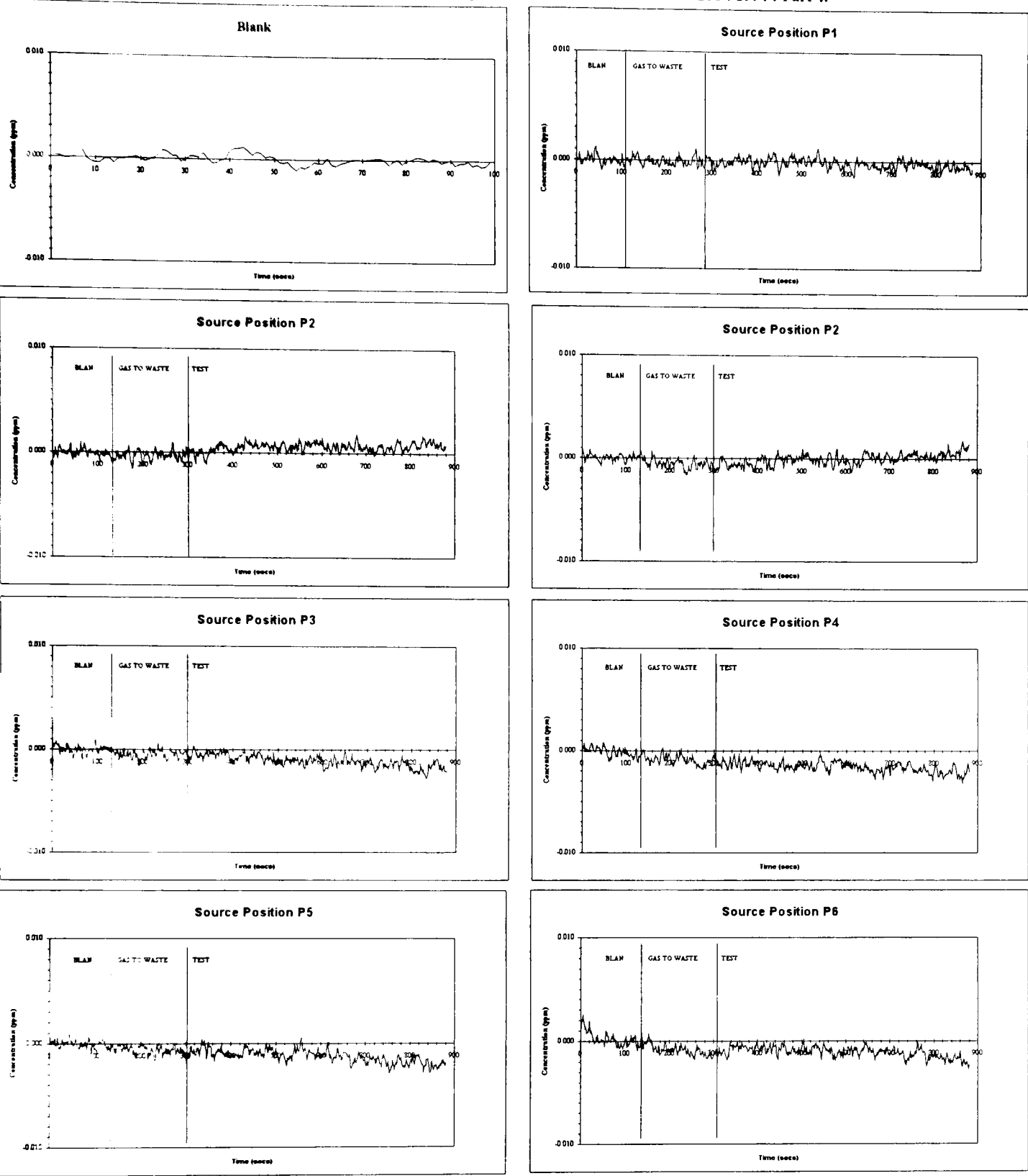
Overall mean face velocity 0.79 m/s

Minimum average velocity at a grid point: 0.69 m/s = 87 % overall mean face velocity

(Figures in small type are standard deviation of 12 measurements from average calculated)

0.82 0.06	0.83 0.03	0.83 0.03	0.82 0.03	0.81 0.03	0.81 0.05	0.83 0.06	0.86 0.03	0.80 0.03
0.77 0.05	0.77 0.03	0.75 0.03	0.74 0.03	0.74 0.03	0.74 0.03	0.79 0.03	0.80 0.00	0.90 0.05
0.75 0.04	0.69 0.02	0.72 0.05	0.72 0.02	0.72 0.02	0.74 0.03	0.76 0.03	0.78 0.02	0.75 0.04
0.82 0.03	0.79 0.03	0.76 0.03	0.74 0.03	0.74 0.03	0.75 0.03	0.79 0.02	0.79 0.03	0.82 0.03
0.83 0.05	0.83 0.03	0.79 0.05	0.84 0.03	0.84 0.03	0.81 0.01	0.87 0.02	0.87 0.02	0.87 0.04

Fig. 3.30 Containment test results on a modified fume cupboard: Infra-red traces of air (sampled in the plane of the sash) when SF_6 was released inside the fume cupboard from positions P1 - P6 according to the method described in BS7258 : 1994 : Part 4.



Prior to the type test, a flow visualisation exercise was performed using water fog generated from an ultra-sonic nebuliser (Kennedy, 1987). This had shown regions of recirculation at the left and right sides of the aperture and over the lipfoil. These appeared to be caused by supports beneath the lipfoil blocking the airflow and causing boundary separation. The net result was air seen to recirculate back towards the aperture in these regions. However, the type test face velocity did not show any regions of high variation. The gas test only indicated a problem when the source was at P2 in the region of the centre of the lipfoil, the traces being very small. None was detected towards the left and right sides with the source at P1 and P3.

In order to ascertain whether gas was actually recirculating to the aperture as seen by water fog a corner probe was detached from its normal position and moved towards the corner in position BIII (Fig. 3.31). There was no tracer gas detected. The funnel was then placed on the work surface so that its open end faced the wall 60 mm away and 60 mm from the plane of the aperture, this being approximately the area of recirculation as demonstrated by the water fog. With the probes arranged in the BS 7258 grid there was no gas detected (Fig. 3.32a). Moving the lower corner probe into the corner position AI again no gas was detected but moving the probe right into the corner in position AII gas tracer was sampled. When the probe was placed on the lipfoil 20 mm from the sash plane (position CII) tracer was still sampled (Fig. 3.32b). When the probe was moved to 50 mm from the sash plane (position DII) there was no tracer sampled (Fig. 3.32c). Equally when the probe was lowered to the lipfoil (position EIII) no tracer was sampled. The probe was then moved towards the corner and approximately 10 mm from the right edge and 10 mm from the lipfoil in the plane of the sash, some tracer was sampled up to 0.01 - 0.02 ppm. Only when it was placed right in the corner was gross leakage detected. With the probe on the lipfoil in the sash plane and 50 mm from the right hand wall there was no leakage detected. It had also been noticed that the water fog collected under the sash handle. With the standard arrangement of equipment and the source in position P6 the top left corner probe was detached and moved towards the sash handle. Near to the handle ~ 5 mm away gas was sampled.

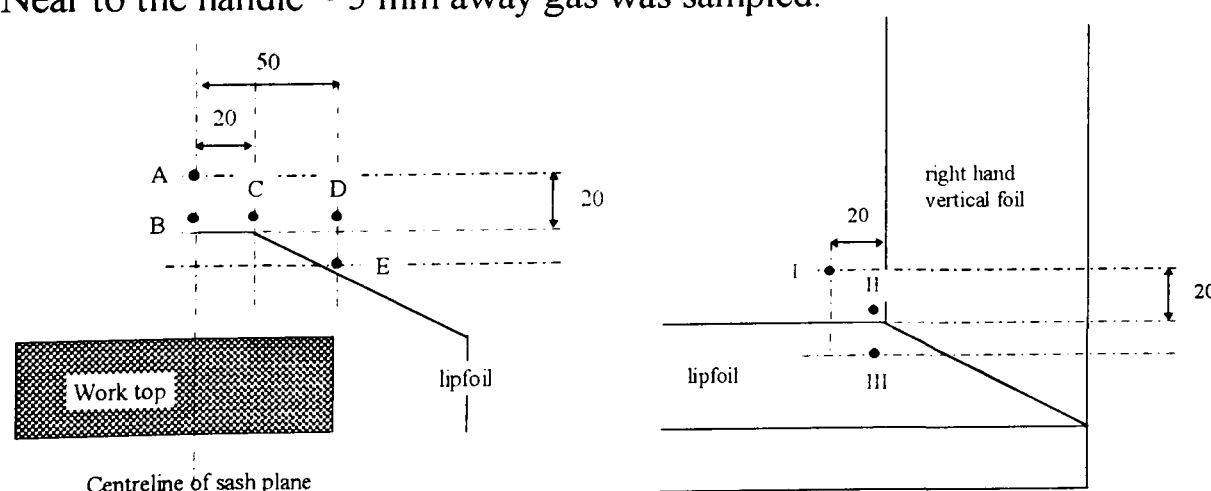


Figure 3.31 Rearrangement of sampling probes to measure potential leakage in the corner of the aperture.

This was repeated for a smaller fume cupboard of the same design in which the recirculation at the edge corners could be demonstrated using the water fog, exaggerated by rough finishing and unsealed gaps. In this case water fog could be seen to move out of the plane in

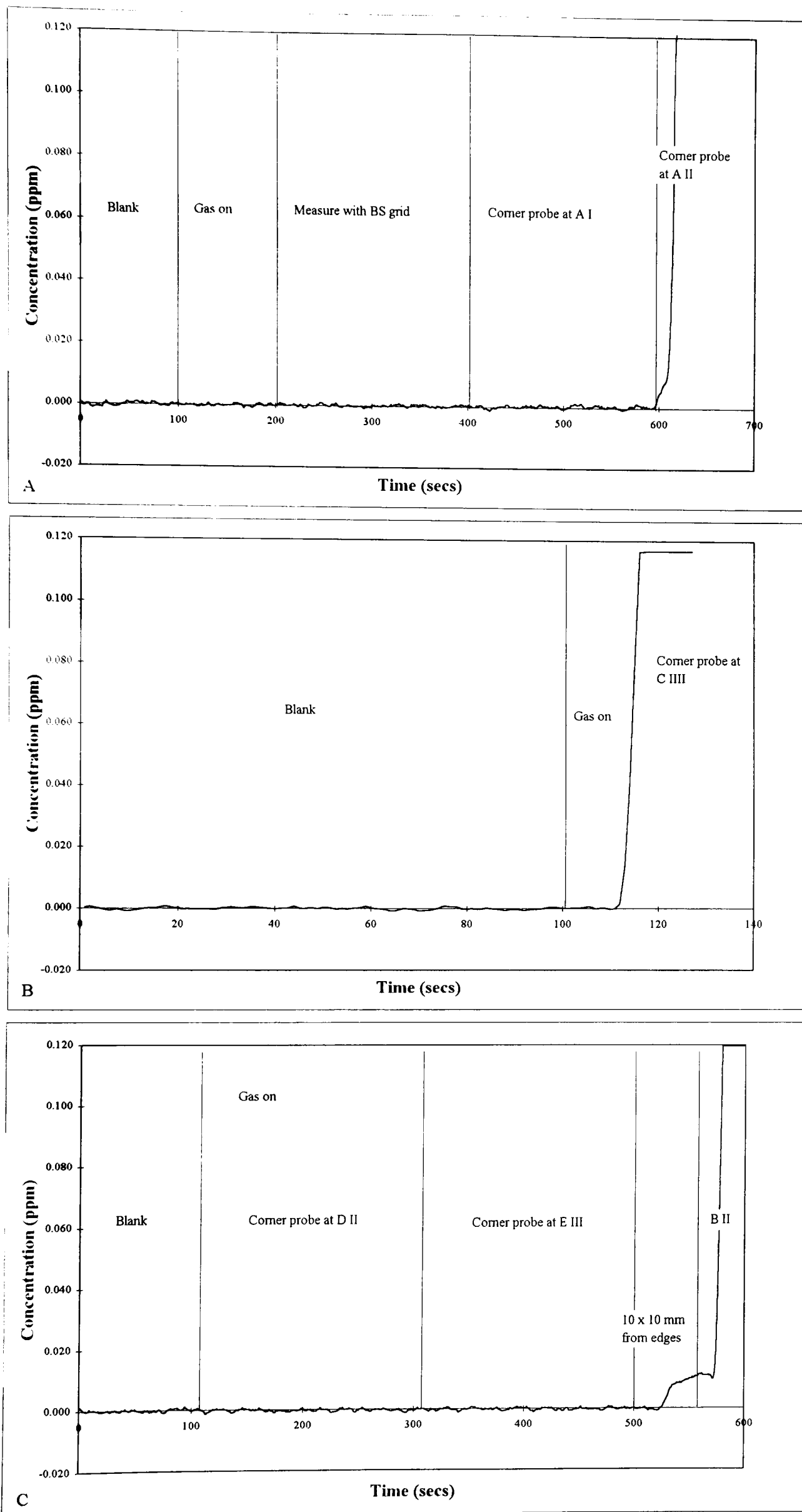


Fig. 3.32 Infra red traces showing the effect of moving a sampling probe into the positions shown in Fig. 3.31.

the wake of an electrical socket fixed to the vertical side aerofoil. Again there was no gas detected in the plane of the aperture when using the BS 7258 : 1994 : Part 4 method. With the gas source in position P3 and using a single probe it was demonstrated that gas was not only detected near the corner but also near to the edges.

This suggested that with the BS grid arrangement, tracer could be recirculated back towards the aperture and around the edges but not sampled. In this investigation gas was not detected until the probe was placed right in the corner.

3.10 Discussion of BS 7258 : 1994 : Parts 1 and 4 and other national standard's testing methodologies used for assessing the performance of a general purpose laboratory fume cupboard

The performance of the Fumair aerodynamic fume cupboard (B1500) used in this study was within the specifications for 'type' testing, 'commissioning' as specified in BS 7258 : 1994 : Part 1. Also using the method recommended for the quantitative assessment of containment in BS 7258 : 1994 : Part 4, no tracer gas was sampled in the plane of the aperture at a face velocity of 0.5 m/s.

For a rapid check on the fume cupboard face velocity, the rotating vane anemometer was adequate and the results were repeatable. For the installation and balancing of several fume cupboards on the same duct a rotating vane anemometer would be considered sufficient at such a stage. The thermistors and hot wire anemometers would be less desirable as they had no averaging properties: variation in velocity at a position could be large and measurements difficult to read. In assessing cupboard performance for "type" testing and subsequently for "commissioning", the fluctuation of readings was an important indication of turbulence and thus measurements with thermal anemometers had to be used. Flow visualisation was also important showing air movements both within and around the cupboard. This was recommended at installation but not as part of the "type, commissioning or maintenance" tests.

The angle to which the sensing head of an "uni-directional" thermal anemometer could be rotated to the line of the flow in the middle of the aperture showed, that not until ~ 30 degrees, was the velocity measured affected giving some tolerance to directional fluctuation in the flow patterns. If there was a cross flow normal to the sensing head, then this would not be identified using an omni-directional probe.

The response times and decay periods of the infra-red gas analyser were affected by the sampling flow rate. In the BS test it was required to be 2 l/min but this produced a very sluggish response to any tracer gas introduced into the sampling system and the decay from the gas cell was so long that any further changes in concentration would be mis-represented.

This has also been found by Fletcher & Johnson (1992) and Bicen (1992). There is no specified dimension of the collection manifold and this would also affect the residence time of tracer gas in the sampling system. The total volume of the sampling system was approximately 5-6 litres, the analyser having a 3-4 litre gas cell. By increasing the flow rate to ~7 l/min using the Miran's own integral pump, the response times were much quicker but perhaps more importantly the decay times were much shorter, the gas cell being purged quicker. This was important with respect to fluctuations in tracer being sampled in the plane of the sash. Initially an instrument response time of 1 second was used but this produced high frequency oscillations. This was smoothed out by increasing the response time to 10 seconds which would not be thought a problem in responding to tracer sampled, as the overall response time of the sampling volume was far in excess of this.

The tracer gas was not completely mixed within the cupboard when released from a single source position. However, as the source was moved over the aperture plane it was assumed that for a completed test the majority of the cupboard working volume was seeded with tracer, albeit not at the same time. There were limitations to this mixing in terms of the position of the source and the sampling grid. If there was leakage from a cupboard possibly by bulk air movement or turbulent diffusion, then tracer from the source position would be expected to mix in this region. This was shown to some extent with the design modifications to the aerodynamic fume cupboard tested causing turbulent recirculation zones at the lower vertical edges and near to the lipfoil. There was tracer sampled in the plane of the sash very near to these edges which did flow past the aperture plane. What was evident was that the position of the BS 7258 sampling grid did not pick this up and only when a probe was placed very near to the corner of the aperture was this evident. Further from the plane of the aperture no tracer was sampled.

This questioned the relevance of sampling in the sash plane. The principle had good foundations, sampling tracer that had the potential to escape as well as that which did escape. However, if no tracer was sampled by the BS 7258 grid arrangement even though there were obvious turbulent recirculation zones bringing tracer to the plane of the sash (shown by flow visualisation), then what was the point of actually sampling in the aperture plane at all?

The ASHRAE and DIN standards sampled a defined distance away from the aperture plane or in the breathing zone of the operator actual leakage. This perhaps gave a much more realistic approach and if the potential leakages at the edges were to escape the cupboard containment then this was an actual leakage.

The re-entrainment of air discharged from the fume cupboard back into the room in which the cupboard was installed was a problem causing raised background levels of tracer making testing of the fume cupboard not possible. This did identify a problem as far as discharge was concerned. Leaking ducts caused a raised background level of tracer. This made meaningful

testing of the fume cupboard impossible. However, as the fume cupboard and associated ductwork can be considered as parts of the containment envelope, ductwork leakage is an important factor.

The release of tracer gas was at a low flow rate compared to the volume of air passing through the fume cupboard. It did not constitute an active challenge to the containment performance of the cupboard but a passive one. In the test room the airflow in and around the fume cupboard aperture was also very stable. As the face velocity decreased and hence reduced the volume flow rate through the cupboard there was no tracer sampled in the plane of the aperture even at a face velocity of 0.25 m/s which was often considered vulnerable to unfavourable environmental conditions which may exist in some installations. It thus did show how stable the airflow and containment was at low flow rates but not how this may be seriously challenged during potential disturbance in on site conditions.

3.11 Key interim conclusions

- There was no minimum performance criteria nor hierarchical structuring of test methods specified in the performance assessment strategy. Emphasis was placed on face velocity testing for type testing, commissioning and for routine maintenance. A quantitative containment test method was optional. Air flow visualisation was only recommended at commissioning.
- The recommended gas tracer test method measured the potential for a fume cupboard to leak, not the actual leakage. It did not identify potential leakages at the lower corners of the aperture, beneath the sash foil or beneath the lipfoil.
- Assessing the containment performance of an aerodynamic fume cupboard at different face velocities, showed that as low as 0.25 m/s no tracer was detected in the aperture plane. This velocity was considered vulnerable to work place disturbances and showed how stable was the airflow and containment at low flow rates in the test room but not how this could be seriously challenged during potential disturbance on site.

Chapter 4 A Study of the British Standard BS 5726 : 1992 Performance Test for Microbiological safety cabinets

4.1 Introduction

For the purposes of this study, the performance assessment of class I and II microbiological safety cabinets was investigated. Class III cabinets were not included because they are not open fronted containment systems and are assessed by a different strategy involving a measure of pressure integrity. The strategy used for assessing the performance of class I and II types involves a hierarchy of tests for 'type' testing, 'commissioning' and for 'routine maintenance'. These are flow visualisation, face velocity and containment tests (section 2.3.2). The main difference between the 'type' test and the other tests of performance is in the measurement of face velocity at each position; for the 'type' test this is over a 5 minute period and for commissioning and maintenance is over a 1 minute period. There is no requirement for the tests to be carried out in a test room but the cabinet has to be installed in a room in which there are no environmental disturbances. The test procedures differ between the different classes of cabinet.

4.2 Methods

4.2.1 Flow visualisation

The visualisation of the airflow using smoke or other visualisation tests such as water fog (Kennedy, 1987), had to demonstrate an inward flow over the whole area of the working aperture. In this study, water fog generated from an 'ultra-sonic' nebuliser (Kennedy, 1987) was used.

4.2.2 Face velocity measurements

The methods used for measuring the inflow through class I cabinets and the inflow and downflow of class II cabinets were those specified in BS 5726 : 1992 : Part 1 : Appendix H. The anemometer used was a rotating vane type with a diameter of 100 mm (Airflow Developments Ltd.) This anemometer and its calibration have been discussed in section 3.8.2.

4.2.3 Quantitative assessment of the performance of class I and class II microbiological safety cabinets: Determination of a protection factor

The methods used were those specified in BS 5726 : 1992 : Part 1: Appendix D. The principle of these tests was to release an aerosol of particles less than 10 μm in diameter and with a settling rate in still air of less than 0.01 m/s, from within the cabinet and which could then be sampled outside the cabinet (section 2.3.2). The challenge droplets/particles were either generated as a monodisperse aerosol composing mainly of single bacterial spores from a nebuliser charged with an aqueous solution, or as a monodisperse aerosol of potassium

iodide (KI) particles derived from droplets of 1.5% KI in 95% alcohol generated from a spinning disc (KI-Discus, Containment Technology Ltd.).

4.2.4 Quantitative assessment of external contamination for class II cabinets

The principle of these tests was to release an aerosol of particles less than $10\text{ }\mu\text{m}$ in diameter and with a settling rate in still air of less than 0.01 m/s , from outside the cabinet, which could then be sampled inside the cabinet at the work surface. The challenge droplets/particles were either generated as a monodisperse aerosol composing mainly of single bacterial spores from a nebuliser charged with an aqueous solution, or a monodisperse aerosol of potassium iodide (KI) particles derived from droplets of 1.5% KI in 95% alcohol generated from a spinning disc (KI-Discus, Containment Technology Ltd.). The microbiological method was that specified in BS 5726 : 1992 : Part 1: Appendix E. The positioning of the KI Discus equipment resembled the microbiological challenge test method specified in BS 5726;1992, Part 1, appendix E as closely as possible. The aerosol was generated outside the cabinet and air sampled within the working area of the cabinet 50 mm from the front edge of the work surface (Fig. 4.1). The protocol was the same as the microbiological tests.

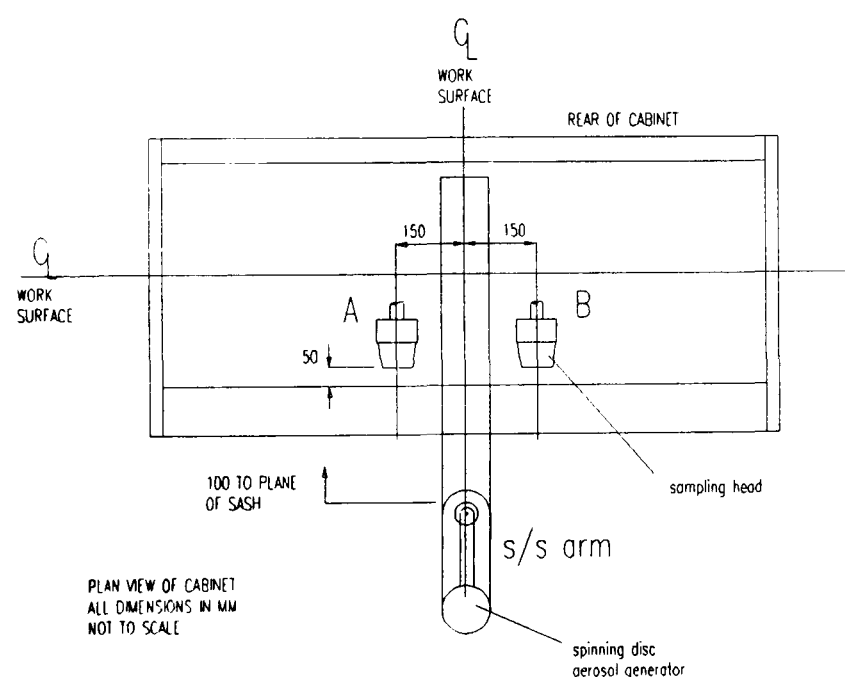


Figure 4.1 Arrangement of equipment for KI external contamination tests.

4.2.5 Quantitative assessment of cross contamination in class II cabinets

The principle of these tests was to release an aerosol of particles less than $10\text{ }\mu\text{m}$ in diameter and with a settling rate in still air of less than 0.01 m/s from one side of the working surface, and which could then be sampled at a defined distance away towards the other side. The challenge droplets/particles were either generated as a monodisperse aerosol composing mainly of single bacterial spores from a nebuliser charged with an aqueous solution, or as a monodisperse aerosol of potassium iodide (KI) particles derived from droplets of 1.5% KI in 95% alcohol generated from a spinning disc (KI-Discus, Containment Technology Ltd.). The microbiological method was that specified in BS 5726 : 1992 : Part 1: Appendix F.

The positioning of the KI Discus equipment resembled the microbiological challenge test method specified in BS 5726;1992, Part 1, appendix F as closely as possible. The spinning disc was placed on the work surface, equidistant from front to back, and the leading edge of the disc placed 50mm in from the side of the work surface (Fig. 4.2). Four samplers were placed so that the open end of each sampler was 37 mm (hole centre) above the work surface and facing the spinning disc generator. They were positioned in pairs one third and two thirds of the width and equidistant from front to back of the work surface; the nearest samplers were 300 mm from the leading edge of the spinning disc. The test protocol was the same as that used for the microbiological tests.

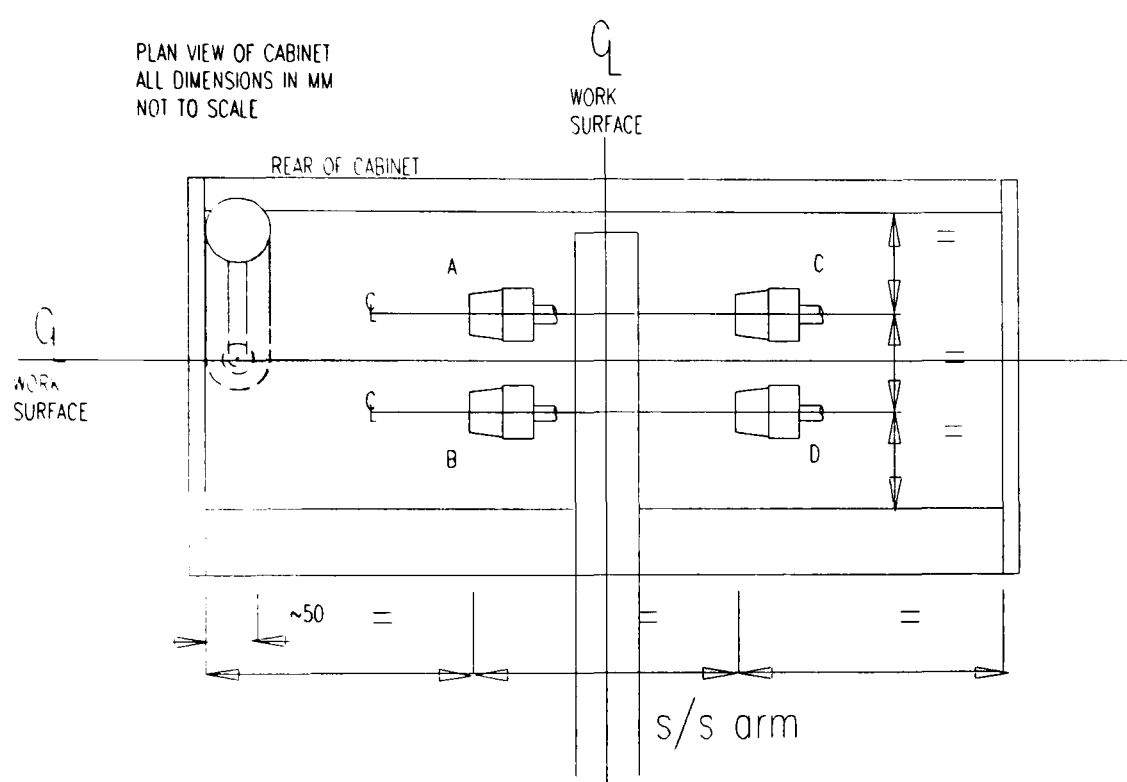


Figure 4.2 Arrangement of equipment for KI cross contamination tests.

4.2.6 Expression of results for type test, commissioning and routine maintenance

4.2.6.1 Flow visualisation

The direction of the airflow using smoke or other visualisation tests such as water fog had to demonstrate an inward flow over the whole area of the working aperture.

4.2.6.2 Airflows

4.2.6.2.1 Airflow (class I cabinet)

The measured air velocities at all points should be between 0.7 m/s and 1.0 m/s and no individual measurement could differ from the mean by more than 20 %.

4.2.6.2.2 Airflow (class II cabinet)

The mean velocity of the downward airflow should be between 0.25 m/s and 0.5 m/s and no individual measurements could differ from the mean by more than 20 %. The mean airflow velocity inward through the working aperture should not be less than 0.4 m/s.

4.2.6.3 Assessment of operator protection factor

For both class I and class II cabinets an operator protection factor was calculated from the measured colonies or particles from each sampler of the five tests and no individual value of the protection factor should be less than 1.0×10^5 . The protection factor was calculated using the following methods:

4.2.6.3.1 Calculation of the protection factor from using the microbiological method

The number of spores in the challenge dose, N , was calculated from the equation

$$N = n_2(M_1 - M_2) - (n_2 - n_1)v$$

where n_1 was the number of spores per millilitre of the initial suspension

n_2 the number of spores per millilitre of the final suspension

M_1 the initial mass of the nebulizer (in g)

M_2 the mass of the nebulizer after the test (in g)

v the initial volume of spore suspension (in ml).

Assume the density of the spore suspension to be 1.0g/ml.

The protection factor, PF, was calculated separately from each culture plate using one of the following equations from Lidwell (1960), which allowed for room ventilation:

$$(a) PF = (N.s)/(10n); \text{ or } (b) PF = (N.s)/(10^4n).$$

where N was the challenging dose

s the sampling rate of one slit sampler, or the combined sampling rate of four impinger samplers (in m^3/min , equation (a), or dm^3/min , equation (b))

n the number of colonies of *Bacillus subtilis* var. *globigii* on the culture plate.

4.2.6.3.2 Calculation of the protection factor from using the potassium iodide method

The number of KI particles liberated, N , was calculated using the following equation:

$$N = (3.1 \times 10^7 \times M)$$

where M was the volume of KI solution dispersed by the aerosol generator (in ml)

3.1×10^7 a constant derived from the droplet size, the sampling flow rate and the speed of rotation of the disc.

The protection factor, PF, was then calculated separately from each filter membrane using the following equation:

$$PF = NV/10^4n$$

where V was the sampling flow rate (in dm^3/min)

n the number of spots on the filter membrane.

In this case $M = 20$ ml and $V = 100$ dm^3/min . Using the above equations and the values of M and V given a protection factor of 1.0×10^5 would correspond to 62 spots on the filter membrane. When calculating the protection factor, if there was one spot on the filter membrane in this case the protection factor would be 6.2×10^6 . If there were no spots on the

filter membrane this would indicate that the protection factor was higher than this, and the protection factor would be recorded as $PF > 6.2 \times 10^6$.

4.2.6.4 Assessment of external and cross contamination

From the results of the microbiological test the total number of colonies of the test organism counted after incubation should not exceed 5 in any test. From the results of the KI test a factor was calculated (section 4.2.6.3.2) using the number of KI particles collected in each sampler and no individual value of the factor should be less than 1.0×10^3 .

4.3 Test results

4.3.1 Class I microbiological safety cabinets

No.	Comment	OPF		Face Velocity (m/s)		
		Average	Worst	Avg	Min	Max
A+	Recirculating	2.8×10^6	1.2×10^6	1.03	80 %	115 %
		$>6.2 \times 10^6$	3.1×10^6	1.10	96 %	101 %
B	Prototype	3.1×10^6	6.2×10^5	1.01	91 %	117 %
		3.1×10^6	6.2×10^5			
		6.2×10^6	3.1×10^6			
C		3.1×10^6	6.2×10^5	1.10	86 %	115 %
D		6.2×10^6	1.6×10^6	1.03	89 %	117 %
		5.0×10^6	2.1×10^6	1.15	95 %	109 %
E		6.2×10^6	3.1×10^6	1.07	89 %	108 %
		1.6×10^6	2.7×10^5	1.08	94 %	111 %
F		6.2×10^6	1.6×10^6	1.15	87 %	113 %
		3.1×10^6	1.0×10^6			
		6.2×10^6	2.1×10^6	1.13	87 %	111 %
		1.2×10^6	5.6×10^5	1.09	90 %	110 %
		6.2×10^6	6.2×10^6	1.11	90 %	117 %
		6.2×10^6	1.6×10^6	1.18	88 %	119 %
		5.2×10^6	1.2×10^6	1.11	95 %	112 %
		$>6.2 \times 10^6$	1.6×10^6	1.13	97 %	107 %
G		1.2×10^6	6.2×10^5	1.14	88 %	111 %
		2.2×10^6	4.8×10^5	1.07	84 %	112 %
		3.1×10^6	7.8×10^5	1.07	88 %	114 %
		6.2×10^6	3.1×10^6	1.15	89 %	108 %
		1.7×10^6	1.2×10^5	1.07	93 %	111 %
		$>6.2 \times 10^6$	3.1×10^6	1.11	93 %	107 %
H		2.1×10^6	6.2×10^5	1.05	86 %	111 %
		1.8×10^6	2.8×10^5	1.04	95 %	108 %
		2.2×10^6	1.6×10^6	1.10	89 %	109 %
		$>6.2 \times 10^6$	1.6×10^6	1.04	96 %	105 %
		2.5×10^6	3.1×10^5	1.06	97 %	102 %

Table 4.1 Class I microbiological safety cabinets. Operator Protection Tests (OPF) using KI. (Maintenance tested unless specified + which is type tested).

4.3.2 Class II microbiological safety cabinets

No. and comments		worst OPF		Cross Contamination		Product Protection		Face vel. (m/s)	Downflow velocity (m/s)						
		KI	microbial	KI	microbial	KI	microbial		avg	min	max				
I	vented sides vented work/surf.	1.3 x 10 ⁵		TNC		2.5 x 10 ⁵		0.76	0.47	87%	115%				
				9.1 x 10 ²				0.70	0.31	77%	123%				
J*		8.9 x 10 ⁵						0.59	0.39	90%	105%				
		3.3 x 10 ⁵						0.63	0.55	89%	111%				
K	ducted outside	7.5 x 10 ⁴		TNC	2		0	0.60	0.37	87%	108%				
		2.3 x 10 ⁵													
	-	6.3 x 10 ⁴			29			0.56							
	-	1.8 x 10 ⁵													
	recir- culating	8.8 x 10 ³										1.2 x 10 ⁶	3.1 x 10 ³	0	0.56
		5.4 x 10 ³													
L		1.6 x 10 ⁵	2.7 x 10 ⁵	TNC	0	2.1 x 10 ⁶	1	0.80	0.32	81%	116%				
M		6.2 x 10 ⁶													

Table 4.2 Class II microbiological safety cabinets. OPF = operator protection factor. TNC = To Numerous to Count. (Type tested unless specified * which is maintenance)

NOTE: All microbiological tests were performed by staff at the Simms Woodhead Memorial Laboratory, Department of Pathology, Papworth Hospital.

4.4 Results and Discussion

4.4.1 Class I and II microbiological safety cabinets

The specified face velocity for class I cabinets in BS 5726 : 1992 : Part 1 is 0.7 - 1.0 m/s. The average face velocity for all those tested, allowing for an accuracy of only 10 % for a rotating vane anemometer (section 3.8.2.1) did not exceed this specification. The fact that all tests indicated higher velocities was because they were all serviced by the same company. All velocities for the class II cabinets tested were within the specifications.

Of the eight class I and five class II cabinets that were tested, only one class II failed to perform to all the minimum levels specified. Visualisation of the airflow into and around the aperture of this class II cabinet, K (Table 4.2) showed brief but infrequent leakage from the top corners and also demonstrated regions of poor containment along the top edge where the movement of an operators arm through the aperture resulted in leakage. Visualisation of the airflow near to the solid work surface demonstrated little resistance to cross-contamination.

Using the microbiological test method, cabinet K was shown to have satisfactory operator and product protection but questionable cross-contamination. Using the KI method the results indicated satisfactory product protection but poor cross-contamination and operator protection. The operator protection tests produced spurious high counts which were not

specific to any one sampler and were marginal between a 'pass' or 'fail' situation. Contamination during the tests was ruled out and the cabinet filter seals were intact.

There were further discrepancies between the microbiological and KI methods for assessing cross-contamination in class II cabinets with solid work surfaces. Apart from cabinet K, when both tests were performed, the microbiological test results gave no cross-contamination, but the KI method results did. For a perforated base the KI results were marginal.

There may be various reasons for the inherent differences between the results of the microbiological and KI tests. For cabinets tested that were equivocally 'good' or 'bad', the performance of both the test methods were shown to have good correlation (Clark et. al., 1981; Matthews, 1985). However, only when there was a marginal failure of a cabinet or when cross-contamination in a class II cabinet was assessed was there any discrepancy. This was most likely due to the method of generation and propulsion of the tracer and the method by which it was sampled, any differences being exaggerated in the marginal case or due to the effects of phoretic forces (thermal or electrostatic) on the droplet/particle as they approached a surface. These are discussed in the following sections.

4.4.2 The effect of particle/droplet velocity

4.4.2.1 Theory

A droplet or particle in motion is subject to inertial forces F_i , frictional forces F_f , gravitational forces F_g , buoyancy forces F_b , phoretic forces F_{ph} and to changes in physical properties due to evaporation E_{vap} . The droplet/particle velocity is thus a function of $f(F_i, F_f, F_g, F_b, F_{ph}, E_{vap})$. Estimation of the path a droplet/particle will take in air following propulsion may be carried out making the assumption that only the inertial, frictional, gravitational and buoyancy forces are acting.

The horizontal stopping distance, X_D , of a droplet/particle (assuming the motion of a solid spherical particle at Reynolds number, Re , $\ll 1$ in a stagnant, suspending viscous fluid, Stokes Law, 1851) due to friction between the droplet and the air (drag force $D = 6\pi\mu_g R_p U_\infty$, where μ_g is the dynamic viscosity of the air, R_p is the particle or droplet radius (m), U_∞ is the fluid velocity far from the particle) and excluding the effect of all other forces would be $(2U_i\rho_p R_p^2)/(9\mu_g)$ and $Re \equiv (2R_p(U_p - U_g)\rho_g)/(\mu_g) \equiv (2R_p U_p \rho_g)/(\mu_g)$ at low air velocities where U_i is the initial velocity (m/s) of the droplet U_p , U_g is the velocity of the gas far from the droplet, ρ_p the droplet density and ρ_g the density of the air (kg/m^3).

The droplet/particle is also influenced by gravitational forces which impart a downward velocity component. However, because of drag, then in still air the droplet/particle reaches a terminal settling velocity where the gravitational and buoyancy forces are balanced against the drag forces on a spherical particle ($Re \ll 1$, stagnant, suspending viscous fluid). This is

calculated from the expression $4/3(\rho_p - \rho_g)g\pi R_p^3 = 6\pi\mu_g R_p U_t$ where the gravitational force = $4/3\rho_p g\pi R_p^3$ and the buoyancy force = $4/3\rho_g g\pi R_p^3$ where, g is the gravitational force per unit mass, or gravitational acceleration constant, ρ_p is the mass density of the particle, and U_t is the terminal settling velocity (cm/s) equivalent to U_p and $U_t \cong 2/9R^2\rho_p g/\mu_g$ where $\rho_p \gg \rho_g$.

In the microbiological test, the velocity of the carrier gas discharged from the reflux blast nebuliser and measured at the front aperture of the cabinet could not exceed the inward air velocity (BS 5726, 1992). Several nebulisers were tested by Matthews, 1985, at 70 KPa (10psi) and shown to have volume flow rates ranging from 3.4 - 9.5 l/min and velocities ranging from 0.05 - 0.58 m/s when measured 5 - 13 cm away from the nozzle in still air. For a Collison nebuliser, commonly used for testing, the initial velocity at a flow rate of 3.4 l/min was found to be ~0.45 m/s (Kennedy, 1988) and the mean droplet diameter emitted from this nebuliser was $< 2 \mu\text{m}$ (Matthews, 1985).

Assuming that the initial velocity of a $2 \mu\text{m}$ droplet with density that of water (1000 Kg/m^3) was propelled from a Collison nebuliser, the velocity of the carrier gas decreased to zero within a very short distance so that the droplet was propelled into still air and that there was no evaporation of the droplet then from these expressions the stopping distance would be 0.005 mm (initial Re 0.06) and the terminal settling velocity 0.01 cm/s. However, the velocity of the carrier gas was much greater than this and the motion of the droplet more likely to be influenced by the carrier gas than by its own inertia.

In the KI method the generation of the aerosol involved the propulsion of droplets from a spinning disc. This had a rotational speed of 58.65 m/s (40 mm diameter disc @ 28000 rpm). It was estimated from the method of Walton & Prewitt (1949) that the diameter of the primary droplet breaking from the edge of the disc was $40 \mu\text{m}$. It was assumed that this droplet would have an initial velocity that of the disc. The stopping distance of such a droplet when propelled into still air, assuming a density that of alcohol (789 Kg/m^3) and assuming no evaporation, would be 224 mm (initial Re 152). However the droplet of alcohol would evaporate rapidly to a nominal particle size of $7 \mu\text{m}$ (Clark & Goff, 1982) with a density of potassium iodide, $\sim 2790 \text{ Kg/m}^3$. The stopping distance of such a particle in still air would then be 24 mm (initial Re 27). For the $40 \mu\text{m}$ particle the terminal settling velocity would be 3.7 cm/s and a $7 \mu\text{m}$ particle 0.4 cm/s.

The change in droplet/particle velocity, U_p , with time, t , (Figs. 4.3 & 4.4) can be determined in the absence of all external forces from the expression: $(dU_p/dt) + \phi U_p = 0$ or $U_p = U_i \exp^{(-\phi t)}$ where U_i is the initial particle velocity, ϕ is the inverse product of the particle mobility B and mass m_p of the particle, $B = U_p/\text{Drag force}$. Using, U_p , the distance travelled by the particle, X_p , with time, t , (Figs. 4.3 & 4.4) can be determined in the absence of all external forces from the expression $\int_0^t U_p dt = \{U_i[1 - \exp^{(-\phi t)}]\}/\phi$.

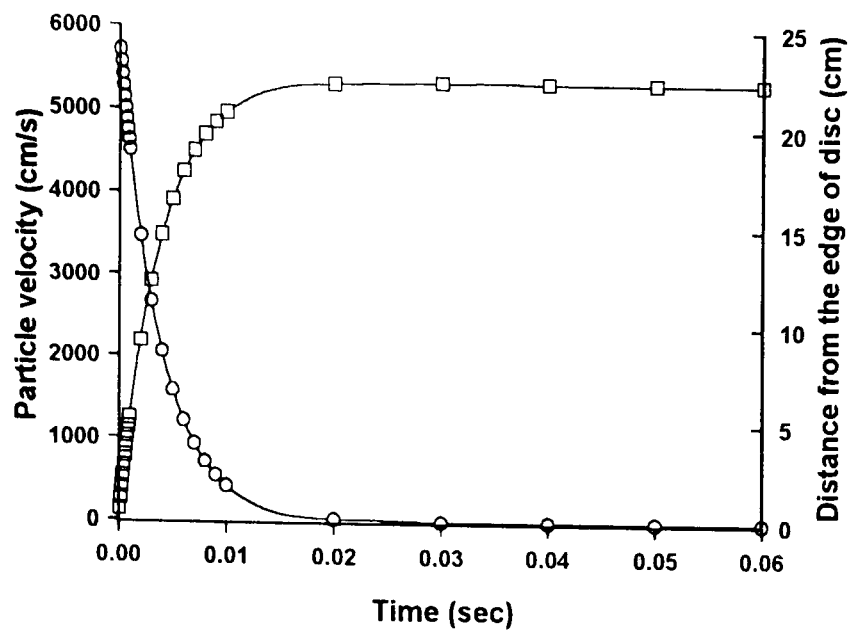


Figure 4.3 Theoretical change in the velocity \circ and horizontal distance travelled \square by a $40\ \mu\text{m}$ KI droplet when propelled from a spinning disc in still air.

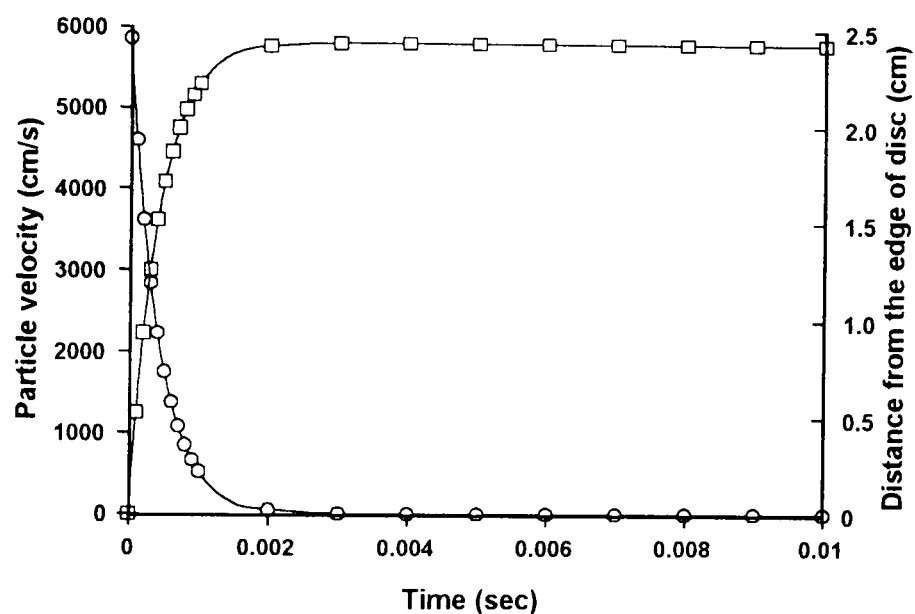


Figure 4.4 Theoretical change in the velocity \circ and horizontal distance travelled \square by a $7\ \mu\text{m}$ KI particle when propelled from a spinning disc in still air.

The evaporation of the KI droplet to the particle is ignored in the previous expressions, but by calculating the two extremes it may be assumed that the physical reality in still air would lie between these curves. A $40\ \mu\text{m}$ droplet with density that of alcohol would thus come to a stop 224 mm from the edge of the spinning disc in ~ 0.03 seconds and a $7\ \mu\text{m}$ particle 24 mm in ~ 0.004 seconds.

The distance travelled X_t and time taken to reach the terminal settling velocity can be determined from the gravitational force $= ma = 6\pi\mu_g R_p U_t$ where $m = \text{density}/\text{volume} = (4\pi R_p^3 \rho_p)/3$, $s = ut + 1/2 at^2$, and $v^2 = u^2 + 2as$ where s is the distance (X_t), u the initial velocity, v the velocity at time t , and a the acceleration (gravitational acceleration, g). Hence $a = U_t^2/2X_t$, $a = 2s/t^2$ and thus $X_t = (R^2 \rho_p U_t)/(9\mu_g)$ and $t = (8R^2 \rho_p X_t)/(18\mu_g U_t)$.

The time taken and the distance to reach the terminal settling velocity are summarised in table 4.3. Figures 4.5 & 4.6 show the resultant theoretical path of the particle following propulsion from the edge of the spinning disc by superimposing the horizontal and vertical distances travelled.

	7 μm	40 μm
X_t	0.0001 cm	0.0071 cm
t	0.0004 s	0.0038 s

Table 4.3 Time and distance for a droplet/particle to reach its terminal settling velocity.

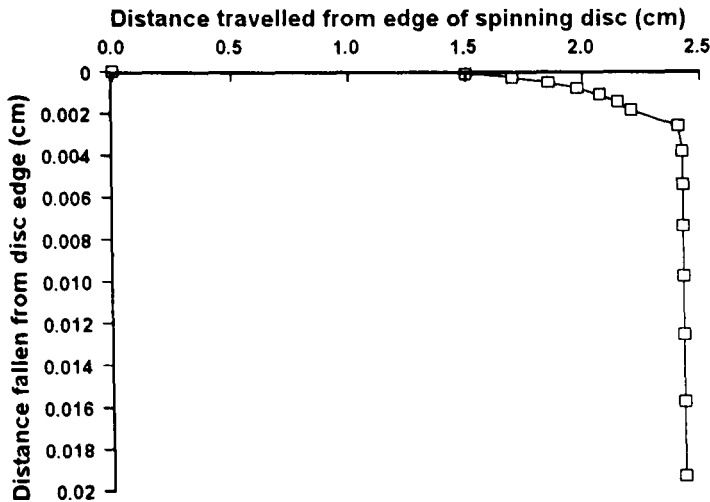


Figure 4.5 Theoretical path of a 7 μm particle as it is propelled from the edge of the spinning disc in still air.

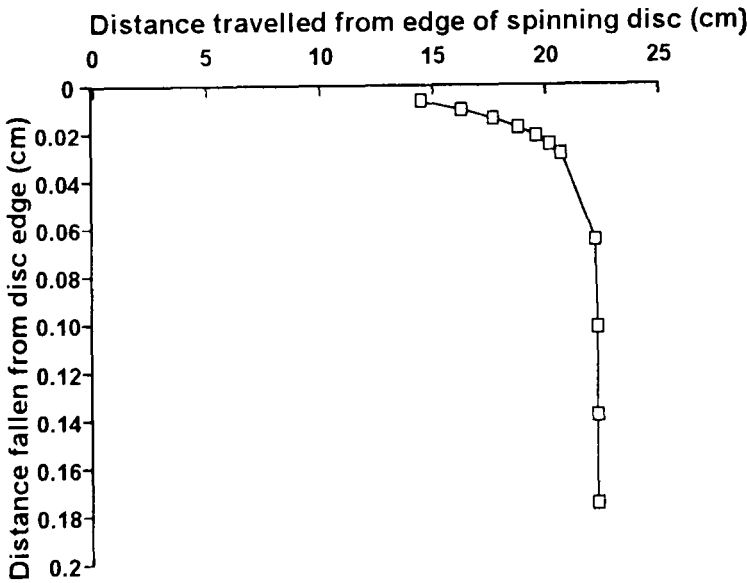


Figure 4.6 Theoretical path of a 40 μm droplet as it is propelled from the edge of the spinning disc in still air.

These analyses assumed $Re \ll 1$. However for the potassium iodide particles because of the high initial velocity the Reynold's numbers were > 1 . This would require adjustment of the drag equation as it deviated from Stokes' Law as a function of Reynold's number. This deviation has been ignored as the velocity would change rapidly and a $7\mu\text{m}$ particle at its terminal settling velocity had a Reynold's number $\ll 1$.

In the KI test method there would be a small effect on the particle due to the capture velocity of the centripetal sampler. The capture velocity can be estimated by the approximation that at

a defined distance away from the opening that the extraction rate $Q = V(10X^2 + A)$ where V is the capture velocity, X the distance from the opening at which the capture velocity applies, A the area of the opening, and Q the volume flow rate through the opening (Everett & Hughes, 1981). The capture velocity from the centripetal sampler decreases very rapidly a short distance away from the opening. As an approximation, the velocity at a distance 1 diameter away from the opening is 1/10th the velocity at the opening.

Figure 4.7 shows the superimposition of the theoretical particle paths and the capture velocity. If it is assumed that these are the paths in still air and the dimension shown is between the edge of the spinning disc and the centripetal sampler as in BS 5726 : 1992, then there is an overlap of the distance a 40 μm droplet will travel and the capture velocity of the sampler. However, this droplet would evaporate to a 7 μm particle and the gap between the capture velocity and the particle stopping distance would increase so reducing any overlap and effect from the sampler.

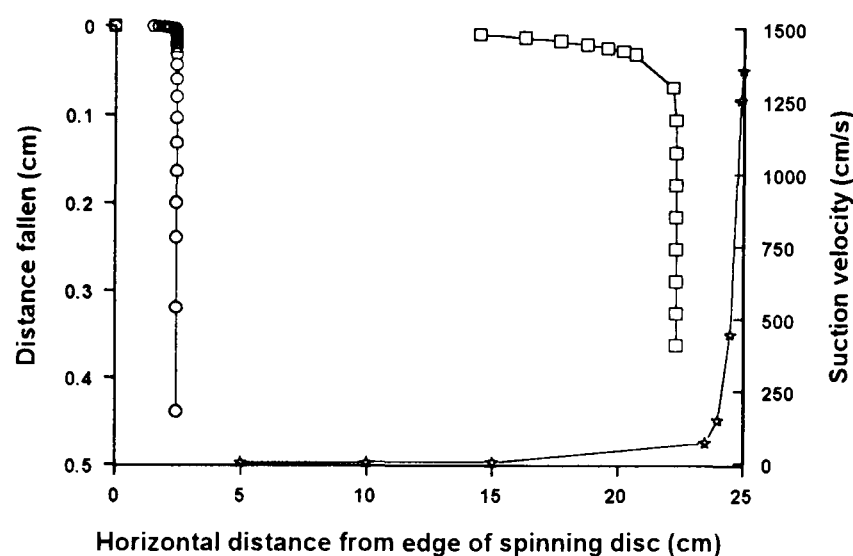


Figure 4.7 Theoretical paths of a 7 μm \circ and 40 μm \square droplet/particle propelled from the edge of a spinning disc in still air and the decrease in capture velocity from a centripetal sampler *.

As the droplet propelled from the spinning disc evaporates the distance travelled before ceasing to be a droplet, h , is proportional to the square of the surface area, S , or to the fourth power of the diameter D ($h \propto S^2 \propto D^4$) (Hidy, 1984). Rooth (1949) stated that the life of a 2 μm droplet of water in dry air at room temperature is 0.006 s and for a 20 μm droplet 0.06 s. This indicates that a 40 μm droplet of water propelled from the spinning disc will still be a droplet when the stopping distance and terminal velocity are reached. However, a droplet of alcohol which is more volatile than water would be expected to have a much shorter life.

4.4.2.2 Experimental

The evaporation of a 40 μm droplet of 1.5% KI/95% alcohol was investigated by measuring the distance between the spinning disc (40 mm from the work surface) and the wall of a cabinet before condensation occurred. With the cabinet switched off and the disc on for 60 s, it was found that only at a distance > 50 mm from the wall did condensation cease. After

many tests in a class II cabinet there was some KI condensation on the sash window 100 mm away which indicated that at around 50 mm distance from the spinning disc condensation ceased.

The effect of settling was then investigated. A filter paper disc (Whatman No.3) saturated with palladium chloride was taped to the cabinet wall and the deposition of KI on the filter paper when released from the spinning disc with increasing distance from the wall observed. With the cabinet switched off and the disc on for 60 s, at a distance of 50 mm from the wall, there was a definite line of KI at a height 2 mm lower than the disc height deposited on the filter paper (Table 3.4). There was also scatter of KI particles above and below this line. With the disc 100 mm from the wall, no major line was evident but there was some scatter. At 150 mm the scatter was much less and only to a height of 22 mm. At 200 mm there was no deposition of KI on the filter paper. This indicated that the horizontal stopping distance was between 100 - 200 mm from the spinning disc. Scatter above and below the major deposition lines may be due to microcirculation of the air, modifying the paths of the droplet/particles and perhaps due to other phoretic forces causing attraction to the surfaces.

Distance between edge of spinning disc and cabinet wall	Major line on filter paper	Top perimeter of scatter
50 mm	38 mm	84 mm
75 mm	22 mm	65 mm
100 mm	no major line distinguishable	38 mm
150 mm	no major line distinguishable	22 mm
200 mm	no line or scatter	no line or scatter

Table 4.4 Change in vertical scatter of KI particles released from a spinning disc with distance.

4.4.3 Phoretic forces

Thermophoretic forces can have an effect on droplet/particle transport in cabinets where the internal temperature in a class II may be higher than ambient due to the heat generated by recirculating fans and lights (Kennedy, 1988). The marginal failure of the class II cabinet, K, was considered to be due to such temperature effects on the challenge aerosol. The internal temperature was 3 °C above ambient, which was within the specifications of BS 5726 : 1992. The operator protection tests were repeated at cooler temperatures, i.e. first thing in the morning, and for a series of five tests none were below 10⁵. The effect of this may not be due solely to the reduction of a thermal gradient between the cabinet interior and the room, but also to the effect of the cooler temperatures on the room airflow near to the aperture.

The generation of an aerosol can impart an electrical charge to the droplets/particles which can result in their attraction to surfaces which are grounded or of opposite charge. Early types of spinning disc generators were equipped with charge neutralisers (Hidy, 1984) in

order to reduce this problem. These electrophoretic forces could be important in surface deposition and leakage mechanisms in and from the cabinet.

4.4.4 Operator protection

When there were clear passes or failures of a cabinet, the microbiological and KI tests were shown to have good correlation. Thus by each method the challenge droplets/particles are presented to a vulnerable area where leakage occurs, producing similar results. However, in marginal cases where the mechanism of leakage is not clear, then the force by which the droplets/particles are propelled may be considered to have an affect.

In section 4.4.2, theory and experimental findings suggest that in still air the aqueous droplets propelled from a reflux blast nebuliser will have a velocity that of the carrier gas, and when the latter is zero the droplet/particle will have no horizontal motion and will settle. In the test method the carrier gas is specified as having a velocity measured in the plane of the aperture to be less than the face velocity. Thus the challenge droplet/particle in still air would perhaps challenge the aperture but if there is an airflow through the cabinet greater than the carrier gas then the droplet will be influenced by this airflow.

A 40 μm KI droplet/particle from the theory would have a horizontal velocity component of ~ 25 m/s in the plane of the aperture in still air. However, it does not remain 40 μm and in practice it would appear that the stopping distance is between 100 - 200 mm in still air. This would challenge the aperture but at a lower velocity. With the cabinet operational then the resistance to leakage of challenge will depend on the face velocity and conditions in the aperture plane. If a cabinet has a face velocity within the specifications and there is no turbulence then the challenge in practice does not penetrate beyond the aperture plane. Assuming a 7 μm final particle size, then the terminal settling velocity will be much less than the face velocity and it would be influenced and suspended by this. Observations of the visible aerosol from a spinning disc (100 mm from the aperture plane) released in an airflow into the cabinet with a face velocity of 0.5 m/s showed it to be swept away towards the extract immediately it was produced.

4.4.5 Cross contamination

There is a discrepancy between the results of cross contamination tests across a solid work surface of a class II cabinet using the microbiological method, indicating a pass, and the KI method, always showing a failure. The relative disposition of the equipment is similar in both methods, there being a 300 mm gap between the source and the first samplers. It would thus seem that there is some inherent difference in either the mechanism of challenge generation/sampling or the physical presence of the equipment. However, which of the methods in use gives the more realistic result?

In most class II cabinets with a solid work tray, the downward airflow divides near to the work surface and travels to the front and back where it is exhausted through extract grills usually in a plane parallel with the work surface. This airflow regime is designed to limit the sideways movement of air across the work surface. However, using water fog to visualise the airflow at the work surface there is a layer within which the air slows down and may recirculate and rise against the downward air. The extent to which this happens varies between cabinets. In cabinet K spurious pockets of air were visualised flowing sideways across the work surface, in cabinet L the rear extract slot was normal to the work surface and created a recirculating air layer above this, level with the top edge of the extract. Cabinet I initially had the extract slots at the left and right sides of the solid work surface which encouraged cross contamination.

In the test methods the challenge aerosol would be propelled into and suspended in this region of recirculating air near to the work surface where the inertia of the droplet/particle would influence how far it may travel horizontally to the samplers. The presence of the equipment on the work surface could also disturb the airflow regime exaggerating the boundary layer around it. The bulk of the centripetal samplers was shown to cause some turbulence around them by water fog visualisation.

The efficiency of the sampling methods would also affect the results. The centripetal samplers actively draw air into them and have a capture velocity which extends from the sampler nozzle. The samplers used in the microbiological test depend on the passive sedimentation of droplets/particles onto the surface of the nutrient medium in a petri dish. The airflow regime in the cabinet results in air passing over the settling plates from which settling of suspended 2 μm droplet/particles is limited and impaction inefficient due to a boundary layer against the medium (Newsom, 1974).

The KI test method thus would seem to be a greater challenge to the resistance to cross contamination than the microbiological method. In reality this may be too severe and normal operating techniques may be represented better by the microbiological method. However, to represent forced propulsion from spillages etc. the KI method would be better.

4.4.6 Particle deposition in the containment test

The deposition of challenge aerosol during a test was greater with the KI method than with the microbiological method. When the KI spinning disc generator was placed on the work surface, as in class I cabinets, KI would be deposited on the surface around the generator (Matthews, 1985; Fletcher & Johnson, 1992). In class II cabinets KI would be deposited on the sash windows and front extract grill. Also KI would condense on the body of the spinning disc generator. This was more likely to be a result of the position of equipment and

the suspension and influence of the airflow within the cabinet on the aerosol rather than due entirely to gravitational sedimentation.

The placement of the aerosol generators in class I and II cabinets means that the droplets/particles are projected towards a solid surface. In class I cabinets with front lips, the aerosol is propelled into the region behind the lip. From flow visualisation there is recirculation of air behind this lip across the cabinet floor and any challenge in this region would be concentrated possibly resulting in coalescence and deposition. In class II cabinets the aerosol is directed at the lower edge of the sash window and there is some impaction of droplets/particles here. As the air is exhausted through the front extract grill then there is KI deposition here also. Challenge droplets/particles deposited on the generator body are likely to be due to impaction of large unevaporated particles as a result of the airflow past the generator.

The result of this is that the amount of airborne challenge is reduced. However, if it is accepted that the same amount of challenge is generated in each case and that deposition is solely due to the airflow characteristics of the cabinet then the comparison of cabinets is not affected.

4.4.7 Contamination during the test

The failure of a cabinet to contain a challenge may be due to leakage from the aperture, from a leak in the cabinet structure or from contamination during the test. Most often leakages and contamination can be sporadic making interpretation of the results of a failure difficult. During a routine containment test on a class I cabinet using the KI method after three consecutive tests the operator protection factors were satisfactory (Table 4.5). On the fourth test the operator protection factor dropped by two orders of magnitude resulting in a fail. This cabinet had been tested on numerous occasions as part of a service contract and presented no problems. Considering this past record and that a further two tests presented no fail it was concluded that the operator had contaminated the test. This was shown by shaking the laboratory coat worn by the operator in front of the samplers which resulted in a failure (table 4.5 test 7).

Test	Sampler A	Sampler B	Sampler C	Sampler D
1	3.1×10^6	$>6.2 \times 10^6$	$>6.2 \times 10^6$	$>6.2 \times 10^6$
2	3.1×10^6	6.2×10^6	$>6.2 \times 10^6$	$>6.2 \times 10^6$
3	6.2×10^6	6.2×10^6	$>6.2 \times 10^6$	1.6×10^6
4	2.1×10^6	3.1×10^6	7.8×10^5	3.9×10^4
5	6.2×10^6	6.2×10^6	$>6.2 \times 10^6$	6.2×10^6
6	6.2×10^6	6.2×10^6	$>6.2 \times 10^6$	6.2×10^6
7	2.8×10^4	5.3×10^4	3.2×10^4	8.1×10^4

Table 4.5 Contamination during a typical KI test. (Shaded boxes highlight failures).

Background contamination was found when on a separate occasion there was more than one class I cabinet being serviced in the room at one time. A normal routine service included changing the pre - filter which was being carried out on one cabinet whilst a KI containment test was taking place on another. The pre-filter was covered in KI which, when carried into the room, resulted in a huge failure of the cabinet being tested to give operator protection factors of 10^2 .

In another instance poor cabinet performance was found to be due to contamination of the spinning disc used in the KI method. When the test was carried out on a cabinet with a past history of high operator protection factors, there were spurious higher counts (Table 4.6). The higher counts (enough to give operator protection factors of 10^4) were confined to the lower samplers.

Test	Sampler			
	A	B	C	D
1	6.2×10^6	6.2×10^6	1.2×10^6	6.2×10^6
2	6.2×10^6	6.2×10^6	3.1×10^6	6.2×10^6
3	$>6.2 \times 10^6$	3.1×10^6	$>6.2 \times 10^6$	$>6.2 \times 10^6$
4	6.2×10^6	$>6.2 \times 10^6$	$>6.2 \times 10^6$	6.2×10^6
5	6.2×10^6	6.2×10^6	2.1×10^6	1.2×10^5
6	$>6.2 \times 10^6$	6.2×10^6	6.2×10^6	6.2×10^6
7	6.2×10^6	$>6.2 \times 10^6$	1.6×10^4	6.2×10^6
8	3.1×10^6	6.2×10^6	6.2×10^6	6.2×10^6
9	$>6.2 \times 10^6$	2.1×10^6	8.9×10^5	9.5×10^4
10	6.2×10^6	3.1×10^6	1.2×10^6	$>6.2 \times 10^6$
11	$>6.2 \times 10^6$	$>6.2 \times 10^6$	5.6×10^5	3.3×10^5
12	6.2×10^6	$>6.2 \times 10^6$	1.6×10^6	6.2×10^6
13	2.1×10^6	6.2×10^6	1.2×10^6	1.7×10^4
14	3.1×10^6	3.1×10^6	1.6×10^4	1.2×10^6

Table 4.6 Contamination during a typical KI test. (Shaded boxes highlight failures).

There was little to suggest from flow visualisation or the face velocity that substantial leakage could be coming from the aperture; there was no outflow of water fog and no environmental disturbance. The nature of the leakage was erratic and contamination of clothing ruled out by test 7. Following this the equipment was rearranged to see if this had any effect. The spinning disc generator was moved from a position parallel to the plane of the aperture to near normal to it, so reducing the obstruction to the flow but this did not change the results (test 8). The feed tube to the spinning disc from the pump which had to pass through the aperture was relocated from the edge of the aperture to the centre of the aperture beneath the artificial arm (test 10) and then above the arm (test 12). However this still did not prevent spurious leakages.

Many of the spots sampled were more varied in size (with some much larger ones) than normal. The test was then repeated on another cabinet without changing the arrangement of equipment (test 14) and this first test showed a significant leakage. It was concluded that there was either something grossly wrong with the room ventilation, which was not obvious, or that contamination other than that due to clothing was occurring. It has been known that intermittent supply of potassium iodide to the spinning disc can cause large droplets to be ejected. However this was not the case but it was noticed that there was a significant amount of crystallised KI at the edges and underneath the disc when still. Previous testing had not produced any problems with the disc becoming contaminated during a run of five tests but cleaning it in this case and keeping it clean resulted in no more spuriously high counts.

It was thus considered that large particles or clumps were detaching from the disc in addition to the normal challenge aerosol and which presented a greater challenge to the cabinet containment. Why this happens is not clear, because the particles would be expected to be deposited behind the front lip, but somehow their path was modified allowing them to challenge the aperture.

4.4.8 Microbiological safety cabinet performance during environmental disturbance

The effect of environmental disturbances on the performance of open fronted contamination control facilities to contain respirable hazards is well documented. However, the inclusion of such effects into a standard test method was avoided because of the difficulty in making such disturbances reliable and repeatable, especially when worker activity was simulated. Barkley (1972) incorporated an artificial arm when testing class II cabinets to disturb the juncture where the inflowing and downflowing air combine and this was incorporated into national standard testing methods. There were further environmental disturbance tests carried out under controlled conditions such as for fume cupboards by Caplan & Knutson (1982) who studied the effect of cross draughts on performance. This was also carried out by Rake (1978) on class II cabinets.

Clark et. al. (1990) studied the effect of worker disturbance on class II microbiological safety cabinets. Environmental disturbance was created by walking past the cabinet and with an operator carrying out manipulations inside the cabinet, such as pipetting, and pouring liquids from one container to another. Also, tests were made with the worker moving away from the cabinet and then returning to it. It was found that only with the worker moving away from the cabinet did the operator protection factors fall below the minimum performance level by an order of magnitude. These procedures were repeated in this study, accepting the variability of using human environmental disturbances. Also a substantial disturbance was created in front of the aperture by creating a draught with an A4 sized board.

i) Walk Past. 6 potassium iodide operator protection tests (BS 5726;1992, Part 1, Appendix D4) were carried out during which disturbance was created near the aperture by walking past the front of the cabinet and inserting and withdrawing arms from the cabinet interior. During the 6th test an A4 board was waved in front of the cabinet.

Protocol: To walk back and forth during a test period, $\sim 0.5\text{m}$ in front of the cabinet working aperture, at a pace of one stride per second (each stride 0.5m in length). Also to insert and withdraw an operators arms from within the cabinet interior working volume twice during the test period; the arms to be manoeuvred as best as possible around the potassium iodide test equipment.

ii) Walk past and draught. In addition to protocol (i), a rigid A4 board was waved horizontally $\sim 1\text{m}$ away from the working aperture in two sweeps at a velocity of $\sim 1\text{m/s}$. This was done in three positions, two at 45° from the left and right sides of the working aperture and one opposite the centreline of the working aperture.

iii) An operator working at the cabinet. In this test, an operator carried out a repetitive and continuous pipetting procedure (e.g. pipetting to and from a multi-well plate and a bottle with a suitable automatic pipette) with the hands and arms remaining within the cabinet throughout the test. The containment test protocol was the same as specified in BS 5726;1992, Part 1, Appendix D4 but the potassium iodide test equipment was re-arranged in order to allow the operator to sit at the cabinet; the stainless steel arm was removed and only two samplers were used, spaced further apart (Fig. 4.8).

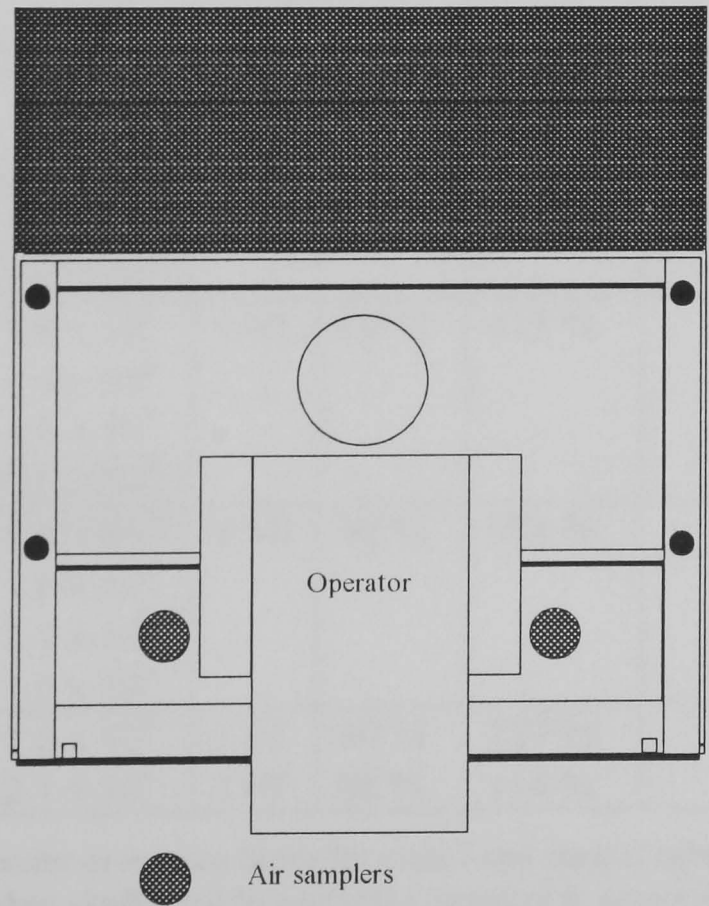


Figure 4.8 Arrangement of air samplers for environmental disturbance tests.

iv) An operator working at the cabinet and moving their arms into and out of the cabinet. In this test, in addition to working within the cabinet as above (iii), the operator moved away from the cabinet (turning to their left), taking a bottle from a bench behind and then returning to the cabinet and continuing to pipette. This procedure was repeated 30 seconds after each return to the cabinet throughout the duration of the test.

As shown in Table 4.7 and summarised in Figure 4.9, there was a decrease in operator protection below 10^5 for tests using protocol iv on the class II cabinet. This disturbance was greater than would normally be expected in a well disciplined laboratory. The presence of the worker just carrying out manipulations at the cabinet (protocol iii) did not result in any leakage at the position of the samplers. However, the results from the use of protocol iv, an operator working inside the cabinet and taking their arms out of the cabinet periodically, caused a decrease in operator protection factor below 10^5 in both the class I and II cabinets tested. This agreed with the conclusions of Clark et. al. (1990). Following this test the laboratory coat worn by the operator was shaken in the laboratory whilst sampling the air showing it to be covered in KI and it was apparent that particles were deposited onto and trapped in the material of the garment so that as the arms move into and out of the cabinet, particles are released within the laboratory. This would also apply to microbiological aerosols. Normal working practice in a safety cabinet should not require the movement of the arms out of the work space and from this investigation it is obvious that an aerosol created during the work process may be trapped in the material of the operator clothing and be carried into the laboratory.

Class	No.	Test	OPF	Face velocity (m/s)			Downflow velocity		
			KI	avg	min	max	avg	min	max
II	L	i	1.4×10^5	0.80			0.32	81 %	116 %
		ii	1.1×10^4						
		iii	1.8×10^5						
		iv	1.2×10^4						
I	A	i	1.8×10^5	1.03	80 %	115 %			
		ii	1.4×10^5						
		iii	4.1×10^5						
		iv	9.0×10^3						
		i	5.4×10^4	1.10	96 %	101 %			
		i	1.6×10^5						
		i	2.1×10^6						
		ii	1.6×10^6						
I	F	ii	1.6×10^5	1.11	90 %	117 %			
I	G	ii	2.1×10^6	1.07	88 %	114 %			

Table 4.7 Effect on the operator protection factor for class I and class II cabinets when there is no environmental challenge, when challenged by protocol i, protocol ii, protocol iii and protocol iv. (Shading highlights failures).

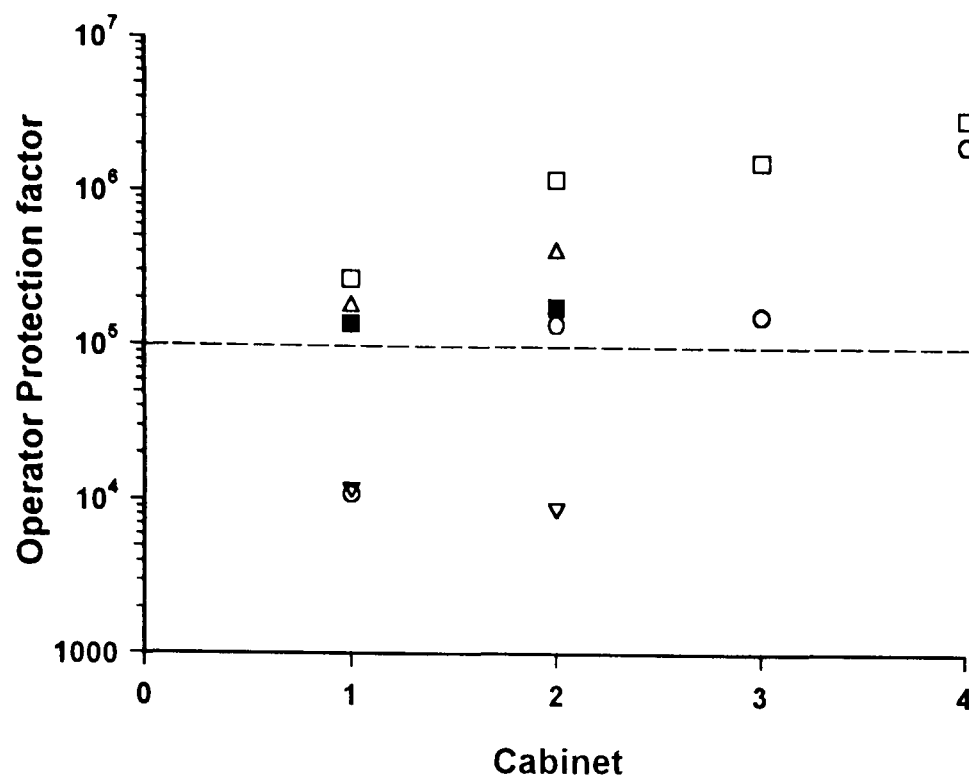


Fig. 4.9 Effect on the operator protection factor for class I (2-4) and class II (1) cabinets when there is no environmental challenge \square , and when challenged by protocol i \blacksquare , protocol ii \circ , protocol iii \triangle and protocol iv ∇

4.5 Key interim conclusions

- There was a hierarchical structuring of the test methods in the performance assessment strategy; flow visualisation, face velocity test with emphasis on a quantitative containment test. For each of these methods a minimum performance criteria was specified and the same strategy was used for type testing, commissioning and for routine maintenance.
- The quantitative containment test method measured the actual leakage from the cabinet. For unequivocally 'good' or 'poor' performing cabinets, the results of containment testing using the microbiological and KI test methods showed good correlation. However, there was some disparity between the two methods for a marginal cabinet and when assessing cross contamination.
- The effect of sedimentation on tracer particles was not thought to be significant compared to the flow rate of air and residence time of air passing through the cabinet. More important was the influence of the air movement on the particle direction and possible impaction.

Chapter 5 The application of a potassium iodide tracer method (KI-Discus) for assessing the containment efficiency of fume cupboards and comparison with the method described in BS 7258 : 1994 : Part 4

5.1 Introduction

At present a quantitative containment test method for assessing fume cupboard performance is not a mandatory requirement of BS 7258 : 1994, but there is a recommended method in Part 4 for those who require such a test. In addition, the KI method laid down in BS 5726 : 1992 for assessing microbiological safety cabinets has been used to assess the containment of fume cupboards. In this chapter, a theoretical comparison and correlation of the principles of the KI test method and the gas method recommended in BS 7258 : 1994 : Part 4 is attempted. Then through practical work such theory is challenged.

Historically the recommended approach for studying the performance of open fronted containment facilities was to measure face velocity and its variation across the plane of the opening; a variation from the average within $\pm 20\%$ was considered acceptable. Flow visualisation using smoke was also recommended for identifying zones of air disturbance and for determining the effects of external disturbances on performance. These methods were usually to demonstrate performance deficiencies and therefore could assist the user in determining the limitations of a particular facility.

The development of a quantitative test of performance however developed differently for fume cupboards and microbiological safety cabinets. The fume cupboard and class I safety cabinet were considered to achieve containment in similar ways (the class II being rather different). The only differences between class I cabinets and fume cupboards was the size of the aperture, cabinets being fixed at < 200 mm (BS 5726 : 1992 : Part 1) and fume cupboards generally around 500 mm and up to ~ 800 mm and safety cabinets had filtered discharges whereas fume cupboards relied on dilution. However all types were designed to offer partial containment and thus could be tested by releasing a tracer inside and measuring what came out into the room. Containment testing progressed quickly for safety cabinets but there was a much slower development of test methods for fume cupboards. Considering the similarities between class I types and fume cupboards, and that both served to contain respirable hazards it was strange that containment testing did not follow a similar course.

It would appear that the intended usage of the facility and occupational health percepts had much to do with this. For safety cabinets the risk of infection and subsequent illness during the pioneering years of research into micro-organisms and disease showed a real problem with the need for containment and subsequently for facilities that could be shown to work. This also brought about a real need for work discipline; the number of organisms required to initiate a disease being as few as 5 for Venezuelan equine encephalitis (VEE) virus. However

with fume cupboards there was no real immediately identifiable health risk and so it could be argued that less care was taken. Fume cupboards were developed to dilute the potential hazard and little was known about levels of toxicity that posed problems, particularly any effects that may not produce problems for many years. In such cases the toxin could be lost in the body systems and potentially stored until a threshold was reached which may result in harm (Vincent, 1990).

A statement in the *Lancet* (1956) (and referred to by Newsom, 1976) was that “ Experience in industry has shown that unless the risk is grave and obvious most people prefer to believe they are the lucky ones”. This was, at the time, very relevant to microbiological safety cabinets but perhaps now is more relevant to the users of fume cupboards. The real or apparent threat (often immediate) from micro-organisms was enough to prompt the development of tests to measure their performance. Many infections involved personnel in a particular research unit and reflected research interests. Several diseases did not occur outside the research laboratory.

For fume cupboards the drive to establish quantifiable performance was less. Barkley (1972) pointed out work by Wright (1964) who quoted Ramazzini (1700) “Chemists boast that they have mastered the art of subduing every kind of mineral, yet they themselves do not come off scot-free from their pernicious influence. They very often bring on themselves the same ailments as do other workers who deal with minerals, and in spite of their persistent denials the colour of their faces reveals the fact”. For many chemicals used, the effect of exposure was not immediate and symptoms could occur several years later. However, the implication of their effects were not known nor could they be traced. This could lead to litigation on the part of employees and with greater awareness of the toxicity of chemicals led to the development of quantitative tests.

The only quantitative test mentioned by Barkley (1972) was that of Papa (1966) who used propane as a tracer. Barkley suggested that the test had to be representative of the type of substance for which the facility was designed to contain. For partial containment facilities control of exposure to aerosols constituting a respirable hazard both gases and particulate tracers were contemplated.

The quantitative test should show a measurable level of performance. In terms of a safety cabinet it was shown that in order to measure a performance of 99.999 %, the challenge must be significantly greater than that produced by common activities. However containment testing of fume cupboards went down the road of using gas tracers instead of particulates and that the release rates of gas was to represent that which may be generated during common activity.

5.2 Qualitative comparison of air flow through fume cupboards and safety cabinets

There is a similarity between the air flow within a class I microbiological safety cabinet and a box fume cupboard (section 2.2.1 & 2.3.1). In both there are large air recirculation zones behind the sash and near to the work surface. In class I cabinets this is exaggerated by a lip at the front of the work surface. The air flow structure within an aerodynamic fume cupboard, although principally the same, is quite different. The presence of rear baffles and aerodynamic entry foils eliminate recirculation zones at the edges of the aperture and across the work surface and there is effective scavenging of the working volume. Within class II microbiological safety cabinets, the air flow structure has no similarity to either class I microbiological safety cabinets or fume cupboards.

5.3 The potential use of particle tracers and the KI test method for assessing the performance of fume cupboards

Doubt was expressed about using aerosols for assessing fume cupboard performance but as particles of small size would remain airborne for a considerable time they were expected to disperse in a similar way to gases in the short residence time of air flowing through the containment facility. Particle deposition and challenge was discussed in section 4.4.2 and 4.4.6 and this would not be expected to be a problem if the particle momentum was low in relation to the air flow velocity. It was shown that at lower airflows and larger particle sizes that natural sedimentation would become a problem (Hambraeus & Sanderson, 1972 ; Shaw, 1972; Whyte & Shaw, 1973; Chamberlain and Leahy, 1978 ; Caplan & Knutson, 1982; Hampl & Shulman, 1985; Clark, 1989). Also if the distance between the source and the sampler was small then the time that the particle was airborne and potentially sampled or influenced by the airflow would be far in excess of the particle settling rate. Other factors, such as the deposition of particles by impaction, would be thought due to the airflow pattern and therefore would simulate reality.

More recently the KI particle tracer test system for assessing safety cabinets in BS 5726 : 1992 : Part 1 was proposed as an alternative for incorporation into BS 7258 : 1994 : Part 4 as a method of containment testing (Clark et. al., 1984: A letter to the BS 7258 working group, *Clinical Research Centre*). There was a sound basis for this owing to way that containment was achieved by class I microbiological safety cabinets and fume cupboards. Fletcher & Johnson (1992) used the KI method on a conventional and a 'vortex' type cupboard. These cupboards gave operator protection factors in excess of 10^5 but the workers discontinued with this method because of deposition of KI on the work surface. They claimed this would reduce the number of challenge particles but did accept that as the protection factor, for any particular type of enclosure, had been chosen in the light of experience in using the test method, then this was not too significant. They also commented on the ambiguity in the BS 5726 document 1979, which has since been revised, of the position of the spinning disc

generator and the samplers, which was not consistent. They further commented on the fact that the method gave an overall figure for comparison but did not indicate where a leakage could occur and scanning the face was considered a lengthy procedure.

Clark et. al. (1987) described a modified test method using KI particles as an alternative to the gas tracer test, backed up by extensive practical use. In the field it was found to give a good indication of a pass or fail (very much as for safety cabinets). This method differed from that for a class I safety cabinet mainly in the detailed disposition of the equipment and in the number of challenge and sampling sites. The aerosol generation and sampling was carried out at varying heights up to the maximum aperture height, and for cupboards wider than 1200 mm the test was repeated at the centres of the left and right halves of the aperture.

5.4 The application of the KI containment test method for the assessment of microbiological safety cabinet performance (BS 5726 : 1992 : Part 1) to the assessment of fume cupboard performance

5.4.1 Aerodynamic fume cupboard performance in a test room

The operator protection factor of the aerodynamic fume cupboard when tested in the test room specified in BS 7258 : 1994 : Part 4 using the KI method specified in BS 5726 : 1992 : Part 1 for safety cabinets (Fig. 5.1) was greater than 1×10^5 giving similar performance to a Class I microbiological safety cabinet (Table 5.1). However, the position of the test equipment in aerodynamic fume cupboards was not thought to give a suitable challenge as the air flow regime was very different to that of the class I safety cabinet, there being a stratification of airflow with limited lateral mixing vertically.

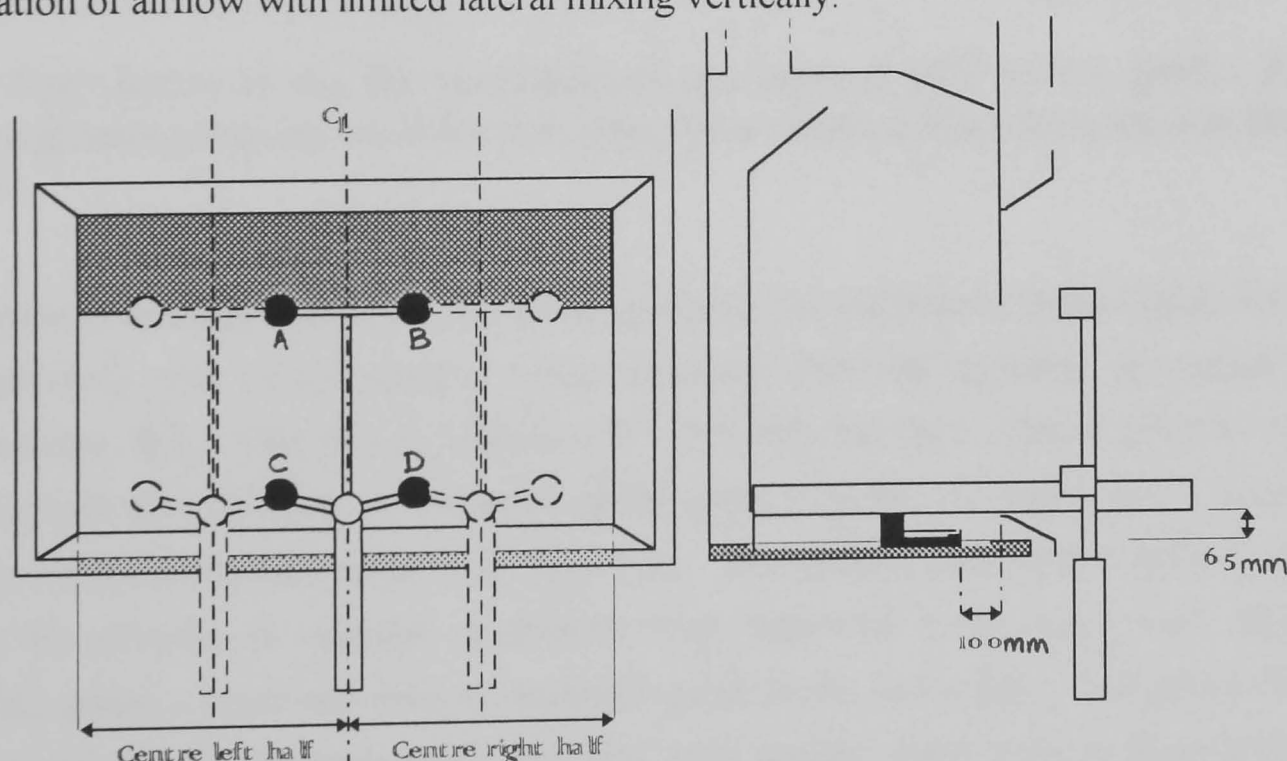


Figure 5.1 Arrangement of the KI equipment (using the method specified in BS 5726 : 1992 : Part 1 for class I safety cabinets) for testing containment of fume cupboards.

Type	Sash Height	Face Velocity	Position	KI Particle counts / Sampler				MAX.	OPF
				A	B	C	D		
Aerodynamic (in test room) (see sec. 3.2)	0.5 m	0.45 m/s	Centre	0	0	0	0	10	6.2 x 10 ⁵
				3	1	4	10		
				1	0	1	0		
			Centre left	1	1	0	4	8	7.8 x 10 ⁵
				1	1	3	6		
				3	2	2	8		
			Centre right	0	1	3	1	5	1.2 x 10 ⁵
				3	5	4	3		
				3	3	3	2		
			Blank	1	0	0	0		

Table 5.1 Operator protection factors, for an aerodynamic fume cupboard in a test room using the equipment arranged in Fig. 5.1. (OPF)

5.4.2 Field survey of fume cupboard performance

The applicability of the BS 5726 : 1992 class I microbiological safety cabinet KI containment test method (section 4.2.3) for use on fume cupboards was assessed in a fume cupboard survey at King’s College London. These fume cupboards were initially graded using a hierarchy of tests including face velocity and flow visualisation (section 2.4, App.4), and then a sample of them were tested using the KI method and an operator protection factor applied. Three repeat tests were carried out for each cupboard and the worst result recorded (Table 5.2). Each cupboard was tested ‘as-used’ which meant that no attempt was made to remove equipment from within the cupboard or prevent normal working practice from carrying on in the other parts of the room where installed.

5.5 Correlation of the KI containment test method (BS 5726 : 1992 : Part 1) with the grading scheme used for assessing fume cupboard performance in the field survey

Correlation of operator protection factor and grade for the cupboards tested (Table 5.2) was $r = 0.65$ indicating that as the graded score improved then the operator protection factor increased (Fig. 5.2). This was significant at $P = < 0.005$, but the r value accounted for $< 36\%$ of the total data variance. Correlation of the grade with the number of spots counted on each filter was not significant at 0.43 (Fig. 5.3). The graphs suggested a general trend to support an increase in operator protection with improved grade score but there were anomalies where a cupboard with a seemingly good grade had a poor operator protection. However, of those cupboards which had very poor grades, there were none with operator protection factors above 10^5 . These included aerodynamic and conventional box type fume cupboards. For many cupboards with good grades but low operator protection factors, the face velocities were below 0.5 m/s. However, correlation of the operator protection factor with the face velocity did not show a strong relationship, having an r value of 0.34 which was not significant (Fig. 5.4).

F/c type	Comments	Sash height	Velocity 250		Velocity 500		Fog score		Grade		OPF	
			m/s	var%	m/s	var%	250	500	250	500	Avg	min
Aerodynamic (Fumair in test room)	Centre	500			0.47	10		1		6	3.6×10^6	6.5×10^5
	Centre Left	500								6	2.3×10^6	7.8×10^5
	Centre right	500								6	2.4×10^6	1.2×10^6
Aerodynamic (Fumair installed in lab)	Centre	500	0.5	8	0.5	8	1	1	1	1	4.9×10^5	1.7×10^5
		250									4.1×10^6	8.9×10^5
Aerodynamic	spinning disc above arm	500	0.81	3	0.43	23	2	2	4	24	6.9×10^5	8.6×10^4
		500								24	2.1×10^6	1.0×10^6
Aerodynamic/portable	Centre	455			0.19	26		3		108	6.0×10^{-2}	5.3×10^{-2}
Box/single sash	Sash full height	715			0.58	-100		3		?	8.9×10^{-4}	1.0×10^{-4}
Box/single sash	Sash 1'	305			0.66	-15		1		1	4.0×10^4	3.2×10^4
	Sash full height	822			0.24	-38		3		108	3.7×10^3	1.5×10^3
Box/single sash	Sash full height	826			0.4	-100		3		?	7.2×10^3	3.4×10^3
Box/single sash	Sash full height	682			0.56	43		1		2	3.1×10^6	5.6×10^5
Box/single sash	Sash full height	715			0.2	-50		3		108	5.6×10^3	8.3×10^2
Box/single sash	Sash full height	710			0.64	-100		1		?	8.6×10^5	3.0×10^5
Box/double sash	Sash A full height	715			0.33	-55		3		72	6.7×10^{-2}	4.1×10^{-2}
Box/double sash	Sash A low speed	685			0.2	-100		3		?	1.2×10^3	TNC
	Sash A high speed	685			0.43	170		3		?	1.4×10^3	7.1×10^2
Box/double sash	Sash B full height	690			0.26	27		3		108	1.0×10^{-2}	1.0×10^{-2}
Box/double sash	Sash A	500	0.65	8	0.34	12	3	3	9	18	6.2×10^3	1.4×10^3
	Sash B	500	0.62	5	0.38	21	3	3	9	54	1.8×10^4	4.7×10^3
Aerodynamic	Tested centre left due to shield in middle	598				-100		3		?	5.2×10^5	1.0×10^5
	Sampler centre left below lipfoil									?	1.6×10^4	8.2×10^3
	Tested centre right due to shield in middle					~				?	1.6×10^6	2.3×10^5
Box/single sash	Tested in front of HPLC equipment	826			0.39	-100		3		?	1.2×10^6	4.1×10^5
	Tested to left of HPLC equipment									?	9.5×10^4	2.8×10^4

Table 5.2 The performance and Operator Protection Factors (OPF) of fume cupboards tested at King's College London. A ? grade was given to a cupboard with a variation in face velocity > 100 %: For statistical analysis this was graded 108. TNC - To Numerous to Count.

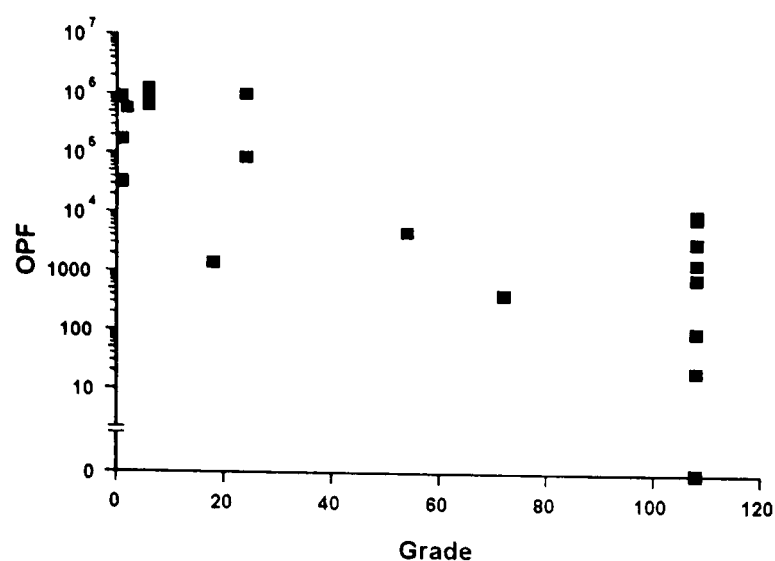


Figure 5.2 Change in operator protection factor with grade.

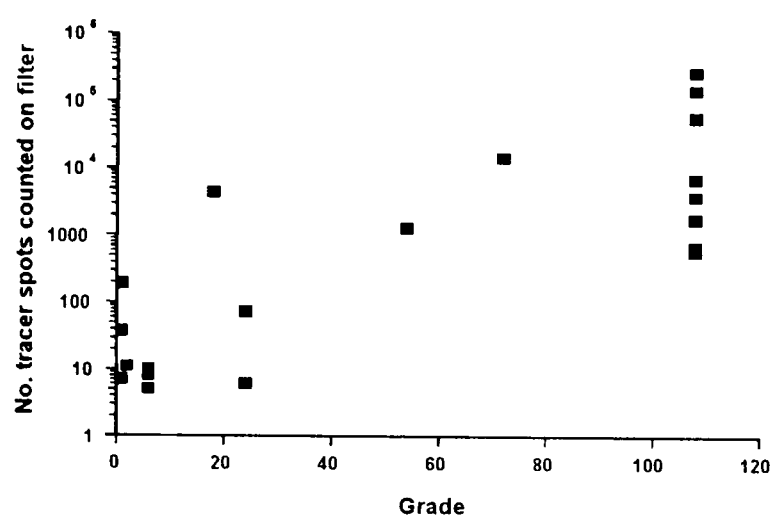


Figure 5.3 Change in the number of KI particles sampled with grade.

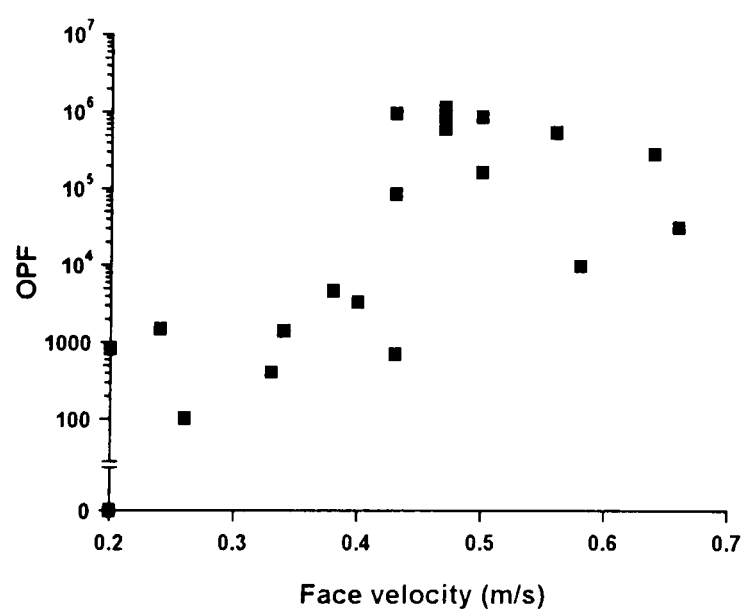


Figure 5.4 Change in operator protection factor with velocity.

There were anomalies in the containment testing results. In the case of an aerodynamic fume cupboard which was used for radioactive work, this had the lower rear scavenging slot blocked by lead shielding and a Perspex[®] shield was positioned in the middle of the aperture, so effectively dividing the aperture into two halves. The position of the cupboard was near to a swing door which, using flow visualisation, was shown to pull air from beneath the lipfoil when opened or closed. The cupboard was subsequently given a low grade. The results using the KI method in the positions as used for BS 5726 for testing class I microbiological safety cabinets did not produce operator protection factors below 10⁵. However,

repositioning a sampler below the lipfoil, in the region of the observed leakage, reduced the operator protection factor by 2 orders of magnitude.

In another case, there was a large piece of equipment inside the cupboard obscuring the right half of the aperture. When tested with the spinning disc generator in the position specified in BS 5726 : 1992, a protection factor above 10^5 was achieved. However, moving the disc to the centre of the left half and repeating the test resulted in the protection factor being reduced by an order of magnitude.

It was concluded that the relative positions of sampler and disc were not appropriate for testing fume cupboards, in the positions specified in BS 5726 : 1992 for testing class I safety cabinets. This arrangement could demonstrate differences in containment performance but there were cases when obvious leakage was not identified.

5.6 Theoretical comparison and correlation of the KI test method (BS 5726 :1992:Part 1) with the gas test method for fume cupboards (BS 7258:1994:Part 4)

The maximum sensitivity for the gas test is 0.001 ppm using a calibrated Miran infrared gas analyser and ignoring the instrument noise. The release rate of 10 % SF_6 gas for a 1.2 m wide cupboard was 0.24 l/min ($4 \times 10^{-6} \text{ m}^3/\text{s}$) and during a test period of 10 mins a total volume of 2.4 litres ($2.4 \times 10^{-3} \text{ m}^3$) was released within the cupboard. The volume of air sampled was 2 l/min ($3.33 \times 10^{-5} \text{ m}^3/\text{s}$) and the total for the test was $2 \times 10^4 \text{ ml}$ (0.02 m^3).

The maximum sensitivity for the BS 5726 : 1992 : Part 1 KI method is achieved when 1 particle is recovered. If the effective diameter of a single KI particle after evaporation of the initial droplet spun from the edge of the spinning disc is $7 \mu\text{m}$, assuming the particle to be spherical, then the effective volume is $1.8 \times 10^{-16} \text{ m}^3$ ($1.8 \times 10^{-10} \text{ ml}$). During a test $2 \times 10^{-5} \text{ m}^3$ (20 mls) of solution are aerosolised which is equivalent to 6×10^8 particles. After evaporation the total volume of particles is $1.08 \times 10^{-7} \text{ m}^3$ (0.108 mls). The volume of air sampled was 100 l/min and the duration of the test was 8 mins 48 secs (8.8 mins), the total volume of air sampled was 0.88 m^3 . If one particle were sampled during a test (the maximum sensitivity) then the equivalent concentration (Volume particle/Volume of air sampled; $1.8 \times 10^{-10} \text{ ml}/0.880 \text{ m}^3$) is $2.05 \times 10^{-10} \text{ ppm}$.

For the microbiological method assuming that the aerosol produced from the nebuliser is monodisperse and the final size of the droplet to be $2 \mu\text{m}$ diameter after evaporation of the initial droplet, then if the droplet is spherical the effective volume is $4.2 \times 10^{-18} \text{ m}^3$ ($4.2 \times 10^{-12} \text{ ml}$). During a test 3×10^8 spores are aerosolised in some 4 minutes minimum, and after evaporation the total volume of particles is $1.26 \times 10^{-3} \text{ m}^3$ (0.00126 mls). The volume of air sampled is 30 l/min for a slit sampler and the duration of the test is 10 mins, then the total volume of air sampled is 0.3 m^3 . If one droplet is sampled during a test (the maximum

sensitivity) then the equivalent concentration (Volume particle/Volume of air sampled; $4.2 \times 10^{-12} \text{ ml}/0.3 \text{ m}^3$) is $1.4 \times 10^{-11} \text{ ppm}$.

The theoretical containment efficiency (CE_{gas} , dimensionless) for the gas tracer method is:

$CE_{\text{gas}} = \{1 - (C_o Q / r)\} \times 100\%$ where r is the release rate of test gas inside the fume cupboard (ml/s), C_o is the concentration of test gas detected in the plane of the sash, averaged over space and time (ml/m³, or ppm) and Q is the volume flow rate through the cupboard (m³/s)

This equation approximates to $\{1 - (C_o / C_i)\} \times 100\%$ where C_i is the concentration of the tracer inside the cupboard.

The equivalent dimensionless containment efficiency for a particle tracer is:

$CE_{\text{particle}} = \{1 - (nQ / NS)\} \times 100\%$ where N (dimensionless) is the number of particles liberated (droplets/s), n (dimensionless) is the number of particles sampled, Q is the volume flow rate through the cupboard (m³/s), and S is the volume of air sampled

Applying this containment efficiency to both the results of the BS 7258 : 1994 : Part 4 method and the BS 5726 : 1992 : Part 1 microbiological and KI methods at their most sensitive level for a facility with a flow rate of 0.3 m³/s it can be seen that the use of a particle is much more sensitive than a gas tracer allowing measurement of performances above 99.999 % efficiency whereas for gas only 99.99 % efficiency is possible (Table 5.3).

Test	Quantity released	Max. sensitivity	Containment efficiency	Recommended limits	Containment efficiency
Gas	4 ml/s	0.001 ppm	99.993 %	0.2 ppm	98.5 %
Microbial*	1.25×10^6 dplts/s	1 colony	99.99992 %	9 colonies	99.999 %
KI	1.14×10^6 ptcls/s	1 particle	99.99997 %	60 particles	99.998 %

Table 5.3 Sensitivity and efficiency of tracer gas, microbiological and KI tracer methods. *The recommended limits can alter depending on the challenge dose.

This can also be shown when using the operator protection factor as an indicator of performance (Table 5.4) as used in BS 5726 : 1992 : Part 1. This was the ratio of transfer indices for the open bench and the cabinet giving an operator protection factor (OPF) which can be used to compare one cabinet from another cabinet: $OPF = Ns / vn$, where v is the rate of the supply of ventilating air (m³/min) (standard 10 m³/min), N is the quantity of tracer liberated (number of particles), n is the number of particles sampled and s is the sampling rate (m³/min)

For gases this may be rewritten as: $OPF_{\text{gas}} = (V_{\text{source}} s) / (V_{\text{sampled}} v)$ where V_{source} is the total volume of test gas released (ml) and V_{sampled} is the total volume sampled (ml).

Test	Max. sensitivity	OPF
Gas tracer	0.001 ppm	2.4×10^4
Microbiological*	1 colony	9×10^5
Particle tracer	1 particle	6.0×10^6

Table 5.4 Operator protection factors achievable using the gas, microbiological and KI tracer methods.
*The OPF may vary as the challenge dose is not fixed (see section 4.2.6.3.1)

If the equipment was at the same position for each assessment method then, ignoring the effects of tracer generation and sampling, the results would be comparable and correlated. However, the fundamental principles of the tests differed. The KI method (BS 5726) challenged the weakest point for containment in the plane of the aperture. That for a class II cabinet was the juncture where inflowing air and downflowing air met and for a class I cabinet the weakest point was considered the lower edge of the aperture. In both cases an artificial arm was used to disturb the airflow. The BS 7258 test did not challenge the weakest point but seeded the working volume of the fume cupboard with the tracer and sampled the passive escape of contaminant.

The position of the tracer source and air samplers differed between the two methods. The KI source was fixed 100 mm from the plane of the aperture in one position. In the BS 7258 test the source was positioned 150 mm from the aperture plane and moved to six positions around the aperture. The KI centripetal samplers had a large sampling flow rate and were positioned 150 - 160 mm **in front of the aperture plane**. The gas probes had a lower sampling flow rate and were positioned in a grid **in the aperture plane itself**. Thus the KI test sampled actual leakage and the BS 7258 test sampled both potential and actual leakage without distinction between them. In terms of sampling the KI test was more closely comparable to the ASHRAE 110 and DIN 12 924 test methods.

For correlation of the KI and BS 7258 containment test methods these fundamental differences had to be taken into consideration. In terms of a pass or fail the questions to be asked were "if leakage was sampled using the centripetal samplers indicating a fail, would this be reflected in the amount of gas sampled and, vice-versa, if a considerable quantity of gas was sampled in the plane of the aperture indicating poor performance would this reflect in the number of particles sampled 150 mm from the aperture plane?".

Theoretical correlations between the results of the containment tests have been given in respect of the plane of the aperture (Bicen, 1993) by extrapolation assuming dilution from a sampling point a fixed distance from the aperture plane to the plane itself. This assumed that concentration levels measured at 150 mm away from the aperture were lower by at least 100 times than those measured in the aperture plane itself. Such assumptions would have to be made if:

1. What was sampled 150 mm from the plane would be sampled in the aperture plane
2. Dilution was applicable to particle transport
3. The mechanism of tracer generation had no effect

This theoretically correlated results from KI tests with the BS 7258 for sampling in the aperture plane but not vice-versa. At the theoretical sensitivities of the KI test, if one particle of KI were sampled 150 -160 mm away from the aperture plane giving a performance efficiency of 99.99997 % then the interpolated efficiency at the aperture plane was far less, 99.997 %. This value was still in excess of the maximum sensitivity of tests using gas tracer. In order to correlate a value of KI with gas then an equivalent amount of gas must be sampled in the aperture plane to give a similar performance efficiency. However the testing philosophies were different and it may be that gas sampled in the aperture plane indicating poor performance would not necessarily leak to 150 mm away and conversely this also had to assume that the particles in the plane of the aperture would escape containment and leak out to the sampling position 150 mm away.

This may be feasible theoretically but are the assumptions correct? A gas would be expected to disperse by turbulent and molecular diffusion. An aerosol of particles will initially disperse like a gas, but the final challenge particles have fixed dimensions, and so an individual particle would not disperse further at the molecular level. In terms of leakage from the aperture plane and sampling a fixed distance from this plane, a single particle leak can be detected whereas for an equivalent volume of gas this would be expected to disperse at the molecular level before reaching the samplers and not detected. Interpolation of this result back to the aperture plane does not mean that there is an enormous number of particles leaking but only one. However by assuming a proportionally greater number in the aperture plane does err on the side of safety.

Another assumption that could be questioned is that, due to the active propulsion of challenge particles in the KI method and only the passive discharge of gas in the BS 7258 method, is there a chance that particles could leak and no gas be sampled in the plane of the aperture? These questions go beyond theoretical realm and would have to be answered practically.

5.7 Use of a nitrogen gas jet to induce leakage from the fume cupboard aperture into the test room for subsequent assessment of both methods

A copper welding tip was used as a nozzle with internal diameter of 3 mm to give a velocity which induced a leakage from the fume cupboard into the test room; the flow rate of nitrogen gas through the nozzle was in the range of 0 - 10 l/min as scaled on a rotameter. The nozzle was positioned inside the fume cupboard supported by a clamp so that the front edge was a set distance from the rear baffle and the work surface.

Leakage was first ascertained using the recommended containment gas test method for fume cupboards described in BS 7258 : 1994 : Part 4 with the source in position P₃, the sampling grid in the plane of the sash and with the nitrogen gas jet positioned inside the cupboard with the front edge of the nozzle 150 mm from the rear baffle (unless otherwise specified) and the centre line of the nozzle directed at and level with the top edge of the source funnel. In addition to induce leakage to the position of the centripetal air samplers as in BS 5726 : 1992, the sampling grid was positioned 150 mm from the plane of the aperture into the test room and the gas test repeated with the nitrogen jet.

jet diameter (mm)	jet flow rate (l/min)	jet velocity (m/s)	cupboard face velocity (m/s)	Source P ₃ (leakage)
Sampling grid in the plane of the sash (jet level with centreline and top edge of funnel)				
2	0	0	0.47	no
	2.8	17.9	0.47	no
	4.7	24.9	0.47	yes
	6.8	36.1	0.47	yes
	8.6	45.6	0.47	yes
3	6	14.2	0.47	no
	7	16.5	0.47	yes
	8	18.9	0.47	yes
Sampling grid 150 mm in front of the plane of the sash				
3	8	18.9	0.47	no
	9	21.2	0.47	yes
	10	23.6	0.47	yes
Centre line funnel and nitrogen jet 15 mm above lipfoil				
3	6	14.2	0.47	no
	7	16.5	0.47	no
	8	18.9	0.47	yes
Centre line funnel and nitrogen jet at centre line of cupboard				
3	6	14.2	0.47	no
	7	16.5	0.47	no
	8	18.9	0.47	yes
Centre line funnel and nitrogen jet 15 mm below sash foil				
3	6	14.2	0.47	no
	7	16.5	0.47	no
	8	18.9	0.47	no
	9	21.2	0.47	yes

Table 5.5 Determination of leakage using SF₆ and the BS 7258 : 1994 containment test method.

A higher flow rate of nitrogen was required to induce leakage near to the sash handle than the other heights of the aperture (Table 5.5). Thus, for tests with induced leakage beyond the aperture plane a jet diameter of 3 mm was used at a flow rate of 10 l/min (23.6 m/s) unless specified otherwise.

5.8 Use of the induced leakage to assess the applicability of the KI containment test method (BS 5726 : 1992 : Part 1) for use with the aerodynamic fume cupboard

The jet nozzle was positioned 250 mm away from the aperture plane (closer to the plane than previously tested) and nitrogen was discharged at a flow rate of 10 l/min to induce leakage from the cupboard at three heights shown in Fig. 5.5. When the jet was in position Nc, above the artificial arm, substantial amounts of KI particles were sampled 150 mm from the aperture plane (Table 5.6). However, with the jet at the other two positions no leakage from the cupboard was demonstrated. From the gas tests it was known that at these sampling positions leakage did occur and it was thus concluded that the position of the KI equipment as specified in BS 5726 : 1992 was not suitable for assessing aerodynamic fume cupboards.

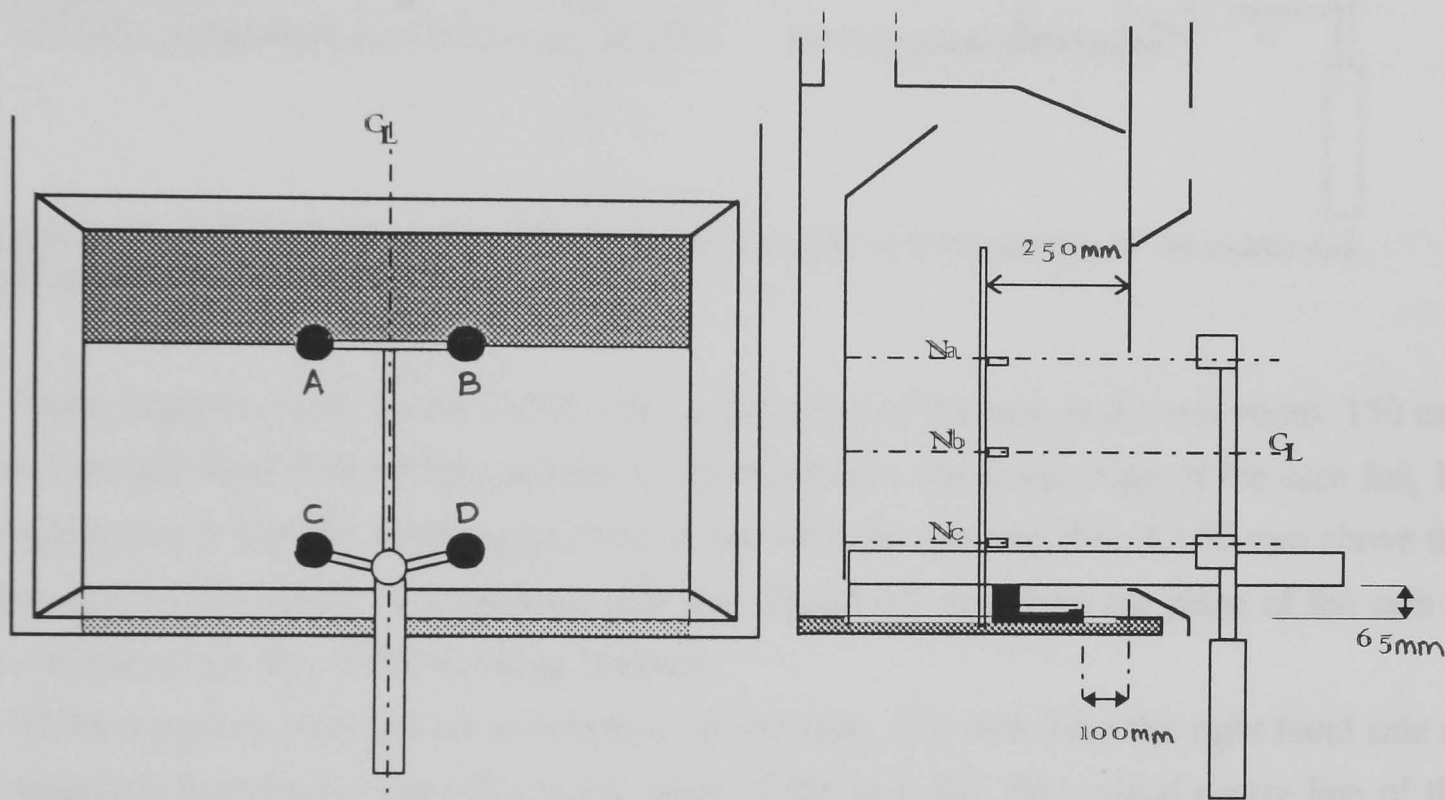


Figure 5.5 Arrangement of the KI equipment as specified in BS 5726 : 1992 : Part 1 for class I cabinets and a nitrogen jet for assessing the applicability of the method.

Type	Sash Height	Face Vel	Position of jet	Sampler				Max	OPF
				A	B	C	D		
Aerodynamic (in test room) (see sec.3.2)	0.5 m	0.45 (m/s)	No jet	13	6	9	6	17	3.7 x 10 ⁵
				7	11	17	3		
				4	8	7	5		
			Room	15	22	19	7	22	2.8 x 10 ⁵
			Na	9	19	20	9	20	3.1 x 10 ⁵
			Nb	19	23	19	8	23	2.7 x 10 ⁵
			Nc	8	20	41	1899	1899	3.3 x 10 ³
			Nc, disc in mid	24	31	244	2002	2002	3.1 x 10 ³

Table 5.6 Number of KI particles sampled in front of an aerodynamic fume cupboard with induced leakage using the BS 5726 : 1992 : Part 1 method. (Equipment arranged as in Fig. 5.5).

5.9 Comparison of the relative position of tracer source and samplers recommended in BS 7258 for use with the KI equipment

It was shown that the disposition of equipment was critical and that specified in BS 5726 : 1992 : Part 1 not suitable (section 5.8). The equipment was then arranged in order to

compare the position of the source and the sampling positions with the gas test as recommended in BS 7258 : 1994 : Part 4 (Fig. 5.6). The following protocol was used.

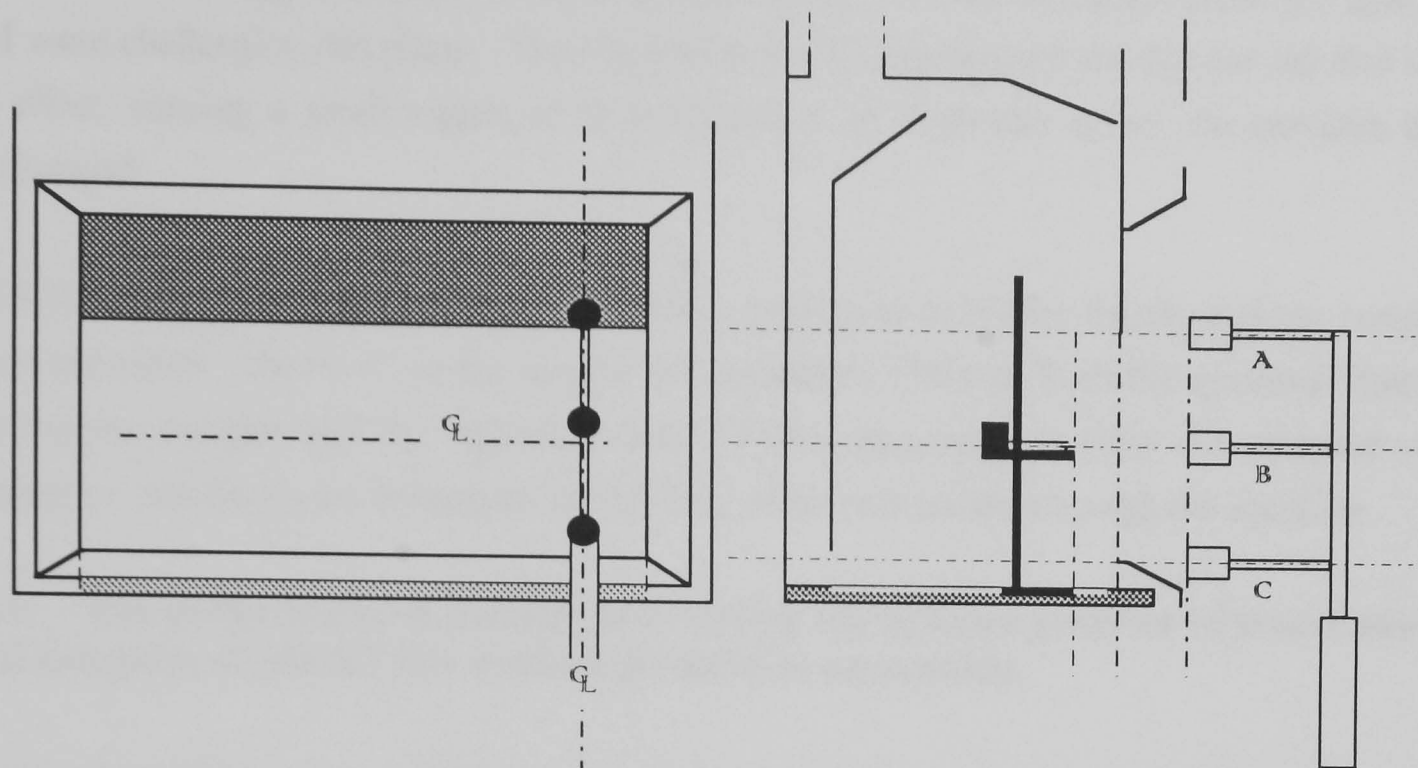


Figure 5.6 Arrangement of the KI equipment for comparison with the position of the source and samplers in BS 7258 : 1994 : Part 4.

- a) Three samplers were placed 150 mm from the plane of the sash in the test room, 150 mm from the right hand side of the aperture A) 50 mm below the lower edge of the sash foil, B) vertical centre line of the working aperture in line with the spinning disc, C) 50 mm above the upper edge of the lipfoil. The spinning disc was placed 100 mm from the plane of the sash in the vertical centre line of the working aperture.
- b) Three samplers were placed in the plane of the sash, 150 mm from the right hand side of the aperture A) 50 mm below the lower edge of the sash foil, B) vertical centre line of the working aperture in line with the spinning disc, C) 50 mm above the upper edge of the lipfoil. The spinning disc was placed 100 mm from the plane of the sash in the vertical centre line of the working aperture.
- c) Three samplers were placed in the plane of the sash, 150 mm from the right hand side of the aperture A) 50 mm below the lower edge of the sash foil, B) vertical centre line of the working aperture in line with the spinning disc, C) 50 mm above the upper edge of the lipfoil. The spinning disc was placed 150 mm from the plane of the sash in the vertical centre line of the working aperture.

Face Velocity(m/s)	Position of equipment	Sampler			Highest
		A	B	C	
0.48	as in (a)	9	10	7	10
0.48	as in (b)	90 %	100 %	3	100 %
0.48	as in (c)	7	1219	5635	5635

Table 5.7 Number of KI particles sampled in front of the cupboard with the equipment arranged as in protocol 5.9 a, b and c. (% indicates the area of Filter coverage).

From the results in Table 5.7 it was clear that sampling in the plane of the aperture (as in BS 7258 : 1994) using the KI equipment was not possible as the samplers were saturated with particles. This suggested that the particles were flung from the spinning disc at the aperture and were challenging this plane. The physical size of the centripetal samplers could also have an effect, causing a small region of air recirculation in front into which the particles were discharged.

With the source 100 mm from the plane of the aperture as in (b) the middle and top samplers were saturated. However, as the source was moved to 150 mm from the aperture plane (c) the bottom sampler had the highest counts. This suggested that either the particles were settling or that they were influenced by the flow of air as it passed through the aperture.

5.10 Use of the induced leakage to establish the relative position of tracer source and samplers of the KI test method for further assessment

In order to establish more representative positions for the KI source and sampling equipment, the spinning disc generator and samplers were positioned at 3 heights to cover the working aperture. A jet of nitrogen gas was used to induce leakage out of the cupboard into the test room from each of 3 heights (Fig. 5.7). The artificial arm was not used as it was considered not to have a measurable effect on disturbance due to the size of the aperture. The following protocols were used.

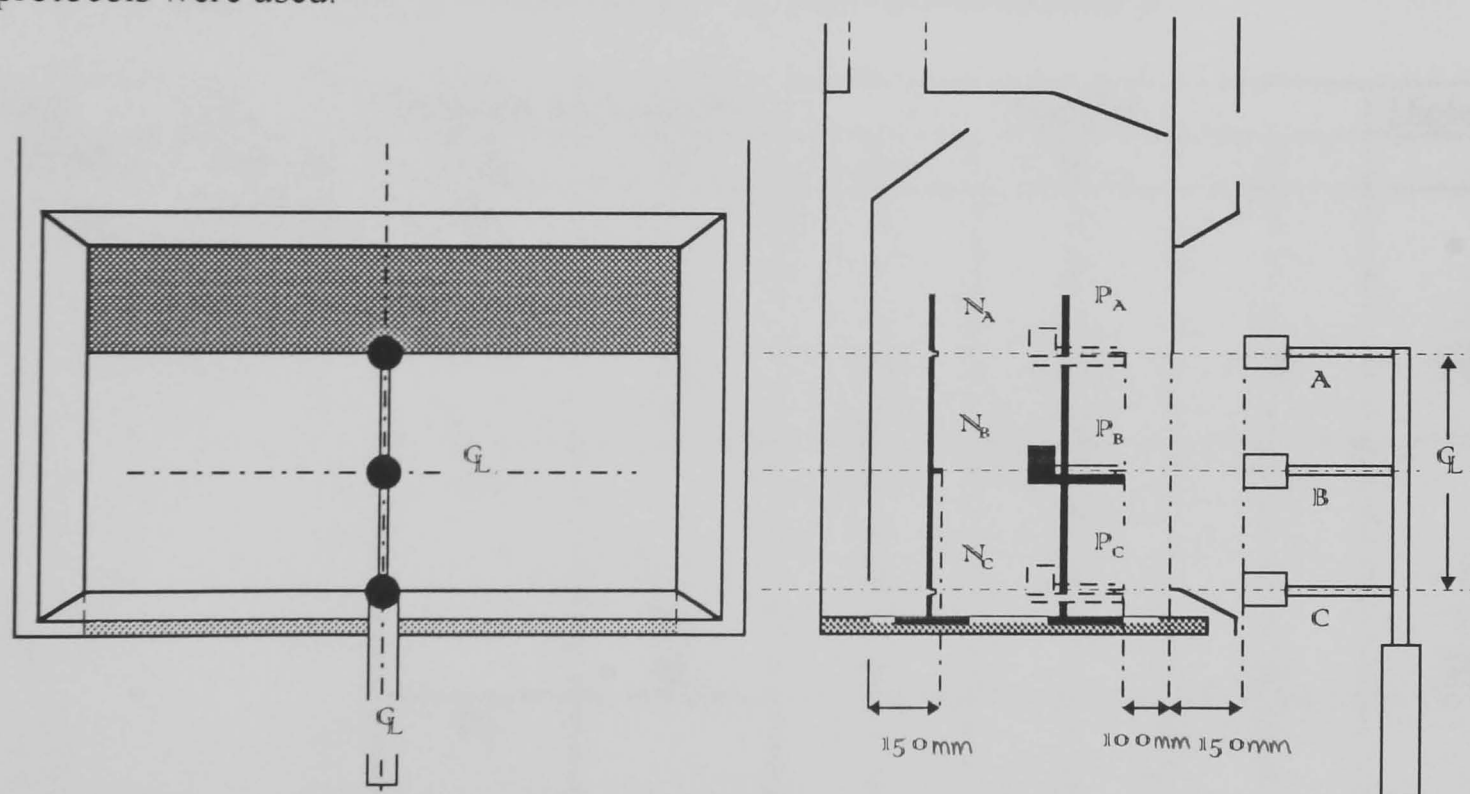


Figure 5.7 Arrangement of the KI equipment and a nitrogen jet for the assessment of leakages from cupboards.

- A single sampler, B, was placed 150 mm from the plane of the sash in the test room, 150 mm from the right hand edge and in the vertical centreline of the aperture, in line with the nitrogen jet, N_B , and the spinning disc, P_B , 100 mm from the plane of the sash.
- Three samplers were placed 150 mm from the plane of the sash in the test room, 150 mm from the right hand side of the aperture A) 50 mm below the lower edge of the sash foil, B) in the vertical centre line of the working aperture, C) 50 mm above the upper edge of the lipfoil.

The nitrogen jet nozzle, N_B, was placed 150 mm from the rear baffle and the spinning disc, P_B, was placed 100 mm from the plane of the sash, both in line with sampler B.

c) Three samplers were placed in the plane of the sash, 150 mm from the right hand side of the aperture A) 50 mm below the lower edge of the sash foil, B) in the vertical centre line of the working aperture, C) 50 mm above the upper edge of the lipfoil. The nitrogen jet nozzle, N_C, was placed 150 mm from the rear baffle in line with sampler C and the spinning disc, P_B, was placed 150 mm from the plane of the sash in line with sampler B.

Face Velocity(m/s)	Jet velocity (m/s)	Position of equipment	Sampler			Highest
			A	B	C	
0.45	14.2	as in (a)		17		17
0.48	23.6	as in (b)	18	5796	4	5796
0.48	16.5	as in (c)	321	2254	80 %	80 %

Table 5.8 Number of KI particles sampled in front of the cupboard with the equipment arranged as in protocol 5.10a, b and c. (% indicates the area of Filter coverage).

d) Three samplers were placed 150 mm from the plane of the sash in the centre line of the aperture A) level with the lower edge of the sash foil, B) in the vertical centre line of the working aperture, C) level with the upper edge of the lipfoil. The nitrogen jet nozzle was placed 150 mm from the rear baffle N_A) level with sampler A, N_B) level with sampler B, N_C) level with sampler C. The spinning disc was placed 100 mm from the plane of the sash P_A) level with sampler A, P_B) level with sampler B, P_C) level with sampler C.

Face Velocity	Jet Velocity	Position of equipment		Sampler			Highest
		disc	jet	A	B	C	
0.5 m/s	23.6 m/s	P _A		3	1	3	3
				1	3	1	
				1	0	3	
				106	5723	28	
				2	1	1	
		P _B		2	3	0	3
				1	2	2	
				2	2	3	
				1	1	1	
				3	1	500	
		P _C		1	1	0	2
				2	2	0	
				0	2	0	
				1	3	1	

Table 5.9 Number of KI particles sampled in front of the cupboard with the equipment arranged as in protocol 5.10d.

e) The effect of the generator bulk on the dispersal of the jet, reducing leakage, was investigated. Three samplers were placed 150 mm from the plane of the sash in the centre line of the aperture A) level with the lower edge of the sash foil, B) in the vertical centre line of the working aperture, C) level with the upper edge of the lipfoil. The nitrogen jet was

placed 300 mm from the plane of the sash N_A) 15 mm below sashfoil, N_B) level with sampler B, N_C) 15 mm above the lipfoil. The jet was then moved to different points around the spinning disc (P_C), described in Table 5.10, to study the effect of the disc generator on the dispersal of the jet. The spinning disc 100 mm from the plane of the sash P_A) level with sampler A, P_B) level with sampler B, P_C) at a level 15 mm above the upper edge of the lipfoil.

Avg. Face Velocity	Jet velocity (m/s)	Sampler			Highest
		A	B	C	
i) Spinning disc in position P _C and nitrogen jet in position N _C in line with disc centre					
0.5 m/s	23.6	9	2	3	9
ii) Spinning disc in position P _C and nitrogen jet in position N _C but in-line with edge of disc					
0.5 m/s	23.6	6	14	1964	1964
iii) Spinning disc in position P _B and nitrogen jet in position N _B but in line with edge of disc					
0.5 m/s	23.6	12	82	5	82
iv) Spinning disc in position P _B and nitrogen jet in position N _A but in-line with edge of spinning disc generator					
0.5 m/s	23.6	18	23	9	23

Table 5.10 Number of KI particles sampled in front of cupboard with the equipment arranged as in protocol 5.10e.

f) When the centre of the spinning disc was level with the nitrogen jet, the bulk of the generator was shown to disperse the jet so reducing the artificial leakage (Table 5.10). Further tests were done using protocol e) but with the nitrogen jet directed past the edge of the spinning disc (Table 5.11).

Avg.Face Velocity	Jet Velocity	Position of equipment		Sampler			Highest
		disc	jet	A	B	C	
0.5 m/s	23.6 m/s	P _A	N _A	50	38	1	50
			N _B	3	437	2	437
			N _C	5	1	0	5
		P _B	N _A	4860	3465	9	4860
			N _B	0	50 %	12	50 %
			N _C	2	100 %	3013	100 %
		P _C	N _A	1	1	20	20
			N _B	0	67	4	67
			N _C	3	0	8748	8748

Table 5.11 Number of KI particles sampled in front of cupboard with the equipment arranged as in protocol 5.10e but with the jet directed at the edge of the disc rather than the centre. (% indicates the area of filter coverage).

In using the KI containment test method, the position of the spinning disc was shown to be critical in the challenge to the face of the aerodynamic fume cupboard. The nitrogen gas jet substantially induced leakage from the face of the cupboard as demonstrated both by the sampling tracer gas and KI released from within the cupboard. With the spinning disc in the positions level with the lipfoil or the underside of the sash foil, a jet induced in the furthest position was not sampled. However, with the spinning disc in the centre of the working aperture, leakage was detected for all positions of the nitrogen jet. For testing purposes the

spinning disc generator and samplers should be placed in all three positions. Due to time and money further tests were carried out with the spinning disc in position P_B and three samplers in positions A, B and C.

5.11 Comparison of the BS 7258 test method results with the modified KI test method results at different face velocities

In section 3.9.6 the performance of the aerodynamic cupboard in the test room was assessed at differing face velocities and no tracer gas was sampled in the plane of the sash even at a lower face velocity of 0.25 m/s. There was some gas detected near to the sash foil at higher face velocities of 0.85 m/s. The assessment was repeated using the KI method with the equipment arranged in the revised position discussed in section 5.9. Three samplers were placed 150 mm from the plane of the sash in the centre line of the aperture A) level with the lower edge of the sash foil, B) in the vertical centre line of the working aperture, C) level with the upper edge of the lipfoil. The spinning disc was placed 100 mm from the plane of the sash in position P_B (Fig. 5.7) in the vertical centre line of the working aperture.

Face Velocity	Test	Sampler position			Highest	OPF
		A	B	C		
0.85 m/s	1	1	6	1	7	8.86 x 10 ⁵
	2	7	4	4		
	3	0	6	4		
0.78 m/s	1	1	1	1	5	1.24 x 10 ⁶
	2	2	5	0		
	3	0	2	2		
0.68 m/s	1	1	0	0	4	1.55 x 10 ⁶
	2	1	3	1		
	3	0	4	1		
0.54 m/s	1	0	5	0	12	5.17 x 10 ⁵
	2	0	12	1		
	3	1	4	1		
0.37 m/s	1	1	3	1	54	1.15 x 10 ⁵
	2	20	45	41		
	3	21	54	31		
0.25 m/s	1	5	6199	15	7567	8.19 x 10 ²
	2	16	7567	15		
	3	8	4830	4		

Table 5.12 Change in operator protection factor with face velocity.

With decreasing face velocity to 0.37 m/s the performance remained above the 10⁵ operator protection factor mark (Table 5.12). However at a face velocity of 0.25 m/s the protection factor decreased by 3 orders of magnitude. These results compared favourably with similar work done on microbiological safety cabinets (Clark, 1989) (Figs. 5.8 & 5.9).

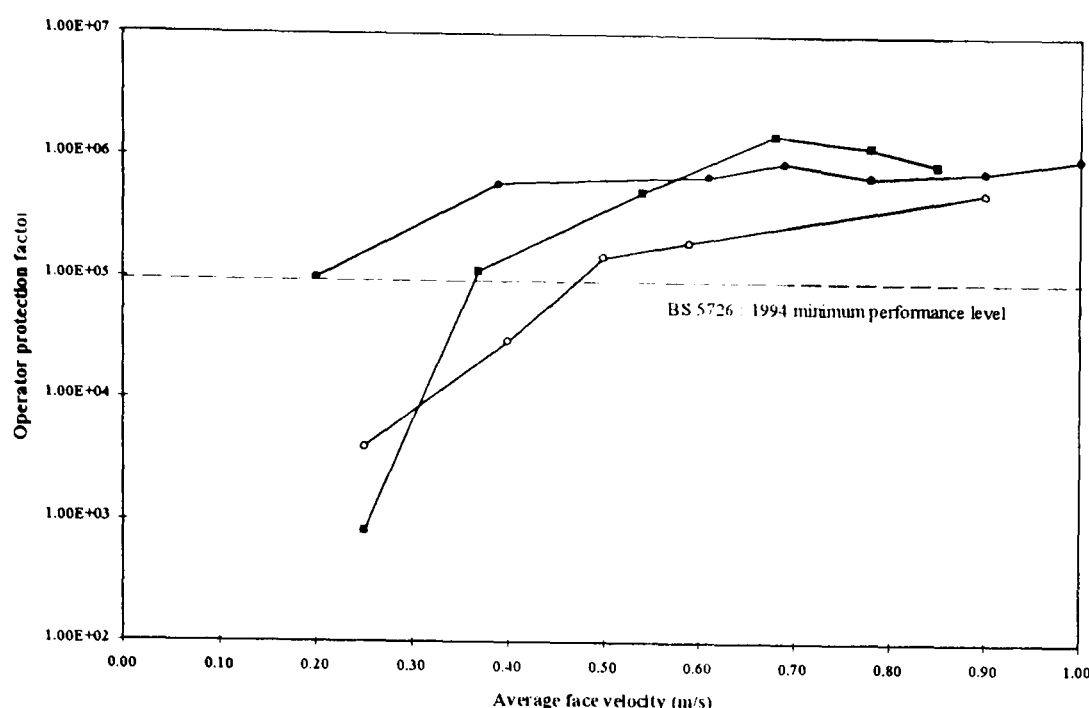


Figure 5.8 Change in operator protection factor for a pre-BS 5726 class I cabinet ○, a BS 5726 class I cabinet with a flared inlet ●, and the aerodynamic fume cupboard ■ with mean face velocity.

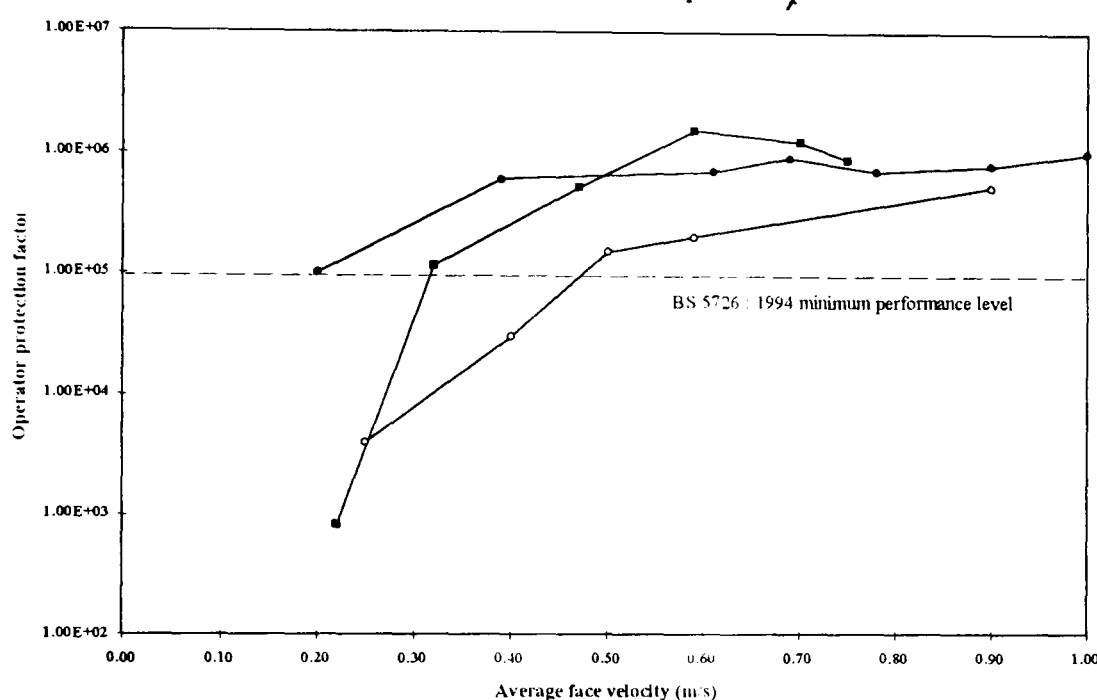


Figure 5.9 Change in operator protection factor for a pre-BS 5726 class I cabinet ○, a BS 5726 class I cabinet with a flared inlet with mean face velocity, and change in operator protection factor for the aerodynamic fume cupboard with face velocity measured in the aperture plane of opposite the source ■.

This reflected the generation mechanism of the KI aerosol (section 4.4.2). The particles were thrown at the aperture and the lower face velocity was insufficient to influence the particle motion resulting in them escaping the containment of the cupboard. As the face velocity increased no particles were sampled.

5.12 Comparison of the BS 7258 test method results with the modified KI test method results during deterioration in fume cupboard performance by design modifications

As discussed in section 3.9.6 the aerodynamic fume cupboard was modified so that there were obvious recirculation zones of air when visualised using water fog. These regions were over the lipfoil in the centre and in the left and right lower corners caused by blockages underneath a modified work surface and lipfoil. Using the recommended gas tracer test in BS 7258 : 1992 : Part 4 only very small amounts of tracer were sampled in the plane of the sash

when tracer was released from position P2 but none was measured with the source at P1 or P3, near the left and right lower edges. Tracer was sampled however in the plane of the sash very near the edges, and it was shown that gas from these two source positions was reaching the plane.

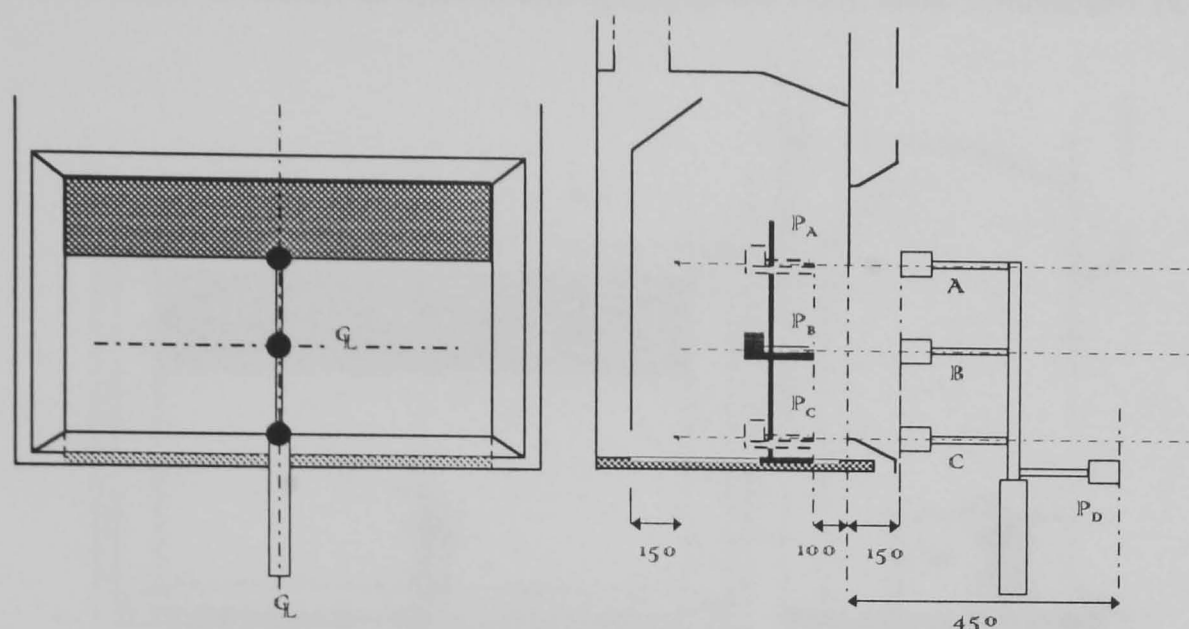


Figure 5.10 Arrangement of the KI equipment and with additional sampler for measuring background.

This was repeated using the modified KI method (Fig. 5.10). This time the background concentration was also sampled. With a release of KI from position P_C in the centre line there was no excessive sampling of particles considering the background level was similar. Thus no significant leakage was concluded to have been measured and that there was re-entrainment of discharge into the test room.

The tracer was then released from position P_C but 50 mm from the right hand edge, 100 mm from the plane of the aperture with the samplers on the same axis. In this case again where substantial recirculation had been observed there was no leakage found. The tracer was then released from position P_A level with the underside of the sash foil and again no leakage was measured.

This either suggested that the challenge was not significant in these areas or that there was no leakage from these regions beyond the cupboard aperture. In order to ascertain whether a disturbance would draw this potential leakage from the aperture an A4 board was waved ~ 1 m from the centre of the aperture and at 45° from the left and right sides. Tracer discharge and sampling was at the centre line of the aperture, and discharge in position P_C. There was again no increase in counts above the background level.

5.13 Comparison of sampling methods for SF₆ and KI particles with common source (Collison nebuliser)

So far had shown anomalies in the generation of the tracer and sampling positions between the two test methods. In this section the performance of the sampling systems as recommended in BS 7258 : 1994 : Part 4 and specified in BS 5726 : 1992 : Part 1 were compared using a common discharge. The source, a Collison reflux blast nebulizer (Fig.

5.11), used a compressed gas to disturb a solution and carry droplets from its surface in the form of an aerosol. This nebulizer was recommended in BS 5726 : 1992 : Part 1 for the dispersal of bacterial spores using a gas, usually oxygen or nitrogen. There was correlative data between release of bacterial spores and KI particles from such a nebulizer (Clark et. al., 1981).

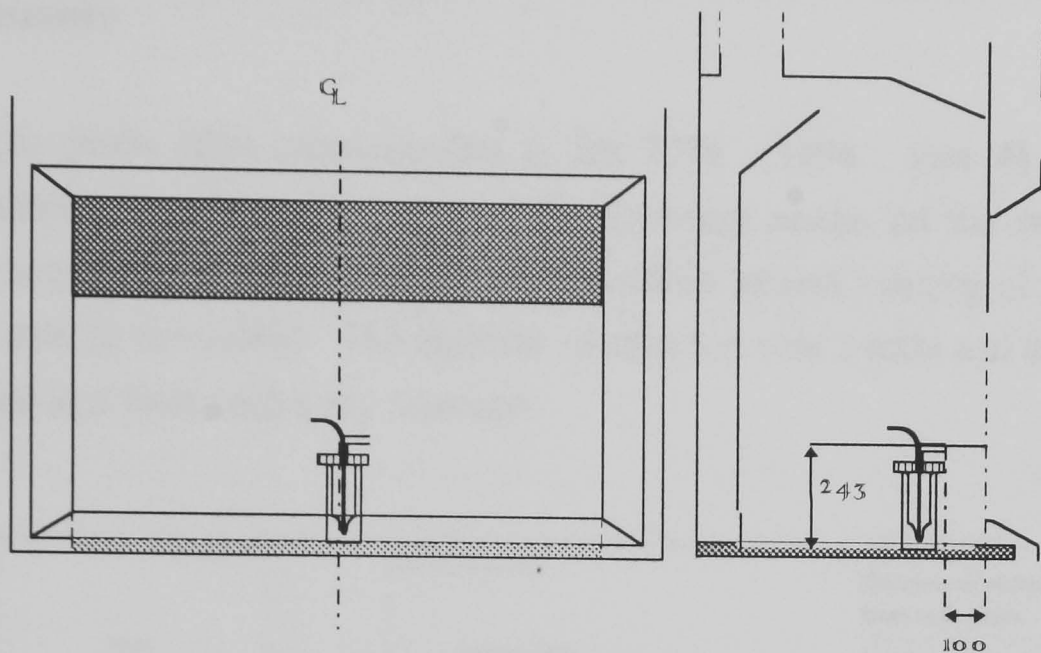


Figure 5.11 Position of a Collison nebuliser in fume cupboard.

In this investigation, sulphur hexafluoride was used as the carrier gas and the solution was 1.5 % KI in absolute ethanol. Initially, sampling of the two tracers was not carried out simultaneously as the KI particles would pass through the infra-red analyser filter possibly damaging the optics within the instrument. However, a system was developed in which this was made possible.

5.13.1 Discharge of SF₆ from Collison nebulizer

The flow rate through the Collison was adjusted to 3 l/min and the face velocity of the fume cupboard was 0.25 m/s in order for the discharge velocity from the nozzle to be greater than the face velocity.

Distance from nozzle along its central axis (mm) (horizontal)															
Distance from nozzle/below nozzle axis (mm) (vertical)															
	0	10	20	30	40	50	60	70	80	90	100	110	120	150	200
0	0.85	0.70	0.65	0.60	0.40	0.20	0	0.05	0	0	0.05	0.05	0.10	0	0
5				0.70											
25					0.60										
30									0.40		0.1				
40								0.30		0.25		0.20			
45						0.50									
55							0.50						0.10		
145														0.05	

Table 5.13 Velocity profile of discharge from a Collison nebuliser nozzle with the fume cupboard turned off (velocity along central axis of nozzle and maximum velocity measured away from the axis).

At 3 l/min the discharge velocity at the nozzle was 0.85 m/s. The maximum velocities were measured below the axis of the nozzle (Table 5.13) suggesting that the gas was sinking towards the ground after discharge.

5.13.2 Concentration of SF₆ sampled in front of the Collision nebuliser with increasing distance

A single sample probe (that recommended in BS 7258 : 1994 : Part 4) was placed at increasing distances away from the front of the discharge nozzle on the same axis. The sampling flow rate was 6.8 l/min which gave a calculated suction velocity of 5.77 m/s (~1.1 m/s measured near to the probe). The duration of each test was 2 mins and 0.006 m³ of test gas was released at 3 l/min with a dry reservoir.

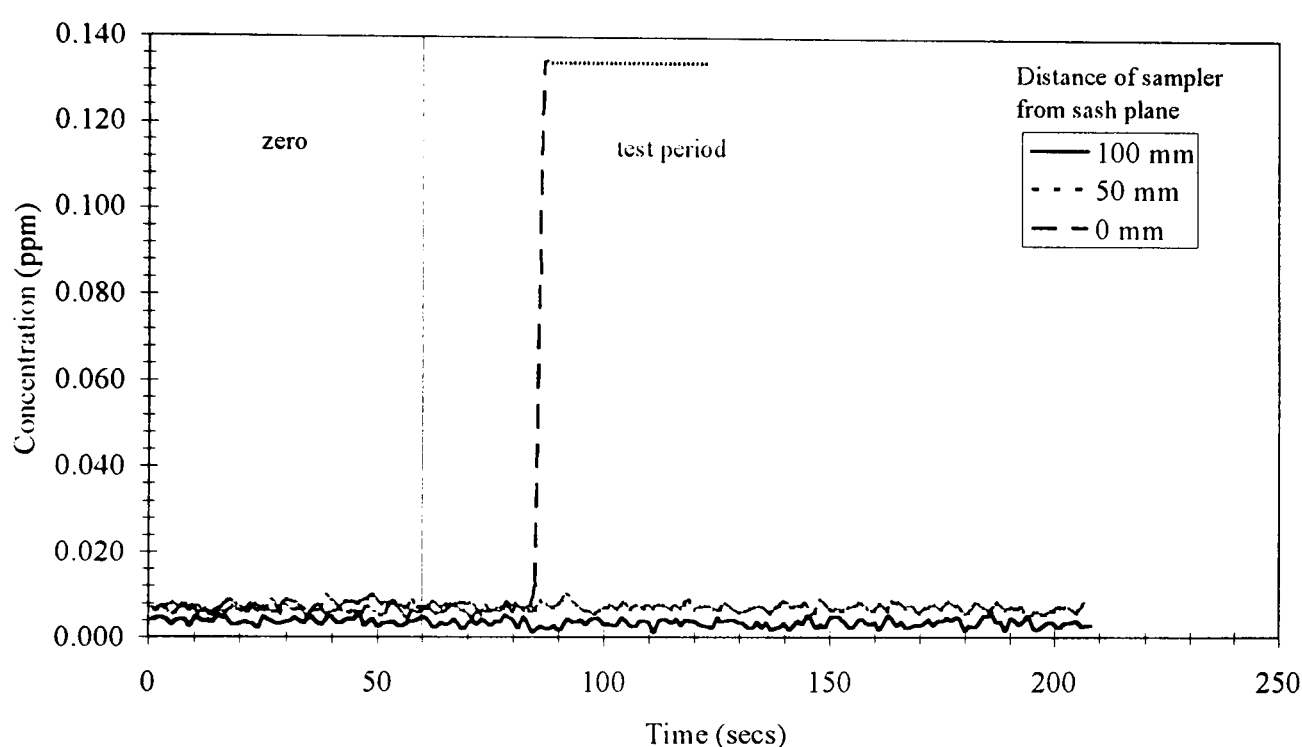


Figure 5.12 The release of SF₆ from a Collision nebuliser, placed in the fume cupboard, at 3 l/min (discharge velocity 0.85 m/s) 100 mm from the sash plane, and measured at increasing distance from the plane using a single sampling probe (BS 7258 : 1994) in line with the Collision jet. Cupboard face velocity 0.25 m/s.

Only when the sampling probe was in the plane of the sash was any gas detected (Fig. 5.12).

5.13.3 No. of KI particles sampled, when released from the Collision nebuliser, with increasing distance

A single centripetal air sampler was placed at increasing distances away from the front of the discharge nozzle on the same axis. The sampling flow rate was 100 l/min which gave a calculated suction velocity of 14.7 m/s (~8 m/s measured near to the sampler).

SF₆ was used as the carrier gas and the Collision was loaded with 75 mls of KI solution. . The carrier gas flow rate was 3 l/min (0.85 m/s). The discharge rate of fluid was ~0.8 ml/min during each test of 2 mins, and an estimated 1.5×10^7 particles were released assuming a particle size of 2 μ m. However, due to the polydisperse nature of the aerosol generated from

a Collison nebuliser, this was a very approximate figure. The particles collected on the filter disc varied in size, all were very much smaller than those released from the spinning disc generator.

Test	Blank	Sampler from sash plane		
		100 mm	50 mm	0 mm
1	2	1	78	100%
2		0	37	
3		1	231	
Highest		1	231	100%
OPF		6.20E+06	2.68E+04	UC

Table 5.14 Number of KI particles sampled at varying distances from the aperture plane when discharged from a Collison nebuliser.

KI particles were detected at all three measurement positions from the plane of the sash (Table 5.14). The filter discs had a purple hue to the background (see section 5.13.4).

5.13.4 Sampling of SF₆ in series with the KI test method

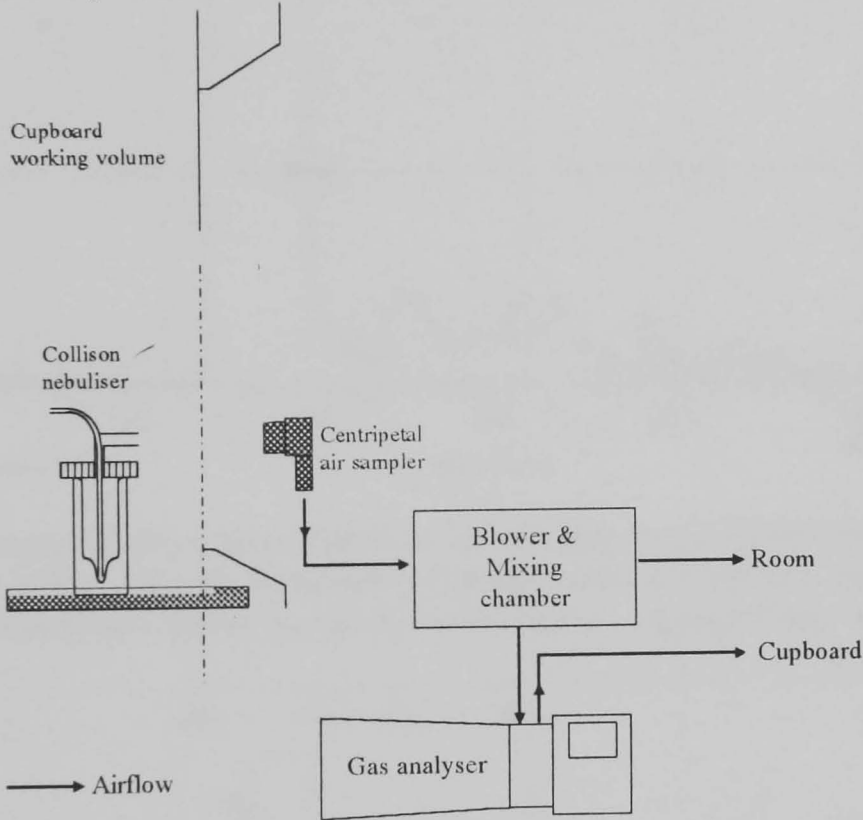


Figure 5.13 Arrangement of the equipment for sampling SF₆ in the KI-Discus sampling system.

The two tracers were sampled simultaneously through the KI sampling system shown in Fig. 5.13. SF₆ was sampled by inserting a BS 7258 probe into the mixing chamber and drawing air through the gas analyser. Initially SF₆ was discharged towards the aperture (face velocity 0.25 m/s) at a rate of 3 l/min (0.85 m/s) from the Collison nebuliser with no liquid present in the reservoir and then repeated using SF₆ as the carrier gas for a KI solution.

Both SF₆ and KI particles were sampled at various distances from the aperture plane on the same axis as the Collison nebuliser nozzle. SF₆ was detected through the KI test system at all measurement positions in front of the plane of the sash as shown in Figs. 5.14-5.17 but no SF₆ was detected, 100 mm from the plane of the sash, using just one BS 7258 probe, in place of the centripetal sampler (Fig. 5.18).

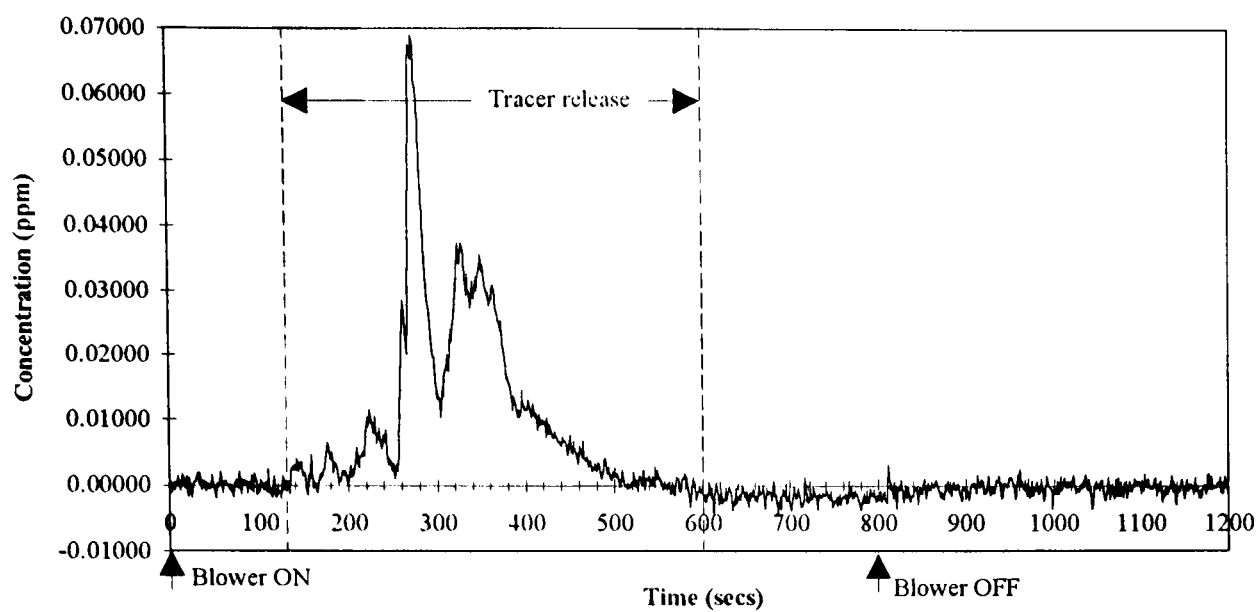


Figure 5.14 Measurement of SF_6 concentration in air sampled by centripetal samplers (100 l/min) 100 mm from the aperture plane. SF_6 released from a Collision nebuliser 100 mm from the plane at 3 l/min (discharge velocity 0.8 m/s). Cupboard face velocity ~ 0.25 m/s.

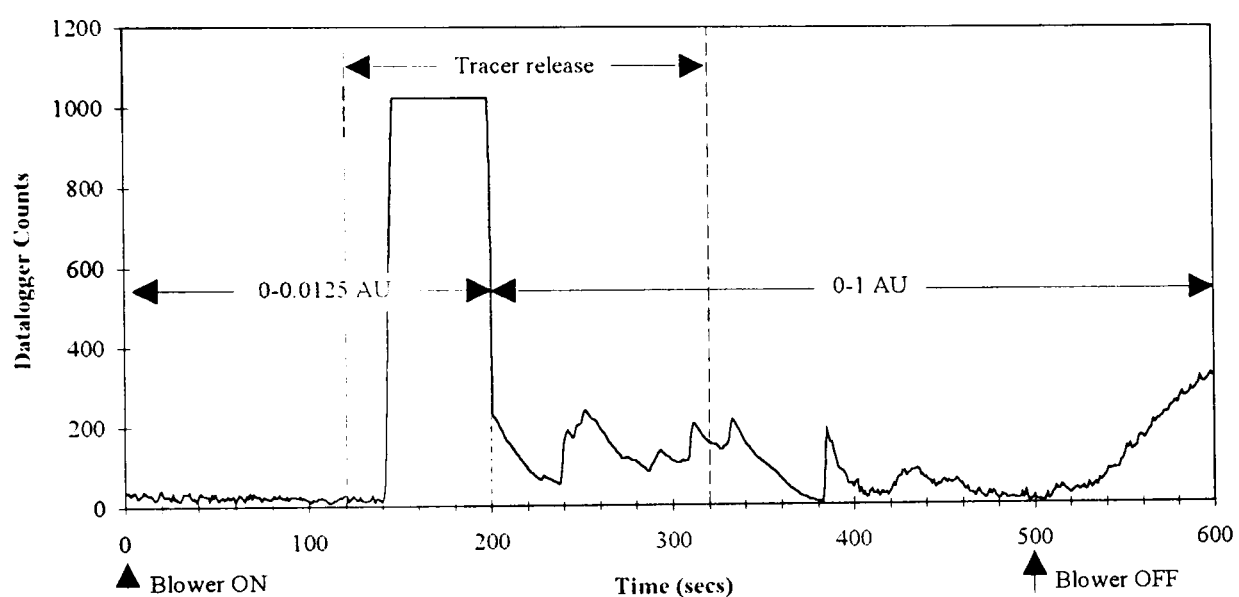


Figure 5.15 Measurement of SF_6 concentration in air sampled by centripetal samplers (100 l/min) 50 mm from the aperture plane. SF_6 released from a Collision nebuliser 100 mm from the plane at 3 l/min (discharge velocity 0.8 m/s) as a carrier gas for KI nebulisation. Cupboard face velocity ~ 0.25 m/s.

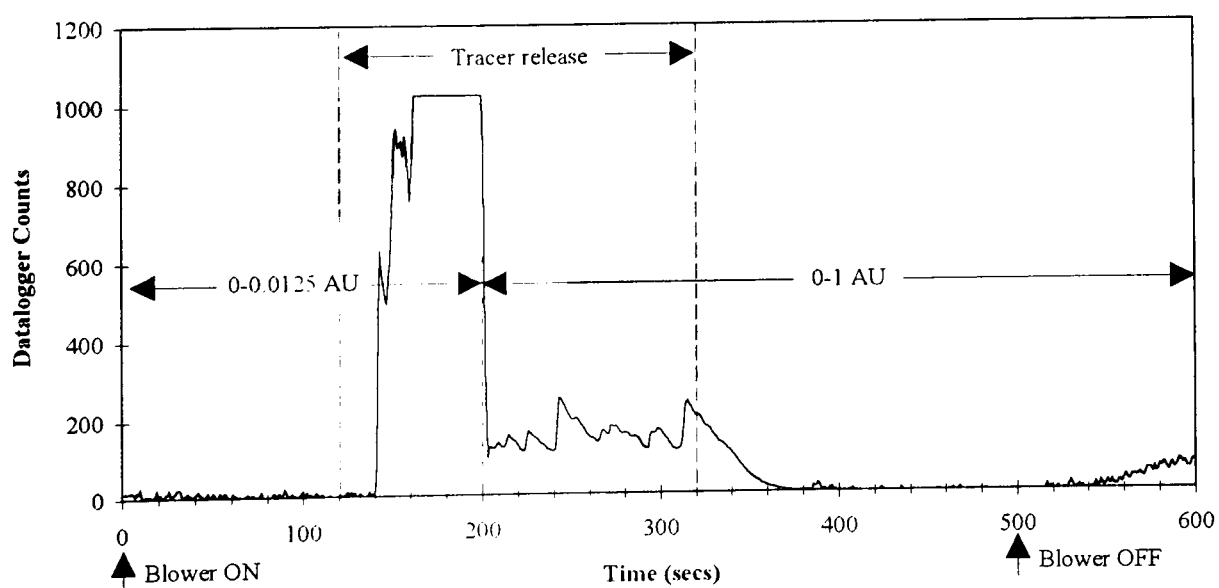


Figure 5.16 Measurement of SF_6 concentration in air sampled by centripetal samplers (100 l/min) 100 mm from the aperture plane. SF_6 released from Collision nebuliser 100 mm from the plane at 3 l/min (discharge velocity 0.8 m/s) as a carrier gas for KI nebulisation. Cupboard face velocity ~ 0.25 m/s.

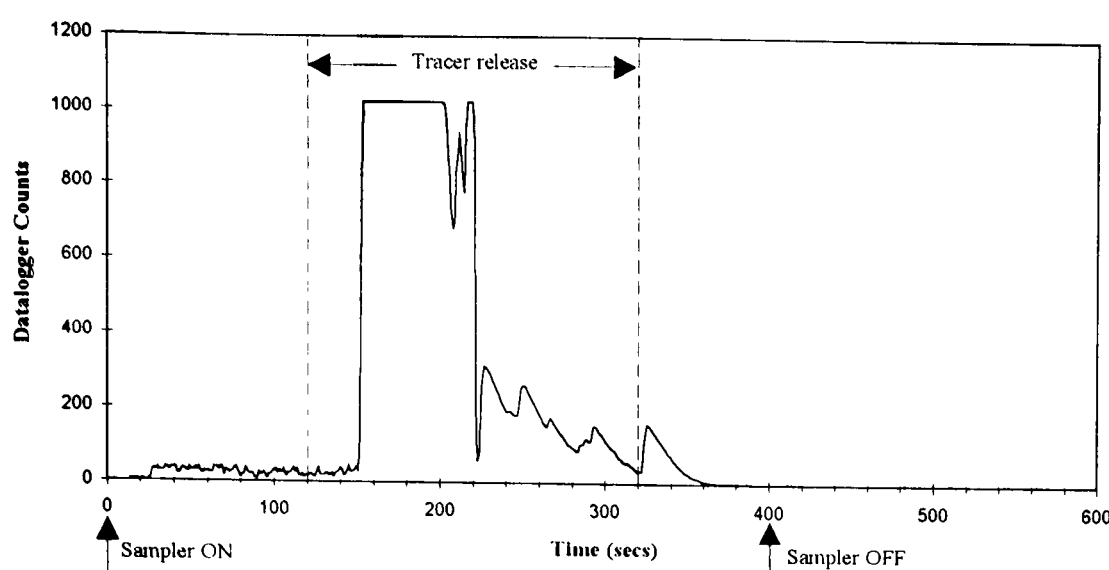


Figure 5.17 Measurement of SF_6 concentration in air sampled by centripetal samplers (100 l/min) 150 mm from the aperture plane. SF_6 released from Collison nebuliser 100 mm from the plane at 3 l/min (discharge velocity 0.8 m/s) as a carrier gas for KI nebulisation. Cupboard face velocity ~ 0.25 m/s.

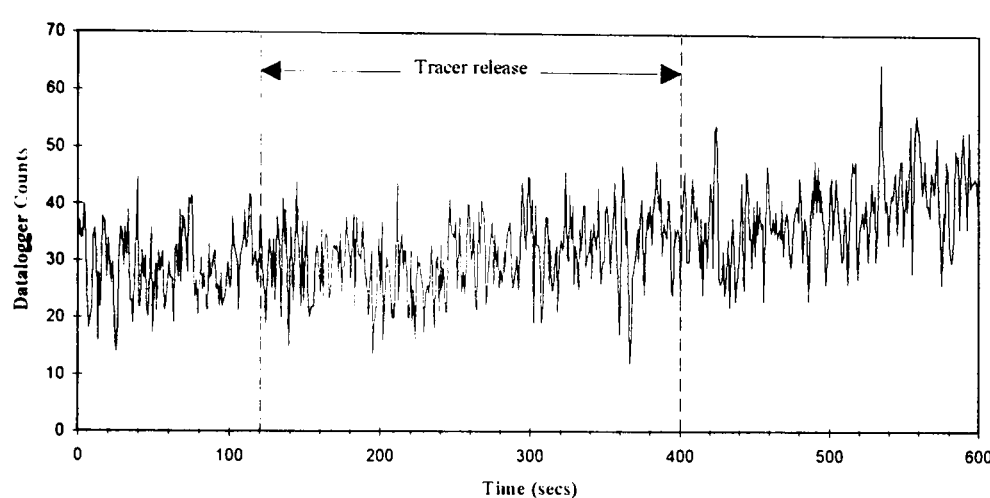


Figure 5.18 Measurement of SF_6 concentration in air sampled through a single probe (BS 7258 : 1994) at 6.8 l/min (5.77 m/s) 100 mm from the aperture plane. SF_6 released from a Collison nebuliser 100 mm from the plane at 3 l/min (discharge velocity 0.8 m/s) as a carrier gas for KI nebulisation. Cupboard face velocity 0.25 m/s.

This discrepancy in the efficiency of the KI-Discus and BS 7258 sampling systems could be due to the much greater flow rate of air drawn through the centripetal sampler and a greater capture velocity. The centripetal sampler used in the KI test system, sampled ~ 15 times the volume of air than the single BS 7258 probe using the gas analyser pump, and a suction velocity theoretically ~ 2.5 times greater, although as measured was ~ 7 times greater. It may also be due to the relatively large bulk of the centripetal sampler, creating a wake in front, which may extend towards the aperture resulting in the entrainment of tracer laden air from a much greater region than the single BS 7258 probe. In terms of the philosophy of BS 7258 : 1994 and BS 5726, the gas probe was used for sampling in the aperture plane of a fume cupboard and the centripetal sampler 150 mm away from the aperture plane of a safety cabinet. The centripetal sampler would possibly sample actual leakages 150 mm from the aperture plane but also potential leakages near to the plane as well.

KI particles were sampled in all the tests but there was a background hue on the filter discs (Table 5.15). For samples at 50 mm there was a dark background, at 100 mm a lighter brown background and at 150 mm no shaded background. This was similar to the earlier results with just particle sampling. With increasing distance from the nebulizer the size of the

spots increased and were much clearer. It was possible, that solution in vapour form was being carried by the gas and not evaporating into single particles, perhaps staining the filter medium.

	Discharge		Face	Distance of equipment		No.	Comments on spot size & background colour
	Flow	vel	velocity	from plane of aperture		spots	
	l/min	m/s	m/s	nebulizer	(mm) Sampler		
	2	0.55	0.25	100	100	?	very faint
	2	0.55	0.25	100	100	29	just visible
	2	0.55	0.25	100	100	29	darker brown background
	3	0.8	0.25	100	50	TNC	lighter brown background
	3	0.8	0.25	100	100	218	varied sizes
	3	0.8	0.25	100	100	398	
	3	0.8	0.25	100	100	539	darker brown background
	3	0.8	0.25	100	100	359	
	3	0.8	0.25	100	150	14	dots bigger
	3	0.8	0.5	100	150	0	

Table 5.15 Number of KI particles sampled simultaneously with SF₆. TNC: too numerous to count

5.14 Comparison of sampling procedures during building re-entrainment

On occasions there was re-entrainment of tracer, discharged from the fume cupboard to the outside, back into the test room. During the release of SF₆ and KI simultaneously during a test, there was a raised background level of KI particles but not of gas tracer. This suggested that either the gas was stripped from the air due to rain (though this would be thought to affect the particles more than the gas), or there was a substantial difference in challenge, the gas tracer being diluted below measurable quantities. This indicated how sensitive the KI particle challenge test was.

5.15 Discussion and conclusions

The air flowing into and within class I microbiological safety cabinets and conventional box type fume cupboards was similar, having large recirculation zones on the work surface and behind the sash. They differed from the less turbulent aerodynamic fume cupboards in which much of the recirculation zones were eliminated or controlled due to the addition of rear baffles and "aerodynamic" features. All these types of facilities had been shown to have variable levels of containment of aerosols when tested using the BS 5726 : 1992 : part 1 method both on site and in a test room.

However, from observation of the air flows in class I safety cabinets it would be expected that measurements in the plane of the aperture of such cabinets using the gas tracer test method in BS 7258 : 1994 : Part 4 would result in tracer being sampled near the edges. Conversely, the use of this method for assessing safety cabinet performance would be limited to cabinets ducted to the outside and would be impossible for assessing those cabinets which were designed to recirculate exhaust air back into the room as the exhaust HEPA filters would not prevent gas penetration.

The use of particle tracers for assessing fume cupboards was considered possible if they were within the size range which constituted a respirable hazard and also remained suspended in the airflow long enough to be a challenge to containment. When development of a quantitative test method for incorporation into BS 7258 : 1990 was considered, the KI test, being used routinely for testing safety cabinet performance according to BS 5726 : 1992, was put forward as a method (Clark et al., 1984). Despite its applicability, the BS committee pursued a gas tracer method instead, and the KI test method was still used for assessing fume cupboard performance as part of service contracts for assessing safety cabinet performance.

In this chapter, the KI test method according to BS 5726 : 1992 : Part 1 was used as a containment test method for fume cupboards, treating them as being similar to class I safety cabinets. This showed that the disposition of the test equipment was important as the fume cupboard had a larger aperture than a safety cabinet, and in aerodynamic cupboards with front lipfoils and rear baffles there was a stratification in air flows which did not mix vertically. Having the KI source on the work surface identified poor cupboards but did not necessarily challenge the entire aperture, especially at the periphery of the aperture such as near the sash handle where potential leakage could occur. It did show weaknesses in regions of recirculation in conventional box type cupboards and also poorly fitted lipfoils on aerodynamic cupboards. This has also been shown by Clark (1989). However, on one occasion there was obvious leakage from beneath the lipfoil shown by flow visualisation but this was not sampled by the normal sampler positions.

As the working aperture of a fume cupboard was substantially larger than those of safety cabinets the artificial arm was considered an insignificant challenge, not disturbing the airflow enough to have a measurable effect, and so was not used. A repeatable disturbance to the fume cupboard containment was achieved using a nitrogen jet which carried air out of the aperture. This showed that the relative disposition of test equipment was inadequate where a challenge from the work surface did not identify a substantial leakage from near the sash and vice-versa. For further testing the KI source was positioned at either of three heights or for repeated tests at one position in the horizontal midline of the aperture. With the source and samplers in these positions it was concluded for a complete test that the KI challenge should come from the work surface, the mid aperture and the region of the sash foil and air sampled at three heights level with the lipfoil, at mid height and level with the sash foil. Ultimately for larger apertures this should be repeated at the left and right sides or have two samplers at each height. This was similar to the lateral disposition of the BS 7258 equipment.

Theoretical correlation of the BS 7258 test method and the KI test method was possible if the equipment was in the same positions for each method. It was also possible, if the equipment was in the position of BS 7258 and the KI test, by interpolation of the amount of tracer sampled at fixed distance from the sash plane to the plane itself. However this made the assumptions that i) the generation of tracer would have no effect, ii) particles would

diffuse and disperse as a gas, and iii) whatever tracer was sampled at a fixed distance from the plane of the aperture by the KI method, this would also be sampled in the aperture plane itself using the BS 7258 method.

Adopting the philosophy of BS 7258 : 1994 : Part 4 for the disposition of the KI equipment, sampling in the aperture plane, was shown not to be possible due to ^{to} saturation of the samplers with KI particles. This was assumed to be due to the particles being propelled at the aperture (the challenge) and to the bulk of the centripetal samplers. It was considered that the position of the KI equipment relative to the aperture plane should be as for BS 5726 and that this had greater similarity to the philosophy of ASHRAE 110 and DIN 12 924 methods for assessing fume cupboard performance.

It was shown that reducing the face velocity of the aerodynamic fume cupboard in the test room gave very different containment results between the BS 7258 : 1994 : Part 4 and the KI method. At a face velocity of 0.25 m/s there was a substantial leakage of KI particles whereas there was no gas tracer measured in the plane of the aperture. This showed that for the cupboard, which was operating in a stable environment there was no challenge of containment by the gas test but the plane of the aperture was actively challenged by particles being thrown out of it. For higher velocities, the inflow of air was enough to prevent the particles from being thrown out of the cupboard but brought gas seeded air below the sash handle so that gas tracer was sampled there.

The aerodynamic fume cupboard was modified resulting in recirculation zones behind the centre of the front lip and at the left and right edges. This was very obvious using fog visualisation. Using the BS 7258 test method, gas tracer was sampled from a source placed in position P2 near the vertical centreline of the lipfoil. With KI generated in the cupboard vertical centreline at its lower position no particles were sampled above the background. Again using the BS 7258 test method no tracer was sampled when released from position P3. However tracer was sampled when a probe was placed very near the corner. It was evident that tracer was passing beyond the plane of the aperture. However, no KI particles were sampled above the background count when the equipment was placed near this region.

From these experiments, the theoretical assumption of interpolating the measurements of tracer 150 mm from the plane of the aperture to the plane itself and correlation with the BS 7258 method was not applicable practically. It could not be assumed that whatever was sampled 150 mm from the aperture plane would be equivalently sampled in the plane itself, that whatever was sampled in the plane would leak out and diffuse, and that the mechanism of tracer generation had no effect. It would seem from these experiments that the fundamental philosophies of the two test are too different for the results to be correlated.

5.16 Key interim conclusions

- Correlation of the BS 7258 : 1994 : Part 4 gas tracer method and the BS 5726 : 1992 KI method for testing fume cupboards was not practicable due to fundamental differences in the tracer used, its method of generation, the disposition of equipment and the sampling methods. The philosophy of the BS 7258 test was to detect potential leakage, the BS 5726 to detect actual leakage.
- For testing fume cupboards using the KI- Discus equipment, the BS 5726 : 1992 : Part 1 method for assessing class I cabinets was modified so that the KI challenge was generated 100 mm from the plane of the sash at work surface height, the mid aperture and the region of the sash foil. Air was sampled through one sampler, 150 mm from the plane of the sash at three heights level with the lipfoil, at mid height and level with the sash foil. For larger apertures, >1.2 m wide, the test was repeated at the centre of the left and right sides.
- Assessing the containment performance of an aerodynamic fume cupboard in a test room using the modified KI method and the BS 7258 : 1994 : Part 4 gas tracer method showed that at a low face velocity, 0.25 m/s, only KI particles were sampled but at 0.85 m/s only gas tracer was sampled. As there was no criteria for a minimum face velocity in BS 7258 then this may be experienced on site and testing using the KI method would indicate a failure, the gas test not necessarily so.

Chapter 6 The application of computational fluid dynamics (CFD) for assessing open fronted containment facilities

6.1 Introduction

6.1.1 What is CFD and how is it used?

Computational fluid dynamics (CFD) is a numerical tool for solving complex fluid flow problems, both supporting and complementing pure experiment and pure theory (Wendt, 1992). The CFD techniques in use today evolved from techniques developed in the 1960's in response to the stimuli of the 'high-technology' aerospace and nuclear power industries. These techniques are now applied to the fields of:

External aerodynamics/hydrodynamics of cars, ships, aircraft etc.

Chemical and process plant, mixing vessels, cyclones, furnace etc.

Thermal hydraulics of nuclear reactors, steam generators, condensers, etc.

Metallurgical processes, strip casting, steel making, solidification.

Internal combustion engines, turbines, reciprocating engines.

Heating, Ventilation and Air Conditioning (HVAC) and the built environment.

Its development has been intimately related to advances in computer hardware, as CFD solutions generally require the repetitive manipulation of thousands, or even millions, of numbers - a task which is humanly impossible without the aid of a computer.

Its application to the built environment enables the user to simulate and analyse air flow, associated heat transfer by convection, conduction and (to a limited extent) radiation, and contaminant dispersal within and around buildings with the objective of improving and optimising the design of new or existing ventilation systems. For the purposes of this study, a PC based software from Flovent (Flomerics Ltd.) was used.

With this software, the user has to input basic data into the computer, via a graphical user interface, to describe the architectural features of the work area/building in 2 or 3 dimensions, the ventilation system (values for inlets and outlets etc.), the internal details (values for temperature etc.) and the properties of the fluid (density, viscosity, specific heat etc.). The user then has to specify whether the solution is steady state (i.e. continuous operation) or transient in behaviour, and that it involves laminar or turbulent flow. From this the software can simulate:

- Natural, forced, or mixed convection systems.
- Problems involving heat transfer within the air, within solid materials, or in both simultaneously (i.e. conjugate heat transfer).
- Heat transfer by convection (within the air), by conduction (within fluid or solid materials), and by radiation between identified surfaces of solid items.

- Contaminant dispersal.

The information from a simulation can then be displayed as vectors, contours or fills. The air flow, temperature and contaminant distribution may be analysed qualitatively or quantitatively, by extracting numerical data and processing this separately using, for example, a spreadsheet.

6.1.2 What are the fundamentals behind CFD?

CFD involves solving the fundamental governing equations of fluid dynamics, the continuity, momentum and energy equations, which are the mathematical statements of the three fundamental principles upon which all of fluid dynamics is based (Anderson, 1992)^{abc}.

Conservation of mass

$F = ma$ (Newton's second law)

Conservation of energy

These governing equations can be obtained in various mathematical forms each of which is important to CFD. In their most general form they are usually a coupled system of non-linear partial differential equations. For air flow simulation, these equations are solved using the field variables:

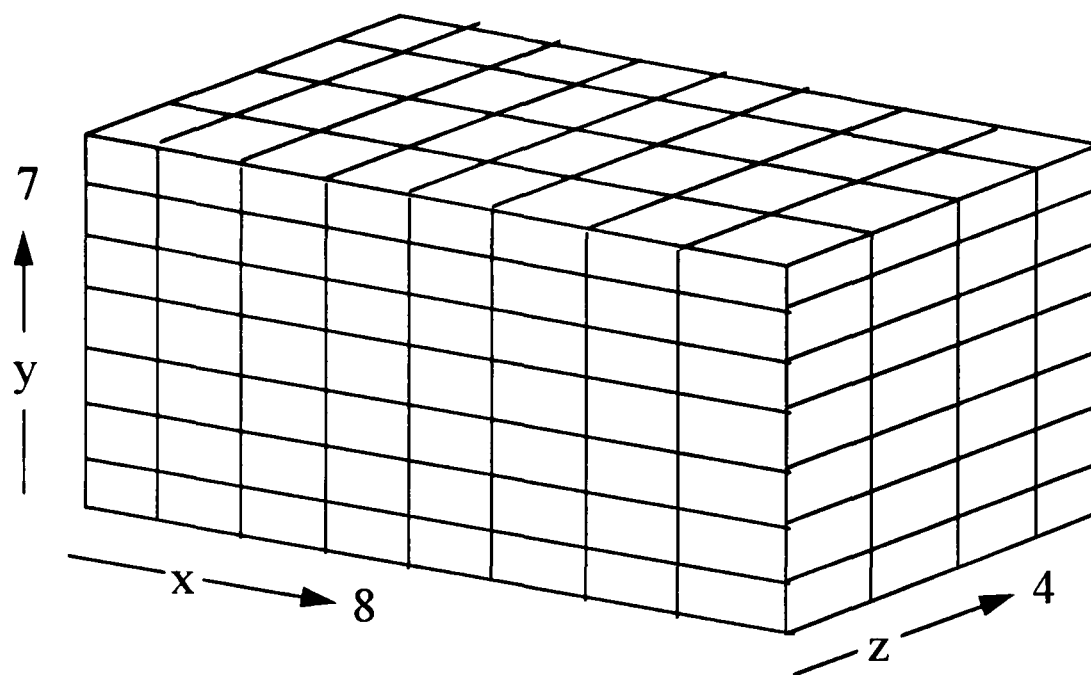
- * u , v and w , the velocity resolutes in cartesian co-ordinate directions x , y and z .
- * p the pressure.
- * T the temperature of the air and/or solid materials.

These variables are functions of x , y , z and time. The values u , v and w satisfy the momentum conservation equations in the three co-ordinate directions. Temperature satisfies the conservation equation of thermal energy. The pressure itself does not satisfy a conservation equation, but is derived from the equation of continuity which is a statement in differential form of the conservation of matter.

These governing equations are solved over the domain of the problem set up by the user. In the building environment, the solution domain encompasses the room or enclosure, or region of interest around a specific piece of equipment. In addition to setting the extent of the domain, boundary conditions have to be described by entering the value or fluxes of the field variables at the domain boundaries and setting the properties of the air.

The governing equations are very difficult to solve analytically and CFD is the art of replacing these governing partial differential equations of fluid flow with numbers, and advancing (marching) these numbers in space and/or time by numerical integration to obtain a final

numerical description of the complete flow field of interest. To solve the partial differential equations, the flow field is split up into discrete points forming a grid, and the equations discretised and expressed in algebraic form at each point. This results in a set of algebraic equations for every discrete point, each of which relates the value of a variable at one point to its value at neighbouring points. The equations can then be solved, using either the finite difference method FDM (Anderson, 1992)^{de}, the finite element method FEM (Dick, 1992)^a or the finite volume method FVM (Patankar, 1981)^b, by marching with respect to the space, influenced by the boundary conditions.



Model 1 Example of a solution domain divided up into non-overlapping and contiguous finite volumes - the solution grid

The expressions in algebraic form and their calculation method constitute the code by which a flow problem can be solved. Flovent uses an FVM method. The domain is divided into a set of non-overlapping and contiguous finite volumes so forming a grid of cells (e.g. shown in Model 1 is a grid of 7 x 8 x 4 cells, 224 in total). Starting with the temperature variable T for example (Flomerics Ltd., 1994), an algebraic equation connects T in one cell to its value in its 6 neighbour cells ($T_1, T_2, T_3, T_4, T_5, T_6$) and its previously calculated value (T_0).

$$T = \frac{C_0 T_0 + C_1 T_1 + C_2 T_2 + C_3 T_3 + C_4 T_4 + C_5 T_5 + C_6 T_6 + S}{C_0 + C_1 + C_2 + C_3 + C_4 + C_5 + C_6}$$

where $C_{(0-6)}$ denote the coefficients that link the in-cell value to each of its neighbour cell values. S denotes the terms that represent the influences of the boundary conditions (if any).

If there are a total of n cells in the integration domain, there are n algebraic equations to solve for each of the field variables T, u, v, w, p , i.e. there are $5n$ equations to solve. Thus, for example, for a grid of 50000 cells there are 250000 equations to be solved.

The simulation is calculated by first initialising the fields of pressure, temperature and velocities. Calculation of the conservation equations over the solution domain (outer

iteration) commences with setting up the coefficients (C) for the temperature field T and then solving the algebraic equations for temperature in each cell in the grid by performing a number of calculations (inner iterations), with $C_{(0-6)}$ constant. This is then repeated for the velocity components u , v and w and then the continuity equations solved for in a similar manner and any associated adjustments made to the field variables. This completes an outer iteration at which stage convergence is checked for. Convergence is reached when the error in the continuity between cells within the domain is small relative to a basal level (residual errors). If the residual errors are large however, then the linking coefficients C are adjusted and the algebraic equations solved once more.

6.1.3 What are the limitations and developments?

Although there are similarities between CFD and the finite element method approach used in structural analysis, the variations encountered between different flows and the complexity of the physical phenomena involved have resulted in CFD being a less mature science than the established structural analysis techniques.

Limiting factors still are the development of models for accurately describing turbulence and setting up of a correct solution grid (Janssen et al., 1992; Purtell, 1995). At present the basic $k - \epsilon$, two-parameter (kinetic energy of turbulence, k , and its rate of dissipation, ϵ), turbulence model which has been around for more than twenty years, continues to form the basis for many codes, although its limitations are well known. Work on improved and different models continues but these require comprehensive tuning and developing. A problem area occurs when varying flows within the solution domain require different turbulent models. Also being developed is the adaptive and automatic concentration of the solution grid into regions requiring the most detailed analysis.

Up until recently in the field of CFD there has been the requirement for code developers and users, the latter still requiring extensive knowledge of which code is relevant to the problem and thus which to apply. In setting up the problem there are a lot of choices for the user. Certain physical assumptions about the fluid flow have to be made all of which may be simplifications of reality, such as is it a stationary or transient simulation, is it a Newtonian fluid and is there a no slip boundary? Parameter settings are required such as the discretisation, the mathematical solution technique, relaxation parameters and stop criteria for the iterations. These settings are the choice of the user and all of them influence the result.

There is also the modelling technique which in importance sits between physical assumptions and parameter settings. Modelling is mathematically describing what physically happens. It discharges itself into models of certain levels of complexity and into models with certain limitations. Examples are the different turbulence models and possible wall functions. The choice of complexity is a balance between what is necessary to solve the problem accurately

enough and what can be done. The chosen parameter settings and chosen mathematical models all influence in one way or another the result.

The grid refinement causes the numerical procedure to be more accurate. At the same time it may influence the way in which the boundary layer is calculated. Sometimes an analytical calculation may help in determining the actual boundary layer thickness. However, in complicated situations it is very difficult to estimate the actual boundary layer thickness at different locations of flow.

Recently there have been developments in both hardware and software bringing CFD to the PC. With it this has allowed the development of software for specific applications, thus reducing the number of choices the user must make in terms of parameter settings and modelling techniques, and perhaps separating further the end user from the code developers.

CFD today still requires development and validation and there are numerous meetings to attempt to focus how this field should develop. As the field of CFD develops in the commercial code market, such findings (Fisher & Rhodes, 1996) include that code users require specific training with major emphasis on fluid flow phenomena and less on the detail of numerical techniques. Also for validation, CFD models still require comparison with physical measurements. Measured data show an inaccuracy, inherent in the used measurement technique. However, calculated results show another kind of "inaccuracy", namely questionable physical assumptions, parameter settings and modelling techniques. Thus application of CFD to a physical problem may still involve the following problems of;

- a) Geometry that is inadequately defined because of design changes, program sensitivity to inadequately defined sections and data collection errors.
- b) Boundary conditions of the flow regime that are not adequately defined.
- c) Fluid properties that are not adequately known, especially in cases of multiphase flow, combustion or chemical reaction.
- d) Lack of knowledge of the flow regimes which may be laminar or turbulent, steady or unsteady, subsonic or supersonic.
- e) Uncertain expertise of the analyst, as there are wide variations in the knowledge and expertise of code users.

Ultimately, comparisons of measurements, calculations and interpretations of results requires a good deal of experience and knowledge (Janssen et al., 1992).

As CFD has evolved and become application specific in the commercial sector, its use in the design and development of HVAC systems has increased. However, there is still mistrust by many engineers as to the accuracy of the results considering the assumptions to be made, but as CFD is improved and developed, with closer comparisons with physically reality, it is being

accepted. Areas where its usefulness is apparent has been in the design of animal houses (Hughes et al., 1996), clean rooms and in contamination control, where knowing the distribution of temperature and potential contaminants is a high priority. Recently it has been used in establishing guidelines for laboratory construction in terms of LEV and fume cupboards (NIH, 1995). This looked at how ventilation design may affect containment of a box type fume cupboard. This was achieved, not from the absolute measurement of simulated contaminant dispersal within the domain, but the effect design changes had on the performance of a base model, reducing the need for numerical accuracy.

In this chapter, CFD is used to look at the potential to assess fume cupboard design and to see whether the CFD model can produce accurate results which compare favourably with physical measurements. Also to assess whether it can distinguish cupboard designs based on disturbances and blockages, and then how physical performance assessment methods may differ by this numerical simulation. Finally, CFD is used to look at the simulation of microbiological safety cabinets where especially in class II cabinets the balance of airflow is critical.

6.2 Two dimensional visualisation and analysis of airflows in fume cupboards

6.2.1 Problem set up of an aerodynamic fume cupboard

For the purposes of this investigation, a PC486 DX66 personal computer (PC) with 8mb RAM was used. In the development of the Flovent CFD simulation it was important to build up the model from a simple problem and then increase its complexity. This meant starting with a 2 dimensional problem and a coarse solution grid with few boundary conditions in order to establish the airflow and then increasing the complexity of the boundary conditions and the refinement of the grid and turbulence model.

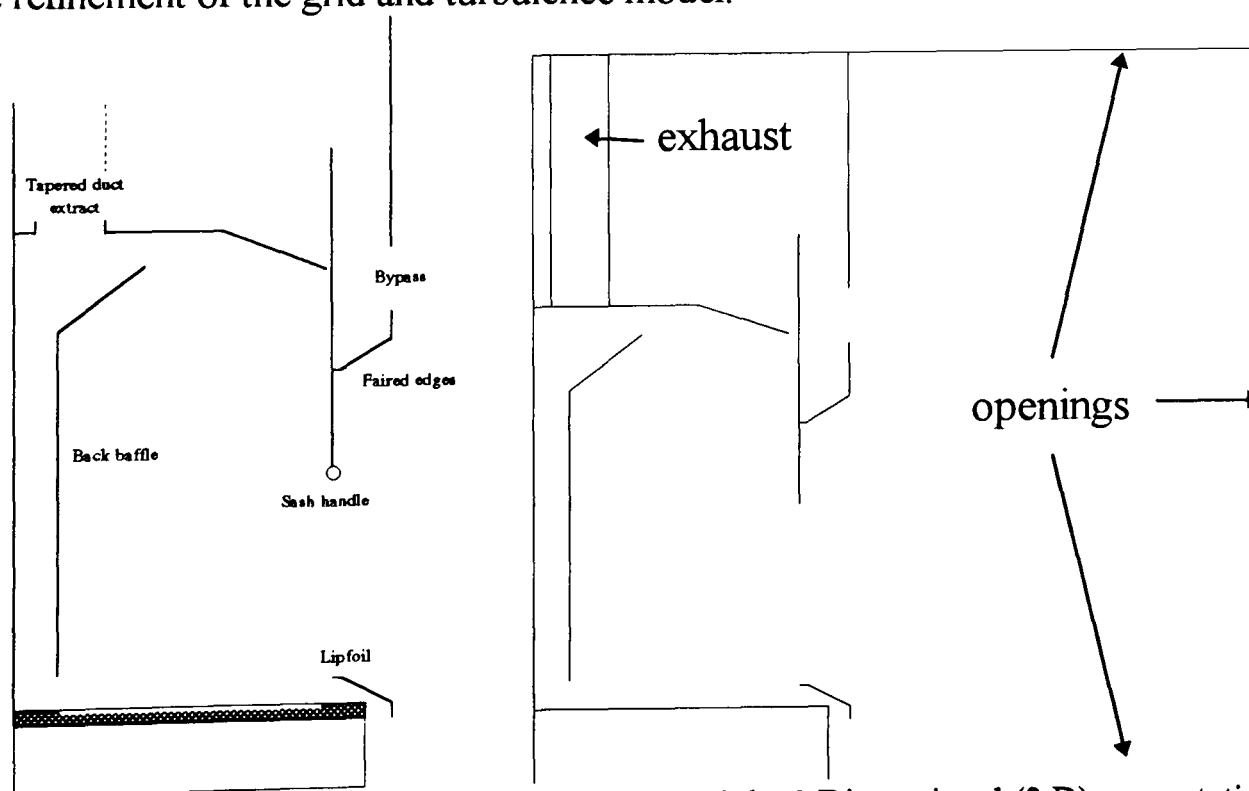


Figure 6.1 Aerodynamic fume cupboard (section 3.2) and the 2 Dimensional (2 D) computational model domain (xy view).

In order to represent airflow into and within a two dimensional aerodynamic fume cupboard the main features were included based on the Fumair fume cupboard used earlier in this study (Fig. 6.1). These included the rear baffle, shaped cupboard roof, bypass and an 'aerodynamic' lipfoil. The lipfoil was represented as thin walls, straight and angled, with a vertical distance of 60 mm between the work surface and the lip. Curves could not be represented. No sash foil was represented in the model. The 2 dimensional solution domain was 1 m deep encompassing the cupboard and part of the room. This room, external to the cupboard had openings specified at the boundaries as passive inlets, as all the air within the solution domain would be exhausted through the fume cupboard. An extract mass flow rate of 0.3 kg/s was used which gave a mean face velocity between the top edge of the lipfoil and the lower edge of the sash of 0.45 m/s. The solution domain was adiabatic at 20 °C and all fume cupboard surfaces were smooth and had no heat transfer.

6.2.2 Effect of turbulence specification and grid refinement

The two dimensional solution domain was overlaid with a grid (38 x 52 cells). This was considered refined enough around the internal surfaces in order to accurately represent flow in these regions, but not too complex which would result in long calculation times (Fig. 6.2). This model was then tested for its sensitivity to the turbulence model settings and to the refinement and density of the grid.

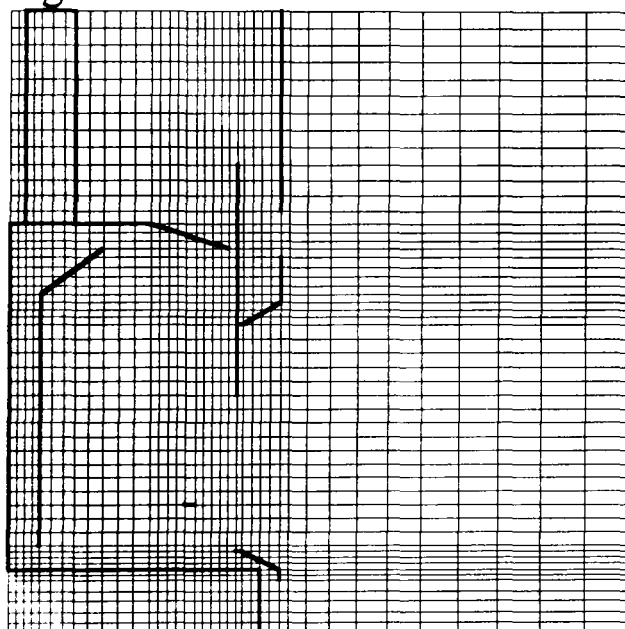


Figure 6.2 2 D Solution grid

Initially a specified turbulent viscosity (revised) value of $0.005 \text{ m}^2/\text{s}$ was chosen based on the air flow through the aperture using the following formula:

$$0.01 \times (\text{density}) \times (\text{characteristic length}) \times (\text{characteristic velocity})$$

This converged quickly (~ 60 mins) to give a flow field similar to that expected in reality (section 6.2.3). The solution was then repeated using a turbulent viscosity value a factor of 4 below and above the initially estimated value and also using the k-ε model. The fixed

turbulent viscosity solutions resolved quickly but the k- ϵ model was substantially longer, both components of the model taking a long time to converge.

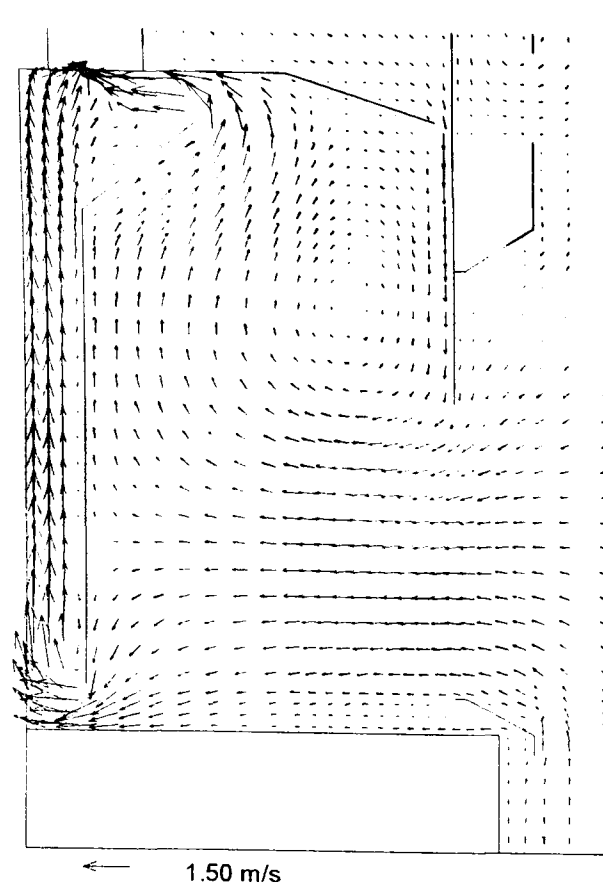
Comparing the results qualitatively (Fig. 6.3) there was little difference between each simulation suggesting no real sensitivity to the turbulence model. By displaying the contour maps over the solution domain for vector speed value (Fig. 6.4) and turbulent viscosity (Fig. 6.5) the solutions were compared quantitatively. There was little difference in vector values between the fixed values for turbulent viscosity and the k- ϵ model. However, there was greater dissimilarity between the contour maps for turbulent viscosity which suggested that the representation of turbulence in the model was dependant on the bulk flow values for turbulent viscosity and not on the turbulent transport between the surfaces and the air; which did not directly involve a fixed value for turbulent transport.

The effect of the turbulent viscosity value was also tested by comparing the x velocity and vector speed values in the plane of the fume cupboard aperture (Fig. 6.6). For each value the profile was different, that using the k- ϵ model gave lower values in the aperture plane and a flatter profile than the fixed value simulations. The solution was concluded to be sensitive to a fixed value for turbulent viscosity based on quantitative comparisons and hence the k- ϵ model was used even though this meant longer solution times.

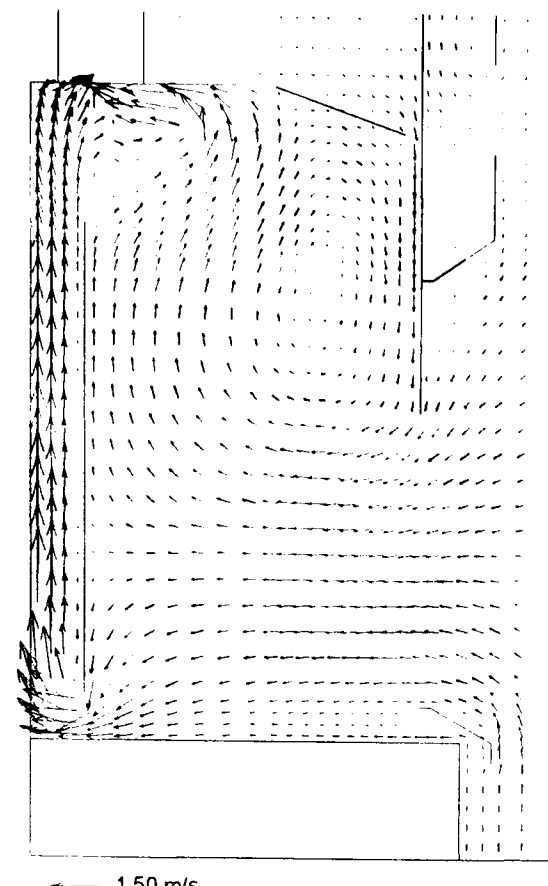
The solution was then tested for dependence on grid refinement. This became a trade off between the accuracy of the solution and the time taken for convergence. There was a point where further grid refinement did not necessarily increase accuracy but substantially increased the solution time. The grid was refined around the important cupboard features, made 'coarser' and made 'complex' (Fig. 6.7).

Qualitatively there was little difference between the vectors for each grid refinement in terms of 'visualisation' of the airflow (Fig. 6.8) and quantitatively in terms of speed contours (Fig. 6.9) and turbulent viscosity contours (Fig. 6.10). Comparing the x velocity and vector values in the plane of the sash showed that increasing the grids complexity increased the values near to the lipfoil and the edge of the sash (Fig. 6.11). This was also shown by refining the 'medium' density grid near to the cupboard surfaces where there was little difference between the 'medium' grids near to the lipfoil and the mid aperture but values near to the sash edge were closer to the very 'complex' grid values for the refined 'medium' grid. The unrefined 'medium' grid produced lower values beneath the lipfoil than the other grid densities or refinements.

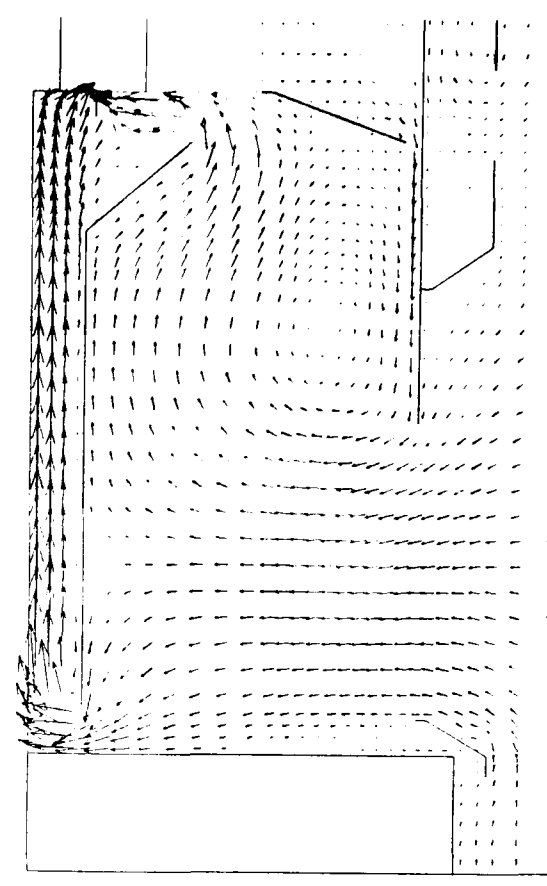
It was concluded that grid density and refinement affected the values near to the cupboard surfaces and in order to not have long solution times as with the very 'complex' grid, the refined 'medium' grid was used.



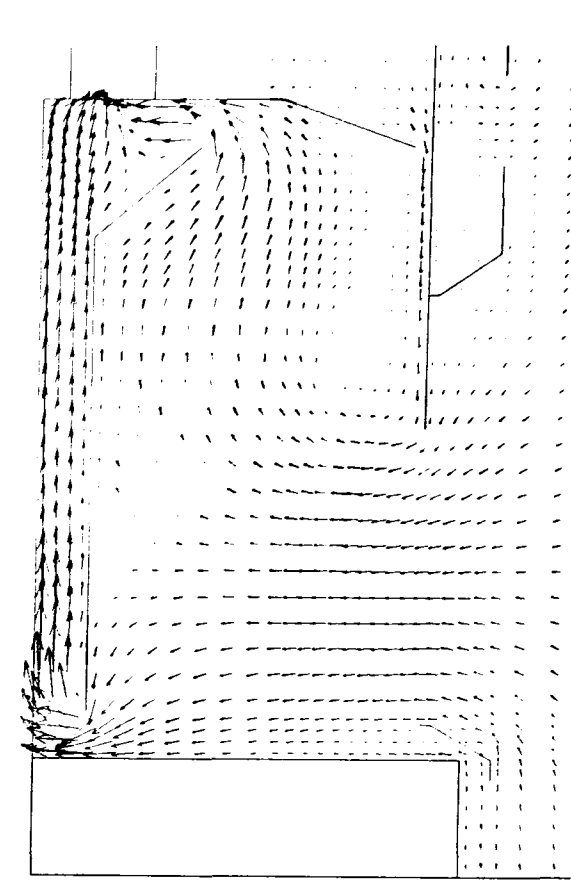
Fixed turbulence 0.005
(revised model)



Fixed turbulence 0.001
(revised model)

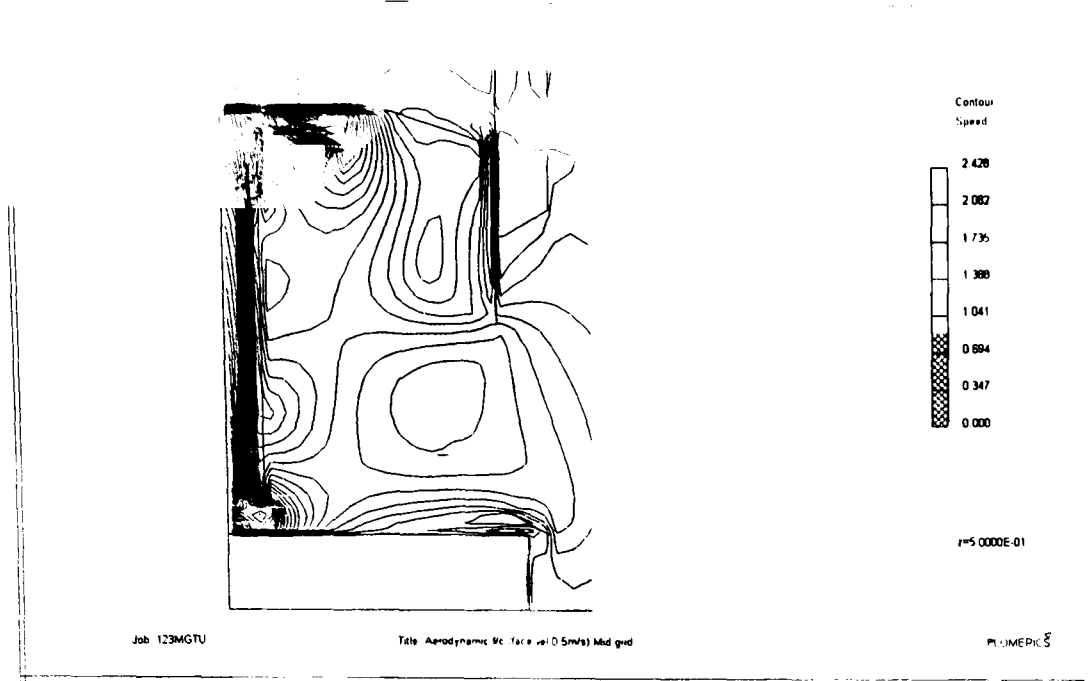


Fixed turbulence 0.02
(revised model)

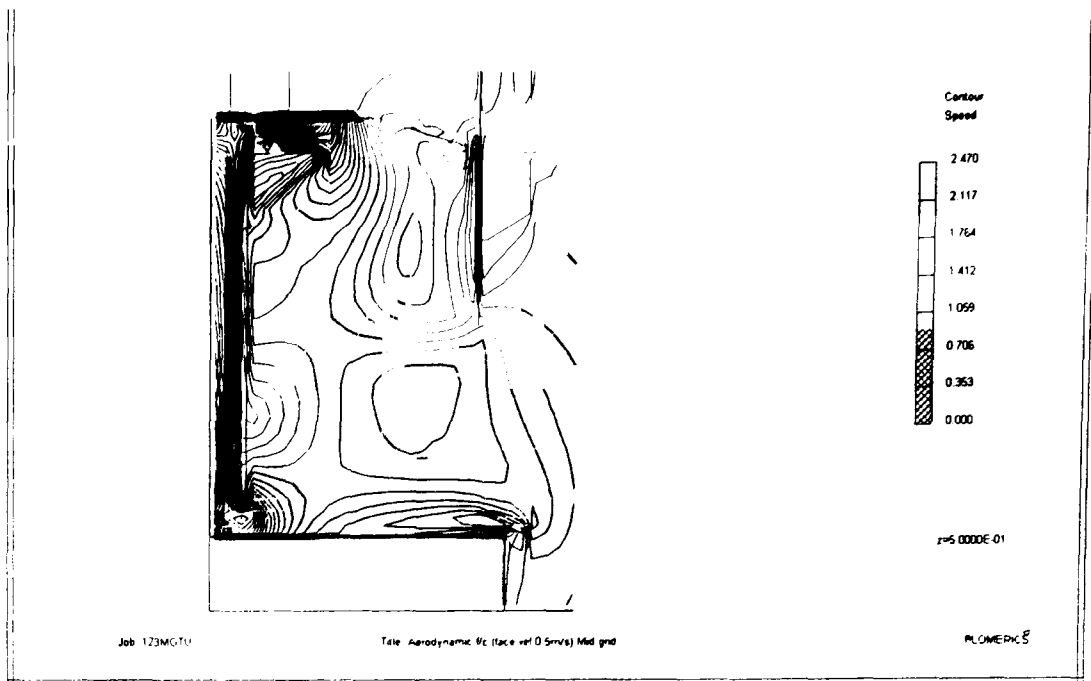


K- ϵ model

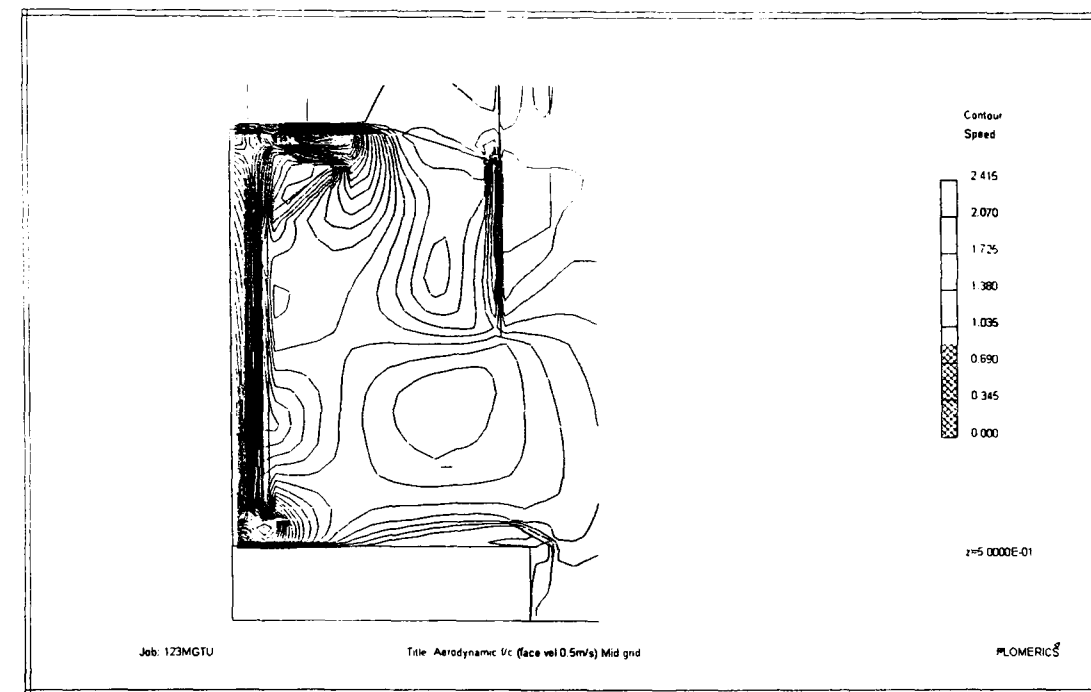
Figure 6.3 Effect of the turbulence model on the airflow vectors (2 D).



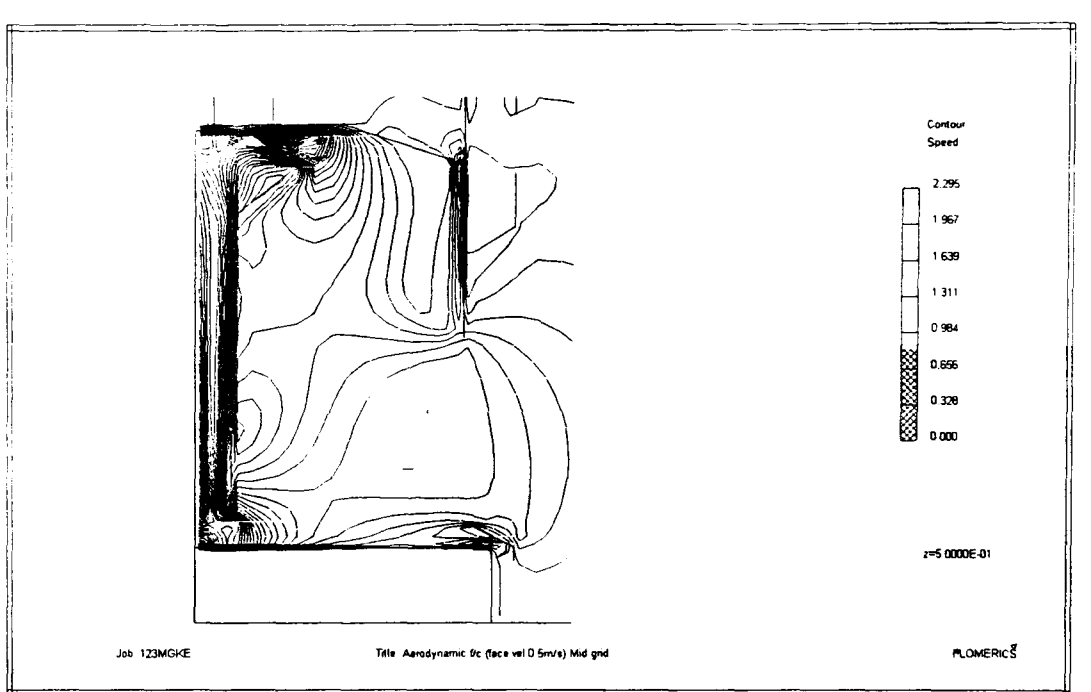
Fixed turbulence (revised model) 0.005



Fixed turbulence (revised model) 0.001

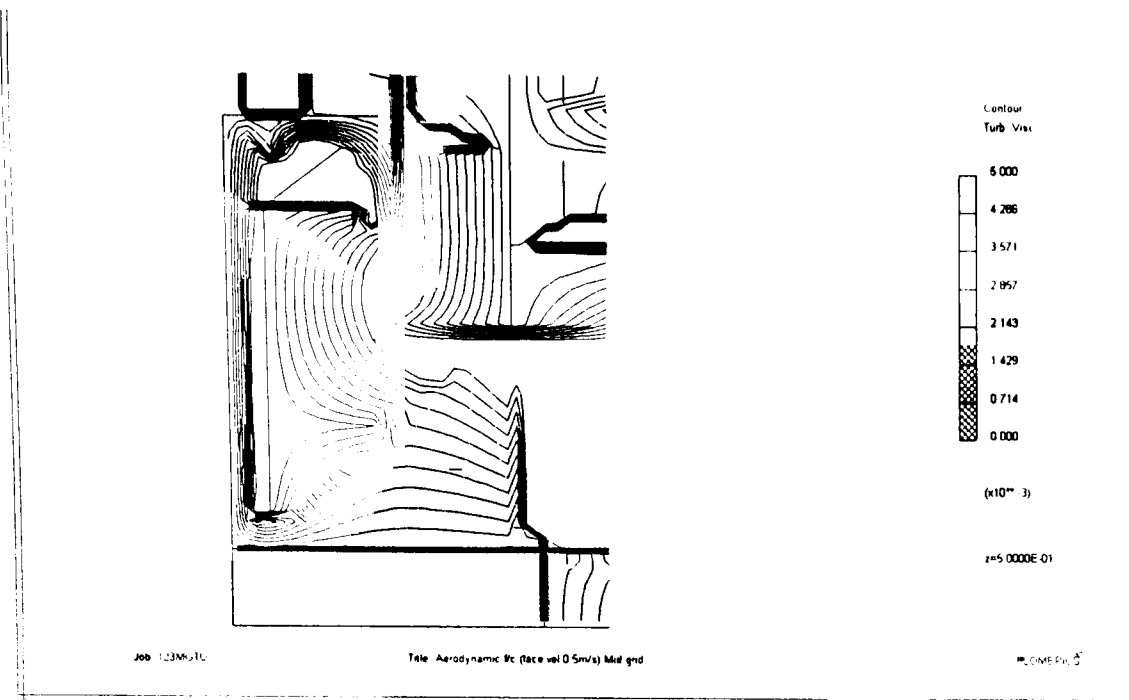


Fixed turbulence (revised model) 0.02

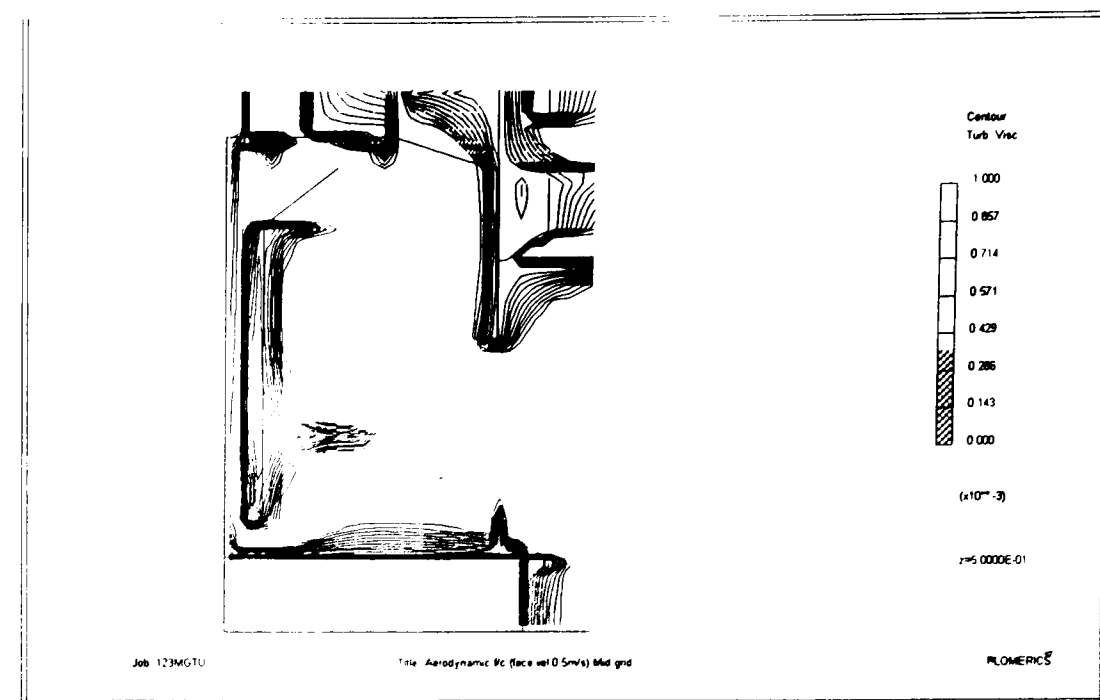


K-ε model

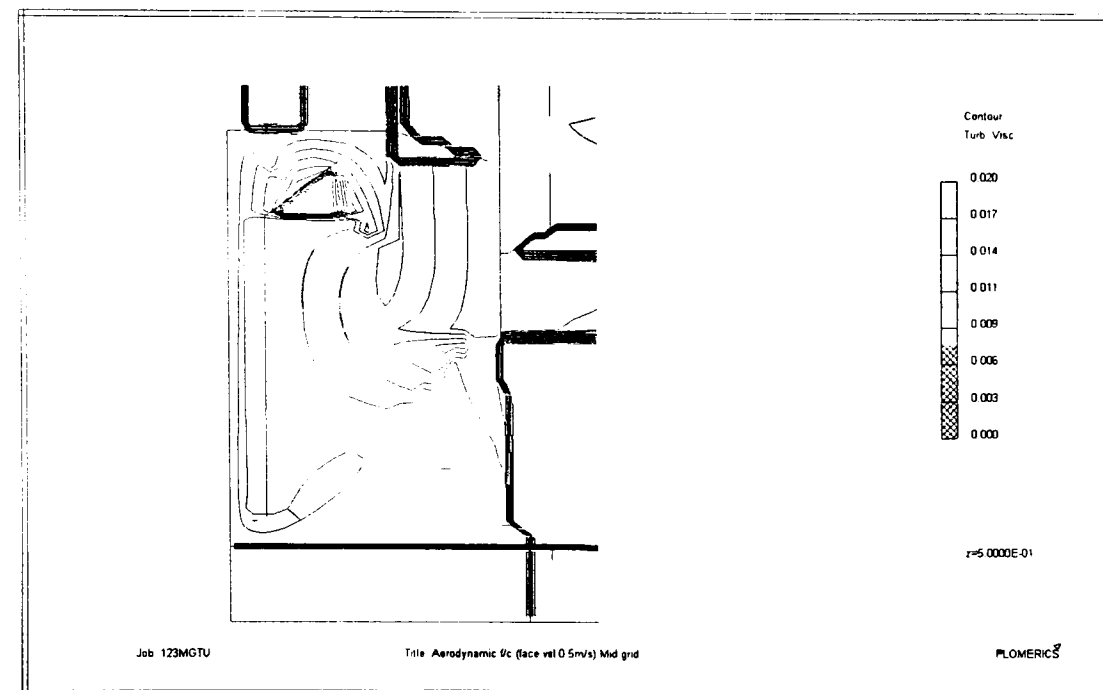
Figure 6.4 Effect of the turbulence model on the airflow speed value contour (2 D).



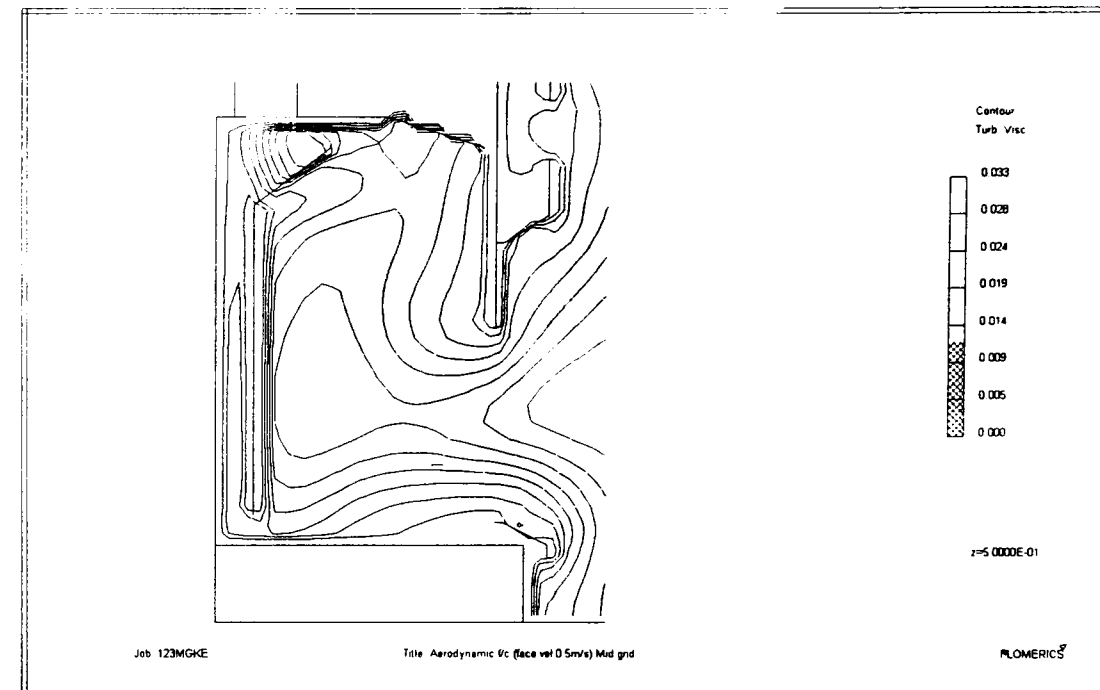
Fixed turbulence (revised model) 0.005



Fixed turbulence (revised model) 0.001

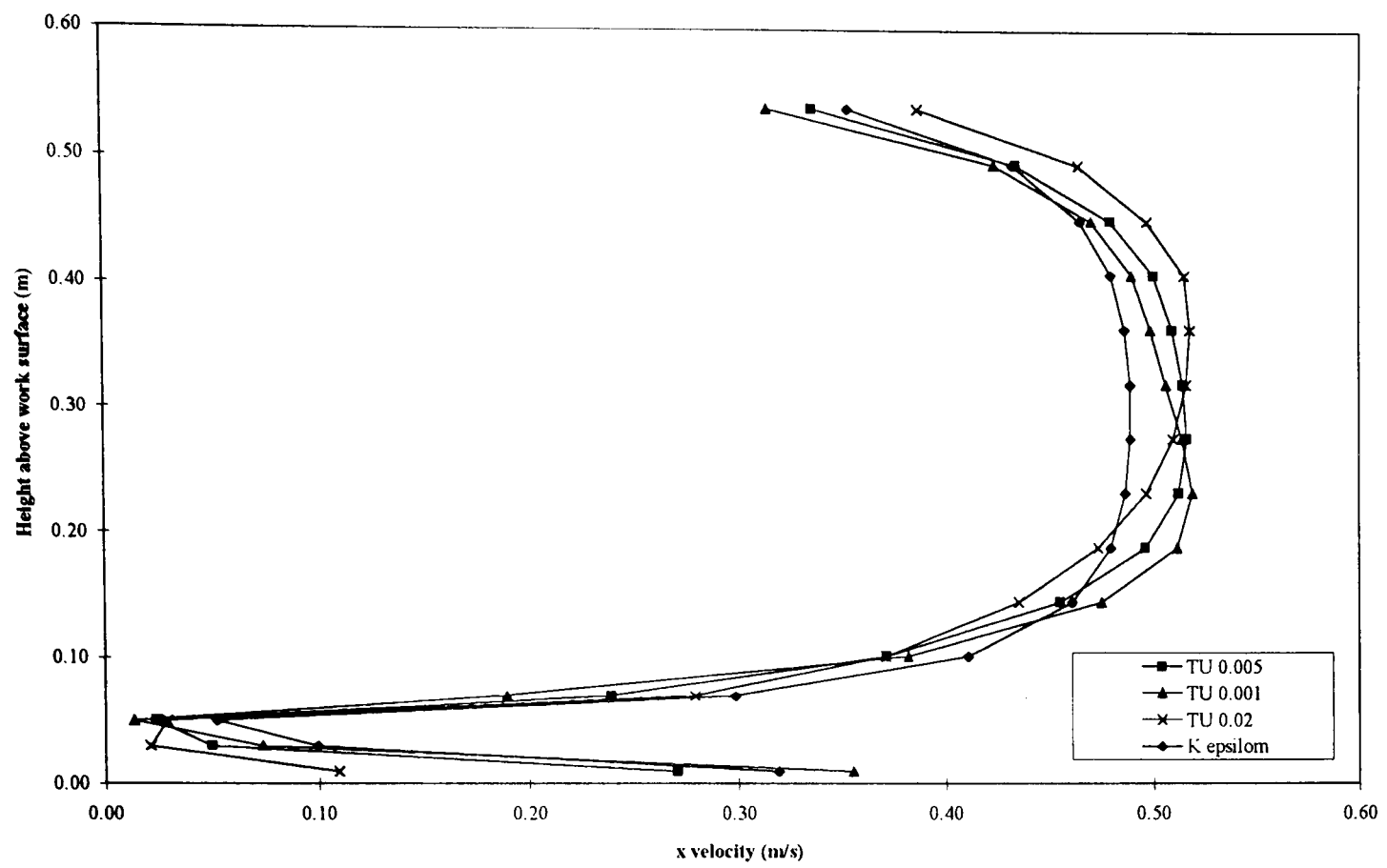


Fixed turbulence (revised model) 0.02

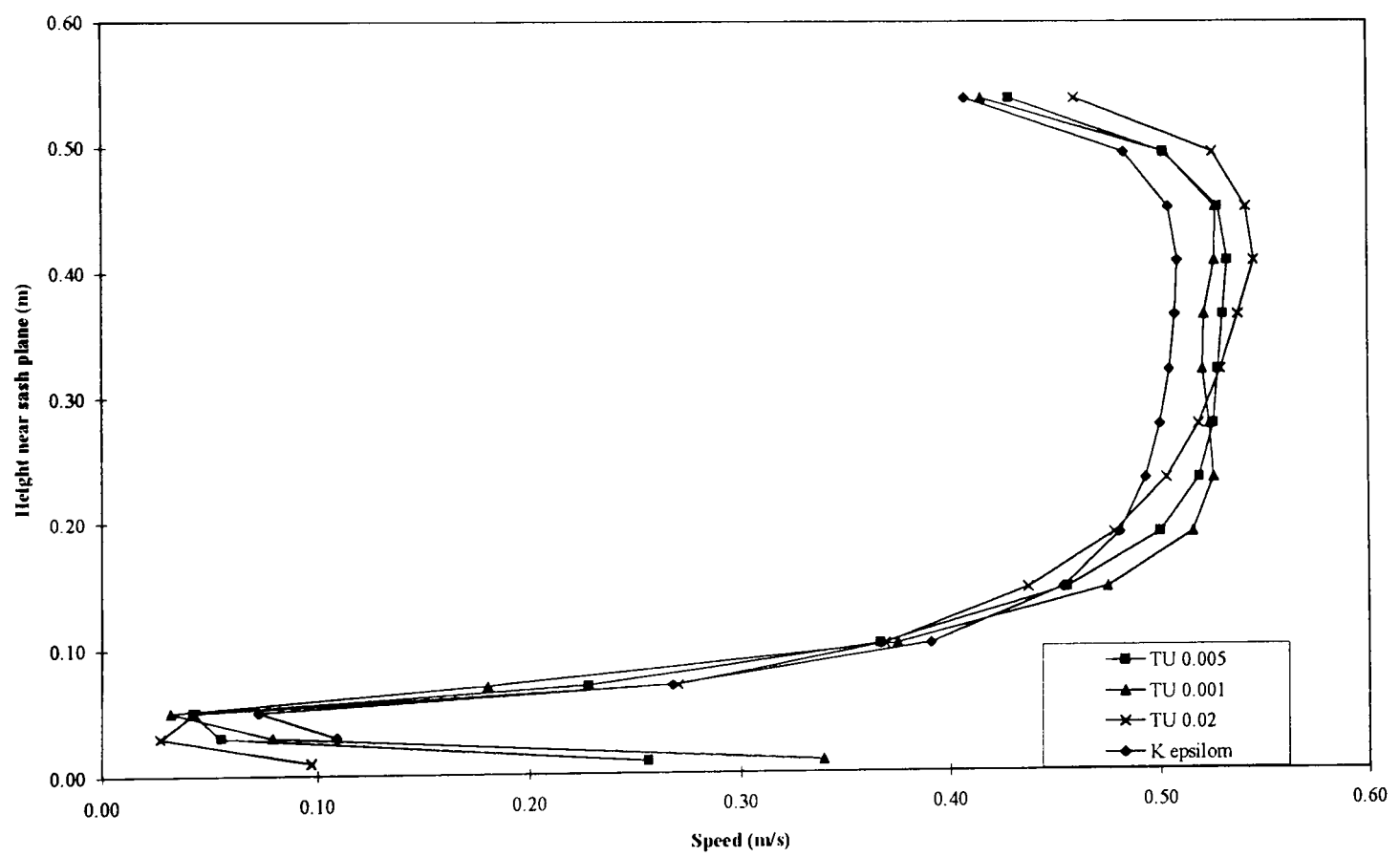


K- ϵ model

Figure 6.5 Effect of the turbulence model on the turbulent viscosity contours (2 D).

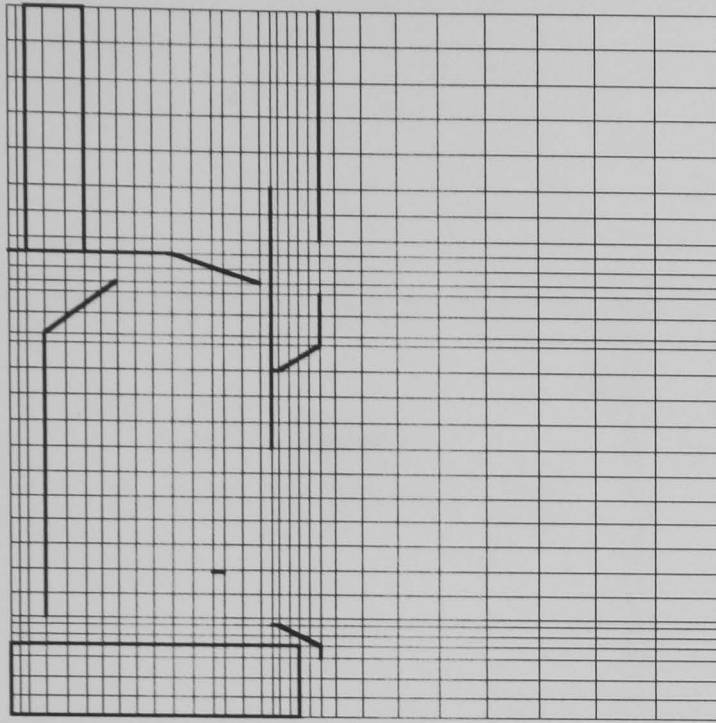


x velocity

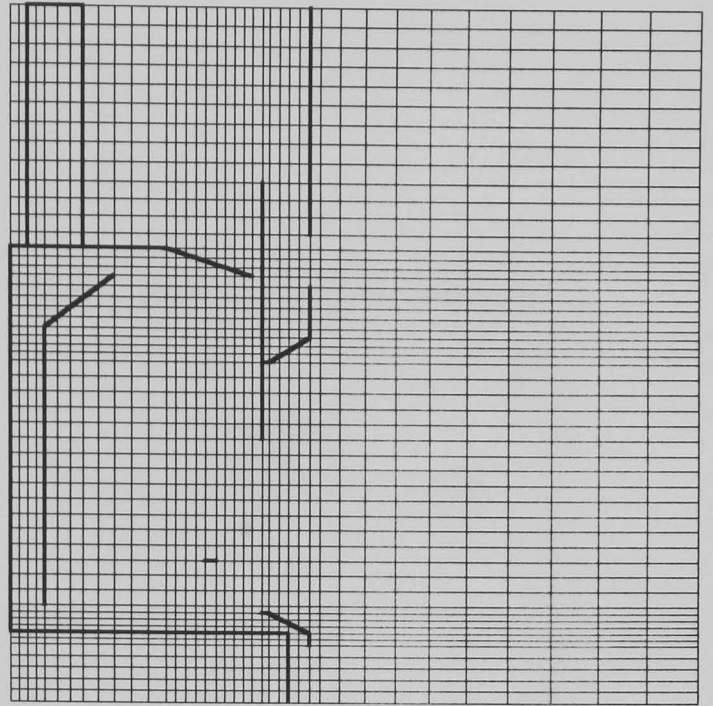


Speed profile

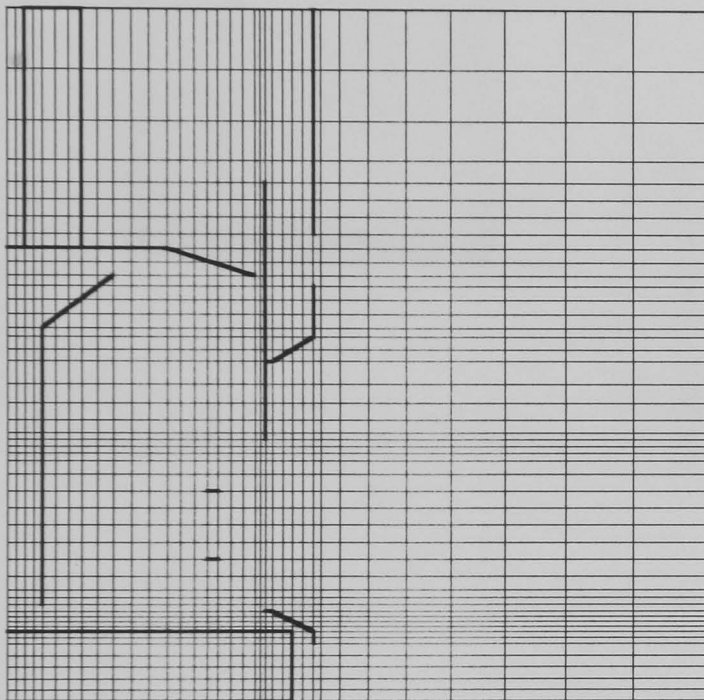
Figure 6.6 Effect of turbulence model on vertical x velocity and speed profiles in the aperture plane (2 D). (TU, fixed revised turbulence model; k ϵ , turbulence model).



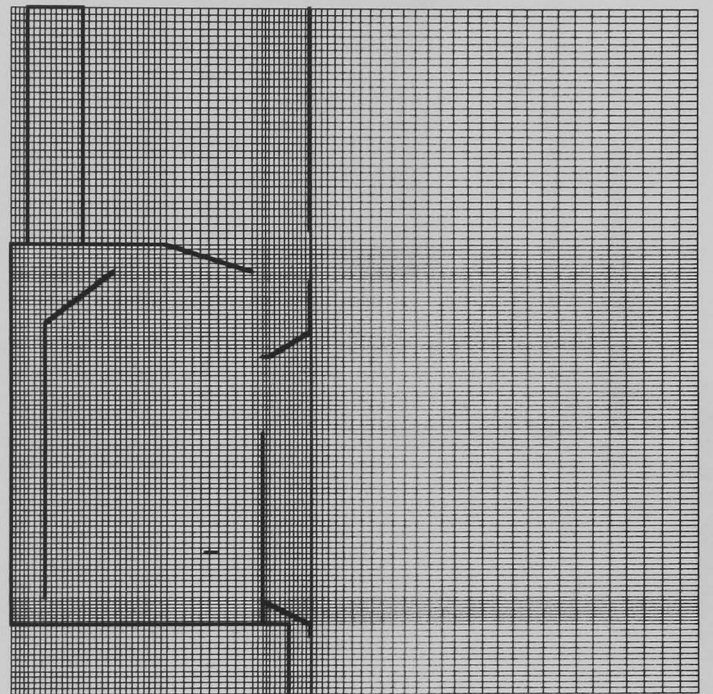
'Coarse' grid



'Medium' grid

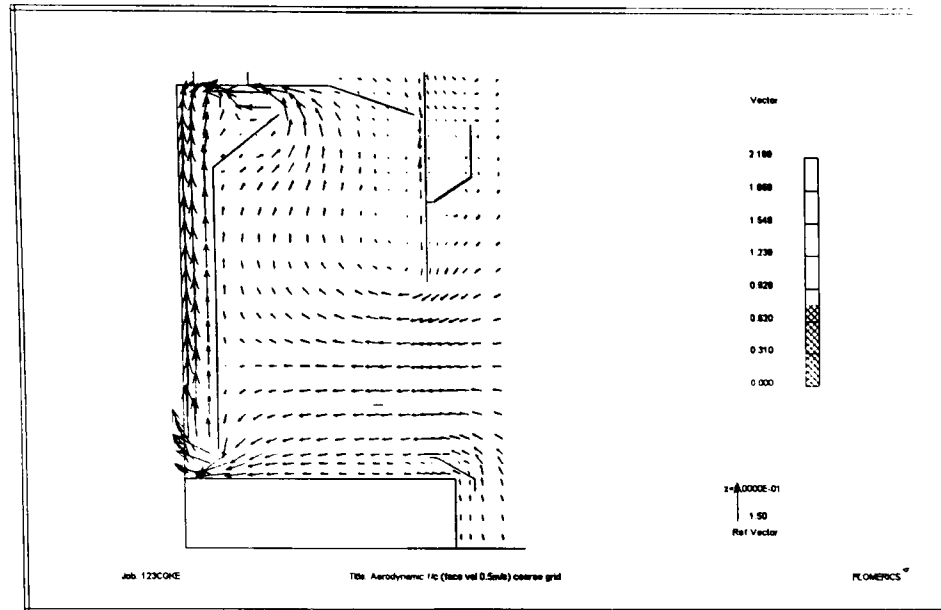


'Medium refined' grid

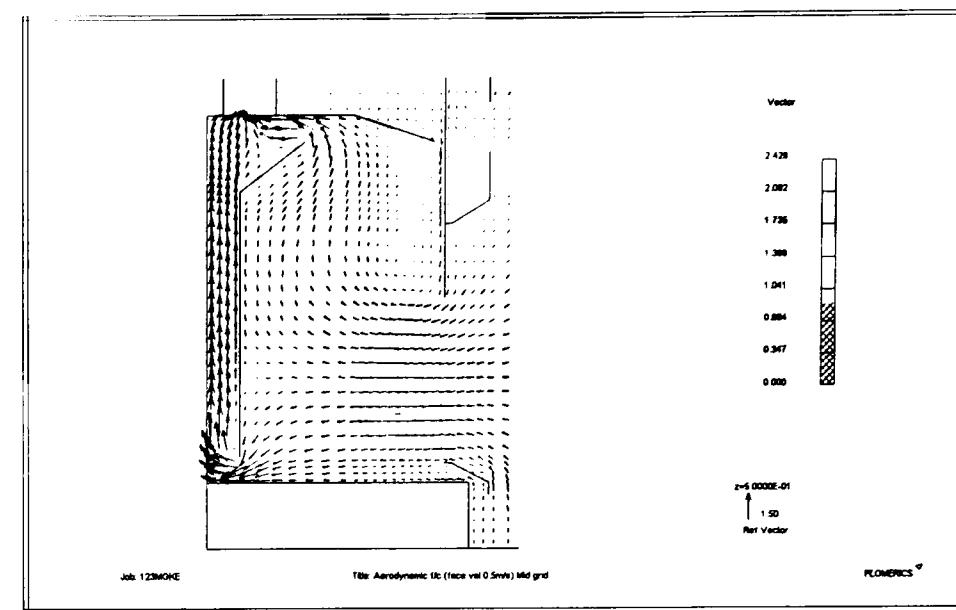


'Complex' grid

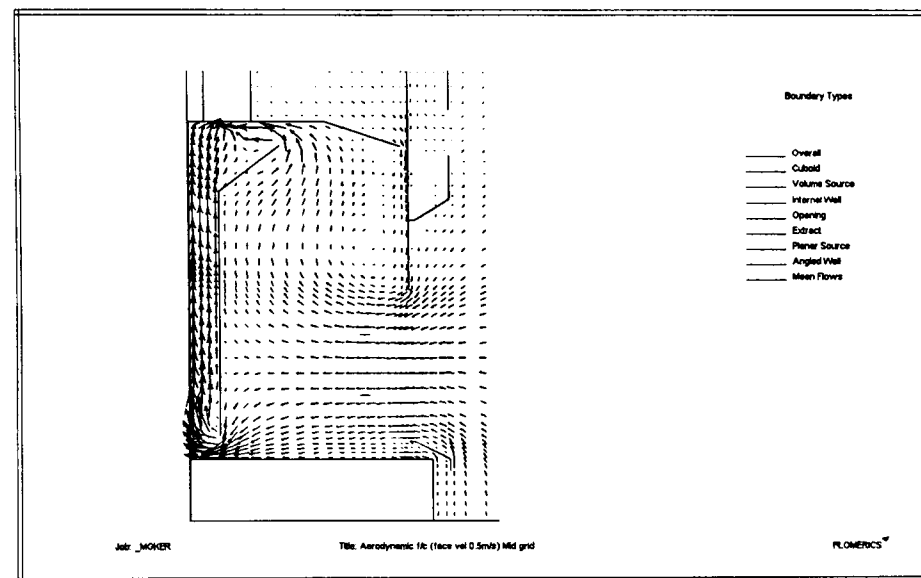
Figure 6.7 Density and refinement of 2 D solution grids.



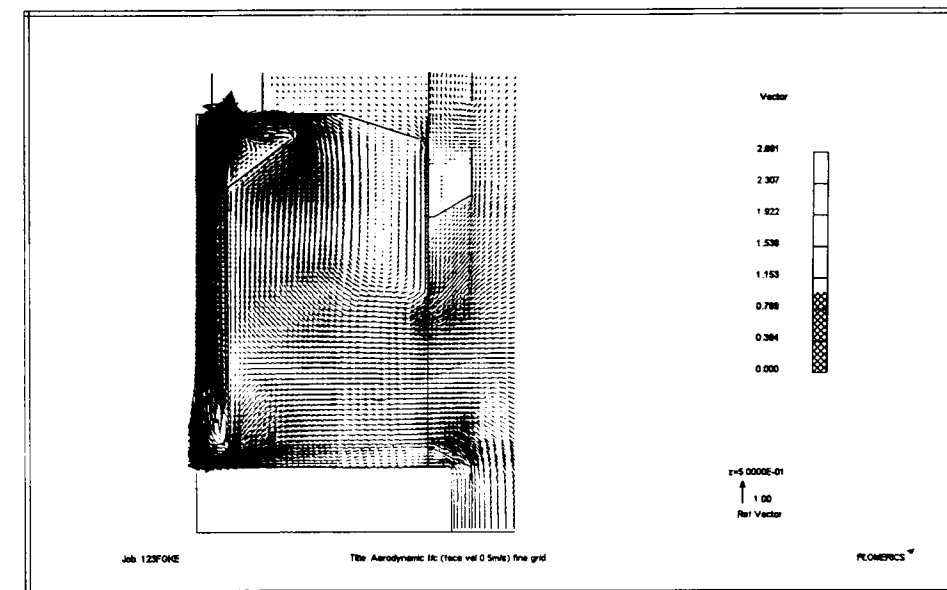
‘Coarse’ grid vectors



‘Medium’ grid vectors

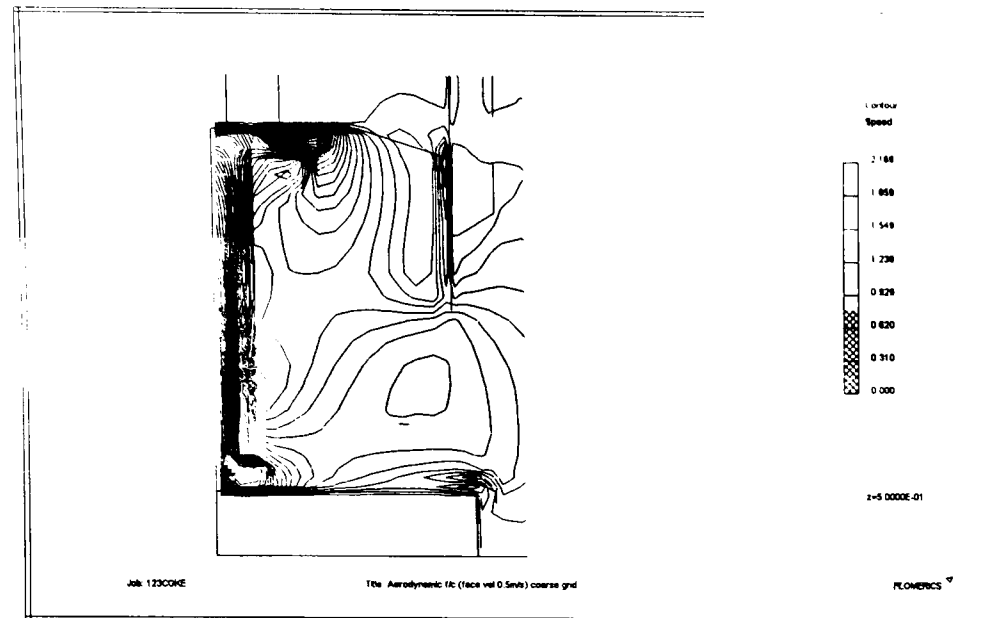


‘Medium revised’ grid vectors

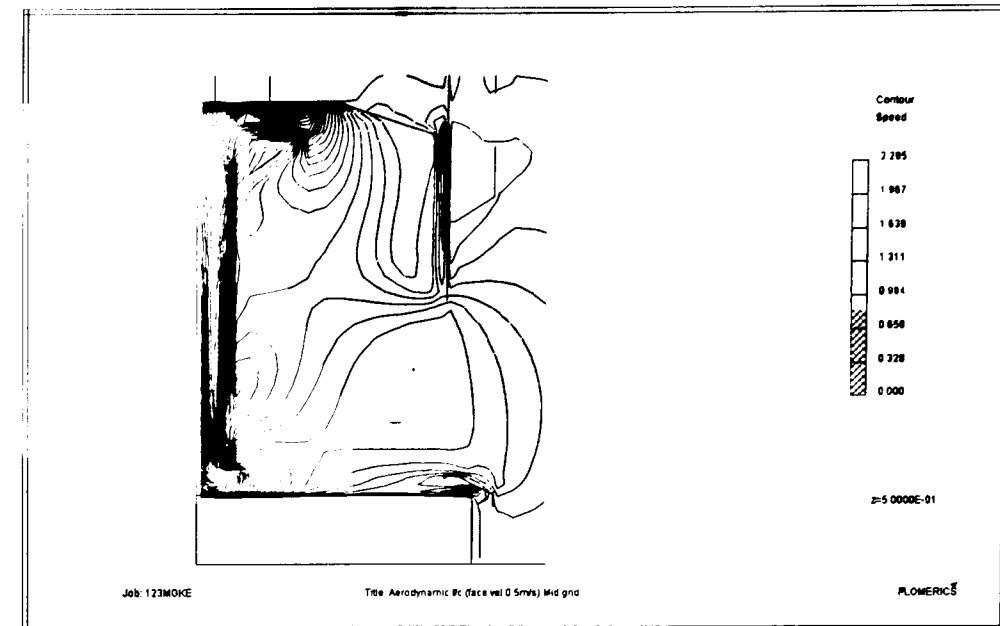


‘Complex’ grid vectors

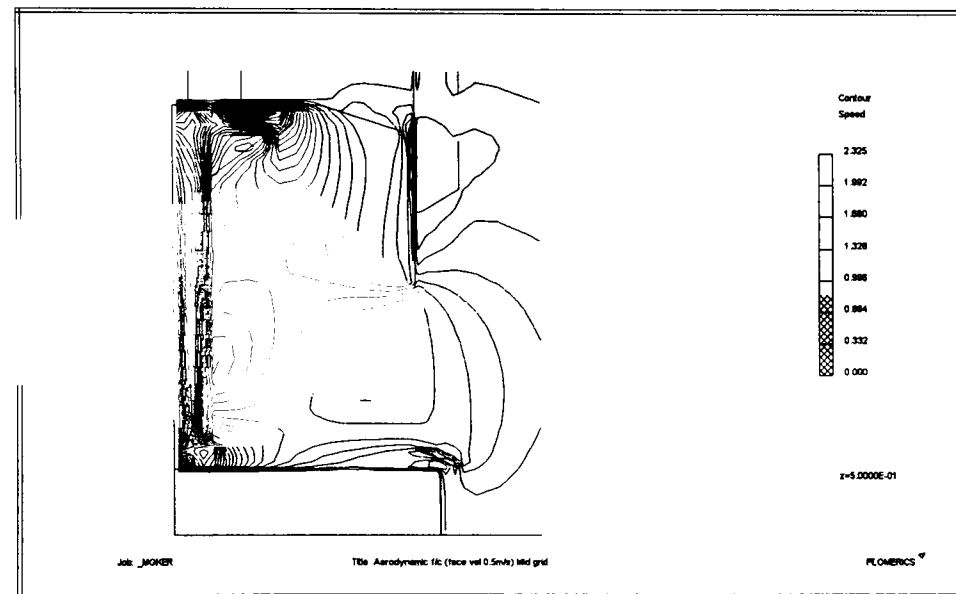
Figure 6.8 Effect of grid density and refinement on airflow vectors (2 D, k-ε turbulence model).



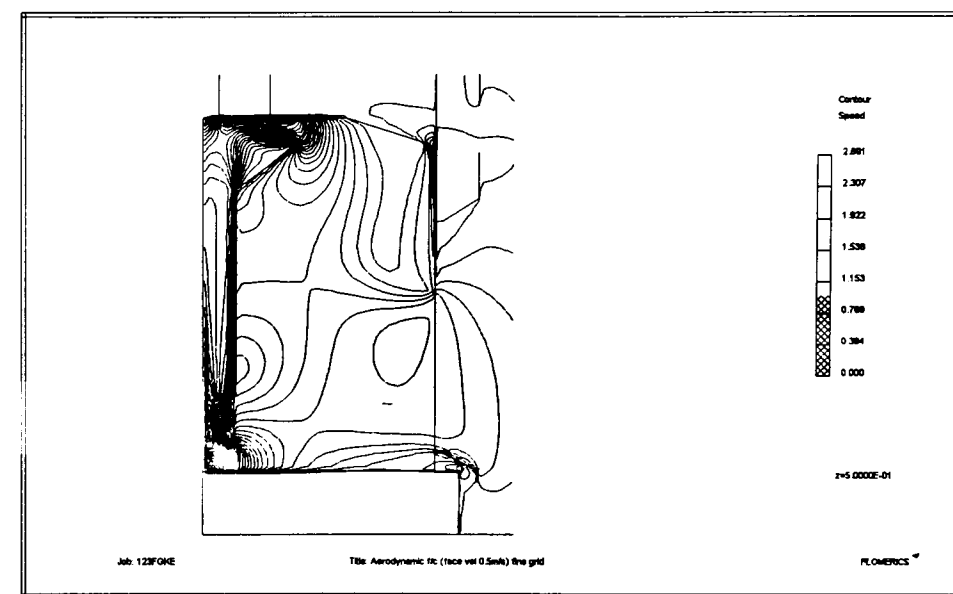
‘Coarse’ grid speed



‘Medium’ grid speed

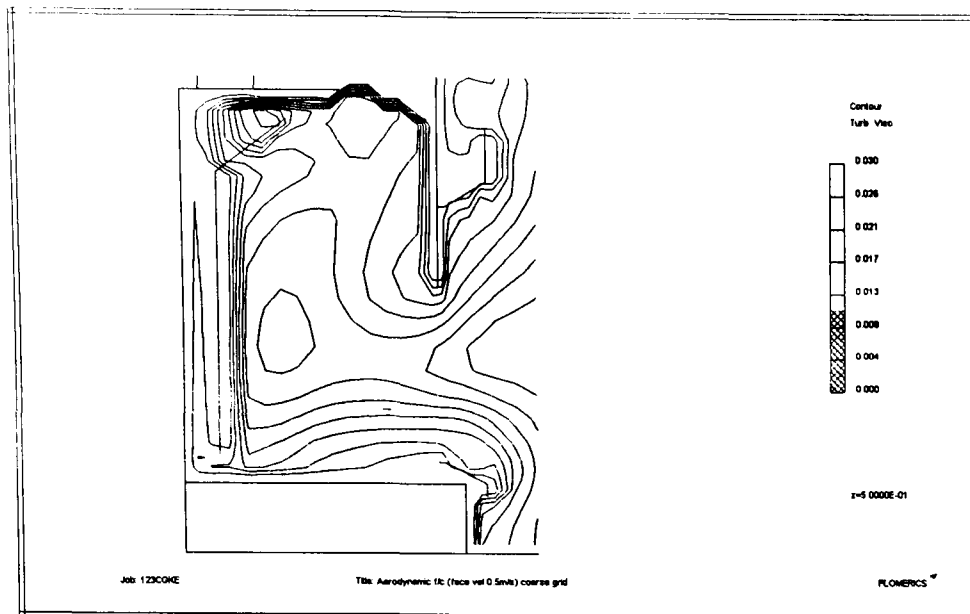


‘Medium revised’ grid speed

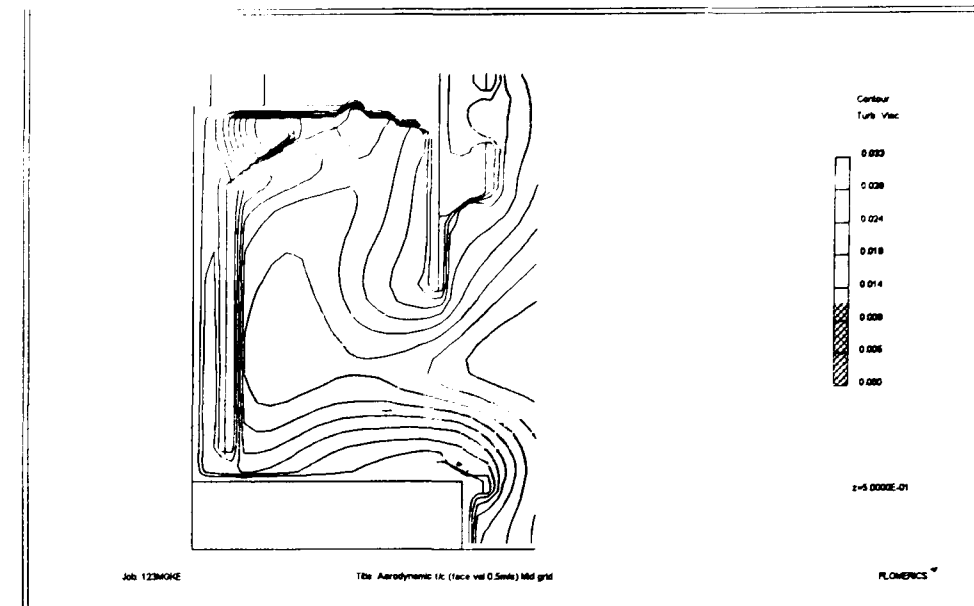


‘Complex’ grid speed

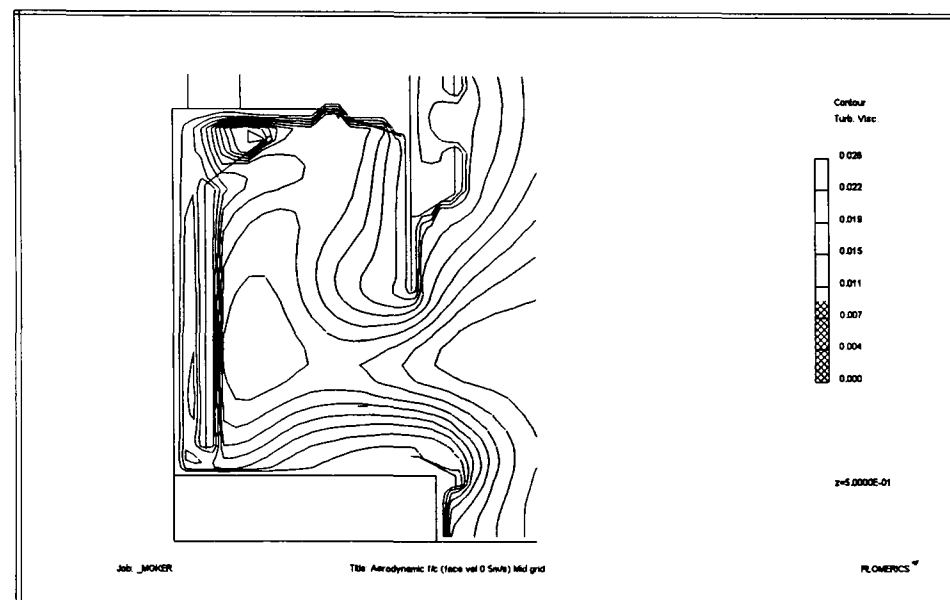
Figure 6.9 Effect of grid density and refinement on airflow speed contours (2 D, k-ε turbulence model).



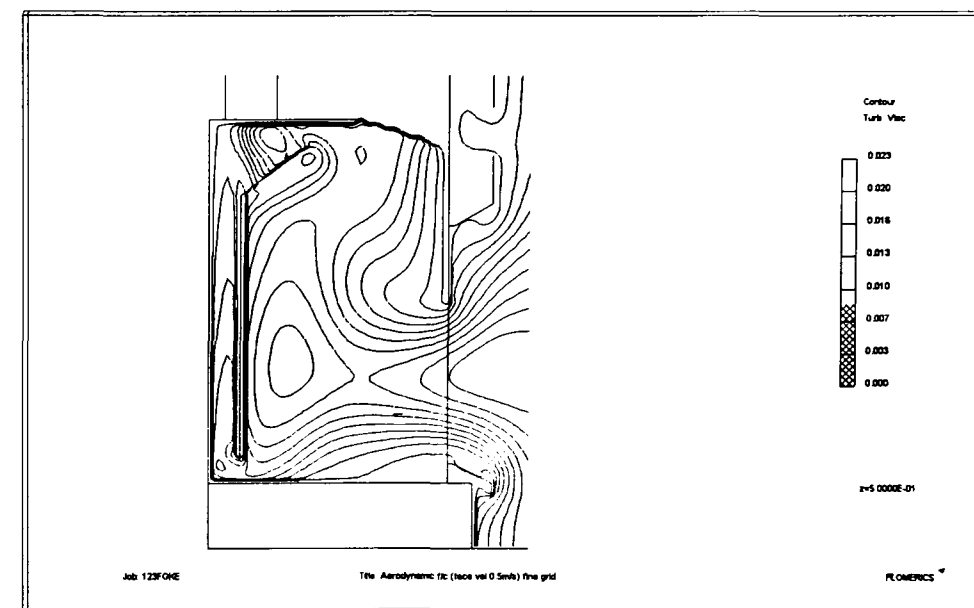
‘Coarse’ grid turbulent viscosity



‘Medium’ grid turbulent viscosity

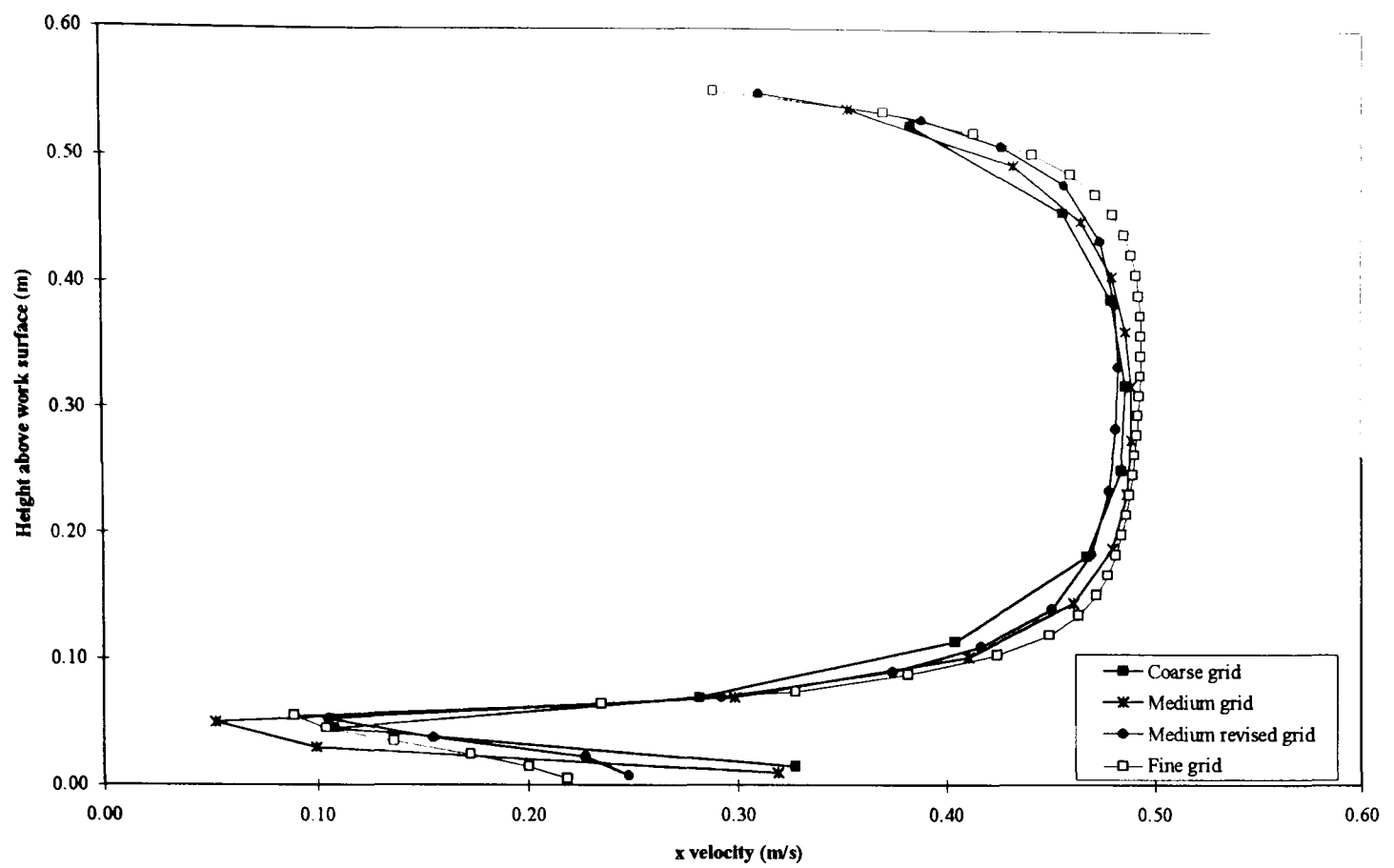


‘Medium revised’ grid turbulent viscosity

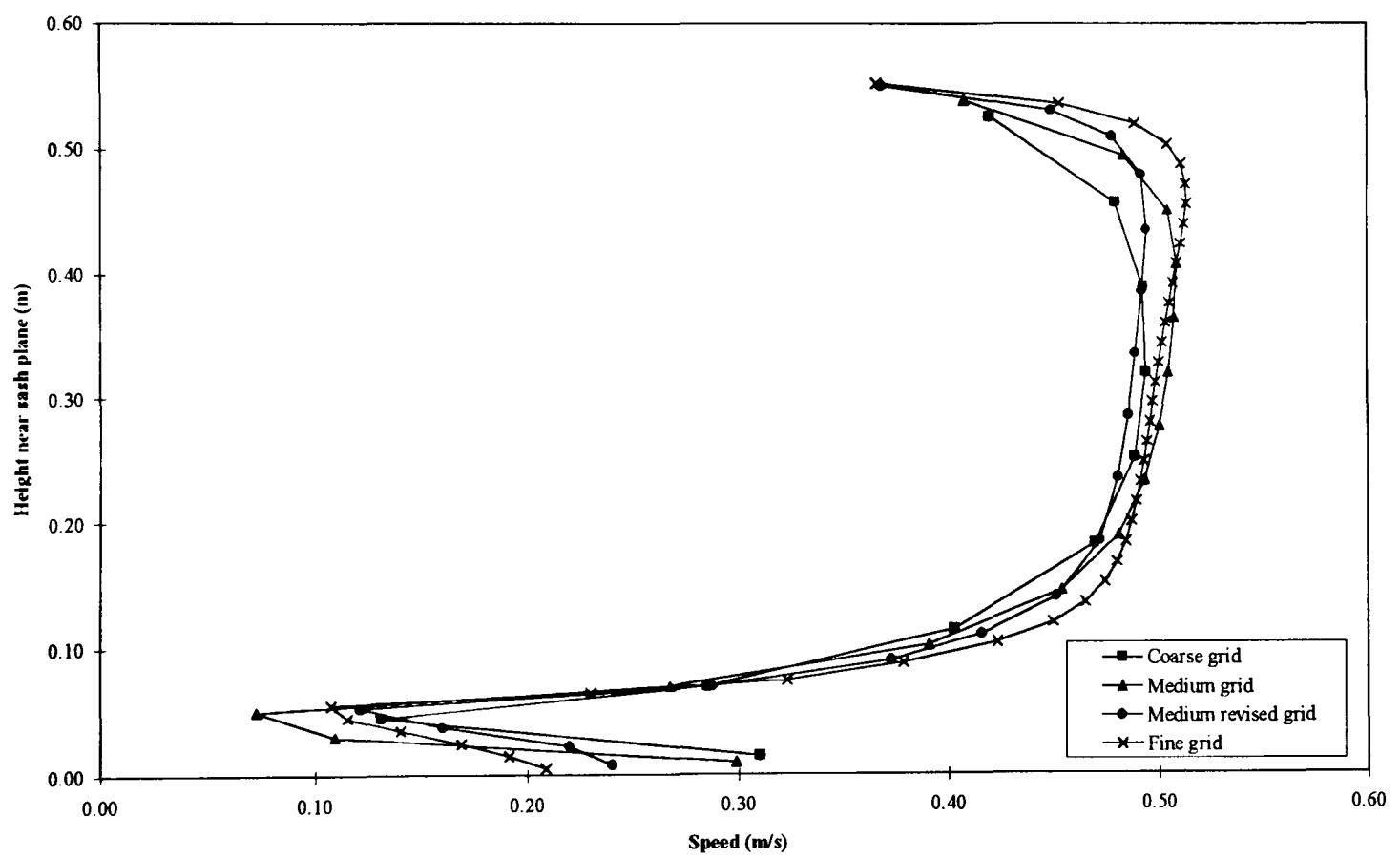


‘Complex’ grid turbulent viscosity

Figure 6.10 Effect of grid density and refinement on airflow turbulent viscosity contours (2 D, k- ϵ turbulence model).



x velocity profiles (Lipfoil 60 mm from work surface)



Speed profiles (Lipfoil 60 mm from work surface)

Figure 6.11 Effect of grid density and refinement on x velocity and speed profiles in the aperture plane (2D)

6.2.3 Comparison of simulation to physical measurements

The air flow through the interior of the aerodynamic fume cupboard was visualised using smoke particles. The fume cupboard had transparent side panels so that the movement of the smoke could be captured on video and subsequently transferred to computer for comparison with the 2 dimensional CFD simulations.

The air flow within the aerodynamic fume cupboard was uniform through the aperture travelling towards the rear baffle (Fig. 6.12). From this flow stream the air separated to either flow to the lower scavenging slot or upwards to the top opening. Behind the sash there was a vortex produced by the sash itself and enhanced by the shape of the baffle, the roof of the cupboard interior and the entry of bypass air down behind the sash. Air flowed over the 'aerodynamic' features of the sash handle and the lipfoil which eliminate boundary separation local to the corners of the sash itself and the edge of the work surface.

These airflows were represented in the 2 dimensional CFD simulation and compared well qualitatively. The 'aerodynamic' sash handle was not incorporated into the CFD model and thus the airflow simulated in this region showed a sharp change in direction which was not observed in reality. The flow past the lipfoil was represented well comparatively.

The two measurement techniques were compared quantitatively. Physical measurements were made in the plane of the sash in the vertical centreline of air velocity using a rotating vane and thermistor anemometer (Fig. 6.13). This showed a profile of lower air velocities near to the top and bottom surfaces, which then increased from the surface but decreased in the middle of the aperture. The 'edge' effects were considered due to the aerodynamic designs where air flow close to the solid surfaces was greater as the distance travelled was further compared to the main stream.

The CFD simulation using the refined 'medium' grid and 'complex' grid did not show this phenomenon both in terms of x velocity profile or vector value in the sash plane (Fig. 6.13). These showed a smooth profile in the majority of the aperture then slowing towards the surfaces. The speed values near to the sash were similar but no aerodynamic sash handle was represented in the CFD simulation. Near to the lipfoil the calculated values decreased nearer to the surfaces but the physical values increased before decreasing near to the surface. The 95 % confidence limits (assuming normal distribution) for the physical measurements become larger nearer to the top and bottom surfaces suggesting increasing turbulence in these regions which did overlap the calculated results.

Beneath the lipfoil there was a large difference between the physical measurements and the calculated values. The physical values showed higher velocities nearer to the lipfoil whereas

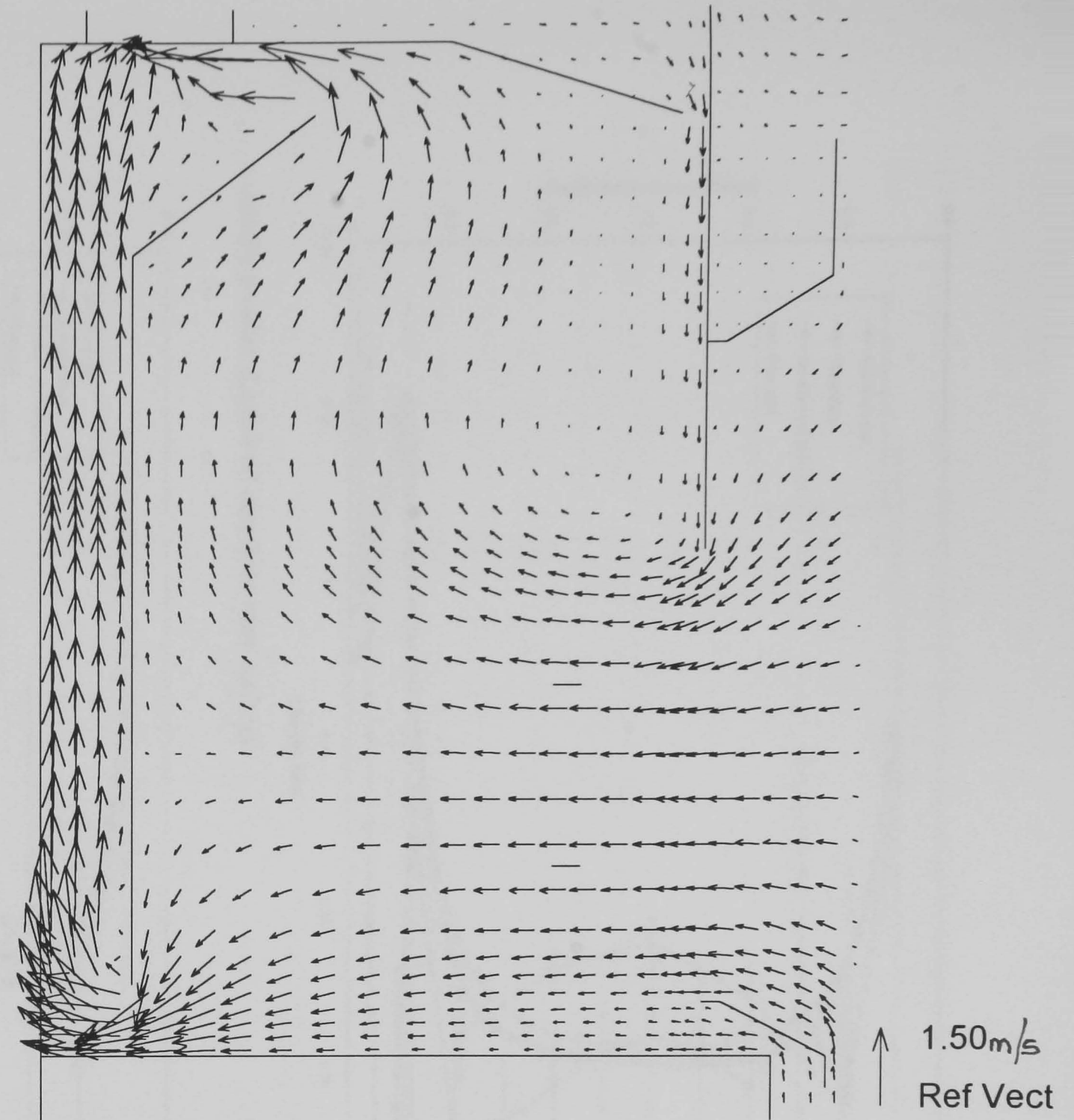
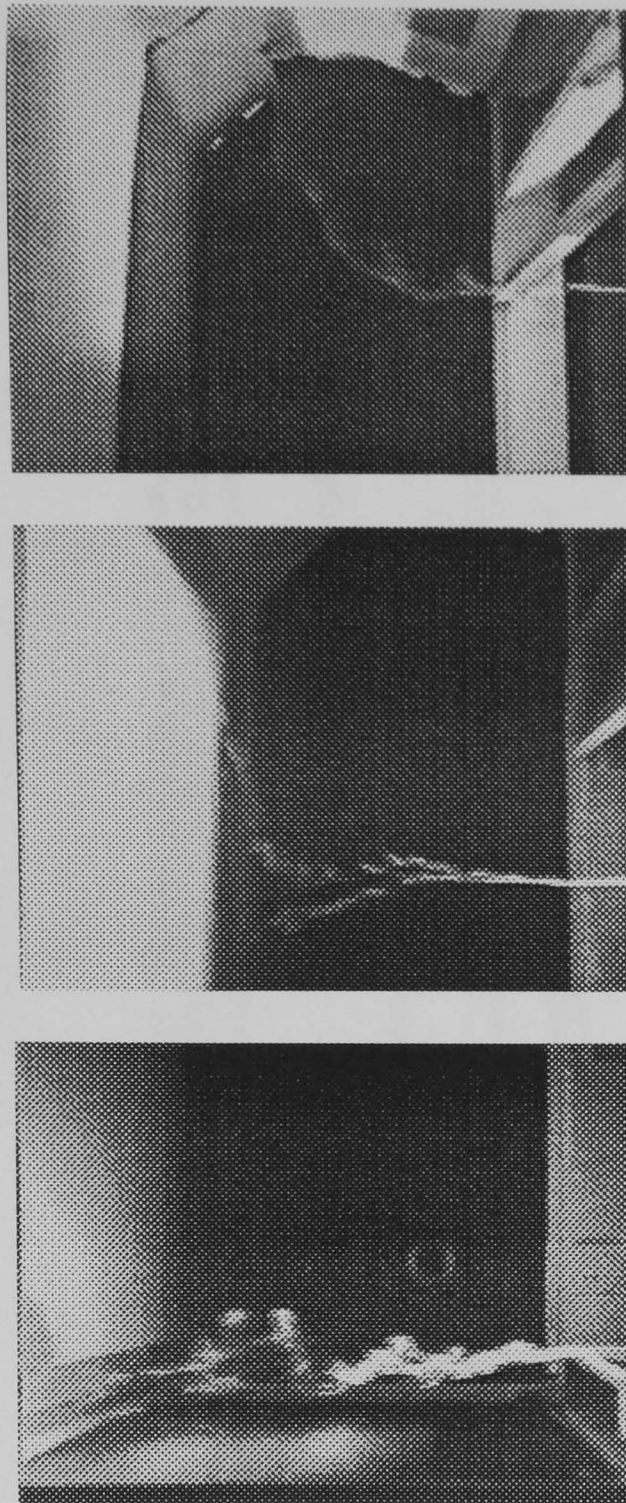
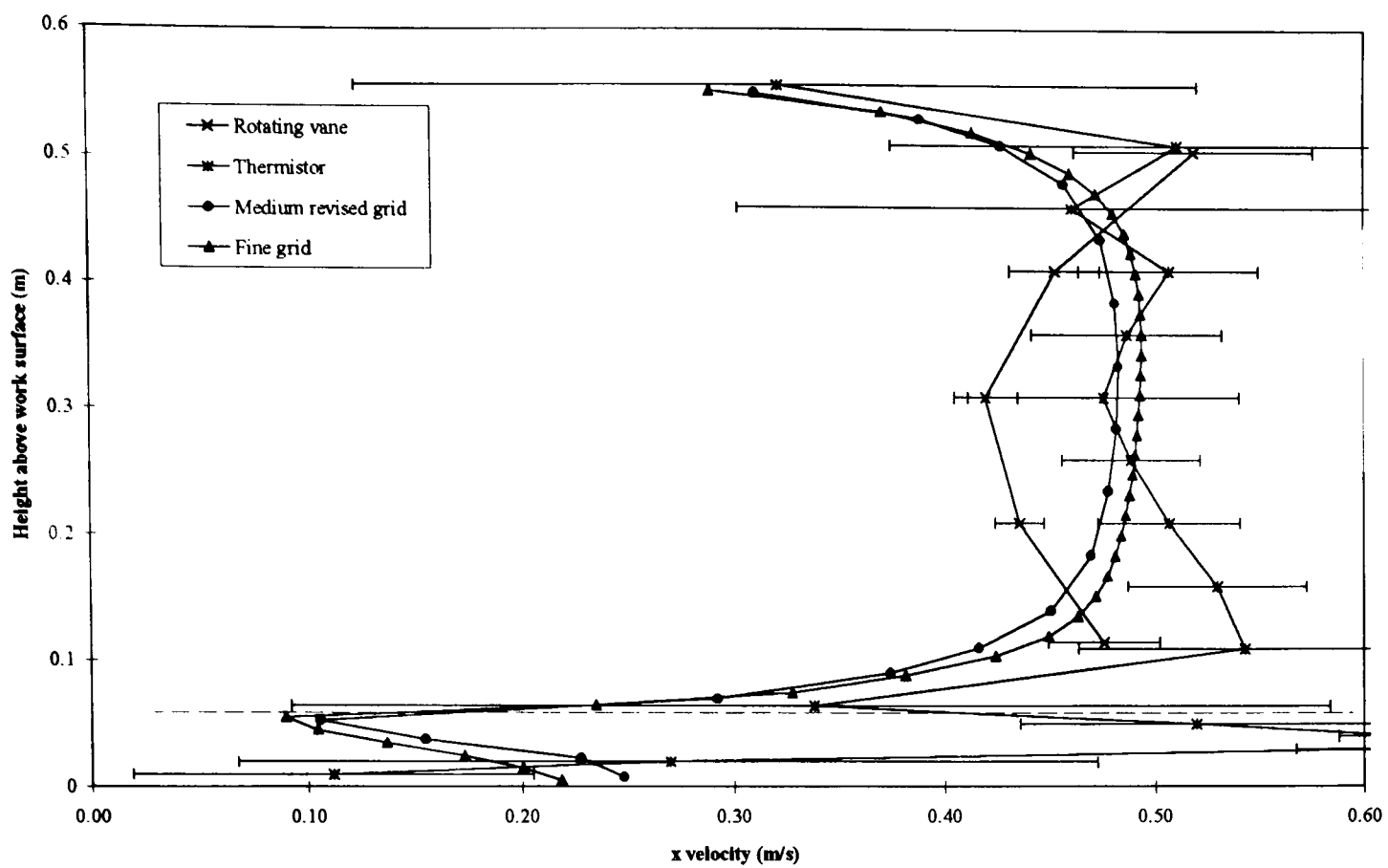
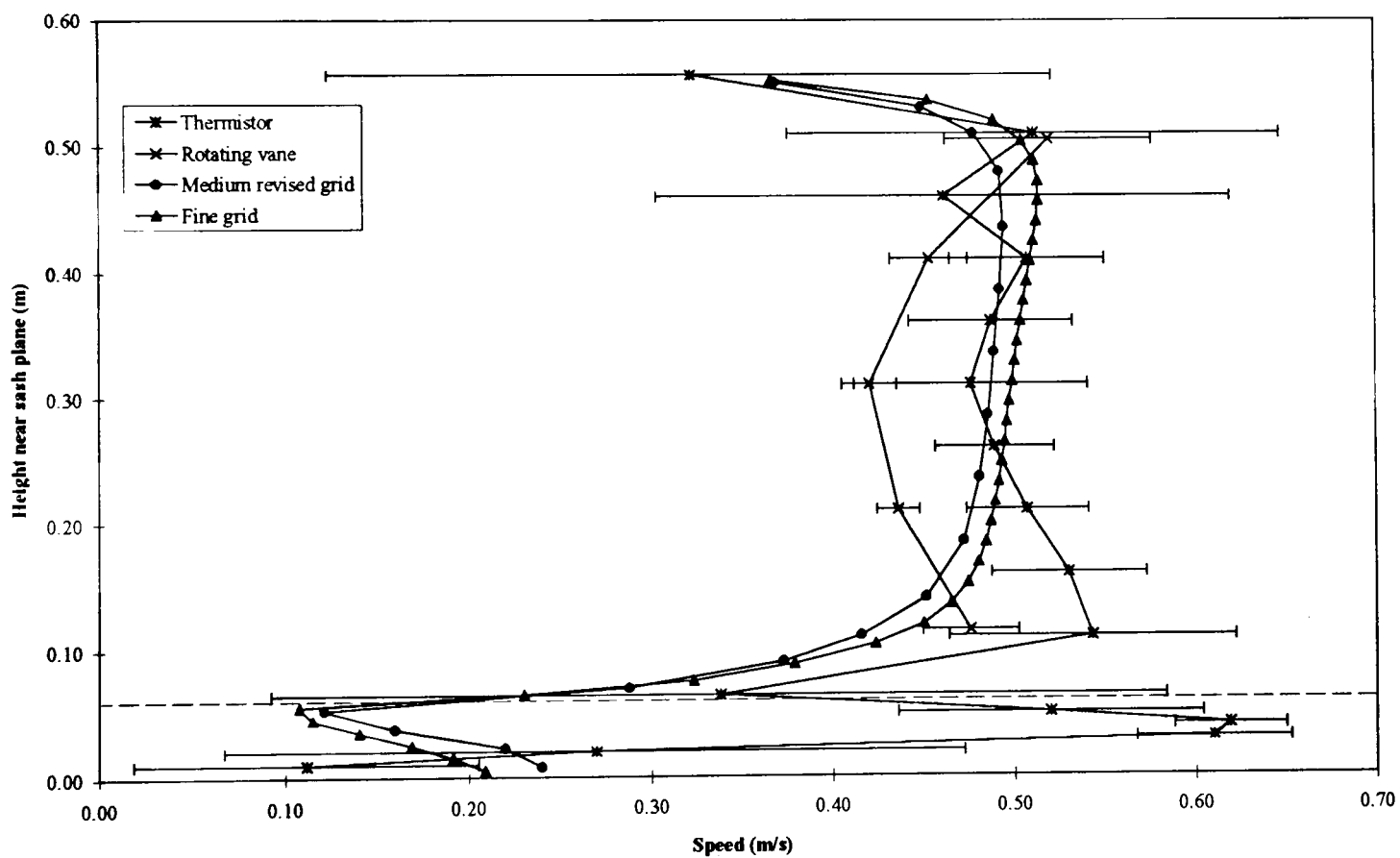


Fig. 6.12 Comparison of airflows within an aerodynamic fume cupboard as visualised using smoke and by 2 D CFD simulation.



x velocity profiles (Lipfoil 60 mm from work surface)



Speed profiles (Lipfoil 60 mm from work surface)

Figure 6.13 Comparison of x velocity and speed profiles in the aperture plane of an aerodynamic fume cupboard using CFD with physical measurements (rotating vane & thermistor anemometers). (Error bars show 95% confidence limits). (2D).

the calculated values were the reverse. The underside of the lipfoil was actually a smooth curve which was not represented in this simulation.

6.2.4 Airflow around individual design features and comparison with the whole flow field

6.2.4.1 Front steps

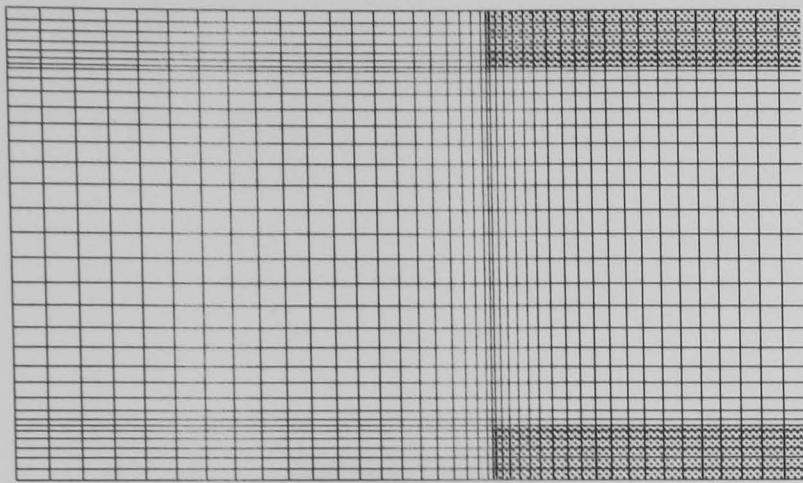
In the previous section the calculated flow field was compared qualitatively with the physical measurements showing good comparison. However, quantitatively values represented in the plane of the aperture were similar in profile but did not completely reflect measured values near to the lipfoil. Also the sash handle was not represented in the CFD simulation. Each of these design elements was studied in more detail as separate 2 dimensional simulations, being able to greatly increase the grid density over the region.

Initially a simple step was simulated (Fig. 6.14) which represented any edge of a typical 'box' type fume cupboard. The simulation was first tested for both turbulence sensitivity and grid dependence. A fixed turbulent viscosity (revised) value determined from the velocity past the edge and the height of the opening was used and the results were a typical air flow pattern of flow separation behind the edge with air recirculating back towards it. The fixed value was varied to a factor of 4 below and above but this had little effect on the 'visualised' air flow vectors. The standard fixed turbulence model was then used which failed to show any recirculation of air past the edge. The effect was also reduced using the k- ϵ model. For the latter model the solution took a long time and the calculated variables did not converge.

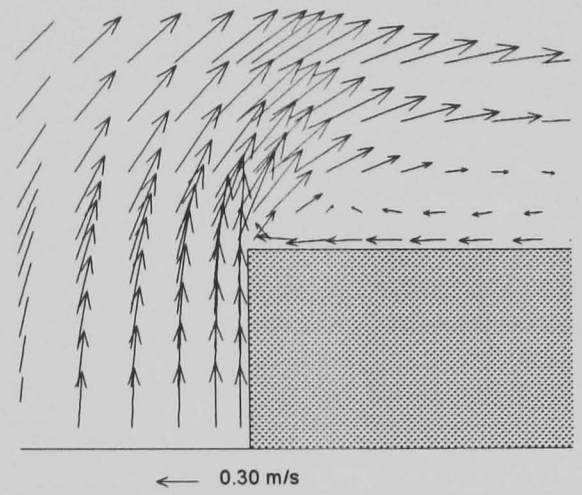
The grid was made 'coarser' with fewer grid cells near to the front edge (Fig. 6.15). This resulted in poor simulation of the recirculation behind the front edge. In the two dimensional simulation of the fume cupboard this level of grid refinement was similar to the 'coarse' grid due to limitations on computation time. It was thus assumed that these flows were a mean estimation of the bulk flow in this region which was sufficient.

The effect of the step size on the development of boundary separation past the edge was investigated. The deeper the block then the less obvious were the recirculation patterns of air past the edge, but the magnitude of the vectors was greater at the edge (Fig. 6.16). For further simulations, the smaller step was used as this 'visually' demonstrated the recirculation zone more. This also reflected the thickness of the fume cupboard work surface tested in earlier chapters.

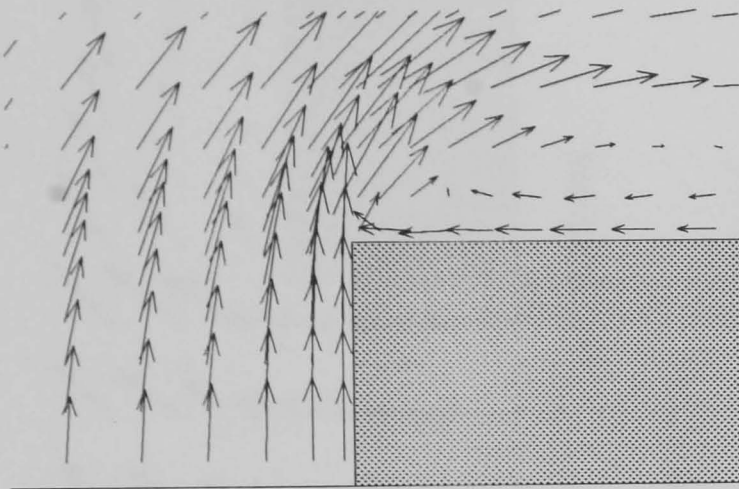
In terms of fume cupboard design, this simulation clearly showed how a step can cause boundary layer separation and potential recirculation of cupboard contents back to the front. The simulation was altered to observe the effect of smoothing out this step on the airflow pattern (Fig. 6.17). A 20° wedge was used in front of the step which eliminated any



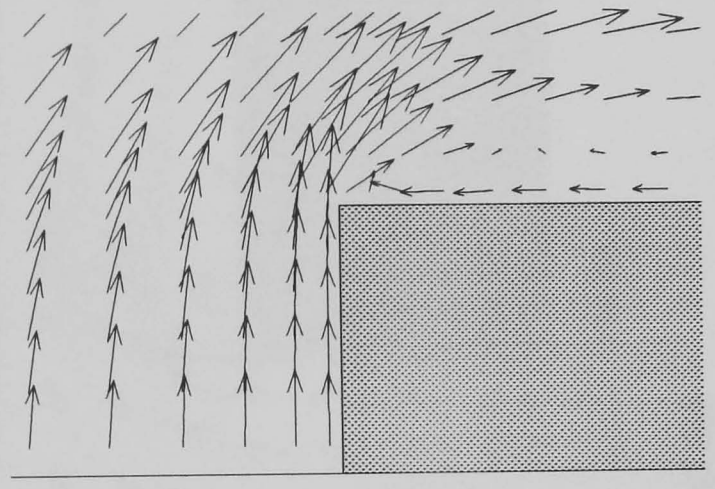
Square edge (35 mm thick)



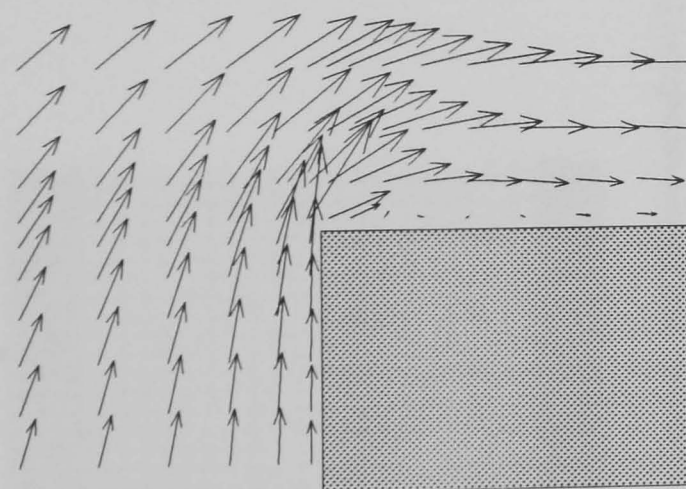
Fixed turbulence (revised model) 0.005



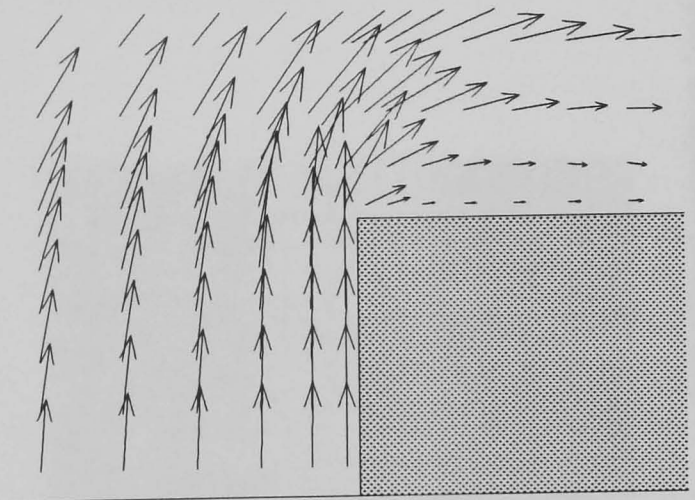
Fixed turbulence (revised model) 0.001



Fixed turbulence (revised model) 0.020



k-ε model



Fixed turbulence (standard model) 0.005

Figure 6.14 Effect of the turbulence model on the airflow around a front step (2 D).

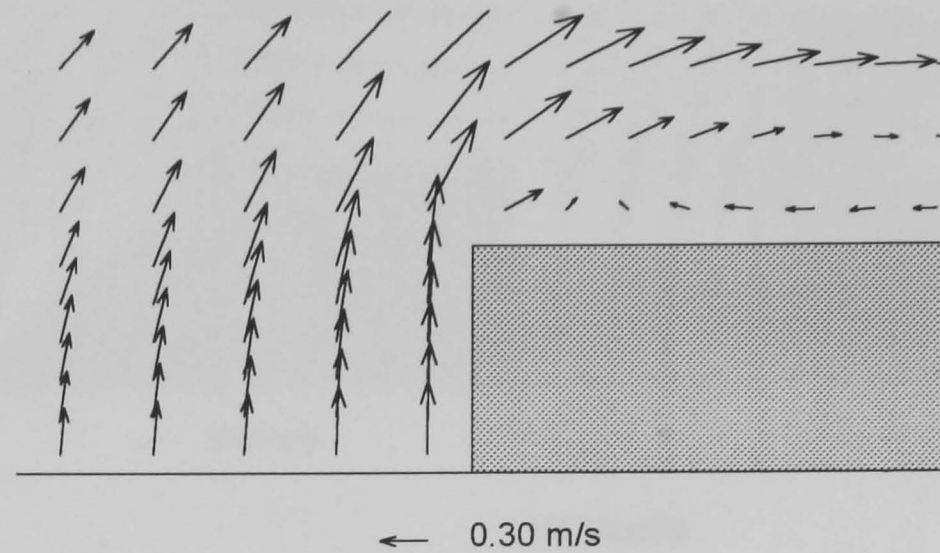
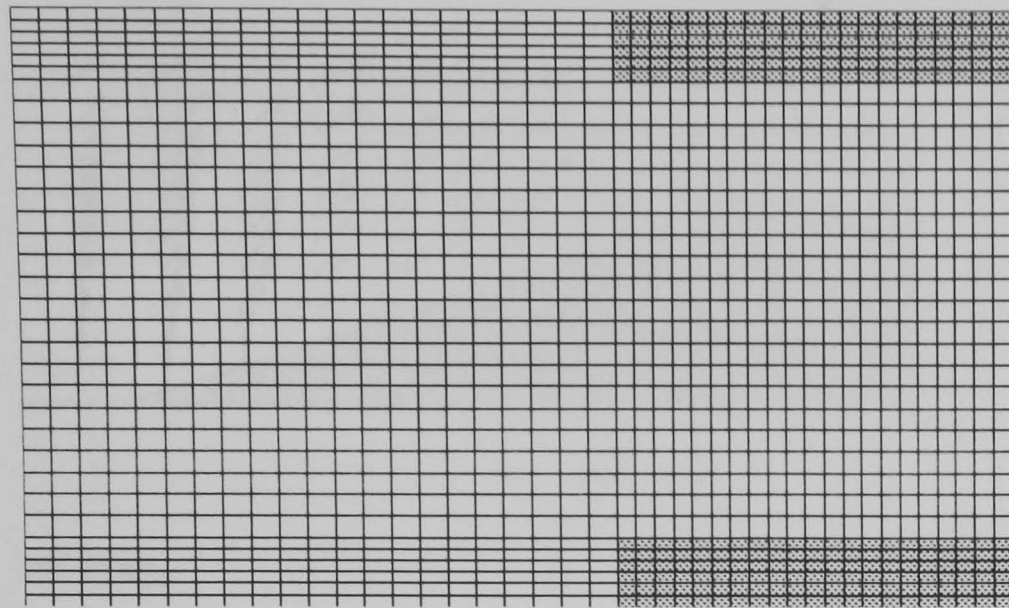


Figure 6.15 Airflow around a front step with a coarser grid (Fixed turbulence (revised model 0.005 (2 D))).

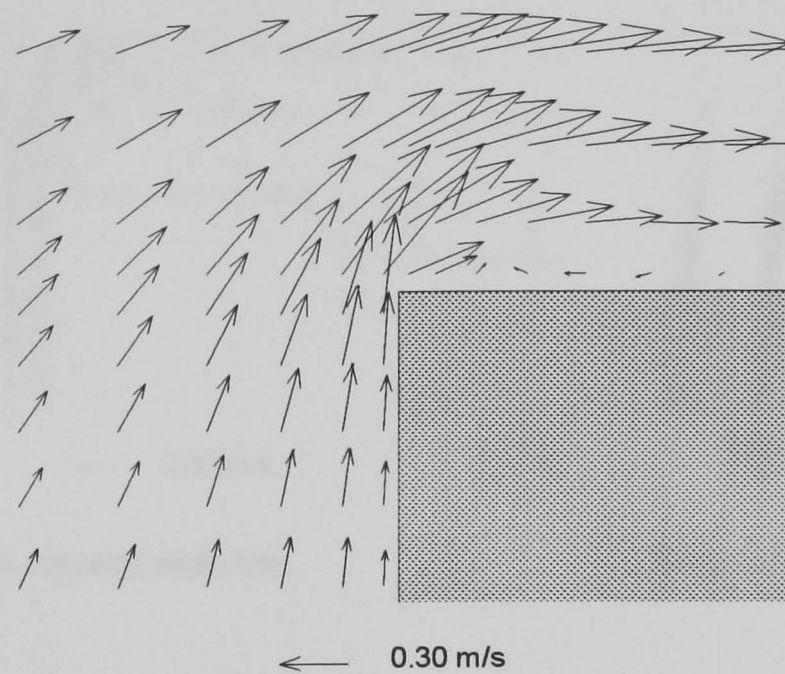
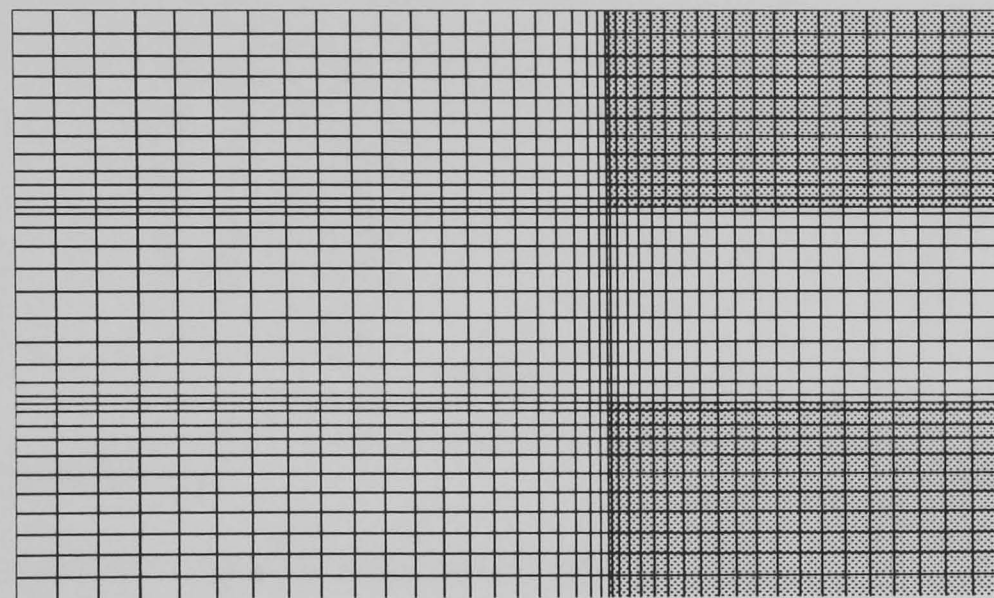


Figure 6.16 Air flow around a front step, twice as thick (Fixed turbulence (revised model 0.005 (2 D))).

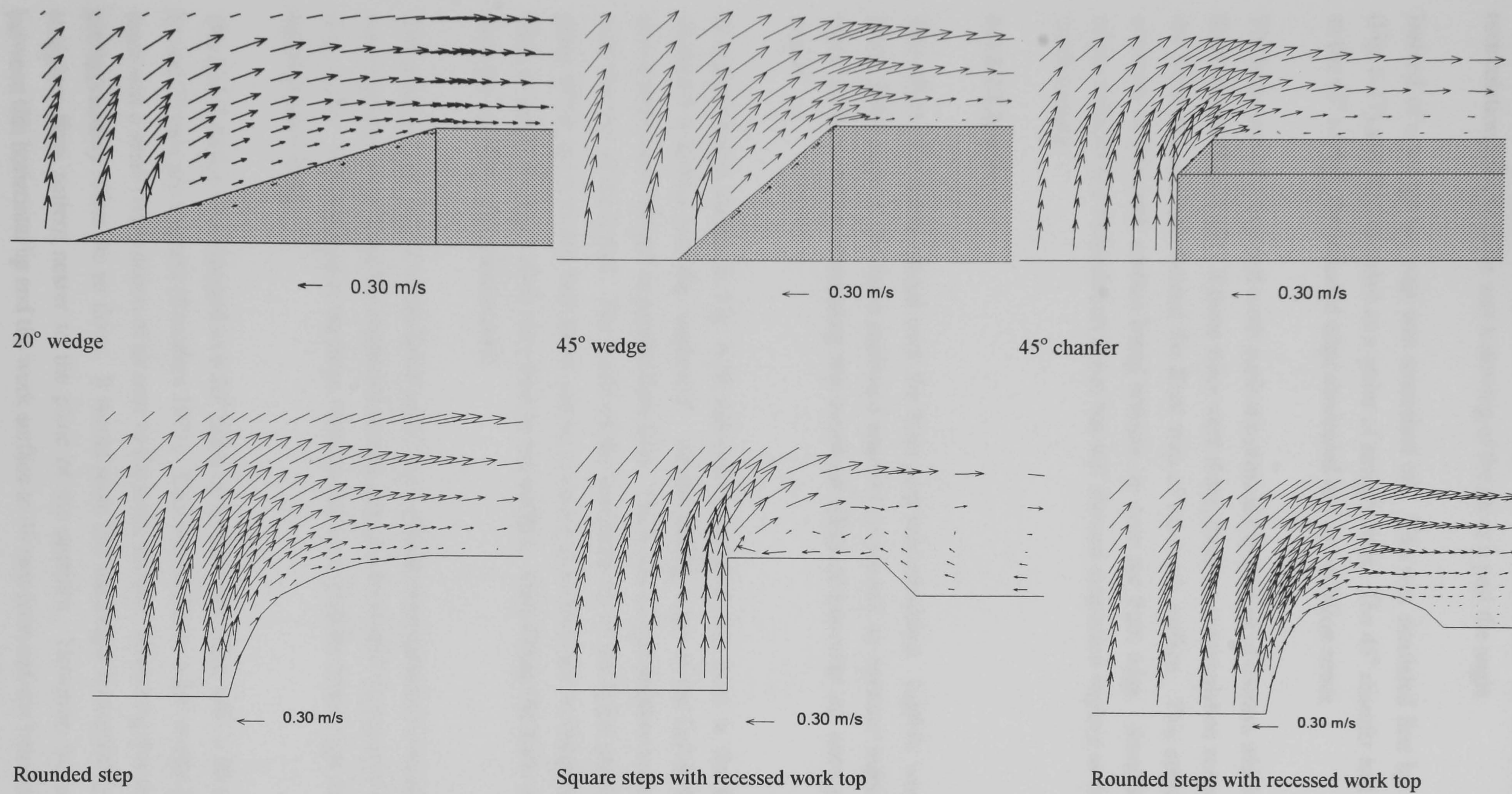


Figure 6.17 Effect of step shape on airflows (2 D).

recirculation zones. The angle was increased to 45° which did not completely reduce the recirculation zone as there was a slowing of the air as it past the angle.

Instead of a wedge the step was smoothed off. This was simulated first by a 45° chamfer (Fig. 6.17) and then rounded as a series of straight lines. The 45° chamfer had similar effects as the 45° wedge, the rounded edge eliminated any recirculation zones.

The inclusion of a recessed work surface increased the number of corners which the air had to flow around (Fig. 6.17). If these steps were sharp, there was recirculation zones not only past the front step but also behind the front step of the work surface. This could result in the contents of the work surface being brought up onto the front edge. Smoothing out these edges reduced the recirculation zones but still showed stagnation regions at the front of the work surface.

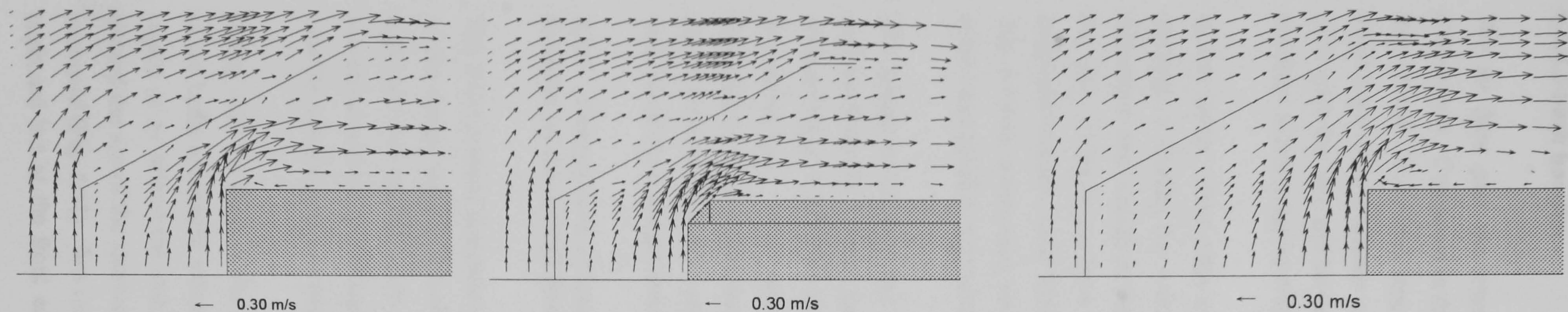
6.4.2.2 Lipfoils

The effect of a lipfoil placed over the front step was simulated. Lipfoils were used at the lower front edge of the fume cupboard aperture to prevent an operator leaning against the work surface and so eliminating any beneficial effect of smoother air entry profiles in this region.

A typical lipfoil shown in Fig. 6.18 reduced the recirculation zone at the front step and displaced it further into the 'cupboard'. At the trailing edge of the lipfoil the air flowing above and below merged as parallel flow lines. There was no recirculation zone of air passing over the top of the lipfoil. The inside of the horizontal lip of the lipfoil usually marked the plane of the aperture and here there was no evidence of air from the working volume flowing back to the front edge, albeit very near to the surface. Chamfering the front step eliminated even the smallest recirculation zone.

The position and 'shape' of the lipfoil could have critical consequences on its effectiveness. It was displaced away from the cupboard so that only the horizontal lip covered the work base (Fig. 6.18). This resulted in the large recirculation zone past the front edge as seen with no lipfoil present at all.

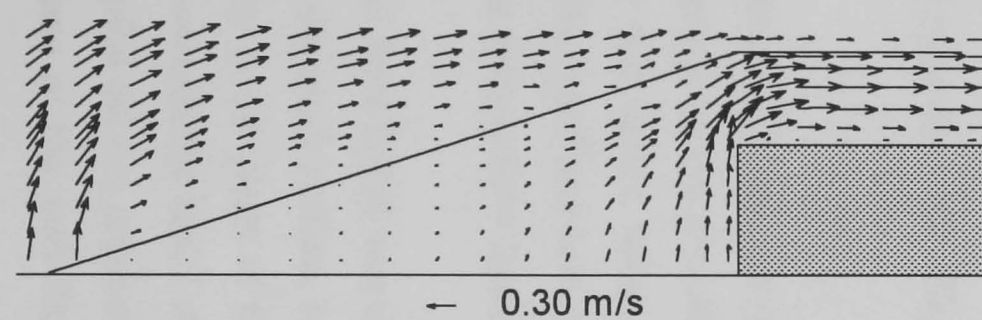
The lipfoil design was changed to a 20° slope up to the front edge, with a 60 mm horizontal lip and 25 mm gap beneath (Saunders 1993). This was similar to a 20° wedge (Fig. 6.17) but there was a small recirculation of air near to the work surface. Increasing this slope to 45° did not appreciably affect the air flows. It would seem that the longer horizontal lip established a straighter flow pattern nearer to the plane of the aperture. However, increasing the gap between this horizontal lip and the work surface to 40 mm removed any beneficial effect (Fig. 6.18).



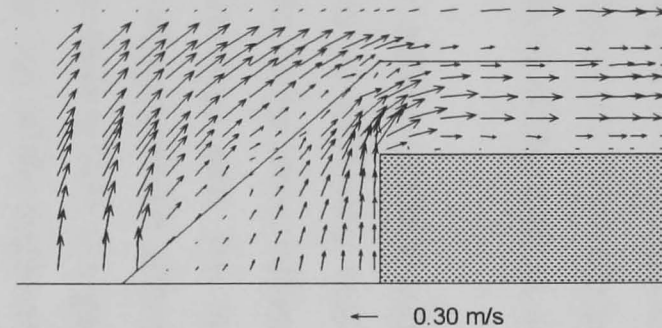
Lipfoil over step (as tested fume cupboard)

Lipfoil over 45° chamfered step

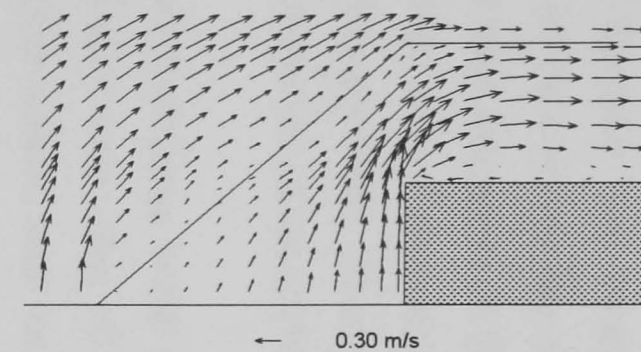
Lipfoil over step but displaced forward



20° lipfoil over step



45° lipfoil over step



45° lipfoil over step but vertically (from 25 to 40 mm gap)

Figure 6.18 Effect of lipfoil design on airflows past a front step (2 D).

6.2.4.3 Sash handles

The air flow past the lower edge of the sash was another critical area in cupboard containment. Compared to the front step of the work surface there was a front step and back step as well. In the back step there was a large change in air flow direction which resulted in larger areas of recirculation of air. However, such recirculation was normal to the bulk flow of air past this step and hence was usually re-entrained. Even so, this was a turbulent region and from which turbulent diffusion could occur out of the cupboard.

At this corner, which often exaggerated the turbulence in the region, was fitted a handle for opening or closing the sash. These devices were often of poor design which increased turbulence and leakage in the region. These handles were usually fitted onto the outside of the sash so leaving a back step and increasing turbulence outside the sash into which cupboard contents could diffuse. This was simulated using the two dimensional CFD model.

Fig. 6.19 show how such handles do not reduce the recirculation of air behind the sash and in some cases result in recirculation zones in front of the sash as well.

The design of handles was improved by adding trailing edges which protruded into the cupboard interior. These had the effect of straightening out the air flow as it entered the cupboard (Fig. 6.19) and modified the recirculation zone behind the sash so that it joined this in parallel lines. Also smoothing out the flow past the sash edge eliminated the local recirculation of air behind the sash. Some designs which although having leading and trailing edges, resulted in stagnant zones behind the sash which, if a gap was left between the foil and sash, could result in turbulence and diffusion out of the cupboard.

6.2.5 Comparison of fume cupboard type and the effect of fume cupboard design features on the overall flow field

The 2 dimensional simulation of the aerodynamic fume cupboard was used to see how each of the design features contributed qualitatively to the overall flow pattern within the fume cupboard and quantitatively as x velocity and vector value in the plane of the sash. The simulation was completed and then the baffle, lipfoil and both subsequently removed. In each case the solution grid was unaltered, and the extract flow rate unchanged.

In Fig. 6.20 the effect of the rear baffle and front lipfoil was clearly demonstrated. Removal of the baffle eliminated scavenging across the work surface, with an increase in the scrolling region of air behind the sash. The velocity in the plane of the sash showed greater values toward the top of the aperture and lower towards the lipfoil compared with the aerodynamic cupboard (Fig. 6.21). Just removing the lipfoil did not appreciably affect the flows within the cupboard but at the front edge in the plane of the sash there was reversal of flow back

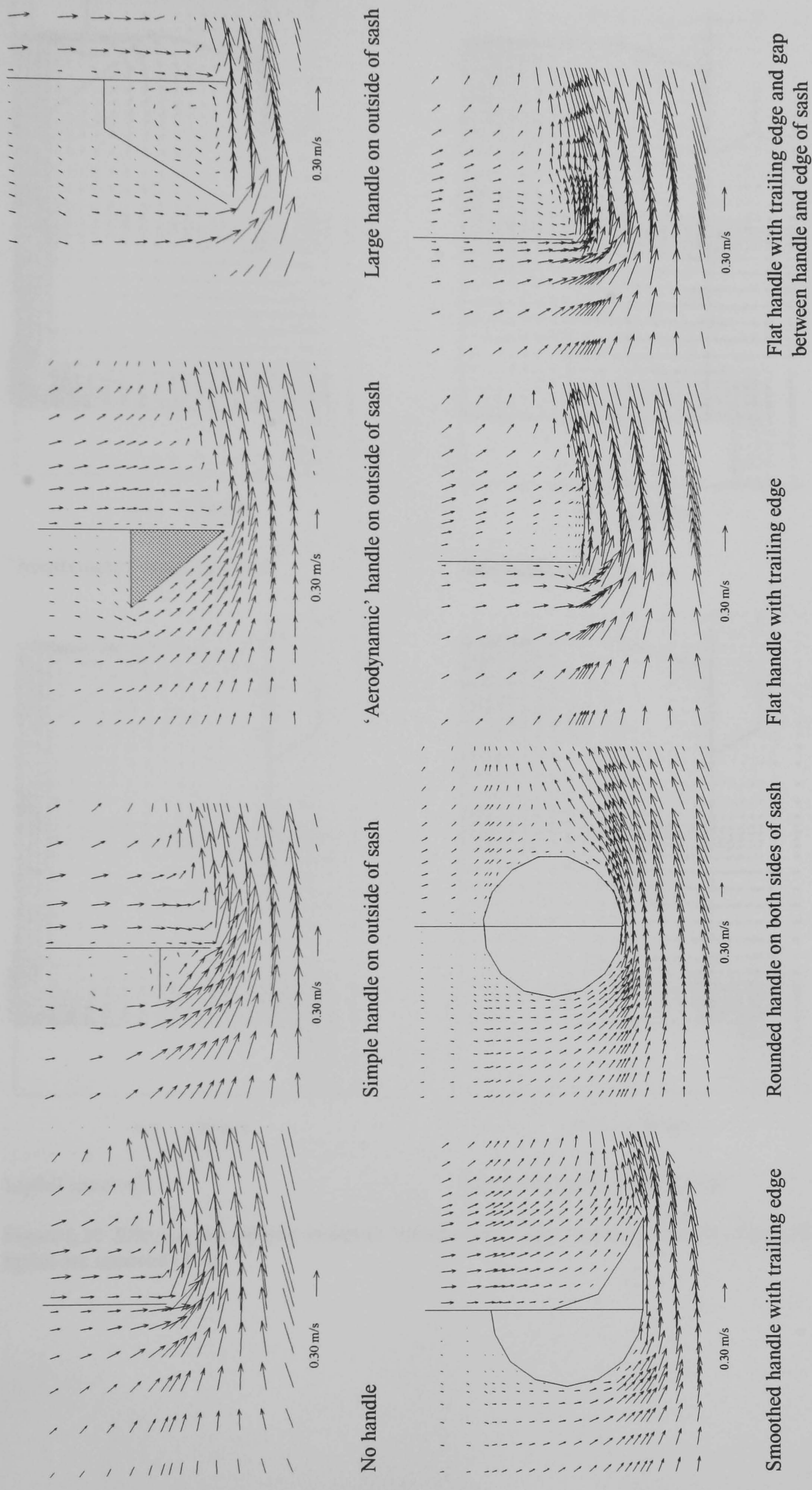
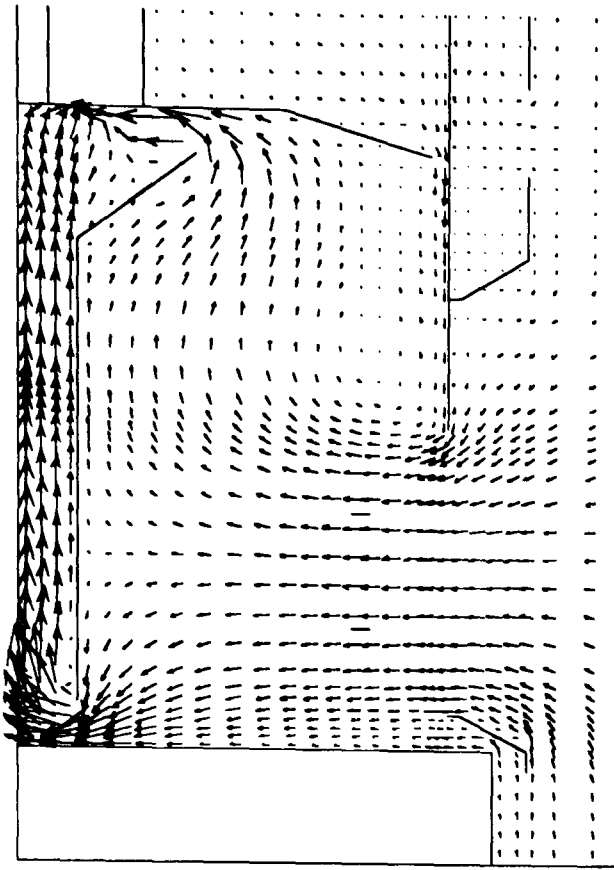
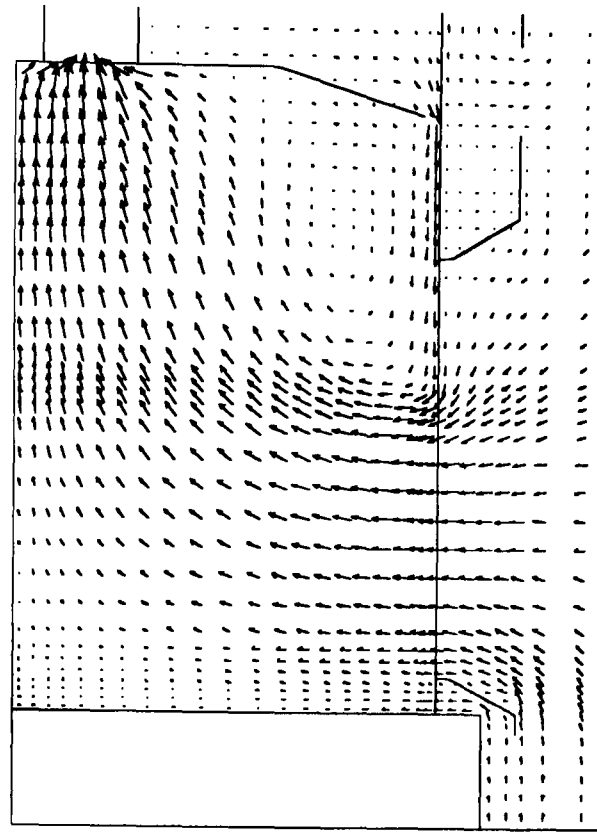


Figure 6.19 Effect of sash handle design on airflows past a sash (2 D).



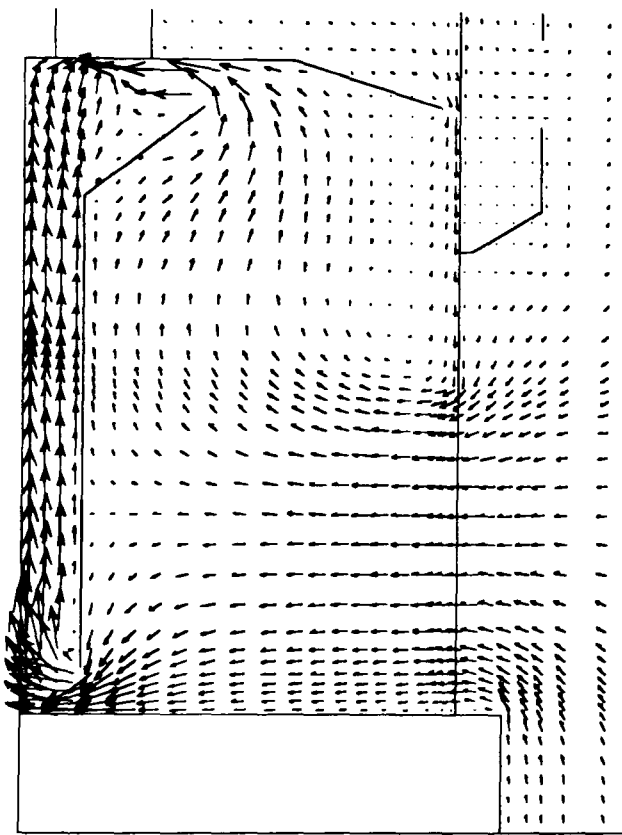
← 1.50 m/s

'Aerodynamic' fume cupboard



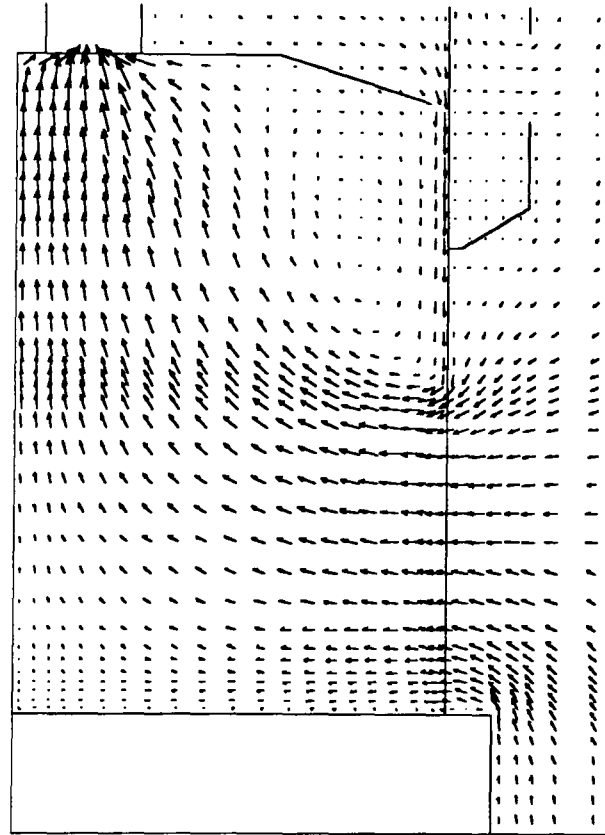
← 1.50 m/s

Rear baffle removed



← 1.50 m/s

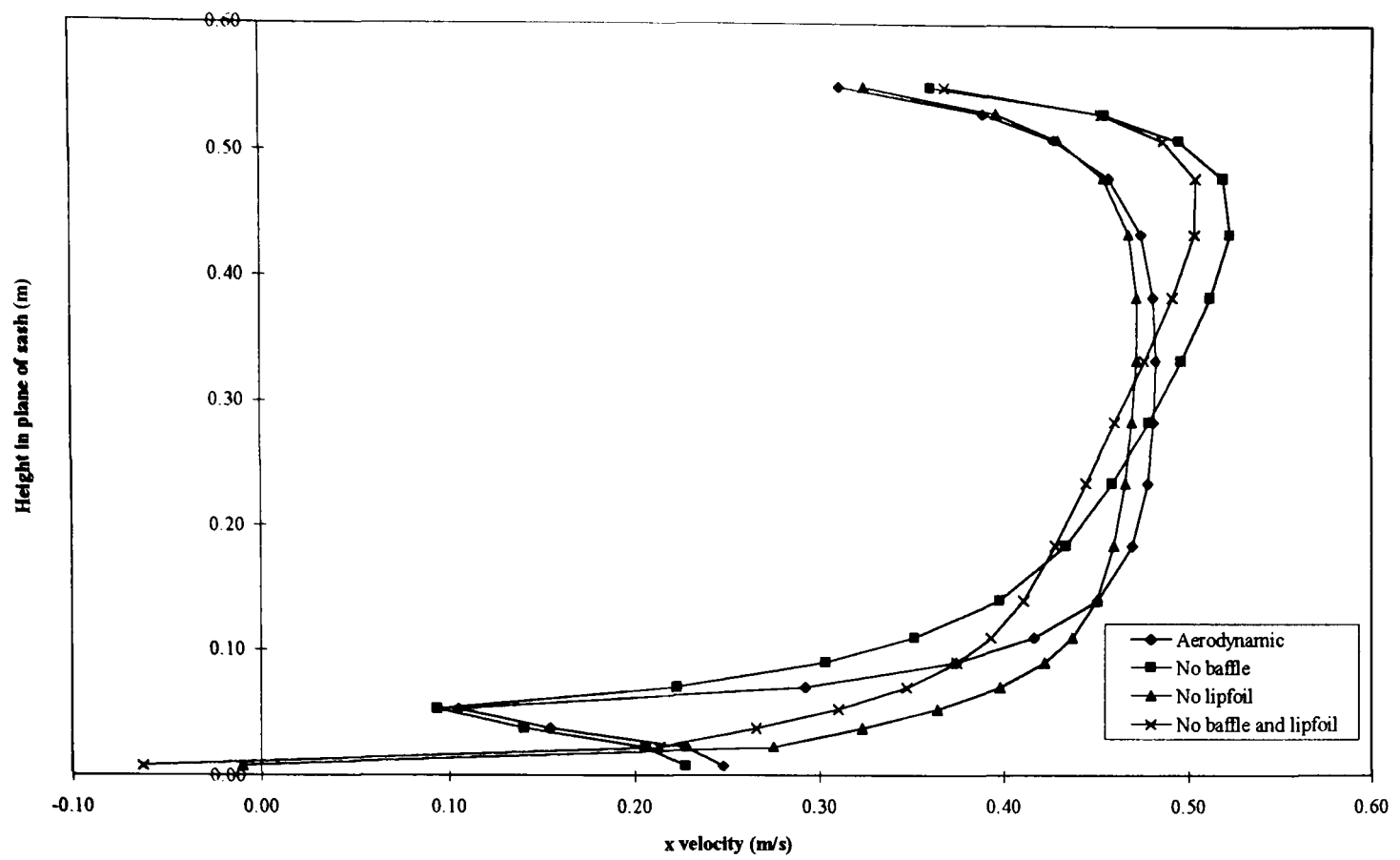
Lipfoil removed



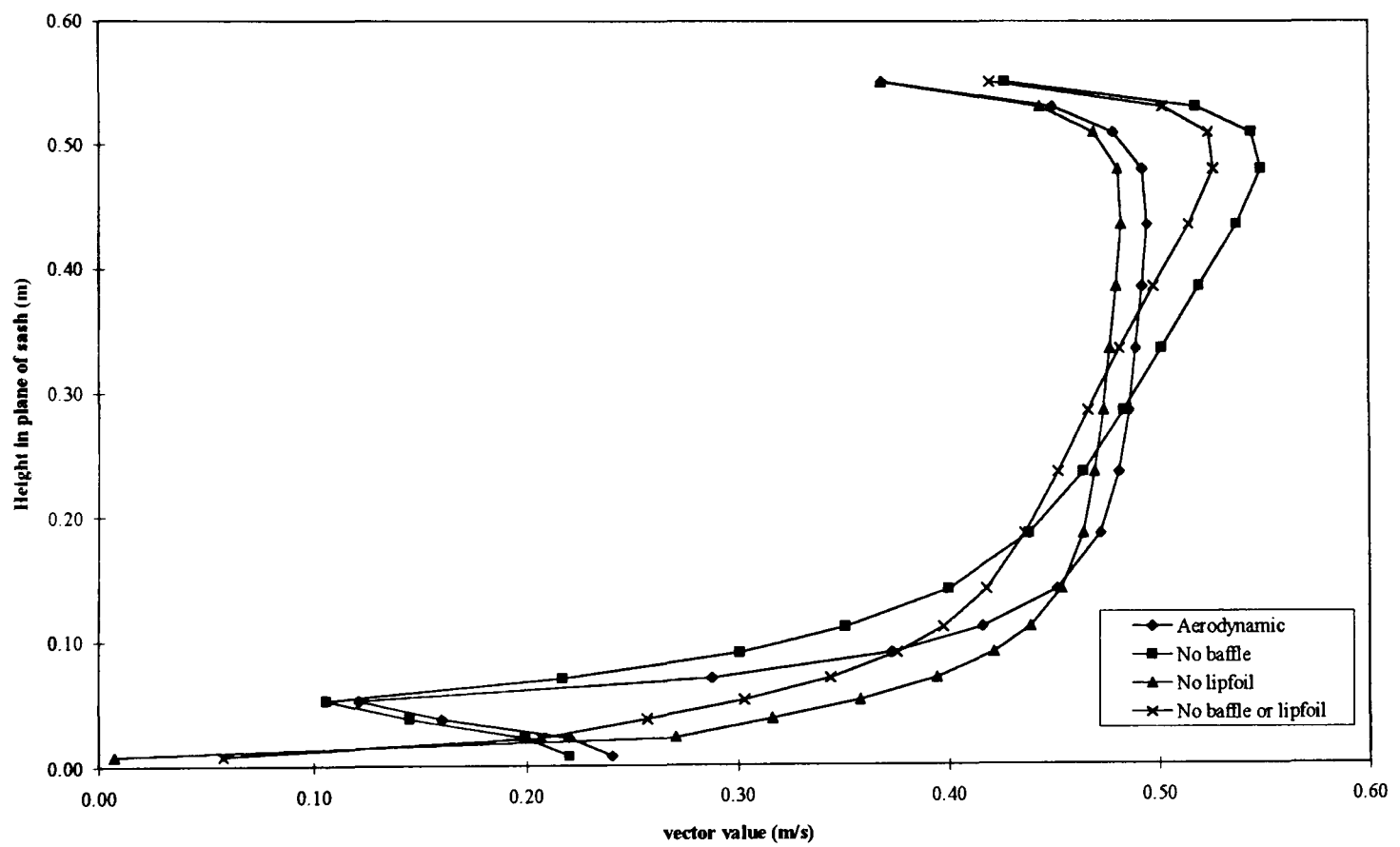
← 1.50 m/s

Rear baffle and lipfoil removed

Figure 6.20 Effect on the airflows within an 'aerodynamic' fume cupboard when the rear baffle and the lipfoil are removed (2 D).



x velocity profiles (Lipfoil 60 mm from work surface if fitted)



Speed profiles (Lipfoil 60 mm from work surface if fitted)

Figure 6.21 Effect on x velocity and speed profiles in the aperture plane of an 'aerodynamic' fume cupboard when the rear baffle and the lipfoil are removed (2 D).

outward beyond the aperture. Removal of both the rear baffle and the lipfoil exaggerated both these effects.

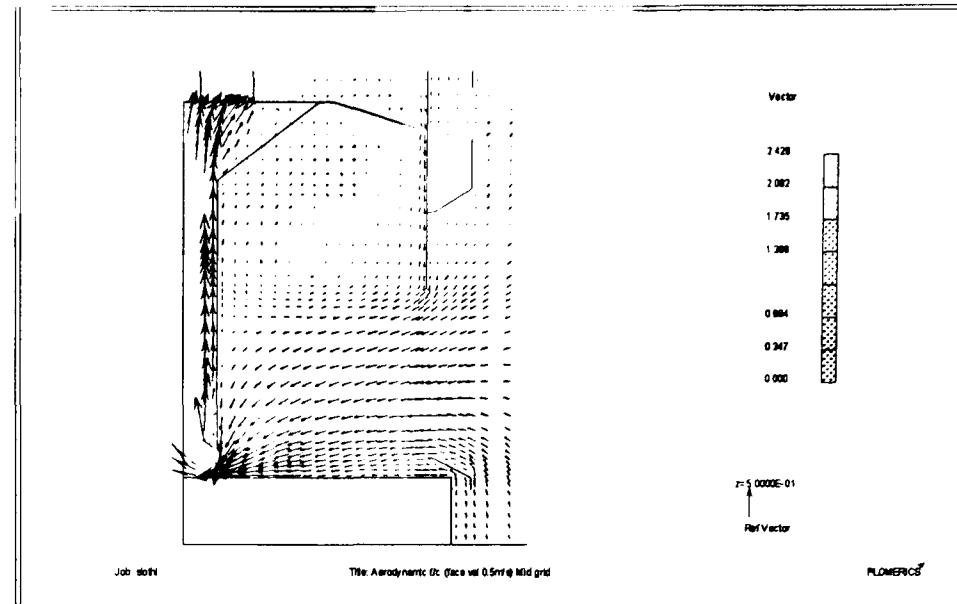
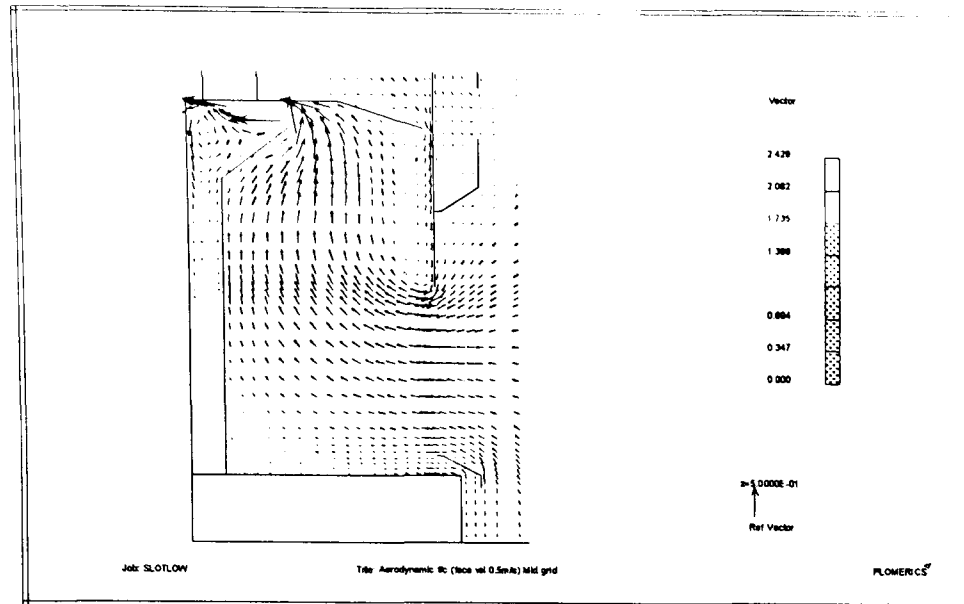
The effect of the distribution of the extract slots in the baffle was crucial to the profile of air flowing through the aperture and distribution within the cupboard. Using the CFD simulation and blocking off the lower scavenging slot this resulted in stagnation of air at the work surface, all the air being exhausted from the cupboard through the upper slot (Fig. 6.22). Blocking off the top slot and leaving the lower scavenging slot open resulted in the stagnation of air in the upper region of the cupboard behind the sash, as all the air was exhausted from the cupboard through the lower slot. These extreme flows were clearly demonstrated by the values of velocity in the plane of the sash showing the different profiles dependant on whether the air was exhausted from the top or bottom of the cupboard interior.

The development of the modern aerodynamic fume cupboard began with simple box type fume cupboards. These were shown in Fig. 6.23 using a 'coarser' grid to simply compare general air flows qualitatively. With no aerodynamic features the air flows were similar to the aerodynamic cupboard with no baffle or lipfoil. There was no scavenging of the work surface and there was a large recirculation of air from deep within the cupboard back to the aperture. There was also a large recirculation of air behind the sash with little purging. The introduction of a slotted straight rear baffle encouraged scavenging of the work surface and a more balanced inflow profile. However, the recirculation zone behind the sash was greater. Introduction of an angled rear baffle so that the extract duct could be placed further forward again encouraged scavenging of the work surface and a smooth entry profile, but also reduced the recirculation zone behind the sash. Further to this was added the shaped entry foils around the aperture to produce a modern 'aerodynamic' fume cupboard.

6.2.6 Modelling the dispersal of a contaminant

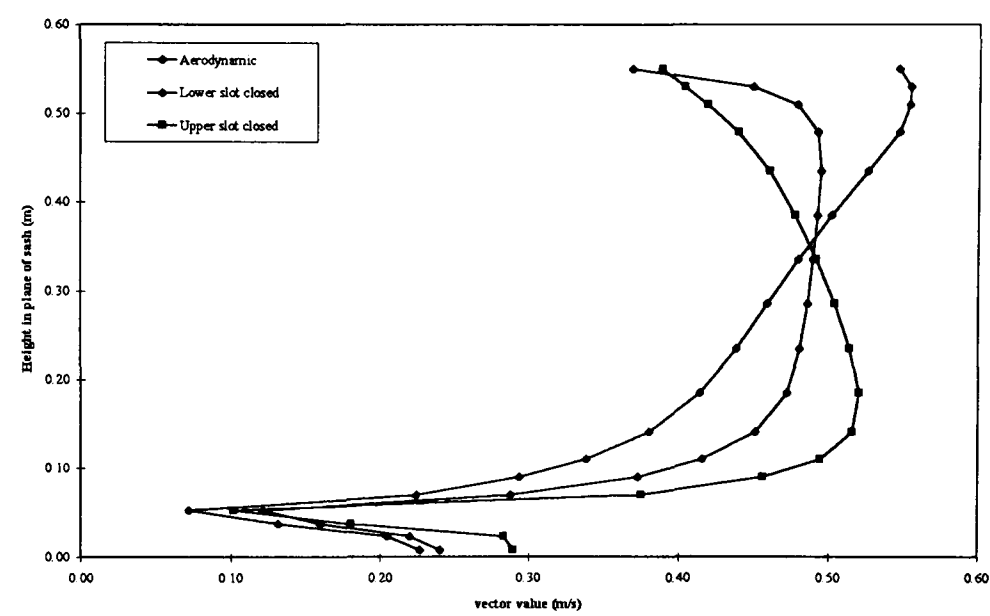
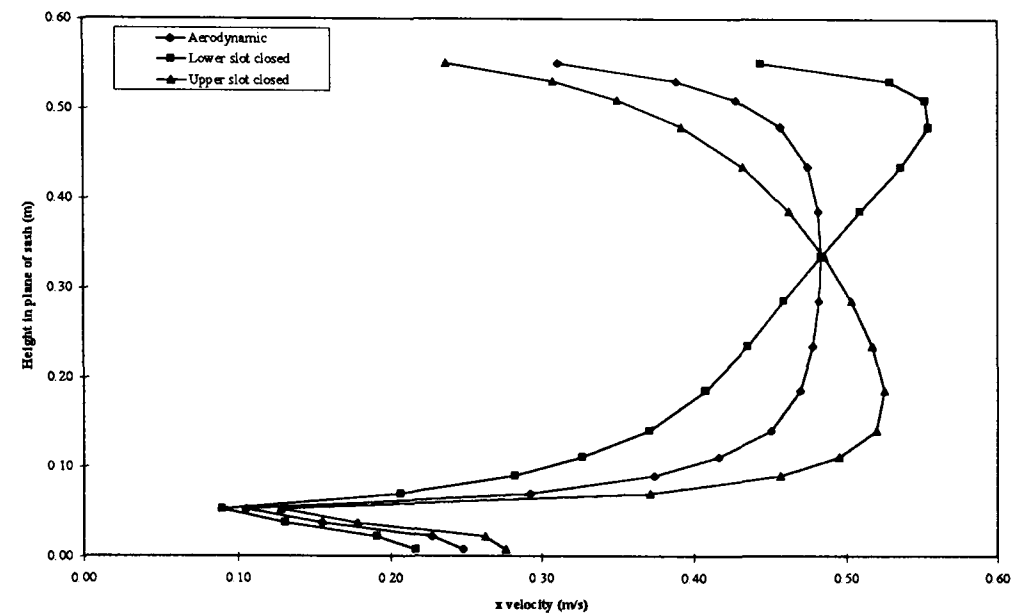
An important tool in CFD was the simulation of contaminant dispersal within the domain. Such a contaminant could be specified as a gas at the same density as air or by using the ideal gas law method as a gas of different density (specified by molecular weight, MW) to air, thus allowing a heavier or lighter than air gas to be simulated. Using the 2 dimensional model set up in the previous sections a volume contaminant source was specified on the work surface to resemble a beaker 150 mm from the front edge. This was 'transparent' allowing air to flow through it and gas at the same density as air was mixed with it at a ratio of $0.001\text{kg}_{\text{contaminant}}/\text{kg}_{\text{air}}$.

The profile of concentration in the plane of the aperture (Fig. 6.24) showed a large difference between simulations using the k- ϵ model and the fixed turbulent (revised) value of $0.005\text{ m}^2/\text{s}$. The simulation of contaminant was much more sensitive to the turbulence model used than was the air velocity. The effect of grid density and refinement was also reviewed using the k-



Lower slot closed

Upper slot closed



x velocity profile (Lipfoil 60 mm from work surface)

Speed profile (Lipfoil 60 mm from work surface)

Figure 6.22 Effect on the airflows, x velocity and speed profiles in the aperture plane of an 'aerodynamic' fume cupboard when the lower and upper slots of the rear baffle are closed (2 D).

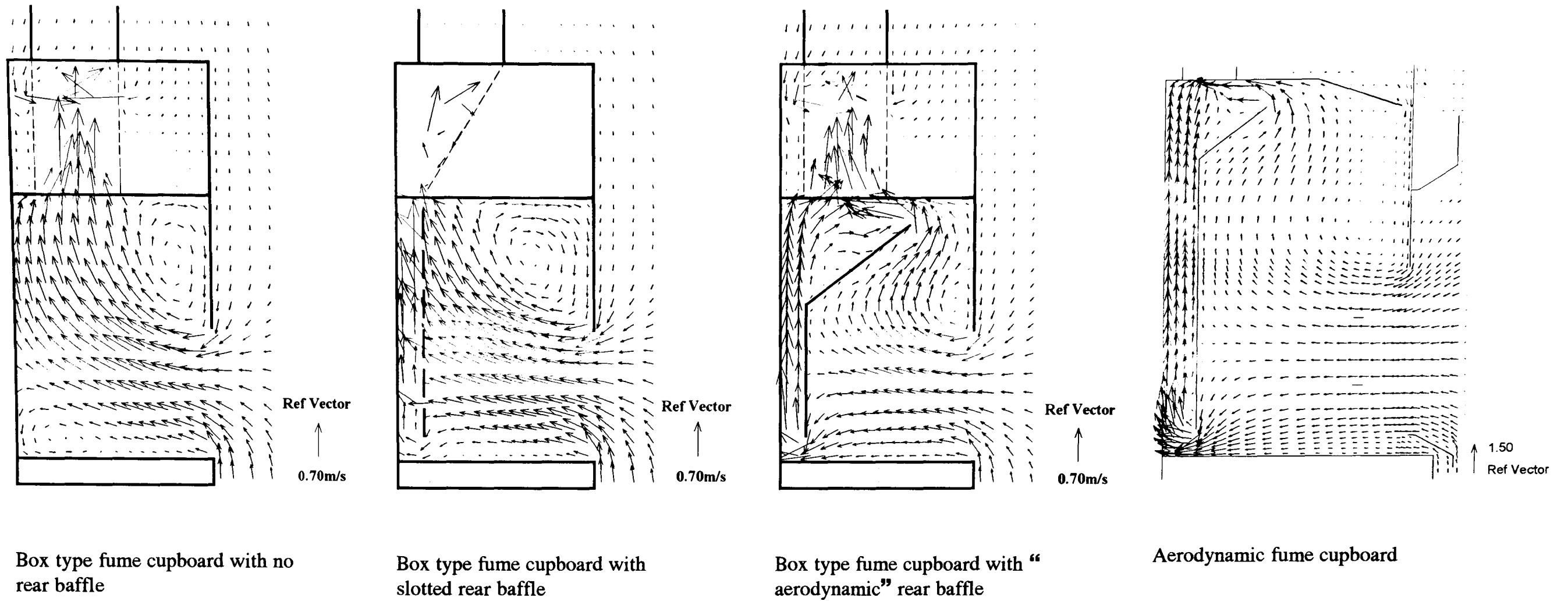


Figure 6.23 Evolution of modern day ‘aerodynamic’ fume cupboard visualised using airflow vectors (2 D).

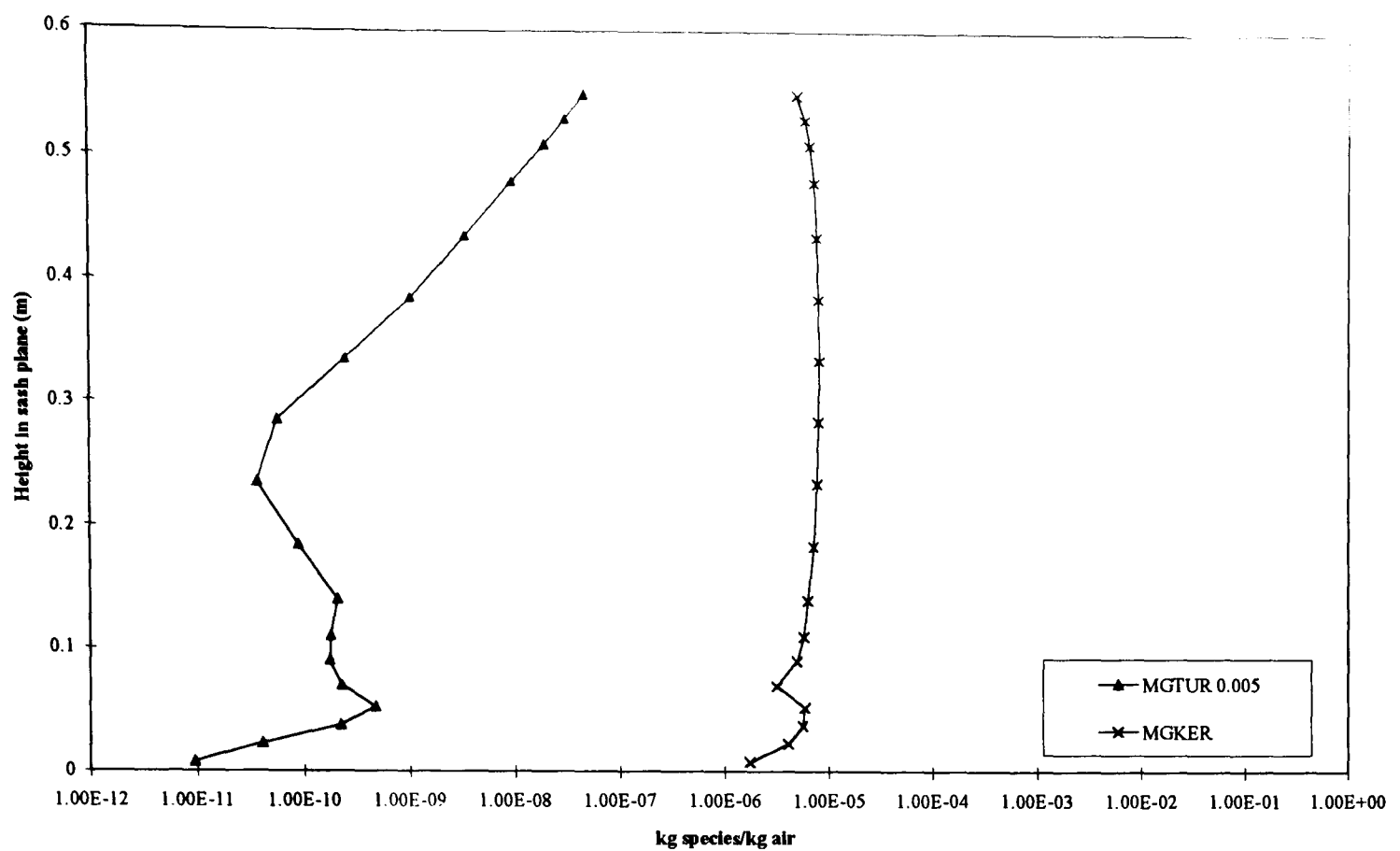


Fig. 6.24 Effect of the turbulence model on concentration profiles in the aperture plane of an aerodynamic fume cupboard (2 D). (MG, medium refined grid; TU, fixed turbulence model; KE, $k \epsilon$ turbulence model)

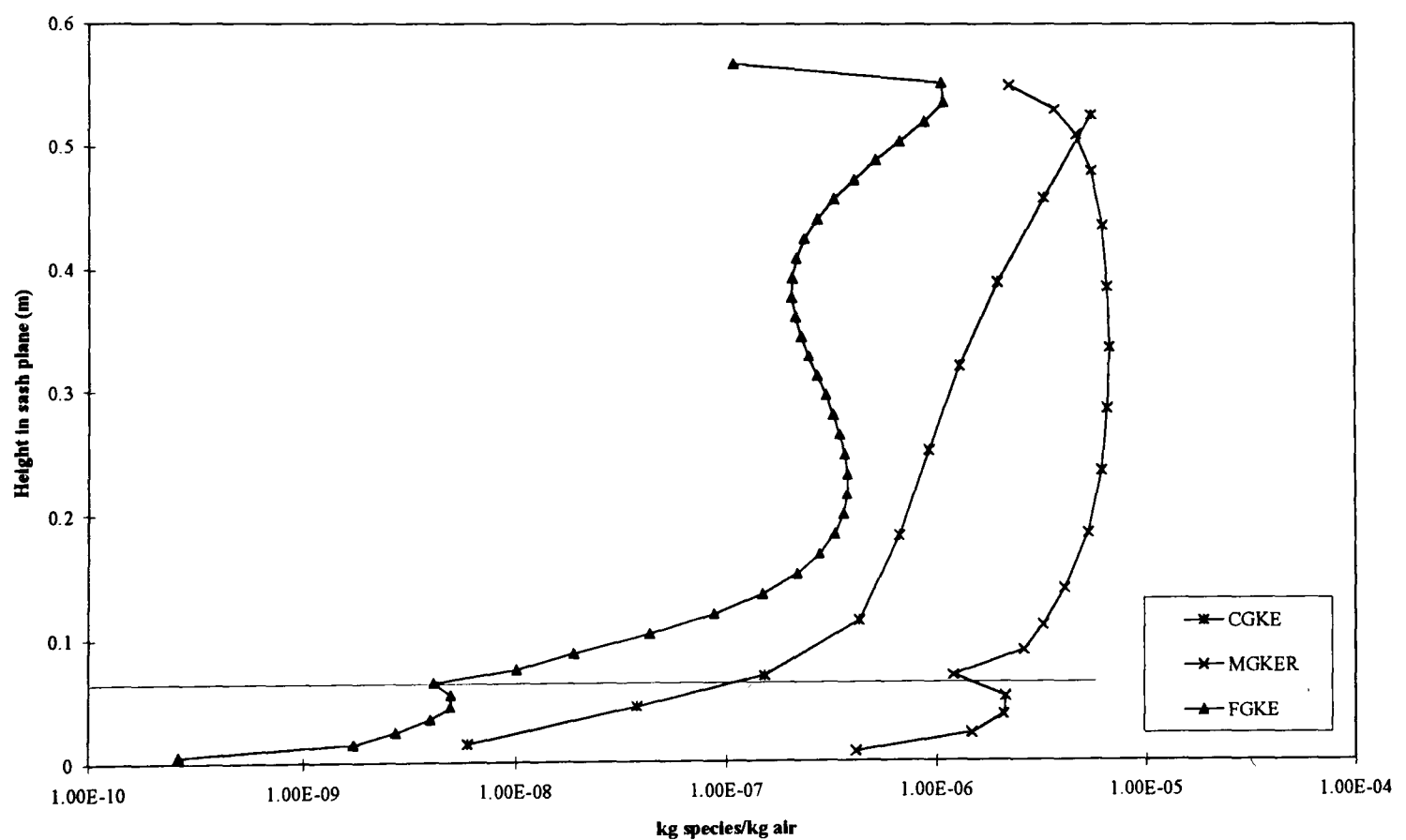


Fig. 6.25 Effect of grid density and refinement on the concentration profiles in the aperture plane of an aerodynamic fume cupboard (2 D). (CG, coarse grid; MG, medium refined grid; FG, fine grid; KE, $k \epsilon$ turbulence model; R, refined grid).

ϵ model and the 'coarse' grid, 'medium' grid and 'complex' grid as used in earlier sections. This again showed that the concentration profile in the plane of the aperture was sensitive to changes in the grid structure (Fig. 6.25).

The refined 'medium' grid was revised further (Fig. 6.26) by increasing the number of cells between the source and the aperture by 1. This substantially altered the concentration profile in the plane of the sash and which more resembled the 'complex' grid results. Two extra cells were added in the y direction of the aperture vertical limits but this only slightly altered the profiles. These further revised grids were then compared to the other grids to establish any effect on the air flow values in terms of x velocity and speed profiles in the plane of the sash. This showed little difference.

The dependence of contaminant dispersal on the turbulence model was demonstrated by simulated diffusion in a 2 dimensional adiabatic tube with dimensions 0.5 m high, 1 m wide and 1 m long rectangular tube with smooth walls (Fig. 6.27). From one end air was extracted and the other end specified as an opening (inlet). The flow through the tube was 0.5 m/s (cupboard face velocity) and with a Reynolds number of 16000. A contaminant (MW of air) was released as a vertical planar source in the centreline of the tube (positive side in the direction of air flow) at a rate of 0.001 kg contaminant/kg air passing through the plane. Contaminant profiles were then plotted at distances upstream of the source.

Changing only the turbulence model appreciably altered the diffusion of the contaminant from the source. The flow in the tube was turbulent and the fixed value for turbulence (revised) of $0.005 \text{ m}^2/\text{s}$ estimated from the density, characteristic velocity and height of the tube, was very different to either the k- ϵ model or fixed turbulent value (revised) of $0.000125 \text{ m}^2/\text{s}$.

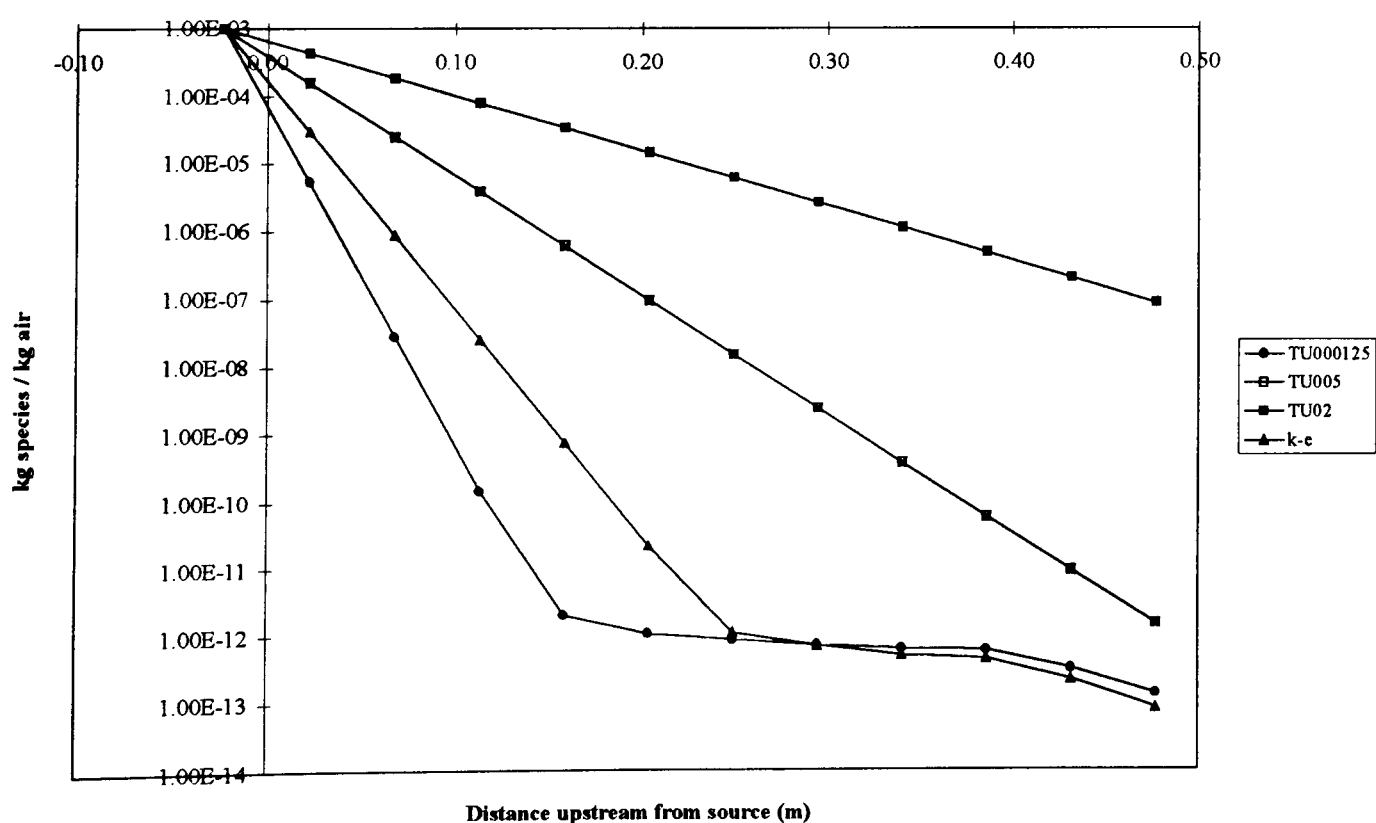
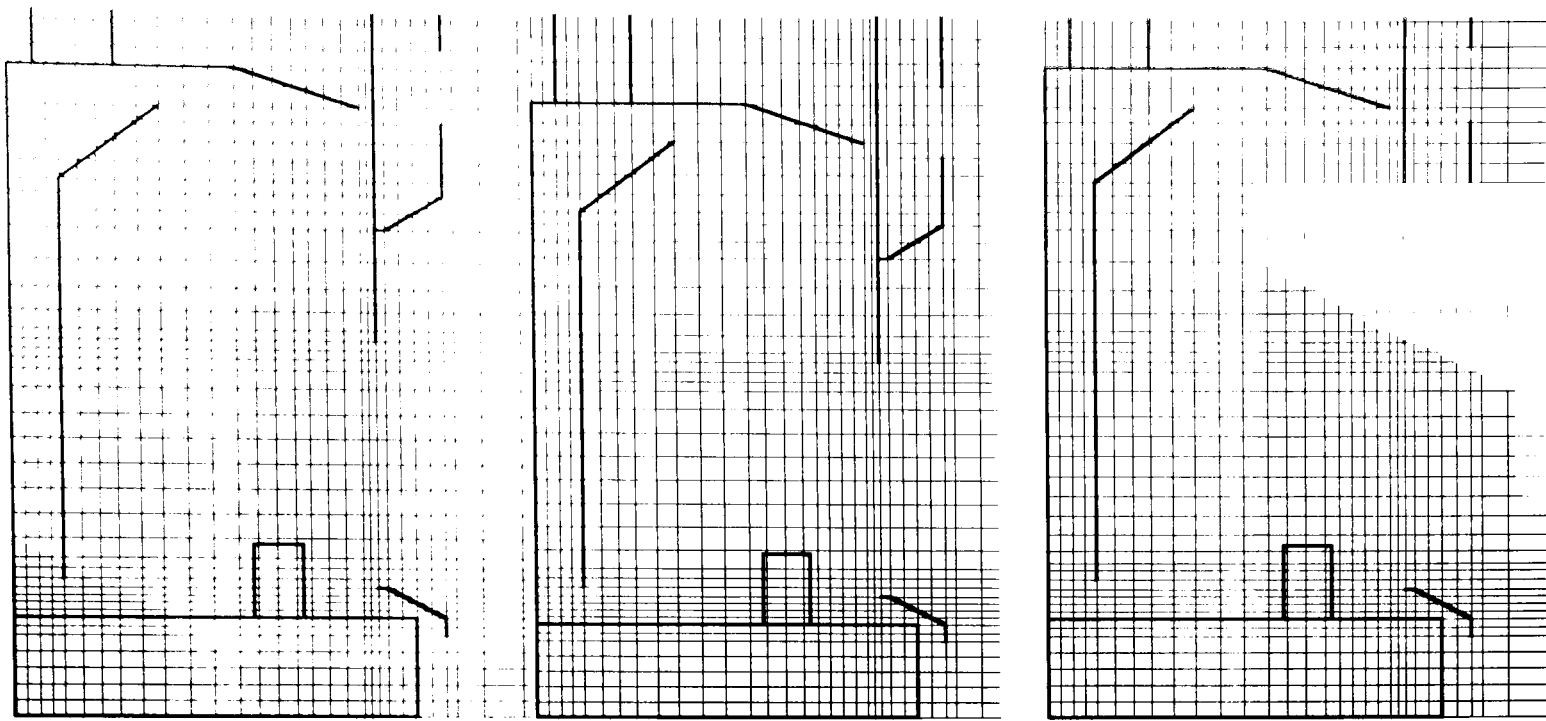


Figure 6.27 Effect of the turbulence model on contaminant diffusion in a straight tube. (TU, fixed revised turbulence model (units m^2/s ; k-e. k ϵ turbulence model).



Existing grid

Increase cells in x direction

Increase cells further in y direction

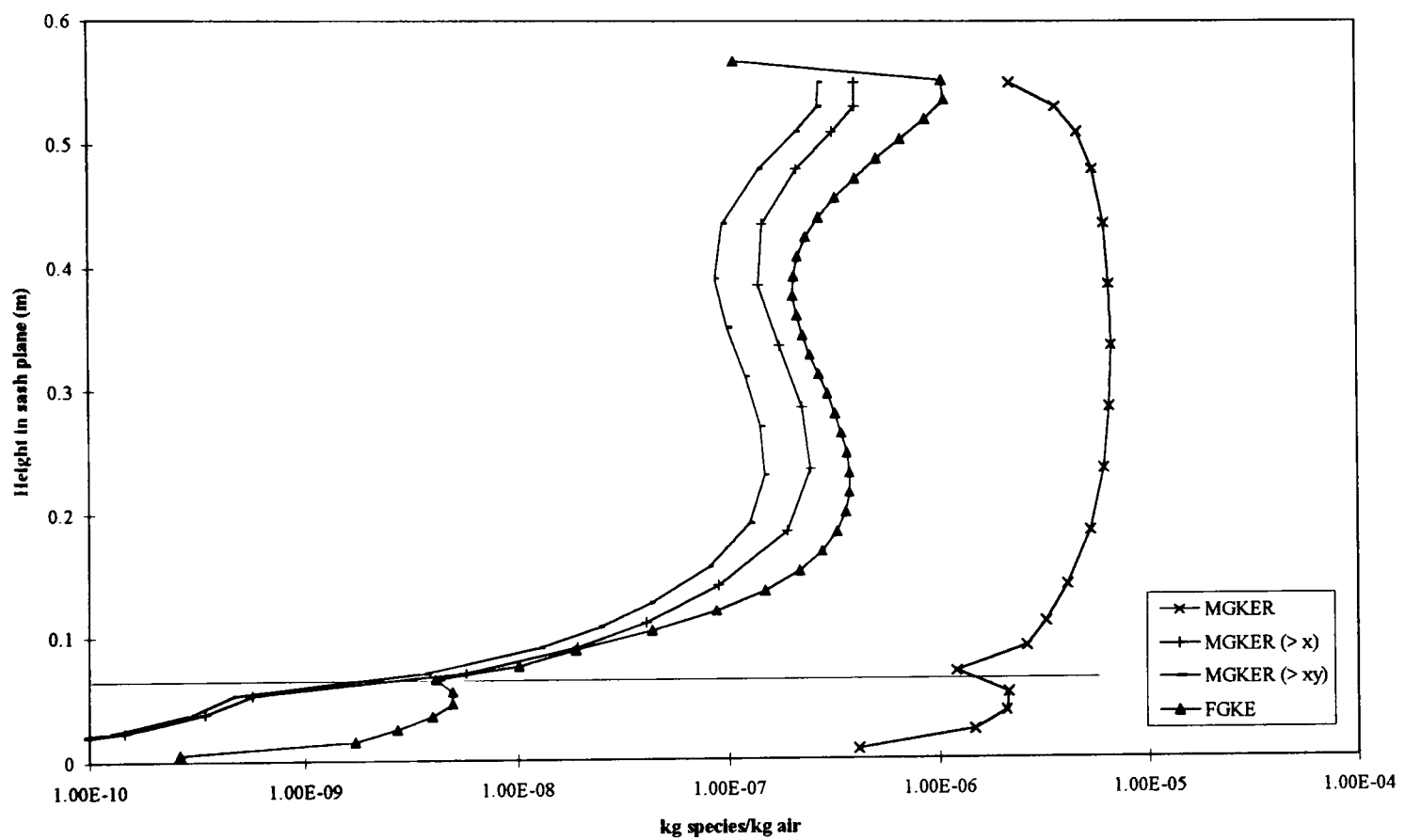


Figure 6.26 Effect of further grid refinement on concentration profiles in the aperture plane of an aerodynamic fume cupboard (2 D) (MG, medium refined grid; FG, fine grid; > x increased grid cells in x direction; > xy increased grid cells in both x and y direction; KE $k-\epsilon$ turbulence model; R, refined grid).

6.2.7 Fume cupboard type compared in terms of contaminant profile

The concentration profile of contaminant in the plane of the aperture of the two dimensional 'aerodynamic' fume cupboard showed higher concentrations near to the sash than the lipfoil (Fig. 6.28). This may have represented the lack of sash handle and increased turbulence in this region. The values were slightly higher than expected in reality but this fume cupboard model was not assessed without the sash handle.

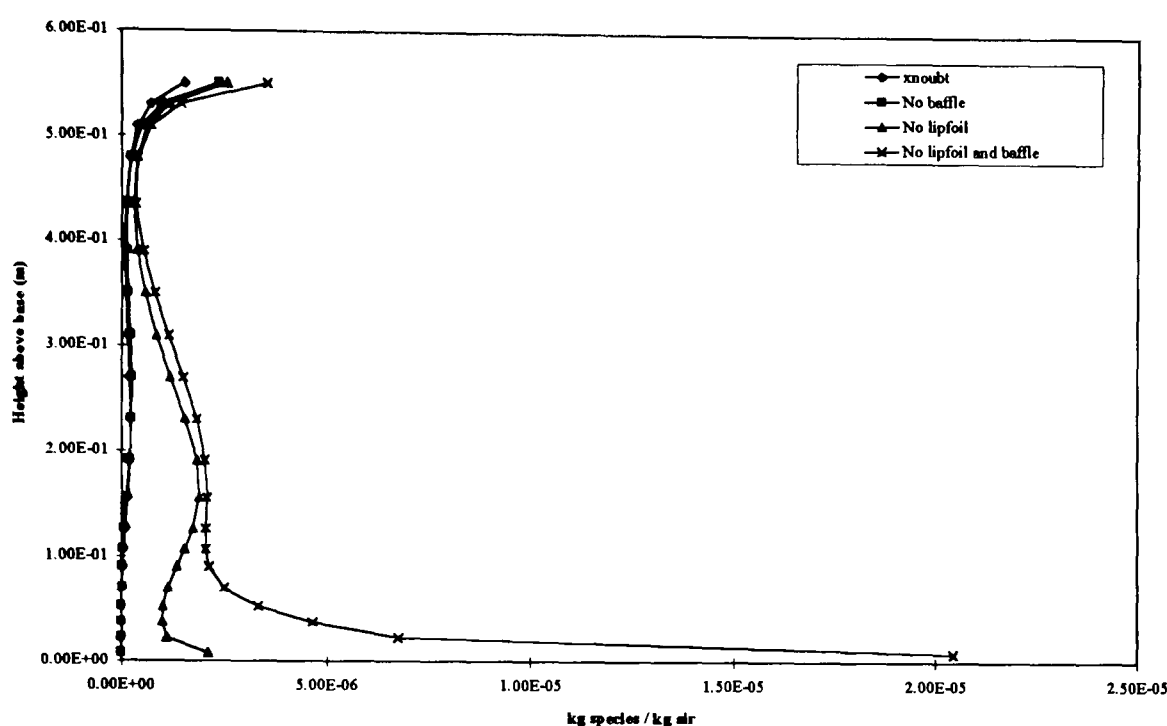


Fig. 6.28 Effect of geometric features on concentration profiles in the aperture plane of an aerodynamic fume cupboard (2 D).

The CFD model was used for comparing the effects of design changes as previously used to compare air flows. Removal of the lipfoil resulted in contaminant moving past the plane of the aperture and out of the cupboard along the work top. The contaminant profile in the plane of the aperture showed considerably higher concentrations near to the work surface. Removing just the rear baffle did not result in any change in the profile in the aperture plane compared to the 'aerodynamic' cupboard, but with both the rear baffle and lipfoil removed gave the greatest contaminant levels near to the work surface.

6.2.8 Discussion and conclusions

The two dimensional simulations were sensitive to the turbulence model specified, the grid density and its level of refinement. Qualitatively there was little difference, for each simulation the general airflow patterns were very similar. However, it was quantitatively where the differences were greatest. The simulation of a contaminant dispersal showed most differences.

The calculated profiles of air flow (x velocity and speed) in the plane of the aperture were similar to the physical measurements but did not reflect accurately edge effects. In the simulation no sash handle was represented but where the lipfoil was simulated there were

differences. The physical measurements showed an increase in velocity as air passed over the top edge of the lipfoil which was not shown in the simulation. The simulation also showed a different x velocity and speed profile beneath the lipfoil. In the simulation, the program was unable to represent curves but only as a series of straight lines which in terms of the whole fume cupboard simulation would produce a grid too complex for this PC based calculation.

However, the two dimensional model of the aerodynamic fume cupboard was used as a base model and the effect of removing the baffle and lipfoil (without altering any of the model parameters) was compared to this base model. This clearly showed the relative contribution of these design features to the overall flow pattern and simulated containment.

The lipfoil and sash handle were studied more closely as separate features from the whole cupboard simulation. This showed in more detail how each may influence local turbulence caused by sharp edges and how a smoothed entry profile may eliminate these. In terms of the whole fume cupboard flow field such local effects were not simulated due to limits on complexity. However, this showed a complete flow field, giving a mean estimation of flow in the more localised turbulent zones.

6.3 The use of a 3 dimensional model to describe and predict the effect of blockage, poor design and disturbance of airflows on the performance of open fronted containment systems (steady state)

6.3.1 Three dimensional model set-up

In order to simulate blockages and disturbance on fume cupboard containment a three dimensional model was set up as a progression of the two dimensional model (Fig. 6.29). The domain was reduced in terms of the volume of room outside the cupboard. This was reduced to ~ 100 mm horizontally and width increased to 1.6 m as the z component. The height was decreased. The same xy grid overlaying the cupboard was used, adjustment was made to the grid beyond the sash (Fig. 6.30) and the z grid was generated with refinement near to the vertical edges. The total number of grid cells was 46530.

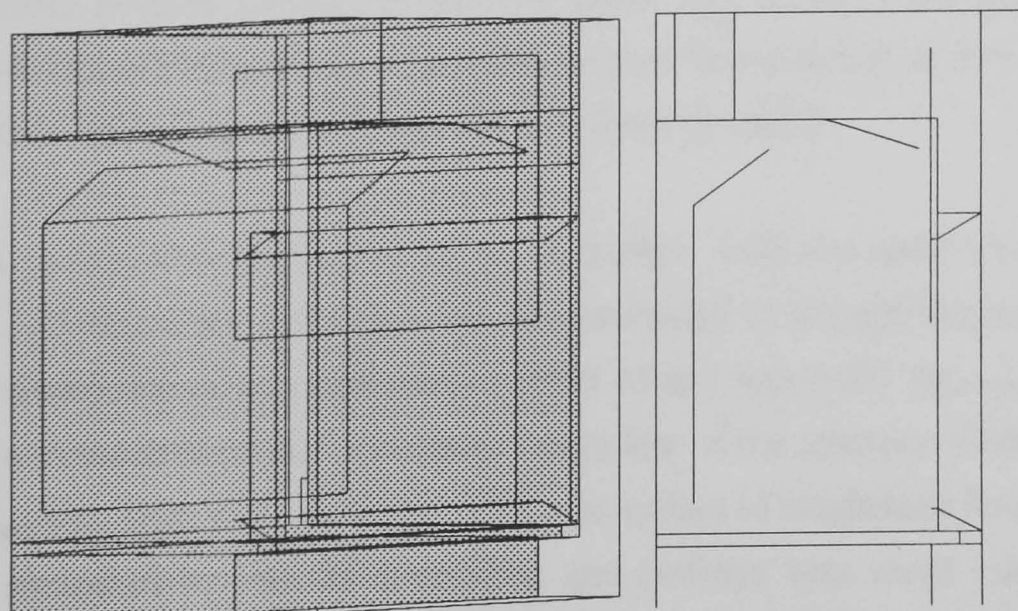


Figure 6.29 3 Dimensional (3 D) model of an aerodynamic fume cupboard.

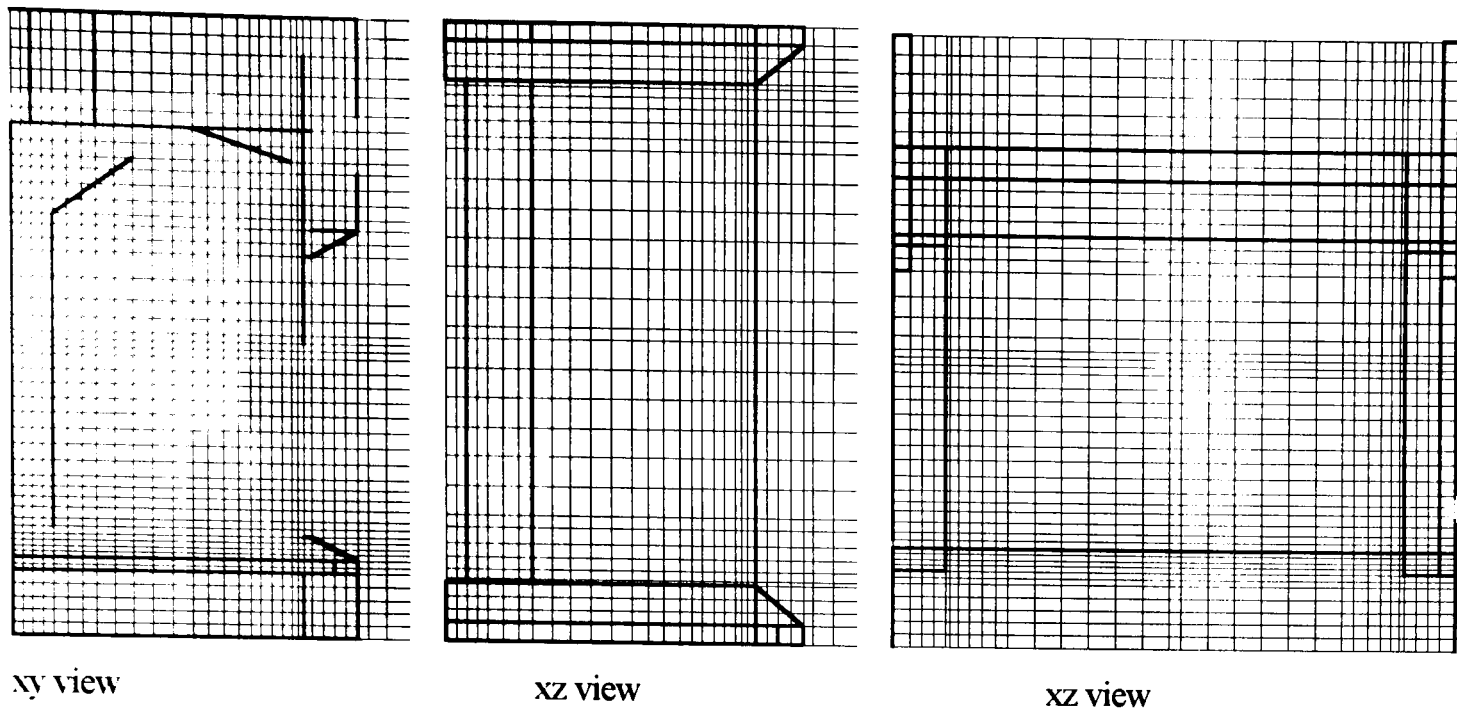


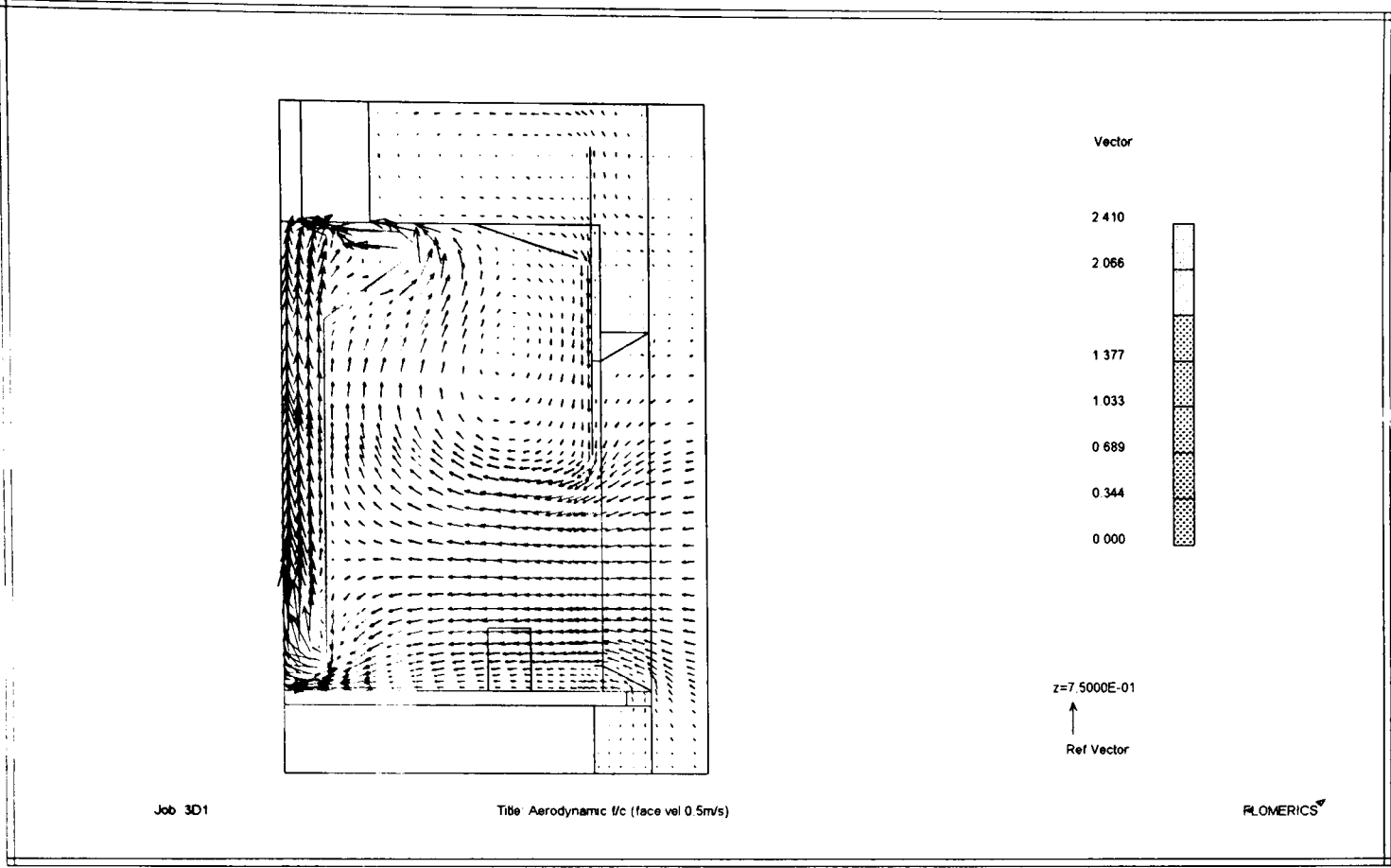
Figure 6.30 Solution grid for 3 dimensional model

For calculation purposes the k- ϵ model was used. A face velocity of ~ 0.5 m/s was estimated, and extract flow rate specified accordingly. The solution domain was again adiabatic. The solution time was approximately 3 days.

6.3.2 Description of air flow and comparison with 2 dimensional simulation and physical measurements

The qualitative and quantitative results using the three dimensional model were compared with those of the two dimensional model. There was no visual difference between the air flows within the cupboard in the xy plane and for the 3D model in the horizontal centre line (Fig. 6.31). The profiles of x velocity and speed for the two models however did differ (Fig. 6.32). They matched each other near to the sash but the 3D model showed a slight drop in velocity in the middle of the aperture which increased nearer to the lipfoil before decreasing again. There was no difference in the x velocity and speed profiles below the lipfoil. In the z dimension (Fig. 6.31) the air flow was uniform across the width of the cupboard being squeezed at the edges to flow straight to the back near to the work surface. At mid height small recirculation zones were shown at the rear of the cupboard against the rear baffle. The x velocity and speed profiles across the aperture plane near to the work surface and in the horizontal centre line of the aperture (Fig. 6.33) showed lower values near to the sides which increased and then decreased slightly with distance from the sides.

A contaminant source was placed on the work surface with the same xy dimensions and position to the 2D model but the z direction was increased to occupy the width of the work surface. The release rate of contaminant gas (MW of air) was $0.001 \text{ kg}_{\text{contaminant}}/\text{kg}_{\text{air}}$ and the resultant profile in the vertical and horizontal centre line of the aperture plane showed values $<1\text{e-}9 \text{ kg}_{\text{contaminant}}/\text{kg}_{\text{air}}$ (Fig. 6.32 & 6.33). This was orders of magnitude less over the whole aperture than simulated by the 2D simulation and perhaps was more comparable to the expected physical measurements. The differences may be explained by increased cells in the z



xy plane (centreline of the aperture width).

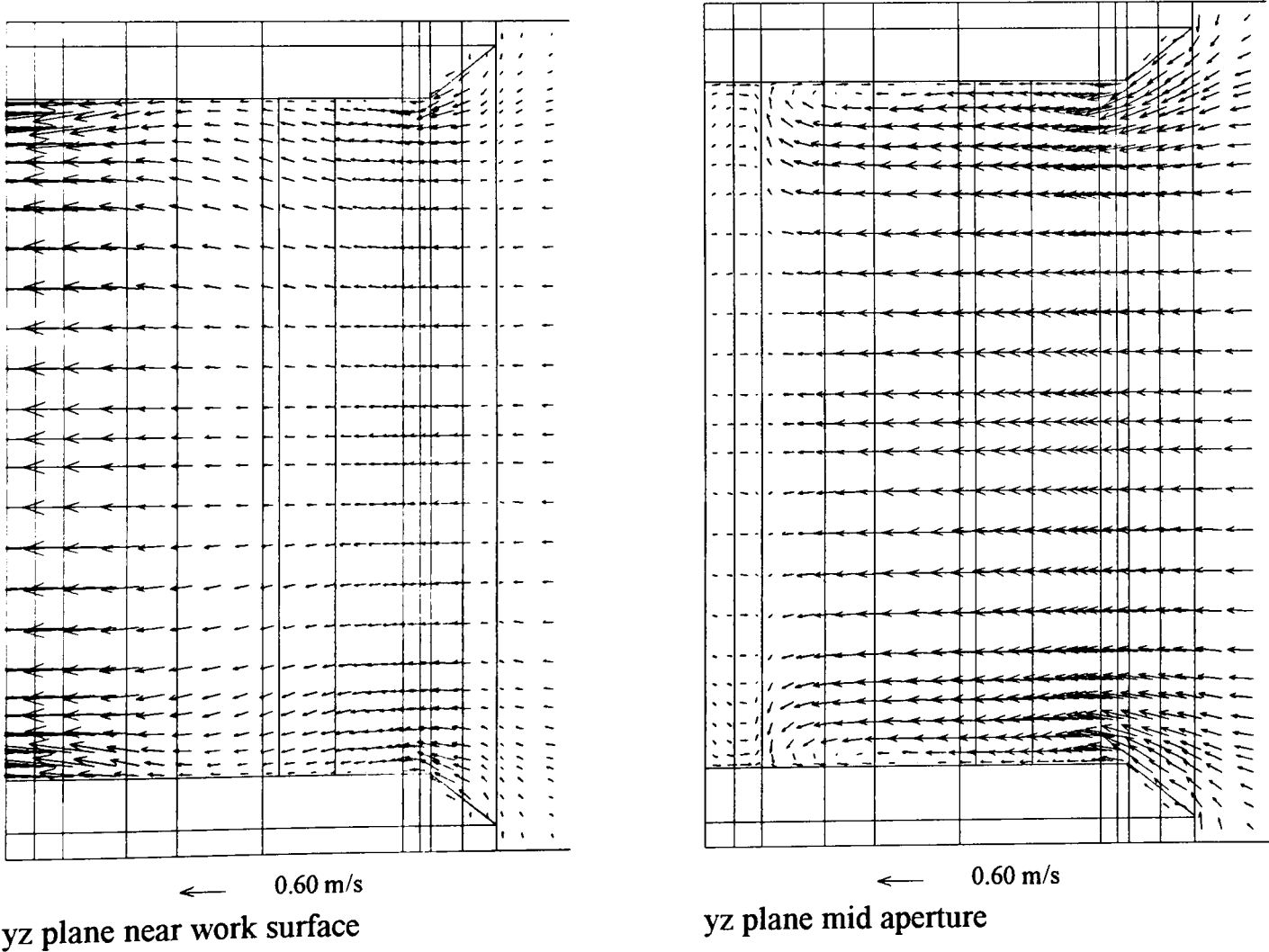
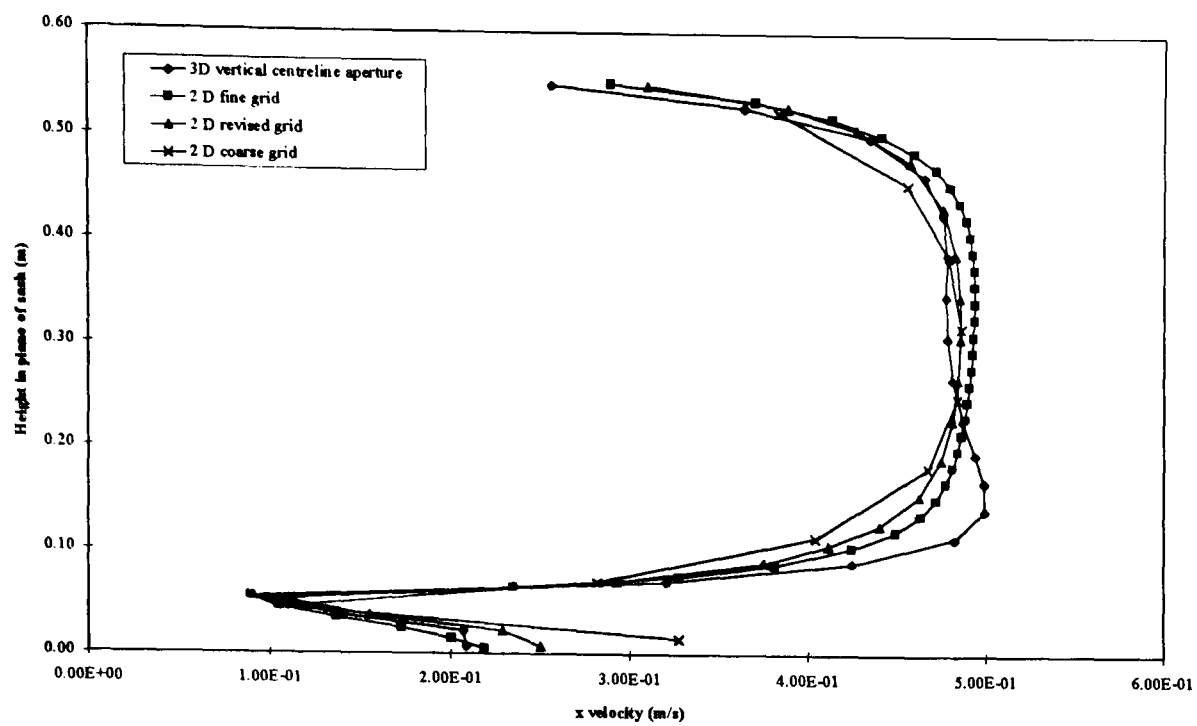
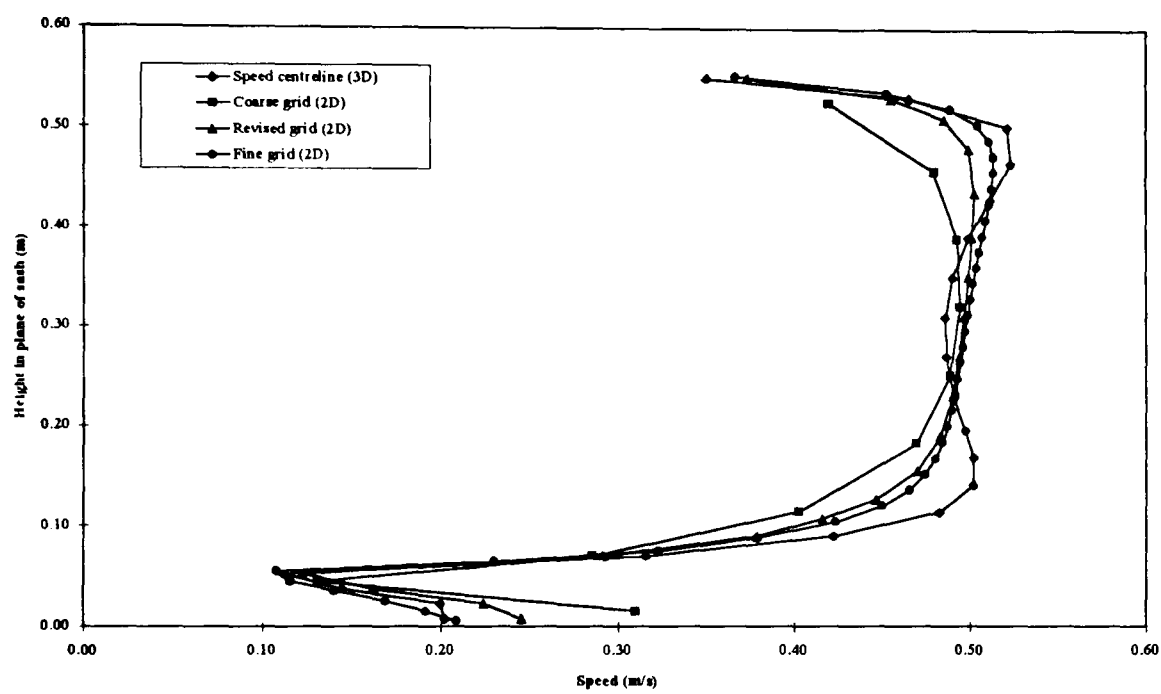


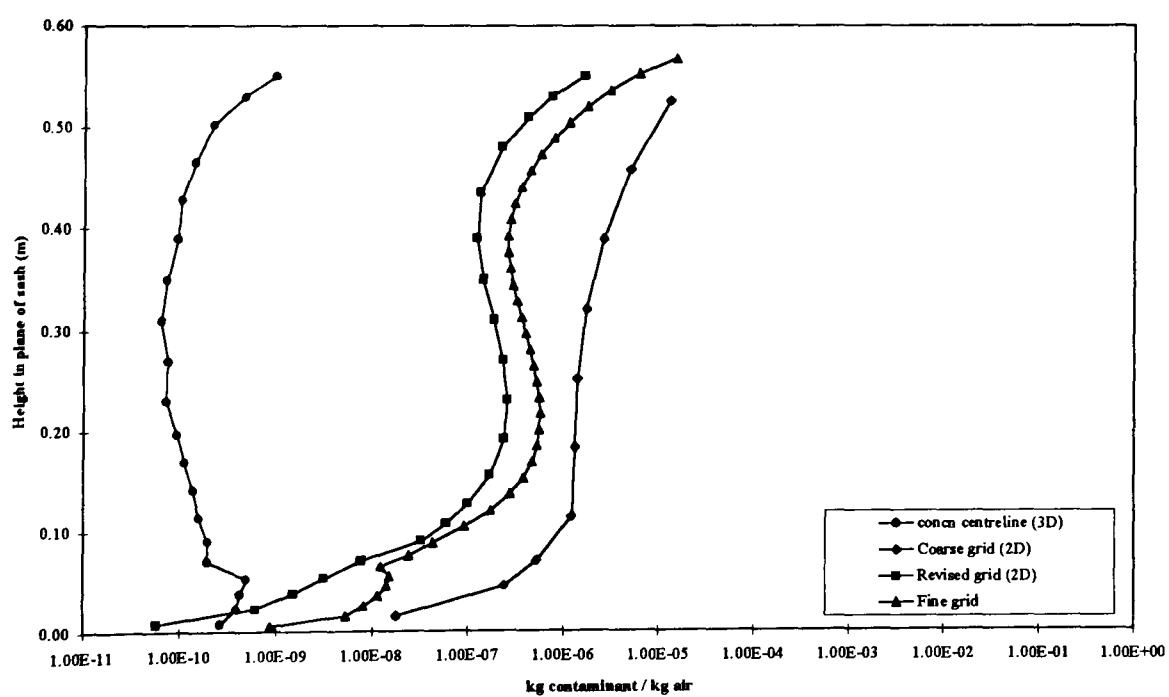
Figure 6.31 Air flow vectors within an aerodynamic fume cupboard (3 D).



x velocity profile

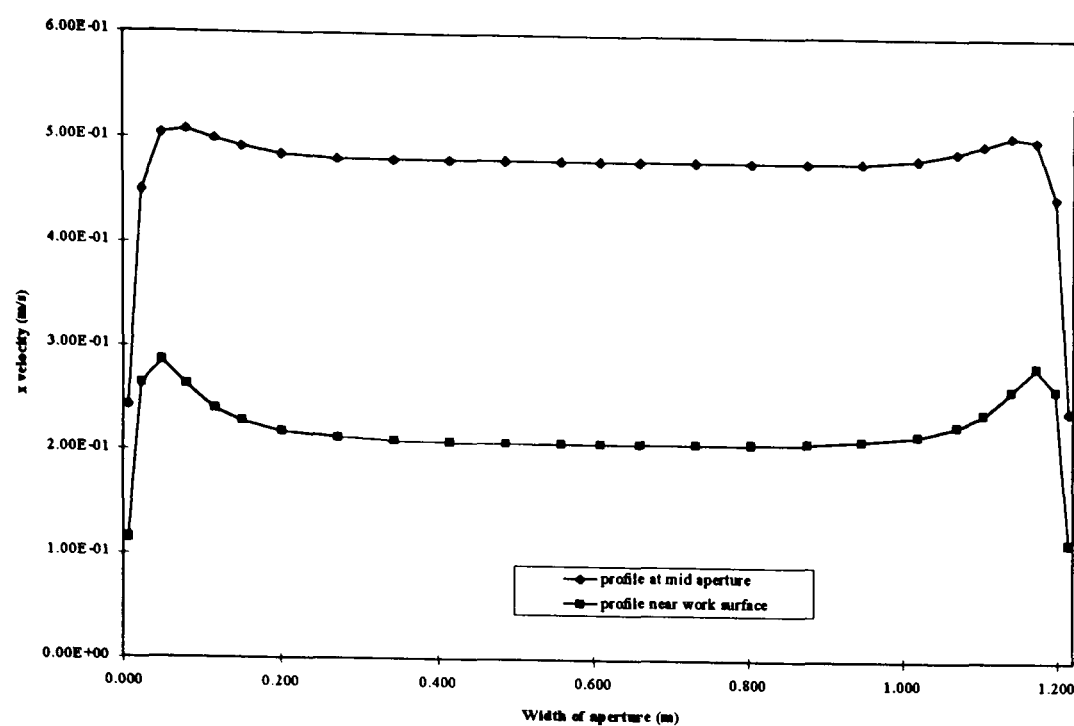


Speed profile

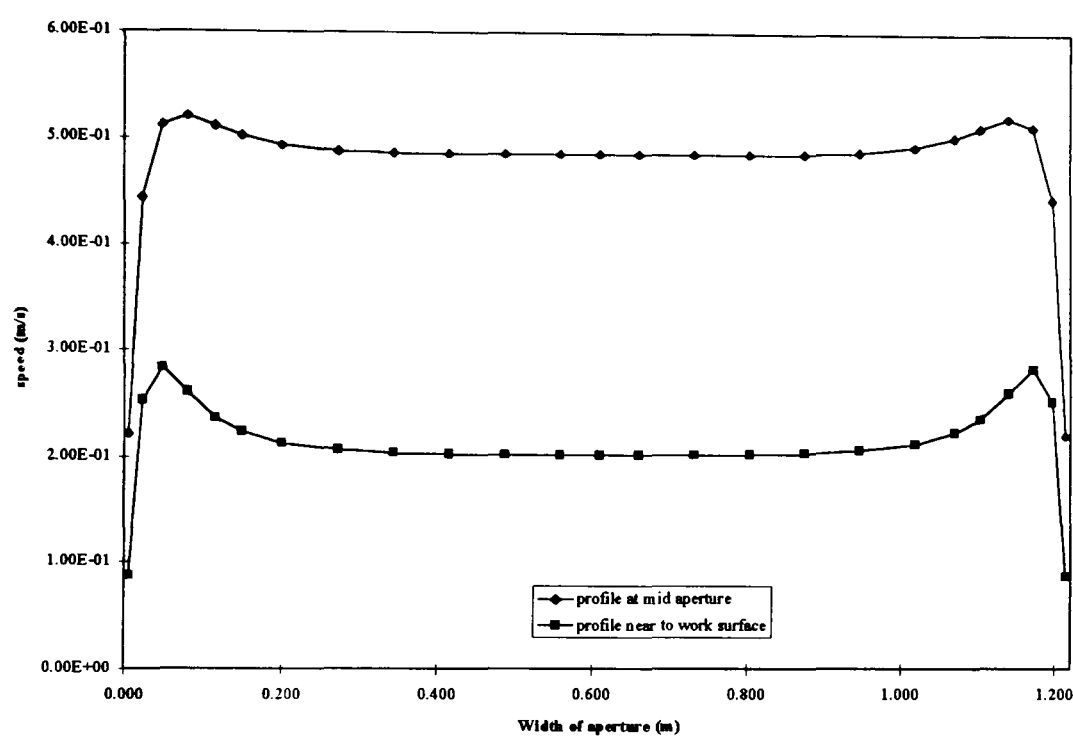


Concentration profile

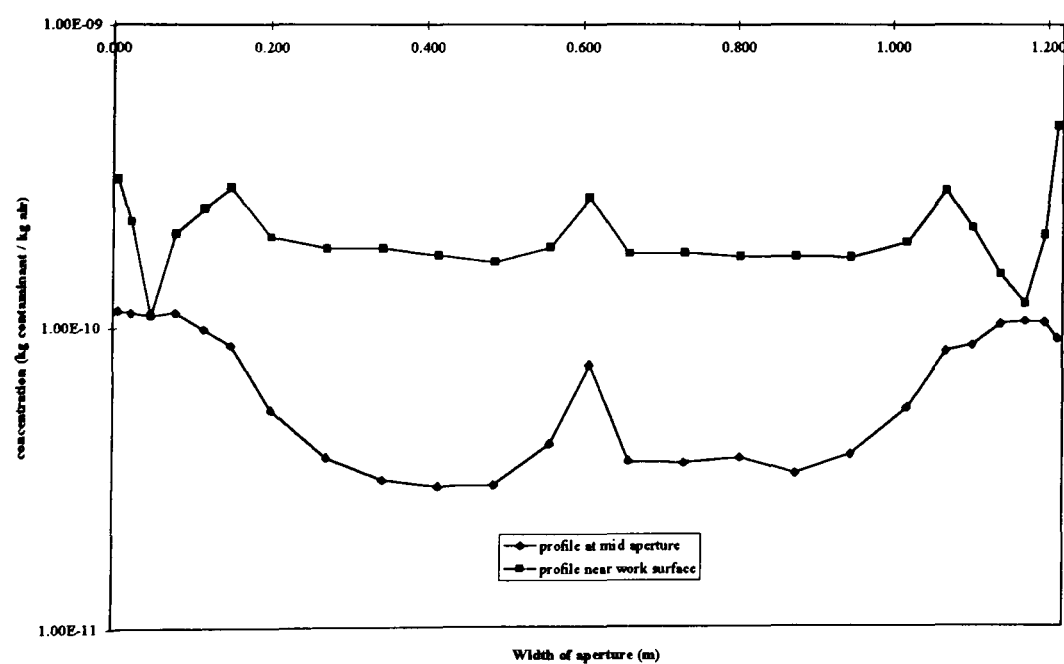
Figure 6.32 Comparison of x velocity, speed and concentration profiles in the horizontal centreline of the aperture plane of the 3 dimensional model with the 2 dimensional model.



x velocity profiles



Speed profiles



Concentration profiles

Figure 6.33 x velocity, speed and concentration profiles across the aperture plane, z direction, near to the work surface and at mid aperture height of an aerodynamic fume cupboard (3 D).

direction over which the turbulent and molecular diffusion was calculated and which also would reflect the change in velocity and speed profiles.

These 3D x velocity and speed profiles were much closer to the physical measurements than the 2D model (Fig. 6.34). However, there were still differences beneath the lipfoil.

6.3.3 Effect of fume cupboard design features on the overall flow field

The effect of removing the baffle and lipfoil on the airflows, as compared using the 2D model, was repeated with the 3D model. Both the baffle and lipfoil were removed. The airflows, x velocity, speed and concentration profiles in the horizontal centre line of the plane of the aperture produced similar results and conclusions as for the 2D simulations.

In the third dimension there was little difference in the air flows at mid aperture (Fig. 6.35), the only difference being at the rear where no baffle was present and the small recirculation zones extend to the back wall. There was greater difference near to the work surface where without the lipfoil or rear baffle the air flowed back towards the aperture from the working volume and where the contamination levels were several orders of magnitude higher (Fig. 6.36) than with the baffle and lipfoil present.

6.3.4 Effect of manikin/operator and blockage on simulated airflow and contaminant dispersal

6.3.4.1 Set up

The 3D simulation was used to study the effects of blockage on airflows and containment. The 'aerodynamic' model with and without the rear baffle and lipfoil was used as the established simulation and a 'square - edge' person modelled standing in front of them (6.37 & 6.38) 1) 84 mm from the aerodynamic lipfoil and 60 mm from the edge of the work surface with lipfoil removed 2) against the edge of the lipfoil and against the edge of the work surface. The simulated person was adiabatic and there was no change of grid or any other parameters.

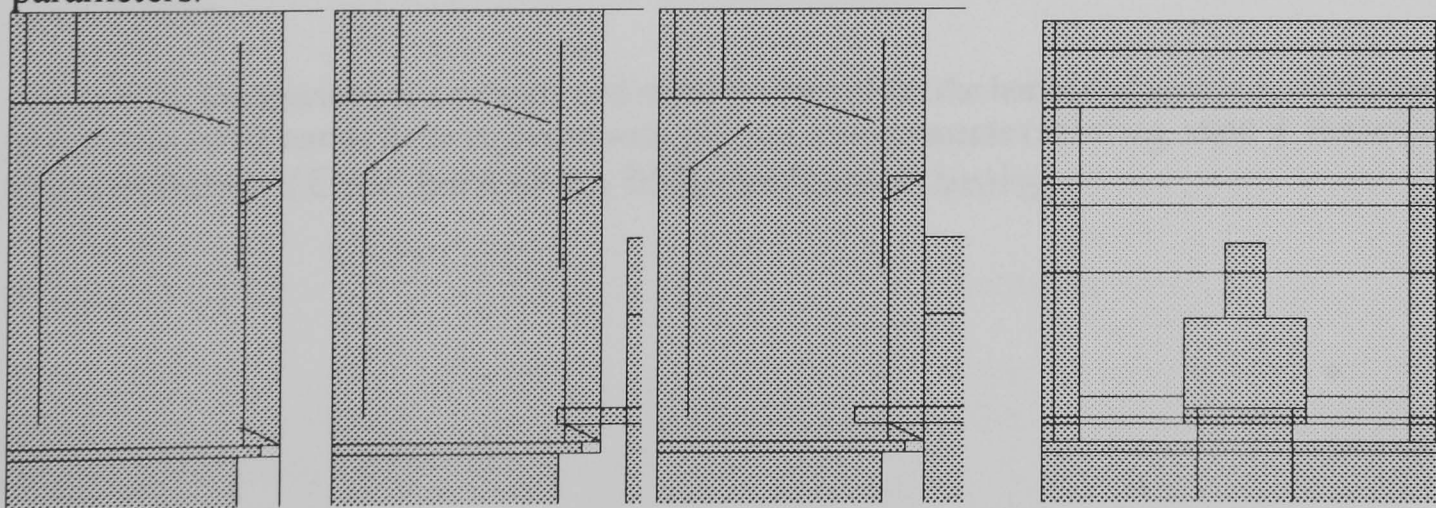
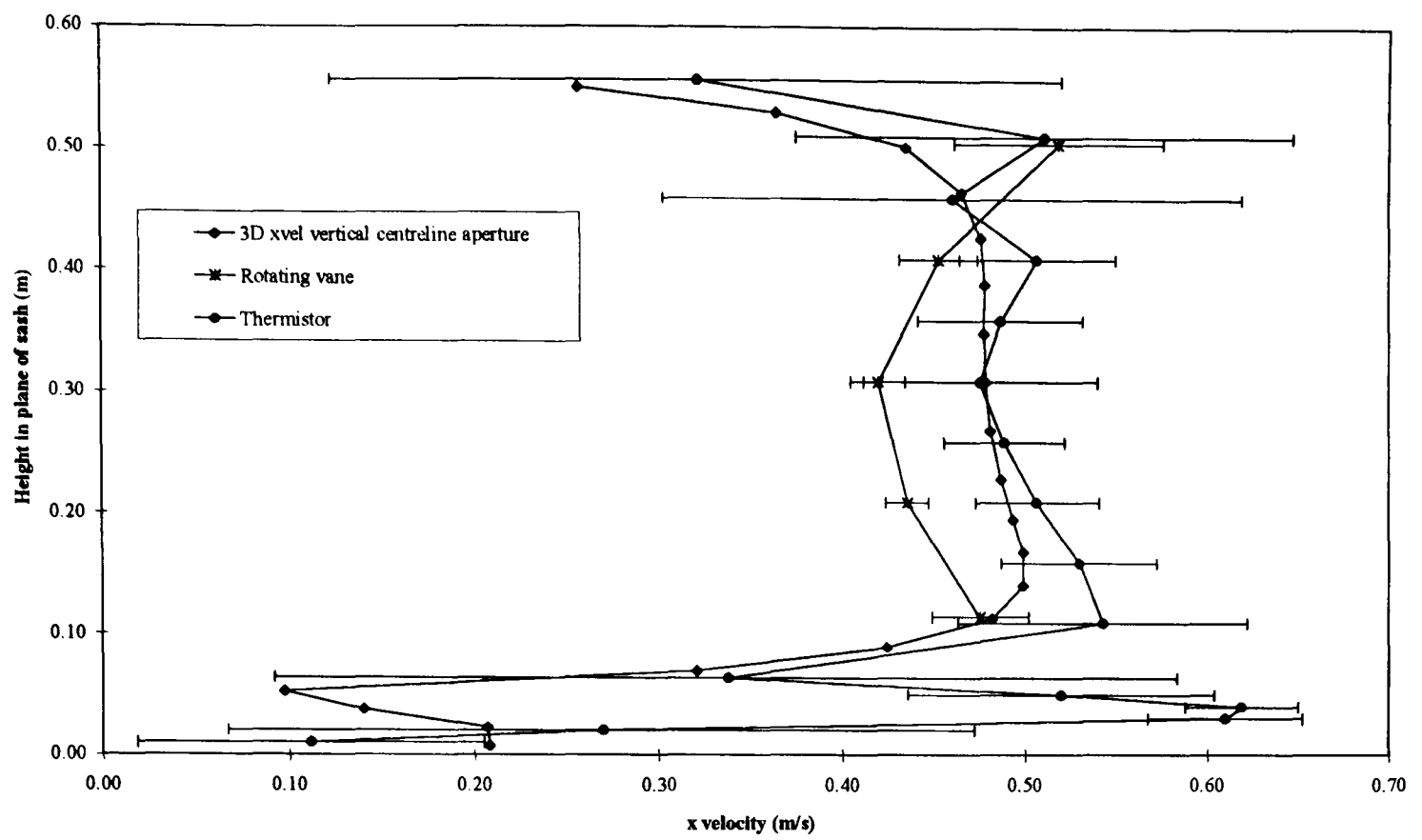
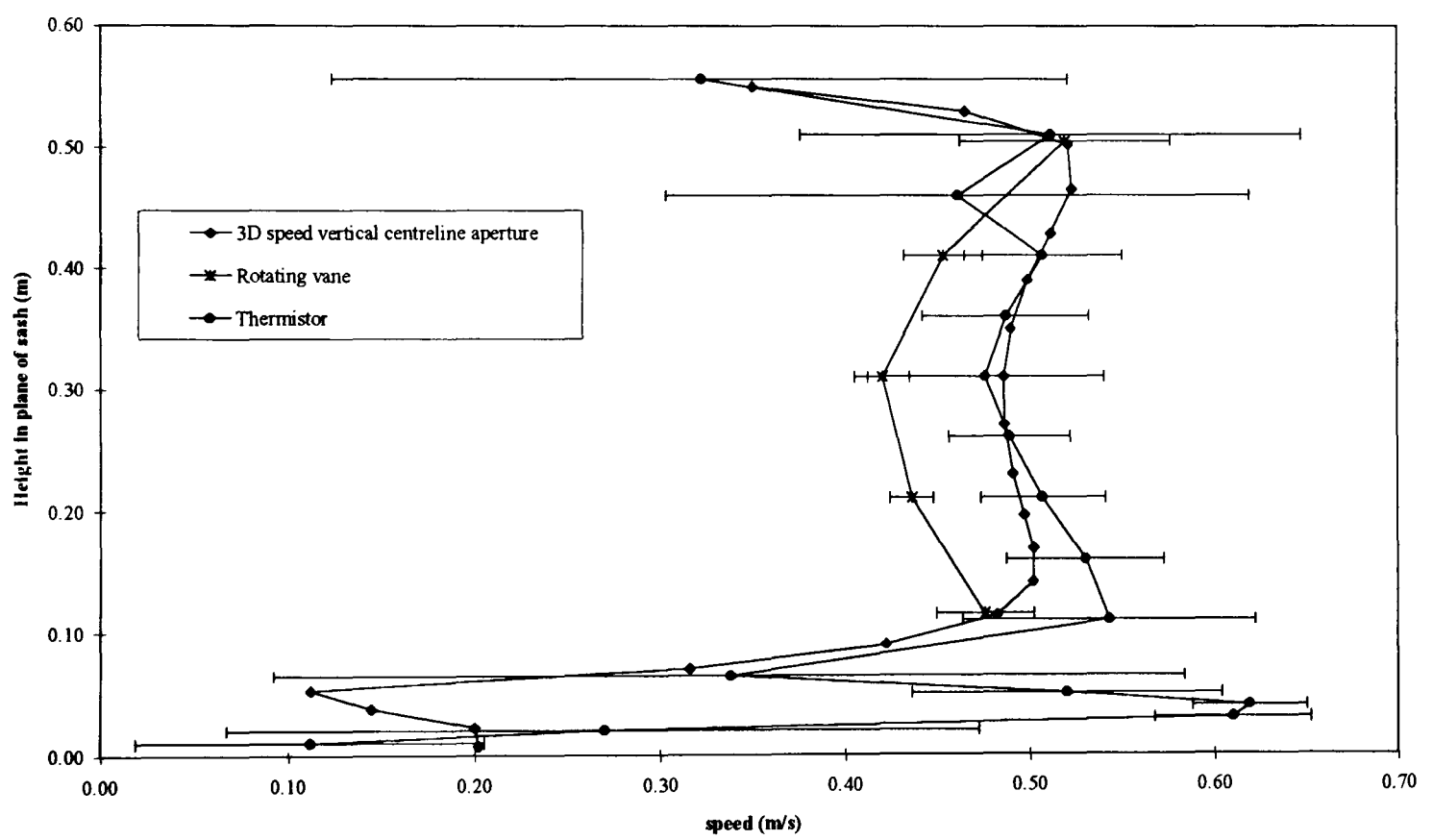


Figure 6.37 xy view of blockage in front of an 'aerodynamic' fume cupboard (3 D).

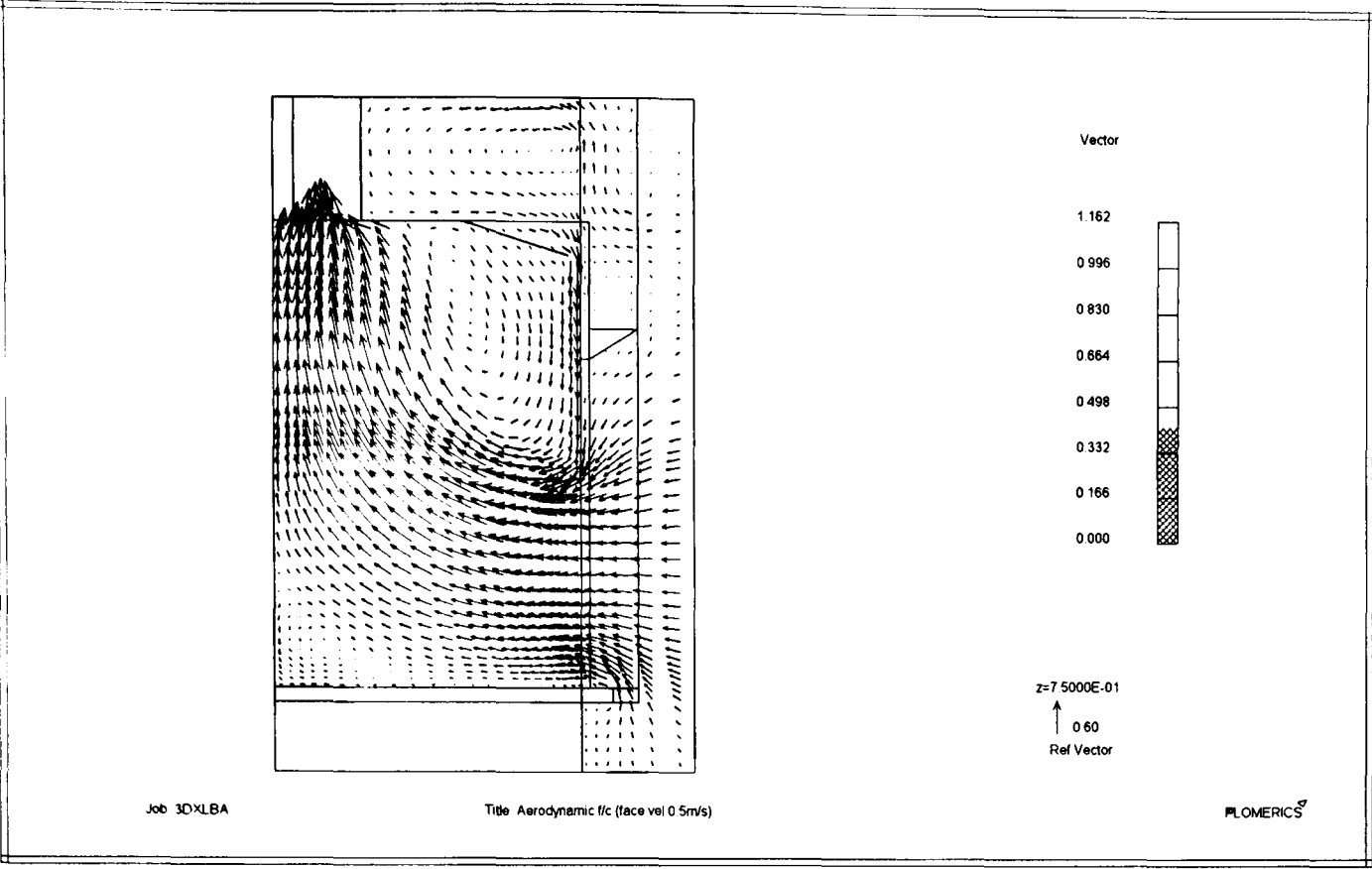


x velocity profiles



Speed profiles

Figure 6.34 Comparison of x velocity and speed profiles in the the horizontal centreline of the aperture plane of an aerodynamic fume cupboard with physical measurements (rotating vane & thermistor anemometers). (Error bars show 95% confidence limits).



xy profile of air flow vectors

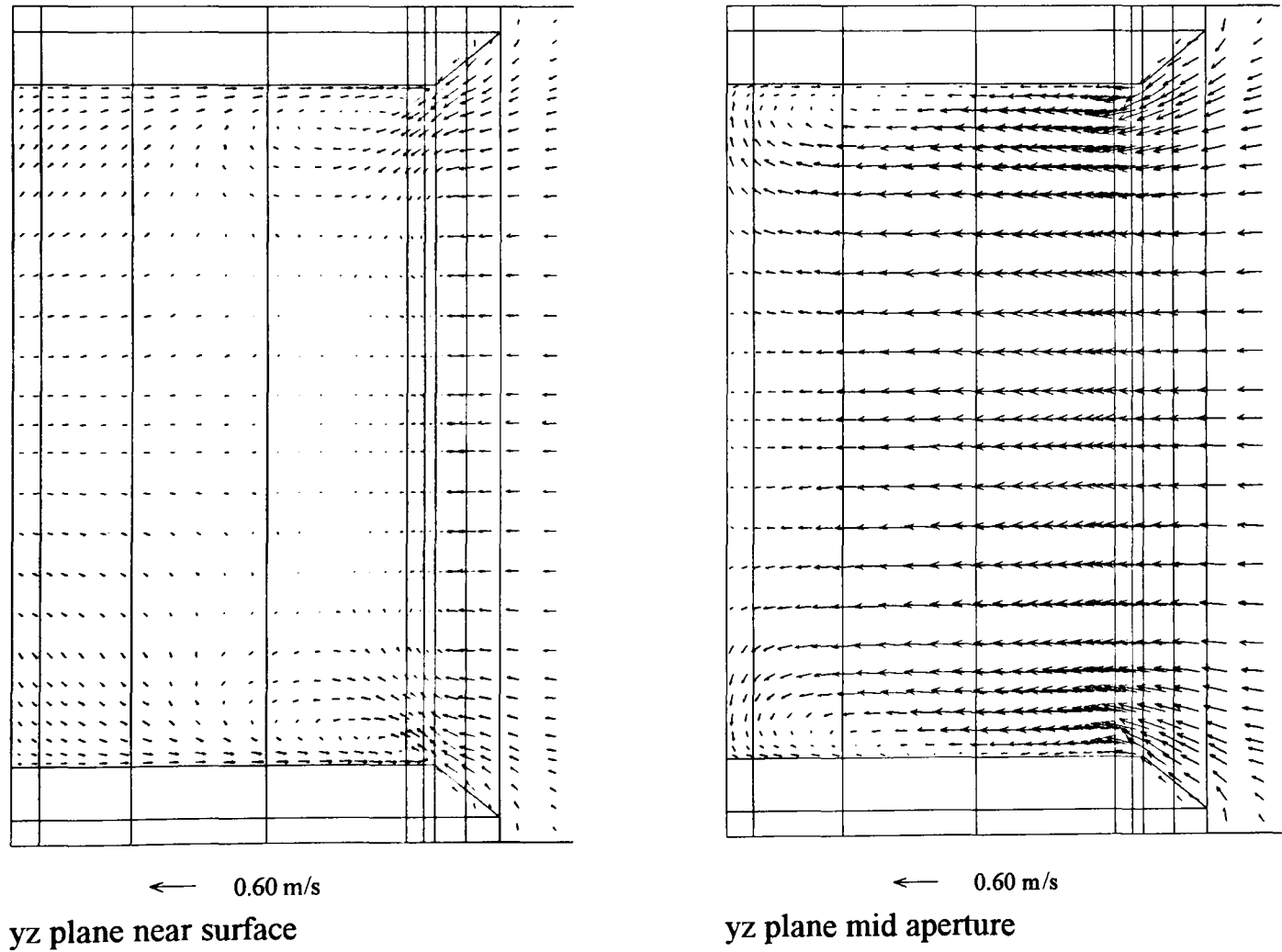
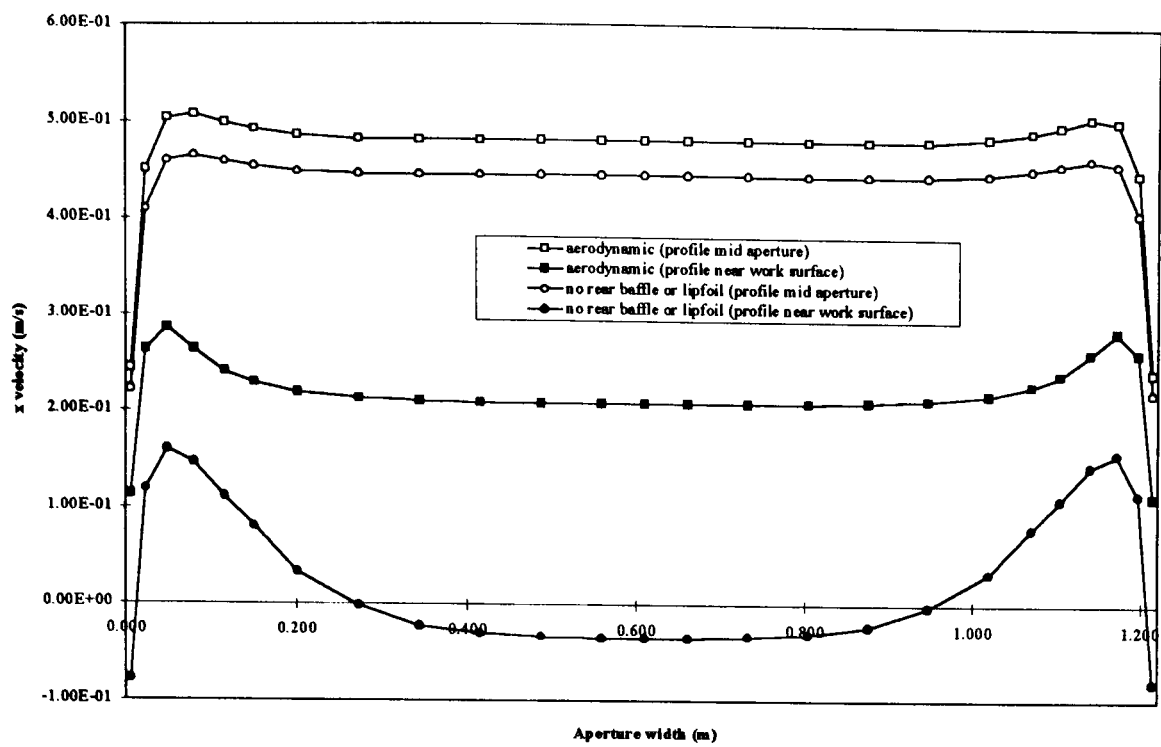
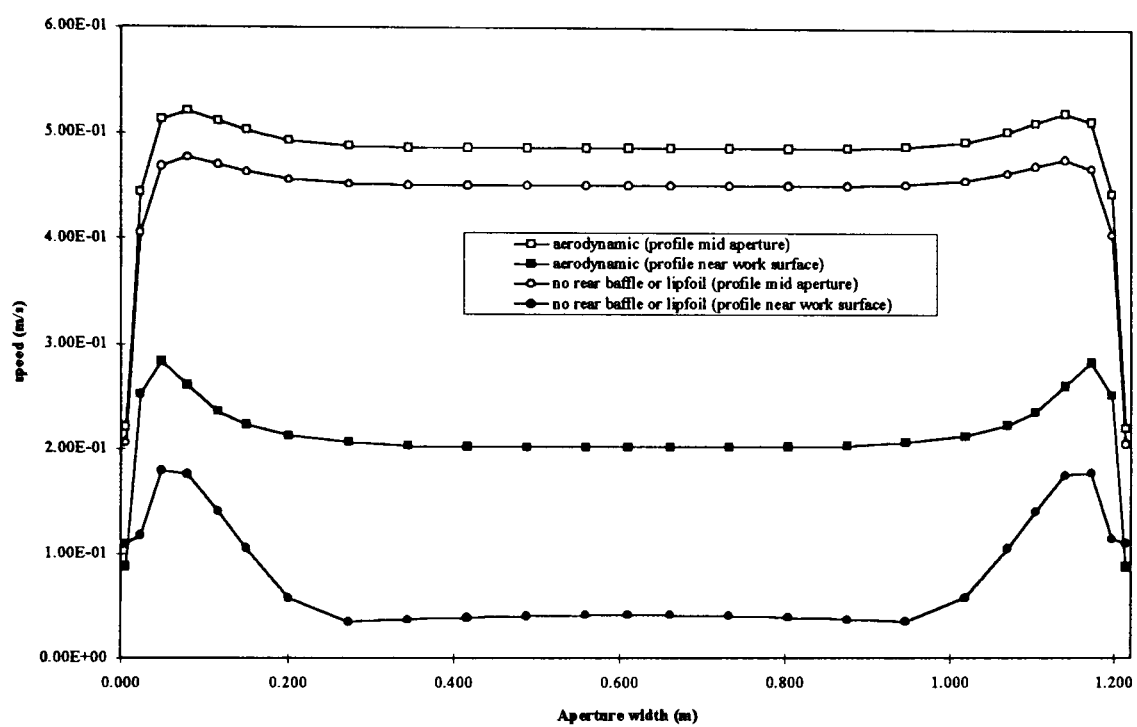


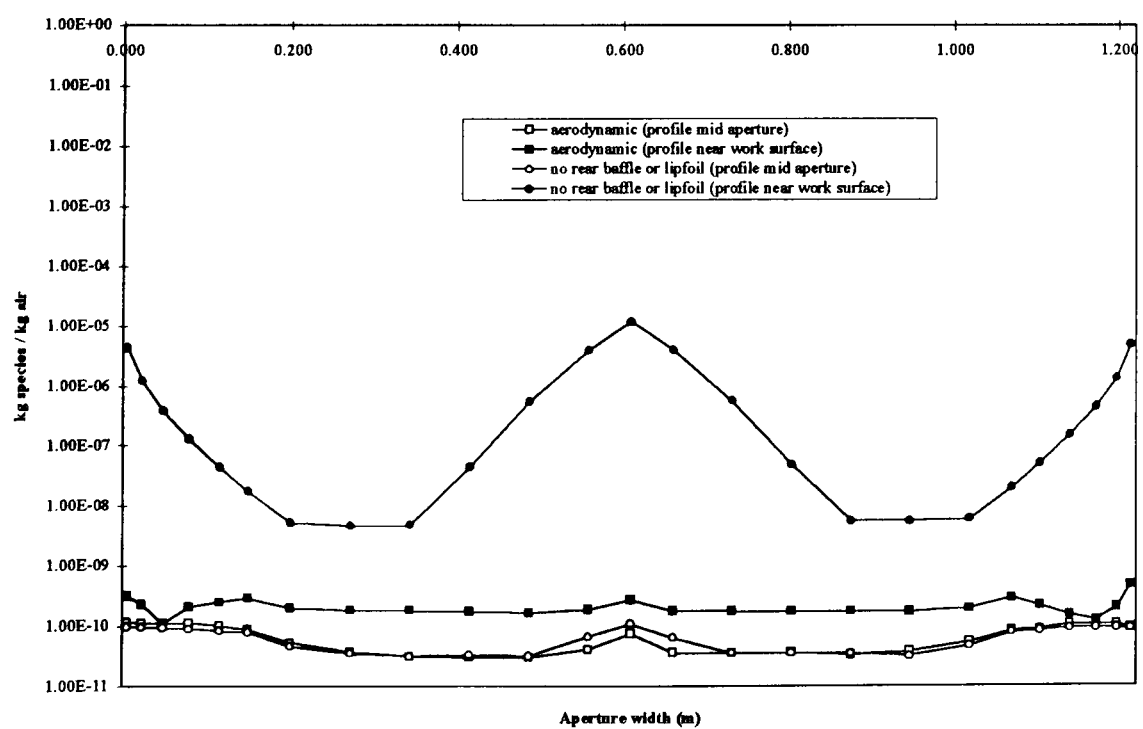
Figure 6.35 Effect on the airflow vectors in the xy plane, centreline of the aperture width, and in the xz plane within an aerodynamic fume cupboard, near to the work surface and at mid aperture height, when the rear baffle and lipfoil are removed (3 D).



x velocity profiles



Speed profiles



Concentration profiles

Figure 6.36 Effect on the x velocity, speed and concentration profiles across the aperture plane, z direction, of an aerodynamic fume cupboard when the rear baffle and lipfoil are removed (3 D).

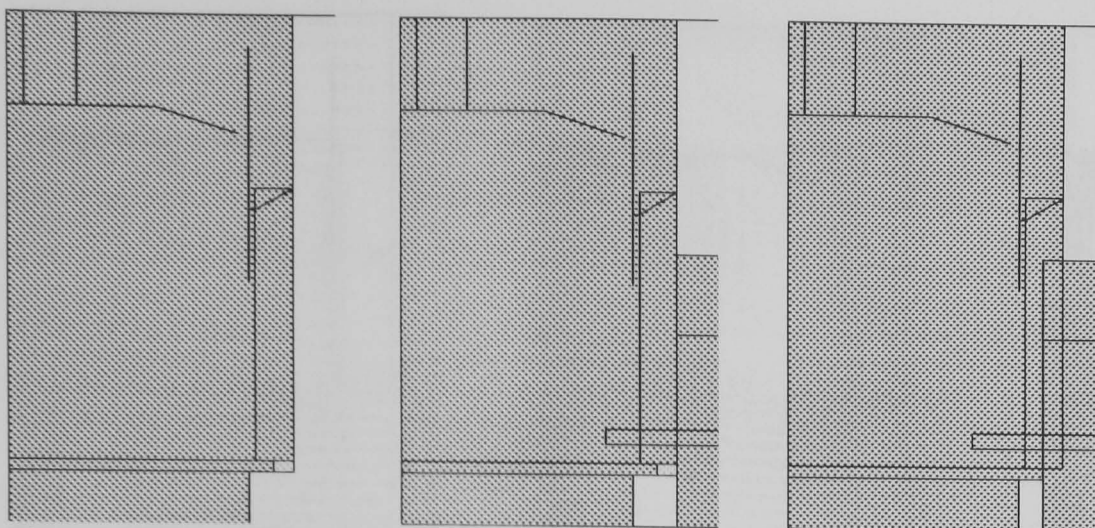


Figure 6.38 xy view of blockage in front of an 'aerodynamic' fume cupboard with rear baffle and lipfoil removed (3 D).

6.3.4.2 'Aerodynamic' fume cupboard

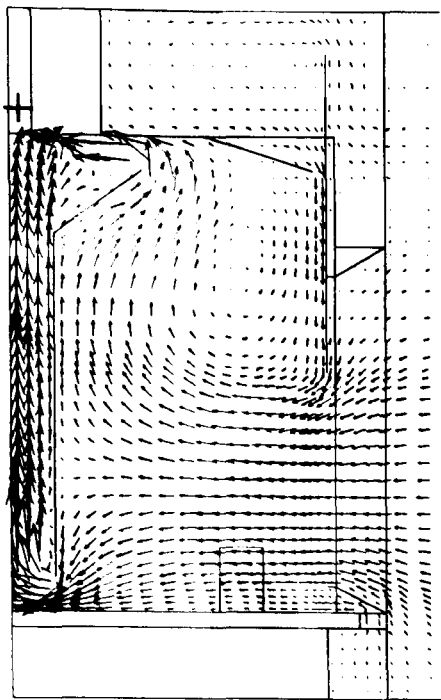
The effect on the airflows is shown in Figs. 6.39 - 6.42. In the vertical centreline of the cupboard aperture the effect of blockage near to the front was to force air to flow up the operator, past the lipfoil, near to the sash where it combined with air flowing down the operator and then into the cupboard. With the person standing against the lipfoil the reverse happened and the majority of airflow was from the top which entered the cupboard but also travelled down the person. The flow beneath the lipfoil was unaffected.

The effect was clearer observing the 3D view. The planes chosen were near to the work surface and at mid aperture. At the work surface with the person standing near to the front there was obvious recirculation zones past the 'square' edges of the person. With the person against the lipfoil no such zones were shown but air flowing over the work surface was more disturbed. In mid aperture at both person positions there were recirculation zones past the person edges and the effect stretched deep into the working volume. This was more observable with the person standing against the lipfoil.

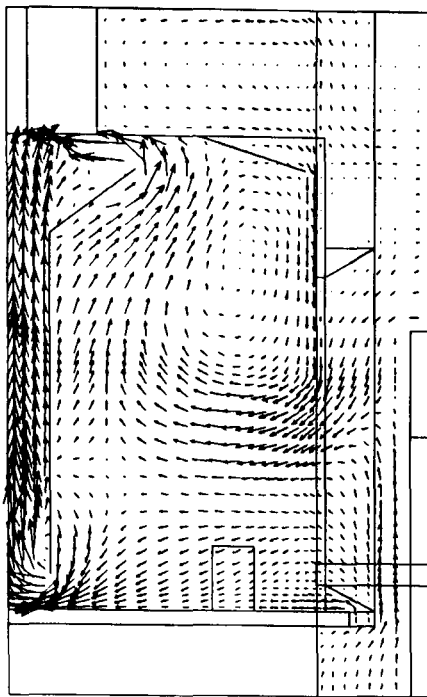
Quantitatively, the profiles in the plane of the aperture showed that in the vertical centreline, the x velocity reduced with blockage in the aperture but beneath the lipfoil remained unaffected. Contaminant release on the work surface as in section 6.3.2 showed that a person standing near to the lipfoil affected the contaminant levels in the aperture plane more than a person standing against the lipfoil. Both caused higher levels near to the sash.

6.3.4.3 'Aerodynamic' type fume cupboard with the rear baffle or lipfoil removed

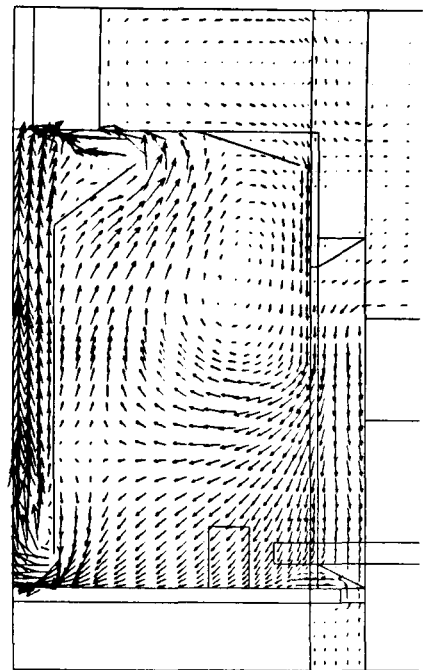
The effect on the air flow near to the person was similar to the aerodynamic fume cupboard (Figs. 6.43 - 6.46). However, there was a much greater effect on the flow within the working volume. Recirculation zones became much more dominant both behind the sash and on the work surface where a large volume of air flowed from the back of the working volume to the front aperture. This was much more noticeable when a person stood against the front edge.



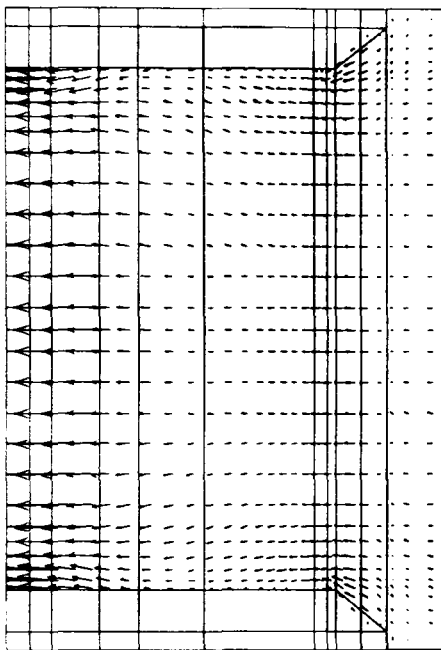
No blockage (xy central plane)



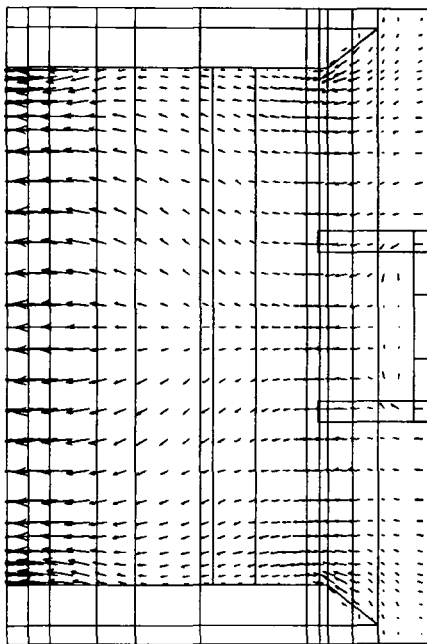
Person near front



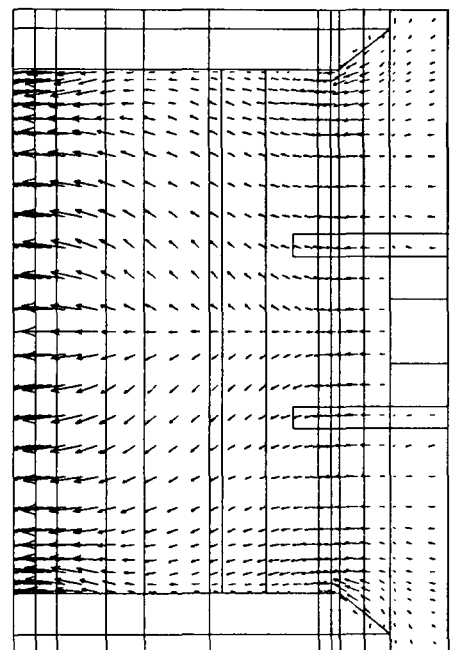
Person against front



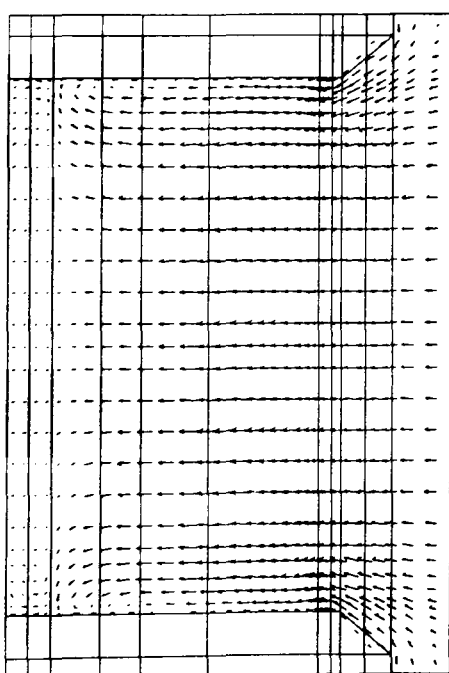
No blockage (yz near surface)



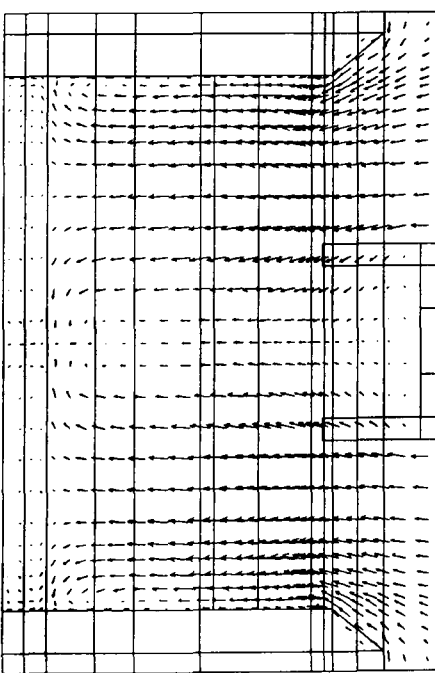
Person near front



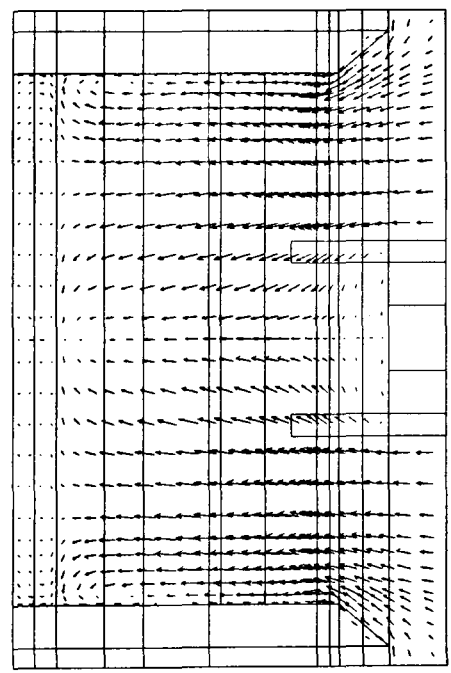
Person against front



No blockage (yz mid aperture)

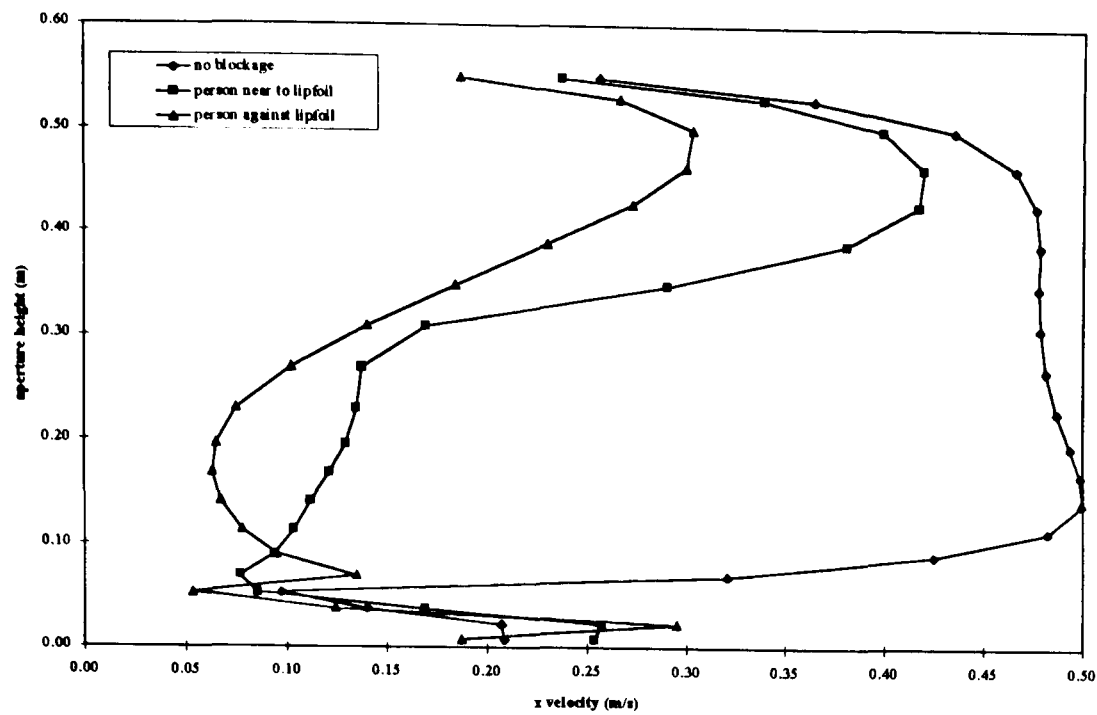


Person near front

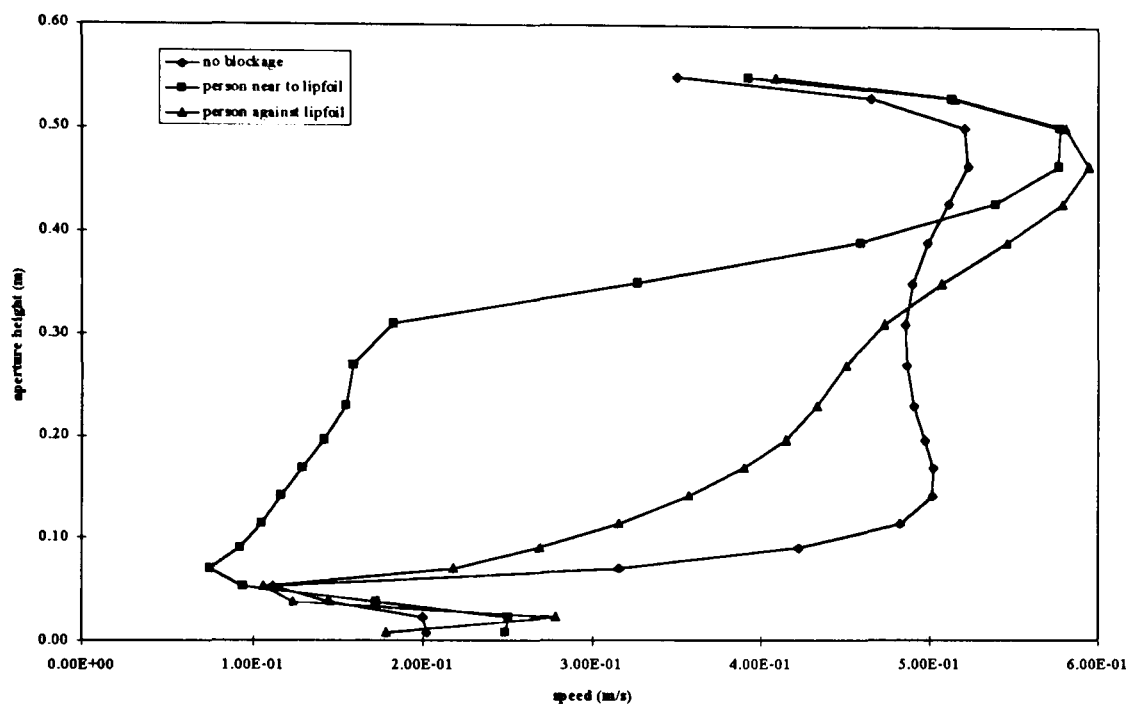


Person against front

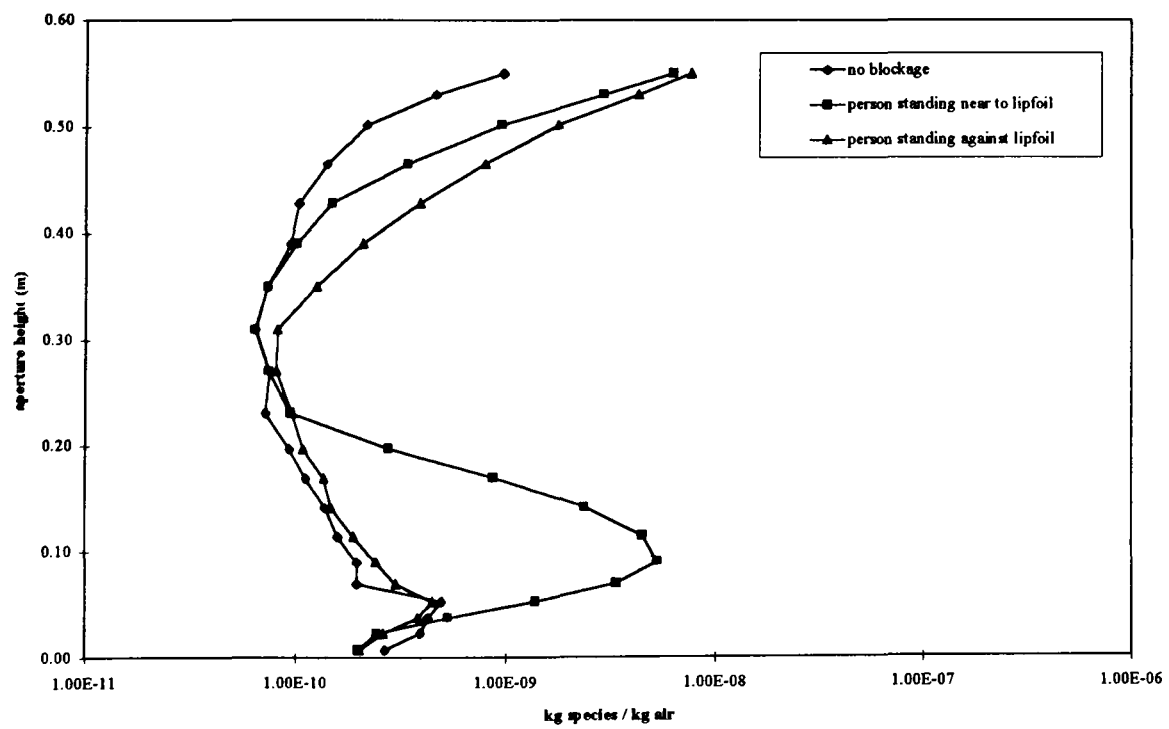
Figure 6.39 Effect of blockage on the airflow vectors in the xy plane, centreline of the aperture width, z direction, and in the xz plane within an aerodynamic fume cupboard, near to the work surface and at mid aperture height (3 D).



x velocity profiles

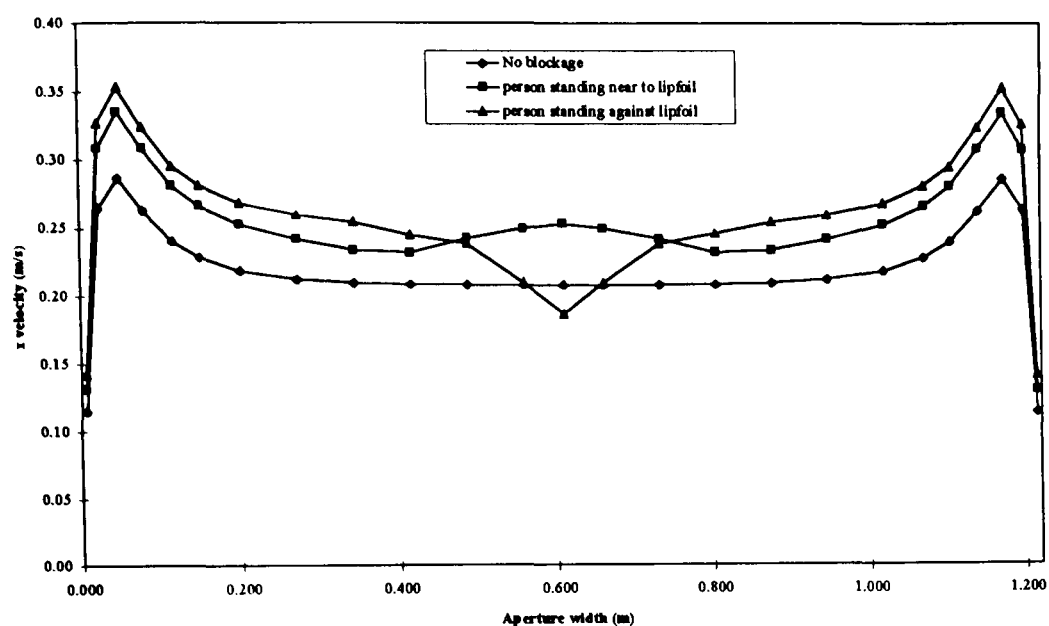


Speed profiles

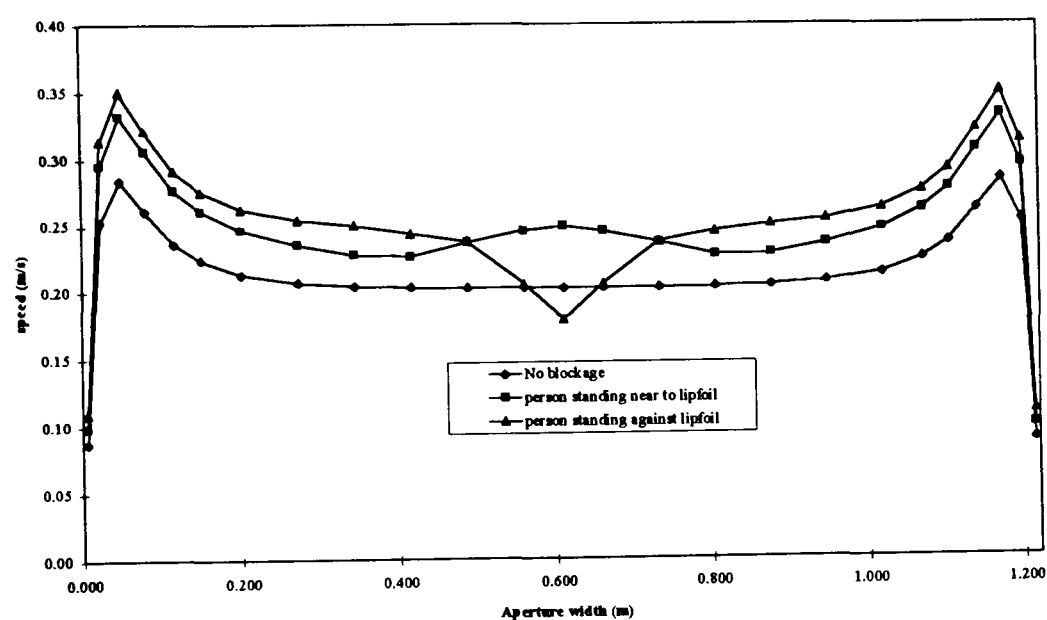


Concentration profiles

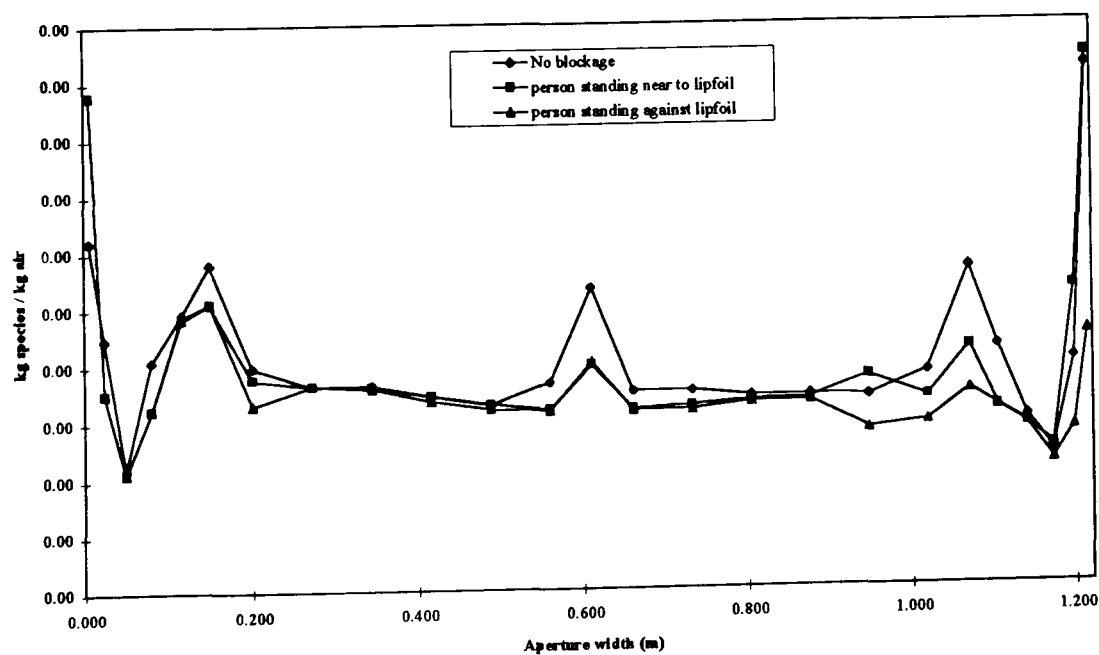
Figure 6.40 Effect of blockage on the x velocity, speed and concentration profiles in the horizontal centre line of the aperture plane of an aerodynamic fume cupboard (3 D).



x velocity profiles

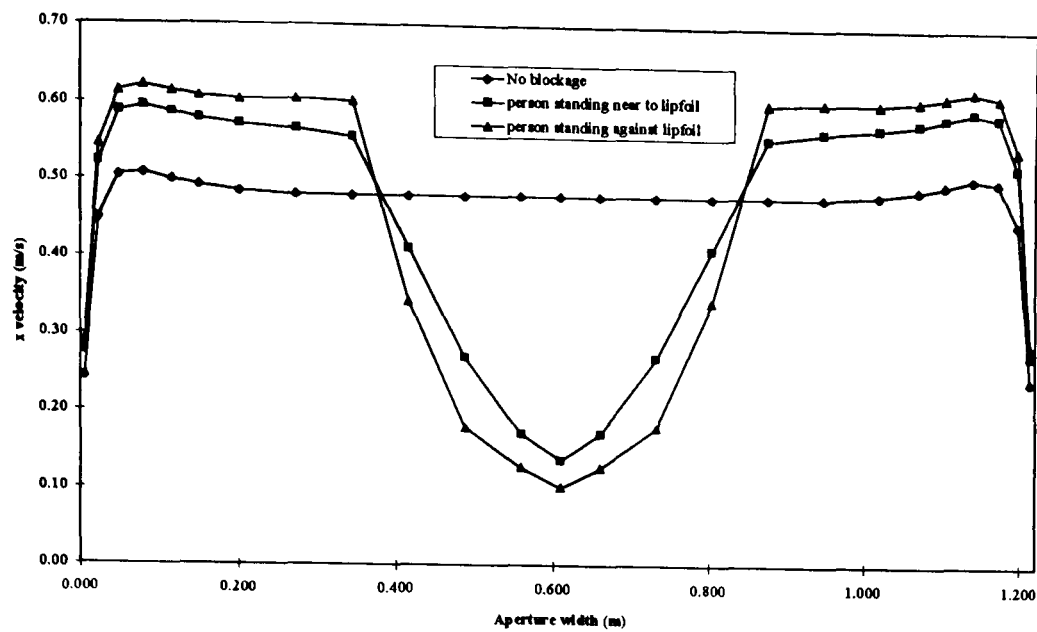


Speed profiles

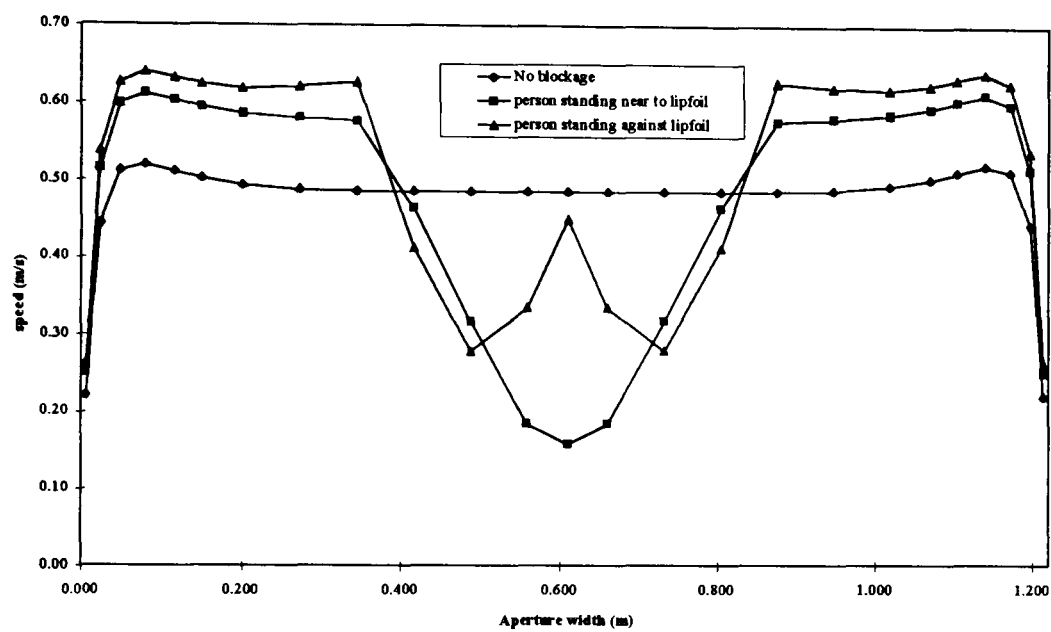


Concentration profiles

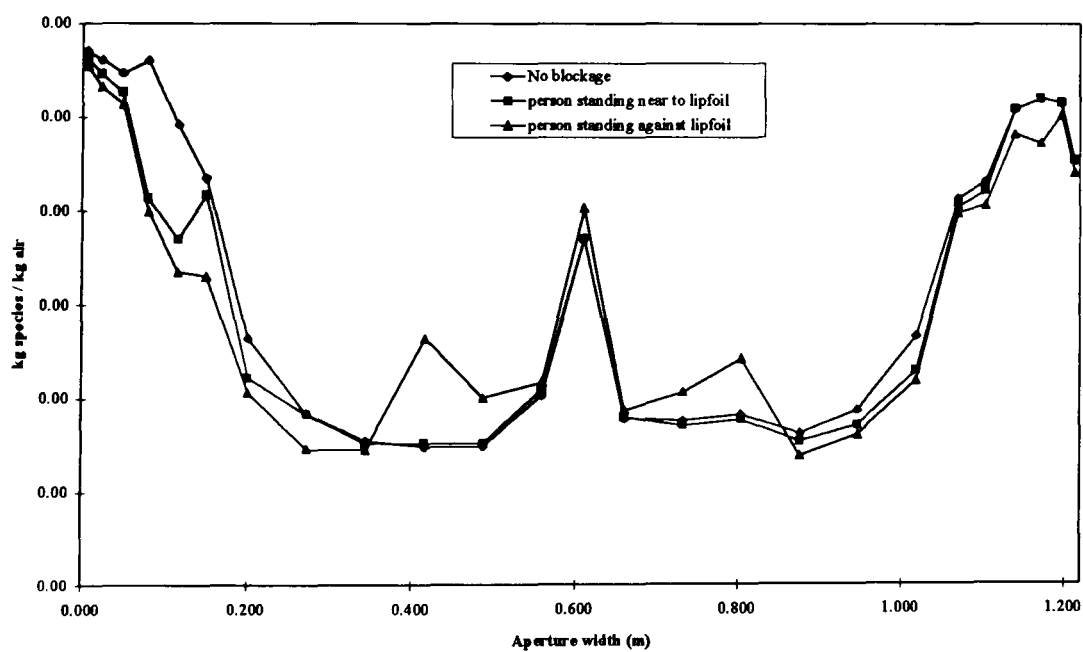
Figure 6.41 Effect of blockage on the x velocity, speed and concentration profiles across the aperture plane, z direction, of an aerodynamic fume cupboard near to the work surface (3 D).



x velocity profiles

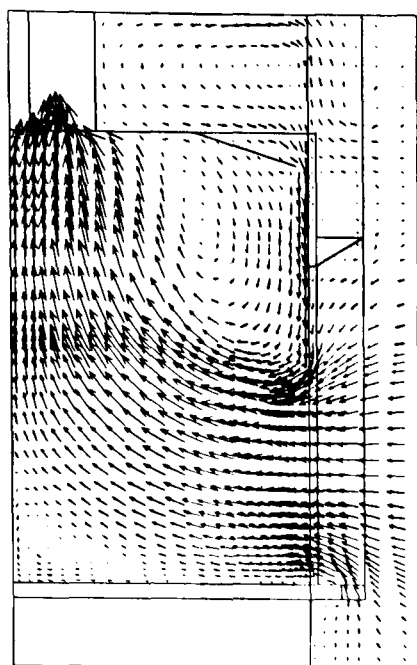


Speed profiles

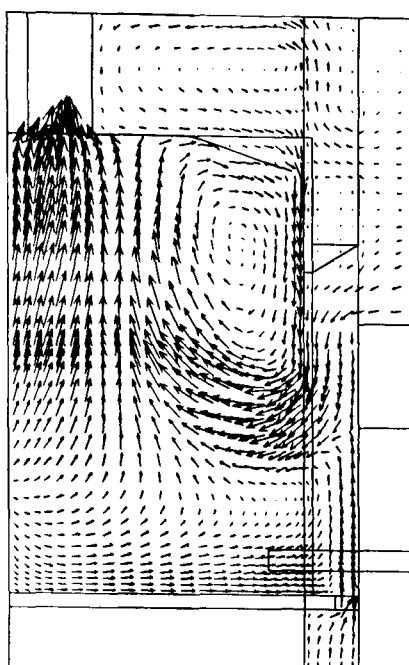


Concentration profiles

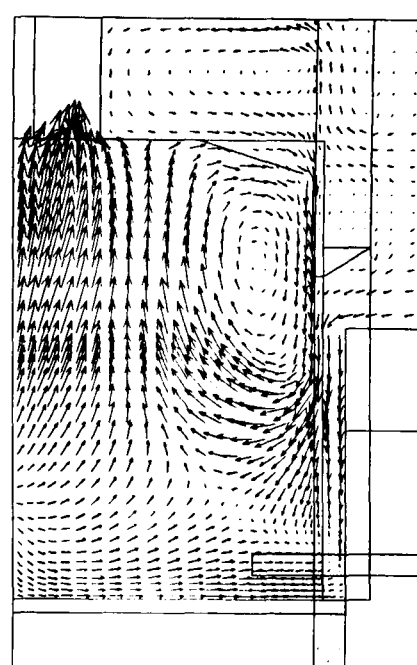
Figure 6.42 Effect of blockage on the x velocity, speed and concentration profiles across the aperture plane, z direction, of an aerodynamic fume cupboard at mid aperture height (3 D).



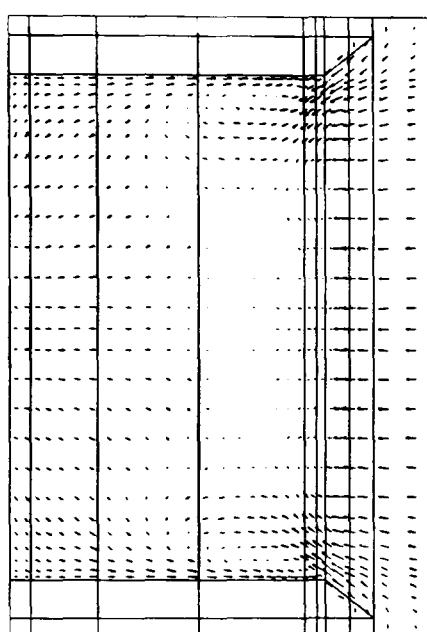
No blockage (xy plane)



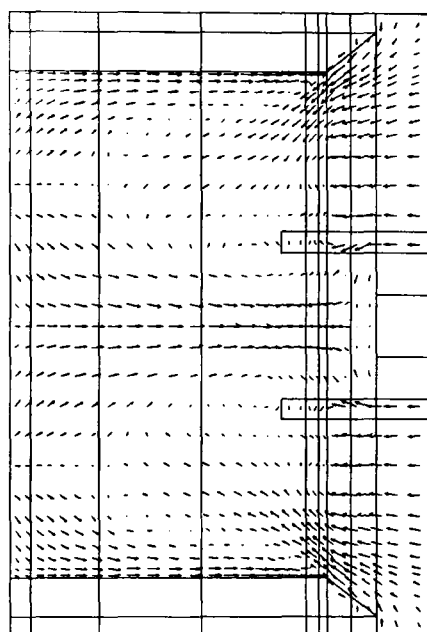
Person near front



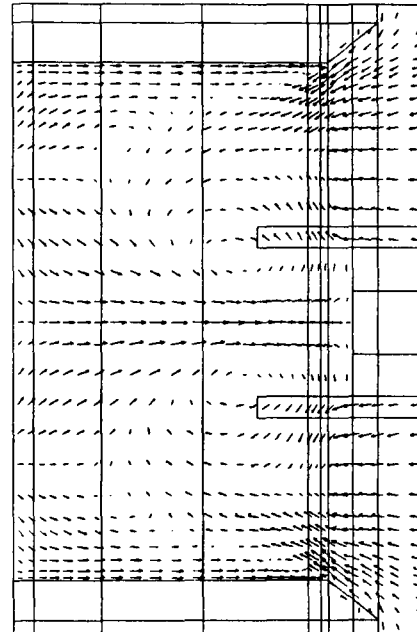
Person against front



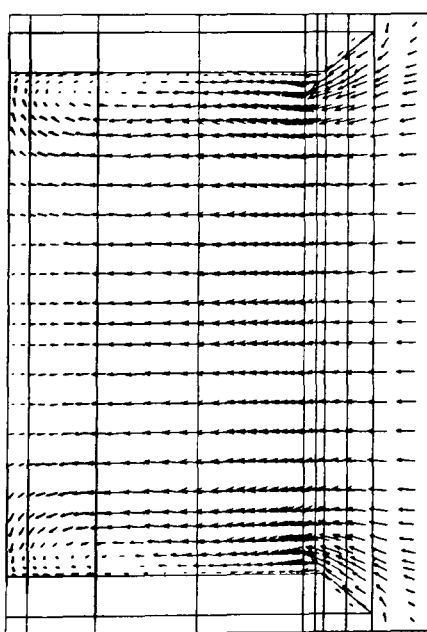
No blockage (yz near surface)



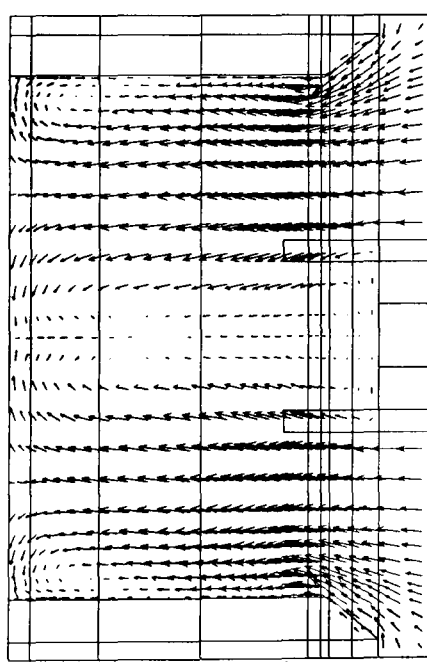
Person near front



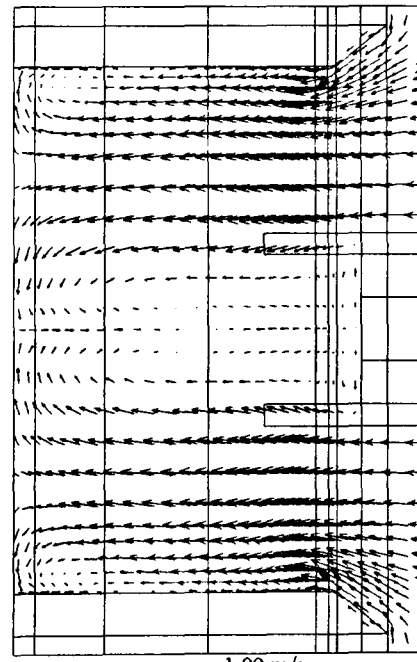
Person against front



No blockage (yz mid aperture)

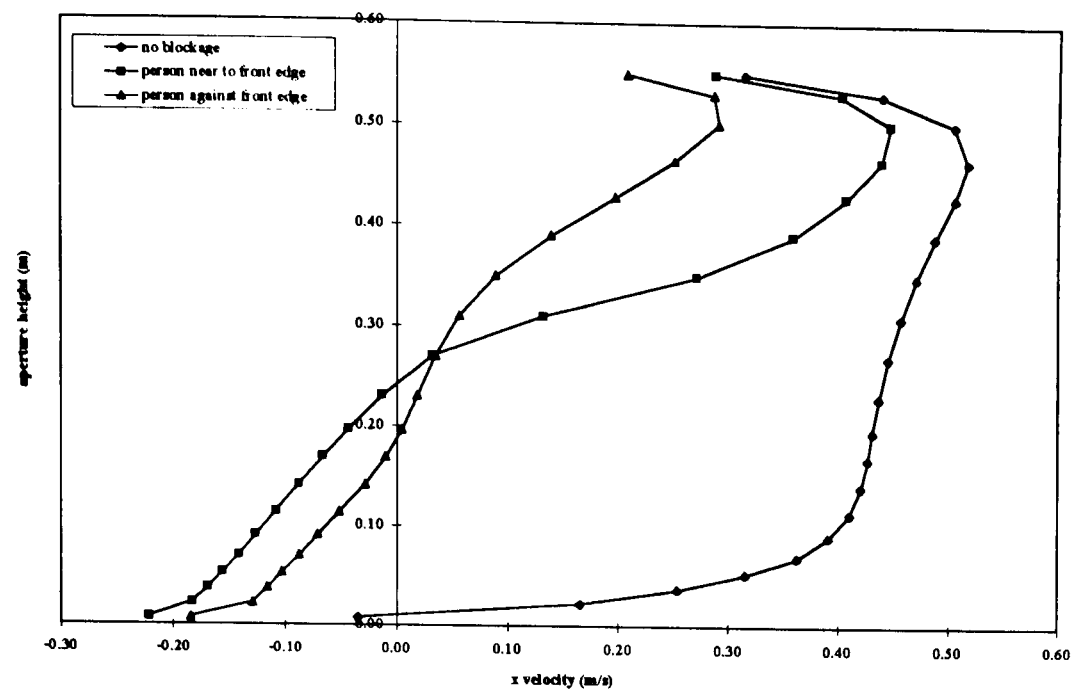


Person near front

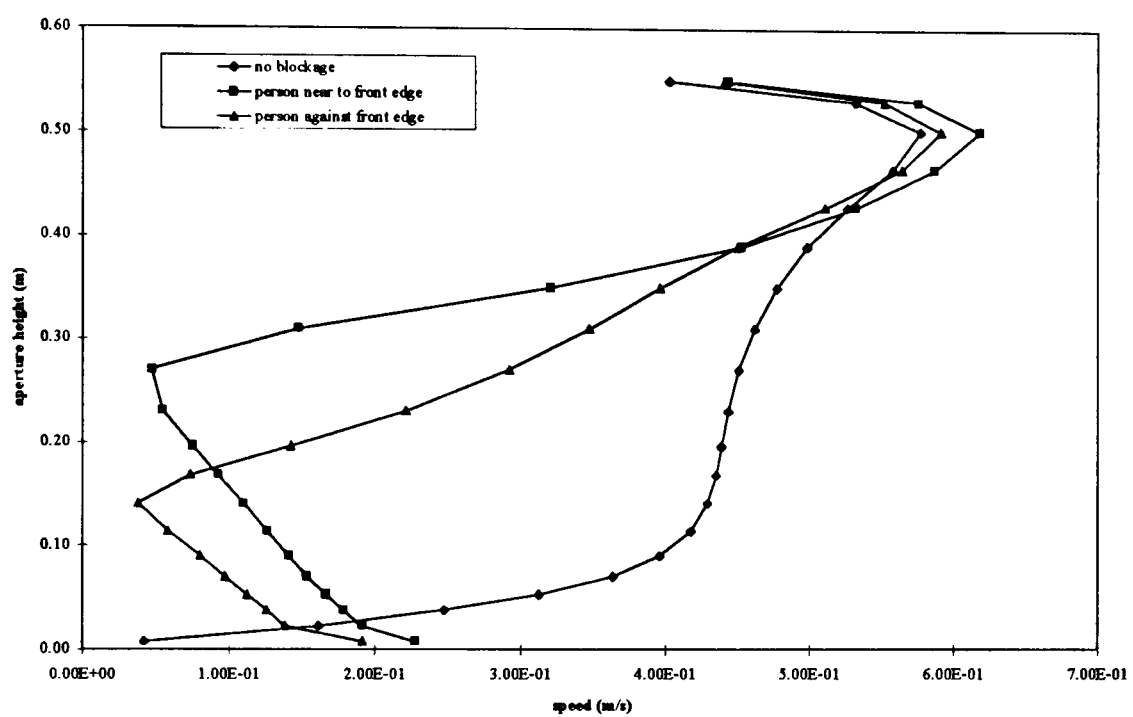


Person against front

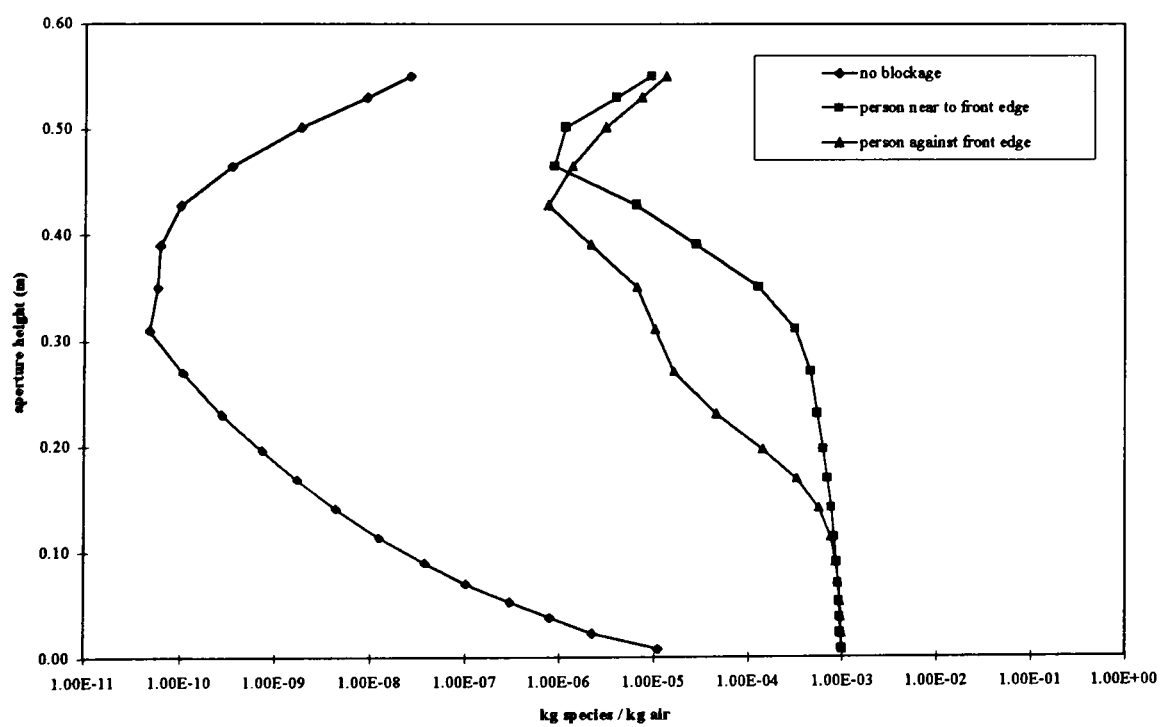
Figure 6.43 Effect of blockage on the airflow vectors in the xy plane, centreline of the aperture width, and in the xz plane within an aerodynamic fume cupboard at mid aperture height with the rear baffle and lipfoil removed (3 D).



x velocity profiles

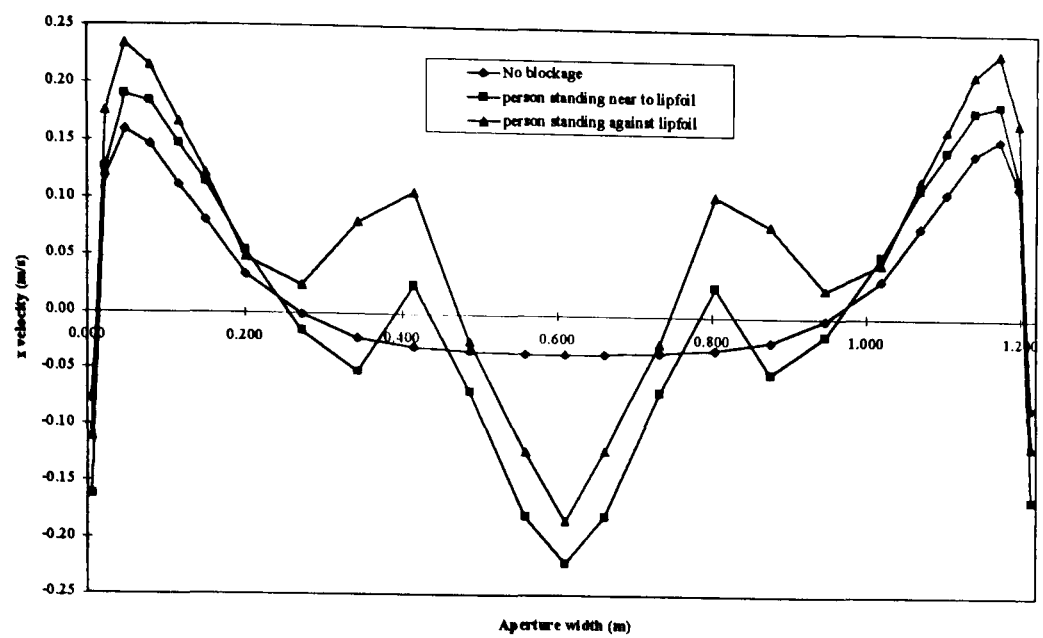


Speed profiles

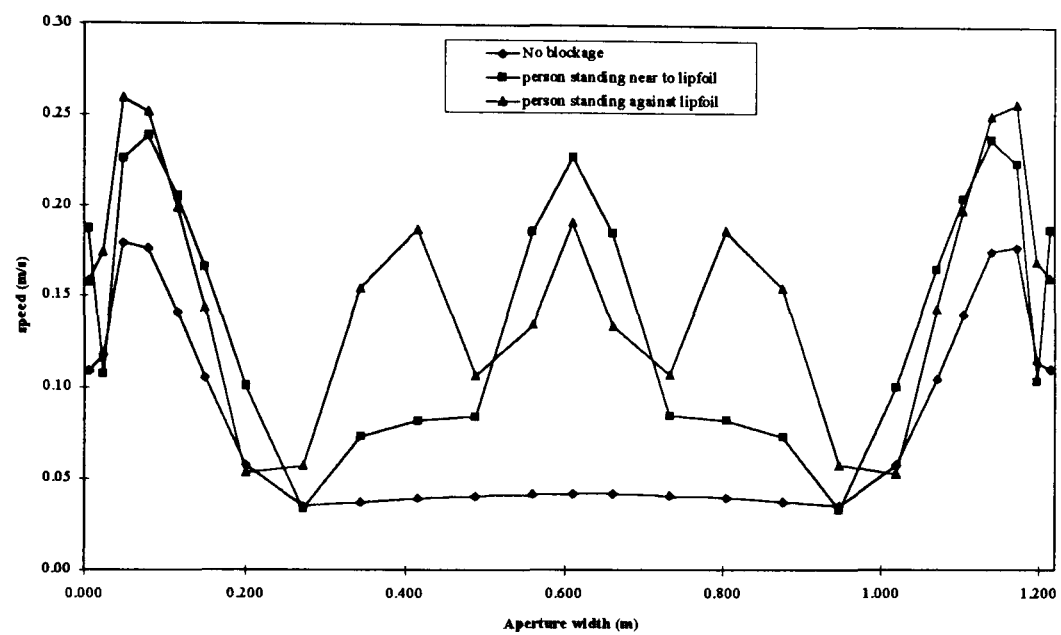


Concentration profiles

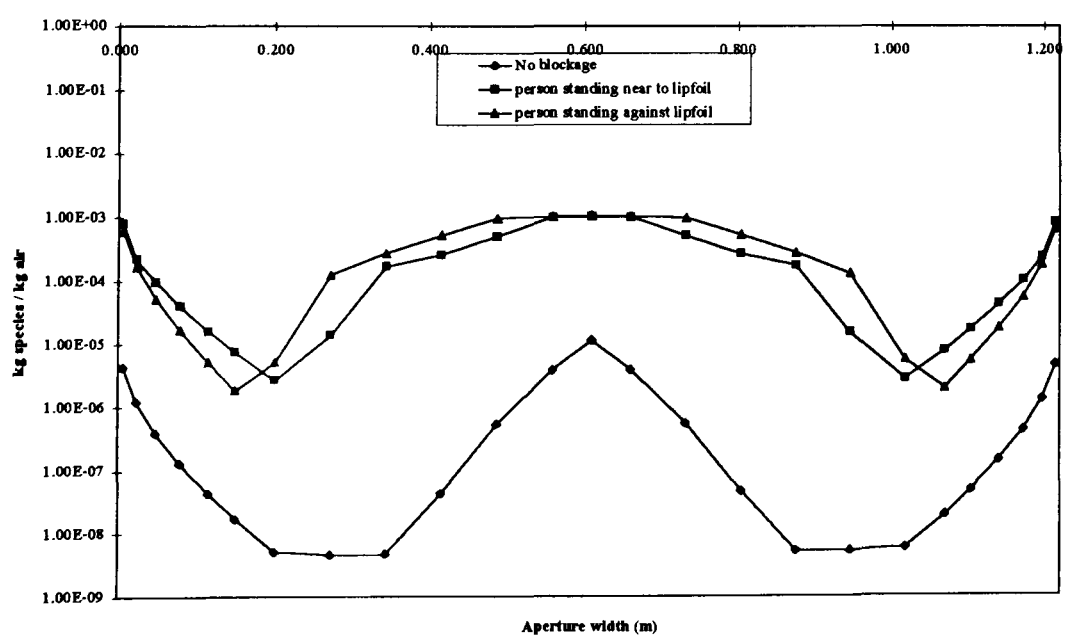
Figure 6.44 Effect of blockage on the x velocity, speed and concentration profiles in the horizontal centre line of the aperture plane of an aerodynamic fume cupboard with rear baffle and lipfoil removed (3 D).



x velocity profiles

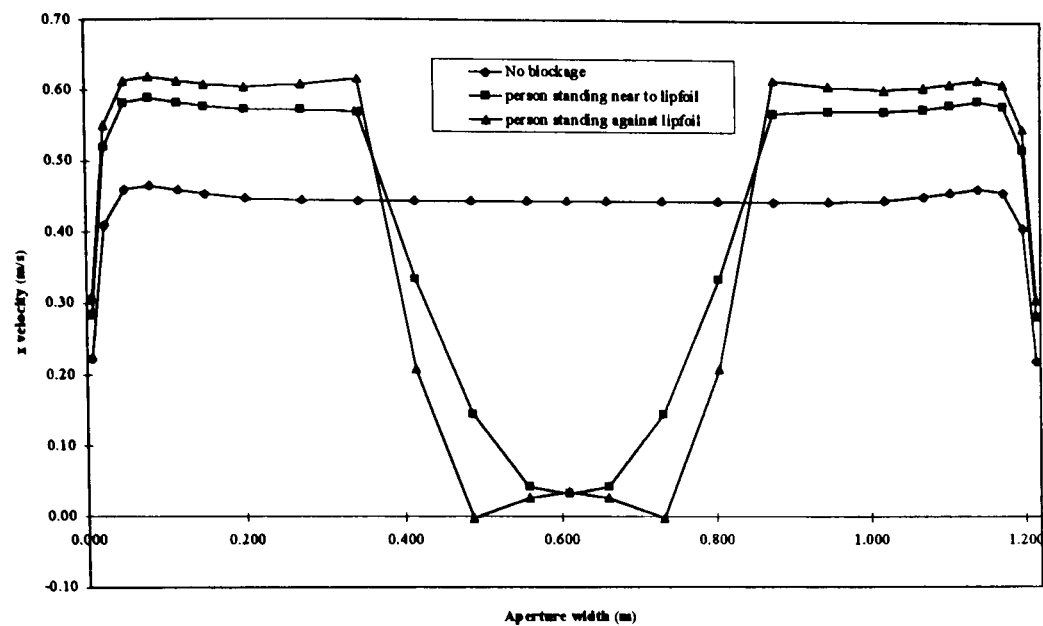


Speed profiles

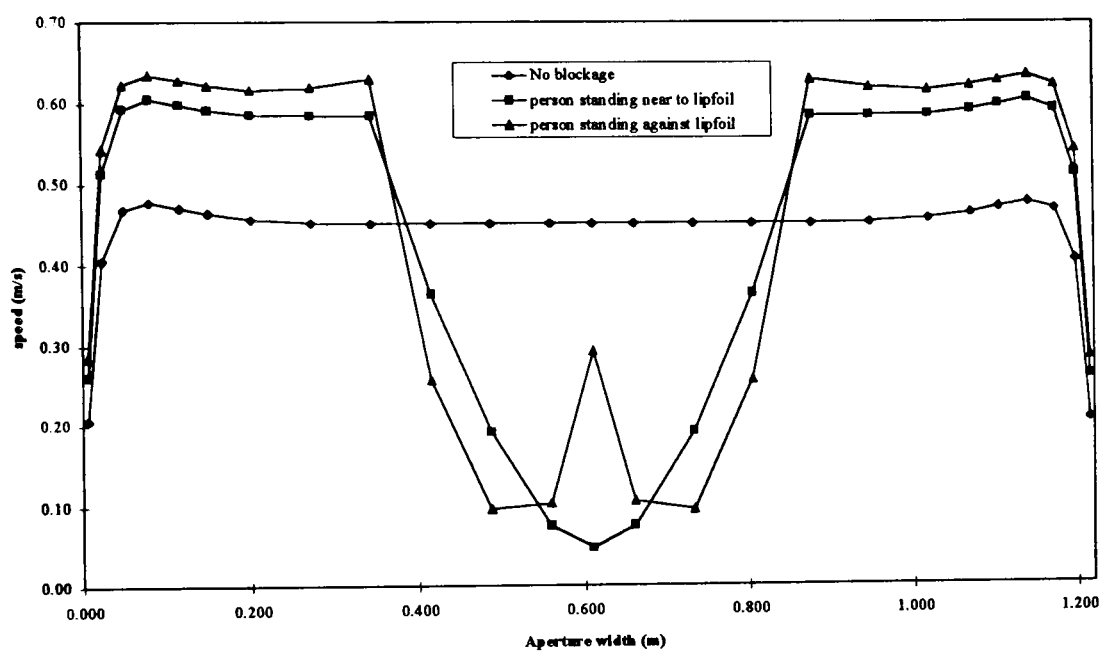


Concentration profiles

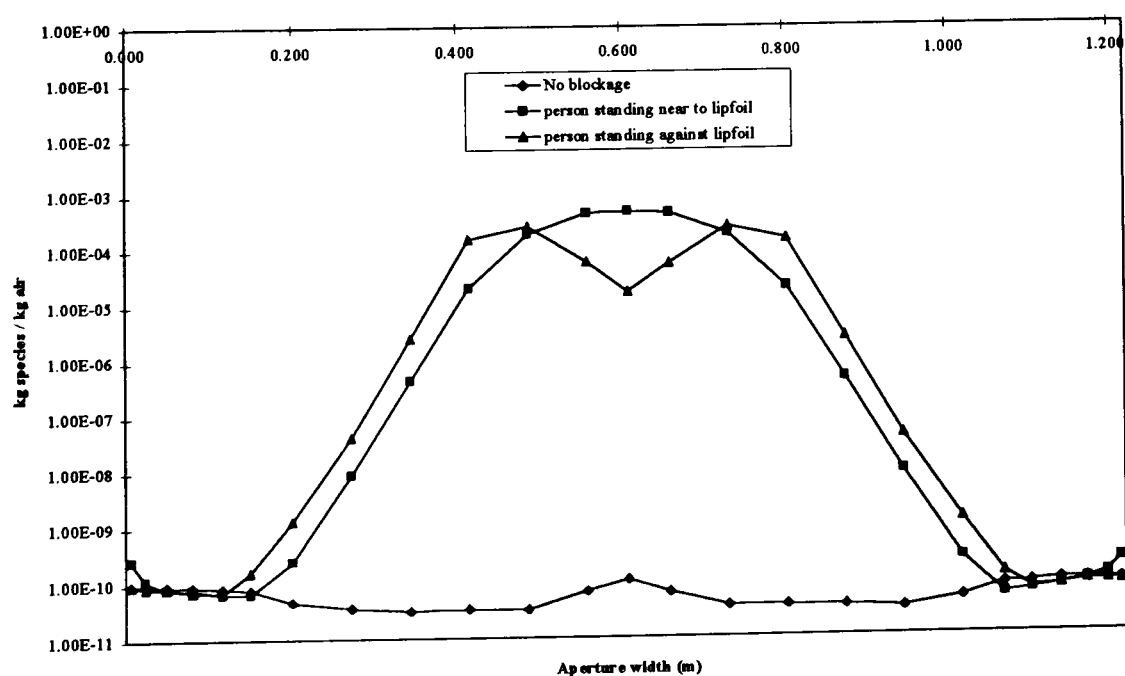
Figure 6.45 Effect of blockage on the x velocity, speed and concentration profiles across the aperture plane, z direction, of an aerodynamic fume cupboard near to the work surface with the rear baffle and lipfoil removed (3 D).



x velocity profiles



Speed profiles



Concentration profile

Figure 6.46 Effect of blockage on the x velocity, speed and concentration profiles across the aperture plane, z direction, of an aerodynamic fume cupboard at mid aperture height with the rear baffle and lipfoil removed (3 D).

These flows were also shown in the third dimension, the z direction, near to the work surface and mid aperture.

The quantitative profiles of x velocity in the aperture plane and the vertical centreline showed the air flow in the lower half of the aperture was affected, flowing out beyond the aperture plane. Concentration profiles clearly showed how the values in the aperture plane for each position of the operator were several orders of magnitude greater than with no blockage. The values near to the work surface were the same concentration as the source itself.

6.3.4.4 Conclusions

The effect of 'aerodynamic' features on resisting disturbance due to blockages was clearly demonstrated; the presence of the rear baffle and the front lipfoil prevented disturbance of the airflow over the work surface. These simulations were considered an exaggeration of the presence of a human standing in front of the aperture as the modelled person was 'square' with smooth surfaces whereas a human is rounded and covered with clothing.

6.3.5 Effect of environmental disturbance on simulated airflow and contaminant dispersal

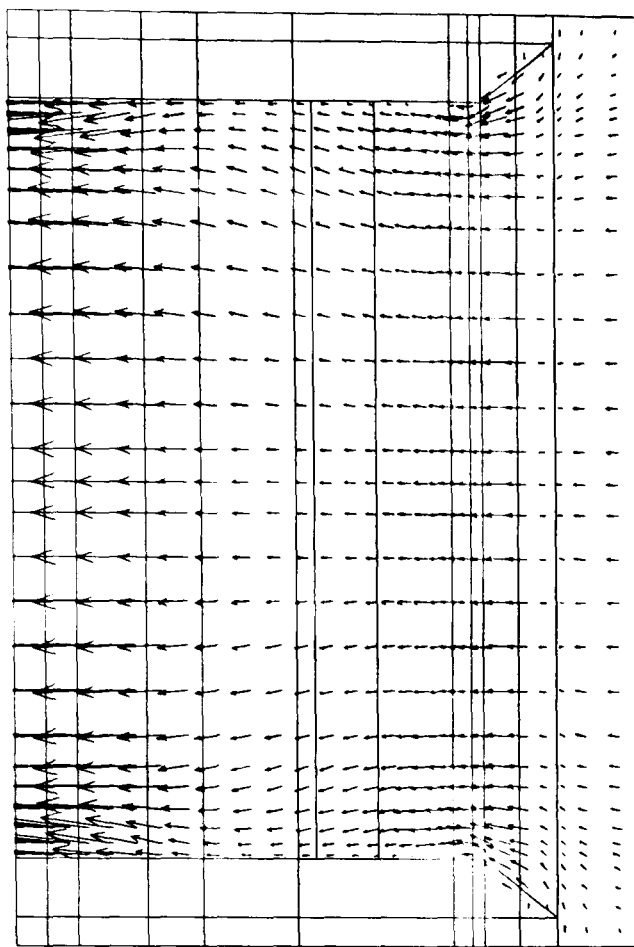
6.3.5.1 Set up

The 3D simulation was used to study the effects of an external air flow across the face of the cupboard on performance and containment. The 'aerodynamic' model with and without the rear baffle and lipfoil was used as the established simulation and the effect of a cross flow shown. The cross flow was specified as a supply encompassing the right side opening of the simulation in front of the cupboard aperture at a velocity of 1 m/s which exceeded the cupboard face velocity.

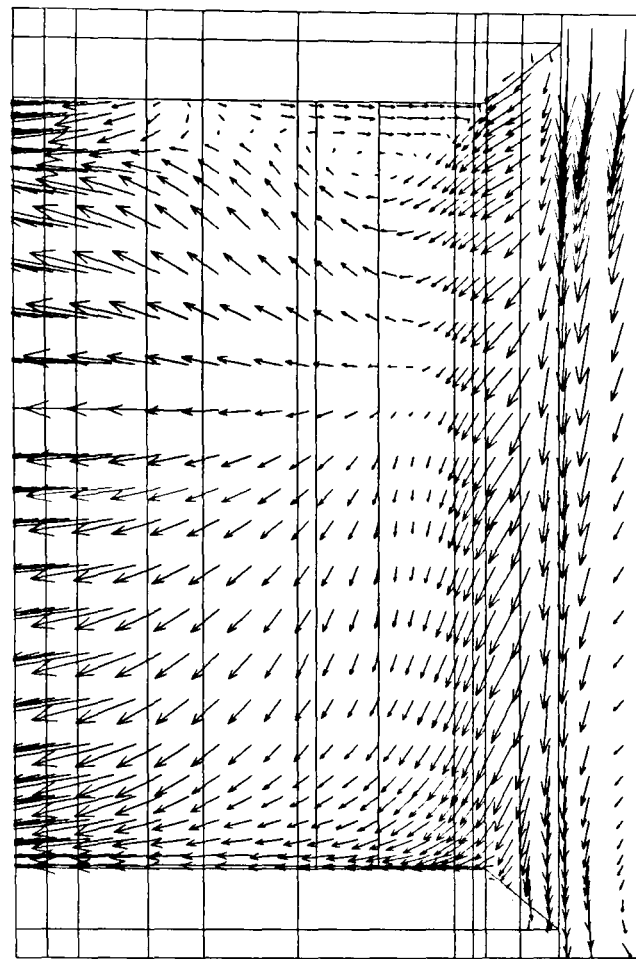
6.3.5.2 'Aerodynamic' fume cupboard

The effect on the air flow was shown in Fig. 6.47. In the xz plane near to the work surface the external air flowed parallel to the lipfoil across the face of the cupboard. This caused substantial disturbance of air flow within the working volume resulting in a small recirculation zone past the nearest edge to the supply and sideways movement of air behind the lipfoil and across the work surface. At mid aperture height the recirculation zone at the near edge was much greater but there was little effect on the air flow over the rest of the working volume.

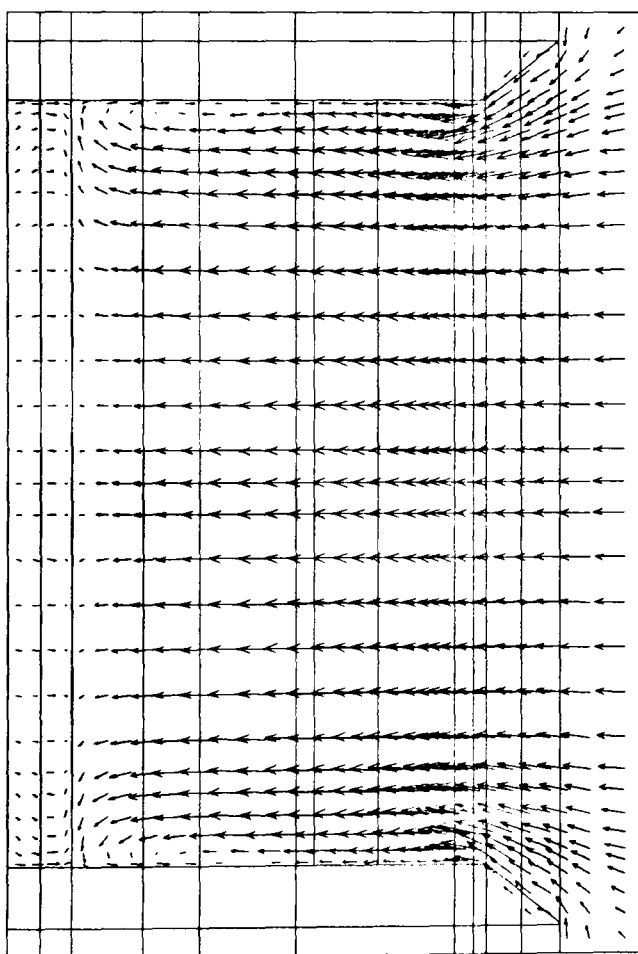
The xz profiles in the aperture plane (Fig. 6.48) showed greatest effect of the disturbance was nearest to the supply of the cross flow. The effect on the concentration of contaminant was greatest near to the work surface.



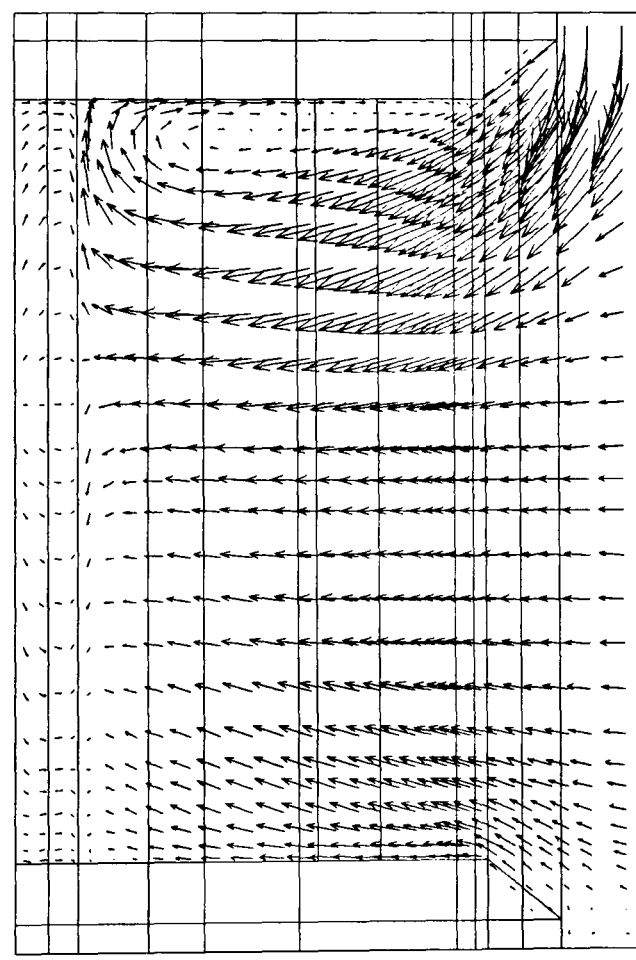
← 0.60 m/s
No disturbance (xz near surface)



← 0.60 m/s
1m/s crossflow

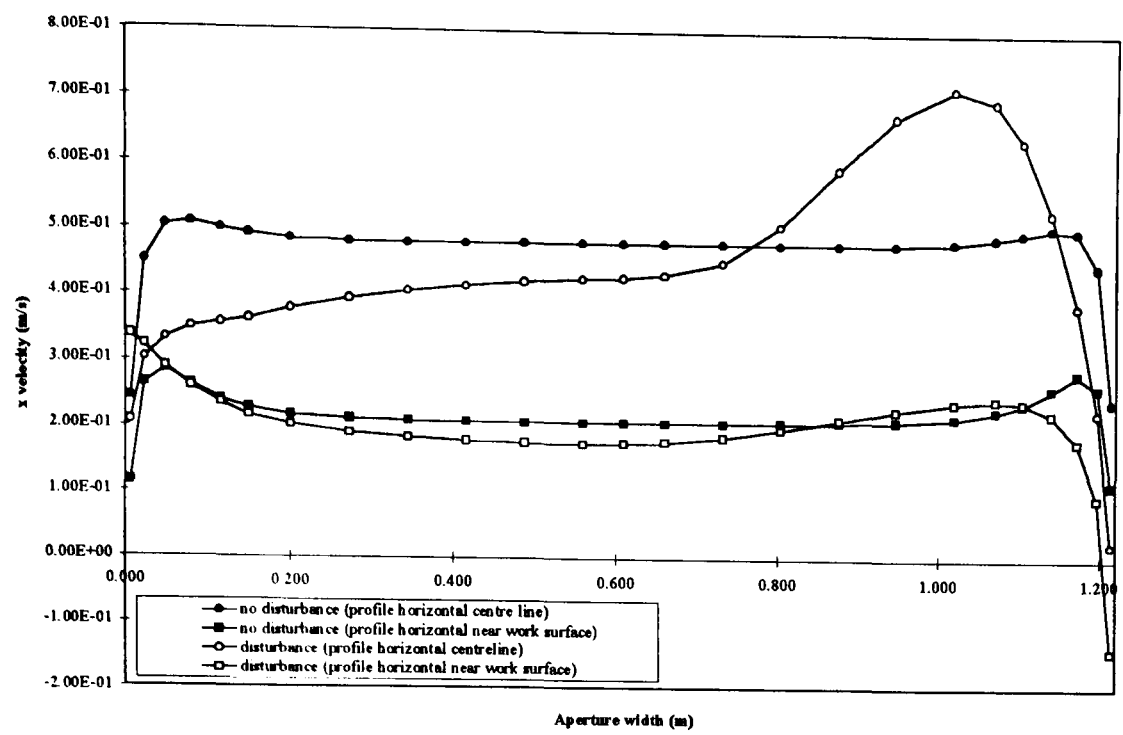


← 0.60 m/s
No disturbance (xz mid aperture)

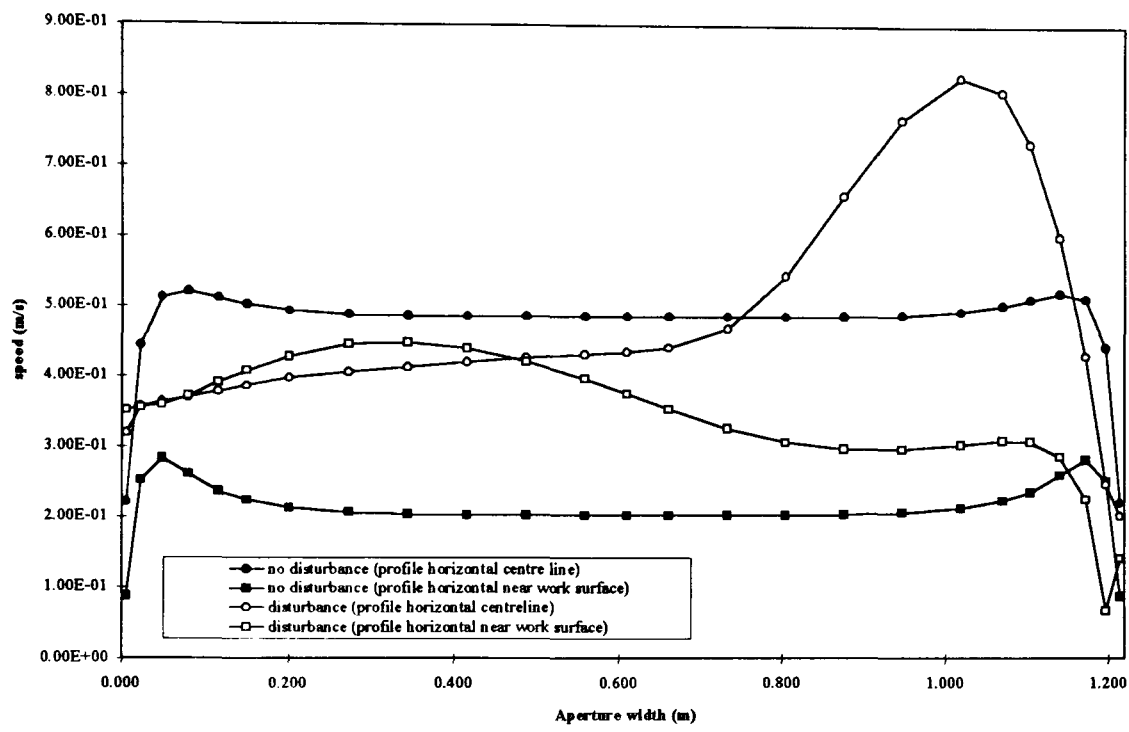


← 0.60 m/s
1 m/s cross flow

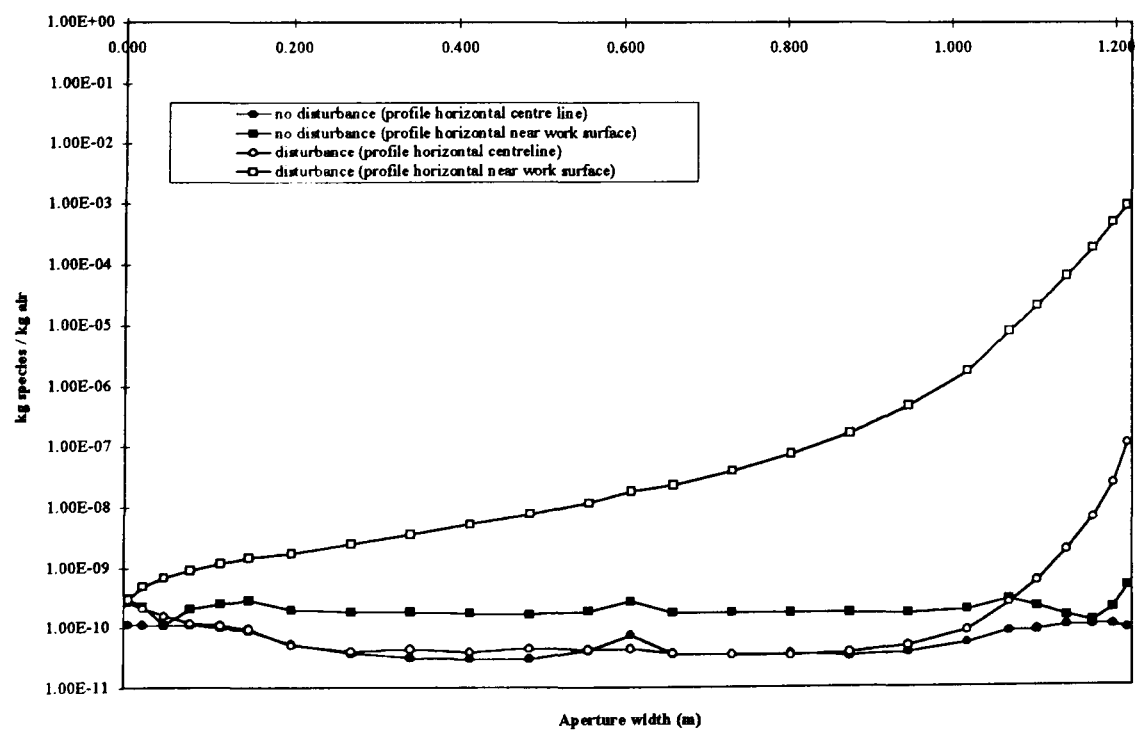
Figure 6.47 Effect of a cross flow of air (1m/s) past the aperture of an aerodynamic fume cupboard on the airflow vectors in the xz plane within the cupboard, near to the work surface and at mid aperture height (3 D).



x velocity profile near work surface and at mid aperture height



Speed profile near work surface and at mid aperture height



Concentration profile near work surface and at mid aperture height

Figure 6.48 Effect of a cross flow of air (1 m/s) past the aperture of an aerodynamic fume cupboard on the x velocity, speed and concentration profiles across the aperture plane, z direction, near to the work surface and at mid aperture height (3 D).

6.3.5.3 'Aerodynamic' type fume cupboard with the rear baffle or lipfoil removed

The effect on the air flow within the working volume was similar at mid aperture height to the air flow within the aerodynamic fume cupboard. However, there was a greater disturbance of the air flow near to the work surface (Fig. 6.49), where the recirculation of air past the edge nearest to the supply was much larger extending further across the work surface and beyond this the air flowed sideways towards the furthest wall.

The xz profiles in the aperture plane (Fig. 6.50) confirmed how the air flow near to the work surface was influenced much more without a rear baffle or lipfoil. In terms of contaminant concentration, the levels were higher across most of the aperture width near to the work surface with disturbance than without. At mid aperture height the concentration nearest to the supply of the cross flow was the same as near to the work surface but this decreased more rapidly with distance across the aperture width.

The simulation was repeated with square vertical edges either side of the aperture, i.e. a 'box' type fume cupboard (Fig. 6.51). With and without disturbance the air flow, x velocity and speed profiles were similar to those of the 'aerodynamic' cupboard with no rear baffle or lipfoil (6.52). However, the contaminant levels were higher with no disturbance, showing greater concentration near to the vertical edges. With a cross flow, the concentration of contaminant in the plane of the aperture near to the work surface was similar to the aerodynamic fume cupboard with no rear baffle and lipfoil. At mid aperture height the concentration across the aperture width was greater.

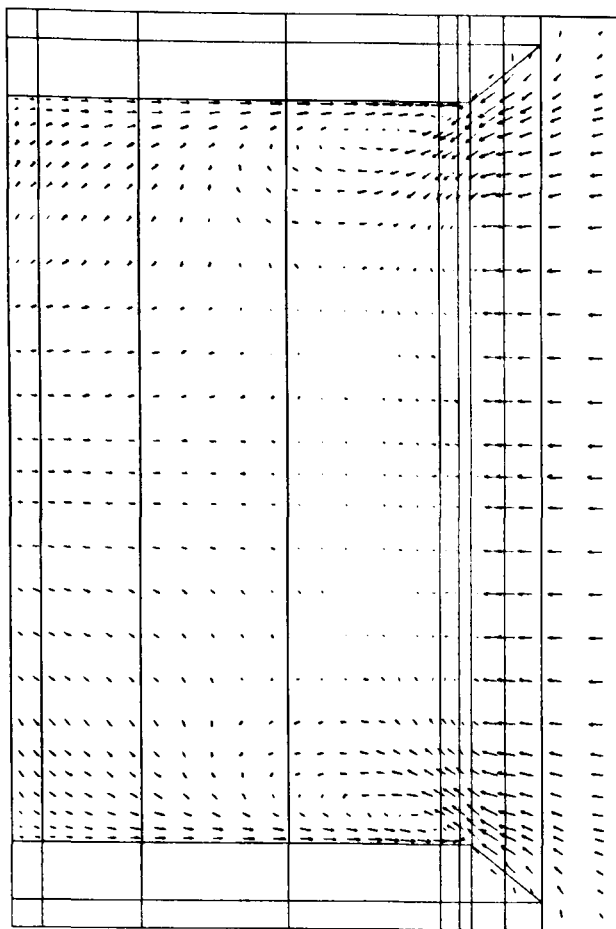
6.3.5.4 Conclusions

An air flow across the face of the cupboard at more than twice the cupboard face velocity was shown to substantially disturb the air flow in the plane of the aperture and within the working volume. However, the removal of the rear baffle and lipfoil resulted in much greater disturbance over the work surface.

6.4 Simulation of the distribution of a contaminant with relevance to British, German and American Standard methods for the assessment of fume cupboard containment

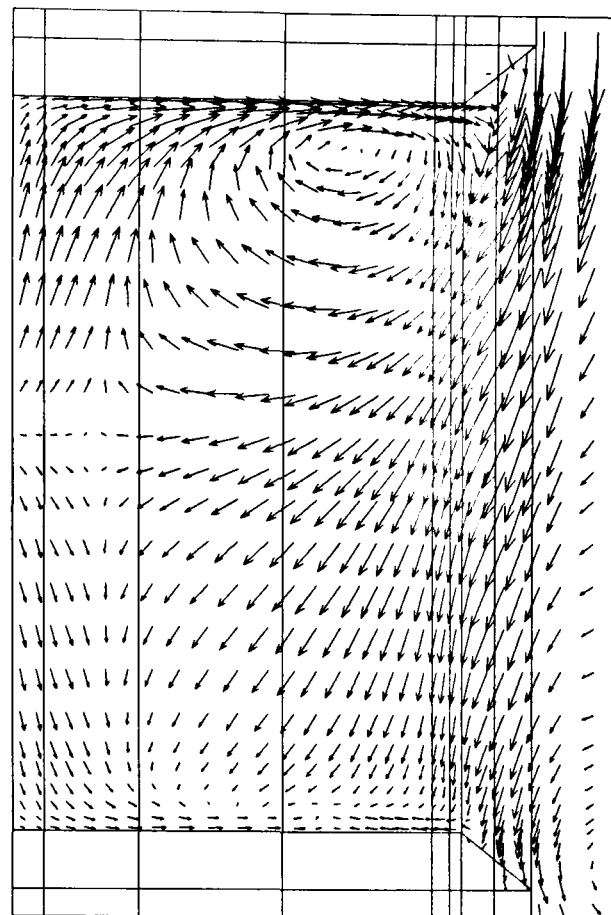
6.4.1 Introduction

In section 2.1 the British, American and German standard methods for the quantitative assessment of fume cupboard performance are described. In chapter 3, experience using the British Standard method (BS 7258 : 1994 : Part 4) is presented. Each of these standard methods utilises SF₆ as the tracer gas which is released within the working volume and sampled for either in the plane of the sash or a fixed distance away. The relative position and type of source generation and sampling differs for each test method and this effects the



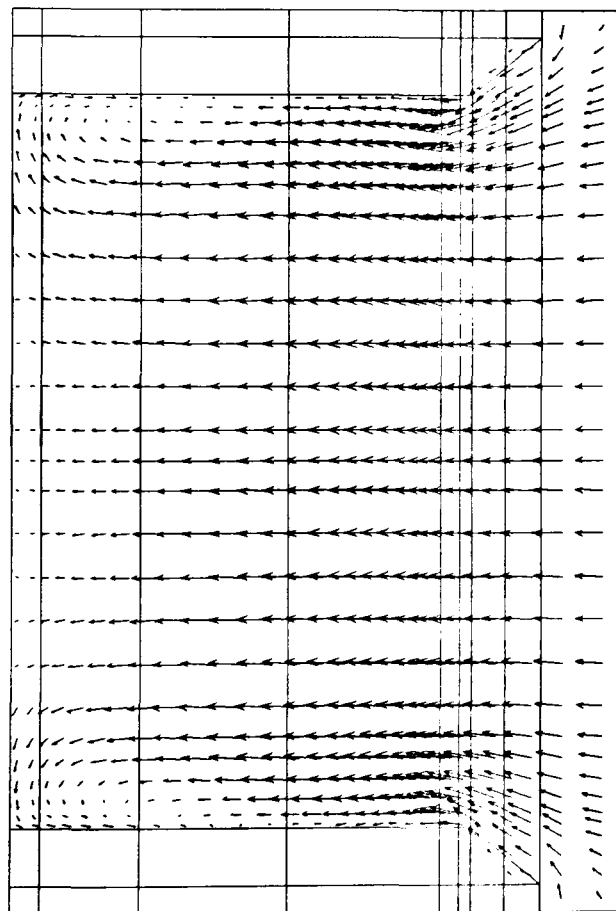
← 0.60 m/s

No disturbance (xz near surface)



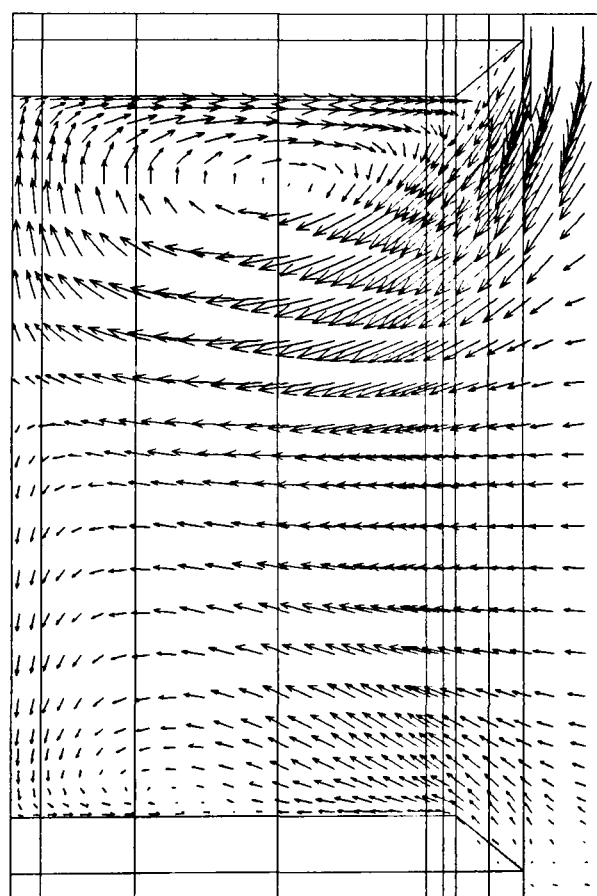
← 0.60 m/s

1 m/s cross flow



← 0.60 m/s

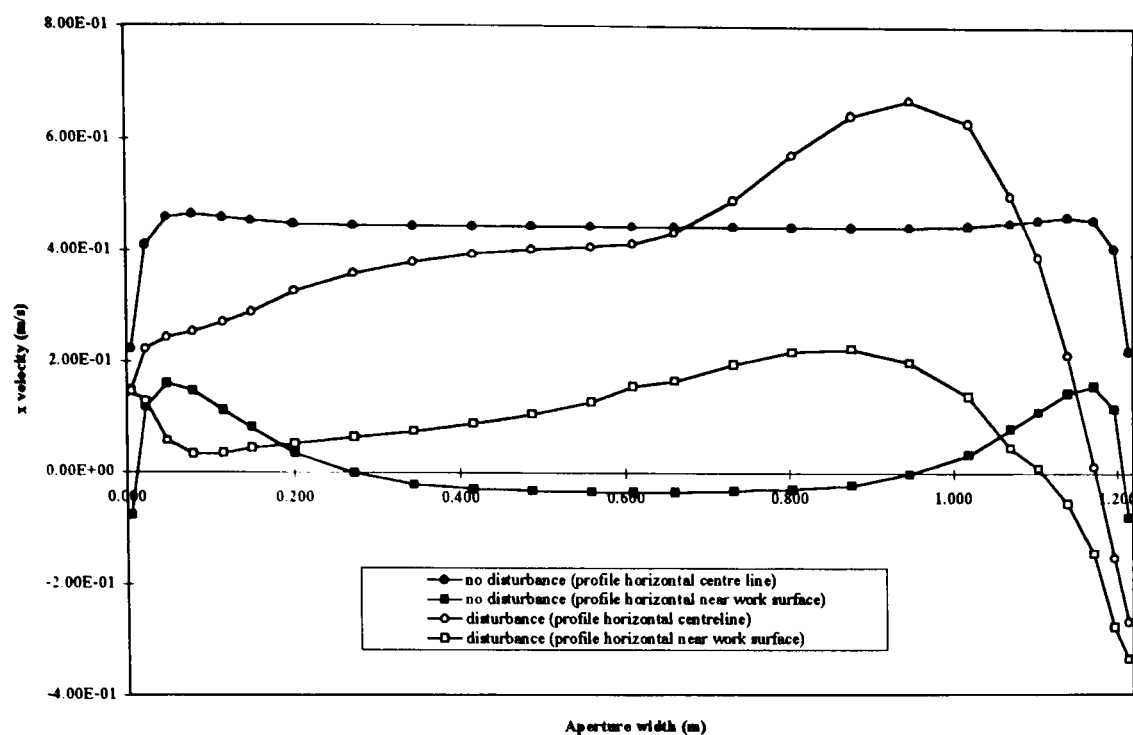
No disturbance (xz mid aperture)



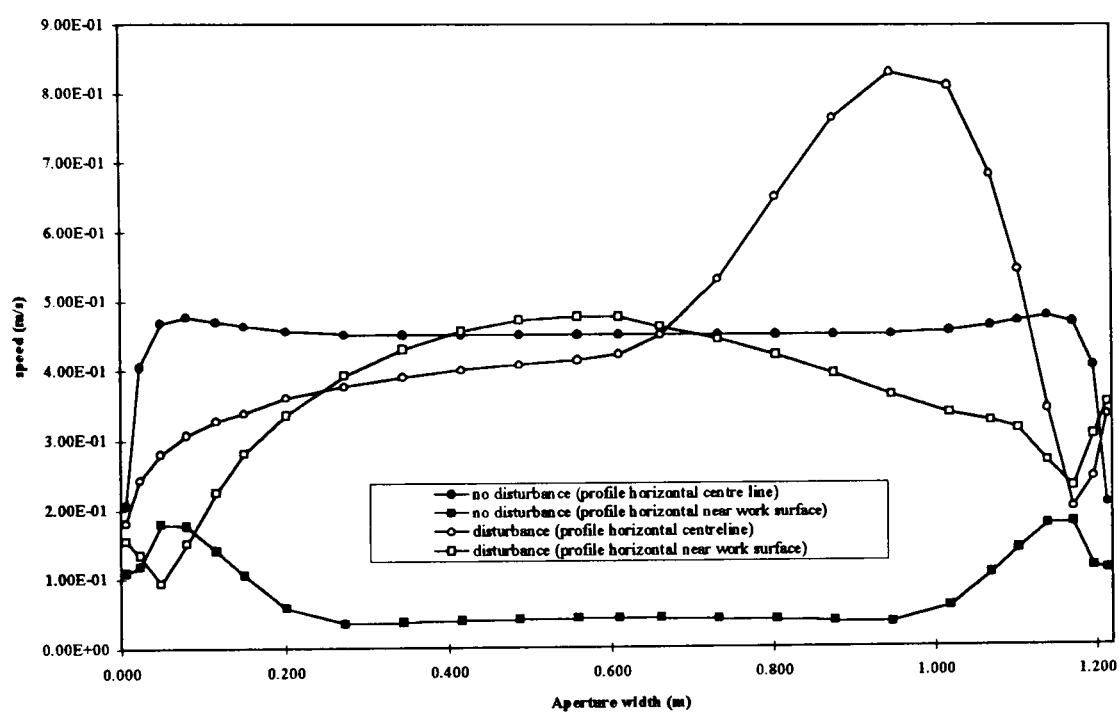
← 0.60 m/s

1 m/s cross flow

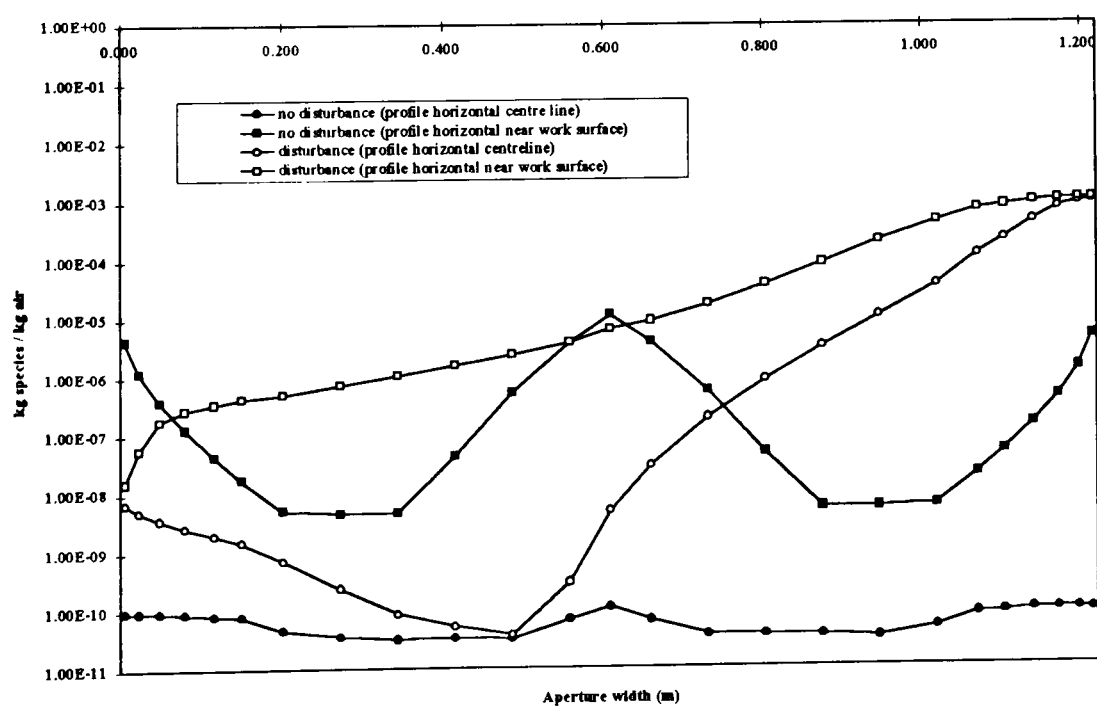
Figure 6.49 Effect of a cross flow of air (1 m/s) past the aperture of an aerodynamic fume cupboard with no rear baffle or lipfoil on the airflow vectors in the xz plane within the cupboard, near to the work surface and at mid aperture height (3 D).



x velocity profile near work surface and at mid aperture height

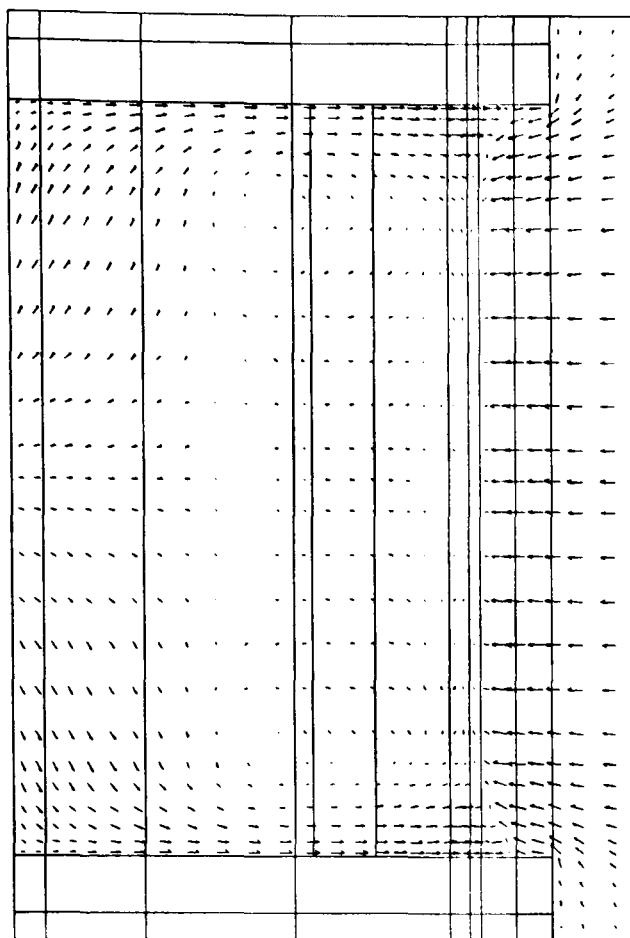


Speed profile near work surface and at mid aperture height



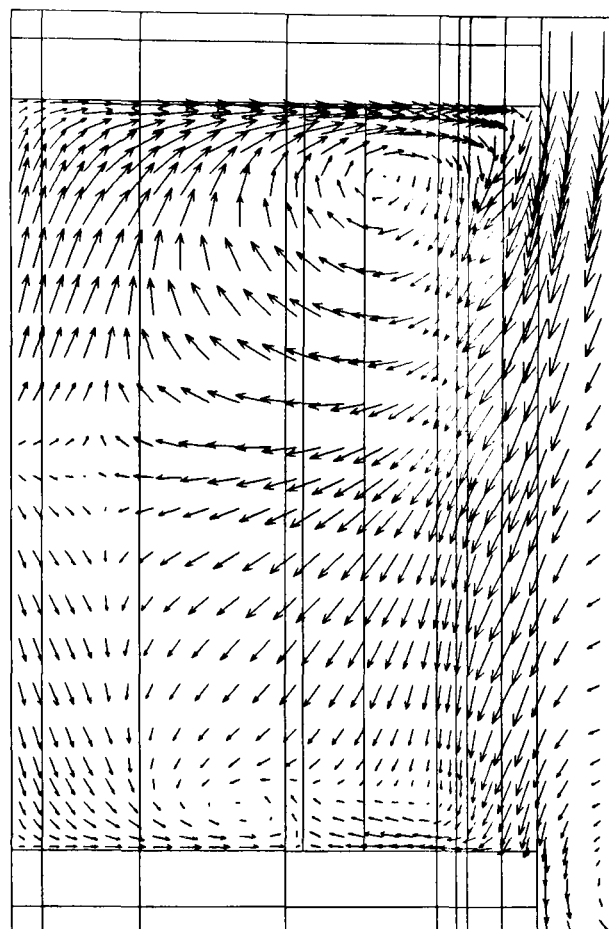
Concentration profile near work surface and at mid aperture height

Figure 6.50 Effect of a cross flow of air (1 m/s) past the aperture of an aerodynamic fume cupboard, with the rear baffle or lipfoil removed, on the x velocity, speed and concentration profiles across the aperture plane, z direction, near to the work surface and at mid aperture height (3 D).



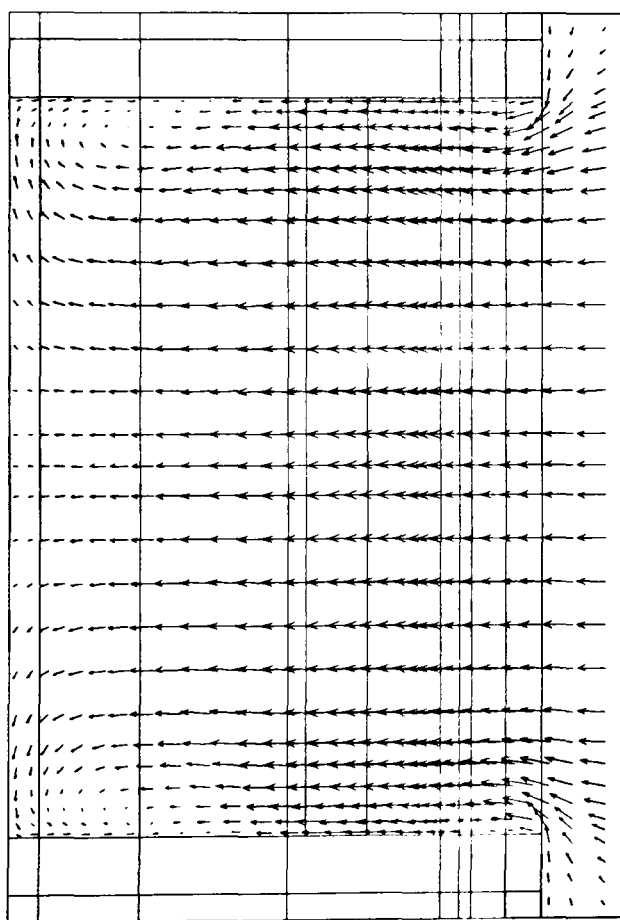
← 0.60 m/s

No disturbance (xz near surface)



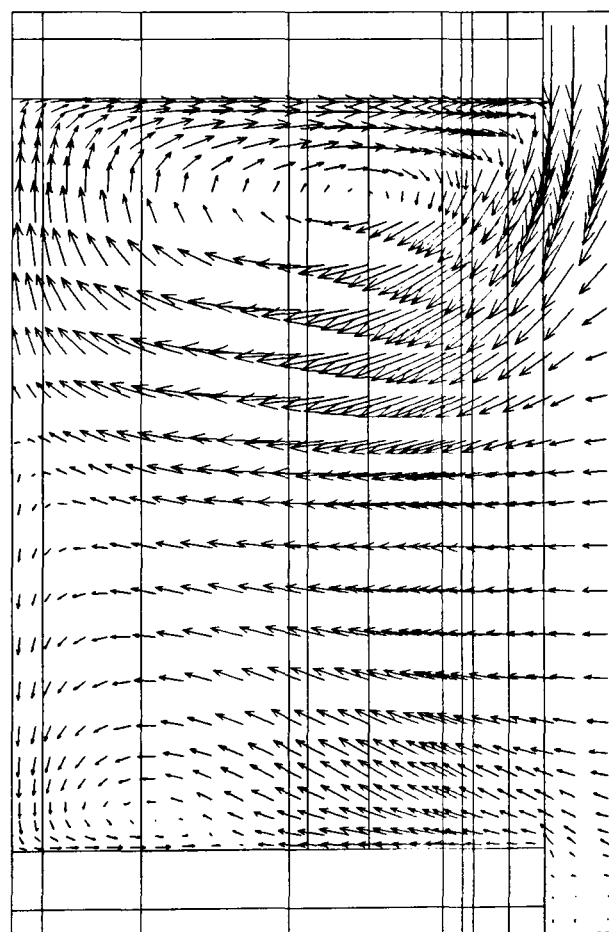
← 0.60 m/s

1 m/s cross flow



← 0.60 m/s

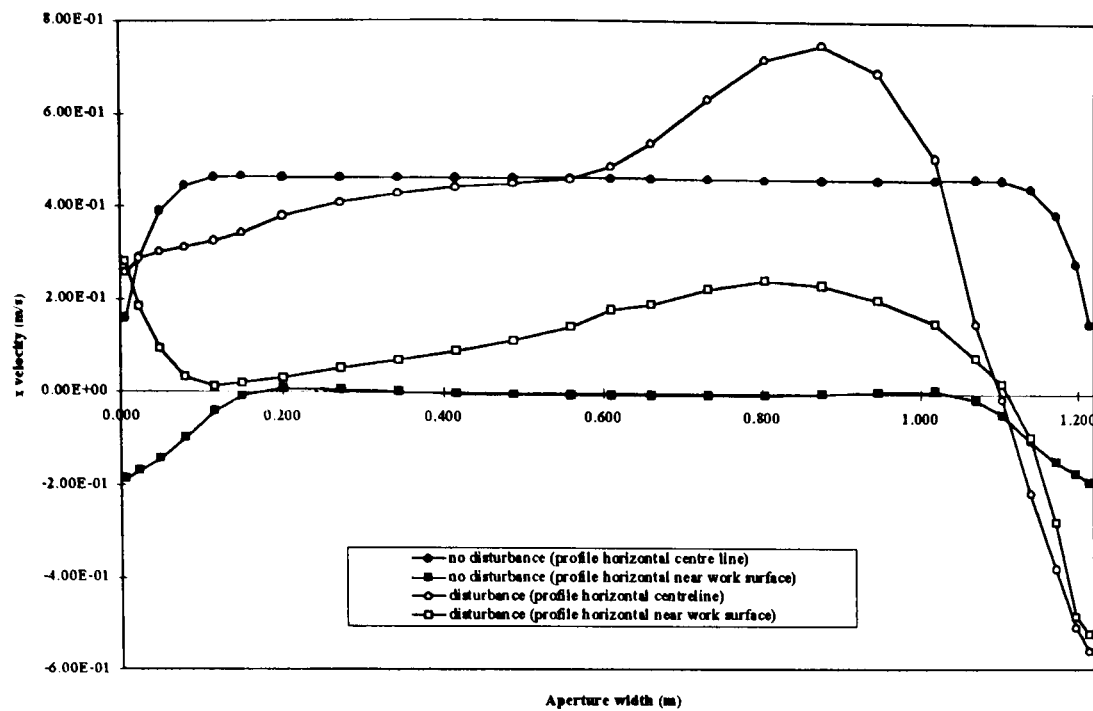
No disturbance (xz mid aperture)



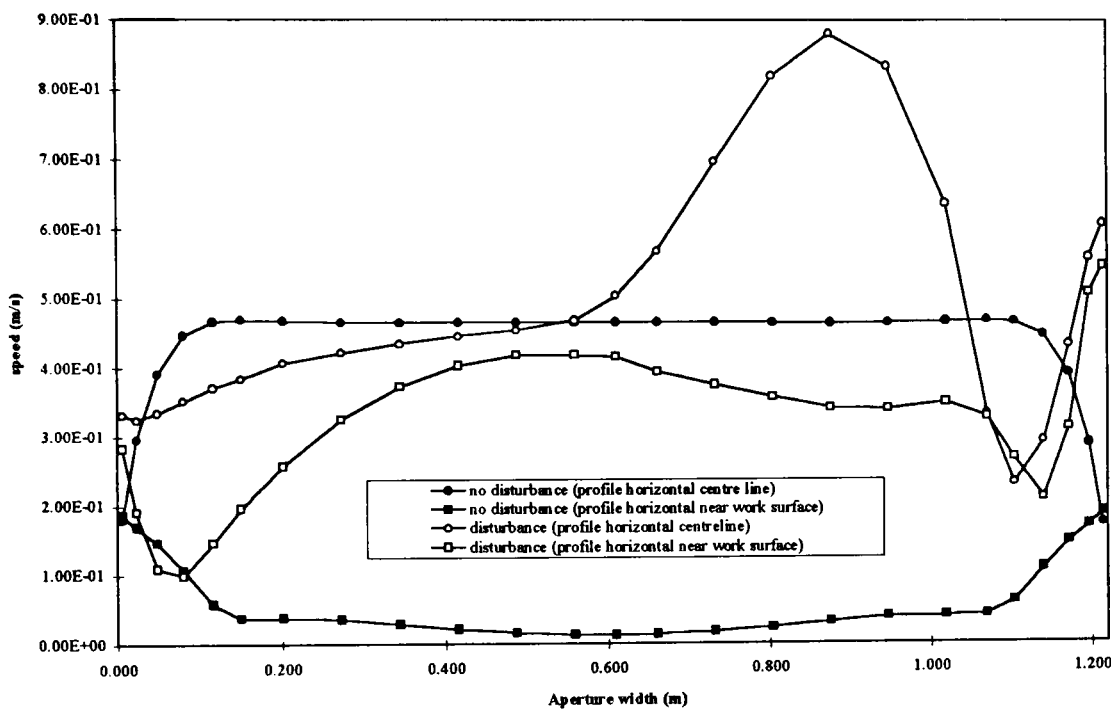
← 0.60 m/s

1 m/s cross flow

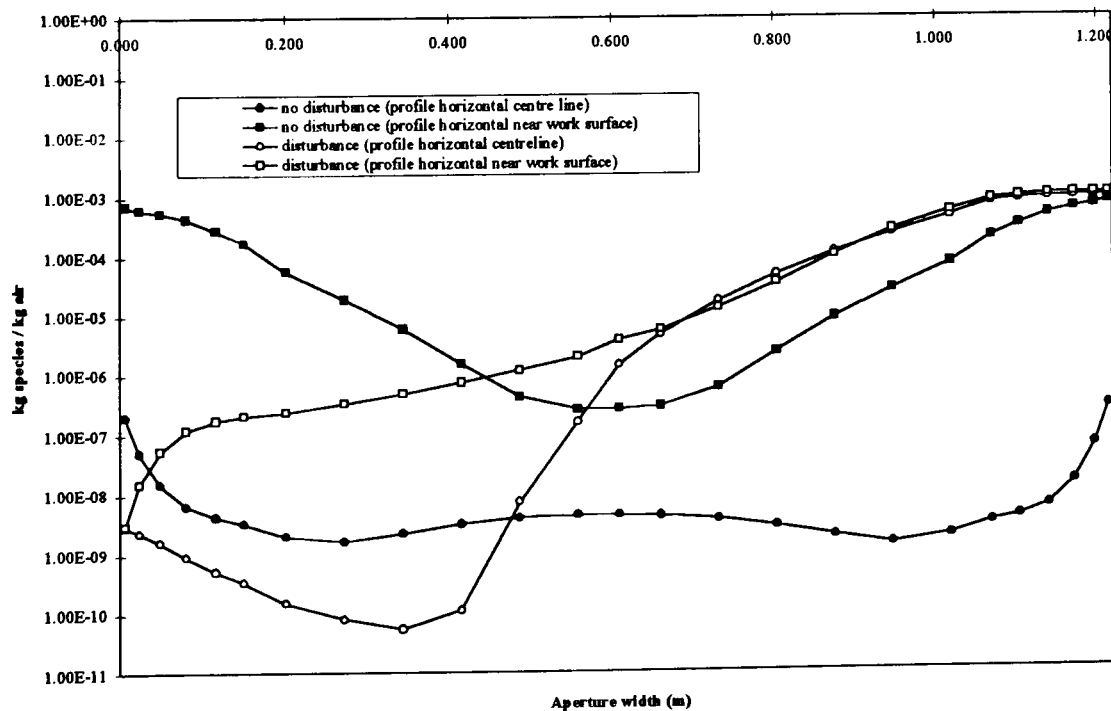
Figure 6.51 Effect of a cross flow of air (1 m/s) past the aperture of an aerodynamic fume cupboard with no rear baffle, no lipfoil and square edges on the airflow vectors in the xz plane within the cupboard, near to the work surface and at mid aperture height (3 D).



x velocity profile near work surface and at mid aperture height



Speed profile near work surface and at mid aperture height



Concentration profile near work surface and at mid aperture height

Figure 6.52 Effect of a cross flow of air (1 m/s) past the aperture of an aerodynamic fume cupboard with the rear baffle or lipfoil removed and with square edges on the x velocity, speed and concentration profiles across the aperture plane, z direction, near to the work surface and at mid aperture height (3 D).

distribution of tracer and possible detection of leakage. As SF_6 is colourless its dispersal cannot be visualised and can only be ascertained by quantitative measurement; comparisons between the methods being based on these measurements. In this section the 3 dimensional CFD model is used to compare both qualitatively and quantitatively the dispersal of the tracer within the working volume by each test method and identification of 'potential' leakages in the plane of the aperture when the rear baffle and the lipfoil are removed.

For each simulation the source is in the centreline of the aperture width in terms of that particular standard method. For quantitative analysis the distribution of the tracer is shown by xy profile in the plane of the aperture and as xz profile at three heights in the plane of the aperture 1) near to the work surface 2) at mid aperture height and 3) near to the sash. The profiles in the plane of the aperture are actually values in the centre of the grid cell 7 mm inside of the aperture plane.

The qualitative contour maps are shown scaled from $1 \times 10^{-8} \text{ kg}_{\text{tracer}}/\text{kg}_{\text{air}}$ to zero values. This is to reflect the sensitivity of physical measuring equipment capable of detecting 1 ppb (v/v). The weight ratio term $\text{kg}_{\text{tracer}} / \text{kg}_{\text{air}}$ can be converted to ppm (v/v) using the following formula:

$$\text{ppm}(v/v) = \frac{m}{m^3} \times \frac{24.04_{@20^\circ\text{C}}}{\text{MW}_{\text{air}}} \text{ where the density of air is } 1.2 \text{ kg/m}^3.$$

For the ASHRAE and DIN tracer ejectors the dimensions and flow rates were approximations from available information. In order to compare the simulations of each of the test methods the solution grid was unaltered so as not to affect the results based on grid differences. However, this meant that the source dimensions would not necessarily line up exactly with the grid, the program would adapt the objects to the available grid (Fig. 6.53, 6.59 & 6.63). Thus the simulations would be an approximation for comparative purposes and not absolute.

6.4.2 BS 7258 : 1994 : Part 4

6.4.2.1 Set up

In the standard test method, the tracer gas (10% SF_6 /90% N_2) was allowed to diffuse out from a funnel 30 mm in diameter at a release rate of 2 l/min/m cupboard aperture width i.e. 2.4 l/min for the cupboard tested. This tracer had a density of 1.7 kg/m^3 . In the CFD model the funnel was represented as a 30 mm square planar source with a mass flow rate of gas at each source position of 0.000068 kg/s, 10% SF_6 /90% N_2 tracer gas concentration $1 \text{ kg}_{\text{tracer}}/\text{kg}_{\text{air}}$. In this simulation the ideal gas law was used and the tracer gas given a MW of 39.8 to reflect the greater density in air.

In the standard test method the source was positioned in 6 places as separate tests. For the purposes of this simulation, first one position was used (P1) and the distribution of the source through the working volume calculated to assess cupboard mixing then for comparison with the other tests a simulation was used with the two sources in the centreline of the aperture width (P2 and P5).

6.4.2.2 Simulations

Qualitatively with the tracer gas released from P1 it was not fully mixed within the working volume near to the work surface or at mid aperture height (Fig. 6.54 & 6.55). This compared well with the physical measurements in section 3.9.3.7 where no tracer was sampled in the lower right half of the working volume when released from P1. However, the tracer was well mixed within the volume of air behind the sash and as the source would be moved to 5 other positions in a test, so covering the aperture, it was considered that the interior working volume would be fully seeded with tracer, albeit at different times.

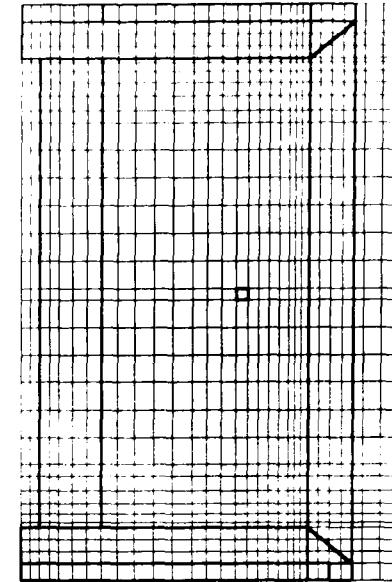
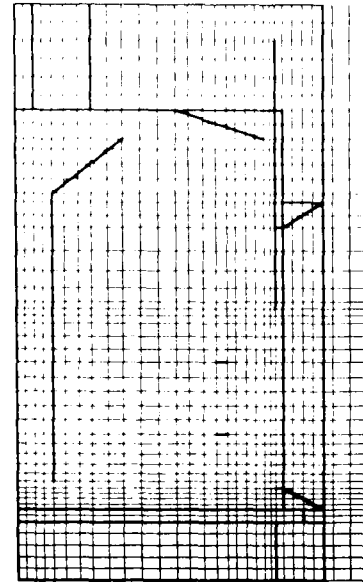
With the source at P2 and P5, in the case of the aerodynamic fume cupboard, much of the working volume was filled with tracer apart from regions near to the left and right walls (Fig. 6.56). For this cupboard model the whole of the aperture height in the centre line was challenged with tracer. From the profiles (Fig. 6.58) there were negligible amounts of tracer near to the work surface or at mid aperture height in the plane of the aperture, but near to the sash there was concentration of tracer several orders of magnitude higher.

Removal of the rear baffle and lipfoil resulted in much greater dispersal of tracer within the working volume, most of the aperture being challenged (Fig. 6.57). The profiles showed greater concentration at the aperture plane near to the work surface and at mid aperture height (Fig. 6.58). At the work surface, there was higher concentration of tracer to the left and right walls whereas at mid aperture height the greatest concentrations were in the xy plane of the sources. Near to the sash the results were similar to those levels with the rear baffle and lipfoil present.

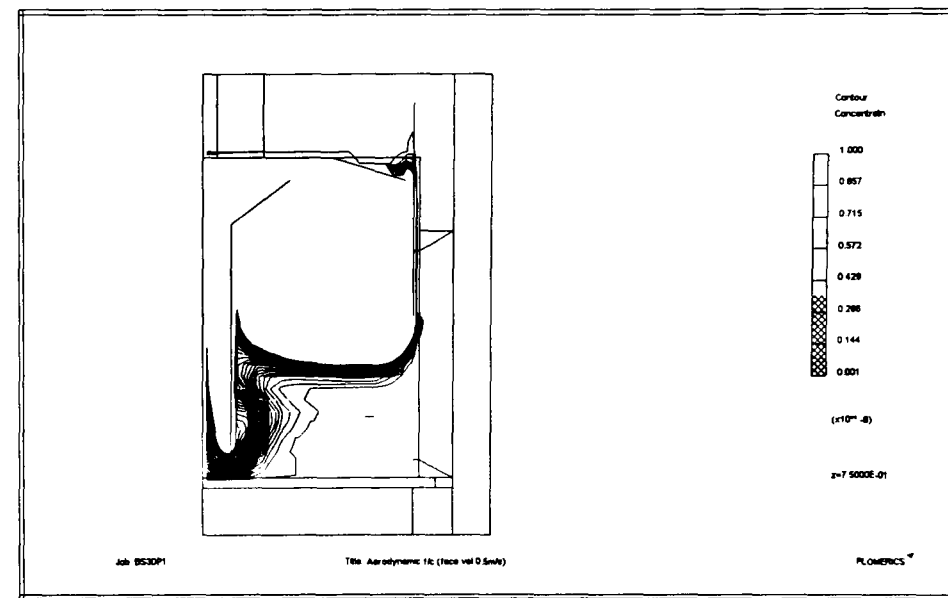
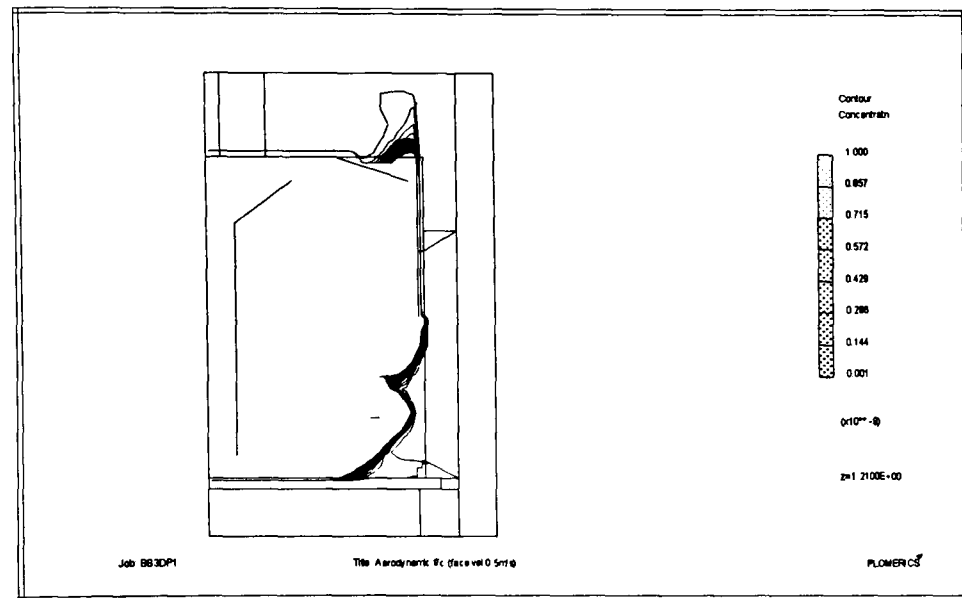
6.4.3 ASHRAE 110 1993

6.4.3.1 Set up

This involved the release of tracer gas from an ejector diffuser 127 mm diameter, 76 mm deep standing ~350 mm with a 90 mm diameter base (these dimensions were approximated from Caplan and Knutson, 1982). The CFD model was represented as a square planar source sitting on a cuboid base. The release rate of SF₆ tracer was suggested to be 1 l/min and as it passed through the base it entrained air to be discharged from the diffuser at ~0.03 m/s with density near that of air. From the dimensions the surface area of the diffuser was 0.043 m² with open area 50 % and the mass flow rate of tracer/air mix from this diffuser, at the density



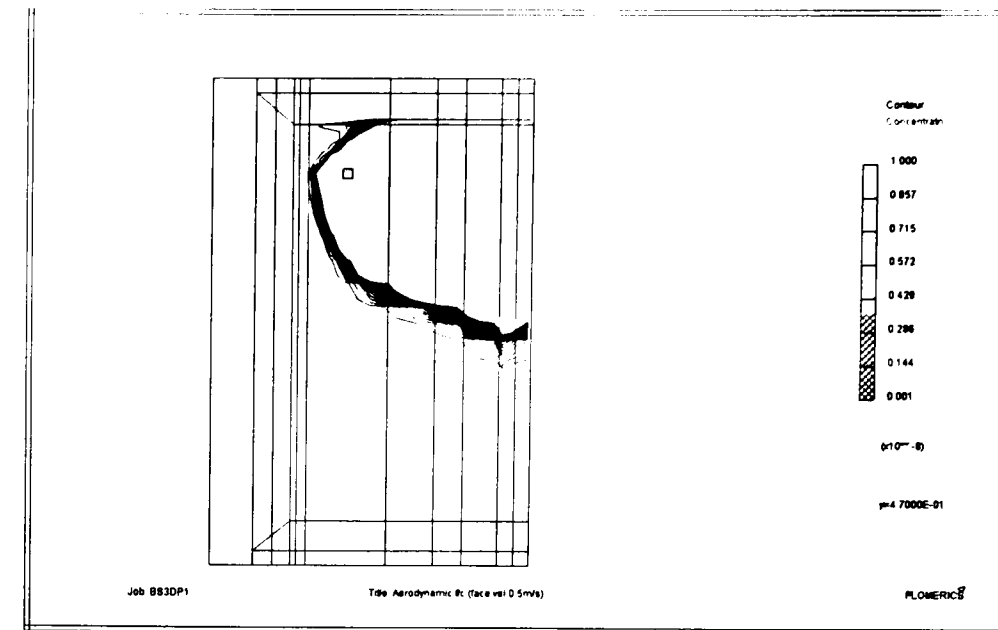
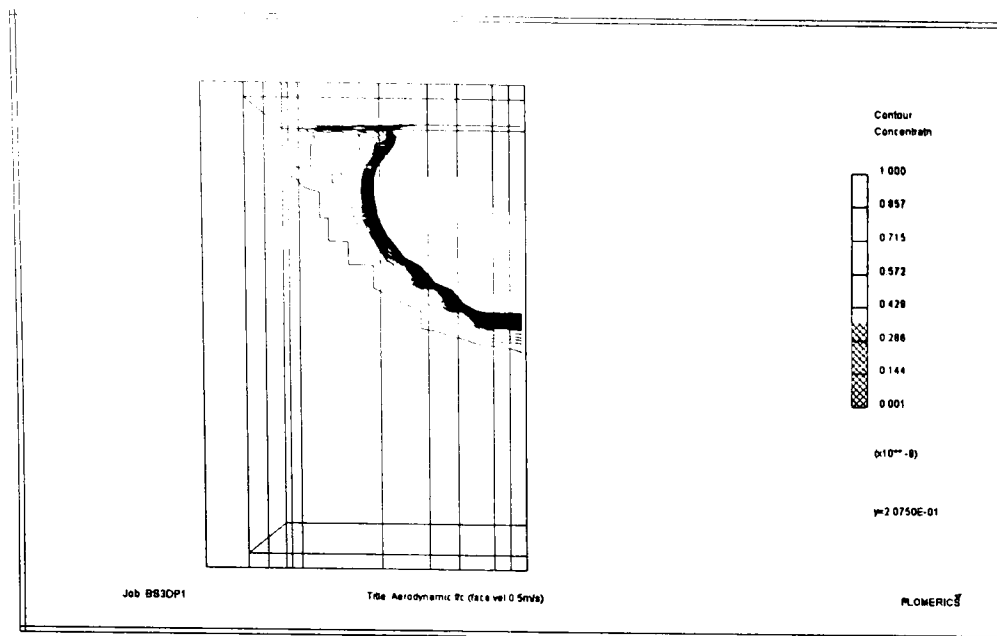
xy plane of source and grids
xz plane of source (source P2 and P5) and grids
Figure 6.53 Position of BS 7258 source in an aerodynamic fume cupboard and solution grid (3 D).



xy plane of source (P1)

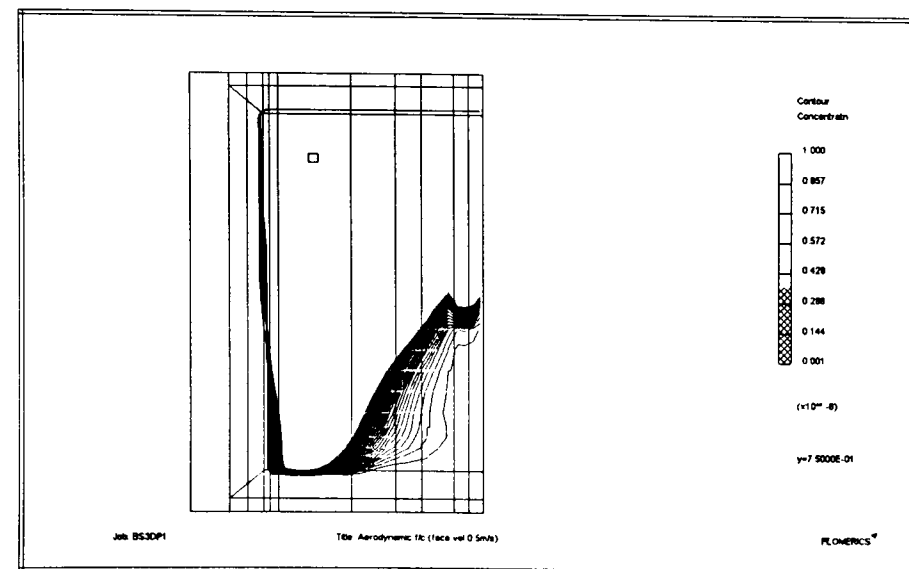
xy plane centre line of aperture width (source P1)

Figure 6.54 xy contours of tracer distribution, in the centre line of the source, when released from source position P1 (BS 7258 : 1994 : Part 4) within the working volume of an 'aerodynamic' fume cupboard (3 D).



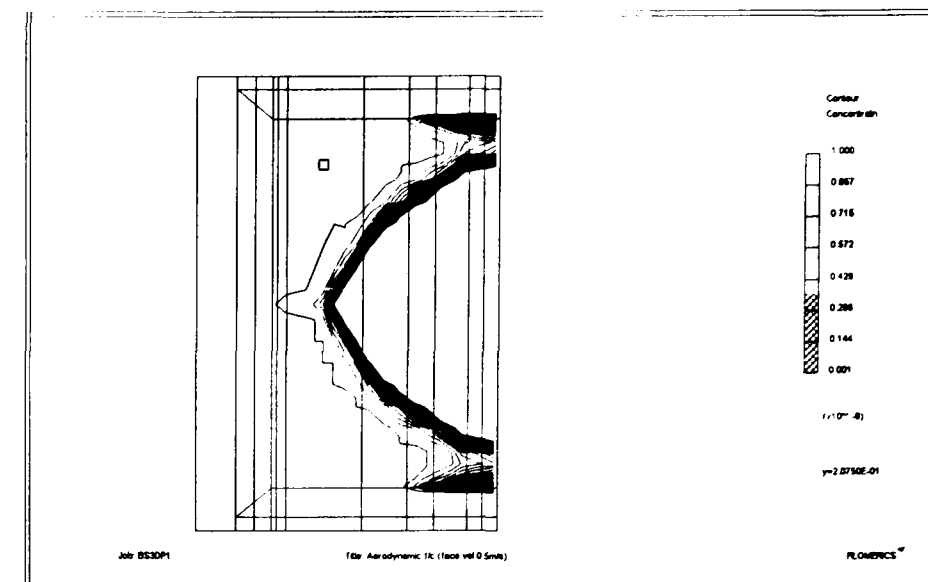
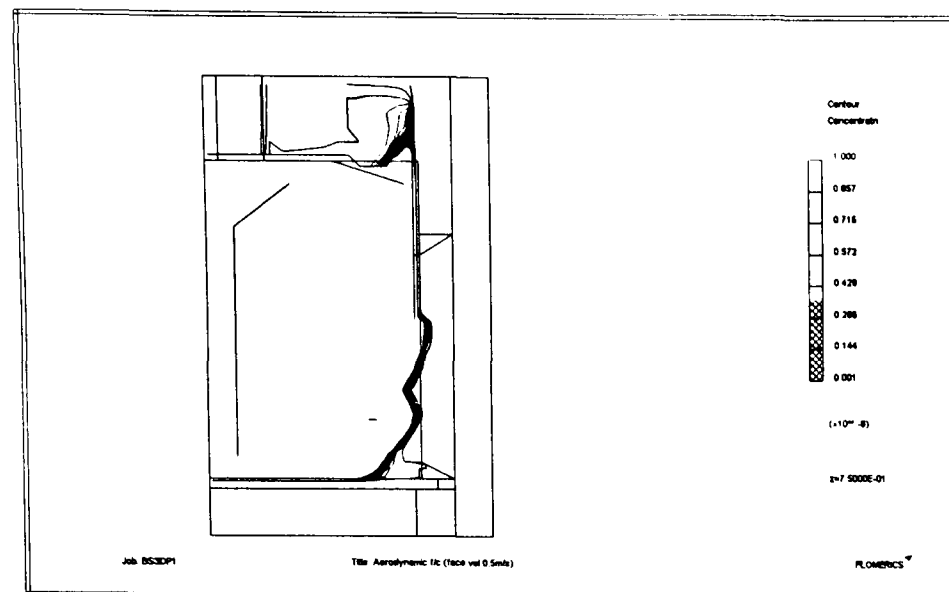
xz plane near work surface (source P1)

xz plane mid aperture height (source P1)



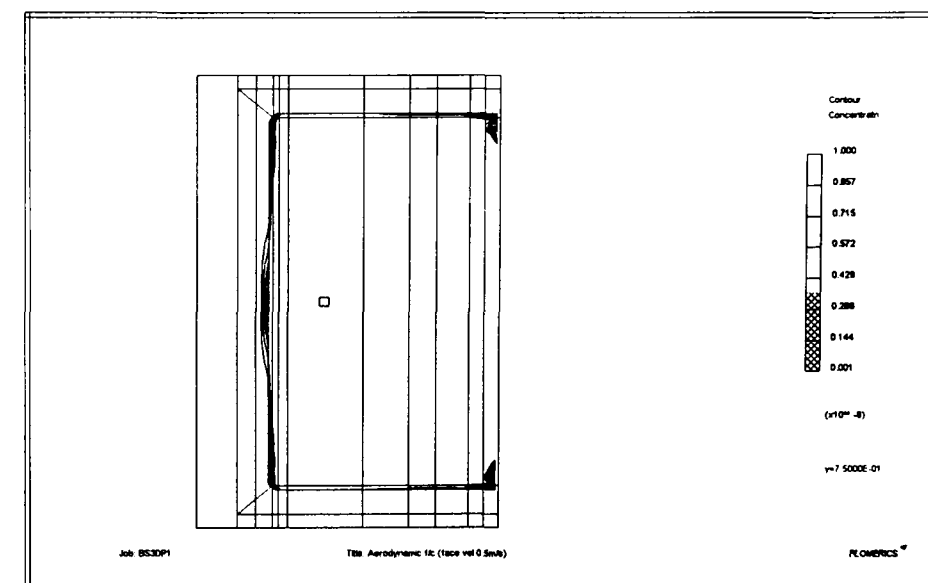
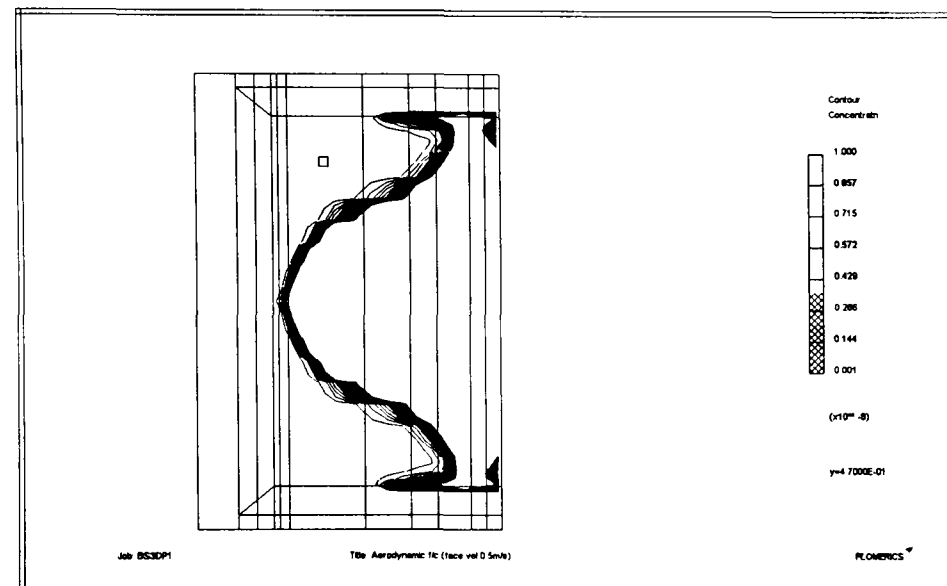
xz plane near sash (source P1)

Figure 6.55 xz contours of tracer distribution inside the cupboard near to the work surface, at mid aperture height and near to the sash when released from source position P1 (BS 7258 : 1994 : Part 4) within the working volume of an 'aerodynamic' fume cupboard (3 D).



xy plane of sources (P2 and P5)

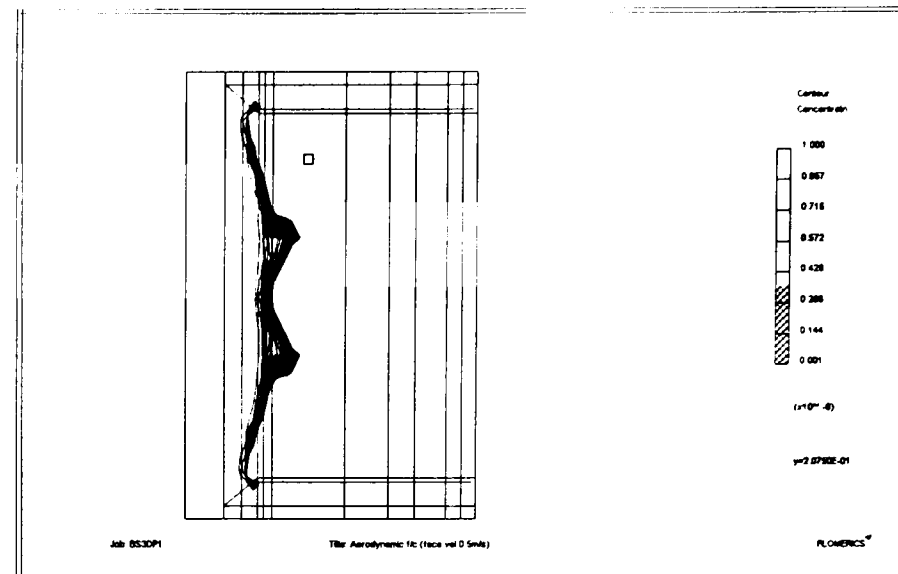
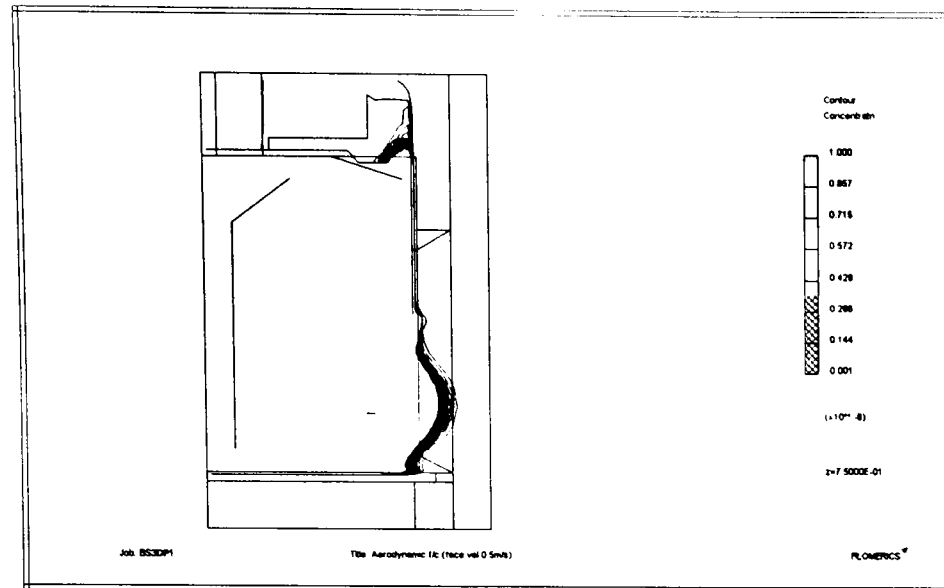
xz plane near work surface (sources P2 and P5)



xz plane mid aperture height (source P2 and P5)

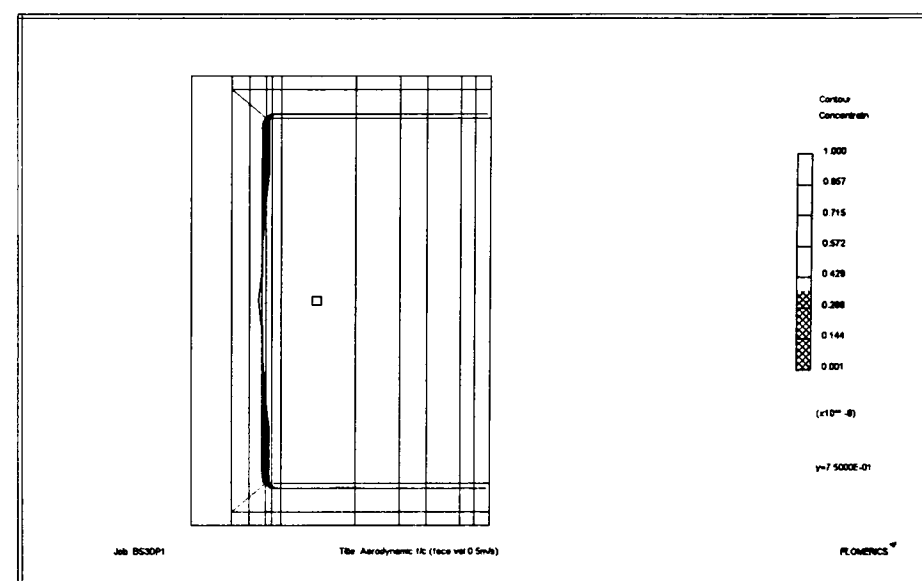
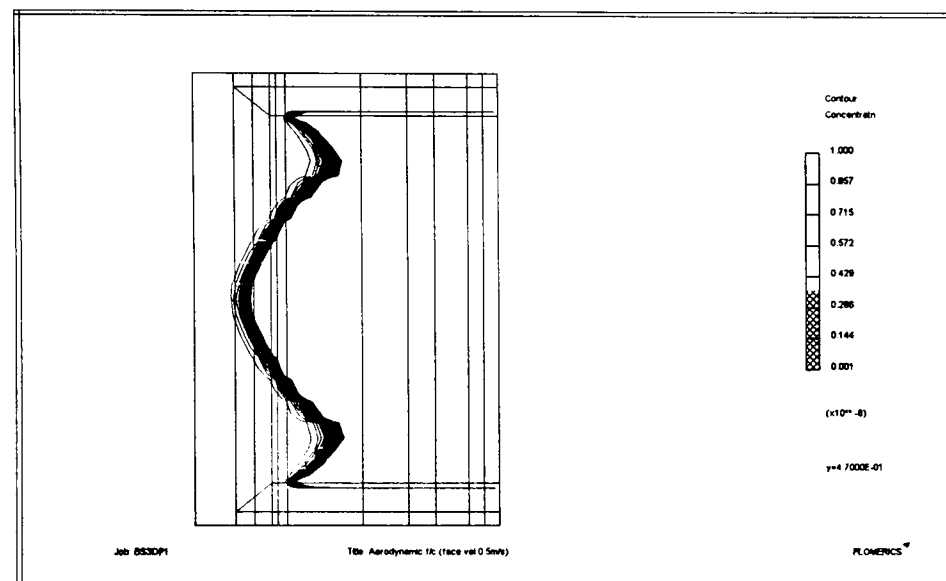
xz plane near sash (source P2 and P5)

Figure 6.56 xy contour, centre line of the source, and xz contours, near to the work surface, at mid aperture height and near to the sash, of tracer distribution when released from source position P2 and P5 (BS 7258 : 1994 : Part 4) within an 'aerodynamic' fume cupboard (3 D).



xy plane of sources (P2 and P5)

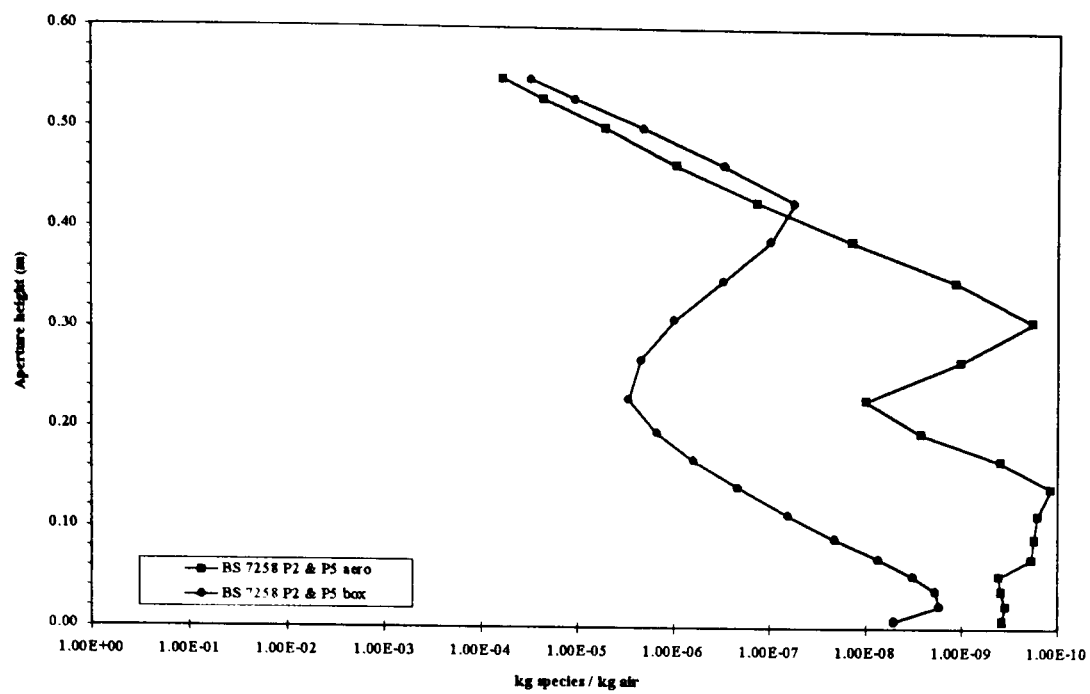
xz plane near work surface (sources P2 and P5)



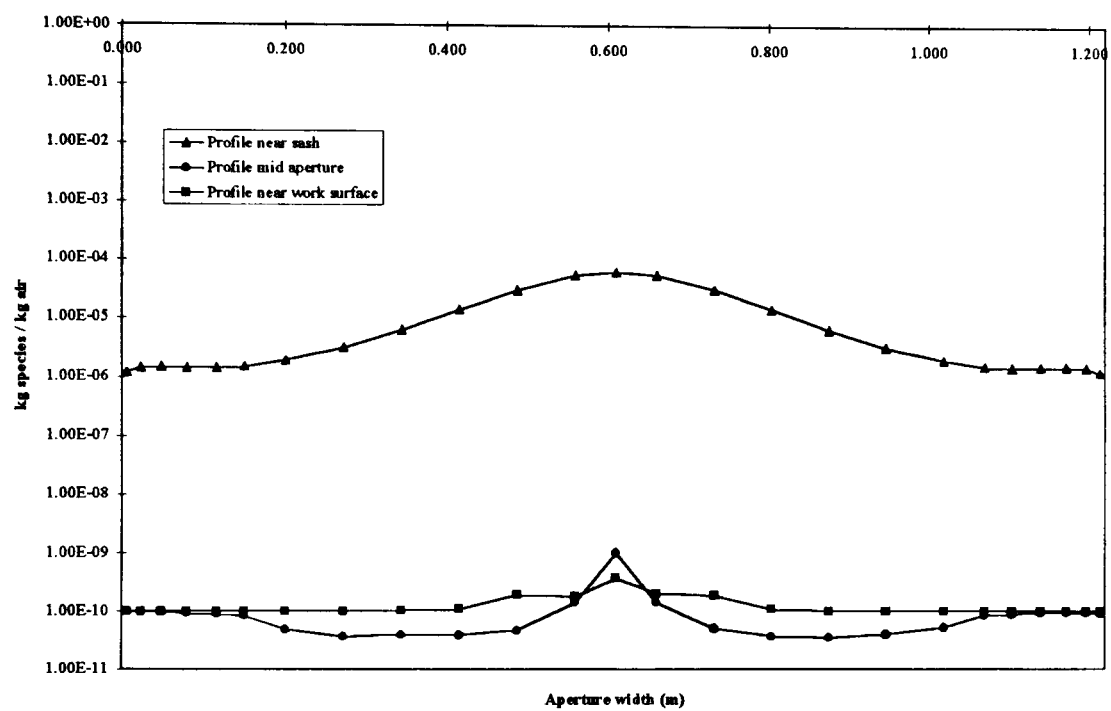
xz plane mid aperture height (source P2 and P5)

xz plane near sash (source P2 and P5)

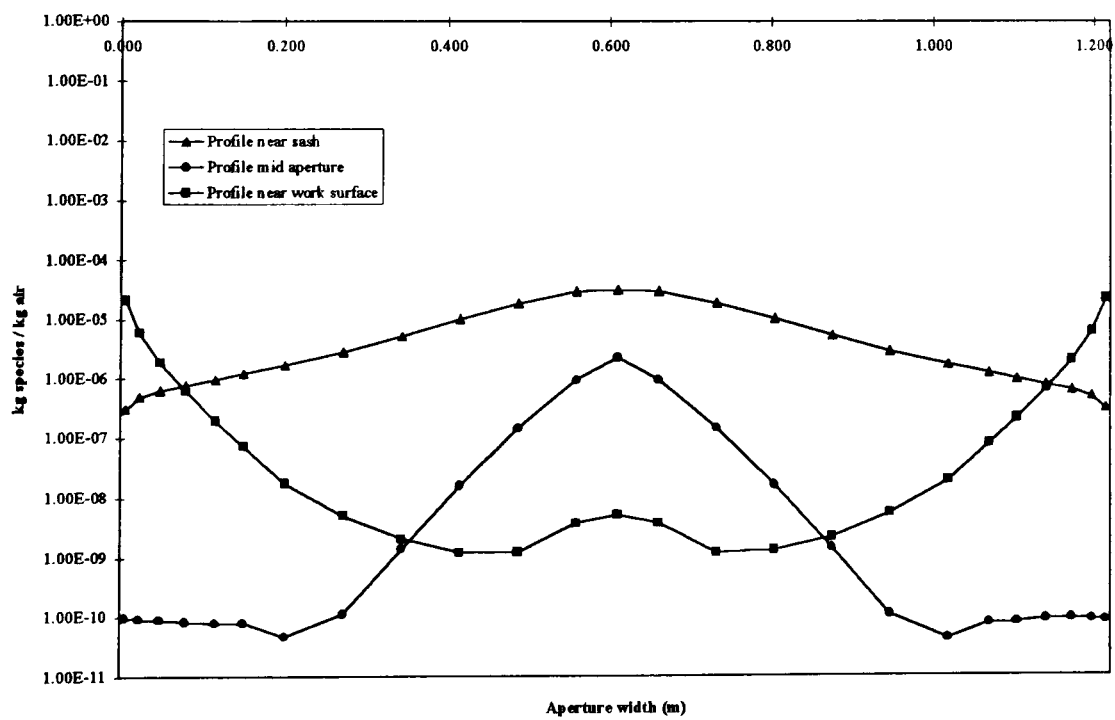
Figure 6.57 Effect of removing the rear baffle and lipfoil on xy and xz tracer contours when released from from source position P2 and P5 (BS 7258 : 1994 : Part 4) within an 'aerodynamic' fume cupboard (3 D).



xy profiles (centre line of aperture width)



xz profile for aerodynamic cupboard



xz profile for aerodynamic cupboard with no rear baffle or lipfoil

Figure 6.58 Effect of removing the rear baffle and lipfoil on tracer concentration profiles in the aperture plane, centreline of the source, and across the aperture plane, z direction, when released from positions P2 and P5 (BS 7258 : 1994 : Part 4) within an aerodynamic fume cupboard (3 D).

of air, was estimated to be 0.0016 kg/s. This gave an entrainment factor of 16 times air to SF₆ and thus SF₆ content 0.0001 kg/s, 0.0625 kg_{tracer} / kg_{air}. In order to diffuse this planar source in 3 dimensions at discharge velocity 0.03 m/s a volume resistance was added above the source with the following settings:

	Loss coefficient	Free area ratio
x direction	2.0	0.2
y direction	1.7	0.5
z direction	2.0	0.2

As the tracer was well mixed with air and may be assumed to equal the density of the air when discharged the solution domain was fixed at a constant density of 1.19 kg/m³, and the ideal gas law was not used.

In the test method the source was positioned in 3 places as separate tests. For the purposes of this simulation, the source was placed in the central position in the centreline of the aperture width.

6.4.3.2 Simulations

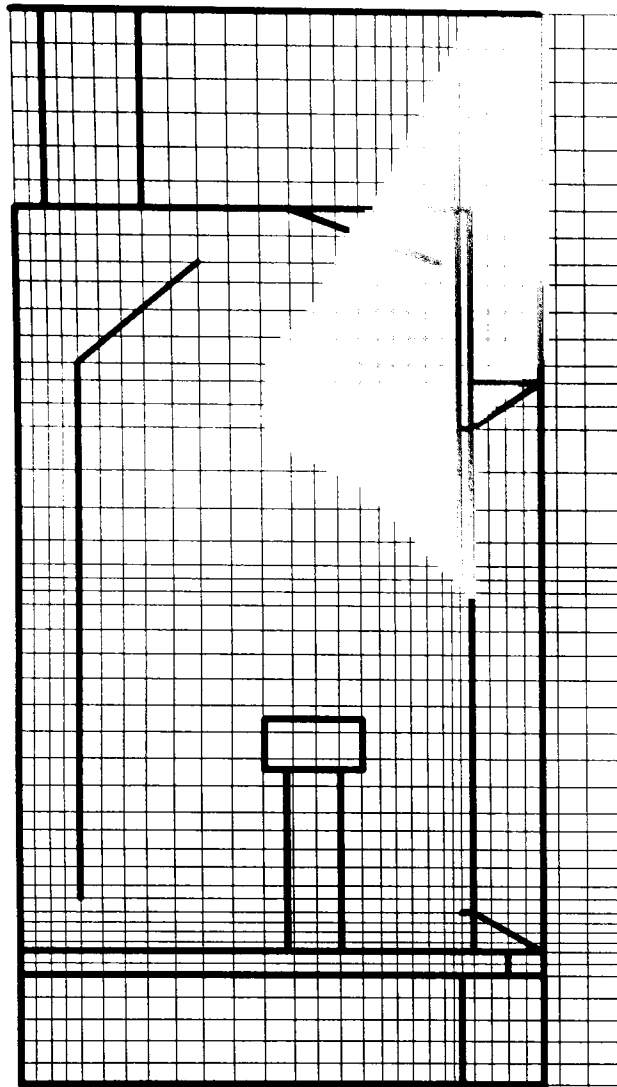
The discharge of air from the ejector did not visually disturb the air flow within the working volume (Fig. 6.59). In the case of the aerodynamic fume cupboard much of the working volume was filled with tracer apart from regions near to the left and right walls (Fig. 6.60). For this cupboard model the whole of the aperture height in the centre line was challenged with tracer. From the profiles (Fig. 6.62) there was negligible amounts of tracer near to the work surface or at mid aperture height in the plane of the aperture, but near to the sash there was concentration of tracer several orders of magnitude higher.

Removal of the rear baffle and lipfoil resulted in much greater dispersal within the working volume, most of the aperture being challenged (Fig. 6.61). The profiles showed greater concentration at the aperture plane near to the work surface and at mid aperture height (Fig. 6.62). At the work surface, there was higher concentration of tracer to the left and right walls whereas at mid aperture height the greatest concentrations were in the xy plane of the sources. Near to the sash the results were similar to those with the rear baffle and lipfoil present.

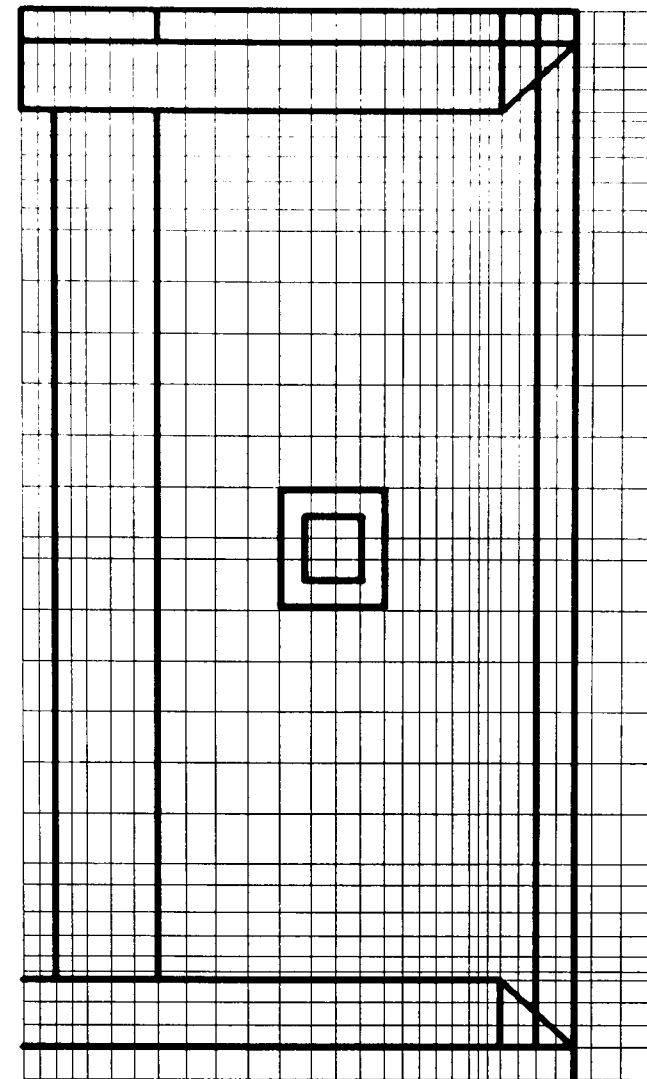
6.4.4 DIN 12 924

6.4.4.1 Set up

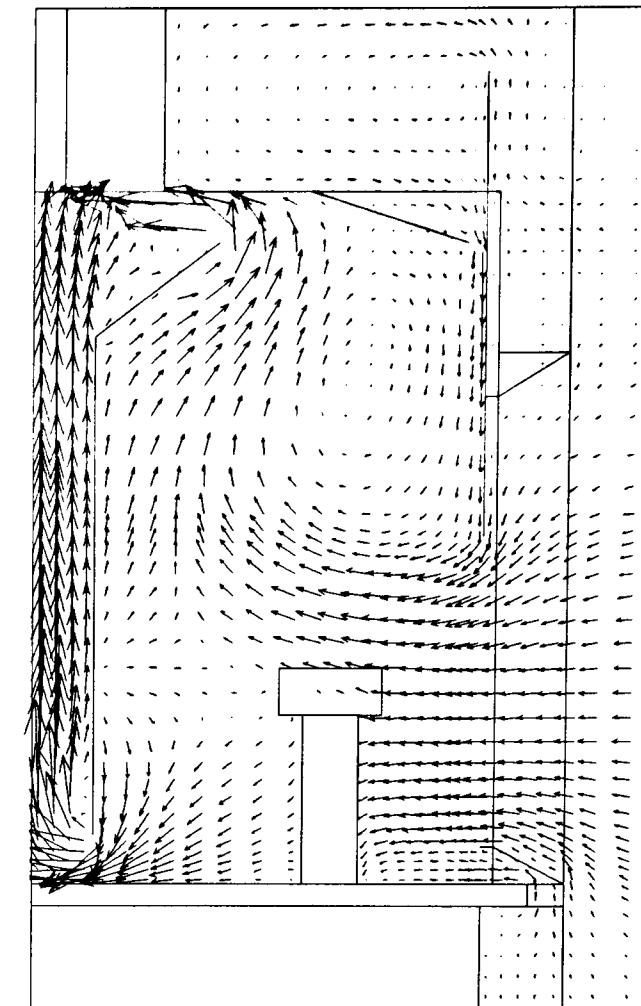
This involved the release of tracer gas from an ejector diffuser 90 mm diameter, 100 mm deep standing 465 mm with a 75 mm diameter base (these dimensions were from DIN 12 924 standard). The CFD model was represented as a square planar source sitting on a cuboid



xy plane of source and grids

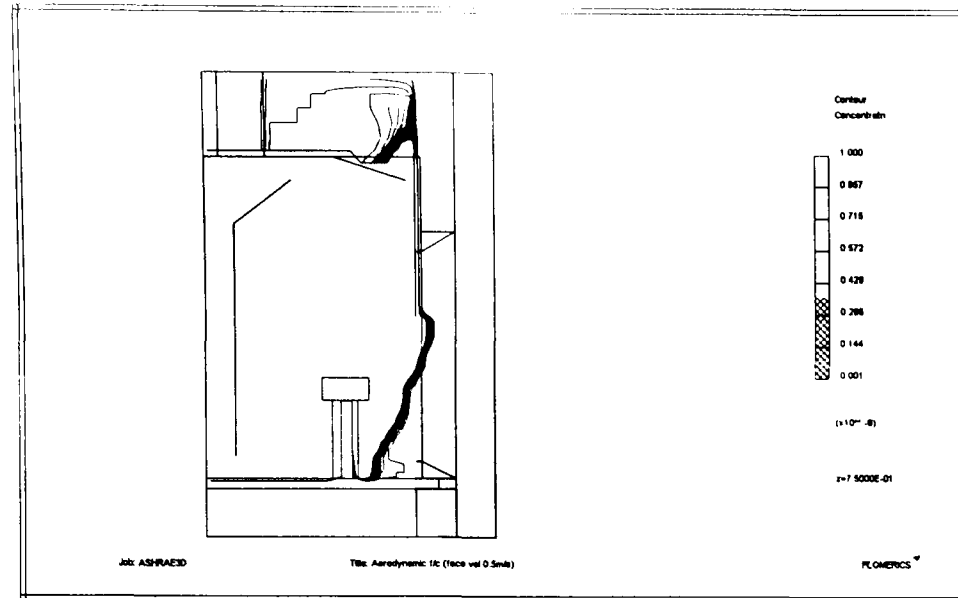


xz plane of source (source P2 and P5) and grids

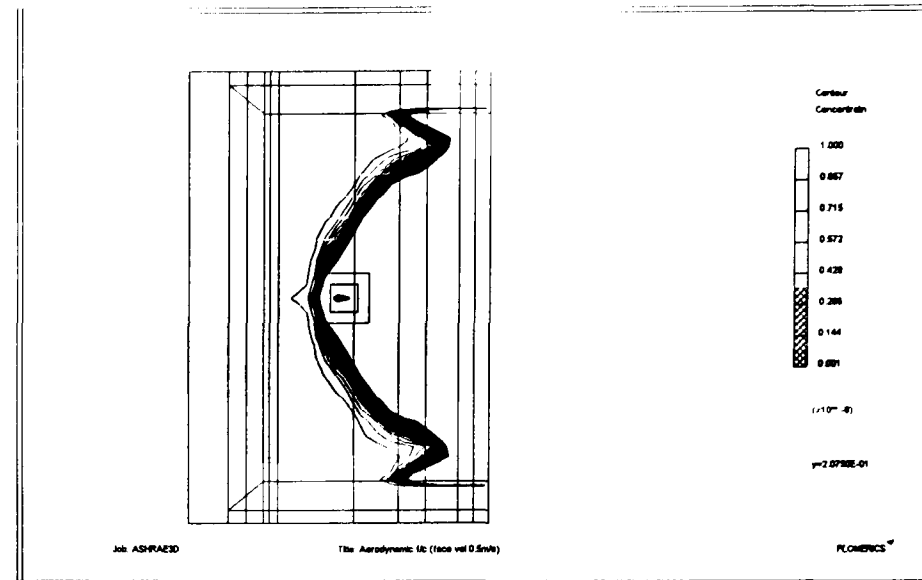


← 1.00 m/s
xy plane air flow vectors

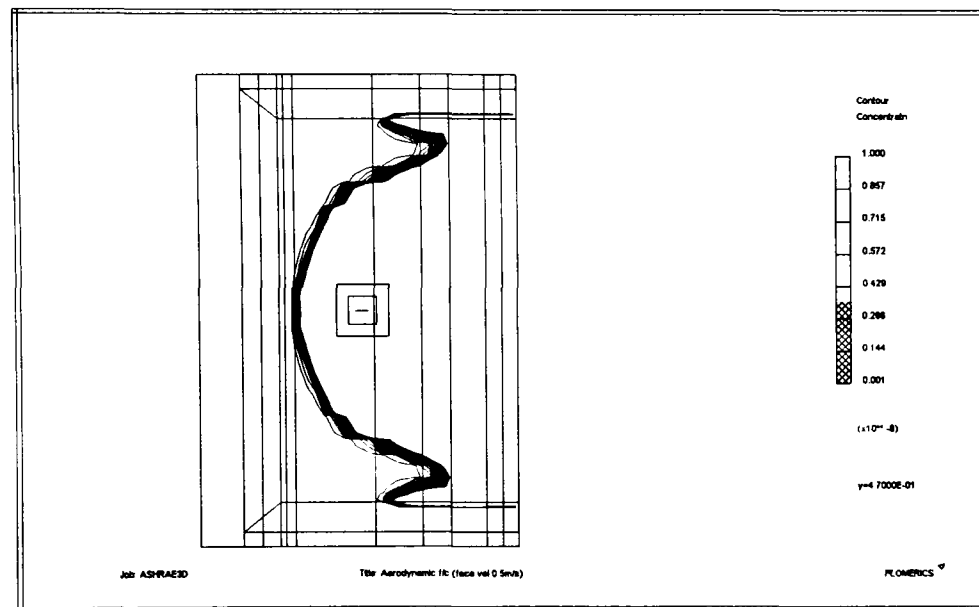
Figure 6.59 Position of ASHRAE 110 injector and solution grid, and airflow vectors in the xy plane, centreline of the source, in an aerodynamic fume cupboard (3 D).



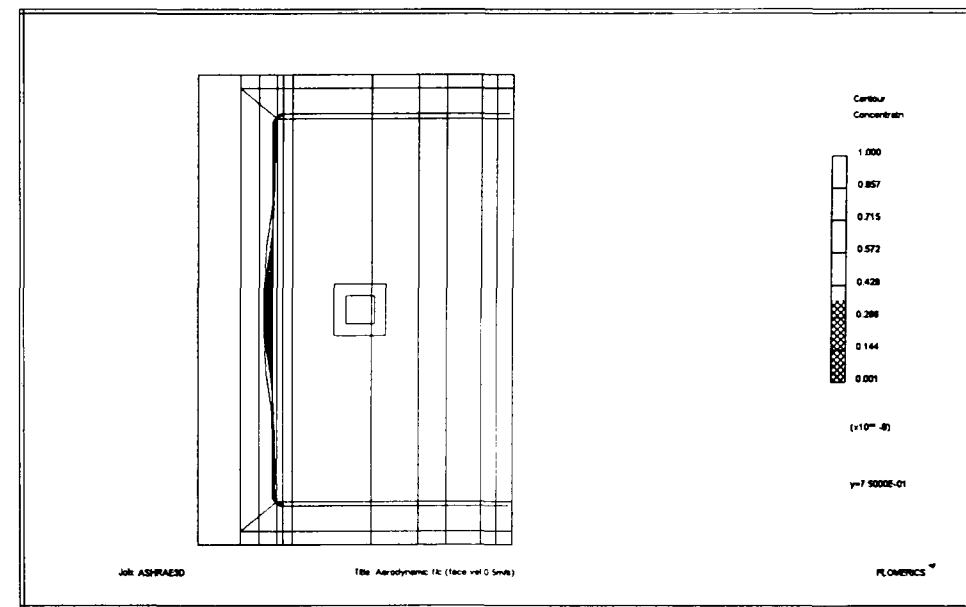
xy plane centre line of aperture width and source



xz plane near to the work surface

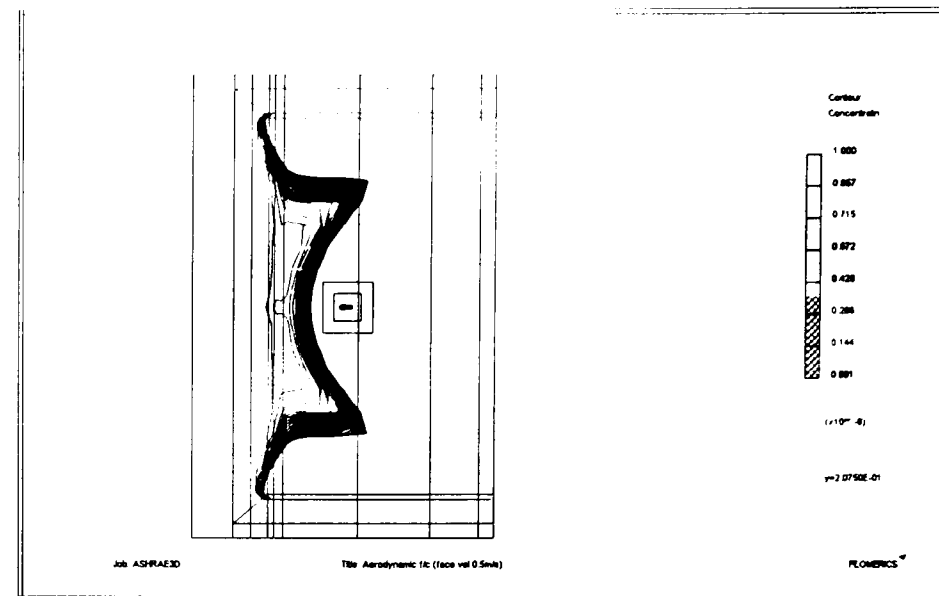
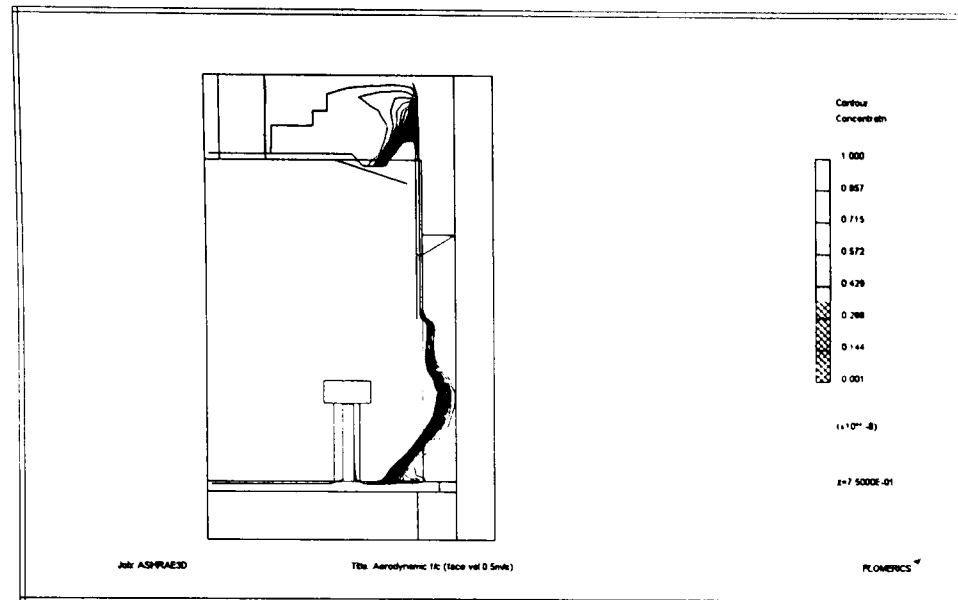


xz plane at mid aperture height



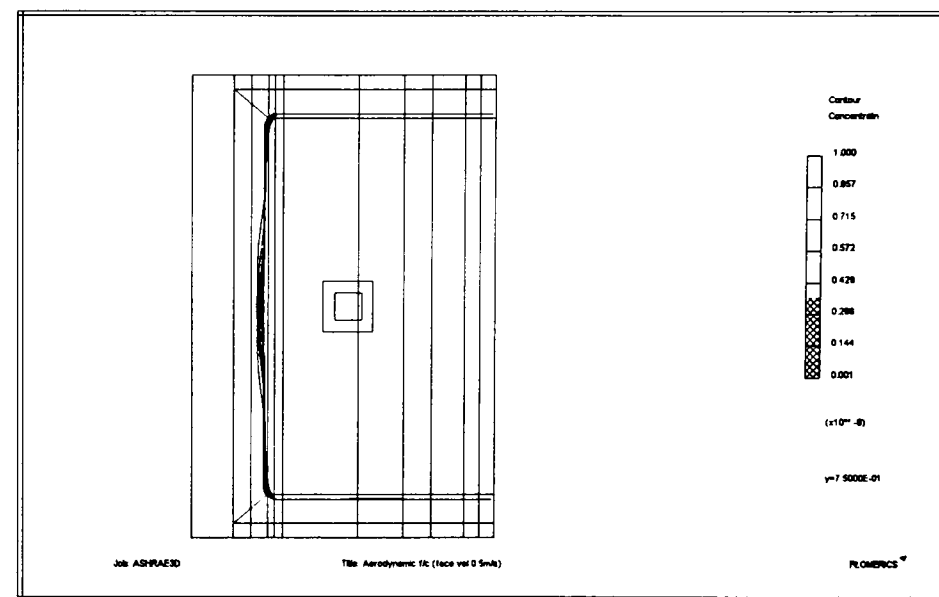
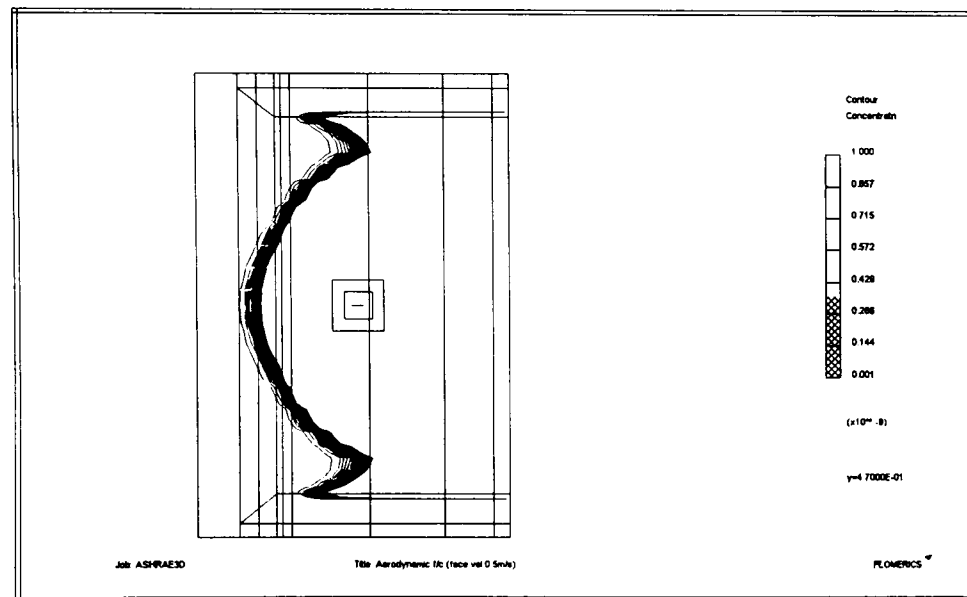
xz plane near sash

Figure 6.60 xy contour, centre line of source, and xz contours, near to the work surface, at mid aperture height and near to the sash, of tracer distribution when released from the central source positions (ASHRAE 110) within an aerodynamic fume cupboard (3 D).



xy plane centre line of aperture width and source

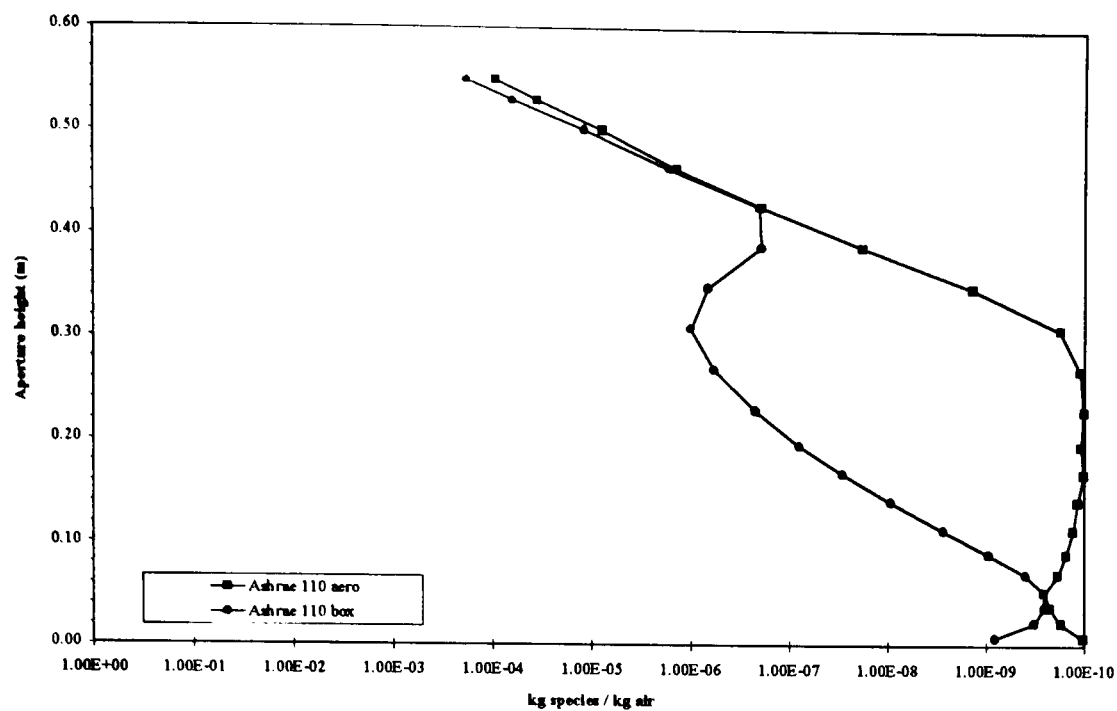
xz plane near to the work surface



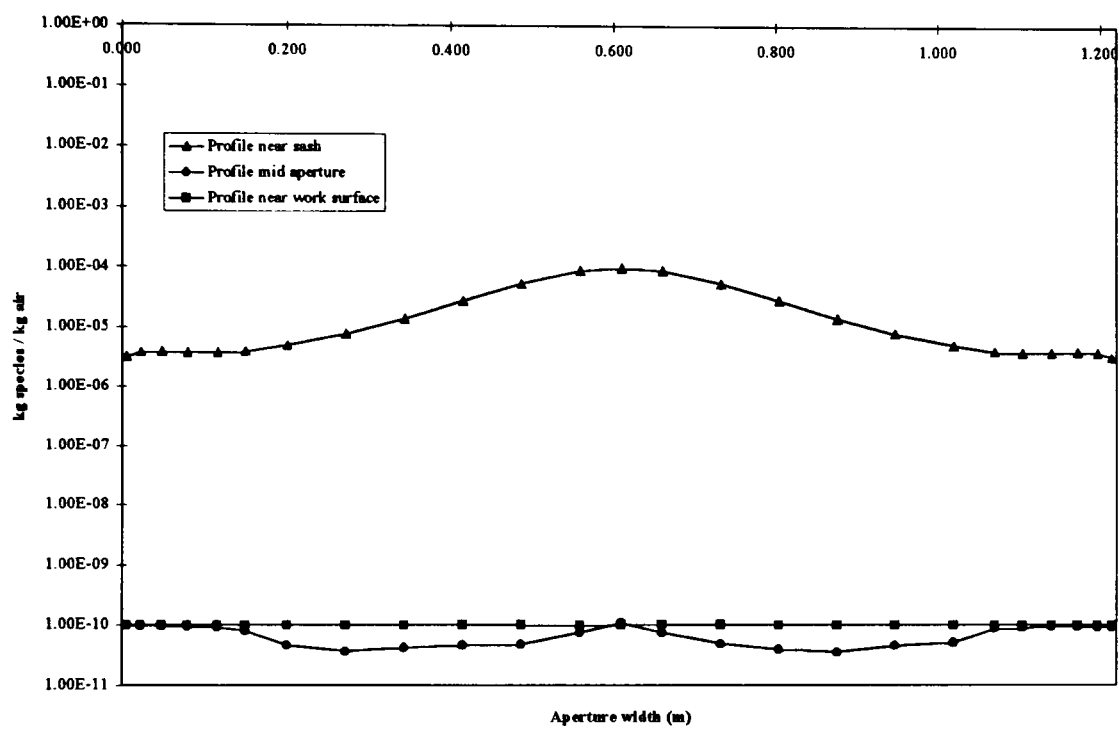
xz plane at mid aperture height

xz plane near sash

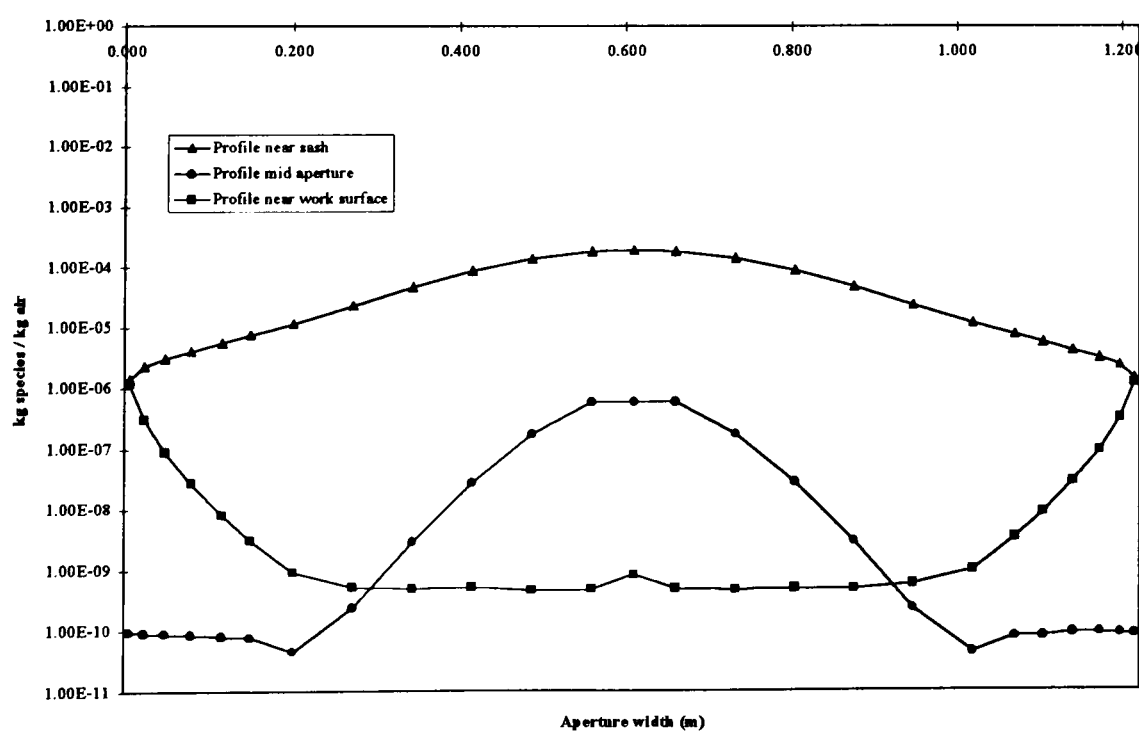
Figure 6.61 Effect of removing the rear baffle and lipfoil on xy and xz tracer contours when released from the central source positions (ASHRAE 110) within an aerodynamic fume cupboard (3 D).



xy profiles (centre line of aperture width)



xz profile for aerodynamic cupboard



xz profile for aerodynamic cupboard with no rear baffle or lipfoil

Figure 6.62 Effect of removing the rear baffle and lipfoil on tracer concentration profiles in the aperture plane, centreline of the source, and across the aperture plane, z direction, when released from the central source position (ASHRAE 110 : 1993) within an aerodynamic fume cupboard (3 D).

base. The release rate of 10%SF₆/90%N₂ tracer was 3.33 l/min per metre length of aperture width and as it passed through the base it entrained air to be discharged from the diffuser at 1 m/s with density near that of air. The plume was described in section 2.2.2 to be ~1 m/s near to the diffuser and then to drop rapidly with distance. From the dimensions the surface area of the diffuser was ~0.015 m² with estimated open area 50 % and the mass flow rate of tracer/air mix from this diffuser, at the density of air, was estimated to be 0.0076 kg/s. The estimated 10%SF₆/90%N₂ content was 0.000094 kg/s, 0.0145 kg_{tracer}/kg_{air}. In order to diffuse this planar source in 3 dimensions at discharge velocity 1 m/s to resemble the plume, a volume resistance was added above the source with the following settings:

	Loss coefficient	Free area ratio
x direction	2.0	0.2
y direction	1.7	0.5
z direction	2.0	0.2

As the tracer was well mixed with air and may be assumed to equal the density of the air when discharged the solution domain was fixed at a constant density of 1.19 kg/m³, and the ideal gas law was not used.

6.4.4.2 Simulations

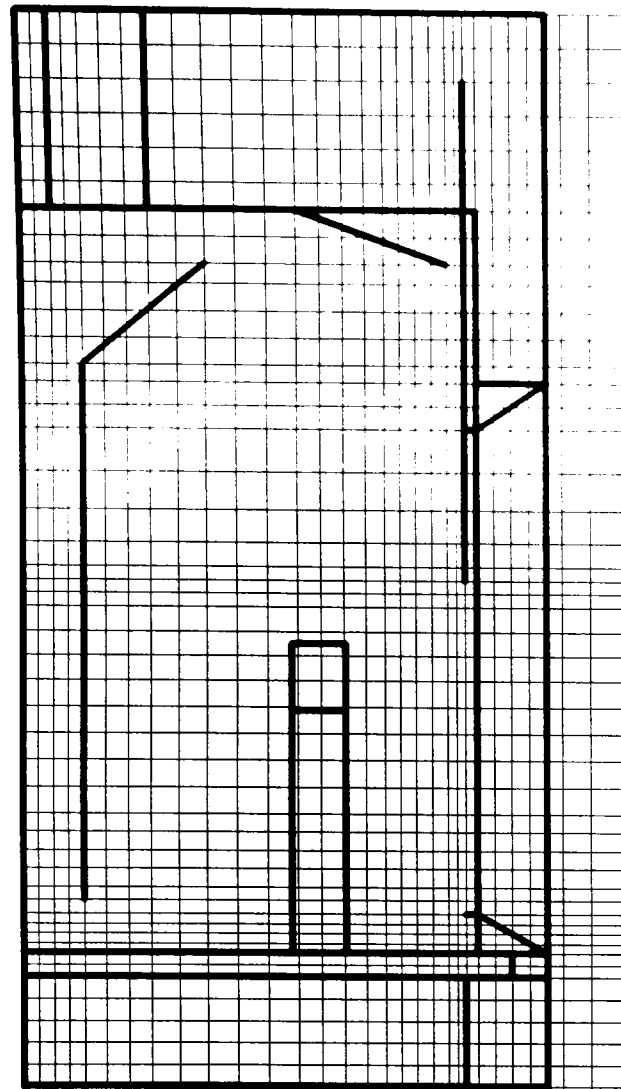
The air flow within the working volume was very much affected by the simulated DIN source (Fig. 6.63). This discharged air into the upper reaches of the working volume. This was reflected in the distribution of the tracer, it being greater in the upper levels with little down at the work surface (Fig. 6.64).

Profiles in the aperture plane for the aerodynamic fume cupboard showed negligible amounts at the work surface or at mid aperture height but, as with the other test methods, much greater concentration was near to the sash (Fig. 6.66).

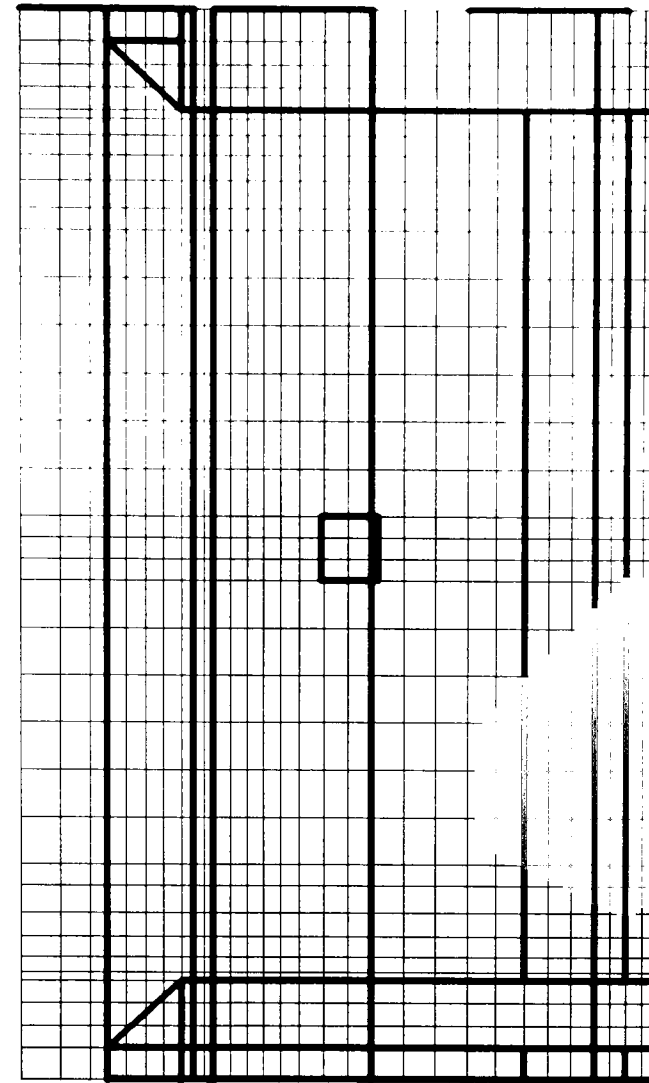
Removing the rear baffle and lipfoil was shown in earlier simulations to result in elevated levels of tracer in the aperture plane near to the work surface (Fig. 6.65 & 6.66). However, the simulation of the DIN source did not show this.

6.4.5 Effect of sash handle on test results (BS 7258)

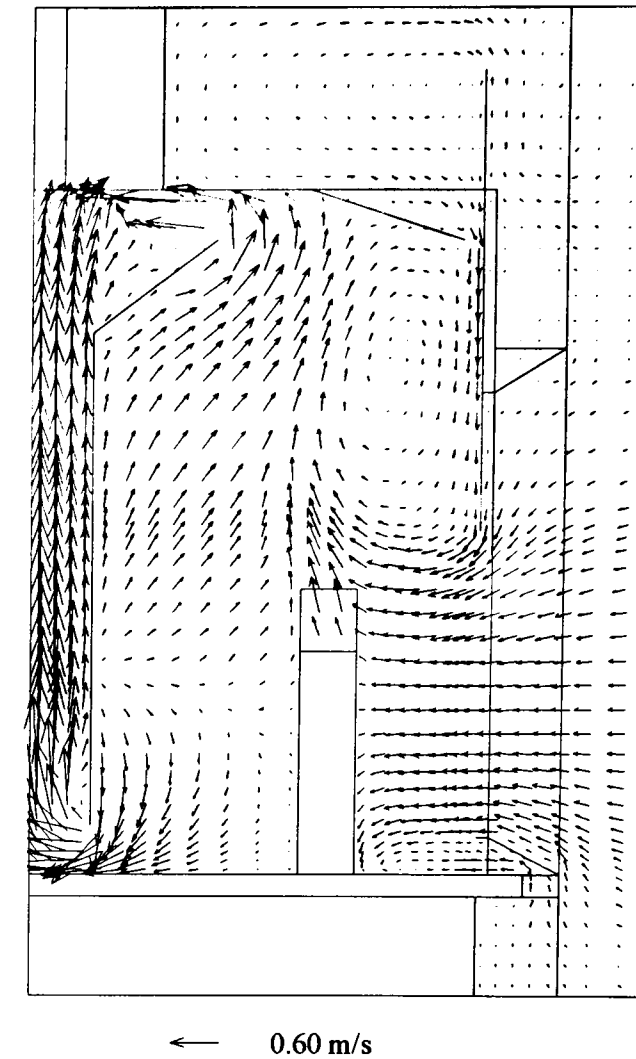
In each of the simulations it was shown there was much higher concentrations near to the sash in the aperture plane than the rest of the aperture. As no handle was or 'aerodynamic' feature was simulated here this was not unexpected. However, the representation of such a feature in terms of the whole model meant too complex a grid. In order to see the effect of a very crude design feature, an angled thin wall was added to the sash which had a trailing edge extending into the working volume. The solution grid was not altered.



xy plane of source and grids

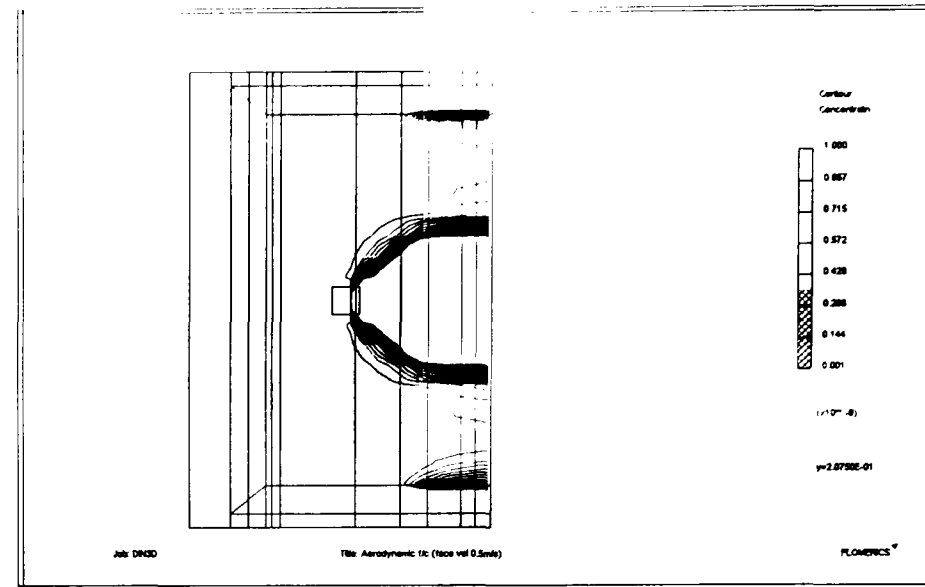
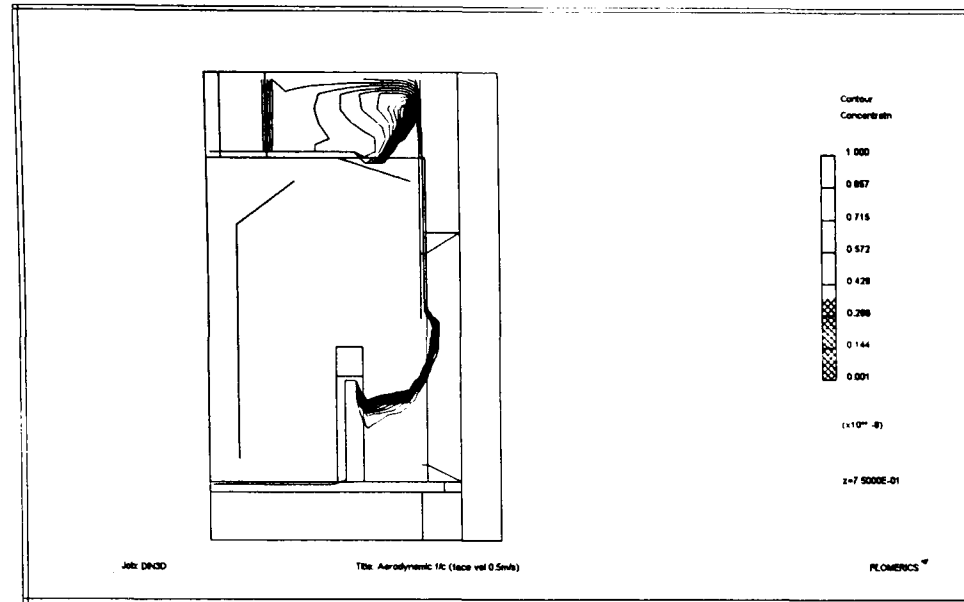


xz plane of source (source P2 and P5) and grids



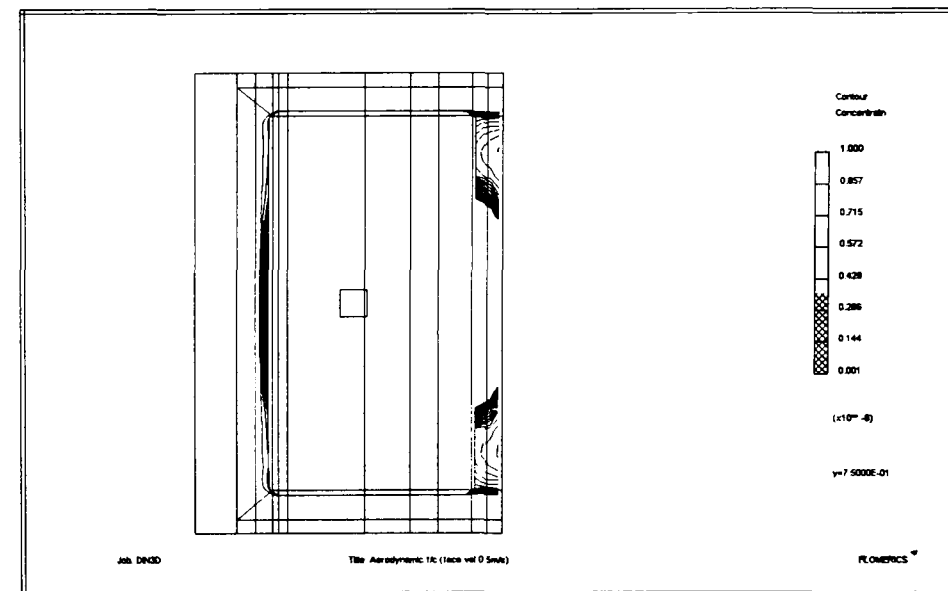
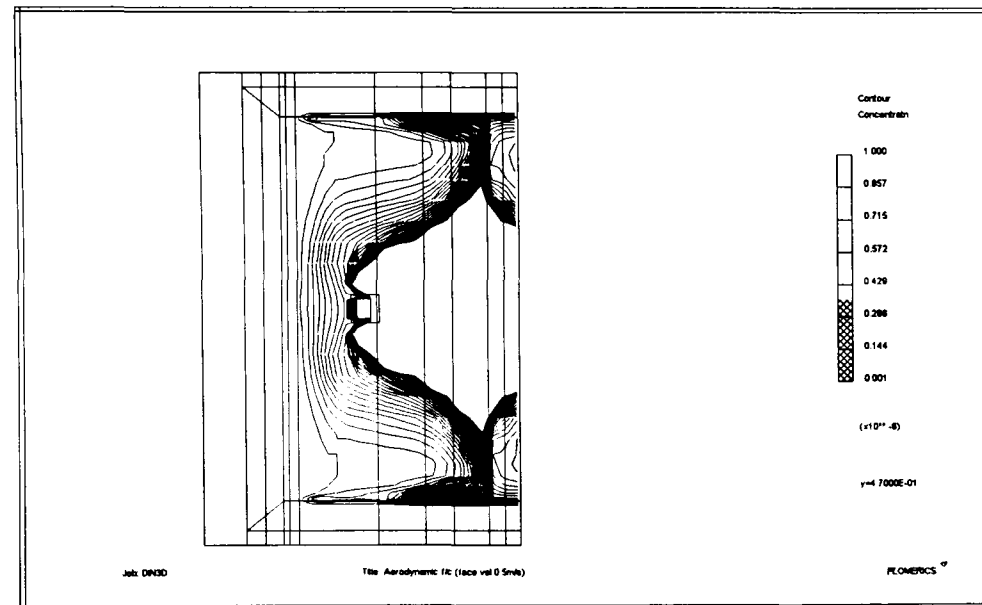
xy plane air flow vectors

Figure 6.63 Position of DIN 12 924 injector and solution grid, and airflow vectors in the xy plane, centreline of the source, in an aerodynamic fume cupboard (3 D).



xy plane centre line of aperture width and source

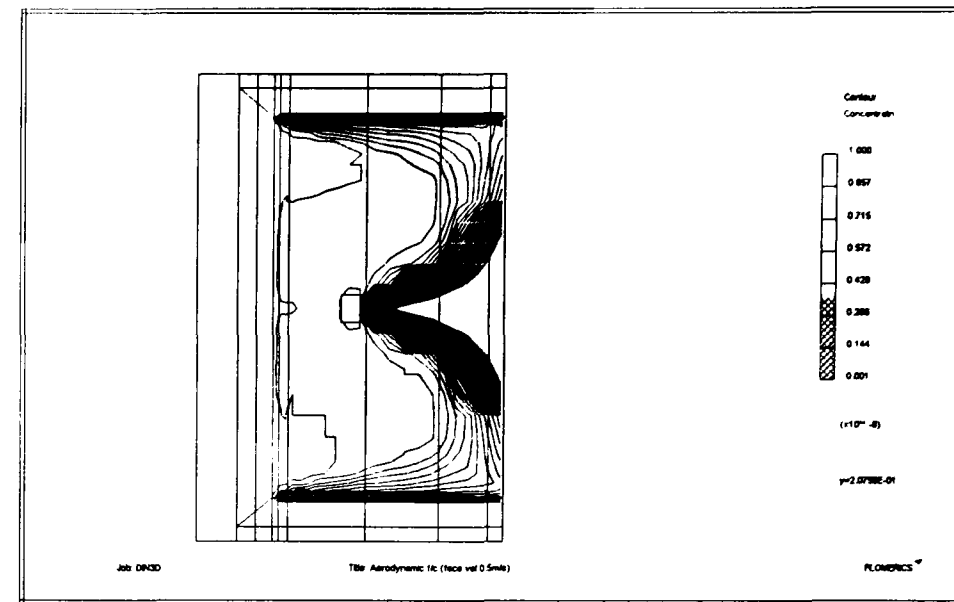
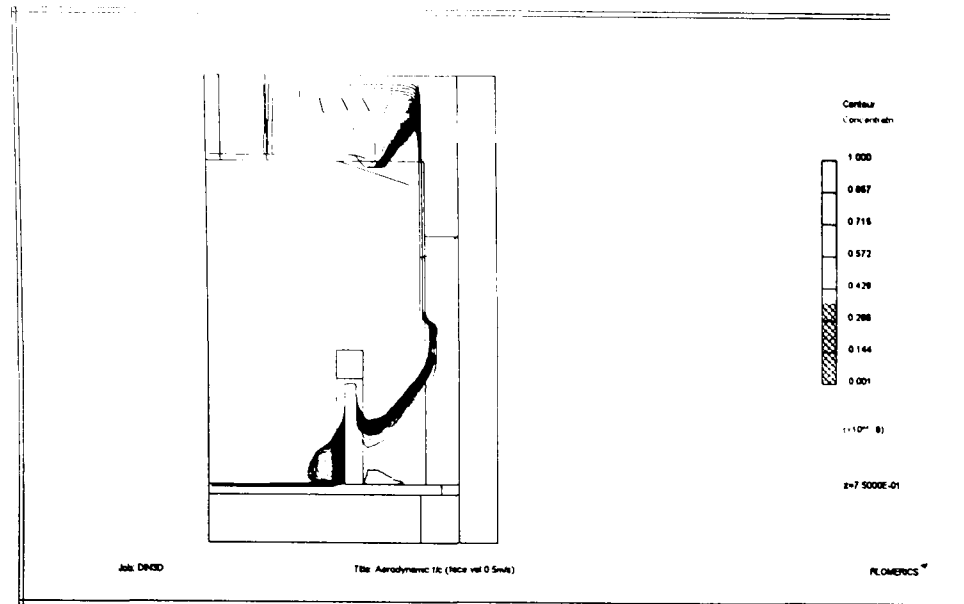
xz plane near to the work surface



xz plane at mid aperture height

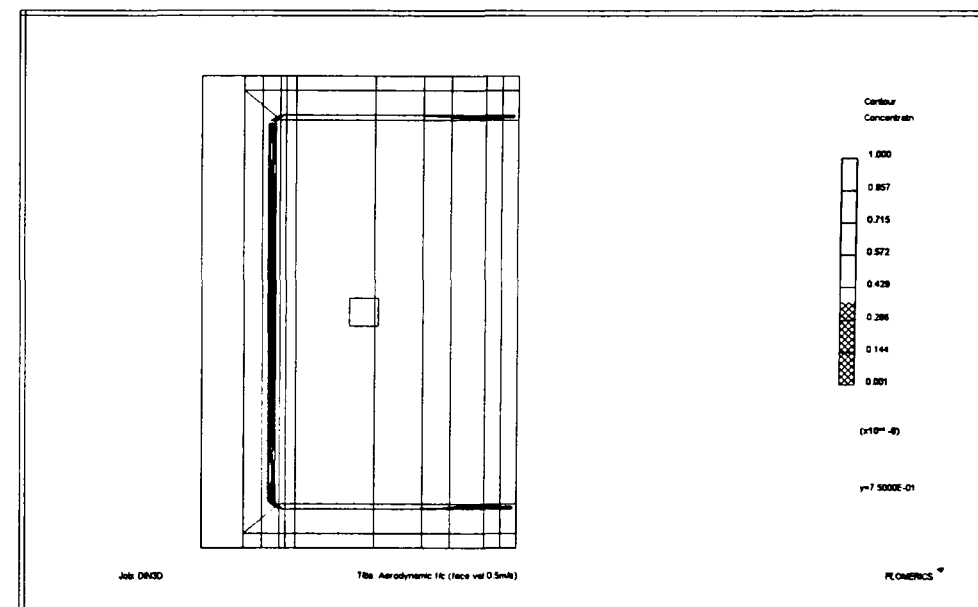
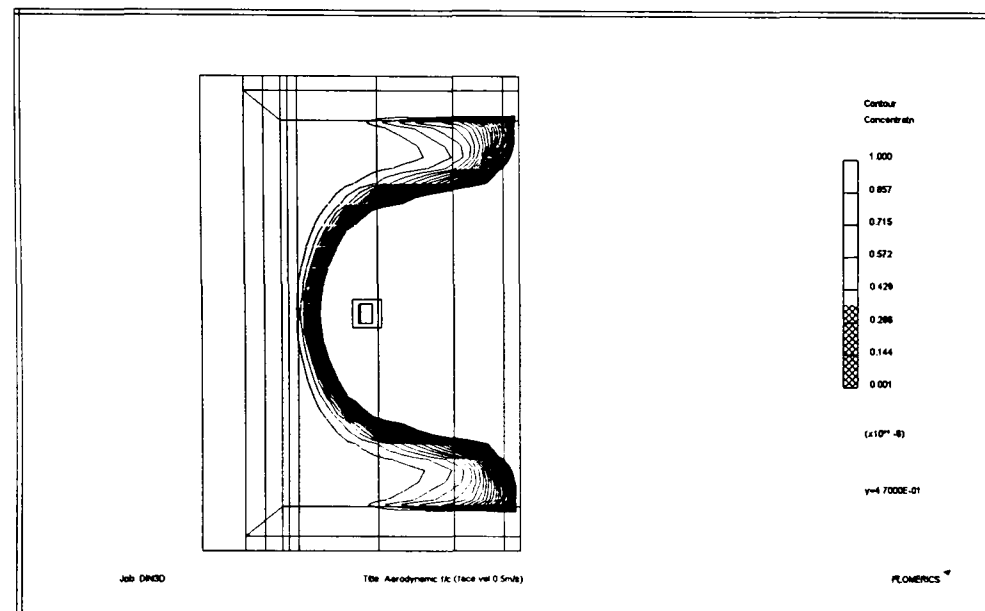
xz plane near sash

Figure 6.64 xy contour, centreline of source, and xz contours, near to the work surface, at mid aperture height and near to the sash, of tracer distribution when released from the DIN injector within an aerodynamic fume cupboard (3 D).



xy plane centre line of aperture width and source

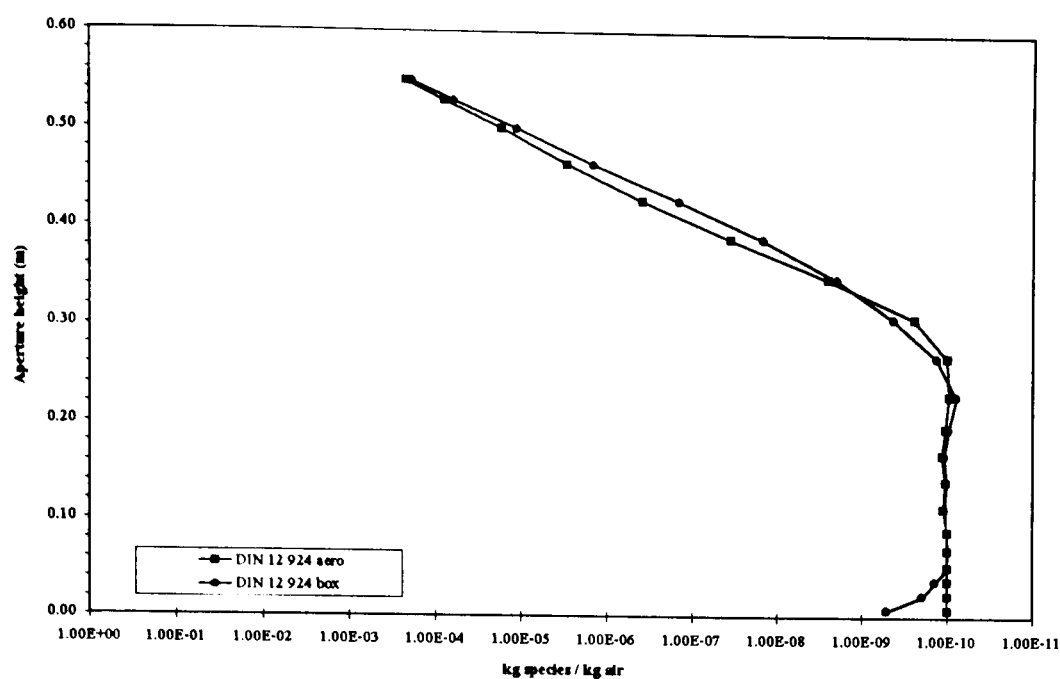
xz plane near to the work surface



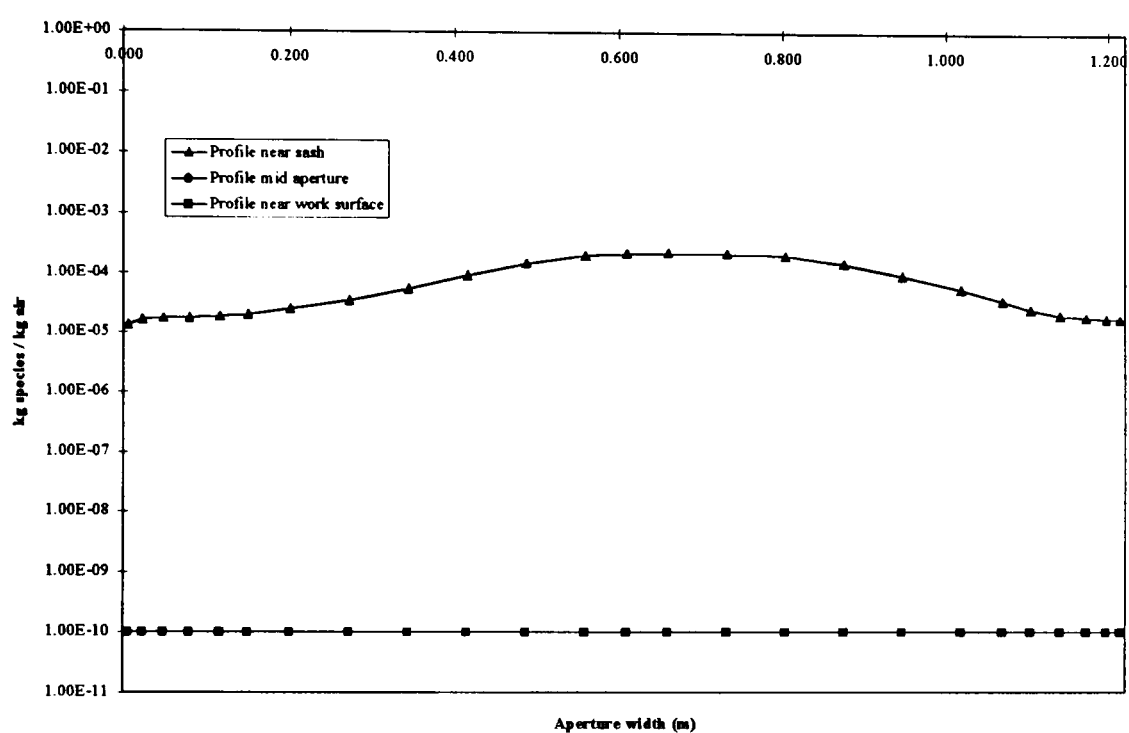
xz plane at mid aperture height

xz plane near sash

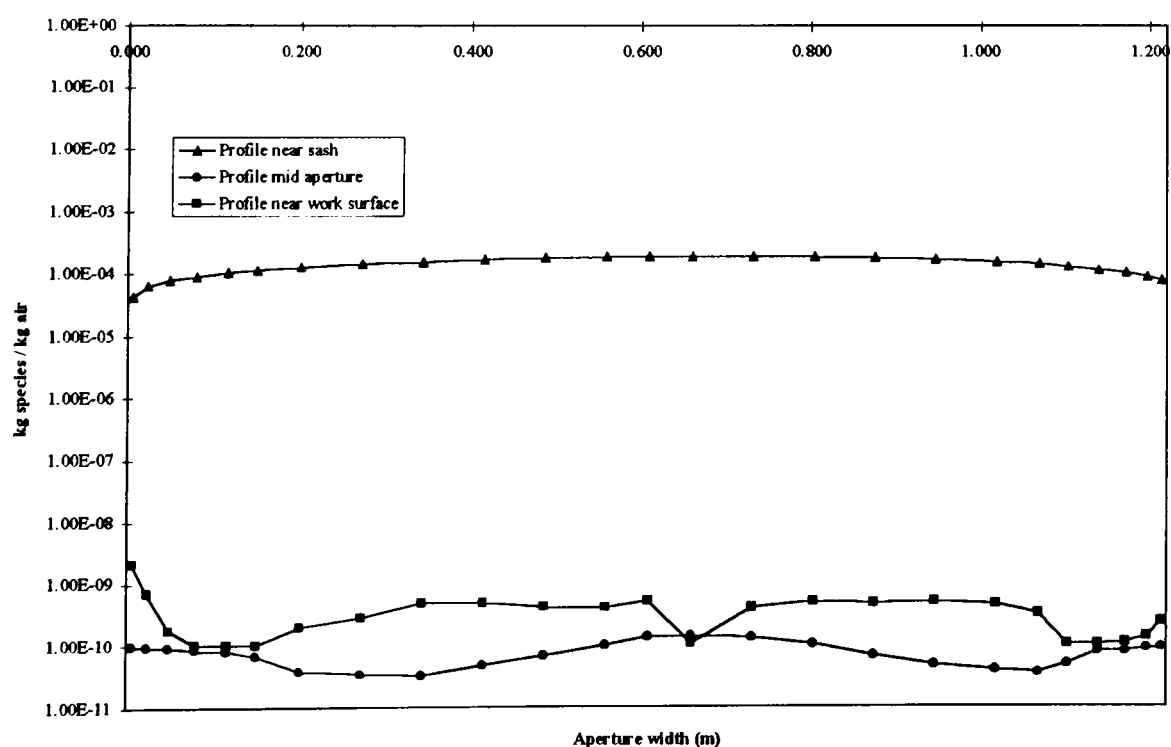
Figure 6.65 Effect of removing the rear baffle and lipfoil on xy and xz tracer contours when released from the DIN 12 924 injector within an aerodynamic fume cupboard (3 D).



xy profiles (centre line of aperture width)



xz profile for aerodynamic cupboard



xz profile for aerodynamic cupboard with no rear baffle or lipfoil

Figure 6.66 Effect of removing the rear baffle and lipfoil on tracer concentration profiles in the aperture plane, centreline of the source, and across the aperture plane, z direction, when released from the DIN 12 924 injector within an aerodynamic fume cupboard (3 D).

Using the BS 7258 source, the presence of this feature decreased the concentration of tracer in the plane of the aperture near to the sash, and was similar to the rest of the aperture plane (Fig. 6.67).

6.4.6 Discussion and comparison of test methods

The BS and ASHRAE simulations produced similar results. The DIN simulation did not result in tracer being dispersed near to the work surface and thus did not show recirculation of air from the working volume of the cupboard back to the aperture plane in this region. This had already been demonstrated by physical measurements (Fletcher, 1992) where it was commented that the DIN source challenged the region near to the sash but not near to the work surface, whereas the BS source, being moved around the aperture challenged all areas.

The concentration of tracer in the plane of the sash was around the maximum sensitivity of physical instruments, 1 ppb. If these simulations were compared to physical measurements, then for the aerodynamic cupboards no tracer would be sampled in the plane of the sash near to the work surface and mid aperture. It would sample and detect tracer near to the sash. However with the sash handle fitted no tracer would be detected in the entire aperture plane. This is what would be expected in reality. On removing the rear baffle and the lipfoil the concentration of tracer was greater in the aperture plane and these levels would be sampled and detected by the physical instruments, as would be expected, indicating poor design.

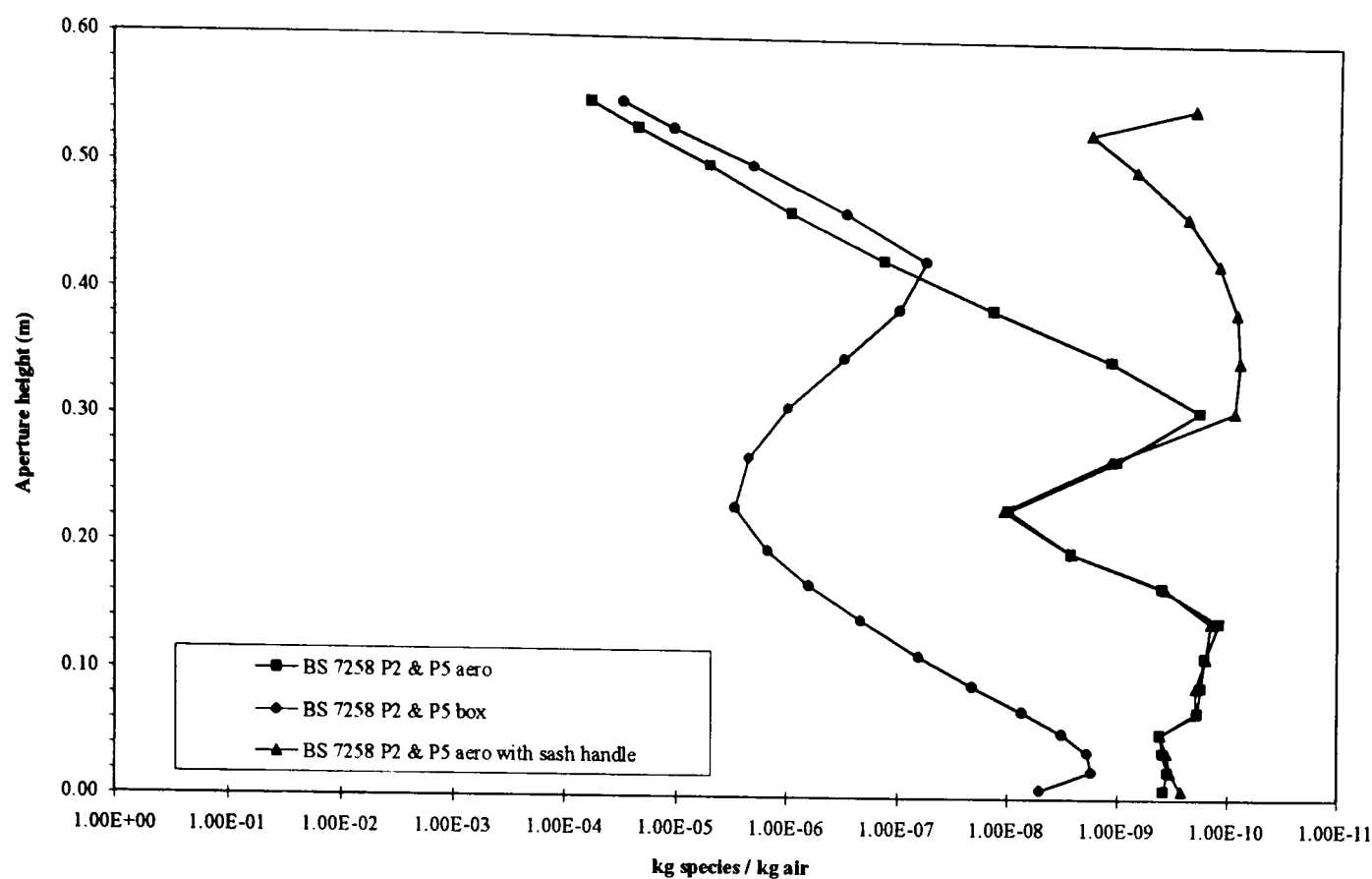
This would suggest that the CFD model was more sensitive than the physical measurements and could clearly distinguish between cupboard designs if poor or good. It could also be used to compare the stability of cupboard designs when disturbed by blockage or cross flows.

The 3 dimensional model gave better results than the two dimensional model. However, it took much longer, over two days to resolve. This is also important in terms of a test and is much longer than the time taken to conduct a physical test, which generally take one hour. However, a more powerful PC would enable the generation of results quicker.

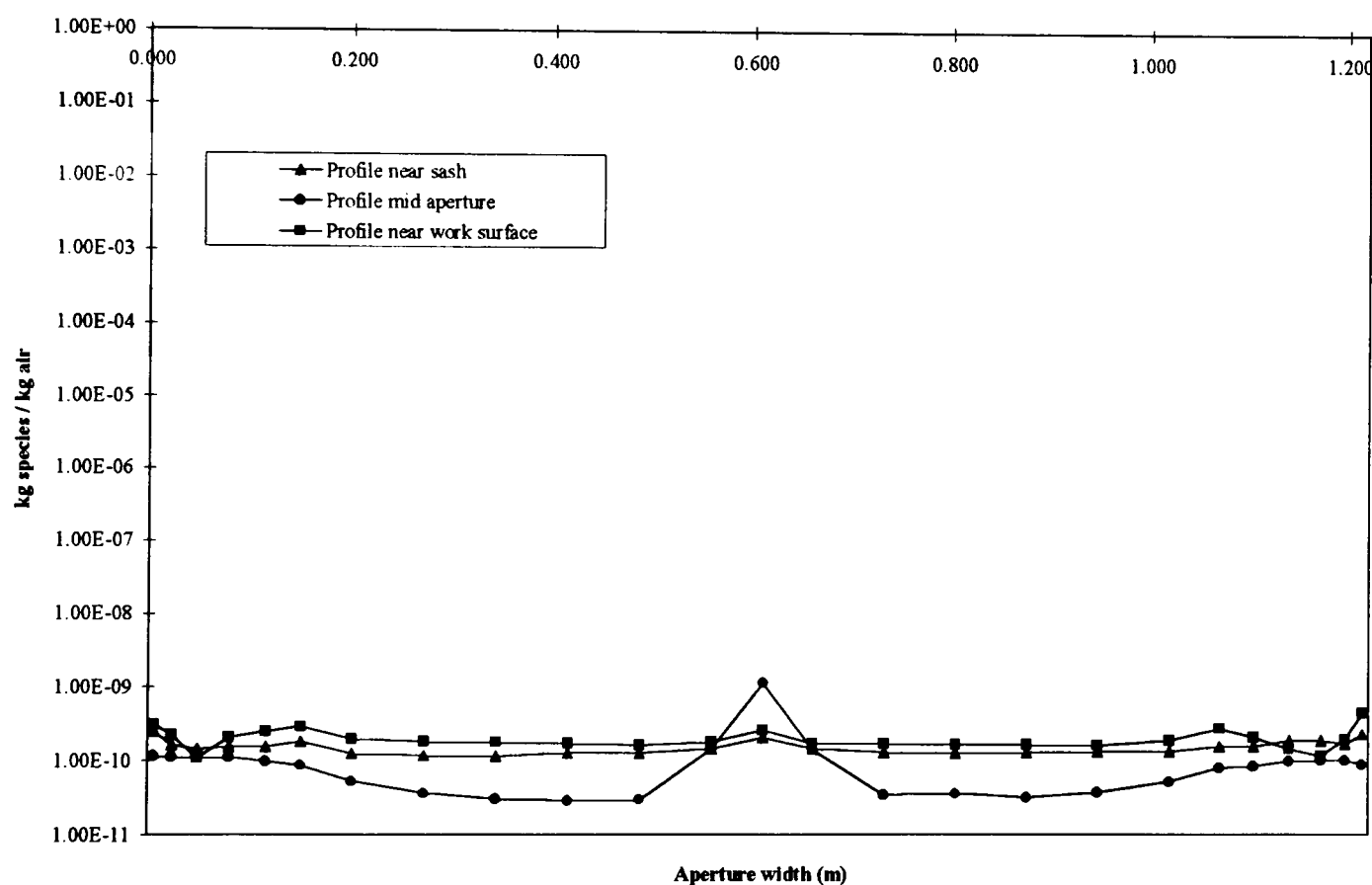
6.5 Two - dimensional visualisation and analysis of airflows in microbiological safety cabinets

6.5.1 Problem set-up

2 dimensional CFD models were used to provide qualitative and quantitative analysis of air flow within class I and class II microbiological safety cabinets. These simulations were adiabatic and had smooth surfaces.



xy profiles (centre line of aperture width)



xz profile for aerodynamic cupboard with no rear baffle or lipfoil

Figure 6.67 Effect of a sah handle on tracer concentration profiles in the aperture plane, centreline of the source, and across the aperture plane, z direction, when released from positions P2 and P5 (BS 7258 : 1994 : Part 4) within an aerodynamic fume cupboard (3 D).

6.5.2 Class I cabinets: Simulation of air flow

The major difference between the class I safety cabinet (section 2.3) and a box type fume cupboard was the size of the aperture which was smaller, narrower and with a fixed height. However little was done to smooth out the air flow into and within the cabinet which resembled those into and within the box fume cupboard. There was turbulence and recirculation of air passed the entry corners of the aperture and no scavenging of the work surface.

This was demonstrated using the CFD model of a class I cabinet with a sloping sash and front lip and with an average face velocity of 1 m/s. There were recirculation zones of air behind the sash and behind the front lip (Fig. 6.68). Air also moved from the back of the work surface to the region behind the lip. This showed that air near to the work surface flowed back towards the aperture. This was also shown by water fog visualisation.

The design of the lower lip resulted in air flowing normal to the direction of flow through the aperture, much the same as air flow past the sash of a fume cupboard. The absence of this lip resulted in air flowing right up to the edge of the work surface (Fig. 6.68)

6.5.3 Class II cabinets: Effect of design and balance on overall flow patterns

The air flow in class II cabinets (section 2.3) was much more complex than a class I cabinet. In a class II cabinet there was a downward flow of air over the work surface and an inflow of air through the front aperture. The balance of these air flows was critical in order to obtain satisfactory operator and product protection. Early work involved both physical and mathematical analysis to get the balance right (McDade et. al., 1968; Akers et. al. 1969).

The use of the 2 dimensional CFD model of a typical class II safety cabinet to visualise the air flow (Fig. 6.69) showed how the balance could be varied between downflow and inflow velocity and the effect on operator and product protection. In a balanced simulation as specified within BS 5726 : 1992 : Part 1 (downflow 0.5 m/s, inflow 0.7 m/s) the x velocity and speed in the plane 100 mm above the lower edge of the sash showed a 10 % deviation at the back and front of the working volume from the average downflow of air; 20 % from front to back. Decreasing the inflow velocity to 0.2 m/s resulted in an x velocity and speed profile 100 mm above the sash edge that was much straighter from front to back of the cabinet interior with little deviation from the average. Increasing the inflow velocity to 1 m/s resulted in the a similar x velocity and speed profile from the front to back of the working volume 100 mm from the sash edge as with an inflow velocity of 0.5 m/s. However at 1 m/s inflow velocity the airflow encroached over the work surface. At a distance of 30 mm from the downflow supply, the profiles were straight for each simulation.

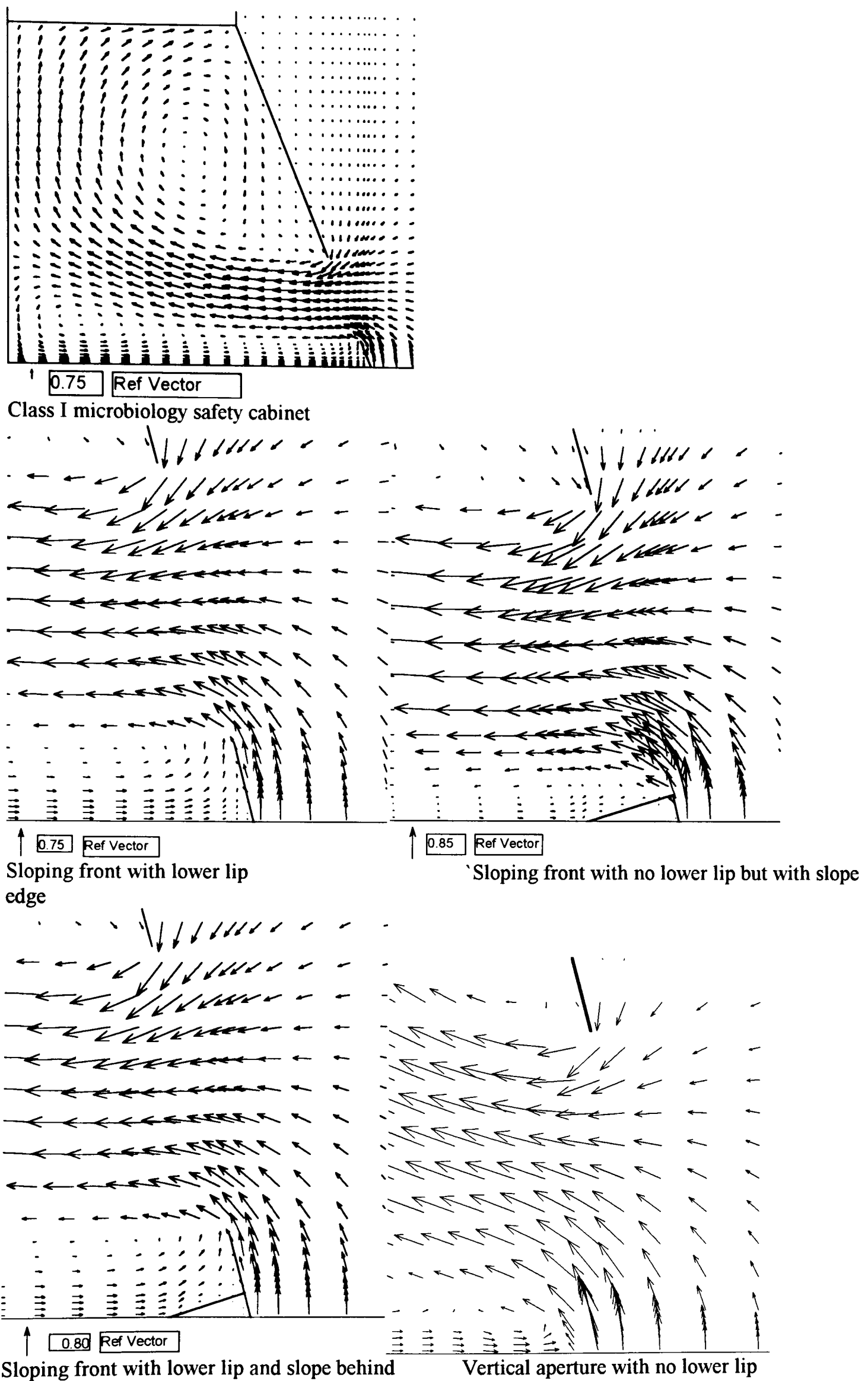
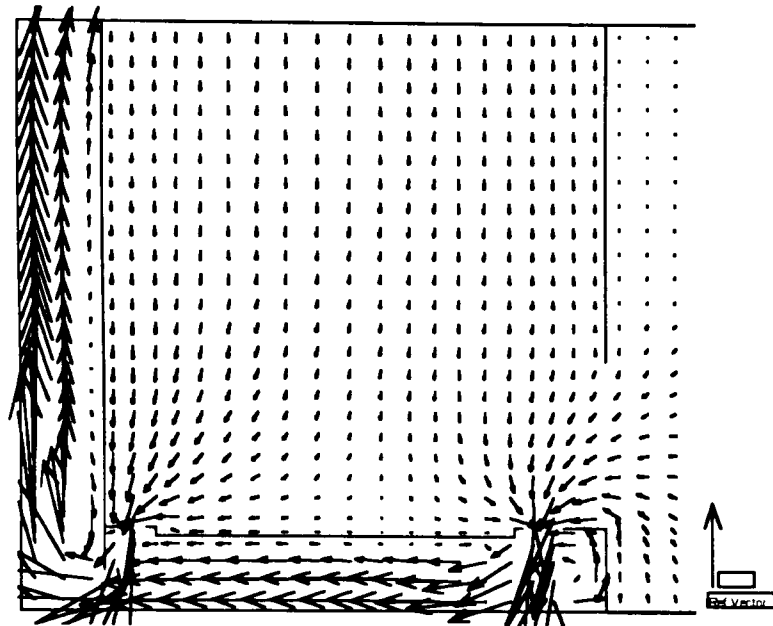
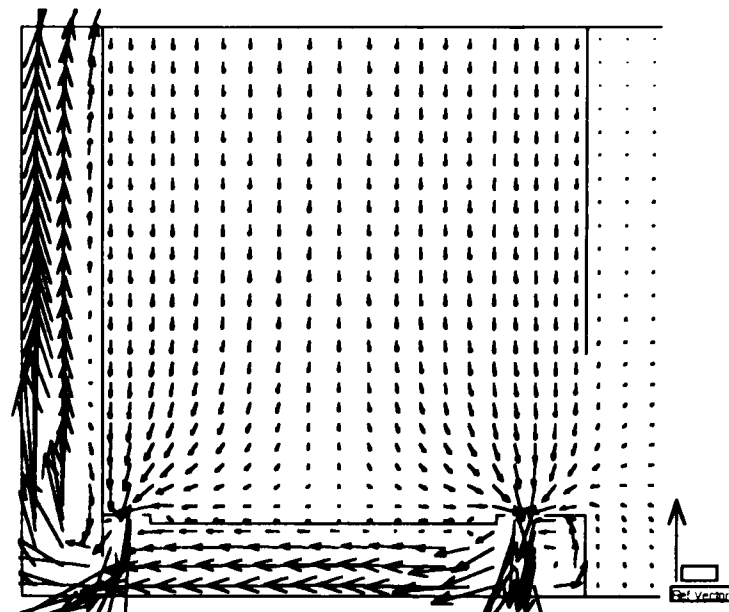


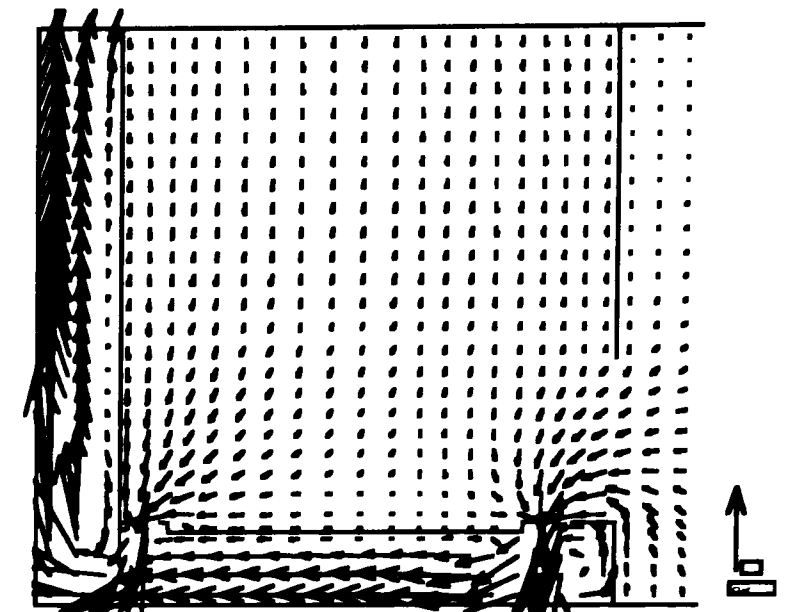
Figure 6.68 Airflow vectors within a class I microbiological safety cabinet with different front lip design (2 D).



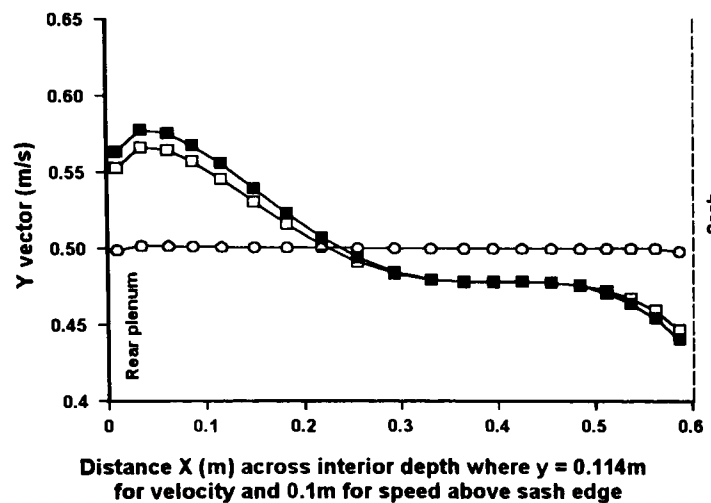
CFD simulated velocity vectors for class II cabinet with downflow 0.5 m/s, inflow 0.7 m/s within specified limits.



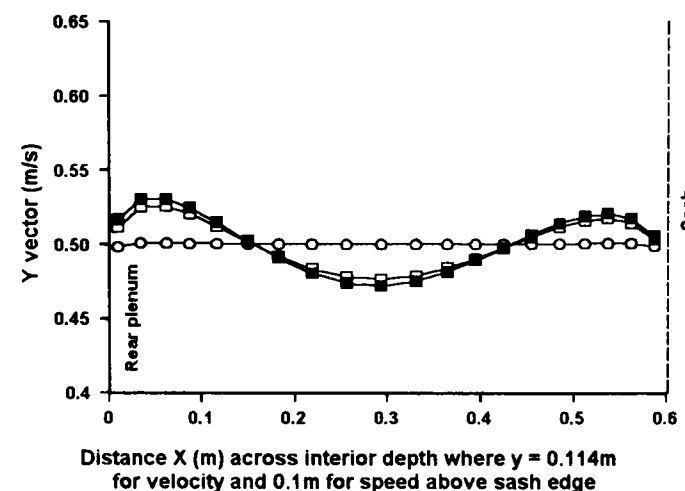
CFD simulated velocity vectors for class II cabinet with imbalanced downflow 0.5 m/s, inflow 0.2 m/s.



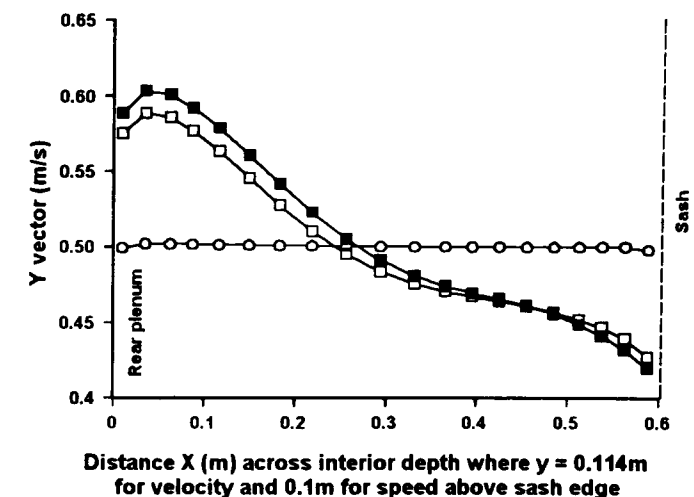
CFD simulated velocity vectors for class II cabinet with imbalanced downflow 0.5 m/s, inflow 1.0 m/s.



Plot of y (vertical) velocity (open) and speed (closed) across a class II cabinet interior 100 mm above the edge of the sash \square , and 30 mm below the supply \circ . Airflows: downflow 0.5 m/s, inflow 0.7 m/s.



Plot of y (vertical) velocity (open) and speed (closed) across a class II cabinet interior 100 mm above the edge of the sash \square , and 30 mm below the supply \circ . Airflows: downflow 0.5 m/s, inflow 0.2 m/s.



Plot of y (vertical) velocity (open) and speed (closed) across a class II cabinet interior 100 mm above the edge of the sash \square , and 30 mm below the supply \circ . Airflows: downflow 0.5 m/s, inflow 1.0 m/s.

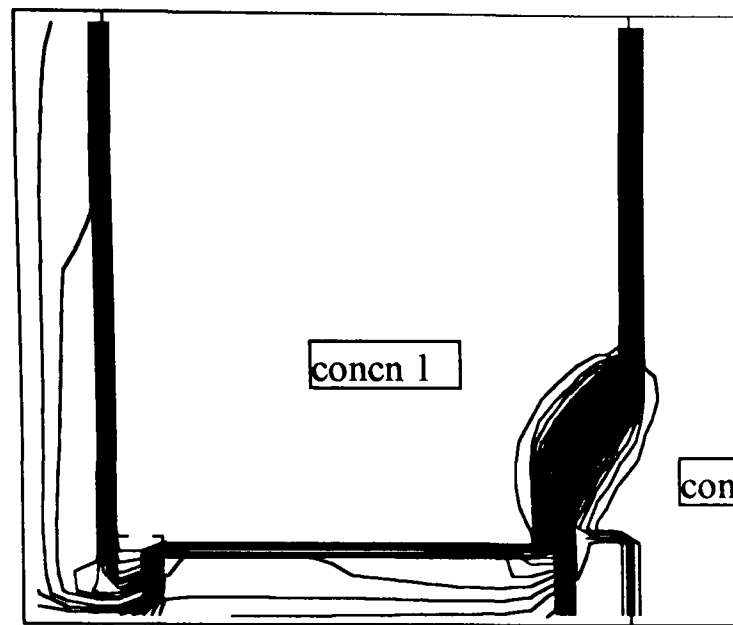
Figure 6.69 The effect of inflow and downflow balance on the airflow vectors and horizontal profiles of x velocity and speed within a class II microbiological safety cabinet (2 D).

A 'tracer gas' was specified as a planar source covering the roof of the cabinet and mixed with the supply air at a ratio of $1 \text{ kg}_{\text{species}}/\text{kg}_{\text{air}}$ for each of the simulations (Fig. 6.70). Using the balanced flow simulation as the base model to which the other simulations could be compared, at a lower inflow velocity (0.2 m/s) greater concentration of tracer was calculated beyond the aperture plane in the room and at the higher inflow velocity (1 m/s), lower concentrations of tracer were calculated over the work surface. Releasing the 'tracer gas' outside the cabinet as a planar source over the opening to the solution domain showed greater concentrations over the work surface for the higher inflow velocity and lower concentrations at the lower inflow velocity.

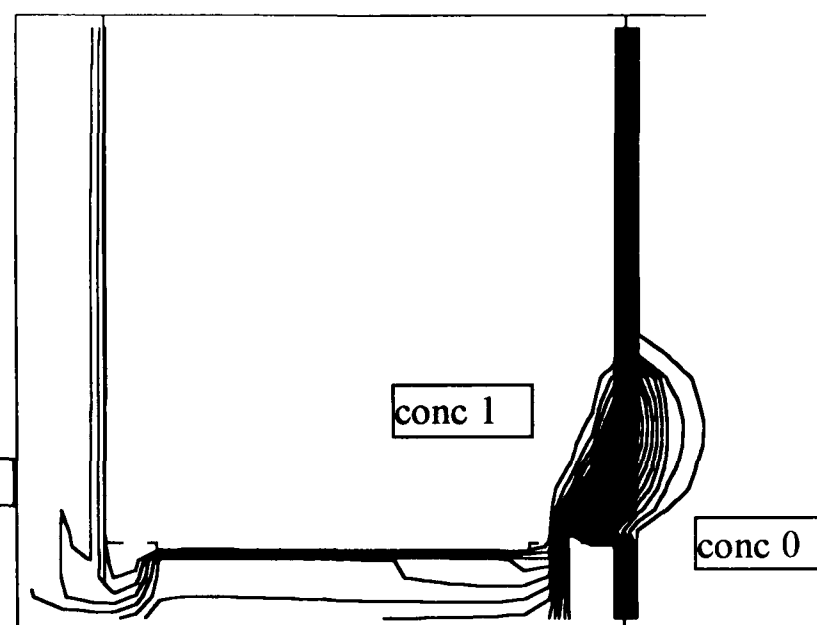
These simple simulations thus showed that for the design of cabinet modelled the inflow and downflow velocities specified in the British Standard were about right and that the model was capable of showing the effect of imbalances.

6.6 Key interim conclusions

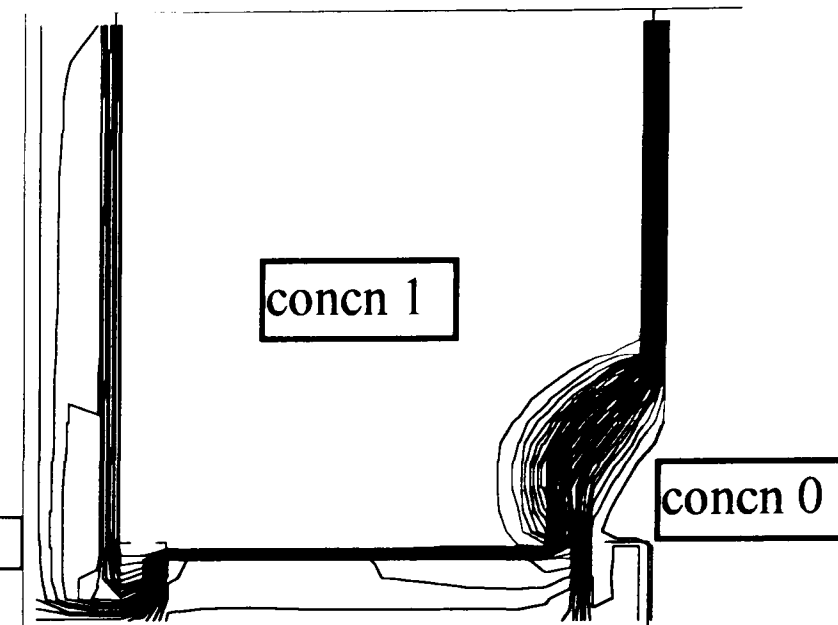
- The Flovent CFD software programme, with its graphical user interface and specific approach to HVAC systems, was simple to input data and boundary conditions. In order to correctly interpret and analyse the results, the user must have a basic understanding of HVAC systems, CFD techniques and its limitations.
- Open fronted containment system simulations showed the relative effect of design features on the overall flow pattern and containment. It clearly distinguished between good and bad designs, comparing well with physical measurements.
- The CFD model was used to compare the stability of fume cupboard designs when subjected to blockage or environmental disturbances. The model could be challenged to see how it performed when installed in normal workplace conditions.



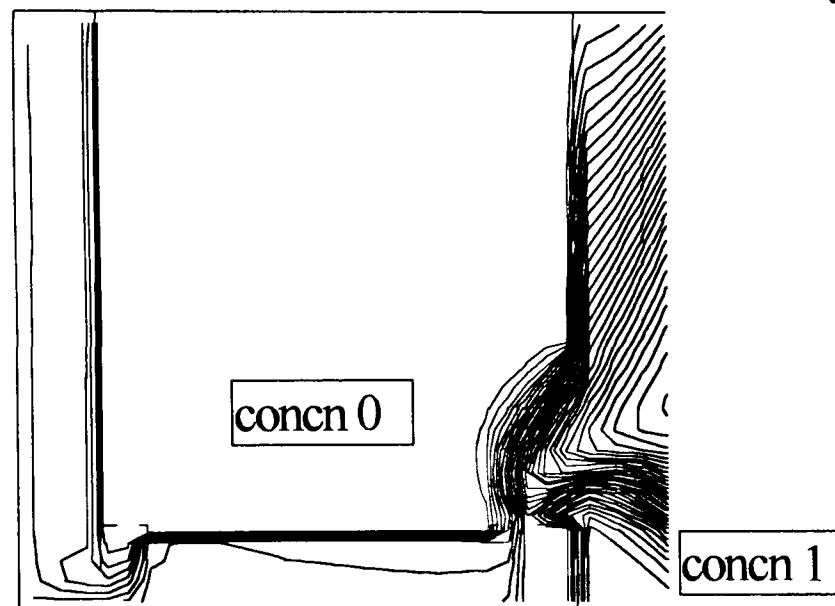
CFD simulation of concentration when released with downflow 0.5 m/s, inflow 0.7 m/s within specified limits.



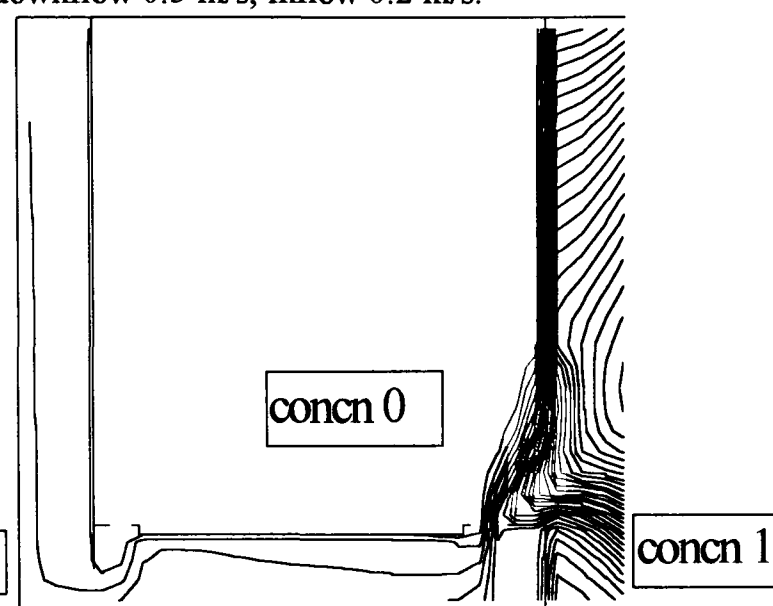
CFD simulation of concentration when released with downflow supply in imbalanced imbalanced downflow 0.5 m/s, inflow 0.2 m/s.



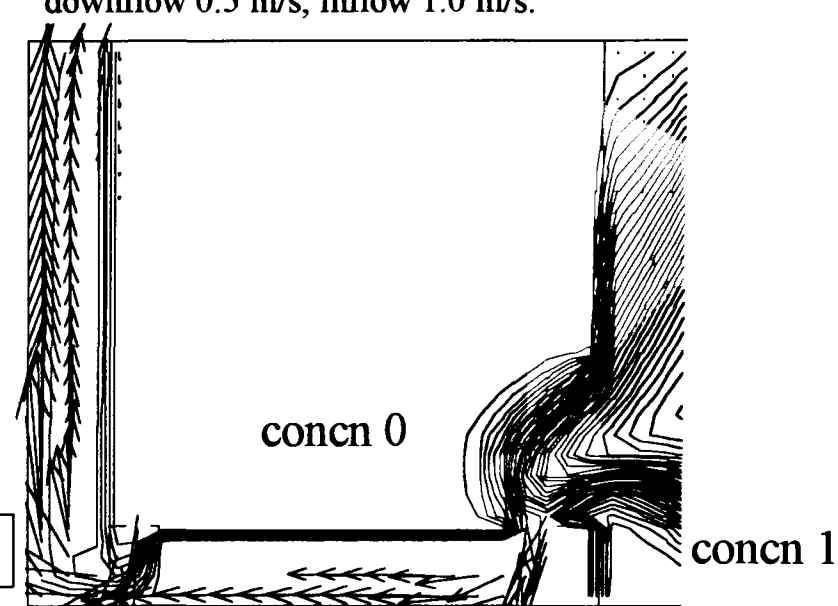
CFD simulation of concentration when released with downflow supply in imbalanced imbalanced downflow 0.5 m/s, inflow 1.0 m/s.



CFD simulation of concentration when released outside the cabinet. Cabinet airflows; downflow 0.5 m/s, inflow 0.7 m/s, within specified limits



CFD simulation of concentration when released outside the cabinet. Cabinet airflows; downflow 0.5 m/s, inflow 0.2 m/s.



CFD simulation of concentration when released outside the cabinet. Cabinet airflows; downflow 0.5 m/s, inflow 1.0 m/s.

Figure 6.70 Effect of airflow balance on the tracer contours within a class II cabinet when released with the downflow supply and when released outside the cabinet (2 D).

Chapter 7 Aerobiological performance assessment of a hospital burns unit

7.1 Introduction

In Chapters 3, 4 and 5 the use of gas and particle tracer methods for the physical measurement of the performance of open fronted containment systems was assessed. In Chapter 6 the application of computational fluid dynamics to the performance assessment of these open fronted containment systems was also investigated. In this Chapter, all these methods are combined to assess a complex containment system for preventing cross-infection in a hospital. The importance of each method for assessing the performance of the ventilation system of a burns unit is investigated and how each method compares for predicting and analysing design changes and remedies to apparent problems. These methods are also compared with the strategies currently used for assessing the performance of operating theatres and ultra clean ventilation systems (viz. by collecting and counting airborne bacteria). In addition, airborne particle counts are made which is a strategy used for assessing clean rooms. There is much similarity between the operation of an operating theatre and a clean room and correlation's have been made (Seal & Clark, 1990). Counting particles in both cleanrooms and operating theatres for assessing performance is included in the Australian National Standard (AS 1386, 1989).

7.2 Historical

The use of ventilation in the operating theatre and intensive care room was needed to control the environment in terms of temperature and humidity, thus ensuring the comfort of the operating team and patient, and the level of suspended matter, in order to minimise or prevent contamination of the wound by the airborne route (Lidwell, 1984).

The ventilation principles used ranged from general ventilation to the advanced concepts of cleanroom technology, depending on the level of surgery or intensive care required. The early operating theatres used general ventilation (Faircliff, 1984) with sufficient air to provide comfortable conditions with respect to temperature and humidity, to dilute the bacteria dispersed by personnel in the operating room, dilute the bacteria in areas adjacent to the operating room and provide control of air movement to ensure minimum transfer of bacteria carrying particles from the adjacent rooms into the operating room.

These conventionally ventilated rooms were improved by using air handling systems to filter the air to remove particles above 5 μm and to distribute the air in a substantially vertical direction over the operating site and sterile instruments (non-laminar flow). Such systems reduced the level of macro-turbulence and increased the dilution of suspended matter at the operating site using the standard supply air volume. This form of ventilation was shown to limit airborne bacteria carrying particles to between 100 - 500 bcp/m³ at the wound site which

was a level compatible with good healing of the soft tissue wounds which were made in the course of general surgical operations. The air velocity in the room was low and room air changes around 20 changes/hr.

This level of airborne contamination was unacceptable for certain types of surgery including orthopaedic prosthesis implant and open heart surgery, and in the intensive care of patients with severe burns where a small degree of contamination could progress to widespread infection. In operations involving cartilage covered joint surfaces or a metallic prosthesis there was no inherent resistance to infection and any bacterial contaminants tended to multiply rapidly. Burn wounds were moist and had protein rich exudate as an ideal medium for bacterial growth but contained no antibacterial factors. In order to prevent wound sepsis clean filtered air had to be provided at the operating zone and in a fashion to minimise the entrainment of organisms from the operating team and to lessen the risk of infectious particles and other suspended matter entering the wound. In these cases the principles of spot protection in cleanrooms using laminar or unidirectional air flow were used and modified.

HEPA filtered air was introduced into the room from a partial surface, i.e. a large area of wall (cross flow), or from ceiling diffusers (vertical flow). This then flowed over the critical zone in a well-defined direction and was exhausted from regions in the room outside this zone. The size of the critical zone had to be large enough to encompass the patient, the table and the instruments. With such systems, as the inlet air was only from a partial area of a surface or wall, the entrainment of air from the peripheral room areas into the clean zone became an important risk factor. There were various methods employed to protect against it which included:

- Curtains of sufficient length at the border of the flow area which extended well below the table or bed to form a canopy.
- A partial canopy in which the ventilation system was altered to encourage air to flow out of the critical zone in controlled manner.
- An established truly laminar displacement flow.

In 1962 Charnley and Howorth designed, for use in orthopaedic surgery, the first of these “ultra clean” ventilation (UCV) systems with an enclosure having full length curtains which separated the service team from the operating team and which provided a unidirectional downward flow of sterile air within the enclosure that was allowed to exit near the floor^(Charnley, 1964). The exhausted air from the enclosure then mixed with the air in the room in a conventional manner. This worked well preventing the entrainment of air from regions outside the clean zone (Lidwell et. al., 1982). However the restrictions imposed by the fixed sides of the enclosure rendered it unacceptable for many types of surgery and to many surgeons.

For ventilation systems fitted with partial canopies, there was still the problem of entrainment as the air exited the canopy, and due to the passage of people into and out of the clean zone. This was approached by using high level extracts on the periphery of the canopy to encourage the air to flow outwards from the canopy at the edges and maintaining a vertical flowing core in the centre. Further development to enhance this flow was to vary the discharge velocity across the clean zone so that there was a higher velocity and pressure in the centre of the clean zone than at the periphery and the air flowed radially outwards, away from the surgical team. The flow regime was likened to an exponential curve and hence termed exponential flow (Ollair Ltd.).

The performance of these systems with normal operating gowns being worn by personnel within the clean zone was shown to be 10 bcp/m^3 (Charnley & Howorth, 1962) near the wound site. In 1973 Charnley developed body exhaust gowns which were made out of occlusive cloth, the microenvironment of the personnel wearing the gown being conditioned by air drawn over the whole body and exhausted via tubes beneath the gown. This reduced the levels of bcp at the wound site to $< 1 \text{ bcp/m}^3$. The gown was modified so that it did not envelope the head but this did not compromise the performance levels obtained at the wound site. New fabrics were then developed which give comparable performance to the Charnley-Howorth body exhaust gowns when used within the clean zone of an ultra clean ventilation unit (Newton et. al., 1991).

The airflow into the clean zone had to be of a high enough velocity to cope with the buoyant convective flows from the surgical team, the patient and the operating lamps, and combat entrainment from areas outside the clean zone from the movement of the personnel. In 1973, Whyte et al. suggested that velocities in the region of $0.3 - 0.5 \text{ m/s}$ be used with no compromise in performance. They examined both crossflow and vertical flow systems concluding the latter provided more stringent cleanness levels as found in cleanroom practice. In 1979, an Australian Standard (AS 2251) was published on UCV design recommending velocities between $0.37 - 0.55 \text{ m/s}$, with uniformity $\pm 20 \%$, with no medical equipment e.g. theatre lights or people present. In 1986, the Department of Health and Social Security put out a draft report on the requirements of UCV systems, recommending vertical velocities measured 2 m from the floor of 0.3 m/s for full walled enclosures (walls terminating 1 m above floor level) and 0.38 m/s for partial walled enclosures (walls terminating 2 m above floor level). These velocities would result in about 400 air changes/hr within the room.

The temperature of the air supplied to the clean zone of an ultra clean ventilation system was important with respect to the thermal comfort of the personnel working and the body temperature of the patient. This had to be below that of the ambient air so that the buoyancy of the air did not cause a problem. The range of temperatures which the majority of people felt comfortable with was in the range $21 - 24^\circ\text{C}$ and $30 - 70 \%$ relative humidity (rh) with air

movement < 0.2 m/s (Clark & Edholm, 1985). However during surgery the personnel were exposed to greater levels of heat in the form of radiation from the lights. A comfortable working temperature for minimum fatigue was found to be between 19 and 20 °C (50 % rh and air velocity 0.13 m/s). However during surgery with open wounds, the heat loss from the body was greater due to radiation and the evaporation of body fluids, and a temperature of 21 - 24 °C was required to prevent surgical hypothermia. In the treatment of burn injuries there was a much larger surface area of tissue exposed resulting in much higher rates of heat loss. In addition a method of treatment was to expose the wound to continuous flowing air in order to enhance the formation of an eschar. This made the control of the temperature critical in maintaining comfortable conditions; to prevent evaporative cooling or sweating. Depending on the form of treatment used, the air temperature could be up to 45 °C (65 - 70 % rh). These conditions made it very uncomfortable for personnel attending the patient.

This elevated supply temperature made the air inherently buoyant and the velocity of the supply had to be increased accordingly to balance the buoyancy but not induce excessive evaporative heat loss. It was a compromise. It was recommended that the UCV have full length walls so as to maintain the flow to 1m above floor level, so lowering the exit point of the supply air into the room (Whyte et. al., MRC recommendations; 1983).

7.3 Review of test methods

The performance of operating theatre and ultra clean ventilation systems were assessed qualitatively, using smoke to visualise the airflow patterns, and quantitatively by measuring the number of bacteria carrying particles (bcp) in the air, based on the number of colony forming units (cfu) (Holton et. al, 1990). The quality of the air was also assessed by measuring the total number of airborne particles; those counts of particles in the size range 5.0 - 7.0 μm correlated with bcp count and in the size range 0.5 - 3.0 μm and > 15 μm corresponded to activity (Seal & Clark, 1990). This was viable for use in the type test, commission and regular maintenance of ultra clean ventilation systems but not for turbulently ventilated operating theatres where the particles may represent to the counter. The DHSS draft report (1986) recommended the use of particle counting in type testing and bacterial counting for commissioning and in-situ testing. The Australian Standard AS 2251 - 1979 recommended assessing the performance as a cleanroom of class 3.5.

The use of gas and particle tracers for assessing cross infection in hospitals was investigated by Foord & Lidwell (1972, 1975)^{ab} and by Hambræous & Sanderson (1972). They used nitrous oxide as a gas tracer and potassium iodide as a particle tracer (from which the KI-Discus method was developed for testing safety cabinets). These studies demonstrated the use of tracers to quantify the isolation of individual rooms within the hospital ward. There was a disparity in the results obtained with particles and gas tracers due to the settling of the

particles, but this could be calculated as effective ventilation. Such tracer methods were never incorporated into standard performance assessment strategies.

7.4 The burns unit and Ultra Clean Ventilation (UCV) system

The burns unit in this investigation was intended to be “isolated” from the rest of a plastic and reconstructive surgery ward in order to minimise possible cross contamination a) either from the hospital ward to the unit or from the unit to the hospital ward and b) between individual rooms within the unit. The movement of air and airborne particles was controlled by maintaining airflow from positive to negatively ventilated regions (Fig. 7.1). Entrances to the unit were through positive pressure airlocks (relative to the ward and unit) and individual rooms within the unit were designed to be at negative pressure with respect to the corridors and airlocks. Barrier nursing techniques allowed the unit to be used for other procedures during the treatment of a serious burn injury in the intensive care room.

The operating theatre, dressing room and intensive care rooms were equipped with ceiling mounted UCV systems with partial canopies. HEPA filtered air at controlled temperature and humidity was blown downwards over a patient nursed on a Low Air Loss Bed (LALB, KCI Mediscus Ltd., Wareham, England) and then outwards into the room producing a clean and controlled environment around the bed (Fig. 7.2). The flow of air away from the bed into the room was augmented by air drawn upwards through extracts in the ceiling around the periphery of the canopy. This air, together with make-up air from a plant room, constituted the UCV supply over the bed (Fig. 7.3). The make-up air was temperature and humidity controlled. The velocity and temperature of the supply air could be controlled between the design parameters of 0.38 - 0.5 m/s and 20 - 40°C respectively.

The proportion of air being drawn from the room back through the UCV determined the net flow of air supplied to the rest of the room. Air in excess of that supplied to the room was exhausted directly to the outside thus creating a negative pressure in the room. The supply air throughout the unit was regulated to give a constant volume flow rate allowing for soiling of the HEPA filters. The pressure within rooms was controlled by varying the exhaust, each room having separate extract systems to allow for flexibility.

The LALB had a temperature controlled flow of air through it to maintain patient comfort. The minimum temperature gain through the bed was 5°C. This temperature rise and some air leakage (some 15% through the stitching) both contributed to the lift of air beneath the UCV canopy.

At commissioning the criteria for performance of the unit and UCV had been to measure the pressure differentials between rooms, establish the recommended exit velocity measured at the edge of the canopy at ambient temperatures which gave a flow rate of 0.1 m/s at the bed

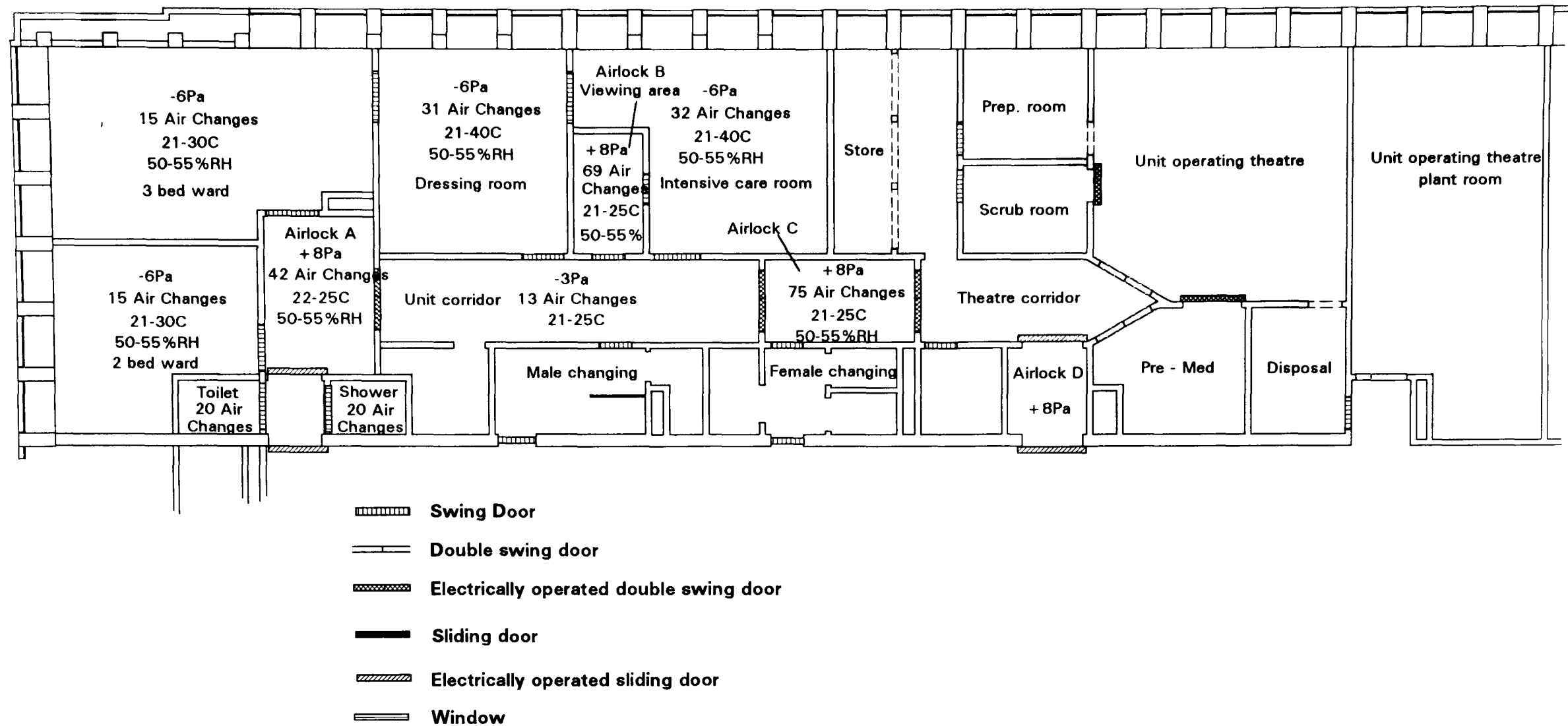


Figure 7.1 The burns unit as designed

surface, airflow visualisation and bacterial counts. At higher UCV supply temperatures the flow rate was increased to maintain 0.1 m/s at the bed surface. Annual inspections involved measurement of pressure and velocity, flow visualisation and bacterial counts beneath the canopy to assess any deterioration in performance.

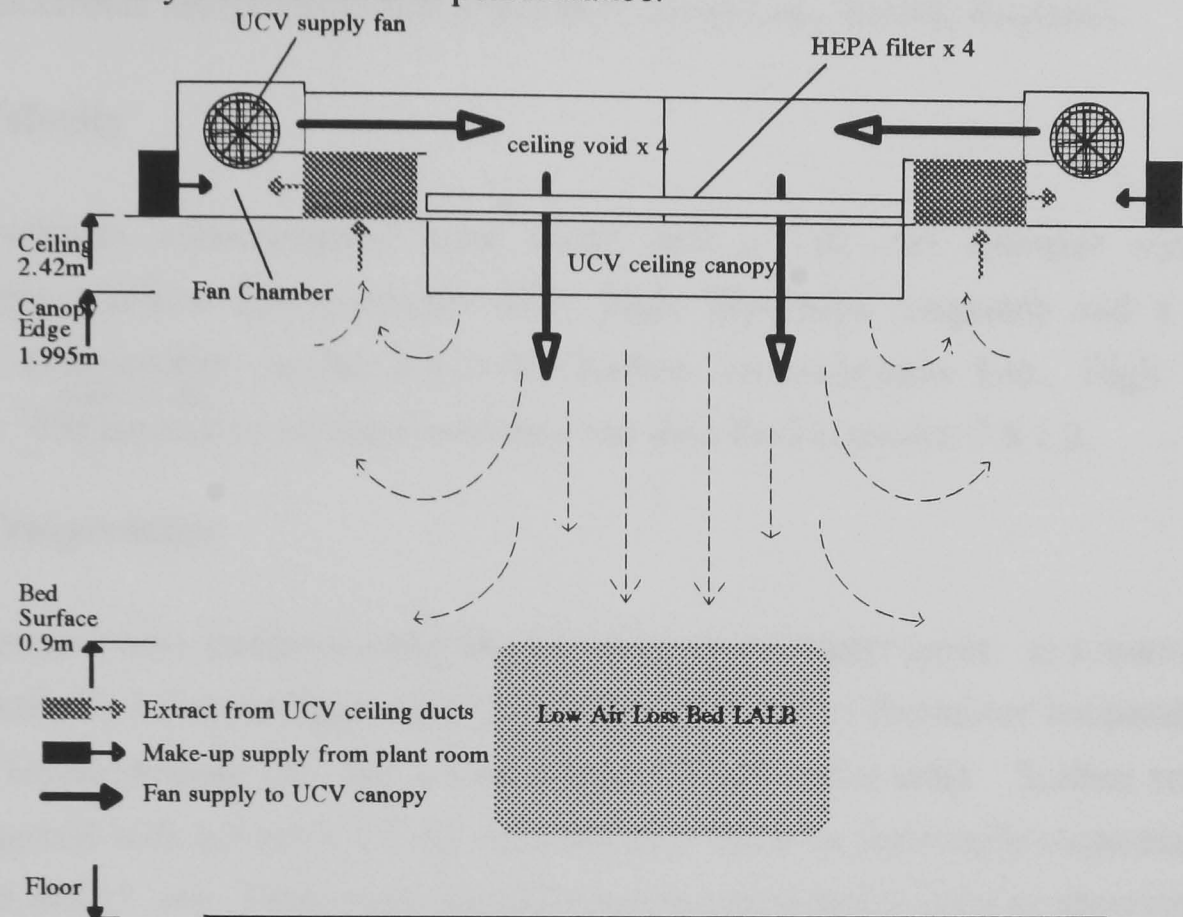


Figure 7.2 Cross section of ultra clean ventilation (UCV) system fitted in the ceiling of the intensive care room showing ducting from UCV extracts to the fan chamber. Fan make up air direction and expected velocity profile over the bed surface are also shown.

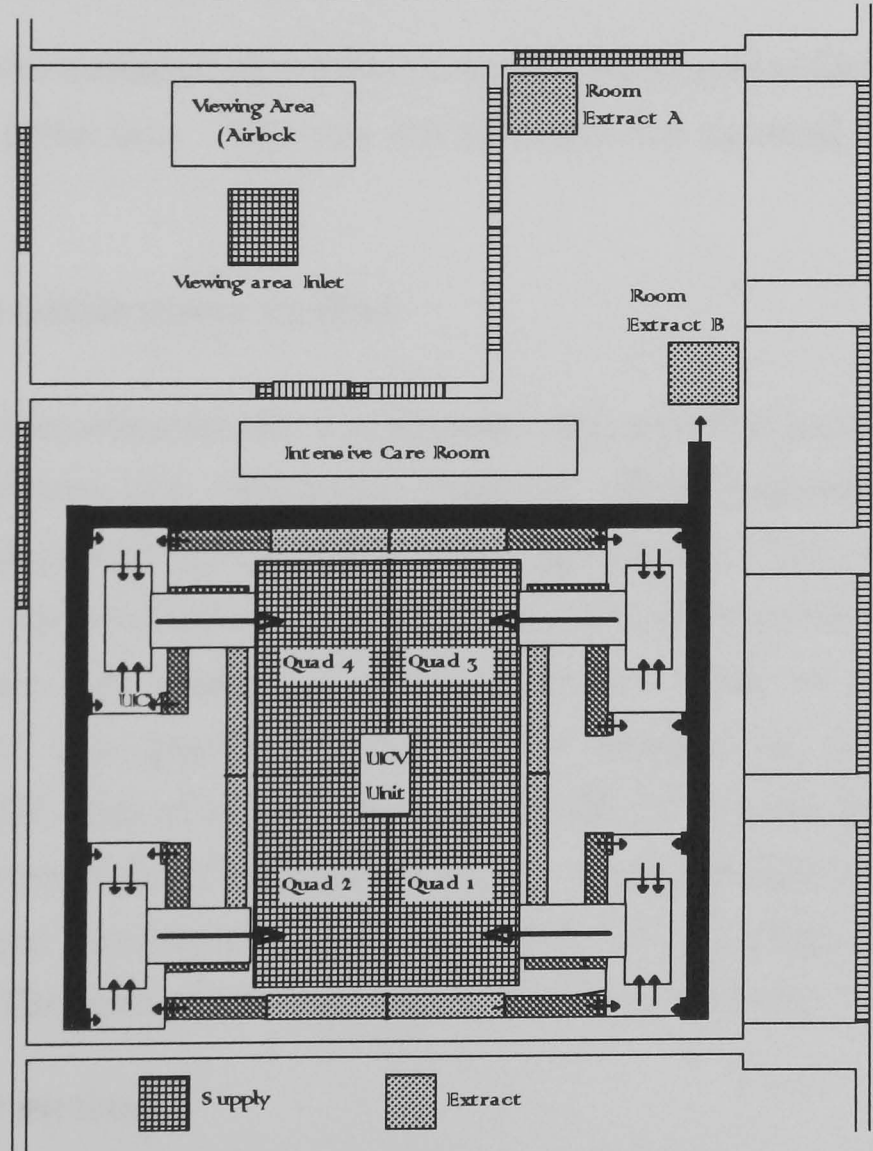


Figure 7.3 Plan view of the ultra clean ventilation (UCV) system fitted in the ceiling of the intensive care room showing ducting from UCV extracts to the fan chamber, fan make up air and room extracts.

7.5 Materials, equipment and methods

7.5.1 Pressure

Room air pressures were measured in the middle of each room in mm water gauge (Wg) using an electronic micromanometer (Furness Controls Ltd., Bexhill, England).

7.5.2 Velocity

Airflow velocity measurements were made with a 110 mm diameter rotating vane anemometer (Airflow Developments Ltd., High Wycombe, England) and a thermistor (thermal) anemometer, model TA-2-15 (Airflow Developments Ltd., High Wycombe, England). The ^{method of} calibration of this instrument was described in section 3.8.1.2.

7.5.3 Temperature

Air temperature was measured using the following thermometer types: a) a mercury in glass thermometer, b) a thermo-hygro unit (Precision Gold) and c) thermistor temperature probes (Airflow Developments Ltd. and a Lee Integer CH-15 probe unit). Surface temperatures were measured with a Raytek ET-III infra-red spot meter (a thermopile measuring radiation between 8 and 13 μ m). These were not calibrated but expected to have an accuracy $\pm 1^\circ\text{C}$.

7.5.4 Humidity

Relative humidity was measured with a thermo-hygro unit (Precision Gold) and a Lee Integer CH-15 thermistor probe unit. This was not calibrated but expected to have an accuracy within $\pm 3\%$ rh.

7.5.5 Potassium iodide tracer method

The spread of airborne contamination was assessed using a particle tracer system (KI-Discus, Containment Technology Ltd., Wimborne, England). This equipment, normally used for assessing the containment of microbiological safety cabinets (BS 5726 : 1992) as described in Chapters 4 and 5, was modified so that the source could be operated independently of the sampling/control unit. A solution of 1.5 % potassium iodide in absolute alcohol was aerosolised to form $7 \pm \mu\text{m}$ particles at a rate of 3×10^7 particles/min. These were sampled in the air at a rate of 100 litres of air per minute with collected particles deposited on a 25 mm diameter filter membrane disc (Millipore UK Ltd.). Any potassium iodide particles on the filter membrane were "developed" in a solution of 0.1 % palladium chloride in 0.1 mol/l hydrochloric acid. The number of brown spots on the filter membrane were then counted.

7.5.6 Gas tracer method

Nitrous oxide gas was used to trace air movement. 5 litres/min of nitrous oxide was released into the unit and which did not exceed the suggested safe limits (the occupational exposure of

nitrous oxide is under review, but a safe limit was considered to be 100 ppm, or 1 %). The tracer gas was measured with a portable infra-red gas analyser (Miran 1A, Foxboro Co. UK). This was a single beam, variable filter spectrometer, scanning the infrared spectral range between 2.5 and 14.5 μm . The instrument was equipped with a gas cell having a path length variable between 0.75 and 20.25 m. The analytical wavelength used for nitrous oxide detection was 4.5 μm and path length of 12.75 m. This gave a calibration (from Foxboro data) of 119.1 (ppm/AU) at the above settings, and minimum detectable limit of 0.04 ppm (based on pathlength of 20.25 m).

7.5.7 Particle measurement

Airborne particle measurements were made using a counter as recommended by BS 4545 for the evaluation of clean rooms. The sample flow rate was 1 $\text{ft}^3\text{min}^{-1}$. Particle measurements were made in the size range from 0.3 μm to >25 μm . This instrument was calibrated by the pharmacy department.

7.5.8 Smoke visualisation

Hot generated oil smoke was used to visualise the movement of air within the unit. The oil used was Shell Ondina oil E.L. light, which is a paraffin based oil of a pharmaceutical grade and which is considered harmless to humans. The oil was thermally vapourised below its ignition point to produce a thick white smoke. This was released through an eight hole smoke comb.

7.5.9 Airborne bacterial sampling

Airborne bacteria were sampled using a Casella slit air sampler (Casella London Ltd., Bedford, England) on an agar plate at a rate of 175 litres of air per minute

7.5.10 Computational fluid dynamics (CFD)

Computational fluid dynamics as discussed in Chapter 6 using software provided by Flovent (Flomerics Ltd., Kingston-upon-Thames, Surrey).

7.6 Results and discussion of the physical measurements made in the burns unit

7.6.1 Air pressures and air flows (as visualised with smoke) within the unit

The manner in which the unit was operated and the measured air pressures around the ward (Fig. 7.4) were found to differ from the design parameters. The main airlock A (generally used for access to the unit corridor and bedrooms) had a small positive pressure relative to the main ward. The doors leading from it to the main ward and bedrooms were kept open.

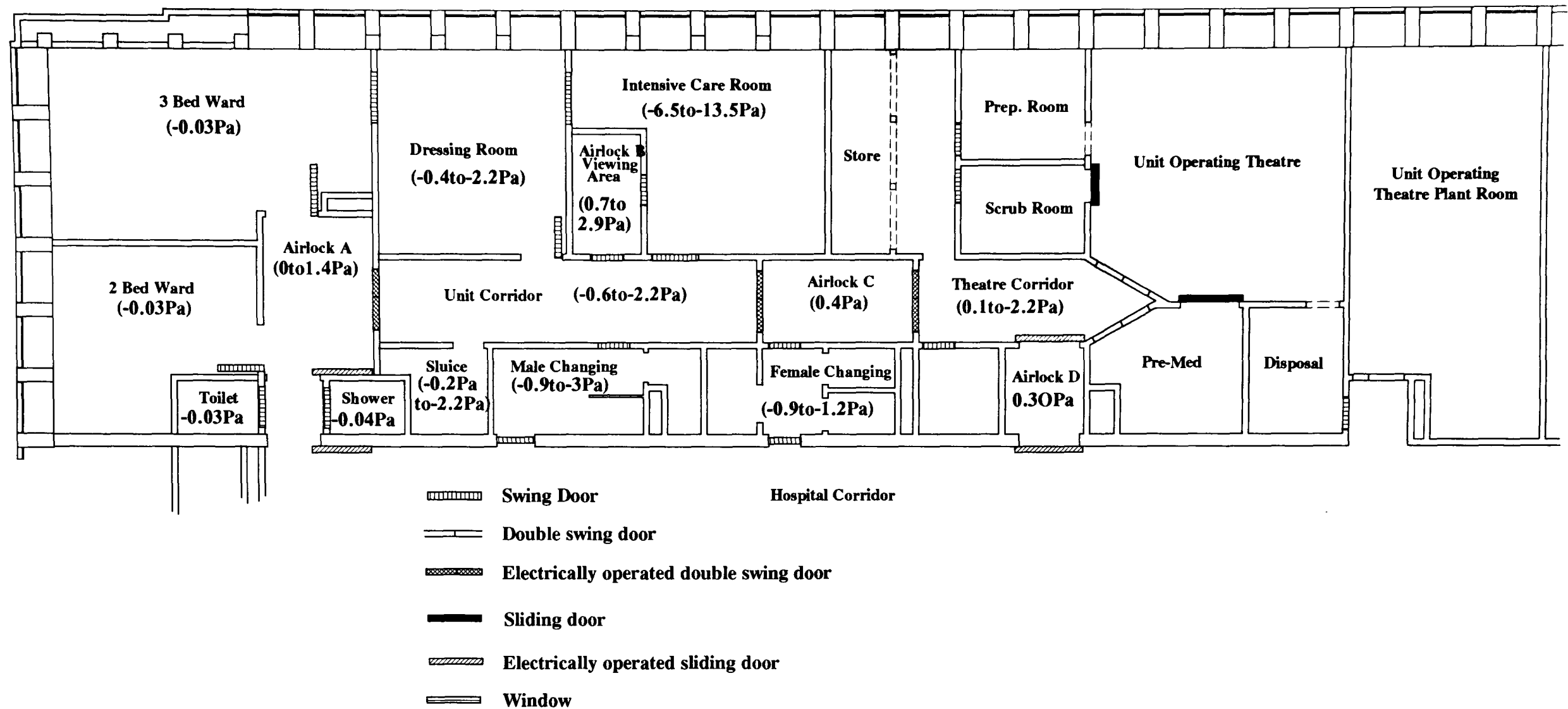


Figure 7.4 The burns unit as used (door positions as commonly found in use)

From the design data supplied, the supply to this airlock should have been +8 Pa with the doors closed. However the lack of positive pressure enabled air to move freely into the airlock from the hospital ward and subsequently into the negatively pressurised rooms leading from it. This constituted a prime route for potential airborne contamination from the hospital ward to enter the unit.

Air flowed into the unit corridor through the double doors of airlock A and along the corridor towards airlock C, and was clearly influenced by the pressure differences of the adjoining rooms. The pressure in both changing rooms was negative with respect to the hospital ward and the corridor. Airborne contamination in these rooms would not be expected to enter the unit. However, there was no control of the opening sequence of the doors. With the door of the male changing room fully open air flowed into the corridor near to the ceiling. This effect was not apparent in the female changing room.

There was little measurable pressure difference (design -6 Pa) between the dressing room (ventilation on standby and the door to the corridor open, as was usual practice) and the corridor, and air flowed into this corridor near to the ceiling.

The viewing area (airlock B) had a positive air pressure much smaller than the design level of +8 Pa. This could have been due to the higher than normal pressure difference with the intensive care room and more air being drawn from the viewing area; little air flowed from the viewing area into the corridor. In the intensive care room the air pressure fluctuated and on one occasion was measured at -13.5 Pa (design -6 Pa). This may have been due to changes in environmental conditions both within the ward and unit but also outside (the room exhaust fans being ducted directly to the outside). Air was drawn into the intensive care room from all doors.

The air flow within the viewing area was dominated by strong jets into the room from the ceiling supply duct which had angled diffusers to direct air across the ceiling towards the corridor door and the opposite window. As a result air moved out of the door (when fully open) and into the corridor. The air flow was near to the top of the door but allowed re-entrainment near to the floor. Opening the door from the viewing area to the intensive care room resulted in air moving into the viewing area near to the top of the opening.

The pressure in airlock C was small (design +8 Pa) and the air was found to flow into it from the unit and theatre corridors. The flow in the airlock was similar to that in the viewing area and was very turbulent with the likelihood of producing re-entrainment at floor level.

7.6.2 Air temperature and relative humidity distribution

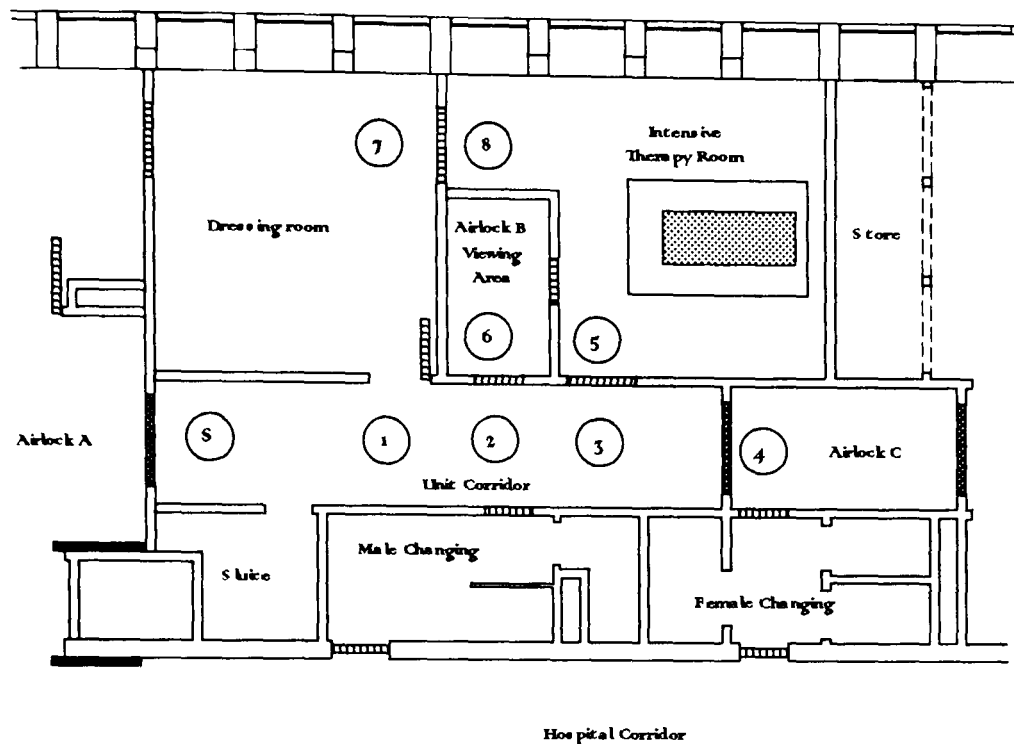


Figure 7.5 Measurement positions of temperature and humidity within the burns unit.

Air temperature and humidity measurements were made within the unit (Fig. 7.5) at three heights; 200 mm from the floor, midway between the floor and the ceiling and 200 mm from the ceiling. From Fig. 7.6, the measured temperature variation within the unit was 22-28 °C (nominal design parameters between 21-25 °C). The measured values of relative humidity ranged between 32 and 48 %. Within the supply/extract ventilated rooms which had environmental control, there was a maximum design temperature of 40 °C (at 55 %RH).

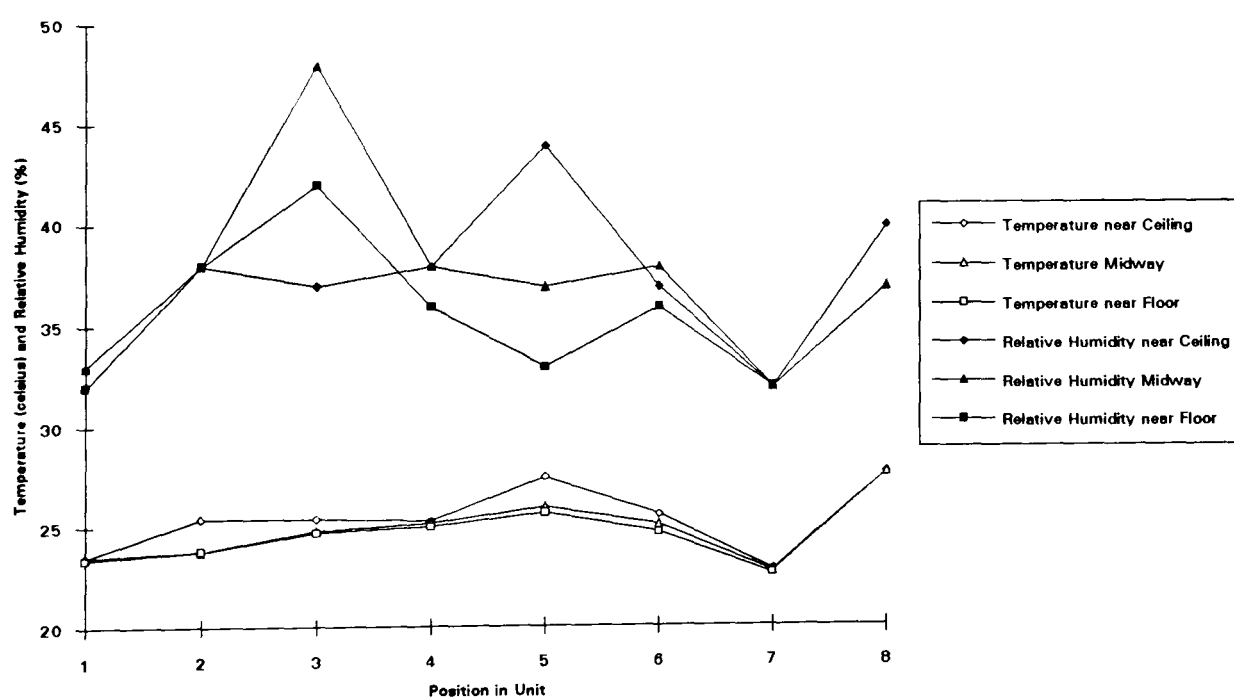


Figure 7.6 Variation in temperature and % rh within burns unit.

7.6.3 Nitrous oxide and potassium iodide tracer measurements

Tracer was released into the unit corridor outside airlock A, position T1 (Fig. 7.7) at a height of 200 mm above floor level, and measured at positions S1-S8 within the unit at three heights, 200 mm from the floor, midway between the floor and the ceiling and 200 mm from the ceiling. Both tracers were released for 5 minutes, nitrous oxide at a rate of 5 l/min and

potassium iodide at a rate of 3×10^7 particles/min. Air was sampled from the start of the release of tracer and carried on for a further 5 minutes after the released was stopped.

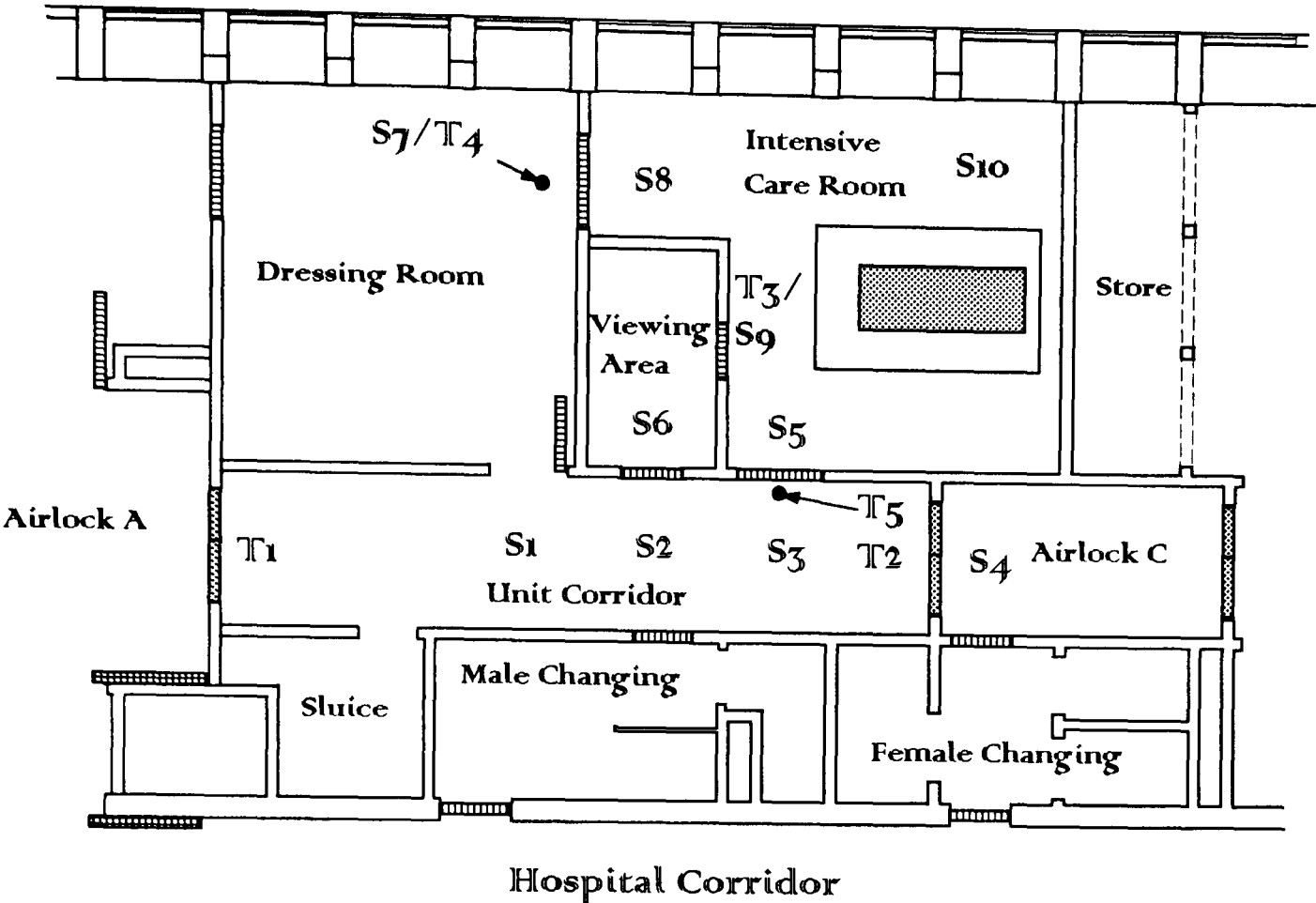


Figure 7.7 Tracer (T) release and sample (S) positions within the burns unit. Tracer was released ~200 mm from floor level. Air was sampled 200 mm from floor level, midway and 200 mm from the ceiling.

When tracer was released from position T1, to represent potential movement of contamination from the hospital ward from this main entrance to the unit, the greatest concentrations of tracer were found along the corridor towards S4 (airlock C), positions S1-S4 (Tables 7.1 - 7.3). In the intensive care room the higher concentrations of tracer were measured near to the door leading to the corridor (S5), indicating movement of air into this room from the corridor. The concentration of tracer measured at the other sample positions within the intensive care room and dressing room were orders of magnitude lower. Potassium iodide tracer was measured in the viewing area but nitrous oxide gas was not detected.

Unit position	potassium iodide (count/m ³)		nitrous oxide (ppm)	
	% disc covered	est. count	Test 1	Test 2
1	50 %	>> 31250	16	77
2	100 %	>> 62500	72	29
3	50 %	>> 31250	101	51
4	30 %	>> 20833	95	54
5	50 %	>> 31250	43	33
6		372	0	0
7		398	27	30
8		5394	23	27

Table 7.1 Concentration of KI particles and N₂O gas in air sampled at floor level from different positions within the unit when released from position T1.

Unit position	potassium iodide (count/m ³)		nitrous oxide (ppm)	
	% disc covered	est. count	Test 1	Test 2
1	100 %	>> 62500	132	93
2	100 %	>> 62500	76	48
3	60 %	>> 37500	98	51
4	20 %	>> 12500	93	50
5		8614	5	5
6		218	0	0
7		247	29	46
8		3221	14	2

Table 7.2 Concentration of KI particles and N₂O gas in air sampled at mid height from different positions within the unit when released from position T1.

Unit position	potassium iodide (count/m ³)		nitrous oxide (ppm)	
	% disc covered	est. count	Test 1	Test 2
1	100 %	>> 62500	101	81
2	100 %	>> 62500	76	49
3	60 %	>> 37500	113	
4		9353	0	50
5		1014	6	0
6		169	0	0
7		847	33	0
8		629	2	0

Table 7.3 Concentration of KI particles and N₂O gas in air sampled at ceiling level from different positions within the unit when released from position T1.

Little potassium iodide tracer was measured outside the intensive care room when released from within it (T3) and no nitrous oxide tracer was sampled (Table 7.4) indicating good isolation of this room from the rest of the unit. When tracer was sampled within the viewing area; both nitrous oxide and potassium iodide were found. Opening and shutting the viewing area/intensive care room door increased the concentration of potassium iodide measured within the viewing area by two orders of magnitude.

Sample position	KI	Gas
S3 (across corridor door, no disturbance)	39	0
Blank	44	
S7 (across dressing room door, no disturbance)	12	0
Blank	9	
S6 (across viewing area door, no disturbance)	25	2.4
S6 (across viewing area door whilst walking into and out of the room)	2272	
Blank	80	

Table 7.4 Concentration of KI particles and N₂O in air sampled outside the room near the corridor door (S3), the dressing room door (S7) and in the viewing area (S6) when released from position T3.

When tracer was released outside the intensive care room near to the corridor door and the dressing room door (Table 7.5) there was considerable movement of tracer into the intensive care room.

Sample position	KI
S5 (across corridor door)	8614
S8 (across dressing room door)	3221

Table 7.5 Concentration of KI particles in air sampled inside the room near the corridor door (S5), the dressing room door (S8) and in the viewing area (S9) when released from position T4 and T5.

7.6.4 Particle counts

Particle counts were made to help in monitoring tracer movement following the release of potassium iodide tracer particles. Potassium iodide tracer particles were released 200 mm above floor level from position T1 and sampled midway between floor and ceiling at position T2 and vice versa. Total particle counts were made at the same time. From Tables 7.6 and 7.7 it would seem that the size of potassium iodide particles sampled from the air are less than 7 μm . However, this count may be low due to errors in counting potassium iodide crystals using an optical particle counter (Wake, 1985).

source	sample	KI source	counts of particles (size range μm)/ m^3						KI sampled
			0.3-0.5	0.5-1.0	1.0-5.0	5 - 10	10 - 25	>25.0	
T1	T2	7.80E+07	4803276	802318	340629	852	714	120	12800
		Blank	3611488	467905	63392	749	682	88	475
T2	T1	6.20E+08	2910014	1541353	1691958	1933	1912	399	62500
		1.60E+08	2903537	1011694 0	387784	1951	1191	205	16342
		7.80E+07	2977049	735053	292071	1028	700	110	14329
		Blank	1163127	685698	135014	1590	1481	322	411

Table 7.6 Concentration of particles and KI in air sampled at midheight position T2 when KI released from T1 (and vice versa).

source	sample	KI released	counts of particles (size range μm)/ m^3						KI sampled
			0.3-0.5	0.5-1.0	1.0-5.0	5 - 10	10 - 25	>25.0	
T1	T2	7.80E+07	1191788	334413	277237	103	32	32	12325
T2	T1	6.20E+08	1746887	855655	1556944	343	431	77	62089
		1.60E+08	1740410	9431242	252770	361	-290	-117	15931
		7.80E+07	1813922	49355	157057	-562	-781	-212	13918

Table 7.7 Concentration of particles and KI in air sampled at midheight position T2 when KI released from T1, adjusted for background (and vice versa).

Airborne particles were also counted to provide an indication of the number of potential airborne contaminants in the unit and ward. Particles can originate from surfaces, people and manipulations and those >5 μm equivalent diameter may potentially carry micro-organisms. Of most interest are those particles up to 10 μm which may be suspended in the air for long periods until they either impinge on surfaces, are inhaled or are vented and of which only a small proportion would carry micro-organisms and that a small fraction of those would be potentially pathogenic.

Counts were made at several sites around the unit and ward at a height ~ midway between floor and ceiling with the sampling head facing upwards. The counts of particles $>5\text{ }\mu\text{m}$ were generally higher in areas where there was most personnel movement, i.e. the progressive care rooms and airlock A (Fig. 7.8). In the corridor and rooms leading from it, and with fewer people present, the number of particles $>5\text{ }\mu\text{m}$ was less. However the number of particles $<5\text{ }\mu\text{m}$ measured in the viewing area and intensive care room was higher than many places with constant and greater personnel movement.

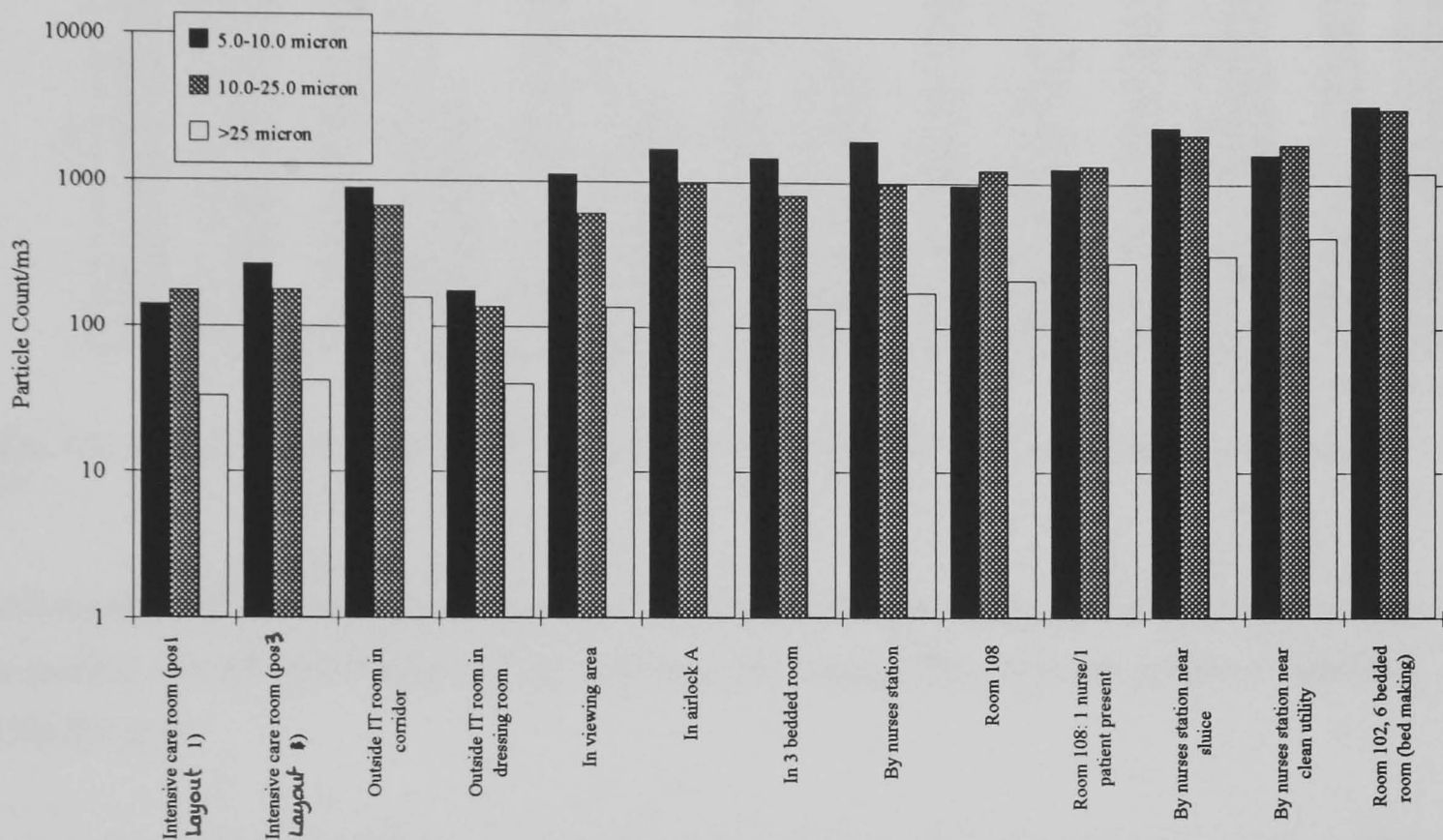


Figure 7.8 Particle counts ($>5\text{ }\mu\text{m}$) at various places within the burns unit.

There was very little change in particle size with height, for example when sampled in airlock A and C, suggesting the air is turbulently mixed. There was a greater number of particles sampled in airlock A compared with airlock C, which is not surprising considering airlock A was in constant use and airlock C was not.

7.6.5 Airborne bacteria

Airborne bacterial counts were made (3 samples) at several places simultaneously with the particle counts in section 7.3.4. Air was sampled for 5 minutes at 175 l/min. The numbers of colony forming units (CFU) recovered (Table 7.8) were several orders of magnitude less than the total number of particles (Fig. 7.9) found at the various sites within the unit and around the ward.

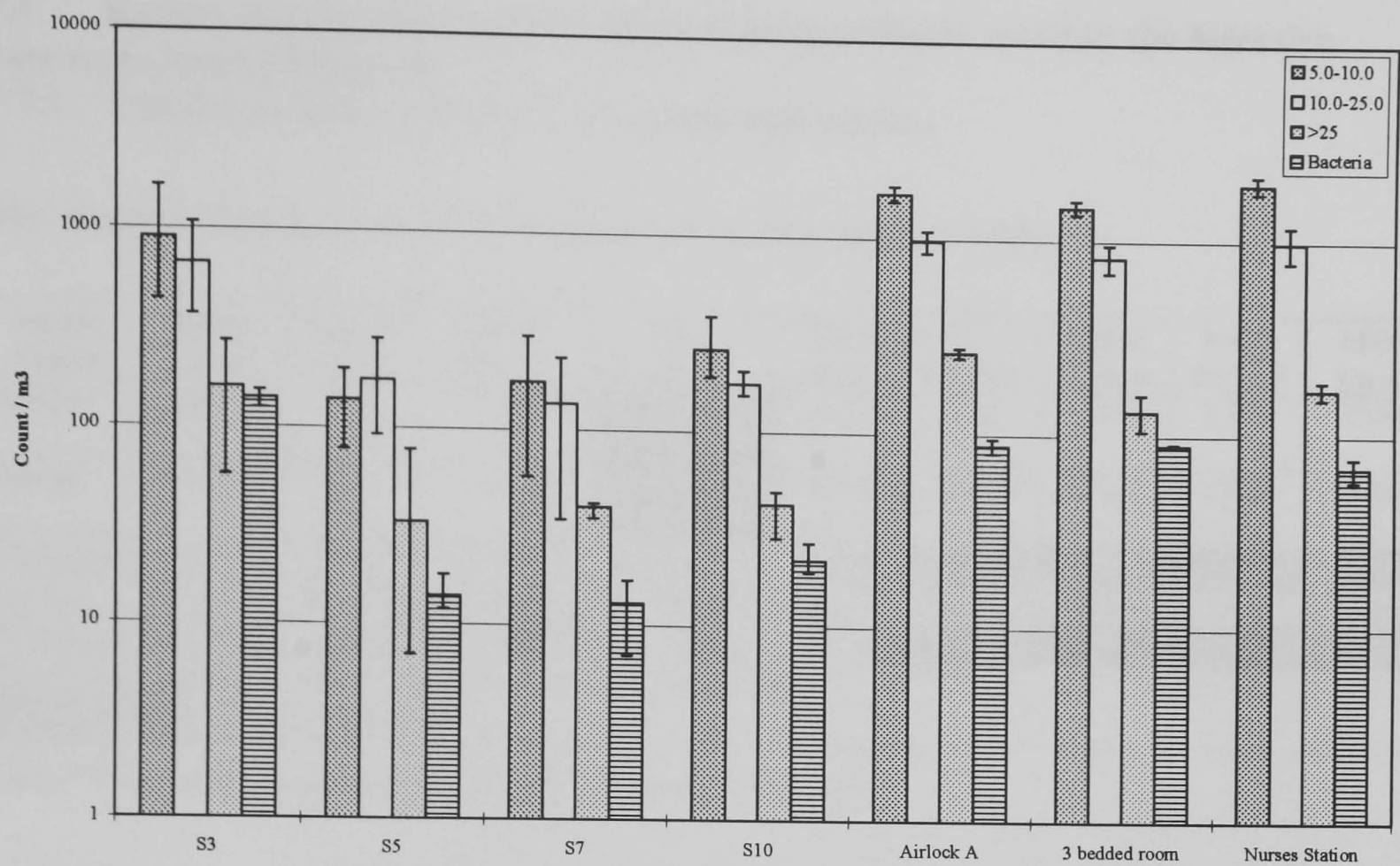


Figure 7.9 Comparison of bacterial counts and total particle counts at various places in the unit and ward

Staphylococcus aureus
Small numbers of *S. aureus* were recovered. These organisms were not from the operator as that person was screened negative but they may have come from another person or persons within the area.

The lowest number of CFUs were found in the intensive care and dressing rooms. The largest number of CFUs were recovered from the corridor.

Position in intensive care room	micrococci	ASB	S.aureus	Fungi	Total CFU/m ³
3	Yes	Scanty			31
	Yes				23
	Yes		1		22
5	Yes				21
	Yes	Scanty			14
	Yes				14
Position in Unit					
In corridor	Yes	Scanty			142
	Yes	Scanty	1		175
	Yes	Scanty			165
In dressing room	Yes				19
	Yes	Scanty			17
	Yes				8
In airlock A	Yes	Scanty	1		109
	Yes			3	93
In 3 bedded room	Yes	Scanty			104
	Yes			2	102
By nurses station	Yes		1		89
	Yes				67

Table 7.8 Number of airborne bacteria (CFU/m³ air sampled) sampled within the hospital ward and burns unit.

7.7 Results and discussion of the physical measurements made in the intensive care room and viewing area

7.7.1 Ventilation and air flows (as visualised with smoke)

The ventilation data acquired in the intensive care room is shown in Table 7.9.

Supply Status	Supply Temp.	Supply %RH	Supply* Vel. (m/s)	Mag. Gauge	UCV Supply	UCV Extract	Room Surplus	Room Extract	Make-Up Air
Design	20.0°C	40-50%	0.38		1.843	1.310	0.533	0.624	0.091
Design	40.0°C	40-50%	0.51		2.474	1.940	0.534	0.624	0.091
Minimum	20.5°C	43.0%	0.35(0.47)	3.3mmWg	1.698				
Normal	33.0°C	39.0%	0.42(0.54)	5.4mmWg	2.319	1.708	0.611	1.104	0.493
Maximum	41.0°C	39.5%	0.52(0.74)	FSD	2.522				
Canopy exit velocity; () velocity measured near grill in canopy									
									Data not measured

Table 7.9 Air supplies and extracts (m³/s) in the intensive care room.

The ventilation, size and construction of the intensive care room determined the air flow pattern within the room. All of the room extracts were at ceiling level. The UCV extracts surrounding the canopy were designed to promote a flow of air out from beneath the canopy circulating back to the ceiling (it was found that the extract duct on the long side of the canopy near the corridor and viewing area was partially blocked and had negligible airflow through it). The room extracts, also in the ceiling, drew air out from the room thereby providing total room ventilation. In effect, all the air in the room flowed up towards the ceiling apart from that directly beneath the canopy.

The most dominant ‘rogue’ air flows within the intensive care room were the draughts into the room. These appeared to come from any opening. The most dominant were from beneath the door to the viewing area, the air moving vigorously underneath the bed and bouncing off the back wall. Draughts from under the other doors into the room and also, to a lesser extent, from around the doors themselves were also notable.

The room was designed to have a negative pressure with respect to the corridor, viewing area and the dressing room. This would create passive make-up movement of air from the surrounding rooms into the intensive care room. The doors were designed to be "leaky" around the frames. However the way in which the air moved into the room was not ideal considering the small size and the position of the canopy ventilation and viewing area. In a large operating theatre such draughts may not be a problem as they can diffuse rapidly into the room air. However, in the intensive care room the close proximity of the walls, canopy and bed resulted in rapid, turbulent and disturbed air which did not diffuse before reaching the bed.

The movement of air over the bed (bed surface 0.9m from floor level) showed a distinctive pattern (Plate 7.1). Fitting an extended Perspex sheet to the head end of the bed helped to prevent the air bouncing off the wall and being re-entrained into the downflowing air from the canopy. This was effective and the air was forced downwards over the whole of the head region of the bed; it then moved outwards from the bed sides and circulated upwards (Plate 7.2) influenced by the extracts around the canopy edge and the room.

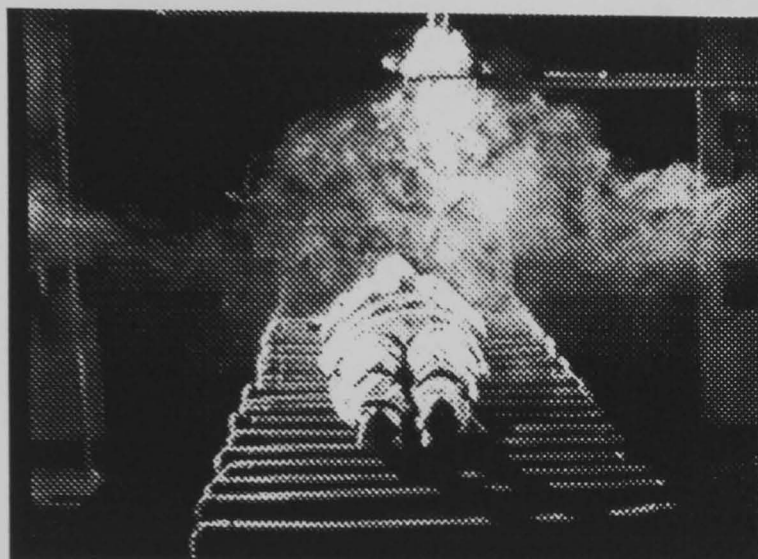


Plate 7.1 Smoke movement over patient lying on a Low Air Loss Bed (LALB).

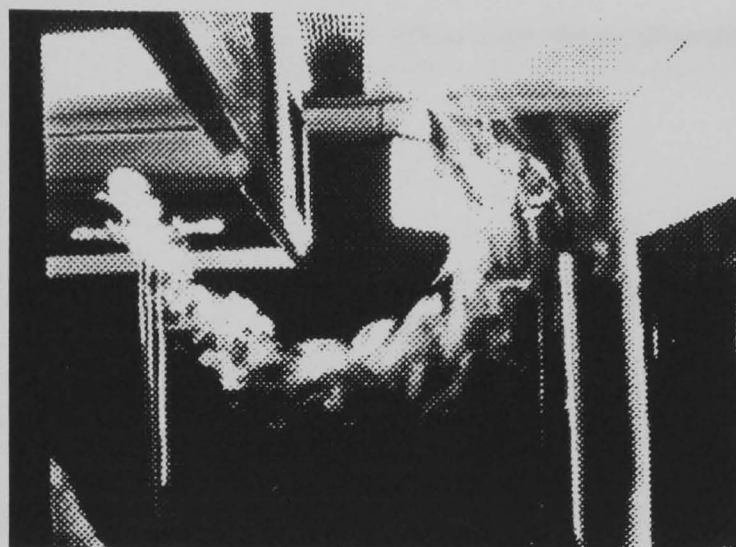


Plate 7.2 Air/smoke flow from under the UCV.

This airflow pattern was not so distinct towards the foot of the bed. There was a general movement of air from the head to the foot end (Plate 7.3) and air flowing downwards from the canopy did not reach the bed surface but was lifted out towards the UCV and room extracts. The bed surface at the foot end was thus 'flushed' with air blown onto the head end, albeit this was still "clean". This appeared to follow the underlying movement of air within the intensive care room (viz. towards the room extracts, moving from around the back of the bed past the corridor wall and foot of the bed, possibly as a result of the dominant draught from under the viewing area door causing recirculation, and on the window side moving into the window alcoves and up towards the ceiling extracts).

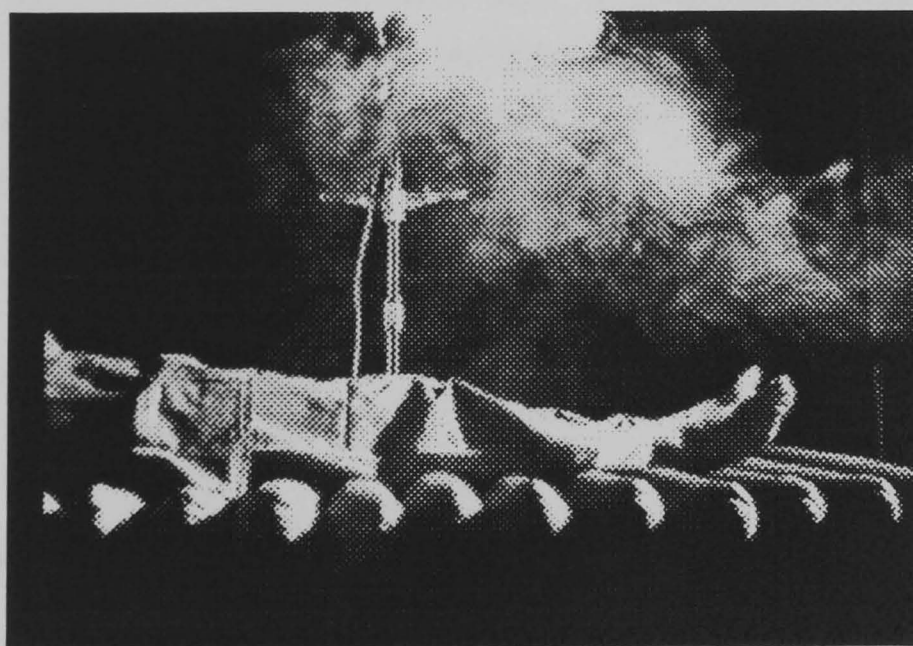


Plate 7.3 Movement of air/smoke from head to foot end of the bed.

7.7.2 Velocity measurements beneath the UCV

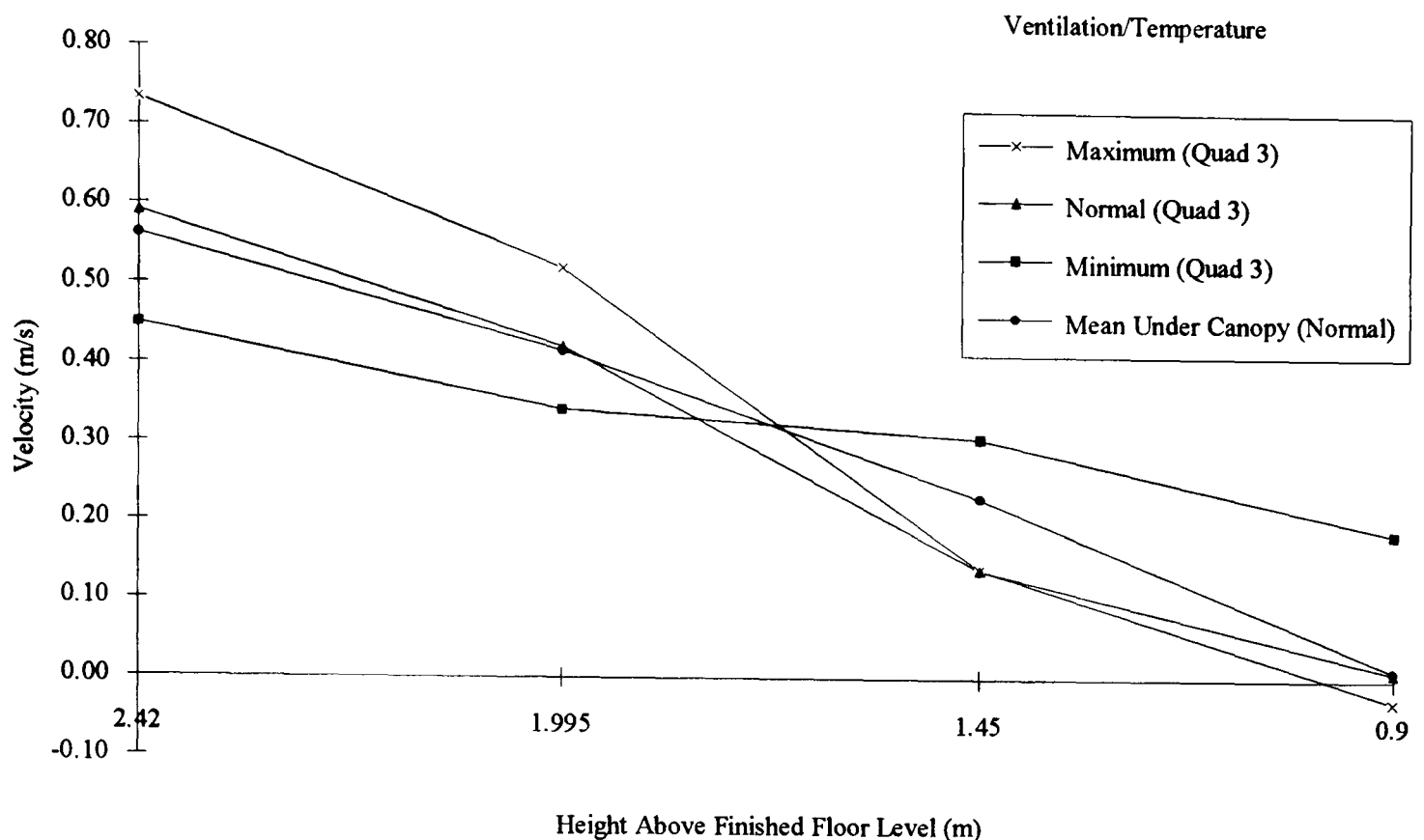


Figure 7.10 Change in mean downflow velocity with height beneath UCV canopy, and variation in downflow velocity beneath UCV (quadrant 3) with changing supply flow rate and temperature.

The mean measured downflow velocity, at normal supply temperature and velocity, near the supply diffuser was 0.56m/s which fell to 0.42m/s at the canopy exit, (Fig. 7.10). However the speed of the air flowing over the bed surface was very low $< 0.1\text{m/s}$ (unmeasurable with the rotating vane anemometer).

With the UCV ventilation on maximum, normal and minimum (measured beneath quadrant 3, Fig. 7.4) the air left the canopy with large differences in exit velocity. However beneath the canopy towards the bed, the maximum and normal measured downflow velocities were similar and at the bed surface the maximum ventilation had the lowest mean average velocity; air was actually measured rising from the bed surface. This could have been because more air was drawn out of the canopy so less reached the bed or that air was bouncing off the bed. Most probably it was the increased temperature of the air at maximum ventilation causing greater buoyancy and forcing air back up towards the canopy. With the UCV ventilation on minimum, there was less stratification of velocity with height, and above the bed surface there was a measurable velocity (average 0.19 m/s).

7.7.3 Air temperature and relative humidity

In the intensive care room, under working conditions but without people in the room, the control panel indicated a supply temperature of $36\text{ }^{\circ}\text{C}$ (40 %RH), and the supply pressure $\sim 5.4\text{ mmWg}$.

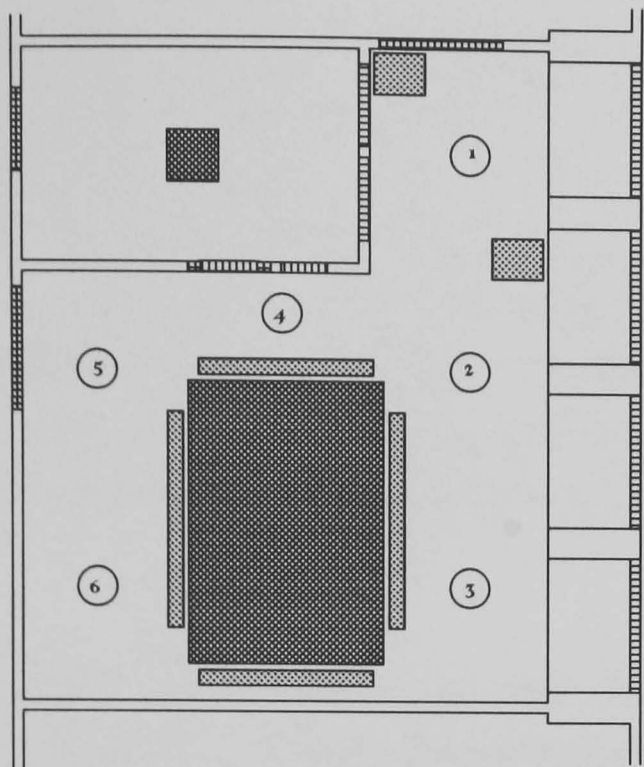
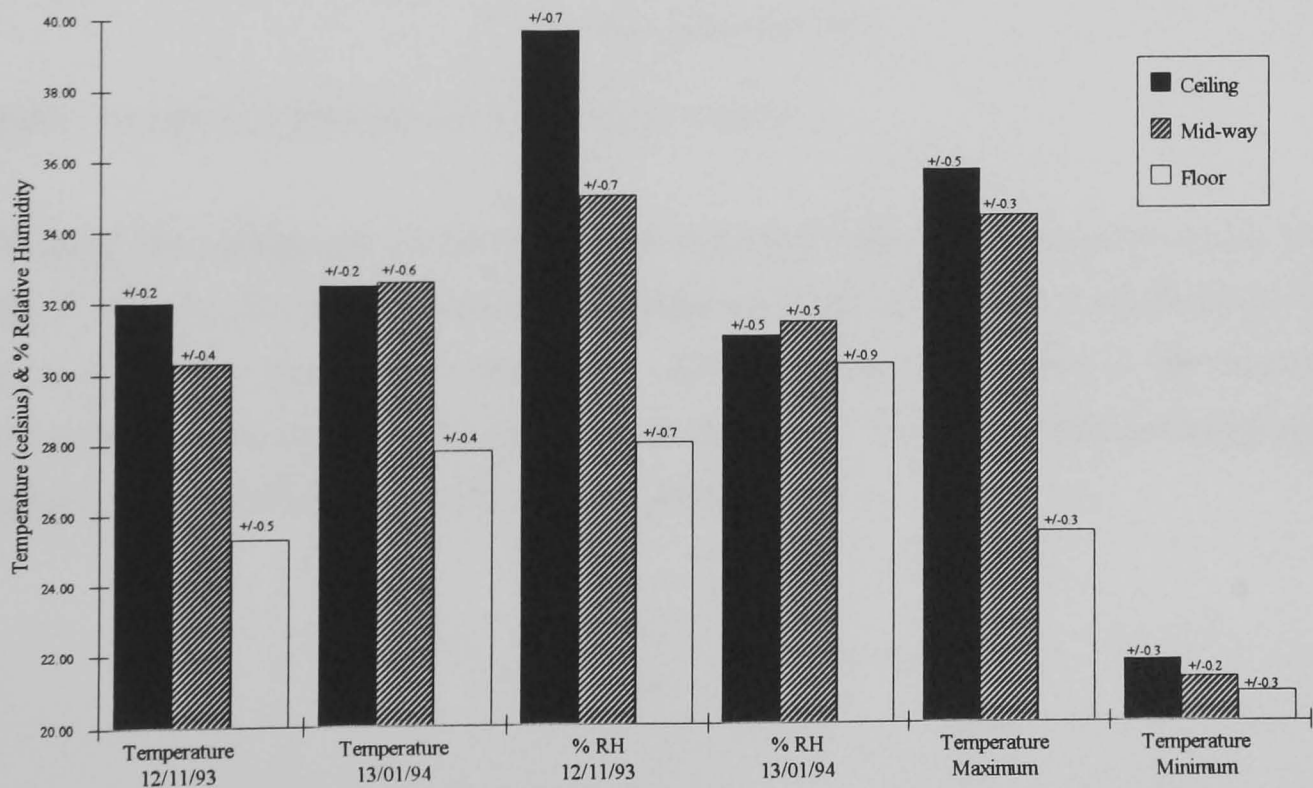


Figure 7.11 Plan view of intensive care room showing the measurement positions for temperature and humidity at three heights; 200 mm from the floor, midway between the floor and the ceiling, 200 mm from the ceiling.

The temperature was measured at several positions within the intensive care room (Fig. 7.11) at three heights; 200 mm from the floor, midway between the floor and the ceiling, and 200 mm from the ceiling. In the areas outside the canopy a temperature stratification was found, the colder areas being close to the floor as would be expected (Fig. 7.12). Temperatures ranged from ~32 °C (40 %rh) at ceiling height to ~30 °C (35 %rh) midway and to ~25 °C (28 %rh) at floor level. The stratification in air temperature was undoubtedly a result of the movement of air through the doors and other openings which were at a lower temperature than the room supply, ~21-25 °C, and cooled the air nearer to the floor. Heat loss through the walls, ceiling and floors also had an effect but perhaps not as great as that due to the forced ventilation. The temperature stratification would make the air more buoyant in the room and enhance the lift of the air towards the ceiling.



Figure

7.12 Variation in temperature and % rh within the intensive care room.

The UCV supply ventilation rates and supply temperatures could be altered in order to control the environment below the canopy and over the bed. The values were discussed in section 7.4.2. Changing the ventilation rates of the UCV had a substantial effect on the average temperatures within the room at ceiling and midway heights which reflected the temperature of the UCV supply and the buoyancy effect of the air. The average temperature near to the floor was unaltered with UCV ventilation at maximum and normal and was dominated by the draughts entering the room. With the ventilation on minimum there was no obvious temperature stratification and the temperature was near to that of the draughts coming into the room.

Under normal operating conditions, the temperature/humidity stratification under the canopy (Fig. 7.13) was not so marked as in the room and the temperatures remained $\sim 33^\circ\text{C}$ (36 % rh). Temperatures over the bed surface ranged from 31.1°C to 32.4°C ($\sim 32.5\%$ rh). The cooler temperatures were to the foot end of the bed, nearest the viewing area room.

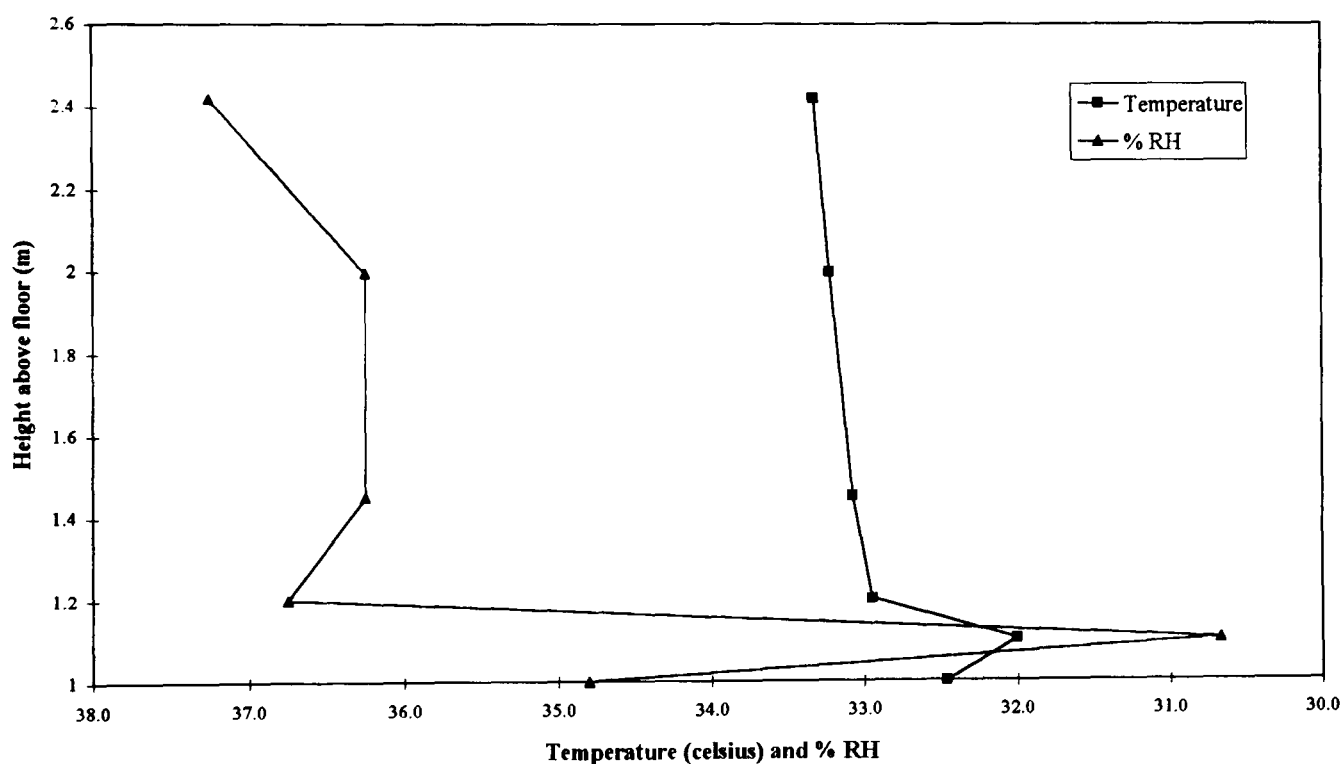
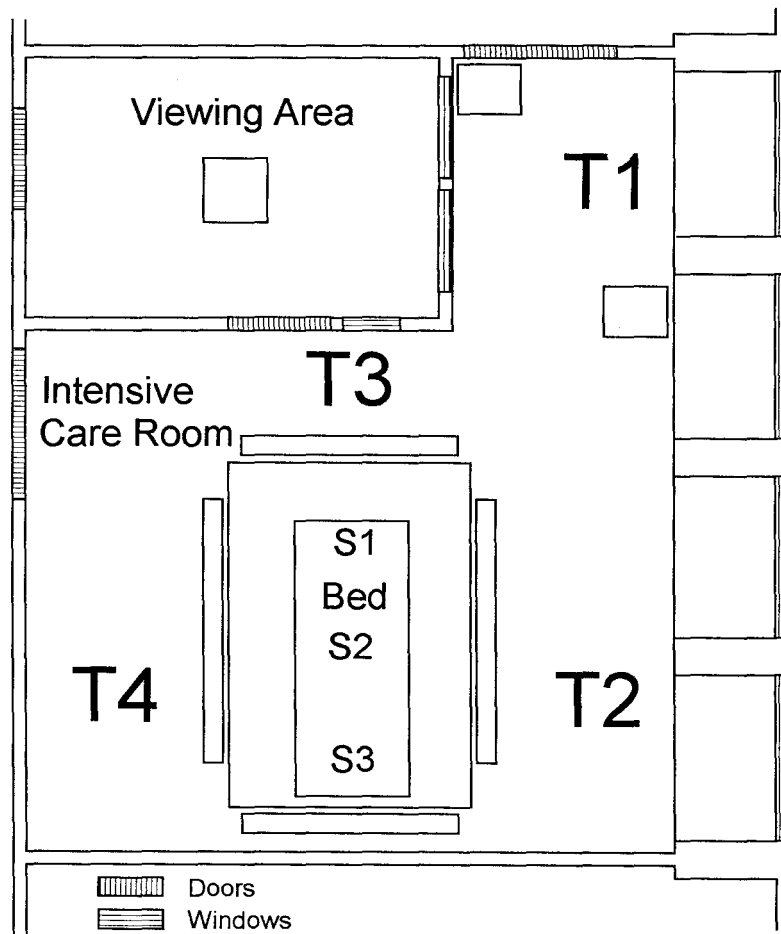


Figure 7.13 Mean temperature and % rh beneath the UCV.

Changing the ventilation of the UCV had a greater effect on the temperature stratification (Fig. 7.14). At the minimum level the temperature did not change significantly, there being only a slight elevation near to the floor. This was likely to be due to the influence of the temperature of the draughts coming into the room and the higher exhaust temperature being discharged from beneath the LALB when switched on.



Layout 1 Tracer release (T) and sample (S) positions within the intensive care room. Tracer was released 200mm from floor level. Air was sampled on the bed surface at the foot end (S1), the middle (S2) and head end (S3).

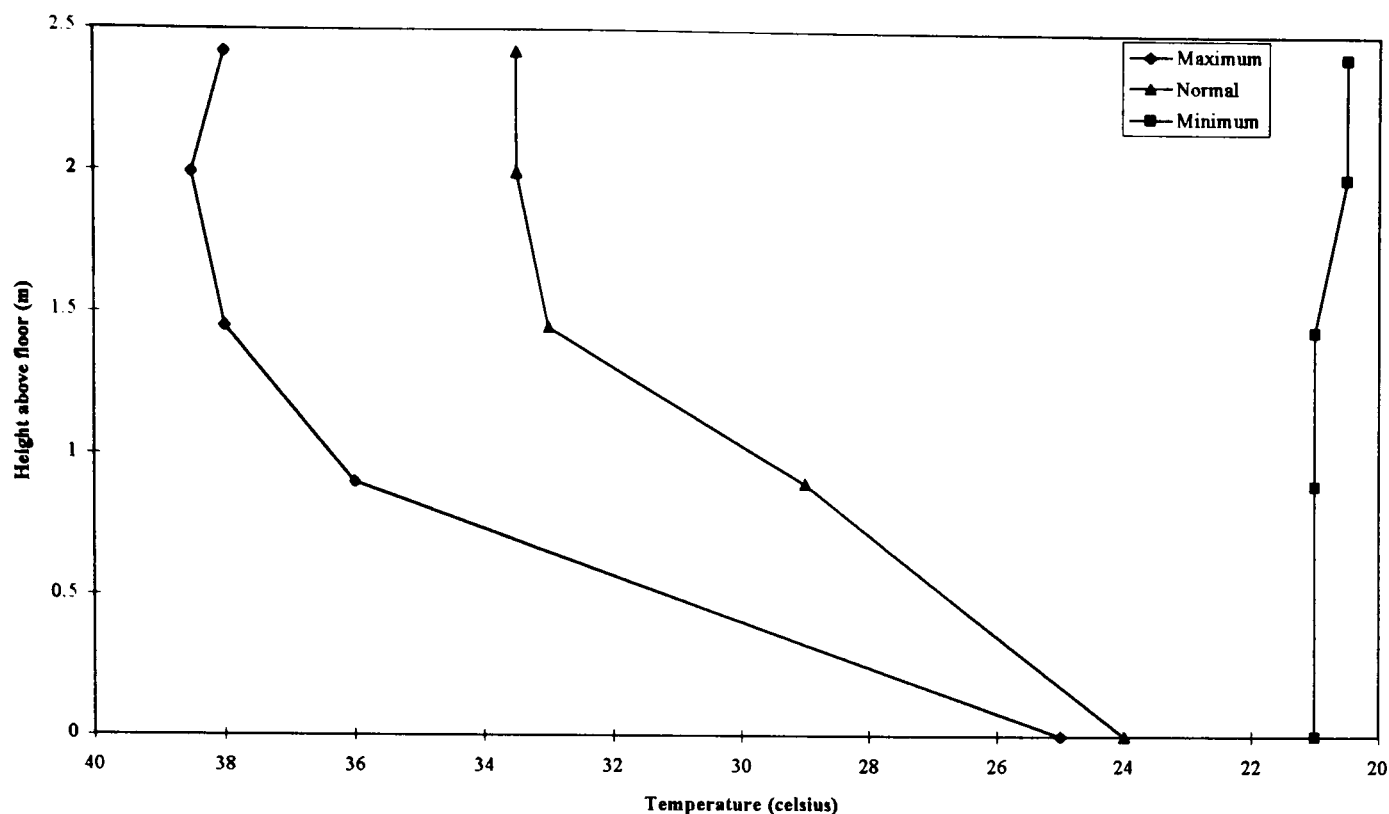


Figure 7.14 Variation of temperature with height beneath the UCV with changing supply ventilation and temperature (measured under quadrant 3).

7.7.4 Nitrous oxide and potassium iodide tracers measurements

Room position	Test	Sample Point on Surface of Low Air Loss Bed (LALB) (Layout 1)		
		Foot End (S1)	Centre (S2)	Head End (S3)
T1	Normal	578	0	0
	During Disturbance	5072	4911	3784
T2	Normal	33	1	0
	During Disturbance	6762	10304	924
T3	Normal	12	2	0
	During Disturbance	732	1399	1040
T4	Normal	5	2	1
	During Disturbance	1566	2158	3273

Table 7.10 The concentration of KI particles sampled at the bed surface (KI/m³ sampled air) with and without disturbance, due to the movement of a person into and out of the ‘clean zone’ near the centre of the bed.

Potassium iodide (KI) tracer analysis suggested a weakness of protection against airborne contamination in the regions towards the foot end of the bed (Table 7.10) where the downward airflow was not as dominant as at the head of the bed. With release of KI particles within the room at four different positions, little was sampled at the middle and head regions of the bed but considerable quantities were found at the foot end. This appeared to be greater when the tracer was released in the position T1 (Fig. 6.7) near to the dressing room door.

When the ‘clean zone’ was disturbed by walking into and out of it (near the centre of the bed), the number of potassium iodide particles measured was several orders of magnitude greater than without disturbance. This demonstrated how particles could be drawn in beneath

the canopy within the human boundary layer over the bed surface (which was observed using smoke).

Room position	Test	Sample Point on Surface of Low Air Loss Bed (LALB) (Layout 1)		
		Foot End (S1)	Centre (S2)	Head End (S3)
T1	Normal	16423	210	0

Table 7.11 Effect of removing restriction in one of the UCV extracts on the concentration of KI particle sampled on at bed surface/m³ of sampled air.

The obstructed UCV extract was unblocked so that the ventilation operated as planned and the tracer tests were repeated (Table 7.11). On this occasion the system was worse, potassium iodide particles being recovered not only at the foot end of the bed but also in the middle as well with no disturbances.

7.7.5 Particle counts

The number of particles measured at various points within the intensive care room did not differ greatly from those measured around the unit and ward (Fig. 7.15). This was not entirely surprising considering the movement of air into the unit from the ward and then into the intensive care room.

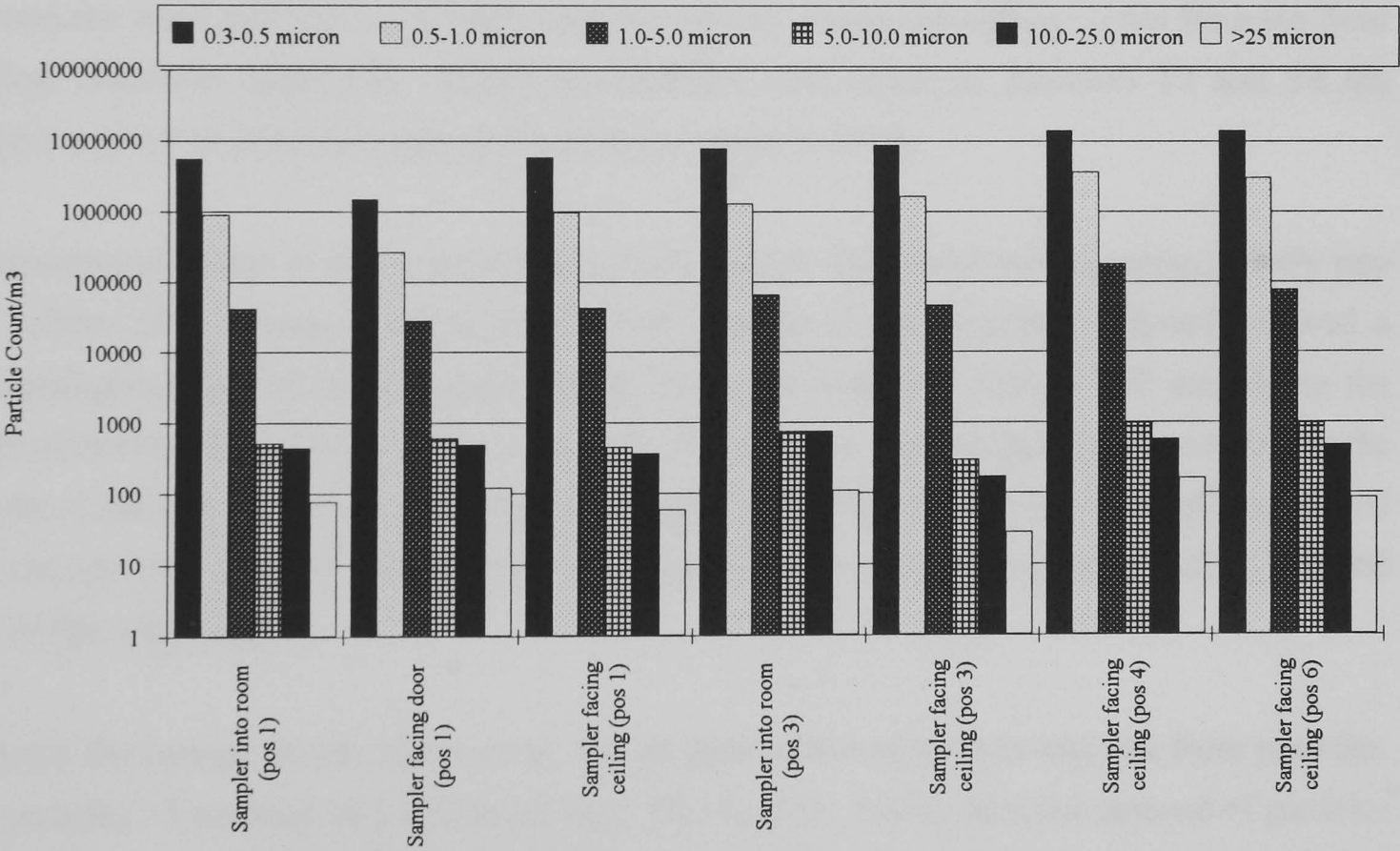


Figure 7.15 Particle counts at various positions within intensive care room. (see Fig. 7.11).

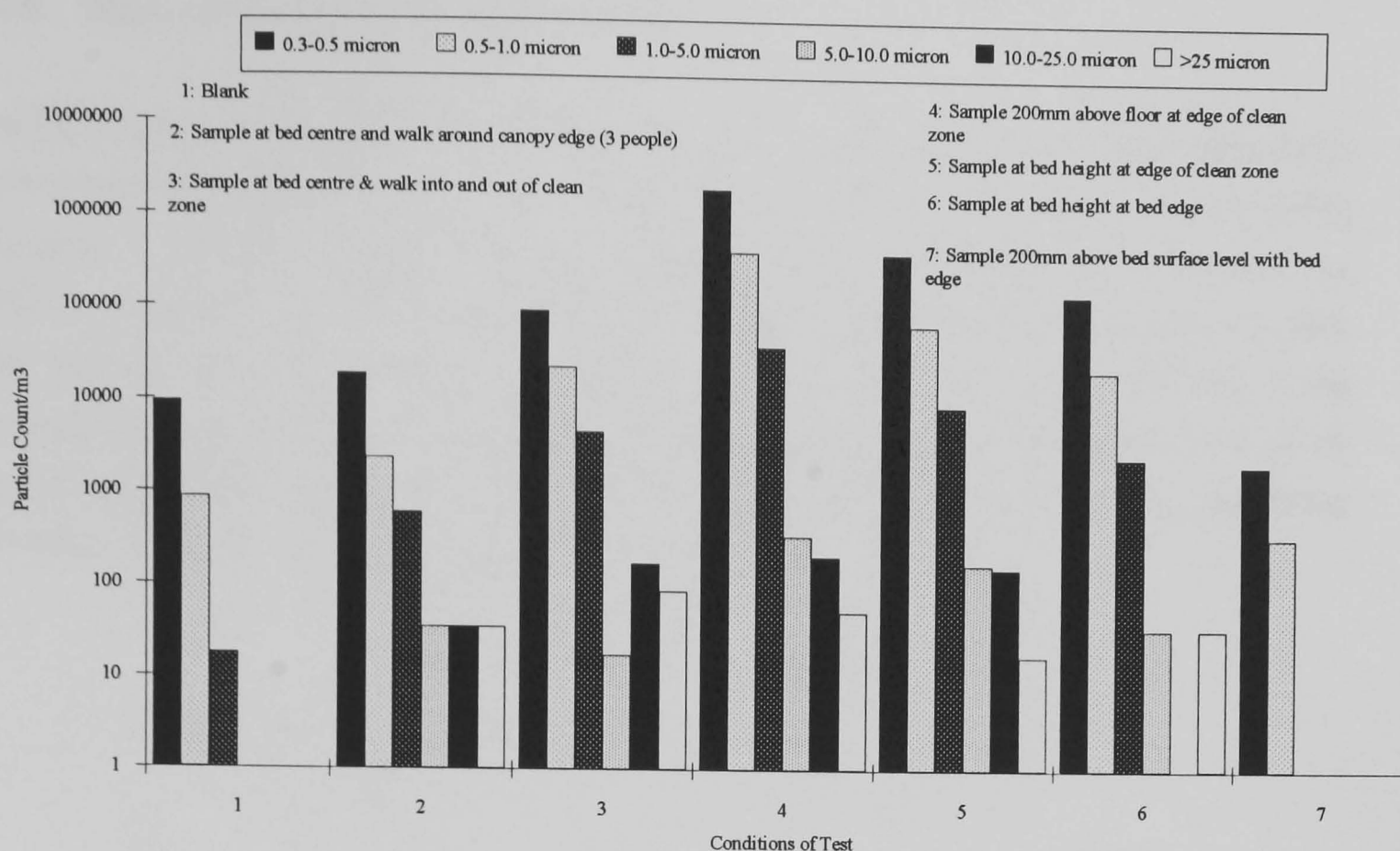


Figure 7.16 Particle size distribution sampled at various points in the intensive care room and under differing conditions.

It was apparent that the position of the particle sampler head had an effect on the number of particles measured. For experimental standardisation purposes, all particle measurements around the ward and unit were made with the sampler facing the ceiling $\sim 0.6\text{m}$ from the floor (unless otherwise specified). Within the intensive care room, at positions T3 and T4 the largest number of particles measured was in the range $5\text{--}10\text{ }\mu\text{m}$.

Measurements made in the intensive care room near to floor level moving progressively into the 'clean zone' towards the top of the bed (middle of side nearest windows) showed a decreasing number of particles (none being measured under the canopy 200 mm above the edge of the bed (Fig. 7.16). There were no particles of size greater than $5\text{ }\mu\text{m}$ measured at the centre of the bed. However during a disturbance of the clean zone by people walking around the canopy edge, a small number were measured which increased as people walked into and out of the 'clean zone'.

Beneath the canopy, in the 'clean zone', the air above the bed surface was free from particles. As particles $>5\text{ }\mu\text{m}$ may be bacteria carrying (Noble et al., 1963), then the absence of particles sampled above the bed surface satisfied the bacteriological requirement of no more than 1 bacteria carrying particle (bcp) per m^3 under the canopy in ultra clean operating theatres. However, around the edge of the bed (up to the top edge) contamination was found which may have arisen from the high number of particles measured within the room. Also, the movement of people under the canopy within the 'clean zone' could have introduced this contamination.

7.7.6 Start-up conditions under the UCV

The UCV was left on standby when the intensive care room was not in use. This maintained a clean environment beneath the canopy with no people in the room, no particles $> 5 \mu\text{m}$ being measured. When the supply ventilation was increased to normal operating conditions, the number of particles $< 5 \mu\text{m}$ measured at the bed surface in the middle increased to a peak after approximately 350 seconds (Fig. 7.17). This may have been due to particles being released from the surface of the HEPA filter as a result of the increased flow rate of air through it, possible leakage of air passed the filter seals or particles on the bed being disturbed. Particles $> 5 \mu\text{m}$ did not increase at start-up.

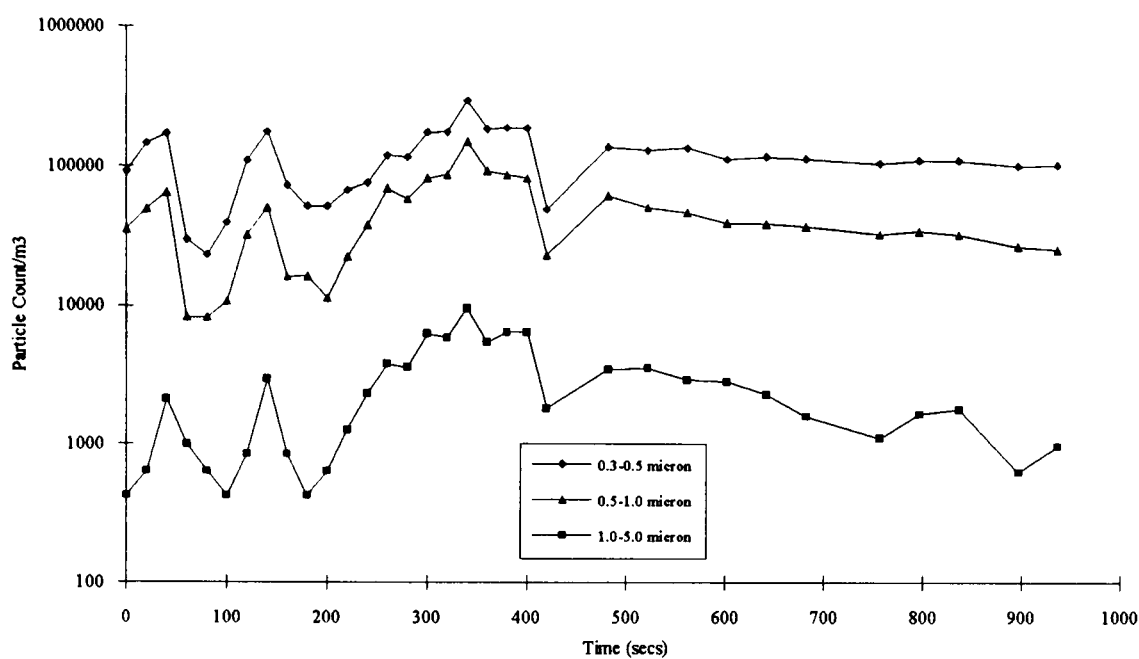


Figure 7.17 Change in particle counts at the bed surface, in the middle (S2), with time during ventilation start-up from standby to normal.

The temperature beneath the canopy (measured next to the mesh, quadrant 3) stabilised reasonably quickly as the supply ventilation was increased to normal operating conditions from standby (Fig. 7.18). A constant value of $\sim 34^\circ\text{C}$ was reached after ~ 40 minutes.

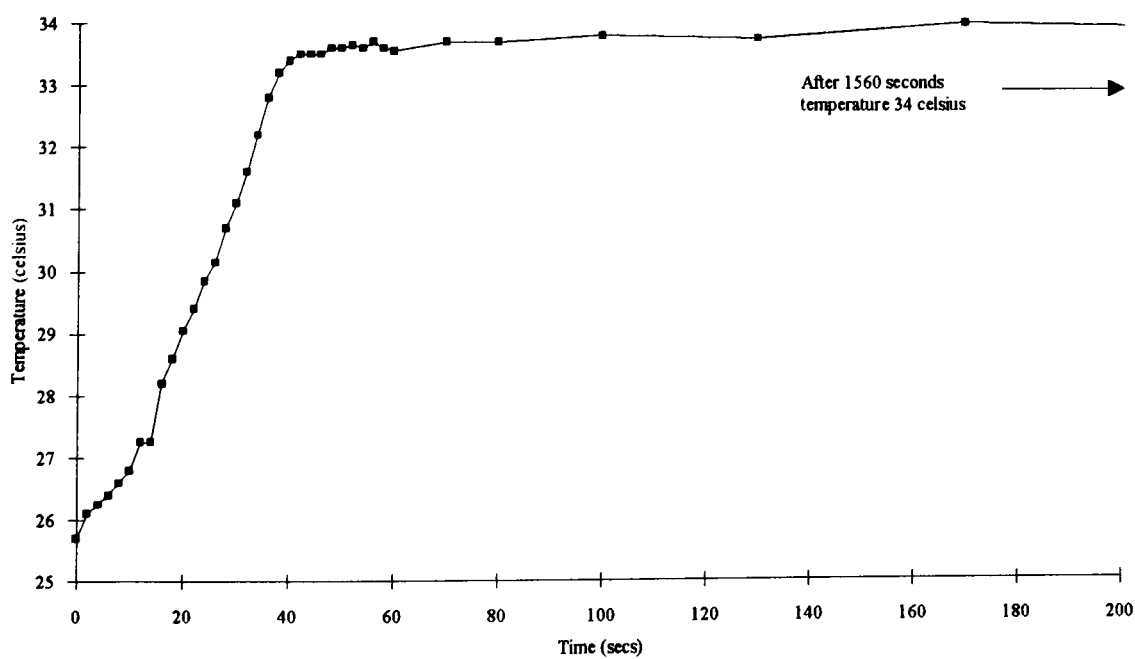


Figure 7.18 Change in temperature with time beneath UCV (quadrant 3) during ventilation start up from standby to normal.

The decay of tracer gas at the middle of the bed surface (Fig. 7.19) indicated the clearance rate of air from the “clean” zone of the UCV. Even allowing for recirculation of the gas through the UCV system, the clearance was of the order of 3 minutes.

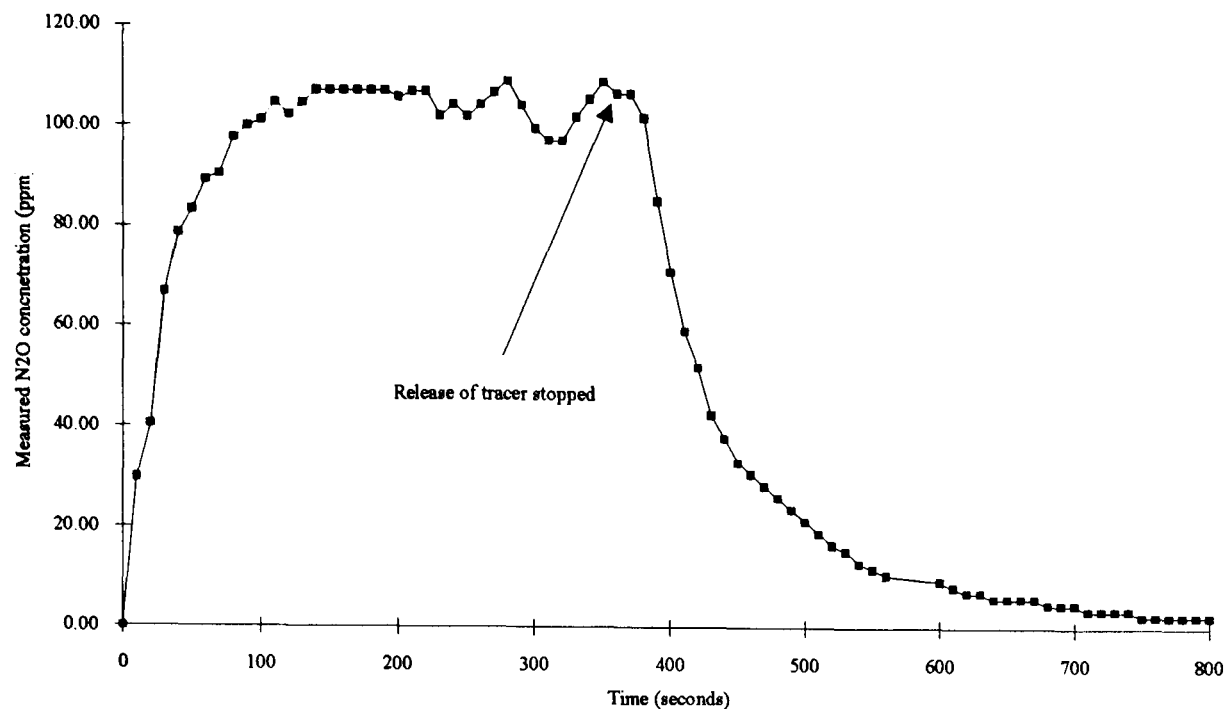


Figure 7.19 Change in N₂O gas tracer measured at the bed surface, in the middle (S2), with time (gas released into UCV extract).

7.8 Conclusions from using physical measurements

7.8.1 Burns unit

The pressures and airflows measured within the burns unit differed from the design specifications because of:

changed plant/control operation and settings

- changed operational procedures (viz. open doors etc.)
- There was effective isolation of the hospital ward from the intensive care room (flow visualisation, gas/particle tracers support this) and potential contaminants did not move from the intensive care room to the hospital ward.
- There was no effective isolation of the intensive care room from the hospital ward (flow visualisation, gas/particle tracers again support this) and potential contamination could move into the intensive care room from the hospital ward.

7.8.2 Intensive care room

- Although measured pressures were similar to the design specifications, the "leaky door" design principle (small areas causing high speed jets) produced draughts which could potentially introduce contamination around the patient.
- There was negligible air flow near to the bed surface at maximum and normal ventilation settings
- Buoyancy effects on the air of the UCV system were apparent.

7.8.3 Entrainment of contamination from staff etc. onto the bed surface in the intensive care room

7.8.3.1 No movement of people in the room

- There was little entrainment of contamination over the bed surface at the middle and head end but more contamination was found towards the foot end.
- The draughts and airflow weaknesses at the foot of the bed were sources of contamination at the bed surface which could be enhanced by environmental disturbance around the canopy, and by air recirculation/movement within the room.

7.8.3.2 People present and moving within room

- The UCV system appeared to be robust when the movement of people in the room was confined to outside the canopy periphery. However, movement in and out of the 'clean zone' allowed contamination to be drawn over the bed surface.

7.9 Results and discussion of air flow simulations within the intensive care room using computational fluid dynamics (CFD) based on physical measurements and design data

7.9.1 3 dimensional problem set-up using measured data

The computational fluid dynamic software (Flovent, Flomerics Ltd.) was not developed for the simulation of airflows within multiple ventilated zones. As the burns unit had a number of zones (viz. operating theatre, intensive care room, dressing room and airlocks) it was not assessed as a whole. Instead, attention was focussed on the intensive care room as this was where the patient would be considered to be at most risk from cross infection for the same reasons most of the physical measurements were made in this room.

The intensive care room was represented as a three dimensional model (Fig. 7.20) over which a solution grid was laid simple enough to limit calculation time but complex and refined enough to represent important ventilation points and obstructions (Fig. 7.21). The measured data at normal ventilation settings were used (viz. 33 °C supply temperature, 0.56 m/s supply velocity, measured at the diffuser and an ambient temperature of 20 °C).

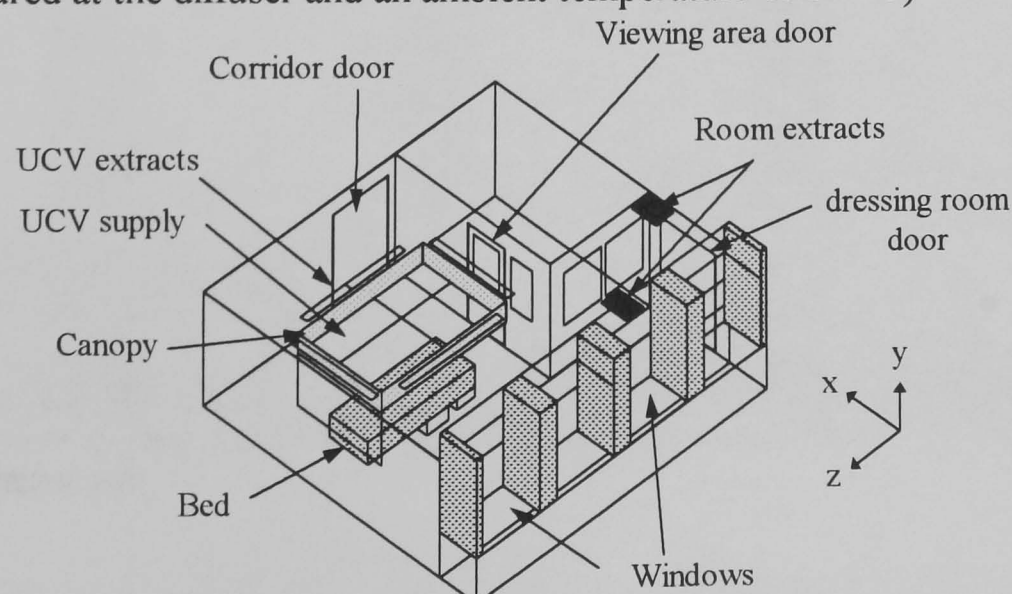


Figure 7.20 Computational 3 - Dimensional view of the intensive care room.

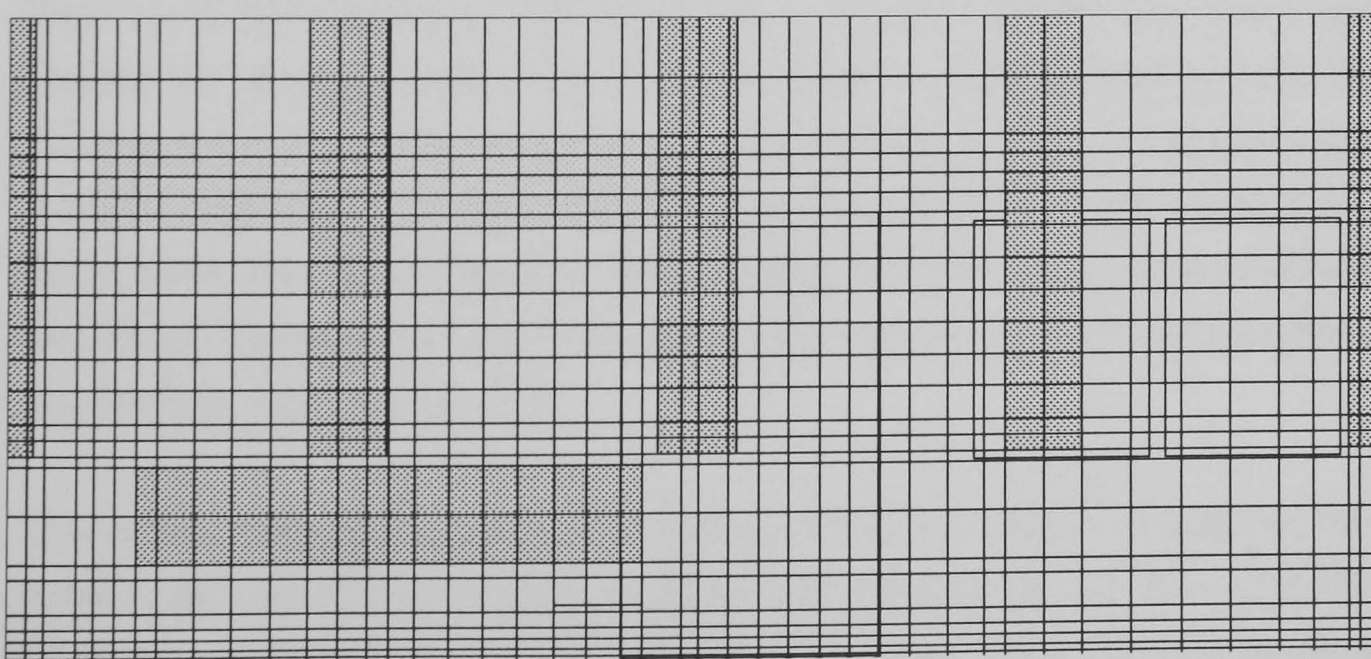
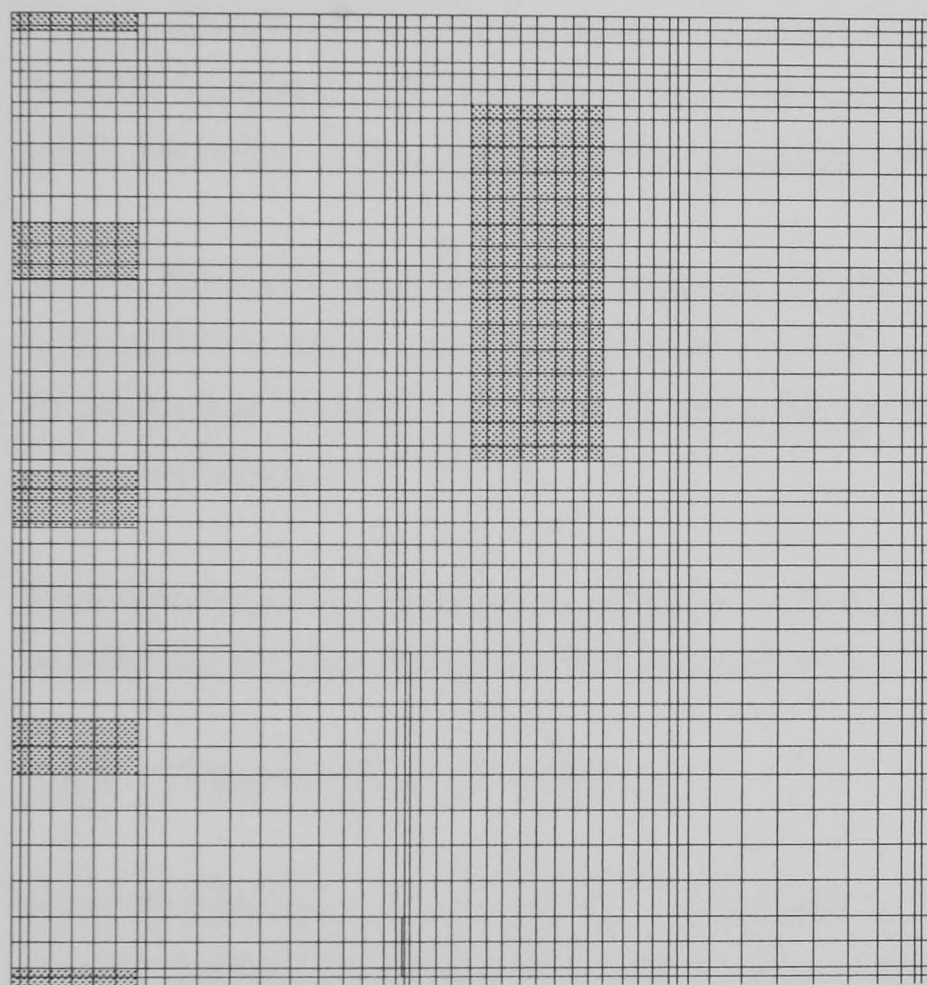
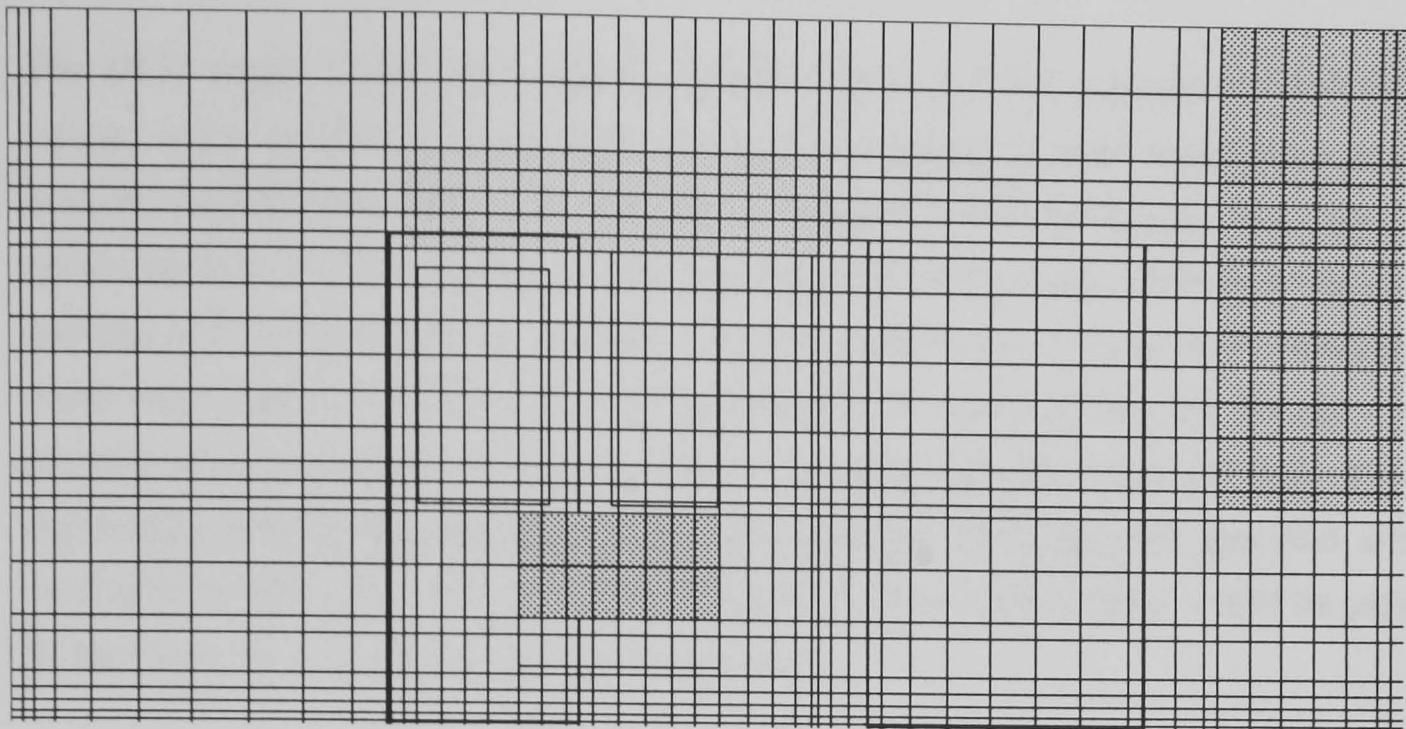


Figure 7.21 End view xy (top), plan view xz (middle) and side view yz (bottom) of intensive care room showing CFD solution grid

The UCV supply, subdivided into quadrants, with two UCV extracts on each side of the canopy were detailed to accurately represent the measured data over these areas. The draughts beneath the doors were specified as supplies with a fixed mass flow rate using the measured data and not simply as openings because the pressure difference varied at each opening and were difficult to estimate. However, there was a small mass imbalance in the room which had to be allowed for by specifying some openings into the domain. From the physical measurements there were numerous draughts into the room (through drawers and cupboards) which were difficult to estimate. Instead, openings were specified around the vertical sides and tops of the doors; the passive air flow around these would be expected to be less than that specified underneath the doors.

Heat losses from the domain through the boundary walls and windows were calculated by the software program using measurements of the external wall temperatures from the Raytek infra - red device or near wall temperatures using the platinum resistance thermometer.

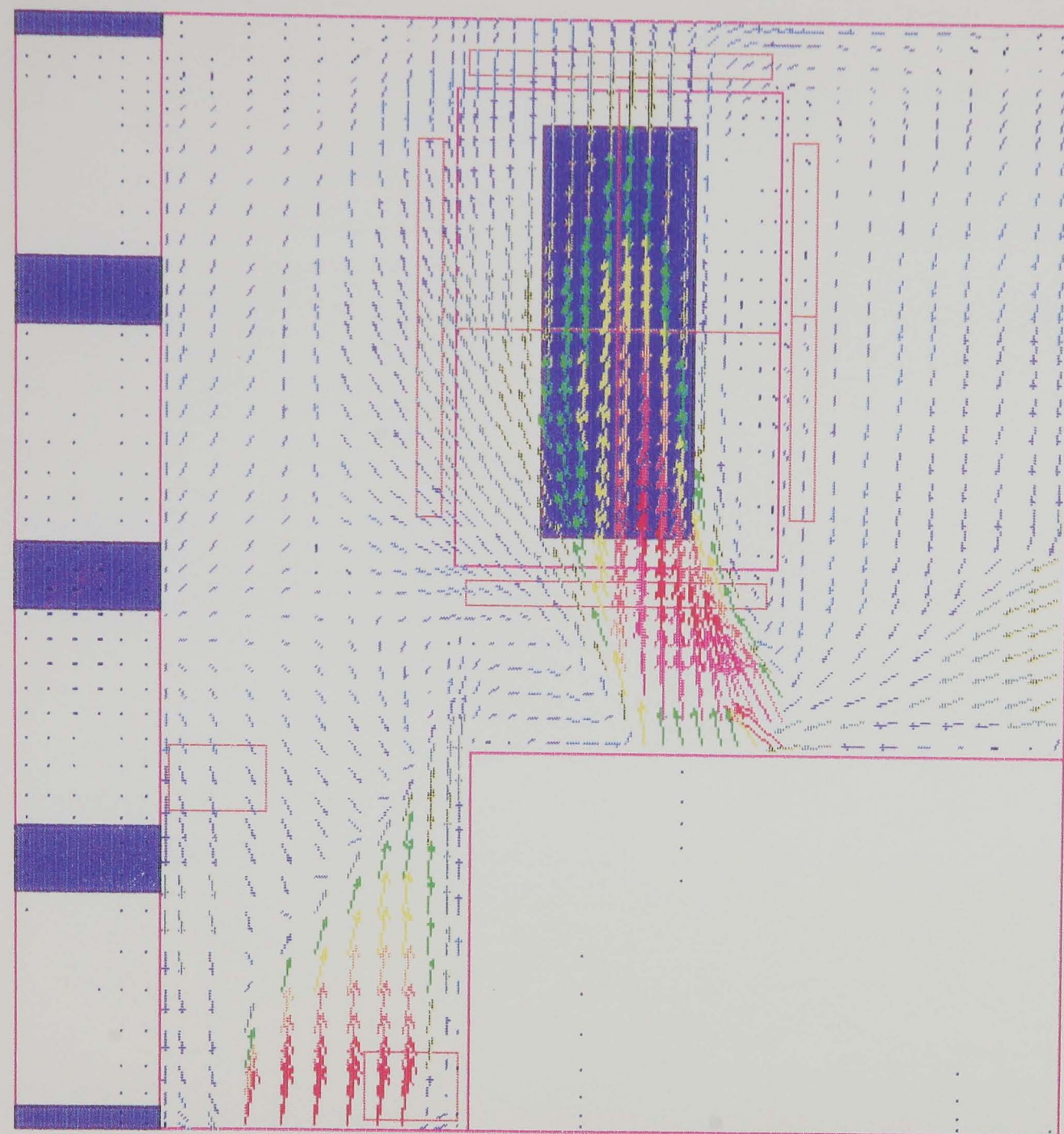
The air flows that were observed within the solution domain using physical measurements were turbulent and for accurate simulation a turbulence intensity was expressed as a multiple of the laminar viscosity, calculated from the characteristic velocity and length of the UCV supply ventilation.

Each simulation was run as steady state, i.e. until an equilibrium within the room was reached, and the solution time was between two and three days on a PC 486, 66 MHz processor.

7.9.2 “Visualisation” of airflows

Once the simulation was complete it was possible to view the air flows within the room as vectors (showing magnitude and direction), from any angle and any plane. It was clear from these views how dominant were the air flows into the intensive care room, moving from beneath the viewing area door into the room, under the bed, around the back wall and past the foot of the bed and viewing area towards the room extracts. It was also clear how the draughts from beneath the doors influenced the flows near to the floor (Fig. 7.22), and how the air flows from the simulated openings around the doors disturbed the air flow near to the foot end of the bed (Fig. 7.23). Near to the ceiling the air flows were influenced by the UCV and the room extracts (Fig. 7.24).

The air flow beneath the canopy and its movement over the bed showed the air moving down towards the bed and being lifted outwards and upwards towards the UCV extracts (Fig. 7.25), the net surplus of air being pulled into the room. The air flow over the bed moved from the head to the foot end, the fitment of the screen at the head end influenced this movement (Fig. 7.26). At the foot end of the bed, air flowing downwards was entrained in the horizontal flow and did not reach the bed surface but was pulled outwards and upwards.



Vector
(m/s)

2.336

2.002

1.668

1.335

1.001

0.667

0.334

0.000

y=2.5000E-02



1.50

Ref Vector

Job: ICRMEAS

Title: Burns Intensive Therapy Room (as measured)

Figure 7.22 Airflow vectors in the xz plane near to floor level in the intensive care room.

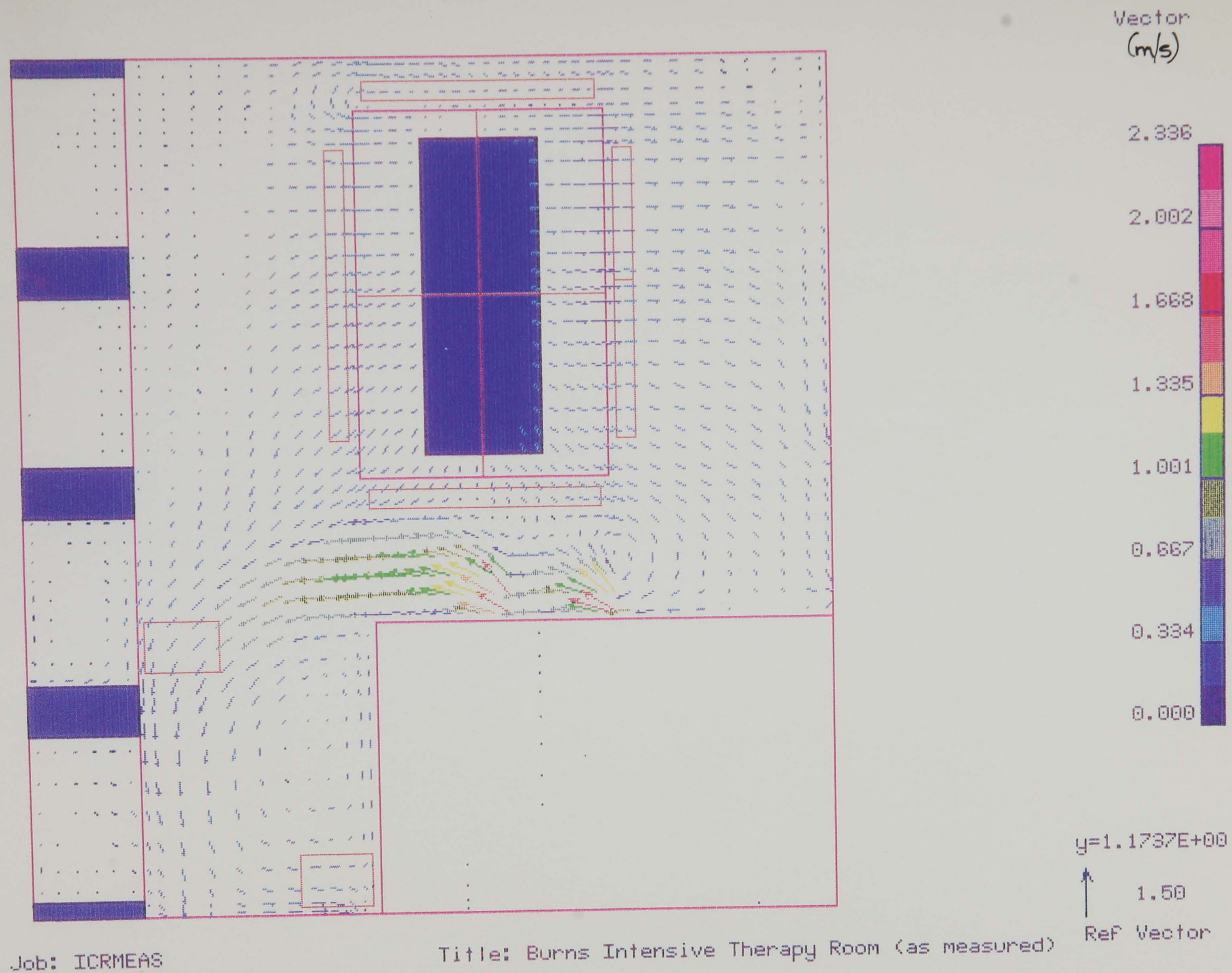


Figure 7.23 Airflow vectors in the xz plane at midheight (near to bed surface height) in the intensive care room.

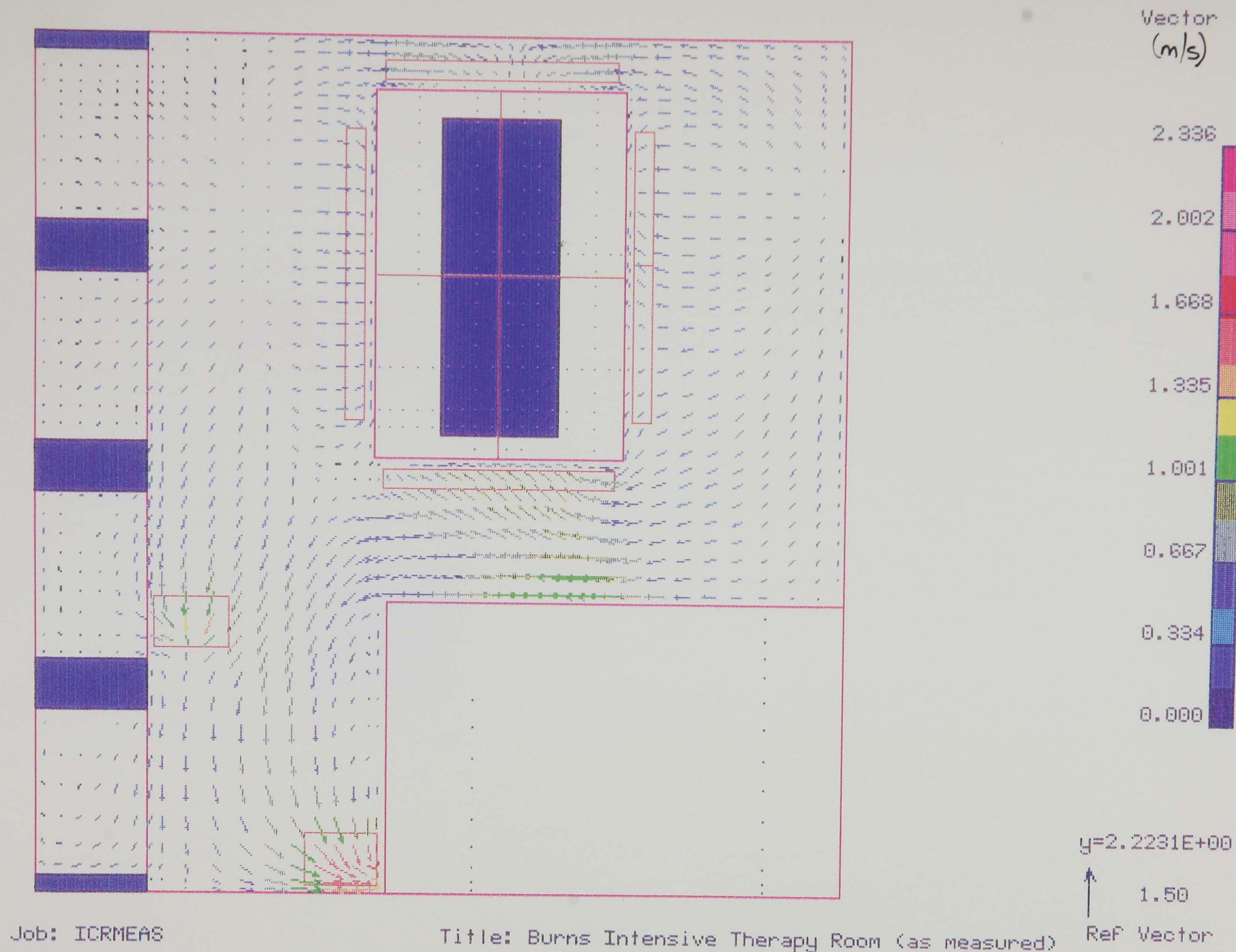
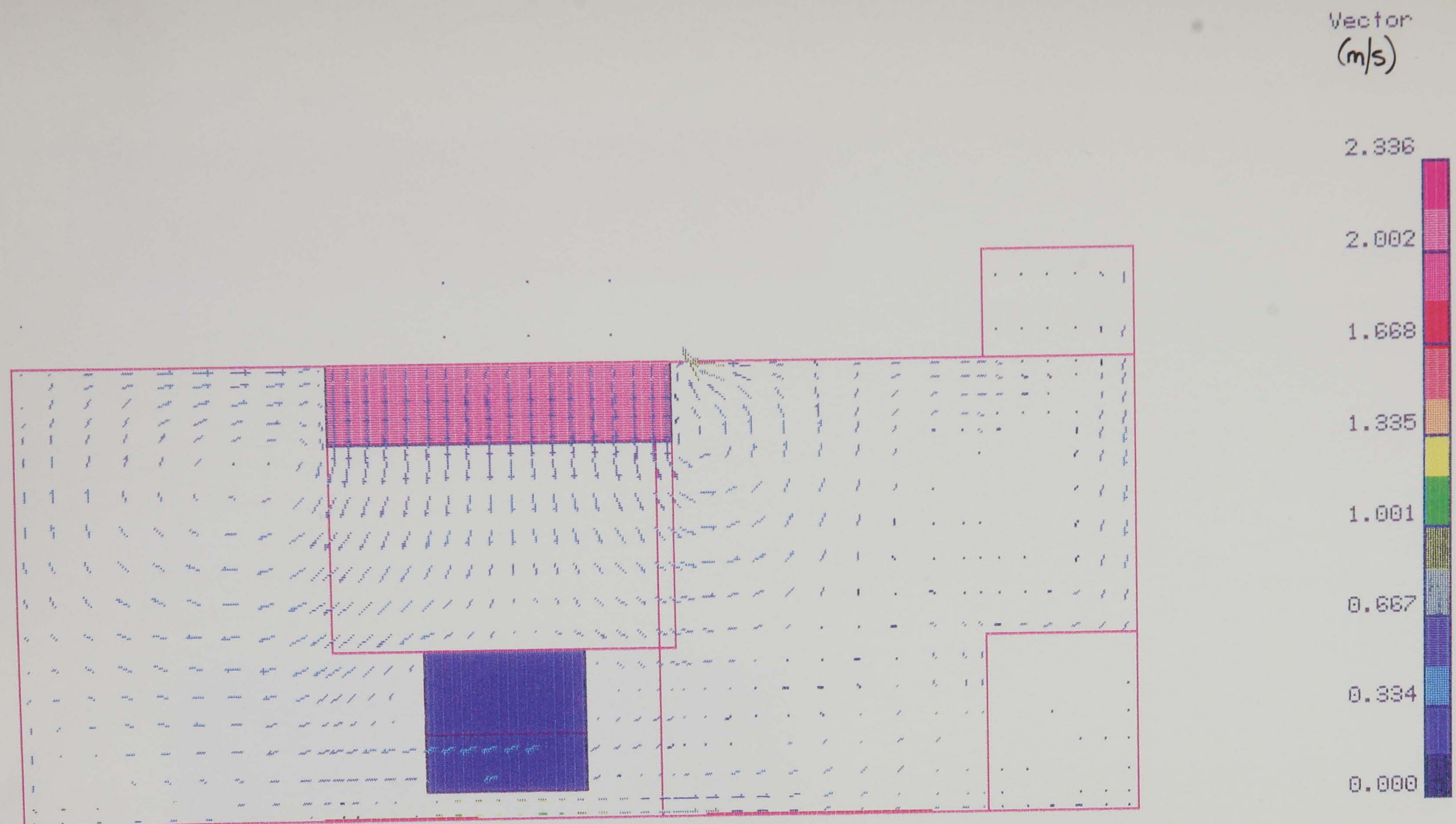


Figure 7.24 Airflow vectors in the xz plane near to the ceiling in the intensive care room.



$z=4.4875E+00$



1.50

Ref Vector

Job: ICRMEAS

Title: Burns Intensive Therapy Room (as measured)

FLUENT

Figure 7.25 Airflow vectors in the xy plane centreline of the UCV.

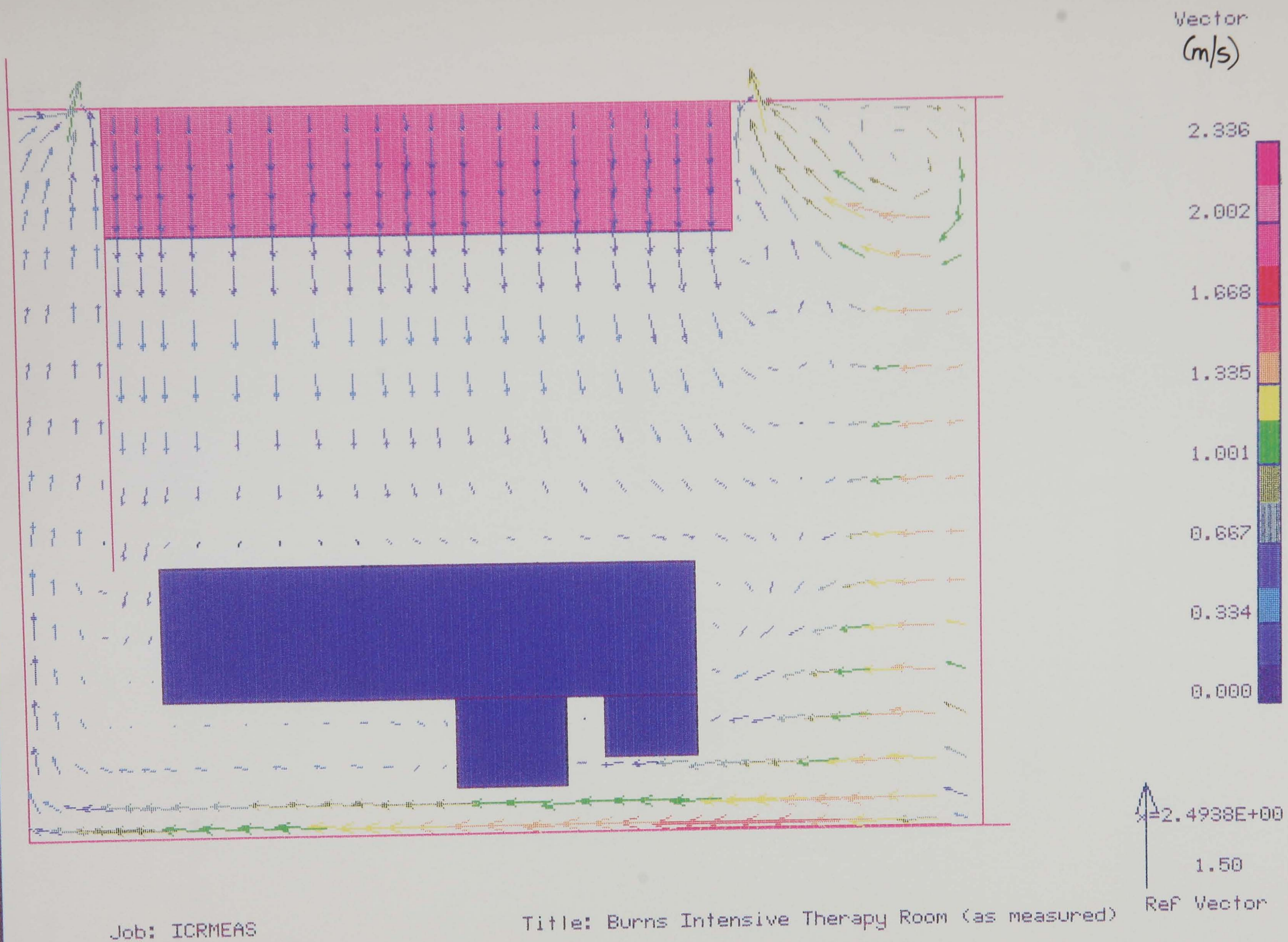


Figure 7.26 Airflow vectors in the yz plane centreline of the UCV.

The area at the foot end of the bed was thus ventilated by air flowing from the canopy at the head end.

7.9.3 Velocity data below UCV

There was no loss in Y velocity or speed over the distance between the supply diffuser and the edge of the canopy (Fig. 7.27). Between the canopy and the bed surface there was a substantial drop in Y velocity and speed and the Y velocity calculated near to the bed surface was < 0.1 m/s. There was a disparity between the Y velocity values and speed values calculated beneath the canopy due to the change in air flow direction from vertical component (Y) to the horizontal components (X and Z). This was further shown when only those values over the bed area were used which showed a vertical component < 0.05 m/s and a speed of 0.2 m/s (Fig. 7.28).

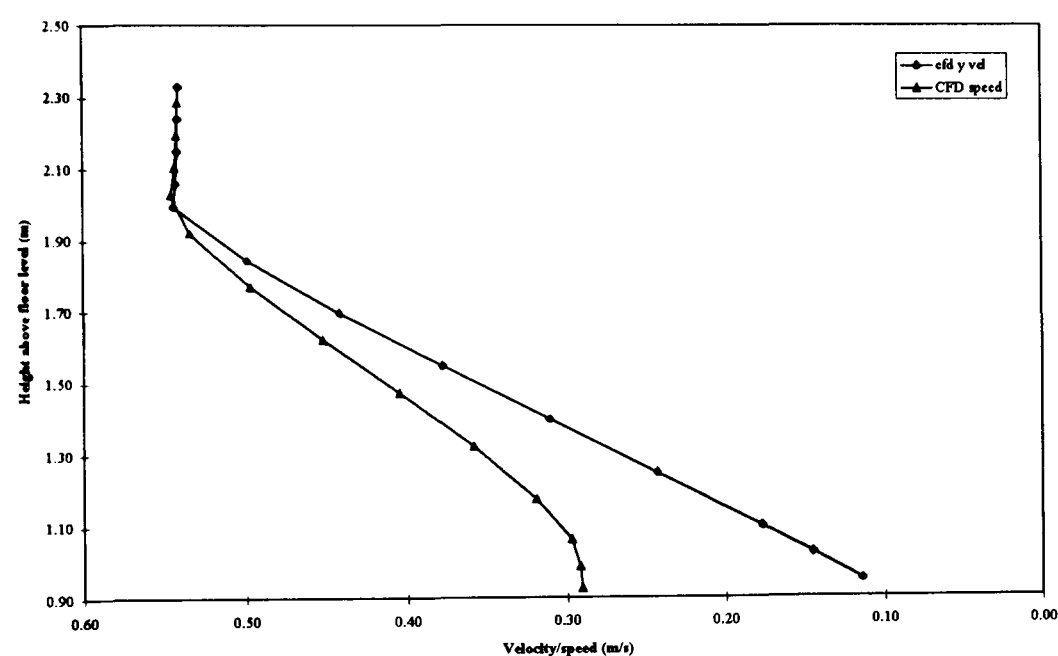


Figure 7.27 Mean y velocity and speed profiles with height beneath the UCV canopy.

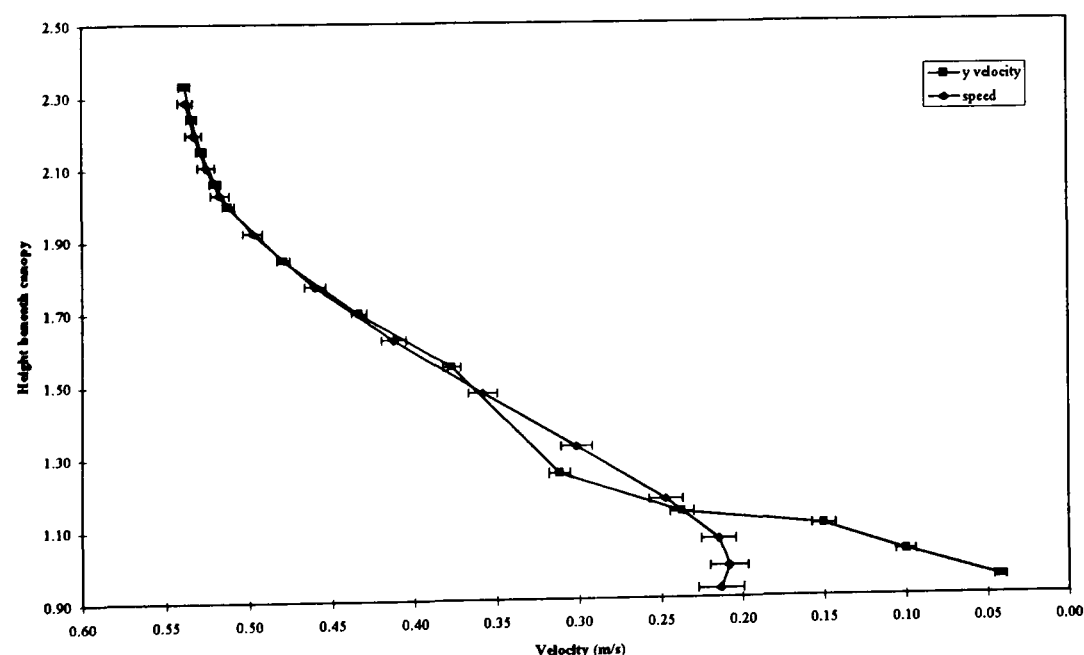


Figure 7.28 Mean y velocity and speed profiles with height beneath the UCV over the bed area only.

7.9.4 Air temperature distribution

The distribution of air temperature within the room (Fig. 7.29) represented those positions used to make the physical measurements (Fig. 7.11). There was an obvious stratification with

height from 30 °C near the ceiling to 21 °C near to the floor. However, the temperature increased to 33 °C in the regions near to the corridor wall and near the windows. This probably reflected the movement of air from the canopy and the limited solution grid refinement near to the ceiling, which was at a lower temperature.

The temperature of the air calculated on the corridor side of the UCV was higher than the window side by approximately 2 °C. This reflected the air movement visualised and the effect of the colder draughts entering the room. This was most marked by the values calculated near to the viewing area door and the dressing room door which were around 6 °C at mid height less than the air temperature on the window side of the UCV. In these regions the draughts at only 20 °C would seem to be having a substantial effect on the room air temperature.

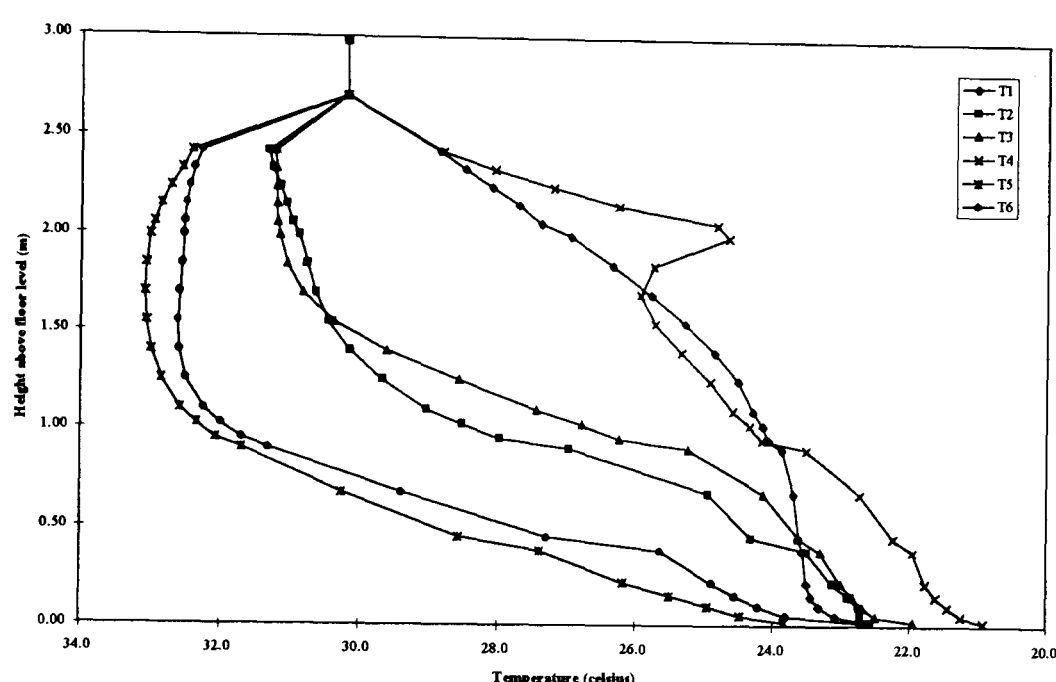


Figure 7.29 Air temperature distribution within the intensive care room. (see Fig.7.11).

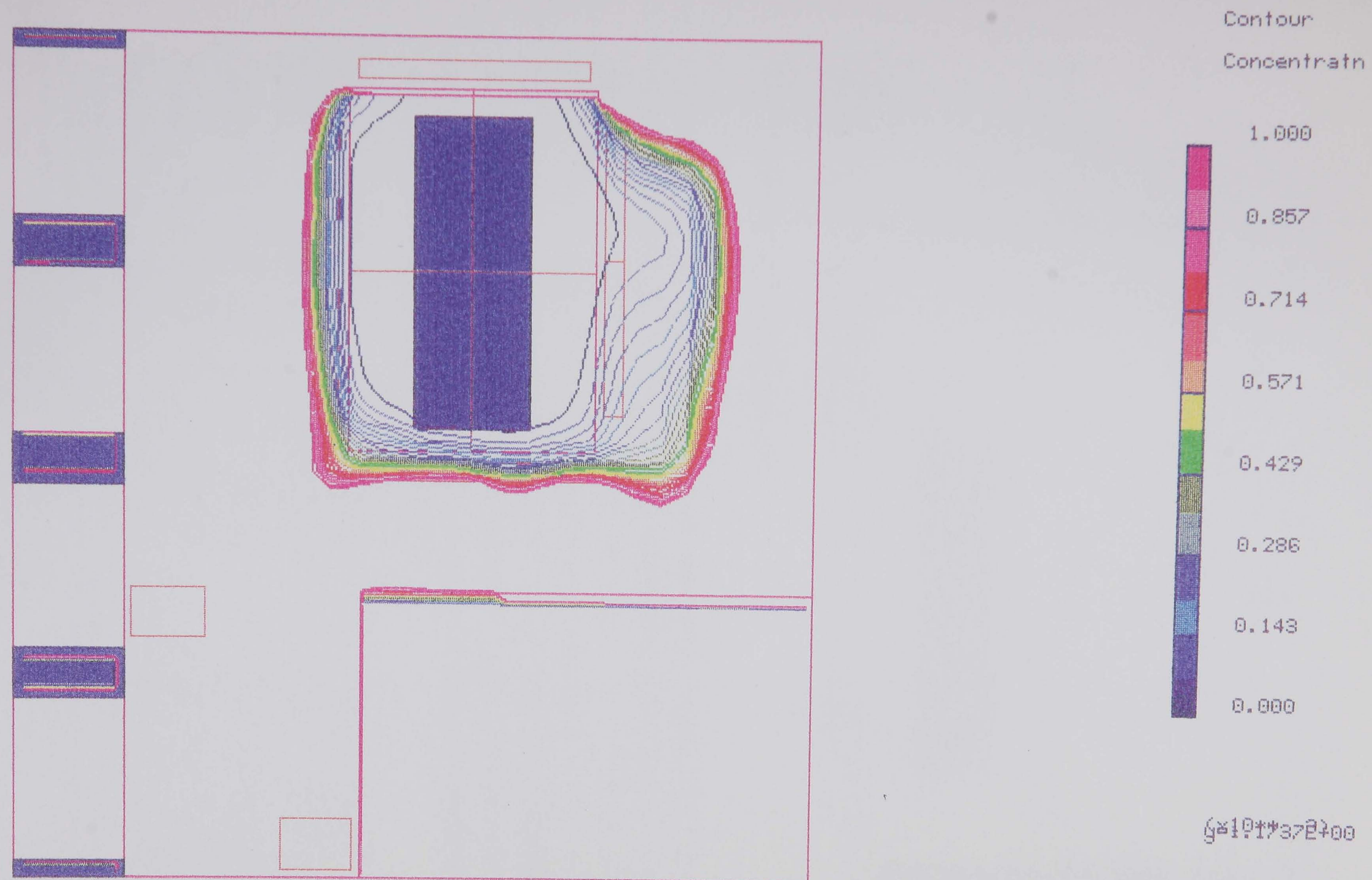
7.9.5 Air temperature data below UCV

There was little change in air temperature with height beneath the UCV canopy area or the area over the bed (falling by < 1 °C).

7.9.6 Distribution of a contaminant

In order to represent the movement of potential contamination into and within the room from the rest of the Unit and to estimate the effectiveness of the UCV to prevent contamination of the bed surface, a massless contaminant source ($1 \text{ kg}_{\text{contaminant}}/\text{kg}_{\text{air}}$) was introduced into the airflows beneath the doors. This source could be distributed with the air only and not be affected by gravity, its diffusion would be that of a gas in air.

The simulation showed that the contaminant became well mixed at steady state within the room and the UCV effectively prevented the distribution or diffusion of the contaminant over most of the bed surface. However, the contaminant encroached beneath the canopy at the



Job: ICRMEAS

Title: Burns Intensive Therapy Room (as measured)

Figure 7.30 xz tracer concentration profiles at midheight (near bed surface height) in the intensive care room when released in the airflows beneath the doors.

edges and near to the foot end of the bed (Fig. 7.30). From the profile from head to foot end over the centre of the bed it was clear that there was contaminant over the foot end of the bed and under both edges of the canopy (Fig. 7.31).

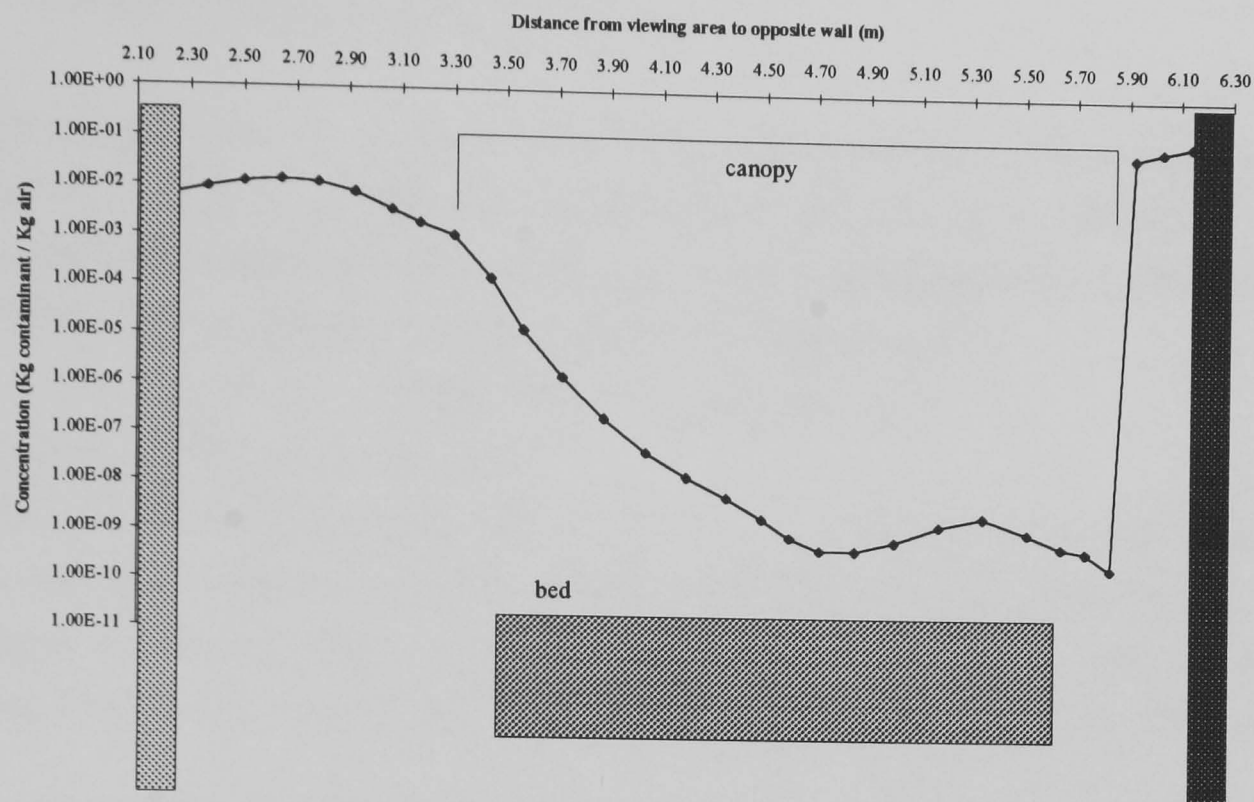


Figure 7.31 Tracer concentration profile along the centreline of the bed surface from the head to the foot end when released in the airflows beneath the intensive care room doors.

7.9.7 Simulation using design data

The simulation was repeated at the normally used supply temperature of 33 °C but the velocity was interpolated from the design specifications at the minimum and maximum settings; 20 °C, 0.38 m/s and 40 °C, 0.51 m/s (Table 7.12). The design criteria was to specify 'leaky' doors in order to allow passive room “make-up” air to pass. This was 0.03 m³/s to pass around the corridor door, 0.06 m³/s to pass around the viewing area door and none to pass around the dressing room door when the two room pressures were balanced. In order to simulate this the air was specified as a fixed mass flow and distributed equally to enter through small gaps around the relevant doors.

Supply Status	Supply Temp.	Supply %RH	Supply* Vel. (m/s)	UCV Supply	UCV Extract	Room Surplus	Room Extract	Make-Up Air
Design	20.0°C	40-50%	0.38	1.843	1.310	0.533	0.624	0.091
Design*	33.0°C	40-50%	0.47	2.280	1.747	0.533	0.624	0.091
Design	40.0°C	40-50%	0.51	2.474	1.940	0.534	0.624	0.091

Table 7.12 Design air supplies and extracts (m³/s) in the intensive care room. * These data are interpolated from the recommended figures at supply temperatures of 20°C and 40°C. They also allow for leaky doors by design which are 0.03 m³/s of air flowing through the corridor door, 0.06 m³/s of air flowing through the viewing area door and none across the dressing room door.

The simulation when completed 'visually' showed very similar results to the simulation using the measured data. There was still the obvious effect of the draughts from around the

periphery of the doors which had a profound effect on the general circulation of air within the room and the disturbance of air flow at the foot end of the bed.

7.10 Conclusions from CFD simulations

- The draughts into the intensive care room dominated the air flows near to the floor and the ceiling mounted extracts which affected the general air movement. This was similar both basing the model on the physical measurements and on the design data.
- There was negligible downflow of air near to the bed surface
- Air flowed from the head end of the bed to the foot end
- Buoyancy effects were apparent
- There were turbulent regions near to the foot end of the bed near to the viewing area
- A massless contaminant source, seeded into draughts from beneath the boundary doors was mixed within the room air and encroached beneath the canopy and the over the foot end of the bed. There was none at the middle and head end of the bed.

7.11 Use of CFD and physical measurements for analysing design changes

7.11.1 Problems identified within intensive care room affecting contamination control performance

- The circulation of air was not ideal due to:
 1. make-up air and draughts
 2. position of ventilation supplies and extracts
 3. buoyancy of supply air
- Limited effectiveness of the air flow pattern beneath the UCV canopy to prevent entrainment of contamination from the room

7.11.2 Proposed design changes

- Alter the room ventilation supply and extract positions
- Diffuse the draughts into the intensive care room
- Move the viewing area door to the side wall of the viewing area
- Extend the UCV canopy nearer to the floor

7.11.3 Effect of room ventilation supply and extracts on UCV performance (2 dimensional CFD simulations)

7.11.3.1 Simulation set up

In order to simulate the effect of changing the supply temperature, velocity and subsequently the effect of the position of the supply and extracts on the performance of the UCV, a simplified 2 dimensional simulation was set up. This used the essential ventilation characteristics of the intensive care room identified from the physical measurements, design data and the more complex 3 - dimensional CFD simulation. It was apparent from these

measurements and data that the higher than ambient supply temperatures and the cooler draughts at floor level resulted in a temperature stratification within the room giving buoyant lift of the air under the canopy and in the room itself. At lower supply temperatures (i.e. minimum settings) there was no temperature stratification and no buoyant effects. In addition the effect of high level extracts was seen to enhance the lift of air flows toward the ceiling. All this was to limit the air flowing down toward the bed surface and to increase the potential of contamination of the bed surface from the room air.

The 2 - dimensional solution domain was a vertical cross section (end on) of the UCV supply / extracts and the bed. The simulations were with open boundaries at each side (Fig. 7.32) and then with solid boundaries but with openings and extracts at either high or level in these walls (Fig. 7.33). The supply temperature and velocity was either 20 °C, 0.38 m/s (minimum setting) or 40 °C, 0.51 m/s (maximum setting). The solution grid shown in Figure 7.34 was laid over the domain and the turbulence model selected was a multiple of the laminar viscosity based on the supply ventilation rate. There was no heat loss from the solid boundaries, but the ambient temperature at the openings and extracts was 20 °C.

In order to simulate the spread of a contaminant species within the domain, this was specified as a planar source of $1 \text{ kg}_{\text{contaminant}} / \text{kg}_{\text{air}}$ at the openings to the domain.

7.11.3.2 Change in UCV performance with supply velocity / temperature (open boundaries)

At the supply temperature of 20 °C and velocity 0.38 m/s there was no temperature stratification in the room, the whole domain was at 20 °C. At the higher supply temperature of 40 °C and velocity of 0.51 m/s there was a 15 °C difference between the air near to the ceiling (35 °C) and the air near to the floor (20 °C). At the minimum setting the air flowed downwards from the canopy over the bed and to the floor (Fig. 7.35). There was sideways movement from the bed surface outward into the room, across the floor and then up to the ceiling mounted extracts. There was negligible distribution of contamination in the domain beneath the canopy and as a profile across the bed surface (Fig. 7.38).

At the maximum used settings the air flowed down from the canopy but barely reached the bed surface (Fig. 7.37) and the vector values were for air flowing upwards from the bed surface. This was the same for the whole domain where the air was flowing towards the ceiling and the recirculation of air into the ceiling extracts was very close to the ceiling (Fig. 7.36). The contaminant species was well mixed within the room and the concentration over the bed surface was the same as at the openings (Fig 7.38).

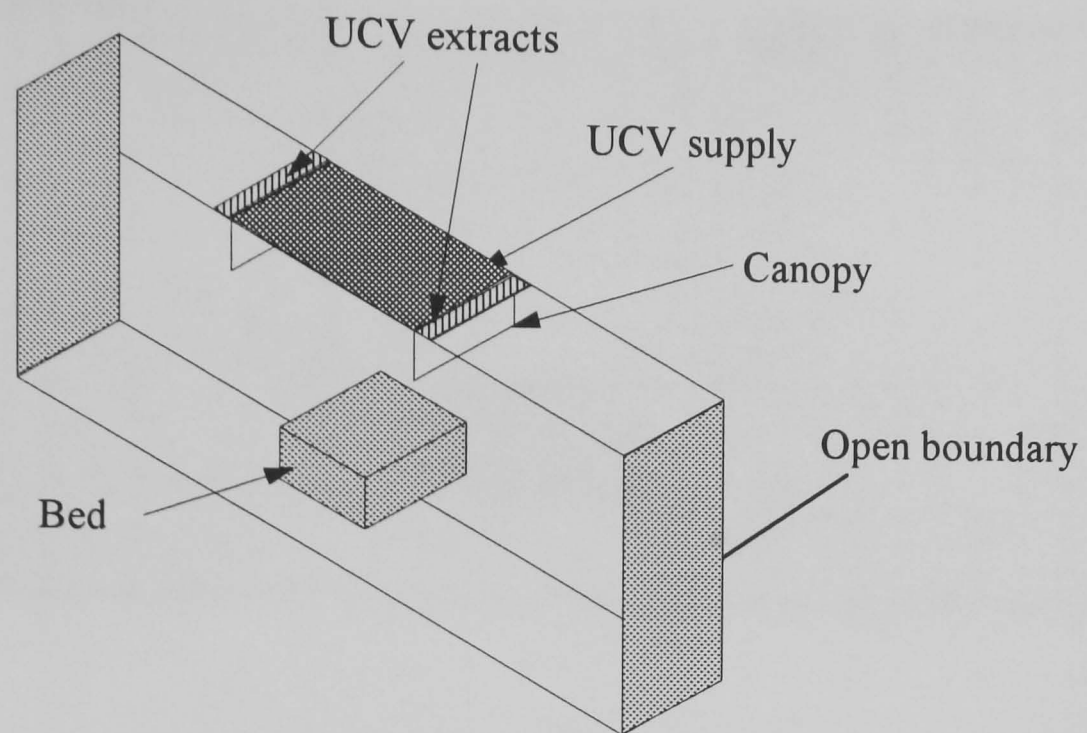


Figure 7.32 2 Dimensional domain of UCV canopy, supplies and extracts. Open boundaries.

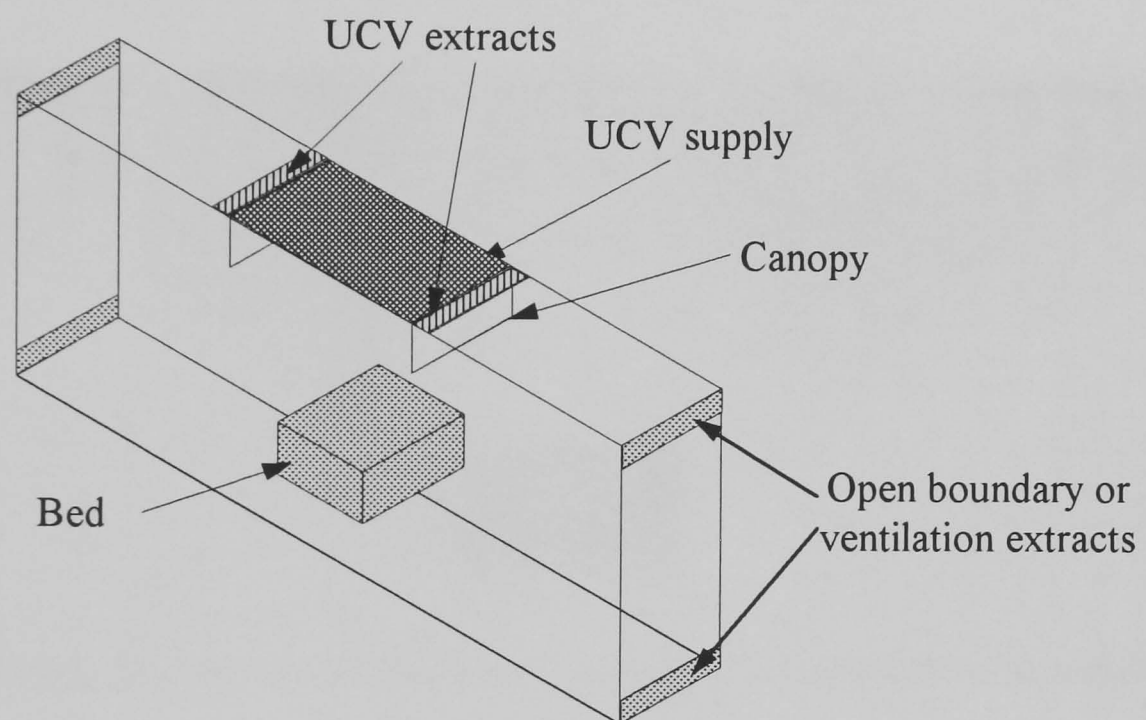


Figure 7.33 2 D domain of UCV canopy, supplies and extracts. High and low open boundaries and ventilation extracts.

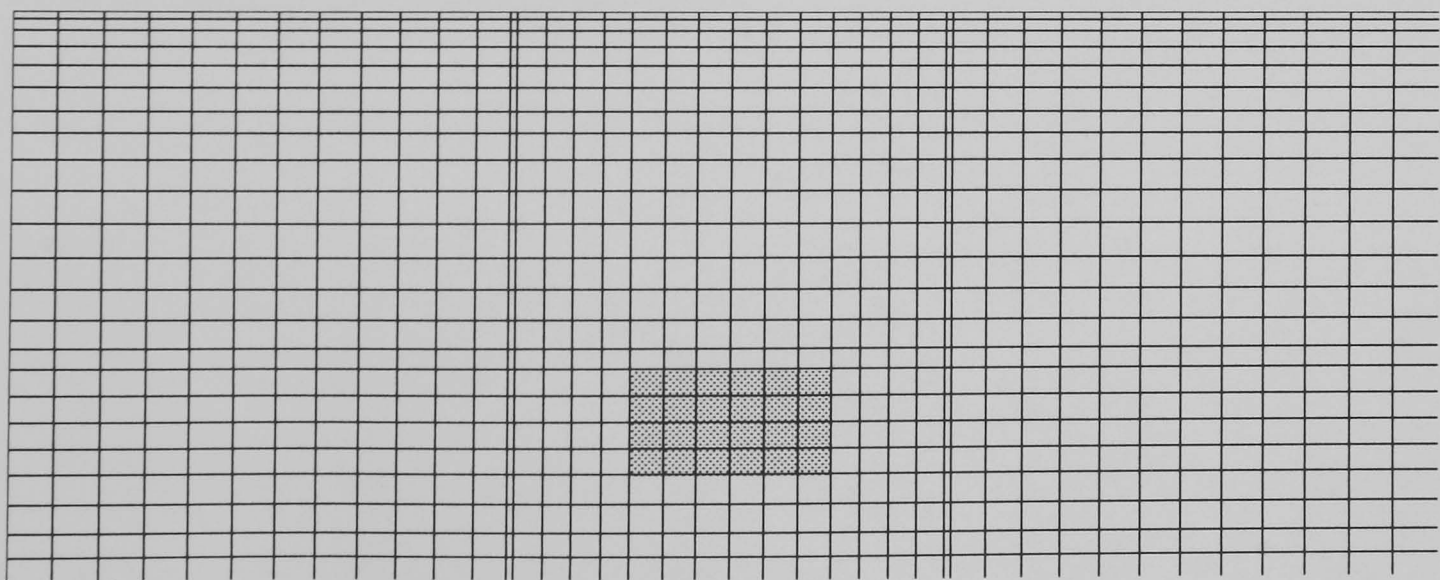


Figure 7.34 Solution grid over 2 D domain.

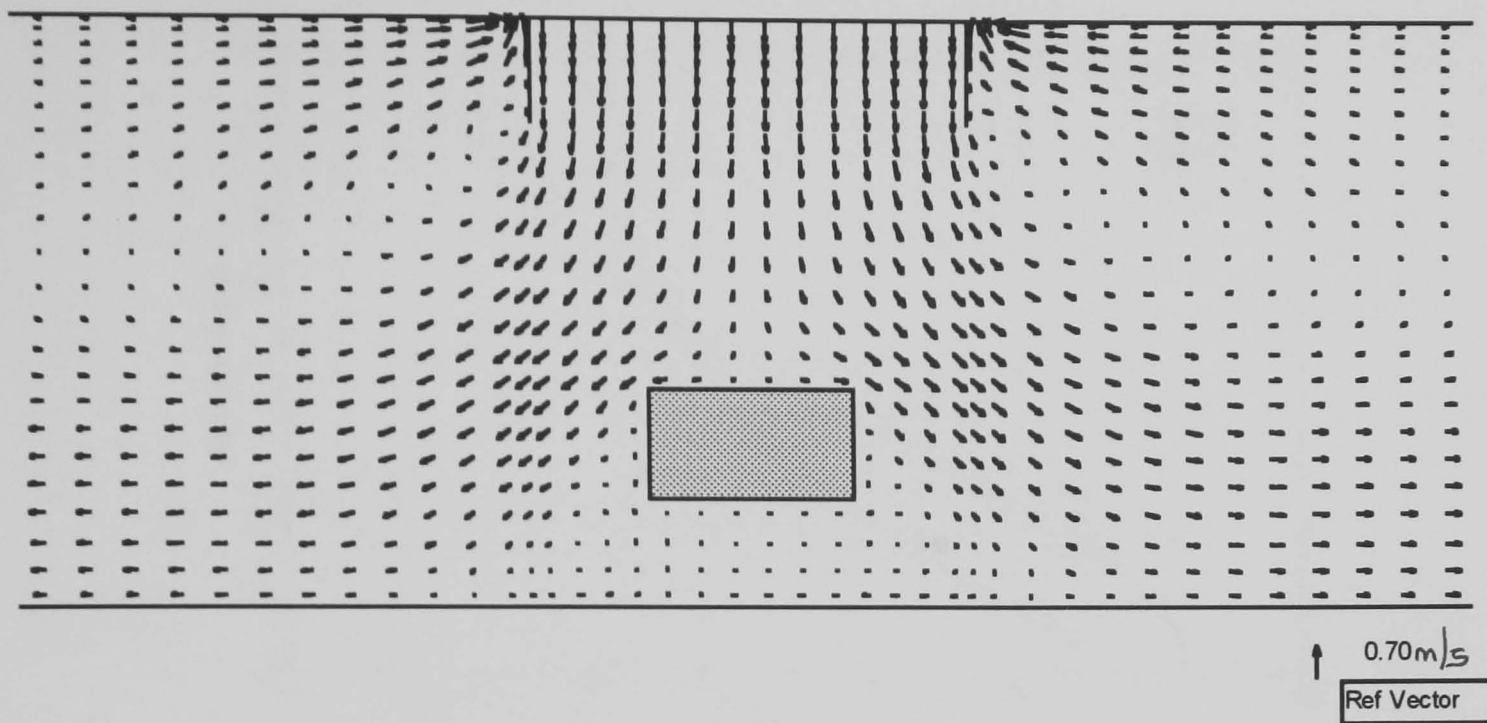


Figure 7.35 2 D simulation of airflows from the UCV canopy at a supply temperature 20°C and velocity 0.38 m/s. Open boundary walls and ambient 20 °C.

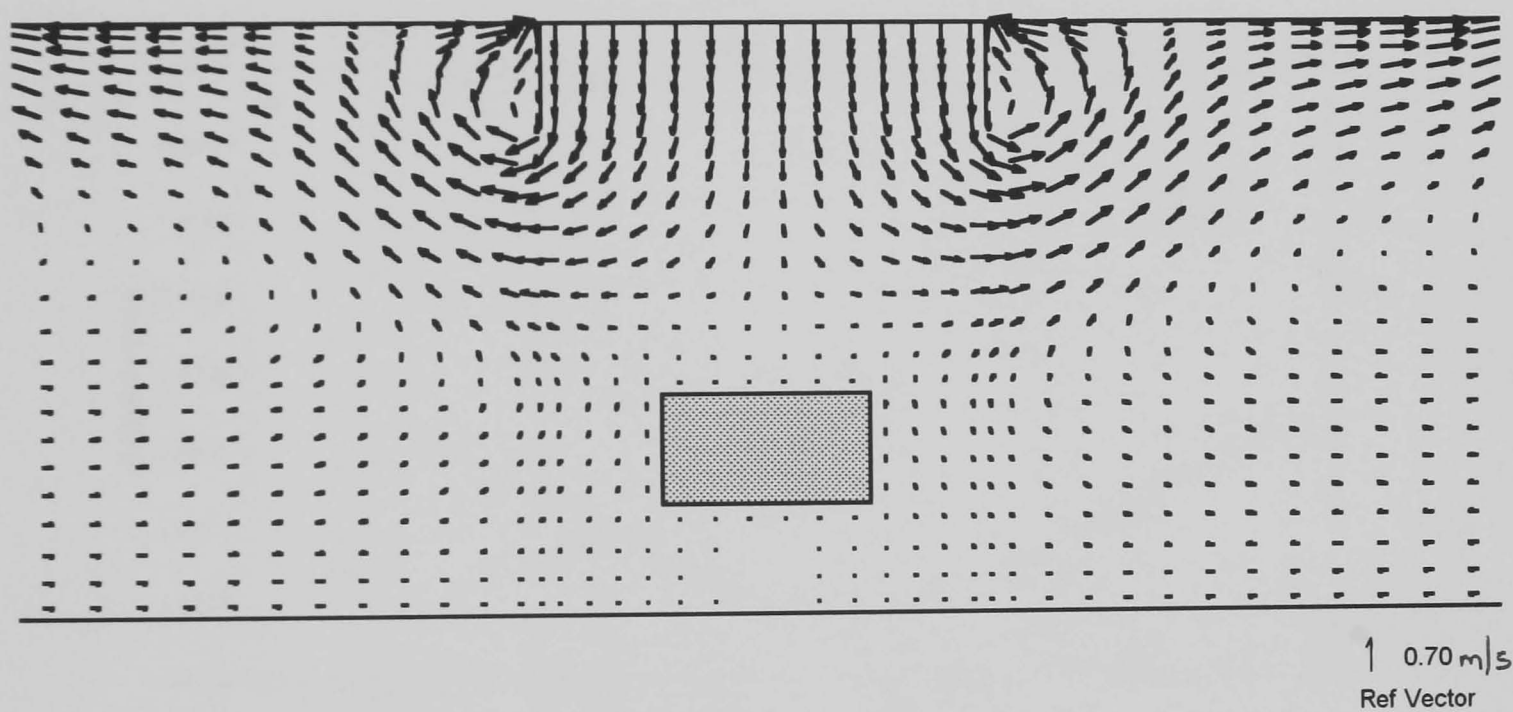


Figure 7.36 2 D simulation of airflows from the UCV canopy at a supply temperature 40°C and velocity 0.51 m/s. Open boundary walls and ambient 20 °C.

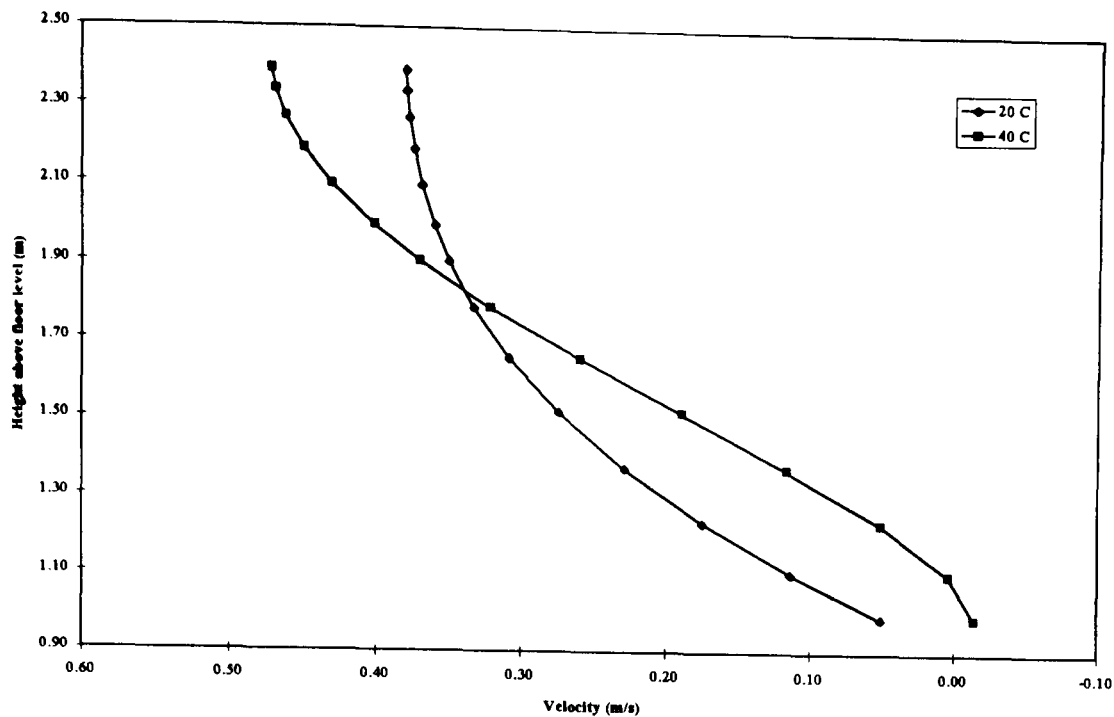


Figure 7.37 Effect of supply temperature on 2 D y velocity profiles with height in the middle of the bed. Ambient 20 °C.

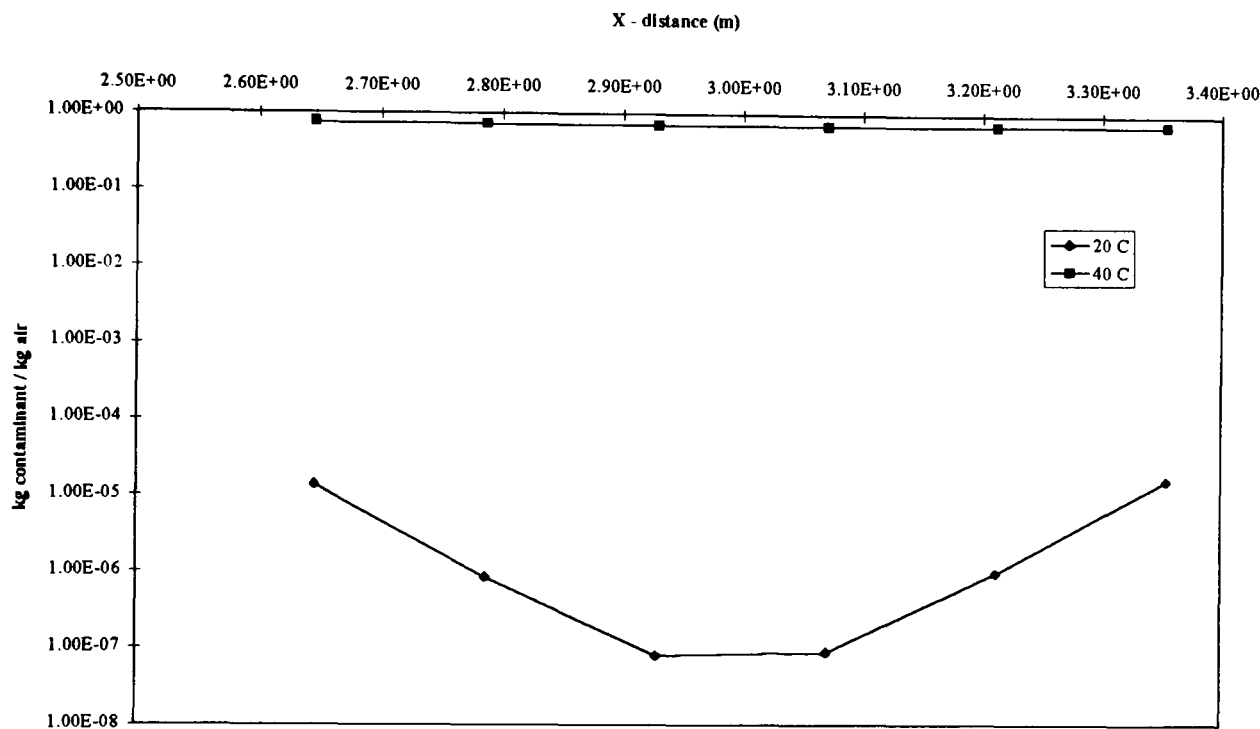


Figure 7.38 Effect of supply temperature on tracer concentration in the xz plane near to the bed surface (when released from the open boundaries in the walls). Ambient 20 °C.

7.11.3.3 Change in UCV performance with supply velocity / temperature (high and low level extracts and open boundaries)

At the minimum used settings, whatever the position of the extract and the openings, there was no temperature stratification within the room as would be expected. With extracts at low level and openings at high level the air flowed over the bed surface and towards the floor, dominated by the low level extracts (Fig. 7.39). There were small air recirculation zones from beneath the canopy to the ceiling extracts which were also influenced by the high level openings. With the high level extracts and low level openings the air flow over the bed surface was visually unchanged but the airflows within the room were (Fig. 7.40). At floor level there were obvious air flows from the openings into the room but these diffused before reaching the bed. The air flowing out from the sides of the bed was pulled to the ceiling and dominated by the ceiling extracts and high wall extracts. Much of the air from the low

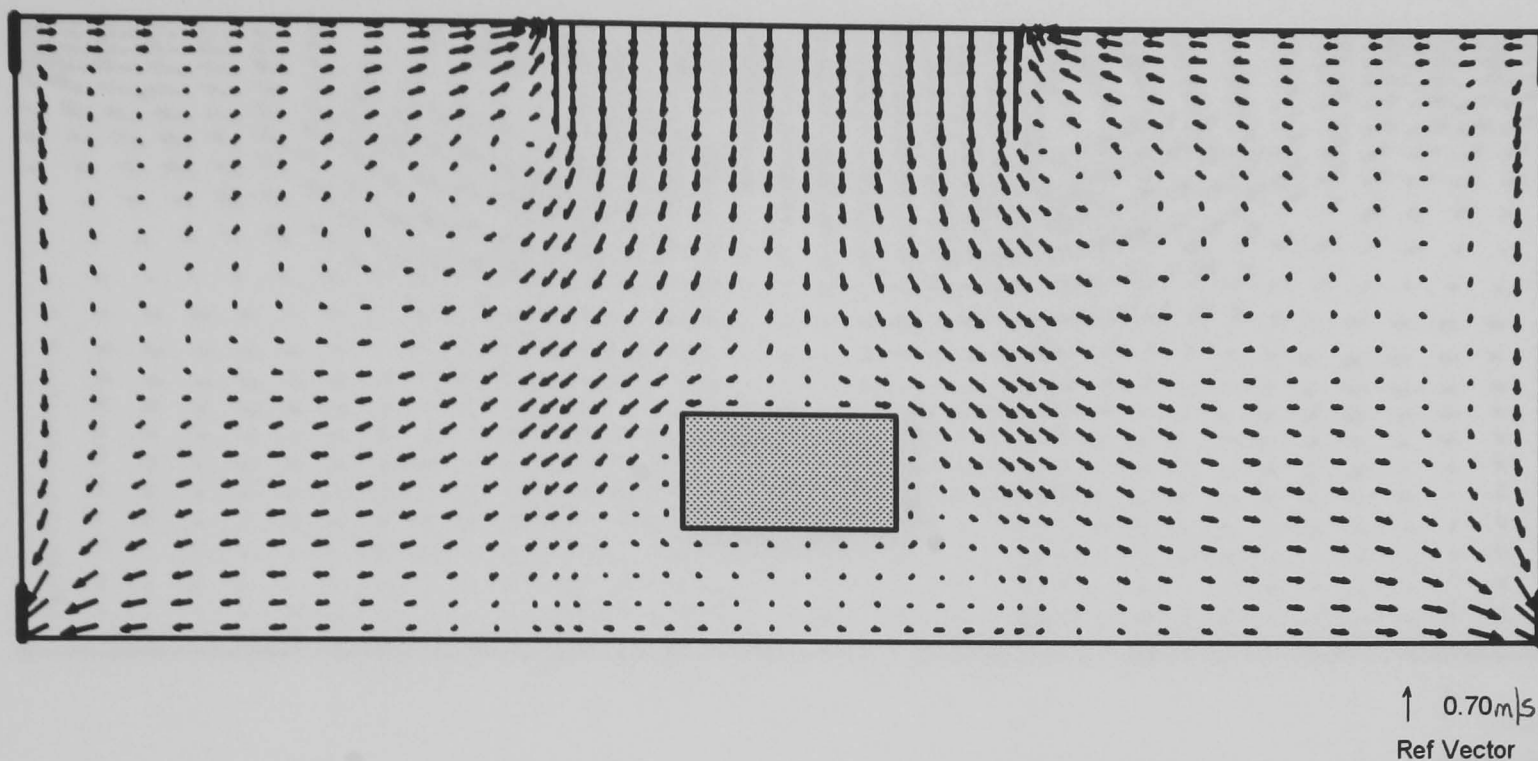


Figure 7.39 2 D simulation of airflows from the UCV canopy at a supply temperature of 20°C and velocity 0.38 m/s. Low level extracts and high level openings on boundary walls. Ambient 20 °C.

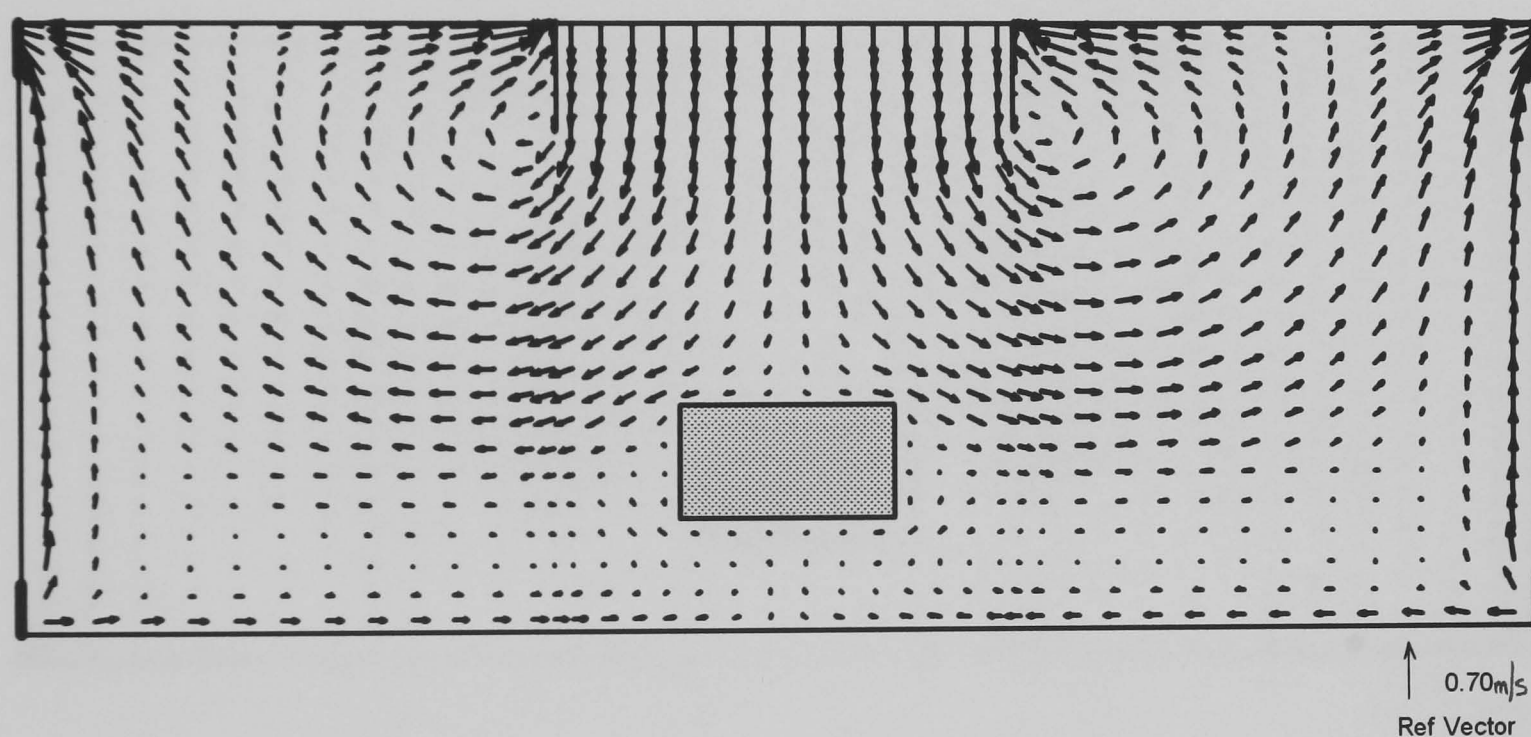


Figure 7.40 2 D simulation of airflows from the UCV canopy at a supply temperature 20°C and velocity 0.38 m/s. Low level openings and high level extracts on boundary walls. Ambient 20 °C.

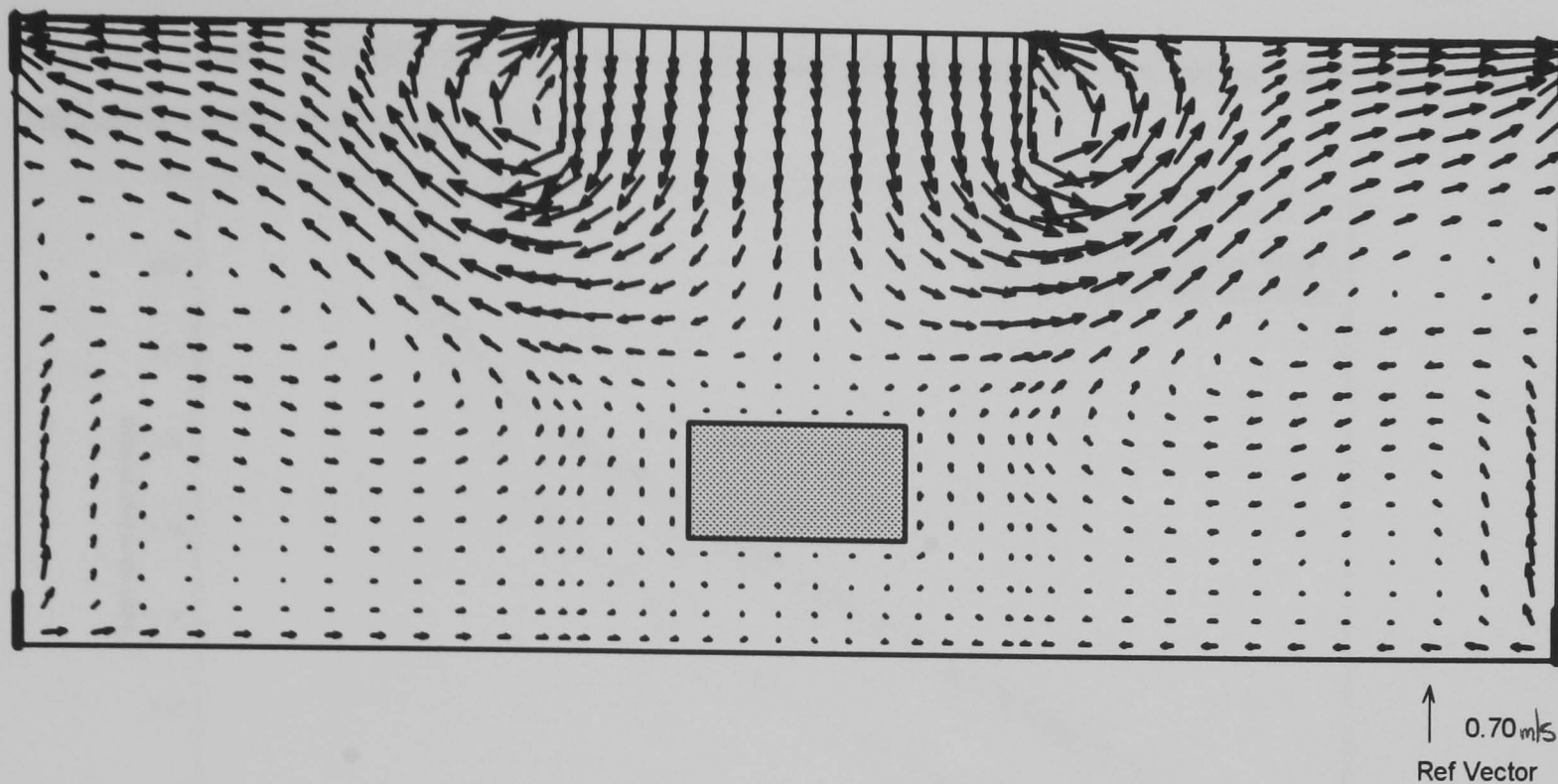


Figure 7.41 2 D simulation of airflows from the UCV canopy at a supply temperature 40°C and velocity 0.51 m/s. Low level openings and high level extracts on boundary walls. Ambient 20 °C.

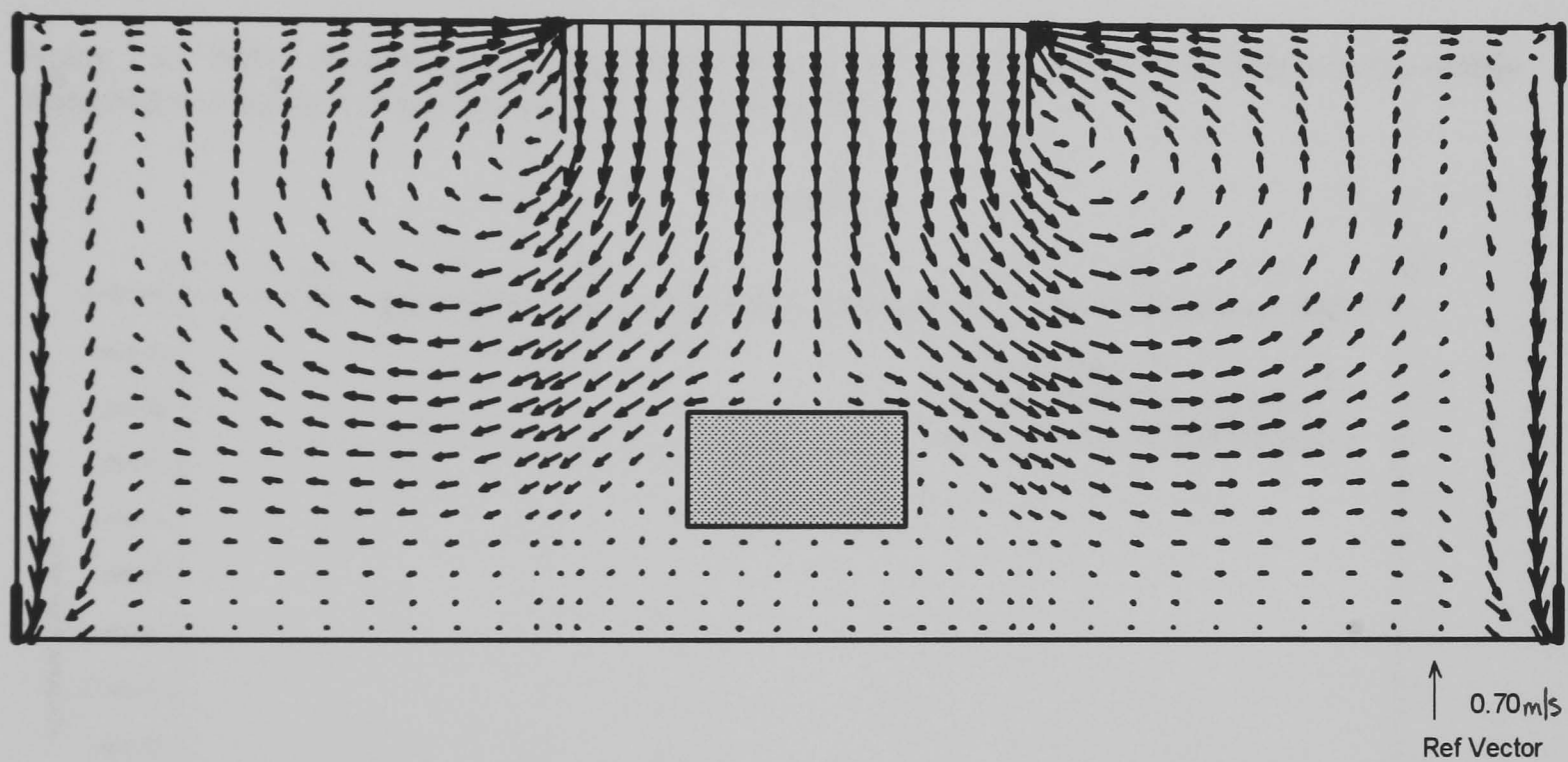


Figure 7.42 2 D simulation of airflows from the UCV canopy at a supply temperature 40°C and velocity 0.51 m/s. Low level extracts and high level openings on boundary walls. Ambient 20 °C.

openings short circuited up the walls to the high level extracts. In either case there was negligible contaminant under the canopy.

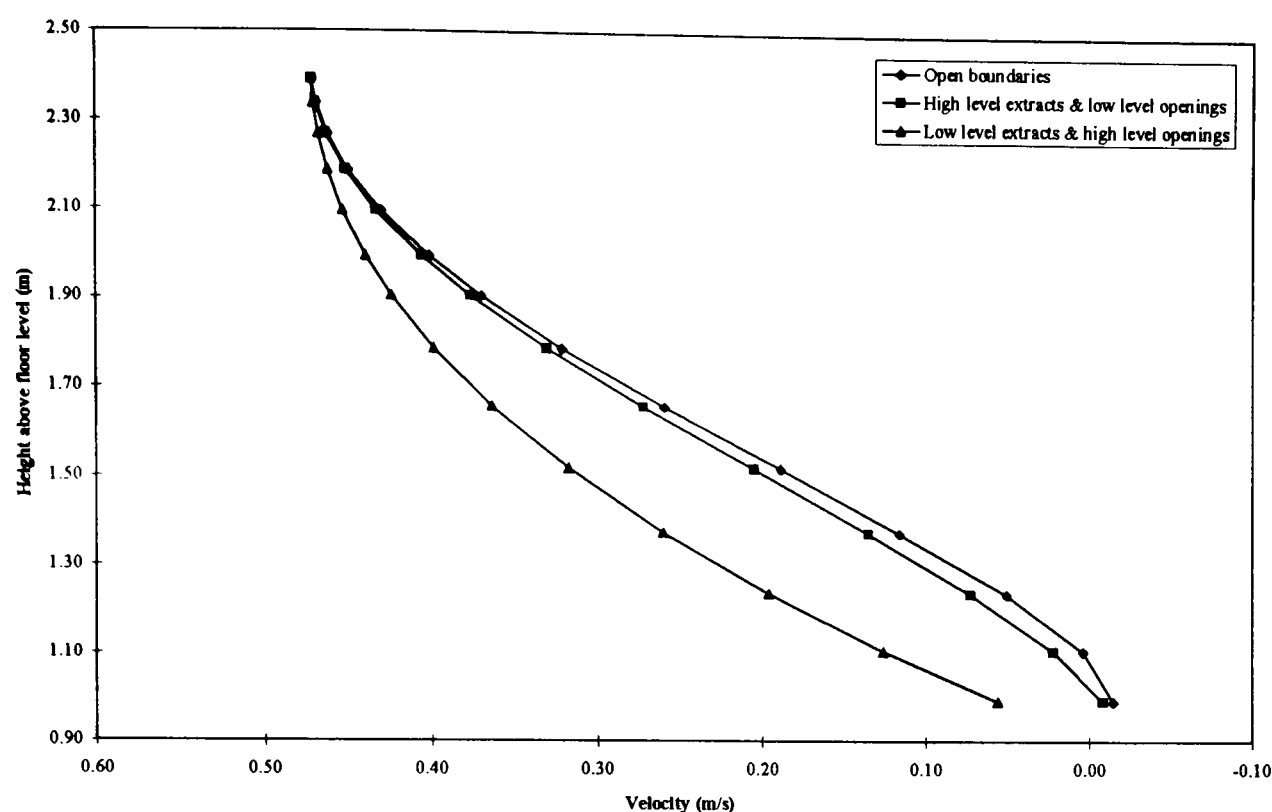


Figure 7.43 Effect of opening and extract position on 2 D y velocity profiles with height in the middle of the bed at a supply temperature of 40 °C. Ambient 20°C.

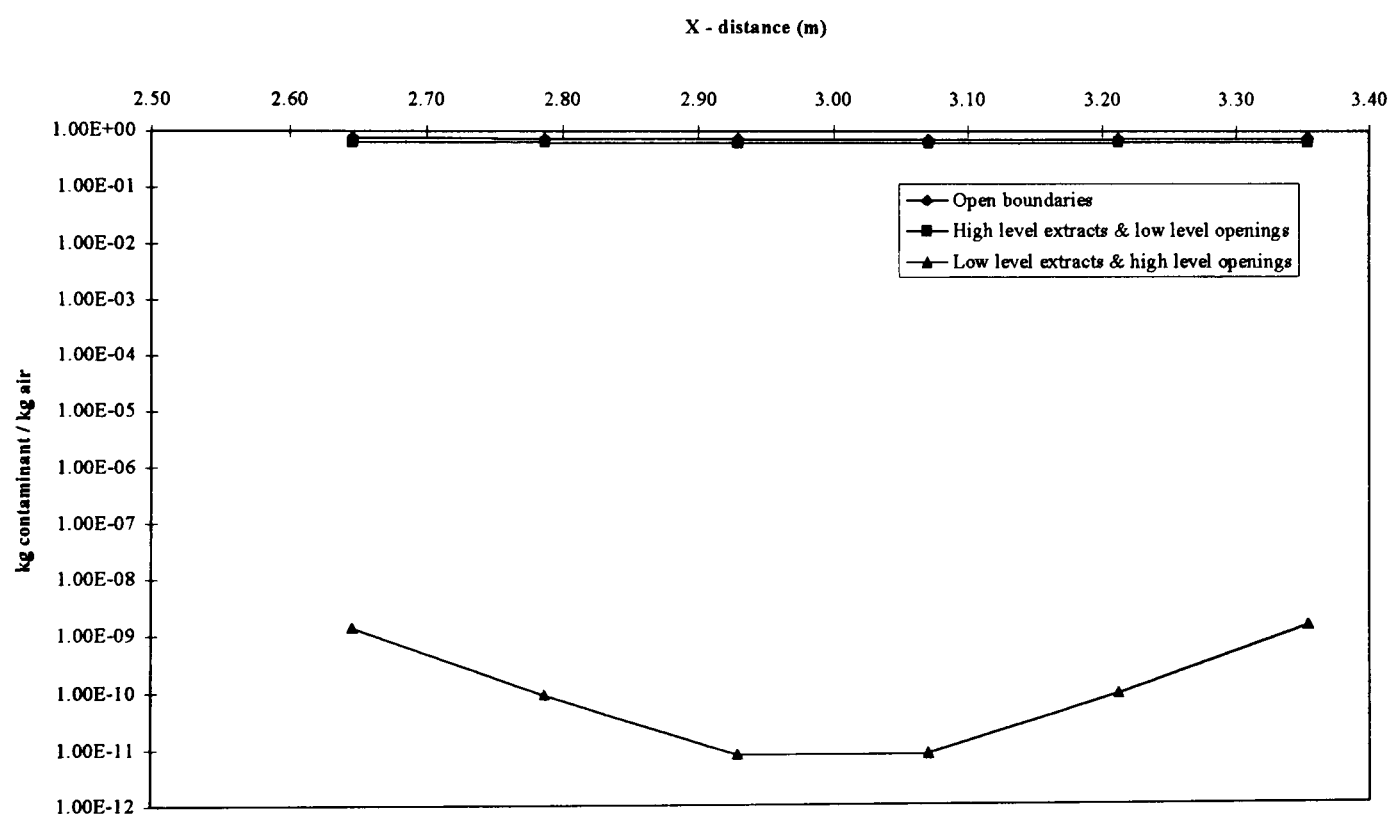


Figure 7.44 Effect of opening and extract position on 2 D concentration profiles across the bed, in a plane near to the surface, when released from the open boundaries at the walls. Supply temperature 40 °C and ambient 20°C.

At the maximum UCV settings and with high level extracts and low level openings the results were similar to those with open boundaries (section 7.8.3.2). There was a temperature stratification in the room of 16 °C from 36 °C at the ceiling to 20 °C at floor level. There was air flowing upwards from the bed surface (Fig. 7.43) and little air flowed from the bed sides or beneath the bed (Fig. 7.41). There was also no effective isolation of the 'clean zone' beneath the canopy from contaminant source released at the low level openings (Fig. 7.44).

With the extract at low level and the openings at high level the temperature stratification within the room was reduced to 1 °C (40 °C at ceiling level and 39 °C at floor level). The airflow under the canopy and above the bed was much more definite, the air flowing over the bed surface, outwards and then pulled down towards the low level extracts (Fig. 7.42). There were definite recirculation patterns of air towards the ceiling UCV extracts and again little air movement beneath the bed. However, the cold air flowing from the high level openings immediately sank to the floor and short circuited towards the low level extract. The effect was that negligible contaminant was distributed under the canopy but followed the air from the opening straight to the low level extracts (Fig. 7.44).

7.11.4 Drafts stopped by “brushes” fitted to drawers/cupboards/doors

As “visualised” both by smoke and CFD, the draughts into the room were considerable. Gaps at the back of drawers and cupboards were sealed up, and the substantial draughts from beneath the doors were diffused by fitment of brushes.

The reduction of this passive make up air into the room increased the negative pressure substantially to ~ -16 Pa (nearly three times the designed level). The pressure in the viewing area was also increased to ~ +6 Pa. There was still a reduced circulation of air around the floor of the room and it was considered this was due to the flow of air from the UCV and that being exhausted from beneath the LALB. The stratification of temperature within the room was not altered and the reduction in draughts did not appear to affect the velocity below the canopy. However, the temperature near to the bed surface was measured at 32 °C under quadrant 3.

The number of potassium iodide particles measured at the surface of the bed was similar to that measured without the door brushes fitted and the UCV extract unblocked. The number measured in the middle of the bed was slightly increased and it was noticed by smoke movement that with the door brush fitted to the bottom of the viewing area door, the force of the draught around the sides of the door had increased at the height of the bed surface.

7.11.5 Effect of diffusing air entry into room through doors (CFD)

Using the CFD model, diffusers were fitted to the doors in order to reduce the velocity at which the draughts entered the room. At floor level, the dominant flows were eliminated and there was a much more defined flow at the foot end of the bed (Fig. 7.45 & 7.46). However the general room airflows at mid height and ceiling height were still dominated by the UCV and room extracts. Seeding the air through the diffusers in the doors still resulted in contaminant encroaching into the region at the foot end of the bed (Fig. 7.47).

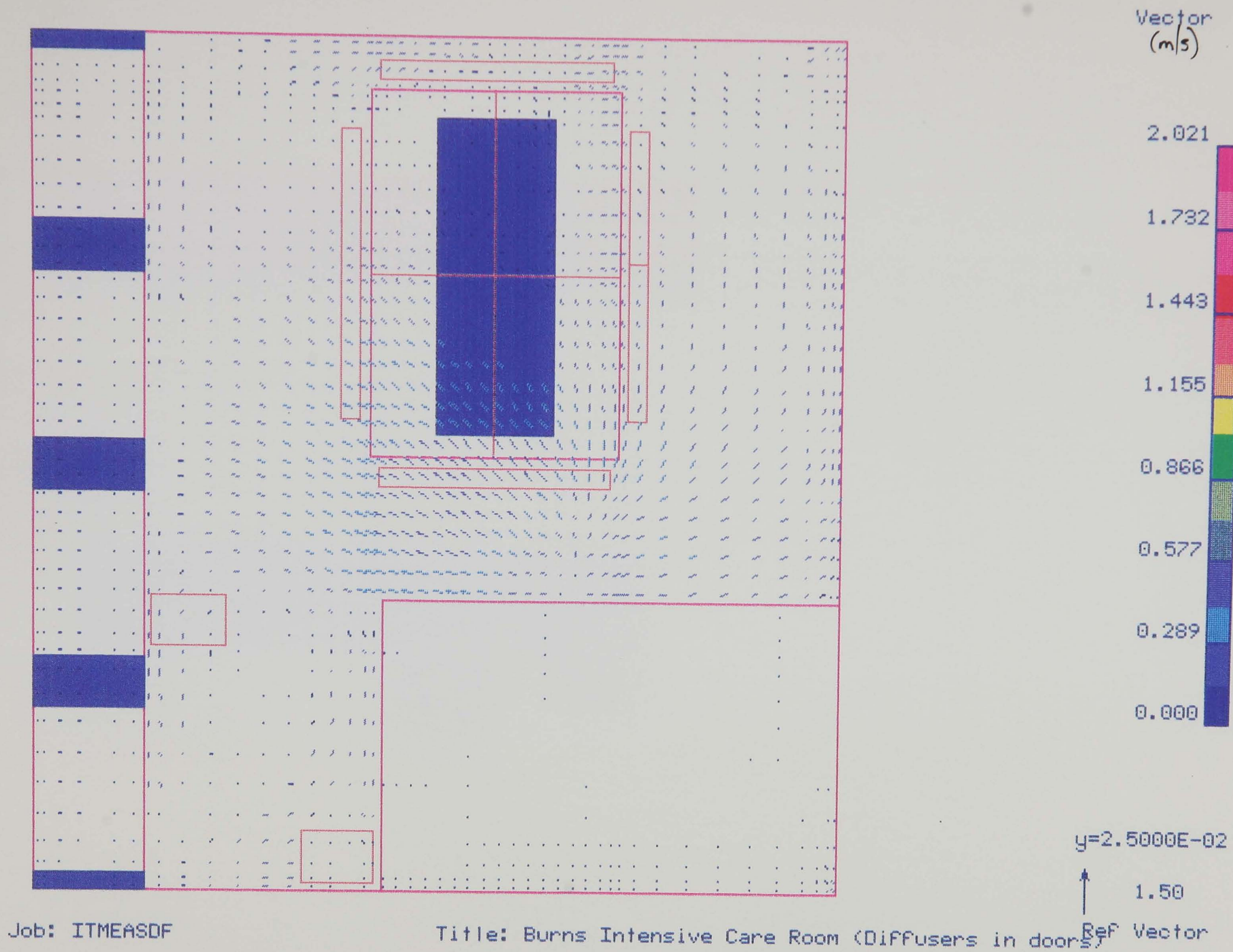
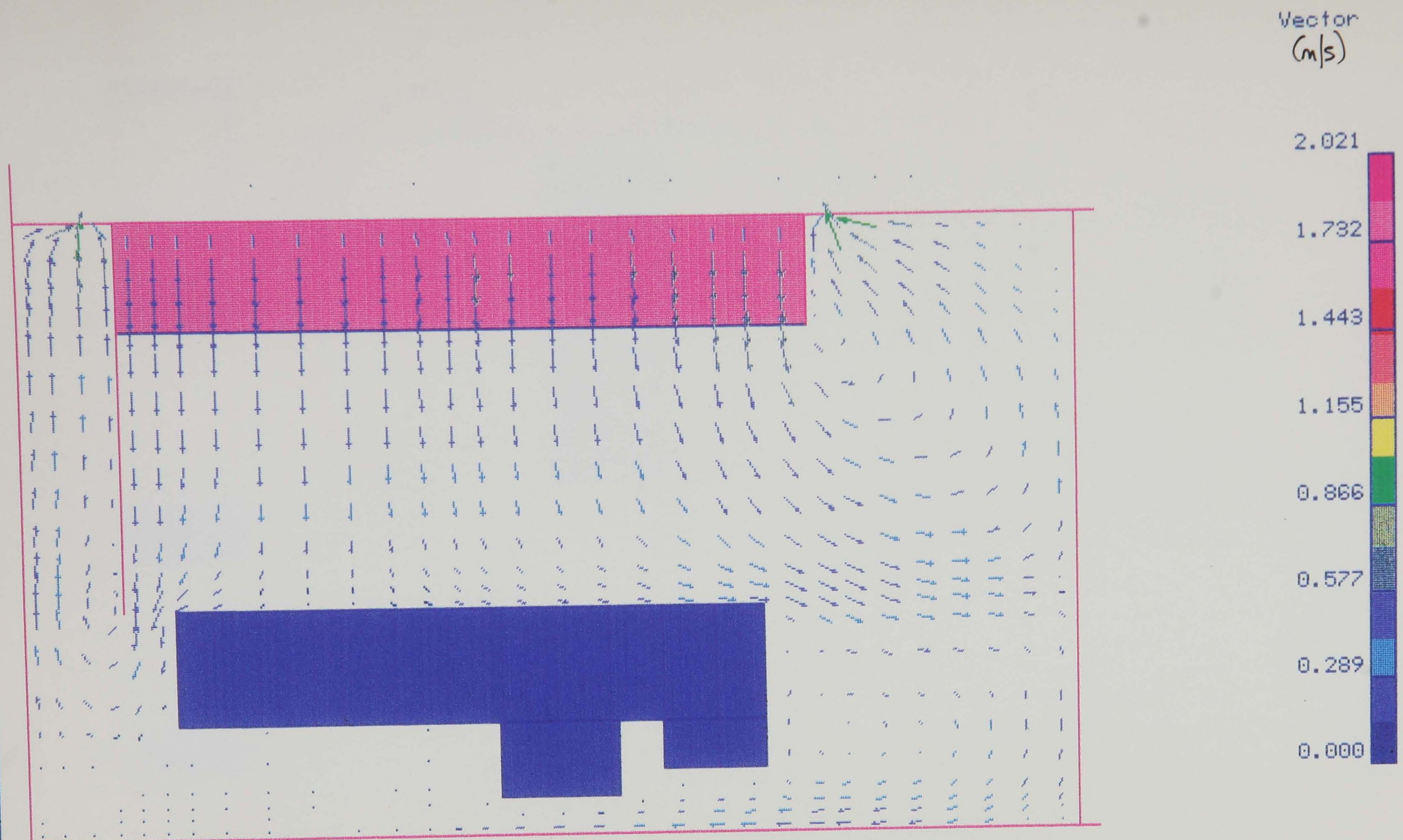


Figure 7.45 The effect of door diffusers on xz airflow vectors near to floor level in the intensive care room when released in the airflows beneath the doors.



$\times = 2.4938E+00$
 1.50
 Ref Vector

Job: ITMEASDF

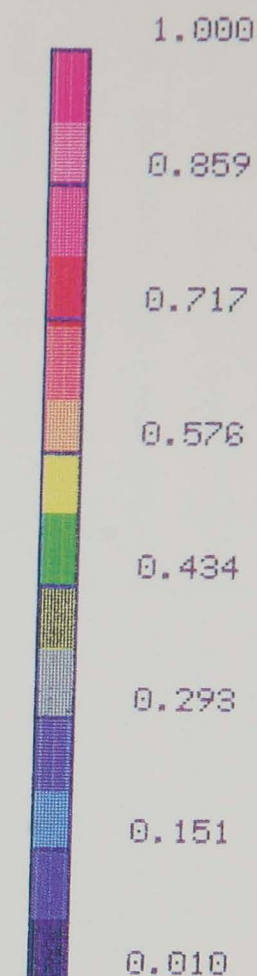
Title: Burns Intensive Care Room (Diffusers in doors)

FLUENT

Figure 7.46 The effect of door diffusers on yz airflow vectors in the centreline of the UCV.



Contour
Concentration



6*10*17462700

Job: ITMEASDF

Title: Burns Intensive Care Room (Diffusers in doors)

Figure 7.47 The effect of door diffusers on xz concentration contours at midheight (near to bed surface height) in the intensive care room when released in the airflows through the door diffusers.

FLUENT

7.11.6 Effect of repositioning viewing area door (CFD)

Using the CFD model, the viewing area door was moved from the original position around the corner to the side of the viewing area. It was assumed that the same airflow / draughts would be present from beneath the door as was observed at its original position. The dominant flows over the floor from the viewing area door where it was positioned were removed. However, the combined effect of the draughts from beneath the dressing room door and the repositioned viewing area door still resulted in considerable airflows over the floor and beneath the bed (Fig. 7.48). The effect of draughts from the corridor was not eliminated.

7.11.7 Canopy extended

With the canopy as fitted, there was negligible airflow at the bed surface. To increase this the canopy was modified; a cardboard extension was fitted which brought the lower edge of the canopy to a height of 1.37 m from the floor thus lowering the exit point of airflow from the canopy nearer to the bed surface.

At all ventilation settings, the measured airflow velocity beneath the canopy decreased little with height (Fig. 7.49). At normally used ventilation settings, the average velocity near to the bed surface was 0.39 m/s with the extension fitted.

At maximum ventilation rate and temperature, extension of the canopy resulted in a higher mean temperature of 29 °C measured at floor level compared with a mean of 25 °C with the canopy as normally fitted. At minimum and normally used ventilation rates, there was little change in room temperature with extension of the canopy.

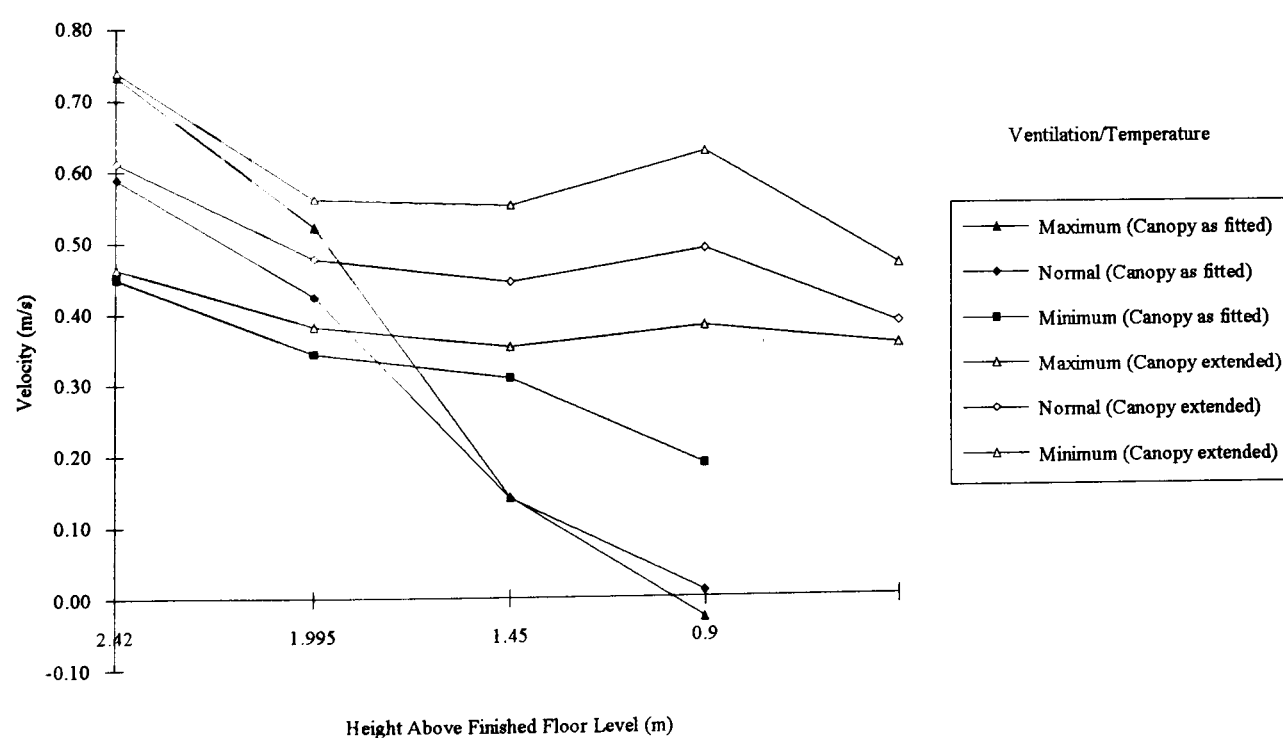


Figure 7.49 Variation in downward velocity beneath the UCV, quadrant 3, with changing supply flow rate/temperature.

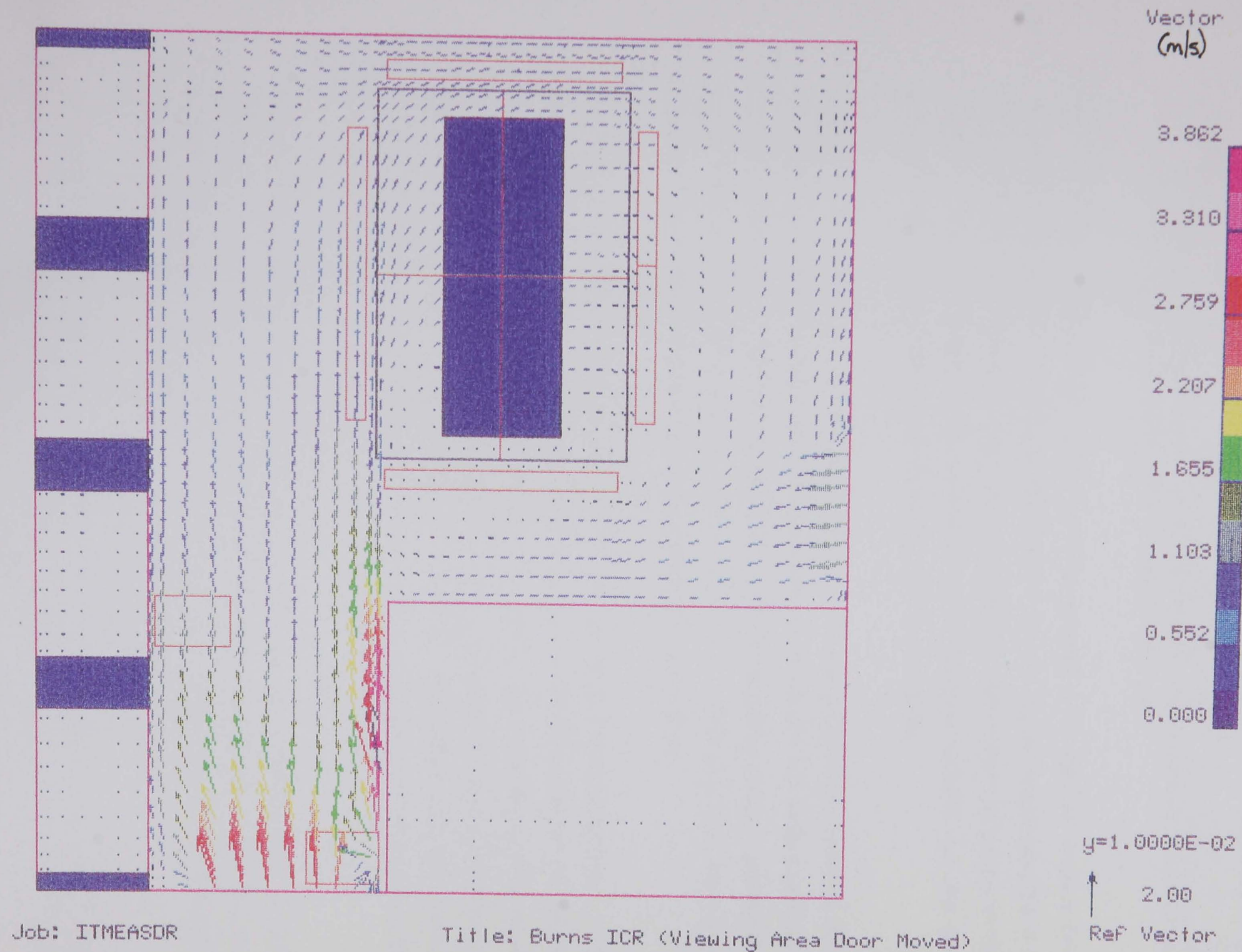


Figure 7.48 The effect of moving the viewing area door on xz airflow vectors near to floor level in the intensive care room.

Beneath the canopy the measured temperature was higher nearer to the bed surface with the canopy extended. Under normal operating conditions, the mean temperature near to the bed surface under quadrant 3 was ~33 °C compared with ~31 °C with the shorter canopy as normally fitted.

	Position of Sampler on Bed Surface (Layout 1)					
	Foot of Bed (S1)		Middle of Bed (S2)		Head of Bed (S3)	
	Extended	Normal	Extended	Normal	Extended	Normal
No disturbance	7	157	10	1.25	1	0.25
Disturbance	92	3533	130	4693	35	2255

Table 7.13 Effect of extending the canopy on the concentration of KI particles/m³ of air sampled at the bed the bed surface when released from within the intensive care room.

The distribution of potassium iodide particles sampled over the bed surface under the extended canopy was more evenly spread (Table 7.13); the higher counts sampled at the foot of the bed under the shorter canopy were not evident. Movement of people in the room resulted in a small increase in the number of tracer particles sampled, but this was some orders of magnitude less than when the canopy was not extended.

There was some evidence of re-entrainment at the canopy periphery (whether or not the canopy was extended) with potassium iodide being found at the bed surface with no people moving in the room. This was slightly more with the extended canopy, potassium iodide being found at the middle and head regions of the bed. This may have been a result of bringing the recirculation of air outside the canopy to a lower level.

Using the 3 dimensional CFD model of the room, the canopy was extended to 1.37 m from floor level. The general airflow movement within the room and at the foot of the bed was unchanged from the normally fitted canopy (Fig. 7.50). However the airflow beneath the canopy was much altered, the supply exit point being pushed further towards the bed surface, increasing the velocity at this point (Figs. 7.51 & 7.52). This produced larger recirculations zones on both the window and corridor sides of the bed sweeping across the floor surface and then into the room.

The distribution of a contaminant through the domain when released from the openings within the draughts mixed thoroughly with the air in the room but encroached less under the canopy in the 'clean zone' than with the normally used canopy (Fig. 7.53). The difference being greatest at the horizontal edge of the extended canopy.

The extension of the canopy to 1 metre above floor level (ending just above the bed surface, 0.9 m) was simulated using the 2 dimensional CFD model (section 6.8.3). With open boundaries there was a temperature stratification within the room of 0 - 14 °C. The temperature near to the ceiling was 34 °C but at floor level ranged from 20 °C to 35 °C. This reflected the lower discharge point of the canopy near to the bed surface. Here the

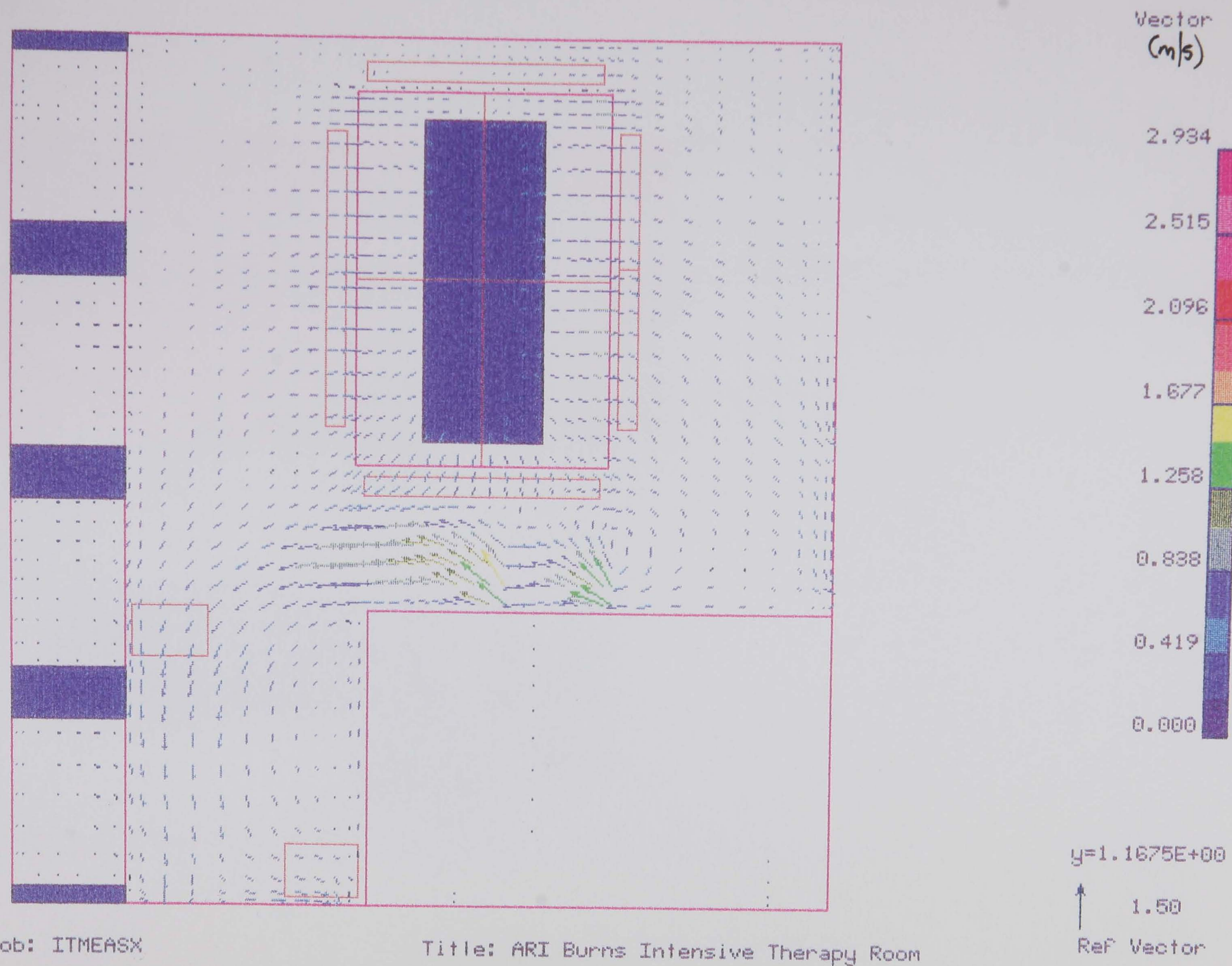


Figure 7.50 The effect of extending the canopy on xz airflow vectors at midheight (near bed surface height) in the intensive care room.

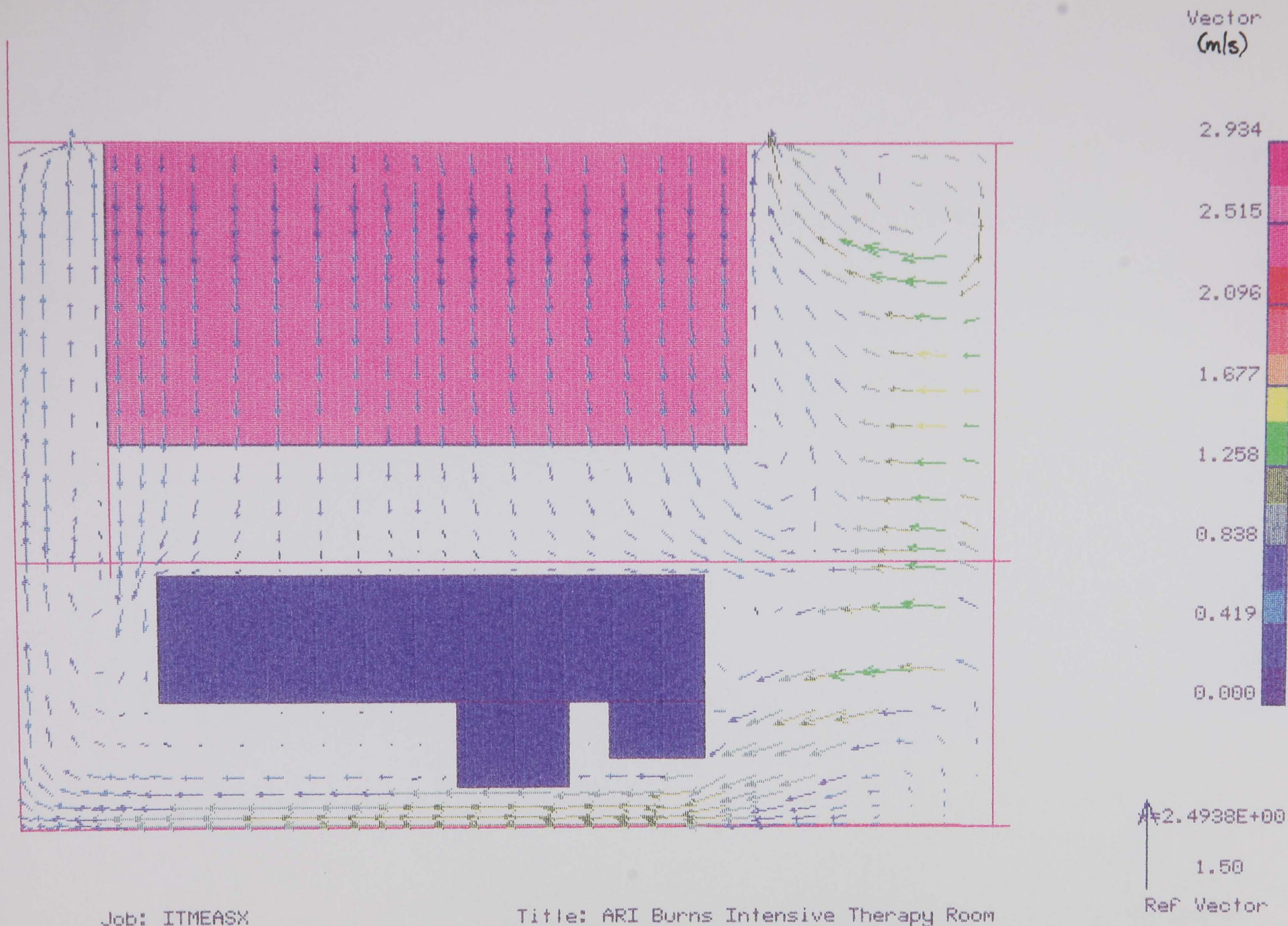
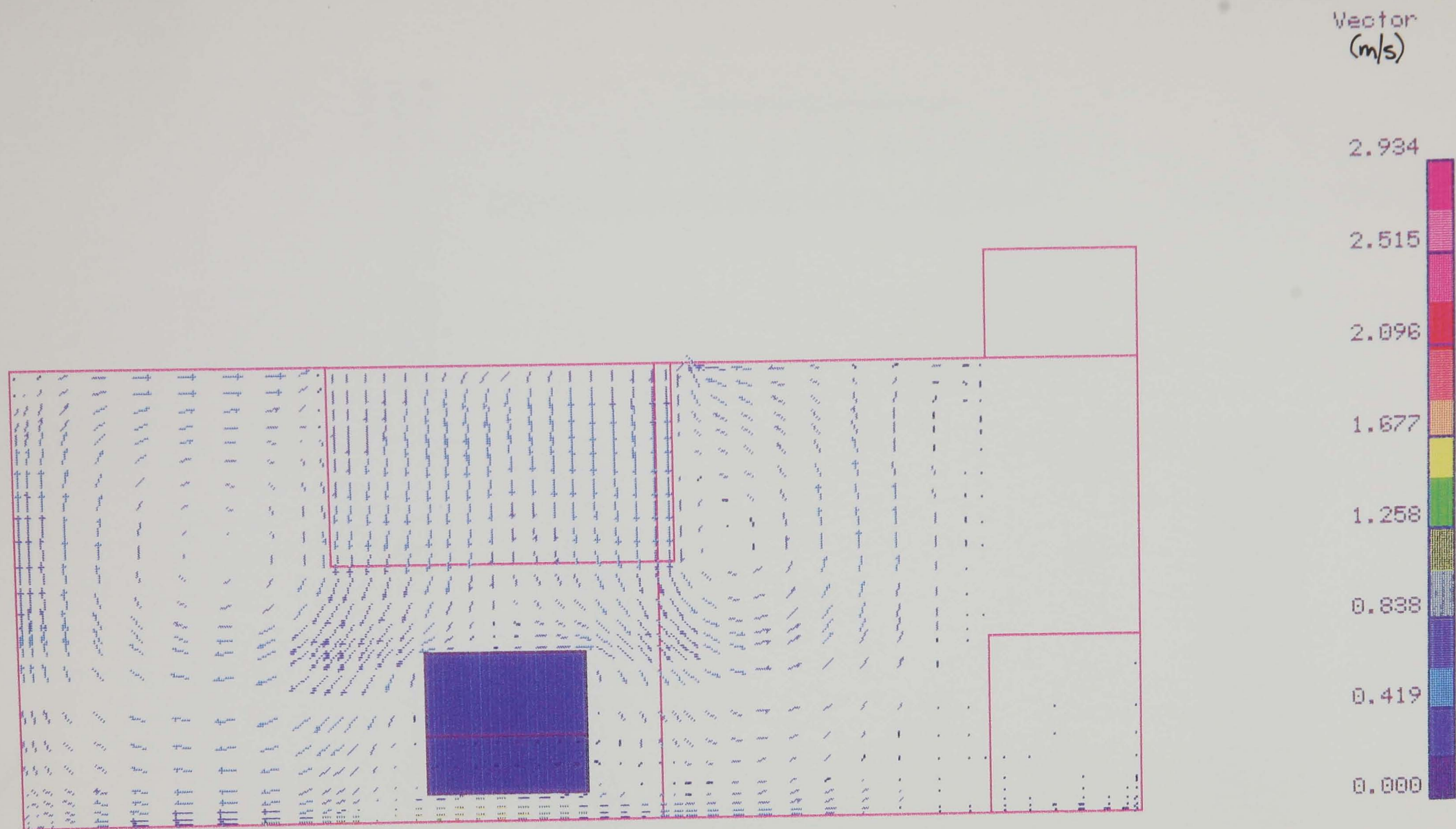


Figure 7.51 The effect of extending the canopy on yz airflow vectors in the centreline of the UCV.



$z=4.5950E+00$



1.50

Ref Vector

Job: ITMEASX

Title: ARI Burns Intensive Therapy Room

FLUENT

Figure 7.52 The effect of extending the canopy on xy airflow vectors in the centreline of the UCV.

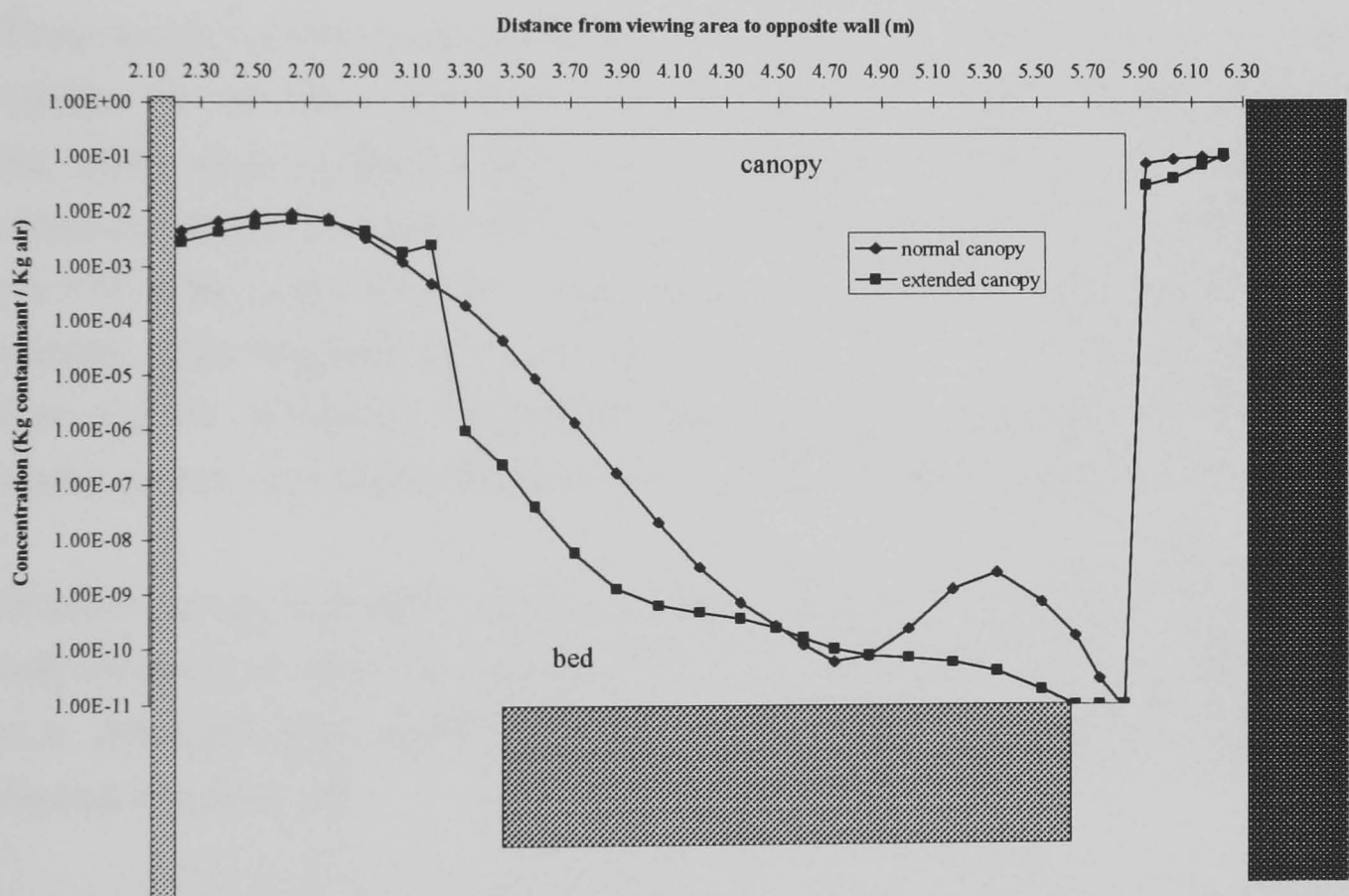
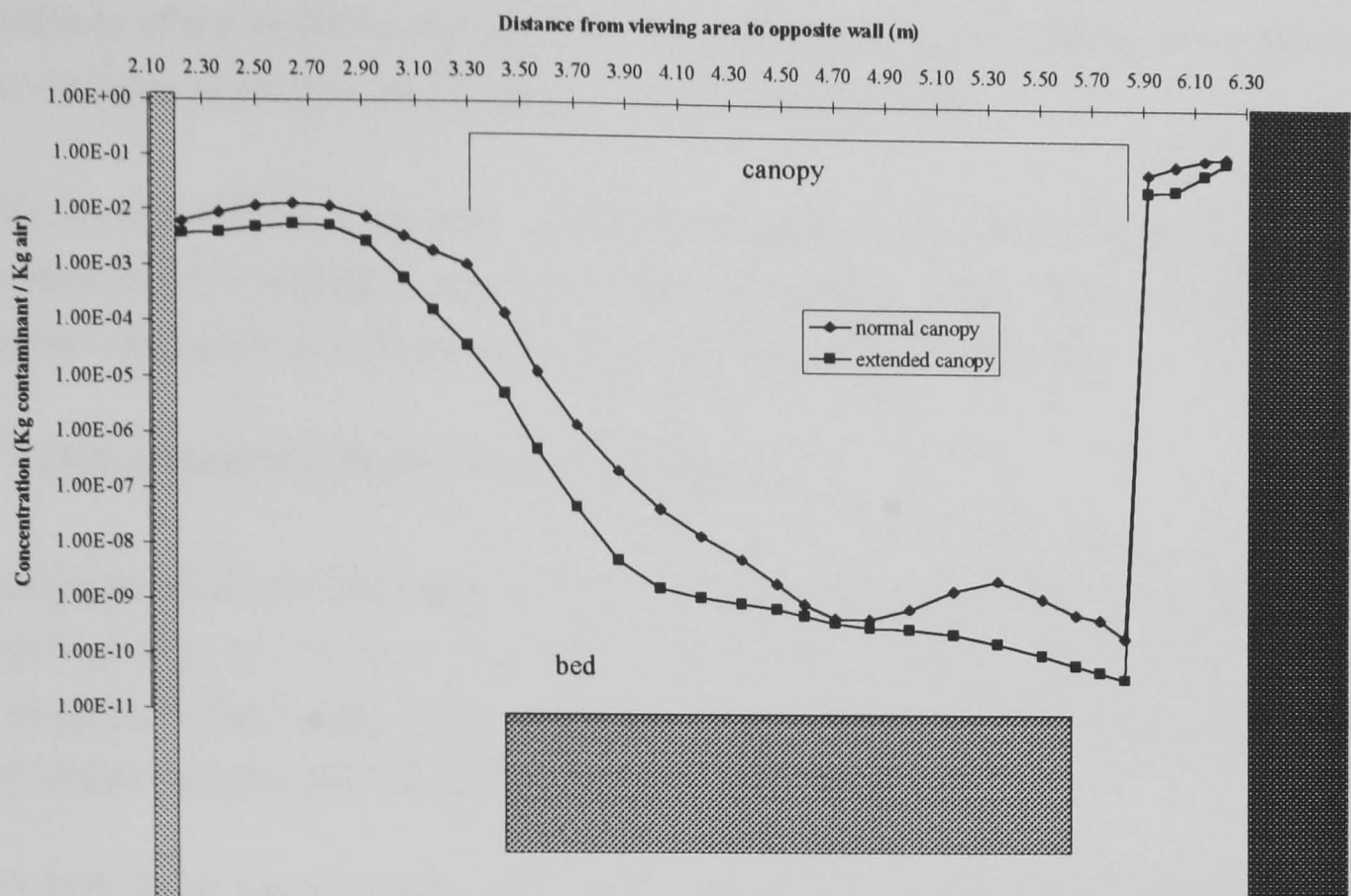


Figure 7.53 Tracer concentration profiles along the centreline of the bed from head to foot end at heights near to the bed surface (top) and at the canopy edge (bottom) when released within the intensive care room.

velocity of the air flow was unchanged from that at the supply diffuser and exited the canopy to circulate to the floor and back up to the ceiling (Fig. 7.54).

Contaminant distribution when released from the open boundaries within the room was well mixed but was negligible underneath the canopy (Fig. 7.55). This was the same whether there were open boundaries, high level extracts or low level extracts.

7.11.8 Extended canopy (foot end only)

Using physical measurements to assess the effect of extending the canopy at the foot end of the bed only, to 1 m above floor level showed results similar to when the whole canopy was extended. That is with no disturbance there was little entrainment of potassium iodide tracer particles onto the head, middle or foot end of the bed surface.

7.11.9 Low Air Loss Bed (LALB) switched on/off, canopy extended/not extended

There was little difference to the measured velocity of the air flowing near to the bed surface whether the bed was switched on or off either with the canopy extended or not. However, the robust nature of these airflows with the bed switched off was questionable. Potassium iodide sampled at the surface of the bed (at a height lower than 0.9 m due to the deflation of the LALB air sacks) with the canopy as fitted was in excess of the upper limits of the test method. This suggested that there was little movement of air in this region in any defined flow and that air moved freely across this area from beyond the clean zone. No tracer measurements were made with the canopy extended and the bed switched off.

With the canopy as fitted the measured temperature at 0.9 m was slightly decreased when the bed was switched off as the temperature of the bed determined the temperature of the air near to it. Extension of the canopy maintained the same temperature near the bed surface whether the bed was on or off.

The substantial amount of tracer and slight decrease in temperature measured at the deflated bed surface under the normally used canopy would be important if the bed was removed and the patient sat in an armchair for example. With the fitted canopy, the air would not be expected to flow as far as a chair and the temperature and contamination levels would be more influenced by the room environment than the sterile air from the UCV.

The effect of removing the bed completely was shown using the 2 dimensional CFD model with open boundary walls (section 7.8.3). At minimum ventilation settings the air flowed towards the floor and there was negligible contaminant underneath the canopy when released from the openings (Fig. 7.56). However, at the maximum ventilation settings there was little airflow beyond the edge of the canopy and contaminant was distributed through the domain

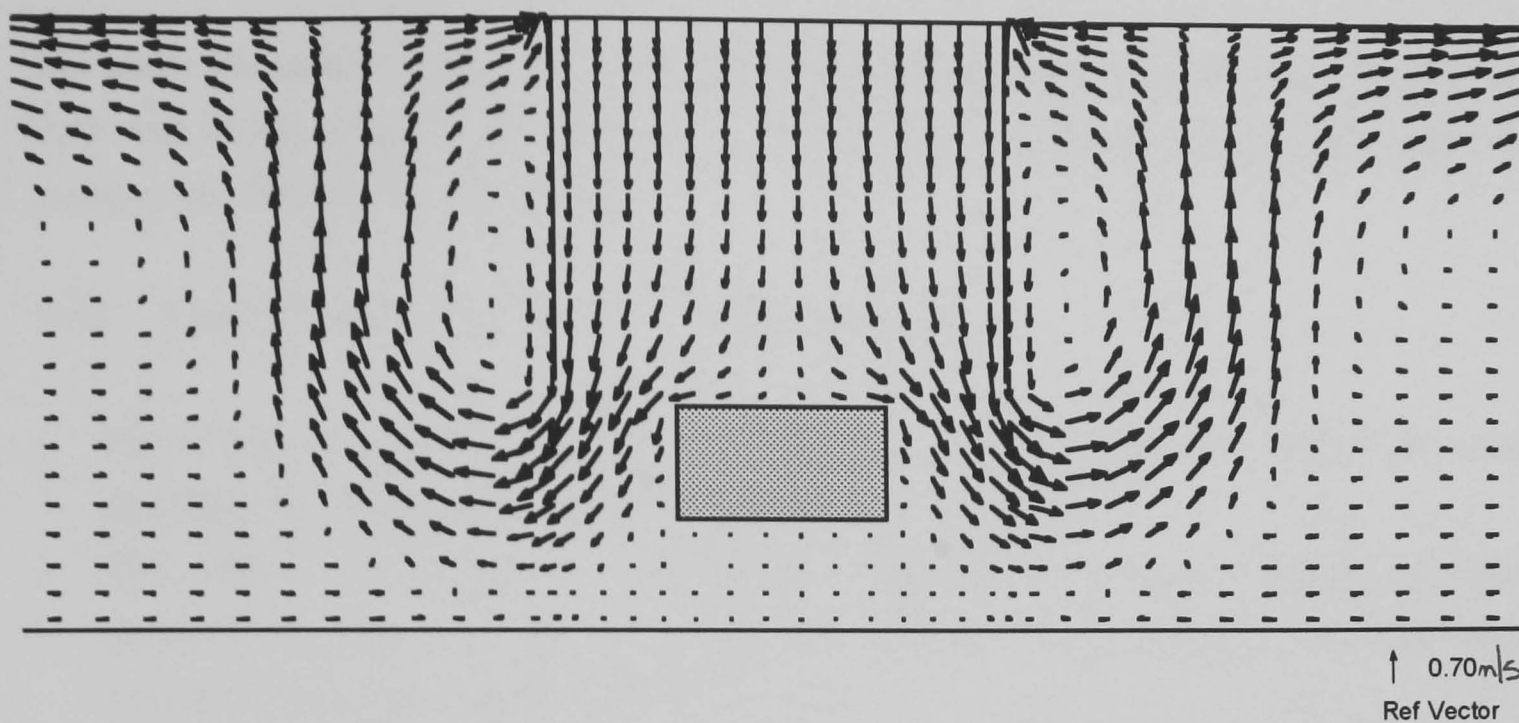


Figure 7.54 2 dimensional simulation of airflow from the UCV canopy (extended) at supply temperature 40°C and velocity 0.51 m/s. Open boundary walls and ambient 20 °C.

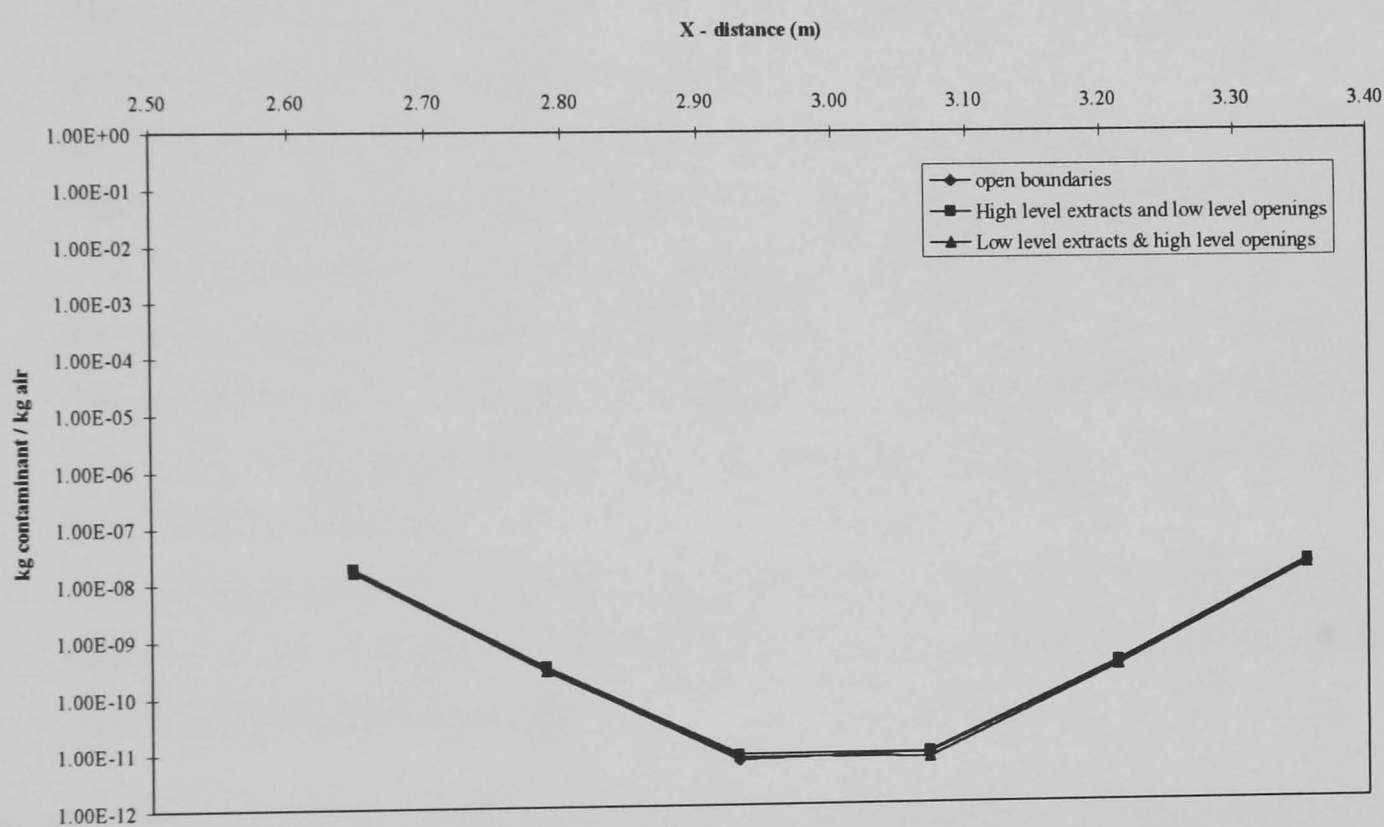


Figure 7.55 2 dimensional simulation of concentration profile under the UCV canopy (extended) at bed height. Supply temperature 40°C and velocity 0.51 m/s. Open boundary walls and ambient 20 °C.

and under the canopy (Fig. 7.57). Extending the canopy moved the exit point nearer to the floor and increased air flow in this region. However there was still contaminant under the canopy near the floor level (Fig. 7.58).

7.12 Conclusions from analysing design changes

- The effect of supply temperature and buoyancy had an enormous effect on room airflows and distribution of room contaminants.
- The effect of room supply / draughts / extracts has a profound effect on room airflows whatever the supply temperature. Having extracts near to the floor level could eliminate the buoyant effects of the air.
- Preventing dominant draughts from beneath doors exaggerated draughts from around the other gaps in the doors. This caused greater disturbance at the foot end of the bed resulting in more contaminant over the bed surface from the room.
- Diffusers in the doors eliminated strong draughts into the room but did not prevent encroachment of contaminant at the foot end of the bed.
- Moving the viewing area door eliminated the effects of draughts at the foot end of the bed but exaggerated draughts from the region of the dressing room door.
- The extension of the canopy had an effect at increasing temperature and velocity at the bed surface and limited the encroachment of contamination over the bed surface.
- The extension of the canopy at the foot end of the bed only, had similar effects to the extension of the complete canopy. This appeared to prevent gross disturbances at the foot end of the bed.
- The presence of the bed had an important effect on the airflow beneath the canopy. Without it the draughts and buoyant effects in the room caused contaminant to be distributed beneath the canopy.

7.13 Discussion of CFD and Physical measurements as containment testing strategies applied to a complex ventilated environment

7.13.1 Physical measurements

Perhaps the simplest and most graphic method that characterised the performance of the Unit and UCV was visualisation using smoke tracer. This gave an immediate perception of the overall performance and identified the most important aspects concerning the ventilation:

1. Whether a ventilation duct was functioning.
2. The general airflow patterns - were they moving in the right direction.
3. Identification of any regions of gross disturbances such as draughts.
4. Visualisation of regions of excessive turbulence for example around the UCV canopy and bed.

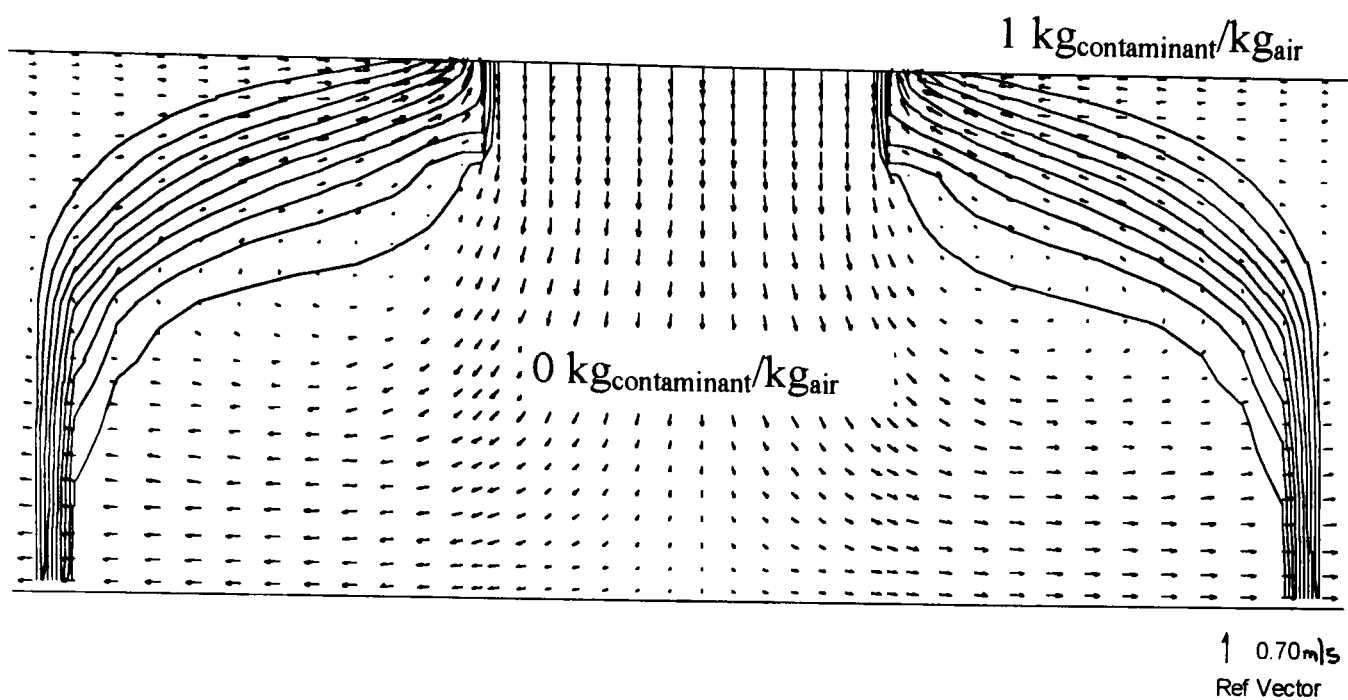


Figure 7.56 2 dimensional simulation of airflow from the UCV canopy at supply temperature 20°C and velocity 0.38 m/s and concentration contours of a contaminant seeded at the open boundary walls. Ambient 20 °C.

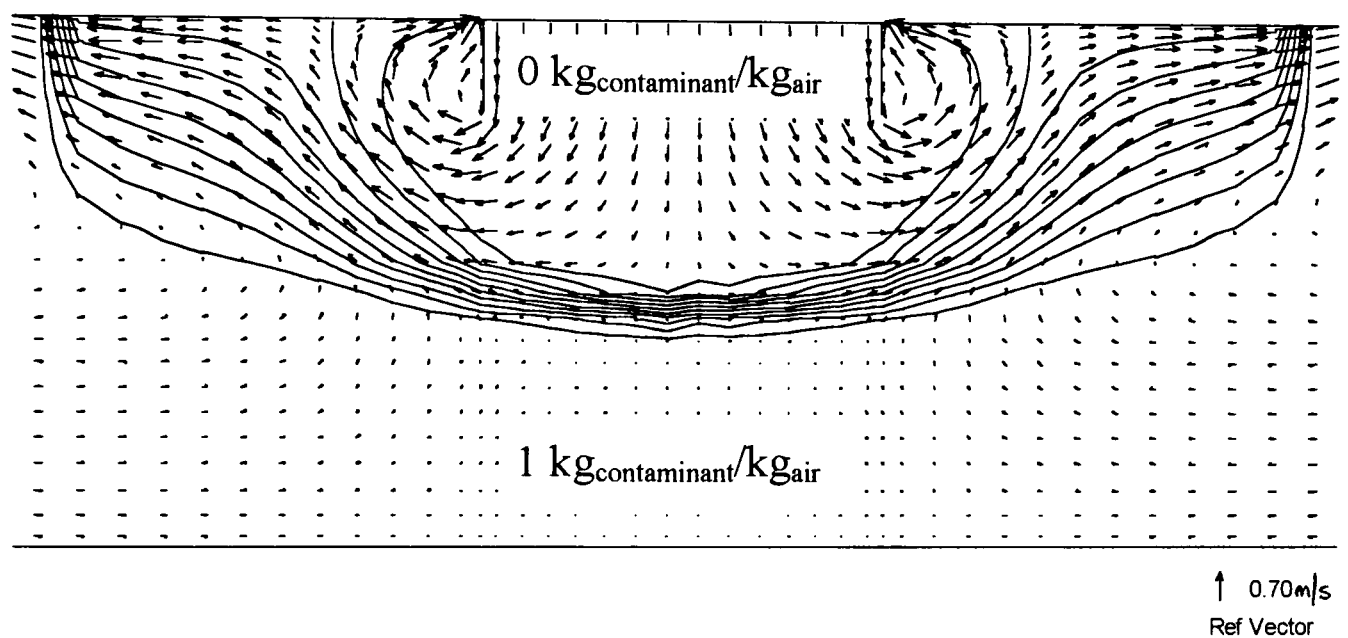


Figure 7.57 2 dimensional simulation of airflow from the UCV canopy at supply temperature 40°C and velocity 0.51 m/s and concentration contours of a contaminant seeded at the open boundary walls. Ambient 20 °C.

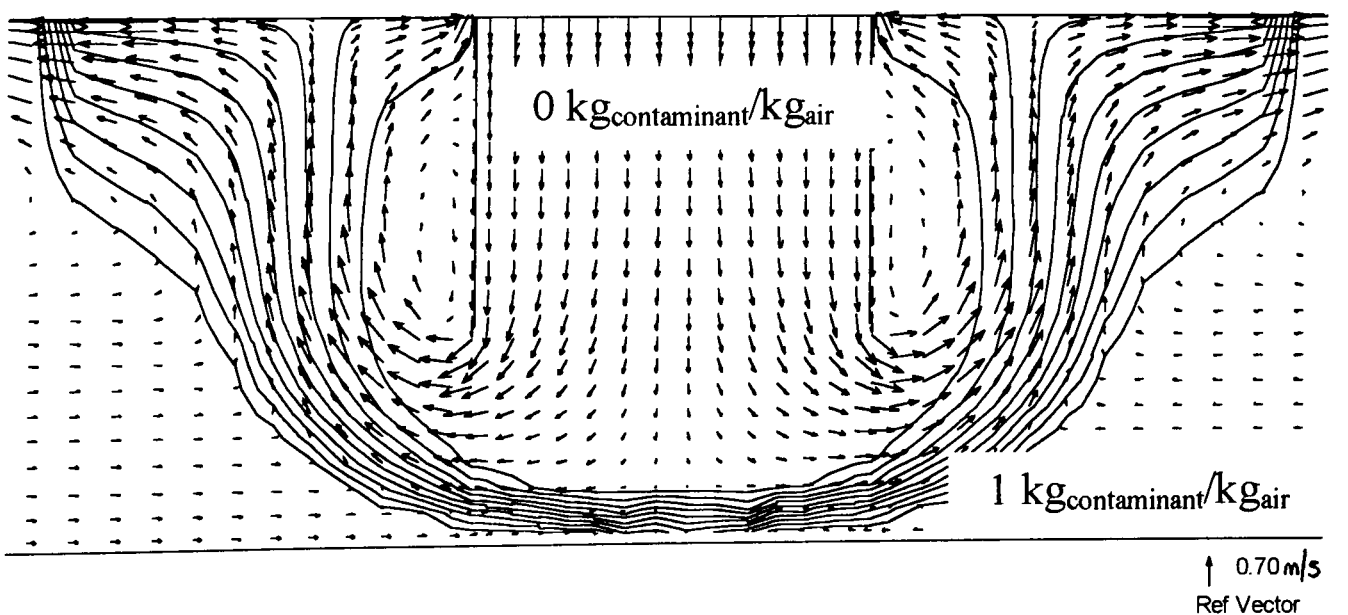


Figure 7.58 2 dimensional simulation of airflow from the UCV canopy (extended) at supply temperature 40°C and velocity 0.51 m/s and concentration contours of a contaminant seeded at the open boundary walls. Ambient 20 °C.

5. Visualisation of the entrainment of air into the “clean” zone beneath the canopy during no disturbance or during the movement of people.
6. Identification of any regions where further quantitative analysis was required.

However, such qualitative analysis was not sufficient to show compliance with design parameters such as air pressures and airflow rates. The use of air pressure, temperature, humidity and air flow measurements showed whether the Unit was built to or being maintained to the design criteria but did not necessarily demonstrate how it performed for controlling cross infection/contamination.

For quantitative assessment, the absolute counts of particles and airborne bacteria demonstrated regions of person activity or excessive turbulence compared to regions of non - activity and stagnation where particle settling was considerable. The number of bacteria sampled from the air correlated strongly with the particle counts $> 5 \mu\text{m}$ (Spearman's rank correlation coefficient > 0.7). Counting airborne particulates and bacteria as a guide to performance has been well discussed in the literature and was used for the assessment of clean rooms and operating theatres, being incorporated into certain National Standards. For the assessment of the UCV in this investigation, such absolute counts gave an adequate assessment of number of particles and CFU below the canopy and at the bed surface during activity and non - activity, and hence the ability to prevent entrainment of potential contaminants from the room, both with no disturbances and when there were environmental disturbances and movement of people. However, these methods did not assess the potential cross-infection/contamination within the Unit or intensive care room between regions. Identifiable strains of micro - organisms carried by the patients were used for this purpose (Williams & Harding, 1969) but the dispersing sources were not under control and the relatively small numbers of identifiable airborne particles dispersed meant that the method was rather insensitive and that observation had to be carried out over a prolonged period.

The use of gas and inert particle tracers provided a much more descriptive method of assessing the Unit and UCV performance in terms of contamination control. These showed how a potential contaminant was distributed within the rooms of the Unit and how well isolated various regions were from the source of the potential contamination. The limitation of these methods (similar for all such methods using point source and sampling of tracers) was the relative positioning of the source and samplers with respect to each other, air mixing patterns, regions of re-entrainment and the re-circulation of air through the ventilation systems. In this investigation it was known that some of the air extracted from the intensive care room was recycled back into the UCV supply ventilation and thus back into the room. This prevented the use of gas tracer for assessing the isolation of the “clean” zone under the canopy from the rest of the room as any gas released in the room would be recycled back into the room through the canopy and there would be a build up in background levels. This was not a problem using particle tracers because they were removed from the air by the supply

HEPA filtration units. However, there was a problem in using particle tracers due to sedimentation and impaction.

The effectiveness of gas and particle tracers for the assessment of cross contamination in the Unit and intensive care room was compared using the transfer index expression. This was derived for both gas and particle tracers by Lidwell (1960) to represent movement of tracer through ventilated areas and to quantitate the effective isolation of the sampling point from the source. The transfer index was the ratio of tracer concentration/amount sampled to the amount released:

$$TI_{\text{gas}} = \frac{Ct}{q} \times 10^{-6} \text{ and } TI_{\text{particles}} = \frac{n}{ZN}$$

where C was the concentration of gas sampled (ppm), t was the sampling time, q was the amount of gas released (m³), n was the number of particles sampled, Z was the sampling rate (m³/s) and N was the number of particles released. The lower the value of the transfer indicated greater isolation of the sampling position from the source.

From early work by Foord & Lidwell (1972, 1975), using gas and particle tracers to evaluate hospital areas, there was a disparity between the transfer indices for both tracers; the particle transfer index indicated between 4 and 25 times greater isolation of the sampling site from the source. This was accounted for by the assumption of sedimentation from well mixed air masses during the time required for the movement of particles between the two positions. This disparity was also found in this investigation; the particle transfer indices were 1 - 2 orders of magnitude less than the gas transfer indices (Table 7.14). However, this was also attributable to the corridor particle transfer indices being based on estimated numbers where the filters were saturated. Also some recirculation of gaseous tracer would be expected in the intensive care room.

Position	Particles			Gas		
	Floor	Midway	Ceiling	Floor	Midway	Ceiling
1	0.0306	0.0613	0.0613	1.848	2.320	1.944
2	0.0613	0.0613	0.0613	0.696	1.152	1.176
3	0.0306	0.0368	0.0368	1.224	1.224	1.200
4	0.0204	0.0123	0.0092	1.296	1.200	1.296
5	0.0306	0.0085	0.0010	0.792	0.120	0.000
6	0.0036	0.0002	0.0002	0.000	0.000	0.000
7	0.0039	0.0003	0.0008	0.720	1.128	0.000
8	0.0053	0.0032	0.0006	0.672	0.048	0.000

Table 7.14 Transfer indices for gas and KI particle distribution in the unit (Fig. 7.7).

There was a similar trend of transfer index with position within the Unit for both particle and gas tracers. These trends correlated strongly ($r > 0.8$) between each height for particles and

gases; there were high transfer index values in the corridor and lower ones through the rest of the Unit. However, the transfer index for both tracers along the corridor was greater towards the ceiling (Fig. 7.59) suggesting that the air was pulled towards the ceiling, considering that the source was 200 mm from the floor. In the regions of the Unit other than the corridor, i.e. across the intensive care room doors, the transfer index was greater near to the floor suggesting that here air was sweeping across the floor with little lateral mixing in the room. This reflected the greater movement of air through the gaps underneath the intensive care room doors than around the vertical and top edges.

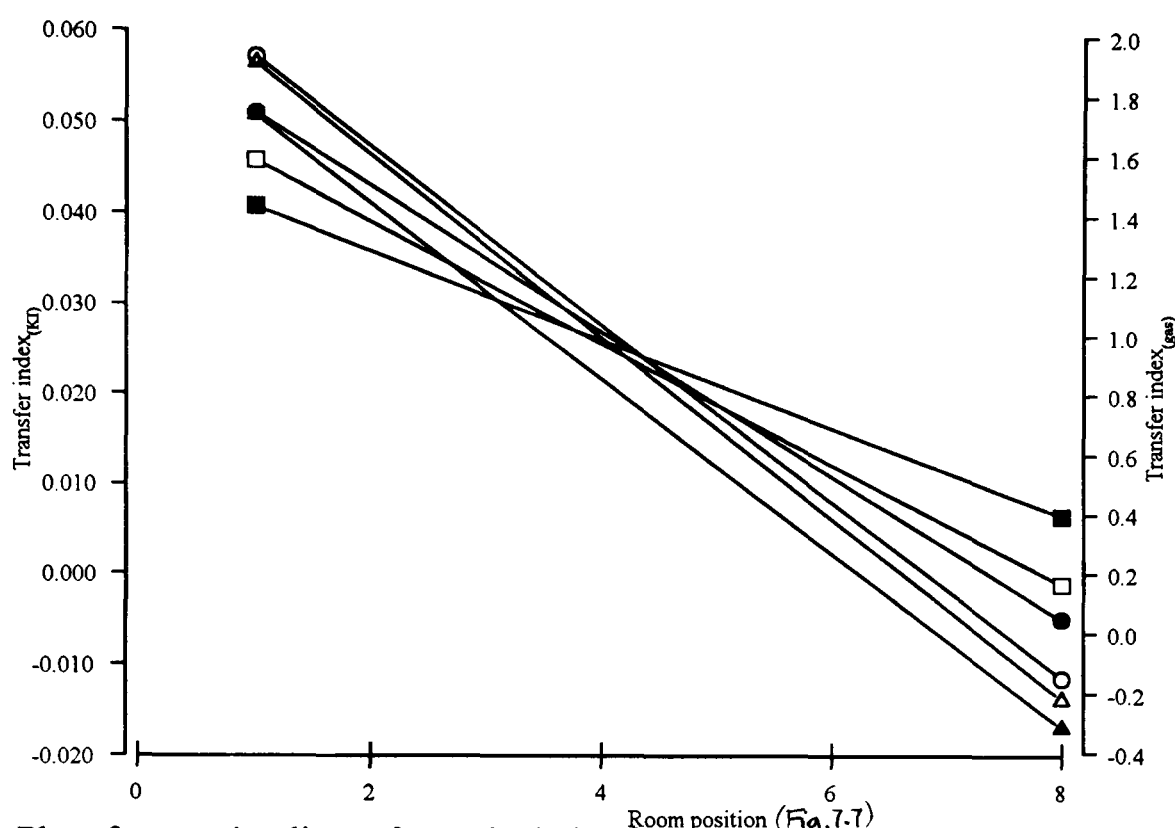


Figure 7.59 Plot of regression lines of transfer index for gas and particle tracers with room position. Gas mid height ●, KI mid height ○, gas floor height ■, KI floor level □, gas ceiling ▲, KI ceiling △.

There was a strong correlation between the particle and gas transfer indices for sampling positions near to the ceiling throughout the Unit ($r > 0.8$). However, this was much weaker for samples taken nearer to the floor where there was poor correlation ($r < 0.4$). At this level, the transfer index for particles was up to 4 orders of magnitude less than for gas. This suggested that due to the greater distance of the sampling positions from the source and the passage of ^{air} around doors there was greater sedimentation and impaction of particles on surfaces. In the intensive care room and viewing area near to the ceiling there was negligible amount of gas sampled although particles were suggesting that the limits of the gas analyser were reached.

7.13.2 Comparison of CFD simulation with physical measurements and use for performance assessment

Similar conclusions on the performance of the Unit and UCV for controlling contamination and comfort were made using both physical measurements and computational fluid dynamics. It was shown that there were undesirable airflow patterns within the intensive care room and at the foot end of the bed, there was little air flow at the bed surface and the buoyancy

resulted in air from outside the canopy encroaching beneath the canopy. The two assessment techniques also lead to similar conclusions as to the effect of changing the room design features on contamination control and general airflow distribution. Extension of the canopy was shown to increase the airflow near to the bed surface and increase the resistance to environmental disturbances of the airflow beneath the canopy. However, they also showed how preventing some of the “rogue” draughts into the room increased others. An important conclusion from both techniques was how some design changes did not solve all problems but highlighted how some design changes created new problems.

The 'visualisation' of the airflows using CFD compared well with the general air flows shown using smoke tracer. The CFD pictures could be superimposed over the smoke pictures taken within the intensive care room and around the UCV and the patterns were very similar both representing the recirculation points of air from beneath the canopy and into the room and up towards the ceiling extracts (Plates 7.4 and 7.5). For smoke visualisation the smoke has to be released in a particular region and photographed before becoming fully dispersed with no resolution of depth. However the advantage of CFD is that it shows the complete flow field or partial field in any plane.

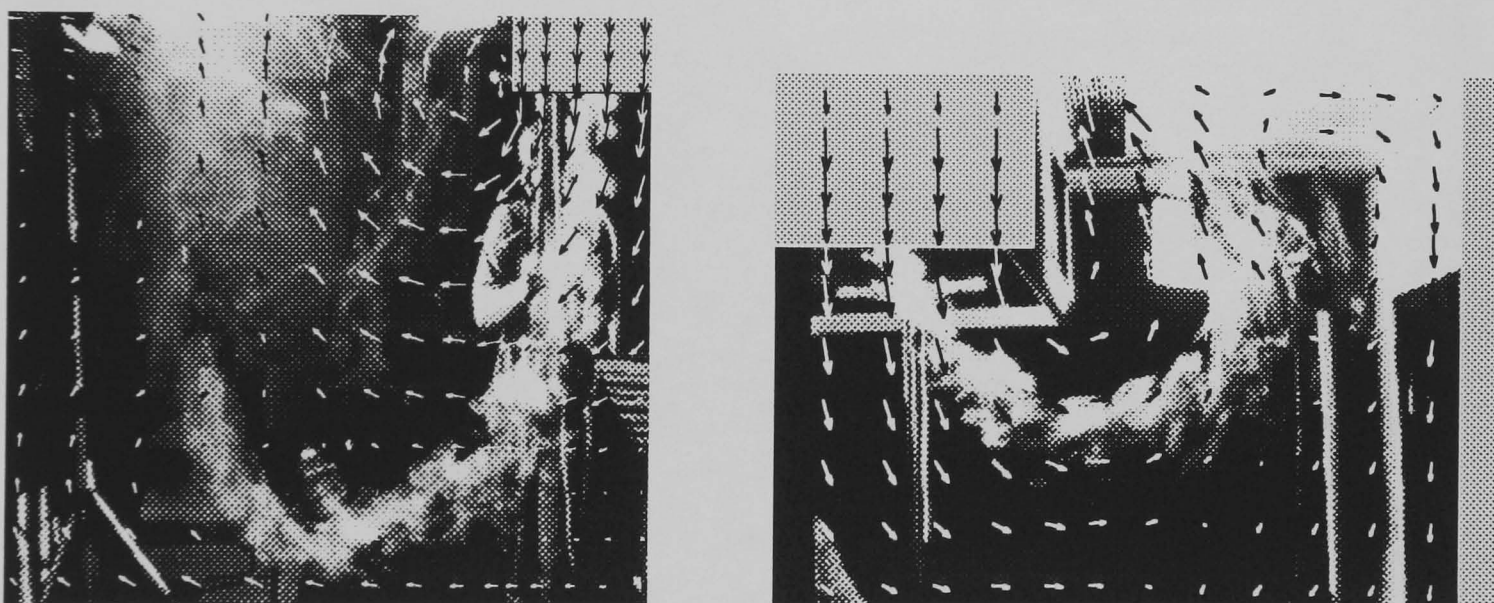


Plate 7.4 & 7.5 Movement of smoke in the intensive care room overlaid with results of CFD simulations, from beneath the canopy to the windows and towards the viewing area, respectively.

As a qualitative tool CFD and physical measurements compare well but in order to be used for performance assessment CFD must give confidence as a quantitative tool. In the absolute values for temperature, airflows and contaminant dispersal there is some disparity between CFD and the physical measurements. However, the relative trends are similar and produce similar conclusions. Allowing for standard errors of measurement the differences between the two systems are much smaller.

Comparing the airflow measurements under the canopy between CFD and measurements using anemometers the trends were very similar (Fig. 7.60). The CFD velocity may be described as X, Y or Z components (Y vertical) and speed. The Y values and measured velocities had the greatest difference at the edge of the canopy which perhaps reflected the

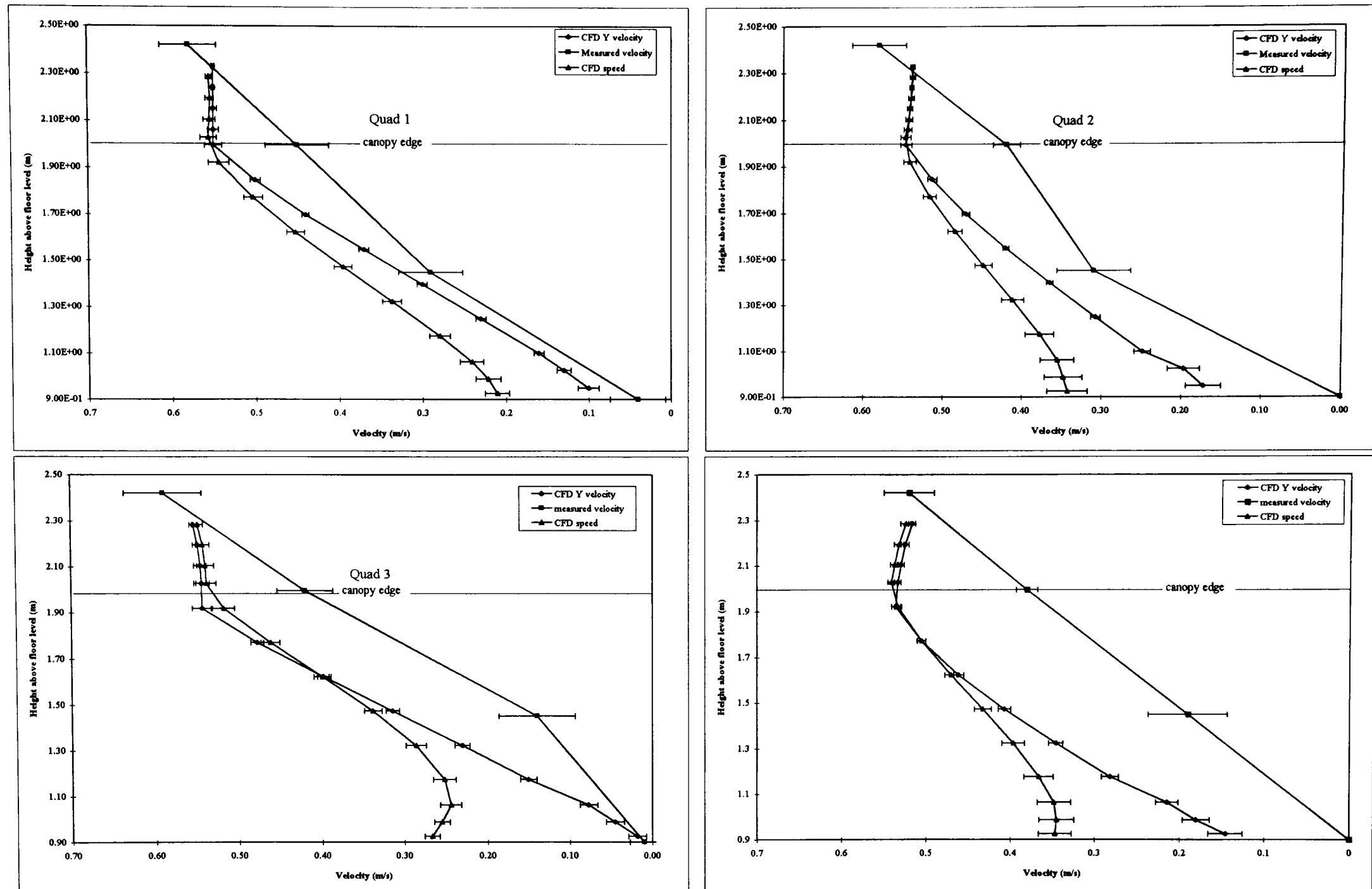


Figure 7.60 CFD Y velocity, speed values and measured velocities beneath each quadrant of the UCV and over the bed surface.

measurement of small jets created by the diffusers so giving a raised value. The profiles were similar below the canopy and showed a reduction in Y velocity and measured velocity towards the bed surface, approaching negligible values. From the speed profiles it is obvious that the airflows were reduced near to the bed surface but also separated more into the horizontal rather than vertical components.

The temperature distribution within the room compared closely between the CFD values and the measured values (Fig. 7.61). Near to the ceiling the calculated results were up to 2 °C less than the measured temperatures. However there was less difference at mid heights and near to the floor. Both methods showed stratification of temperature within the room and both methods indicated higher temperatures near to the corridor than the rest of the room. The greatest difference in the results was in the regions in front of the viewing area and dressing room doors where the CFD values were much lower at mid height and the former lower at floor level. This was considered due to the draughts from around the doors at a temperature of 20 °C so lowering the temperature within the room in this region. It may be that these draughts were mis - represented in the problem setup.

Monitoring the dispersal of a contaminant within the room gave similar conclusions from both methods; identifying the encroachment of room air under the canopy near to the foot end of the bed. An advantage of the CFD model was that the spread of the contaminant could be 'visualised' over the whole domain or any particular region in any plane. It also enabled the position of the source to be simply altered in order to observe the effect of source position. For physical measurements the relative position of the source and samplers may be critical to each other and to the room ventilation points. The CFD model could be used to select the most suitable positions at which to position the source and samplers for physical tracer measurements. The limitation of the CFD model was the simulation of a disturbance. Moving boundaries such as people were not part of the model and as such the effect of someone moving into and out of the canopy could not be represented. As seen from using physical measurements the movement of people has a profound effect on the transport of potential contaminants under the canopy.

The CFD model has so far been compared to the measured data. However the CFD model was also based on these measured data and has been shown to compare well. If the measurements were not available and the airflows could only be anticipated, how 'realistic' would the simulation be? Using only the design data gave conclusions similar to the physical measurements and simulation based on the measured data. However it did not identify problems such as unwanted draughts through drawers or any other departures from the design. It was also difficult to anticipate how the air would enter around designed 'leaky' doors and thus what effect this would have. A fundamental point is that although a simulation based on the design data will give results as expected in reality, it does not allow for the fact, commonly experienced, where the design criteria are not met. It is thus relevant

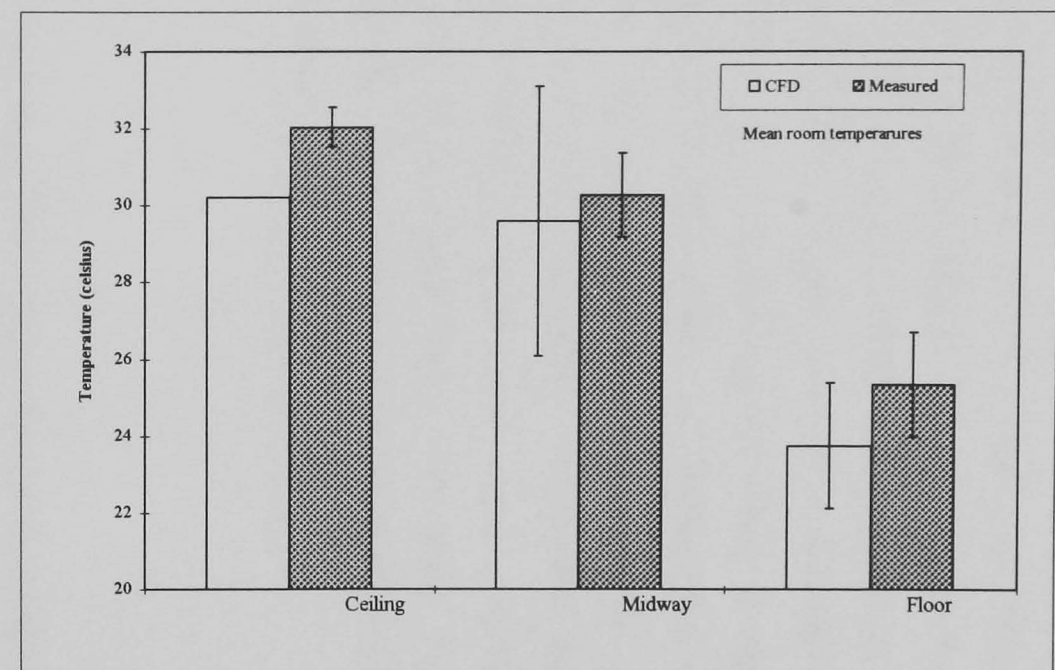
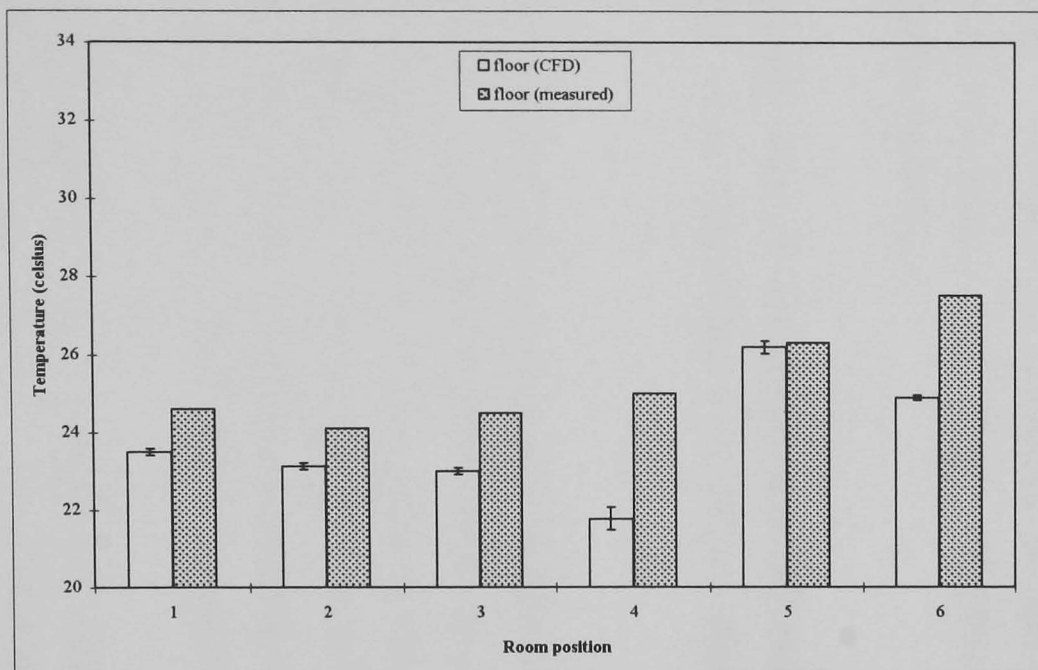
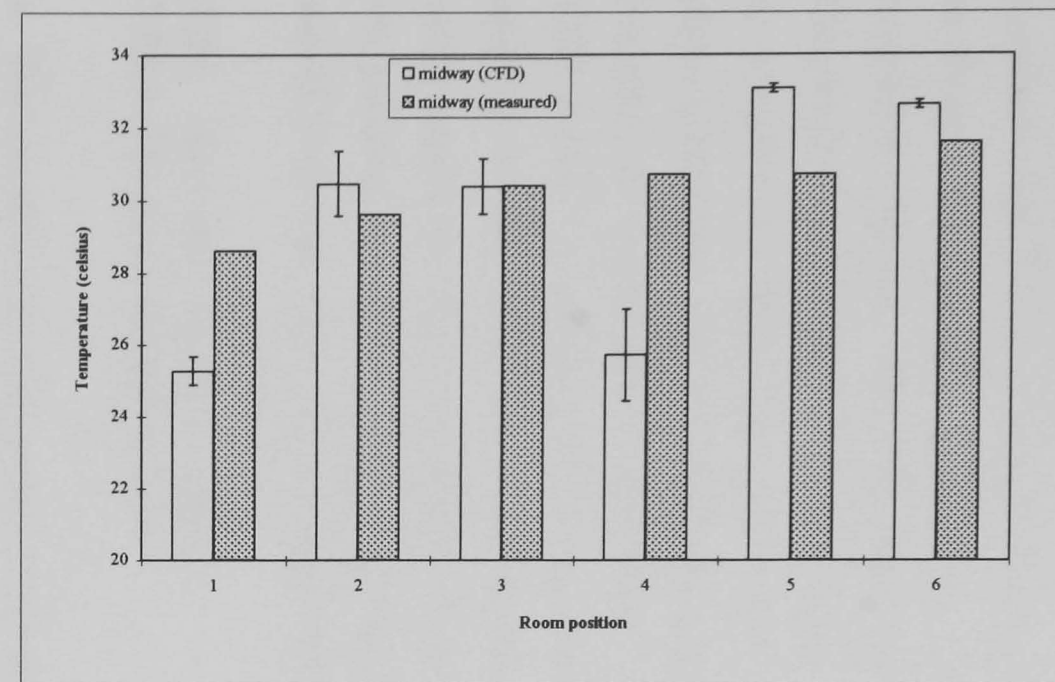
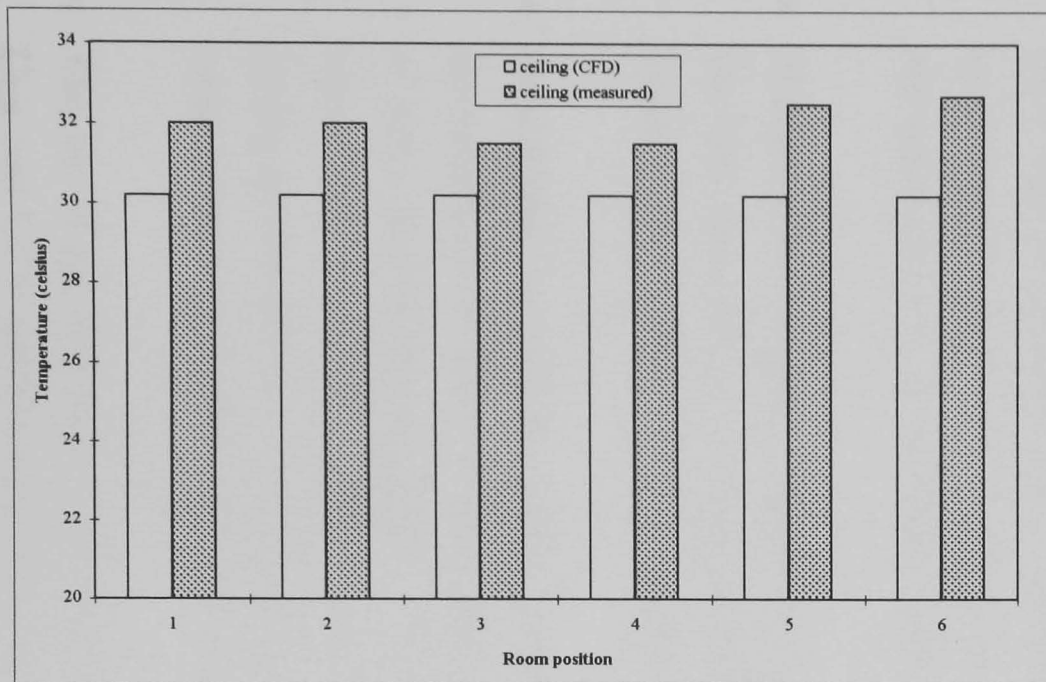


Figure 7.61 CFD calculated and measured temperatures within the intensive care room. (CFD 95 % confidence limits show the spread of data for several grid cells at each position at ceiling height, midway and floor height, and for spread of mean temperatures in room at each height). (For room positions see Fig. 7.11).

in predicting how a design will function but not necessarily how it actually functions when built, and it is still necessary to carry out tests to validate and commission a facility.

The CFD model showed great potential in predicting the effect of design changes. The simulation was fine tuned using the physical measurements and then used as an analytical tool to observe the effects of changing the ventilation characteristics of the room and the airflow beneath the canopy. The conclusions from these changes gave the same conclusions as using the physical measurements but the changes were much simpler to set up and relatively faster to compute and make conclusions using CFD. An example was the effect of moving the viewing area door to another part or changing the position of the room extracts and openings. For physical measurements to be made this would require major building work but using the CFD model the results could be gained quickly and with little effort. It was also shown that alterations which may have been thought beneficial to performance could actually reduce performance and thus be a costly mistake if physical measurements were used. In addition the potential number of detailed design changes that could be made using the CFD model would be greater than could be undertaken using physical measurements.

7.14 Key interim conclusions

7.14.1 Physical measurements

- The simplest and most graphic method that characterised the performance of the Unit and UCV was visualisation using smoke tracer. This gave an immediate perception of the overall performance and identified the most important aspects of the ventilation. It was not sufficient to show compliance with design parameters.
- The use of air pressure, temperature, humidity and air flow measurements showed whether the Unit was built to, or being maintained to the design criteria but did not demonstrate performance for contamination control.
- Quantitative assessment using absolute counts of particles and airborne bacteria demonstrated the effects of personnel activity or excessive turbulence compared to regions of non - activity and stagnation. They showed the UCV to have good performance in maintaining low numbers of particles and bacteria below the canopy and at the bed surface during activity and non - activity. However, these methods did not assess the potential for cross-infection/contamination between regions within the Unit or intensive care room.
- The use of gas and particle tracers provided a more exhaustive method of assessing the Unit and UCV performance in terms of contamination control. These showed how a potential contaminant was distributed within the rooms of the Unit and how well isolated various regions were from the source of the potential contamination.

7.14.2 Comparison of CFD simulation with physical measurements and use for performance assessment

- The CFD simulations using the design data and measured data, gave similar conclusions to the physical measurements. However, the simulation based on the design data did not allow for deviations from the design criteria. CFD was thus relevant in predicting how a design would function but not necessarily how it actually did function when built, and it was still necessary to carry out physical tests to validate and commission the facility.
- The CFD model showed great potential as an analytical tool for predicting the effect of design changes. It was shown that alterations which may have been thought beneficial to performance could actually reduce performance and thus be a costly mistake if physical measurements were used.
- CFD had the advantage over physical measurements in being able to ‘visualise’ the airflows and contaminant dispersal within the intensive care room in any region or any plane. For the assessment of cross contamination the CFD program enabled the position of the source to be simply altered in order to observe the effect of source position. For physical tracer measurements the relative position of the source and samplers could be critical to each other and to the room ventilation points. The CFD model could be used to select the most suitable positions.

Chapter 8 General discussion and conclusion

8.1 Contamination control equipment and assessment strategies

The damaging effects of gas and particulate contaminants can be a critical factor in industry, scientific research and healthcare. Contamination control systems, used for reducing the exposure of vulnerable sites to such potential contaminants, have to be assessed in order to ascertain whether they function correctly and achieve the required level of protection. In this study open fronted containment systems, used to limit exposure of the operator/product to airborne contamination, and Ultra Clean Ventilation (UCV) systems, used to reduce contamination of wounds during surgery and burns, have been investigated. The performance of these systems and the strategies and methods used for their assessment have been investigated.

A strategy incorporates several methods to give an overall indication of performance, each method providing limited information on its own. There are qualitative and quantitative methods and the relative importance of each and how they compliment each other is critical to the strategy. The key question is, do they give representative information about the function of contamination control systems?

Another problem is the standardisation of testing strategies and component methods for the assessment of similar types of contamination control systems. Most often the strategies adopted as National Standards for specific types of equipment do not have the same philosophy (section 2.2.2, 2.3.2), which is not a problem as long as the different test methods yield comparable results but is a problem when they don't. Therefore, for the design, production and international marketing of contamination control equipment, testing to each National Standard is required. This is time consuming and increases costs.

8.2 Open fronted containment systems

For the assessment of fume cupboards the ASHRAE 110 1993/SAMA LF 10 1980 test strategy is the most extensive involving smoke visualisation, face velocity and containment testing. The BS 7258 : 1994 strategy places main emphasis on a complex face velocity test with only a recommendation for containment testing. The DIN 12 924 test strategy places emphasis only on containment testing. The French and Australian standards have no containment test. The DIN and ASHRAE test strategies are the only ones to specify minimum performance criteria.

There is a great difference in the methods used, each with a different philosophy. In each containment test, tracer gas is released within the working volume of the cupboard but through different injector devices. The ASHRAE and DIN tests use a manikin and require sampling for leakage at a fixed distance from the sash plane. The ASHRAE test requires

sampling in the breathing zone of the manikin. The DIN test requires sampling through a grid encompassing the aperture. The BS test has a different philosophy requiring sampling in the sash plane itself, thus measuring potential leakage. All these tests may be used for type testing or on site.

For the assessment of microbiological safety cabinets (MSC) there is not such a diversity in the strategies incorporated in National Standards, emphasis being placed on a containment test. However, there are some differences in the methods used but the BS 5726, NSF 49, DIN 12 950 and JAS 1981 containment test methods are very similar, each using bacterial spores released inside the cabinet and sampling for leakage at a fixed distance from the sash plane. In BS 5726 there is a further option of using KI particles instead of bacterial spores. The BS 5726 strategy, similar to the others, is based on a hierarchical structure of flow visualisation, face velocity and then containment testing. In each of these strategies, unlike those for fume cupboards, there are minimum performance criteria that the safety cabinet must achieve. Each of these microbiological safety cabinet test methods uses a hierarchical strategy at type testing, commissioning and routine maintenance.

The assessment of leakage from safety cabinets at a fixed distance from the aperture plane is similar to the ASHRAE and DIN fume cupboard test methods but not to the BS 7258 method. However, there is a great difference in the philosophy of the tracer generation methods. The aerosol used in the safety cabinet test is a much greater concentration of spores/particles than would be experienced during normal working conditions and challenges the weakest point where containment is considered to be achieved. In class I cabinets this also results in further dispersal within the working volume. The gas tracer challenge is a passive release designed to reflect working conditions and to disperse within the working volume.

The results obtained from these test strategies may not be comparable and thus results from testing a fume cupboard or safety cabinet may indicate different levels of performance depending on the method used. In the development of BS 7258 : 1994 : Part 4, a limited comparison of fume cupboard assessment methods suggested little practical correlation between DD 191 and DIN 12 924 containment test methods. There has been correlation of the microbiological and KI test methods in the BS 5726 containment method. However there has been no practical correlation of fume cupboard and safety cabinet test methods and no comparison of assessment strategies.

The basic principle of operation of open fronted containment systems is similar, all achieving containment by enclosing the source in a chamber and manipulating the air flowing through it. It would appear that a common strategy could be used for testing all types and with methods that yield comparable results. Box type fume cupboards and class I safety cabinets can be considered to achieve containment in similar ways and it may be possible to compare the

performance of fume cupboards and safety cabinets using the gas and bacterial/particle tracer tests.

The BS 5726 KI method, and a modification of this method (Clark et. al, 1987), have been used by some workers with confidence for testing fume cupboards but the principle has not been formally accepted as a standard alternative to gas testing for fume cupboards. It is however, still used on fume cupboards as part of service contracts on safety cabinets. In this study, the BS 5726 : 1992 assessment strategy has been revisited and an attempt to correlate the results obtained when using the KI test method and the BS 7258 : 1994 method have been made.

A survey was carried out on the fume cupboard stock at King's College London (KCL) to evaluate the type, condition and performance. A hierarchical test strategy involving flow visualisation and face velocity was used, from which each fume cupboard was graded. This strategy was crude but designed to yield information on those cupboards *in-situ* that were not working at all, those that had poor performance and those that were satisfactory. No containment test was included at that stage because it was considered not to yield any additional relevant information and was not therefore cost-effective.

Of 221 cupboards surveyed at KCL there were aerodynamic and wooden box types, with one, two or three sashes, with some opposing. It was found that there was a large variation in performance. There were those that were switched off and did not work at all (unknown to the users), those in which the variation in face velocity across the aperture was extreme, those with very low or very high face velocities, those which were cluttered with almost total obstruction of airflow, those in which the airflow was visibly poor due to poor siting and those which were satisfactory.

With the sashes at normal working heights there was no significant difference in terms of graded performance between the aerodynamic and box type cupboards; the aerodynamic cupboards were expected to work better. This indicated that the majority of fume cupboards in this survey were installed and used in a way that was far removed from the ideal conditions in a test room and, perhaps, the conditions at commissioning. There appeared to be little understanding by the user of the principles of fume cupboard containment, the effects of equipment bulk within it, of personnel movement and of environmental disturbances near to the aperture. There were also problems in the manner in which make up air was introduced into some rooms, which on occasions involved the opening of windows resulting in draughts.

It was concluded that no real performance assessment strategy had previously been applied to the majority of cupboards given the diversity of type, condition and performance even though the college had its own strategy and BS 7258 was available. For satisfactory performance, the user had to know how the facilities functioned and that work discipline was very

important. Of those that had been tested by the college strategy or to BS 7258, none had been assessed by containment testing.

This was not necessarily representative of all institutions and in those where strict testing and user awareness was required, better performance would be expected. This did reflect though peoples attitude to an unidentifiable risk, not necessarily treating performance seriously. It also reflected the notice given to the available BS 7258 and guidelines which did not specify any minimum performance criteria. From discussions with fume cupboard users in the KCL survey, it seemed that microbiological safety cabinet testing was much better received and the user had more respect for its use. This was most probably due to an identifiable risk and perhaps to clear performance guidelines.

BS 7258 : 1994 was investigated. There was no hierarchical strategy and different protocols were used for type testing, commissioning and routine maintenance testing. These were designed only to indicate a decline in performance and not to establish any minimum performance levels. Flow visualisation was suggested only at the commissioning stage and the inclusion of a containment test was only a recommendation at any stage. The results of using the complex grid for measuring face velocity in type testing and commissioning were not significantly different, questioning the relevance of such a complex grid for type testing.

The BS 7258 : 1994 containment test protocol showed that the fixed flow rate through the gas analyser was too low and the response times too long. The tracer gas was not fully dispersed within the cupboard when released from a single source position. As the source was moved over the aperture plane, it was assumed that for a complete test the majority of the cupboard working volume was seeded with tracer, albeit not at the same time.

This investigation also suggested that the type test was far removed from the *in-situ* case. The face velocity was reduced to 0.25 m/s, a velocity known to be vulnerable to environmental disturbances. However when tested there was no leakage. This showed how stable the airflow and containment was at low flow rates in the ideal conditions of the test room but not how this could be seriously challenged during potential disturbances on site. Further limitations of the method were shown when the fume cupboard was modified and no leakage was measured in the plane of the aperture near to the sash handle and in the lower corners, although this was demonstrated using water fog. Only by rearrangement of the grid and position of source was tracer sampled in these regions. It appeared that in the stable environment of the test room the sampling grid did not measure edge effects where tracer may have leaked out and was most likely re-entrained back into the cupboard. *In situ* this may have been carried into the room.

The re-entrainment of air discharged from the fume cupboard back into the test room from ducting was also a problem resulting in raised background levels of tracer. This made testing

of the fume cupboard meaningless and identified a problem in discharge, but as the fume cupboard and ducting were considered to be the containment envelope then this was an important factor.

BS 5726 : 1992 was also investigated. In this, the hierarchical structure of flow visualisation, face velocity and containment testing was the same for type testing, commissioning and routine maintenance testing with little change in protocol and with clear performance criteria. For quantitative assessment there was a choice of two methods; microbiological and KI, which for unequivocally 'good' or 'poor' performing cabinets yielded similar conclusions. However, for marginal cabinets which may have been shown occasionally to fail the minimum performance levels of containment and cross contamination by the KI method, there was a disparity; the KI method indicating a failure in performance, the microbiological method indicating satisfactory performance.

This was looked at theoretically and practically which indicated that the difference in generation and sampling methods may have been exaggerated in these cases. The generation of KI challenge had greater momentum than the microbiological challenge. The final droplet/particle size had terminal settling velocities less than the velocity of air flowing through the cabinet. Therefore the final challenge would be suspended and influenced by the cabinet airflow. It was considered that particle deposition in the test was by virtue of the airflow pattern and cabinet design resulting in impaction, settling in stagnant regions or any other force acting and not entirely due to particle/droplet settling alone. Thus the challenge was always the same, losses during the test being a result of the cabinet performance.

It was also shown that an indicated failure of a cabinet could be due to contamination only. This was shown to be relatively easy and as spurious as actual leakage. Such contamination was of clothing, cleanliness of equipment and the testing of more than one cabinet in the same room at any one time. The effect of environmental disturbance was also investigated which showed that in the absence of cross draughts, the movement of an operator's arms out of the cabinet could result in a serious breach of containment where aerosol droplets/particles generated in the working volume could be trapped in the material of the clothing.

From this work it was evident that there were limitations in both containment test methods for the assessment of fume cupboards and microbiological safety cabinets. The theoretical possibility of testing microbiological safety cabinets using the method in BS 7258 1994 : Part 4 was attempted. If the cabinets were ducted outside then this may have been possible. A class I cabinet had similar airflow characteristics to a box type fume cupboard, but compared to a modern fume cupboard, the design was poor. Using the BS 7258 method could possibly result in tracer being sampled in the sash plane. This needed further investigation. However, the design of class I cabinets was shown not to leak within the specifications of BS 5726. This was considered to be due to the small opening and high face velocity. Perhaps the

design of class I cabinets should be reviewed? However, class II cabinets have become more popular and perhaps the days of class I cabinets are numbered? Work with the BS 7258 containment test method for testing microbiological safety cabinets was discontinued because it was not considered to be practicable. The effluent air of many safety cabinets is recycled back into the room and the exhaust HEPA filter would not remove the gas from it. This made testing meaningless.

The theoretical possibility of testing fume cupboards using the KI method was attempted by correlation with the BS 7258 : 1994 : Part 4 method. This was shown to be possible if the equipment was placed in the same positions for each method. Using the position relative to the sash plane the results could be interpolated with respect to the amount of tracer sampled at a fixed distance away from the sash plane to the plane itself. However, this made the assumption that i) generation of tracer had no effect, ii) that the particles diffused and dispersed as a gas, and iii) whatever tracer was sampled at a fixed distance away from the aperture by the KI method would be sampled in the plane of the sash using the gas method. It was also shown that the particle tracer method was much more sensitive than the gas tracer method. This theory was challenged in practice.

BS 5726 was applied to fume cupboards. The test method was first used in the KCL fume cupboard survey on a small selection. The equipment was positioned as for a class I cabinet, considering a box type cupboard was similar to a class I cabinet. The results of this however did not show a strong correlation with the flow visualisation grading and face velocity results. There were anomalies where a cupboard with a good grade had poor containment and of those cupboards tested which had very poor grades there were none with operator protection factors $> 10^5$. The grade was only an indication of performance whereas the KI test provided more quantitative data with greater sensitivity. However, on a couple of occasions out of the 16 cupboards tested there was an obvious problem with the position of the KI equipment not identifying regions of obvious leakage.

It was considered that the position of the equipment for BS 5726 class I cabinets did identify poor performing fume cupboards but did not sufficiently challenge the entire aperture and was not suitable for aerodynamic cupboards. This was shown using an artificial disturbance in an aerodynamic cupboard. A jet of nitrogen gas was used to entrain air from within the cupboard out through the aperture and thus to challenge containment during a test. This confirmed that there was no vertical mixing from the work surface and there was no challenge near to the sash where leakage could occur.

Whereas a box type cupboard may be like a class I cabinet the flow regime in an aerodynamic fume cupboard was not. In this the scavenging of air from the work surface was separate from that behind the sash with little mixing resulting in a vertical stratification. Any tracer released from the work surface was immediately swept away with no dispersal into the region

behind the sash. This may not be the weakest point where containment is achieved, which was the philosophy for testing class I cabinets, i.e., beneath an artificial arm, past through the aperture and the subsequent dispersal within the working volume. Due to the size of the aperture, the artificial arm was not considered effective and excluded from the tests. Therefore, it was considered that the whole aperture should be challenged vertically i.e. to include tracer generation both near the work surface, at mid aperture height and near to the sash handle.

The equipment was rearranged so that laterally the KI challenge was generated 100 mm from the plane of the aperture at each of three heights. On the work surface or level with the lipfoil where fitted, at mid aperture height and in the region of the sash handle. Air was sampled through single samplers 150 mm from the plane of the aperture level with the KI generator. This would be conducted in the centre line of the aperture but as in BS 5726 for apertures wider than 1.2 m the test would be repeated at the centre of the left and right halves. It was considered to have two samplers at each at fixed distances either side of the vertical centre line of the source.

The limitation of this method was the number of replicate tests to be conducted at each position according to BS 5726. If this were done at each height then 15 tests would be required for each position across the aperture making a possible 45 tests in all (approximately 450 minutes in total); this would be impractical. The reason for 5 replicate tests seemed to derive from the viability of spores used in the microbiological test but this was not a problem in the KI test. As the BS 7258 gas test assumed a test period of 10 minutes for each of the 6 positions (60 minutes total), perhaps the 5 replicate tests was not necessary for the KI method. Over a 5 test run only one test might show a failure. More work needs to be done in adjusting the number and duration of tests and observing the effects on results. This could be achieved by pooling all the data from service technicians using the KI method, to establish after how many tests a failure was evident and from this seeing if all 5 tests were required. For the ASHRAE test for fume cupboards at one position it was stated that a failure usually occurred in the first 5 minutes of testing.

The arrangement of the BS 5726 equipment was altered to simulate the positioning of the BS 7258 equipment relative to the sash plane. This resulted in the samplers being saturated with KI particles. This suggested that the particles were thrown at the aperture and the sampler bulk and capture velocity had an effect. The efficiency of the two sampling methods was also compared but showed a great disparity. It appeared that the KI samplers were much more efficient at sampling the tracer gas than the BS 7258 probe.

In practice the KI particles were shown to challenge the plane of the aperture and would not be expected to diffuse as a gas due to the relatively large size compared to gas molecules. The results of the KI and BS 7258 tests were compared at varying face velocities. At 0.25 m/s only KI was

sampled beyond the aperture plane but at 0.85 m/s gas was sampled only in the aperture plane. This showed that i) what was sampled at a fixed distance away would not necessarily be sampled in the plane itself by the other method and vice versa and ii) the gas test was passive and the KI challenged the containment at low face velocities. The low face velocity would be vulnerable to environmental disturbances and although the gas test indicated how stable the cupboard was operating in the test room environment, the KI method demonstrated how fragile it could be. As there was no criteria for a minimum face velocity in BS 7258 then this may be experienced on site, and applying the KI method would indicate a failure, the gas test not necessarily so.

From this work it was concluded that the containment testing philosophies of the BS 7258 : 1994 containment test method and the BS 5726 : 1992 KI method were fundamentally different in terms of sensitivity, tracer generation and sampling methods, and as long as no minimum face velocity for fume cupboards was specified then no correlation of the two test methods was achievable and no further work was carried out. In terms of the equipment layout relative to the sash plane there was a greater similarity between the KI method and the ASHRAE and DIN gas tracer methods, albeit there was still a difference in the challenge. Further work is needed to compare these test methods in static conditions and more importantly during environmental disturbances to challenge containment.

However, the present work showed the importance of using an assessment strategy, especially that used for assessing safety cabinet performance, which should be applied to fume cupboards in terms of type testing, commissioning and routine maintenance. This strategy consisted of three clear stages.

STAGE 1: Flow visualisation, followed by

STAGE 2: Semi quantitative and quantitative tests involving absolute measurements such as face velocity and a measure of turbulence, then

STAGE 3: Quantitative tracer tests

The importance of flow visualisation was paramount. The collection of data on airflow velocity and turbulence was also important. Both these indicated whether the system was working or not and that it met design criteria. However quantitative methods were required in order to quantify performance. Comparing the National Standards for open fronted containment systems in section 2.2.2 and 2.3.2, where applicable, STAGE 1 and STAGE 2 were consistent, only the method of application and detail being a criteria. The greatest variability was in the philosophy and methods used for STAGE 3. If from this strategy minimum performance criteria were specified then there may have been more scope for comparison of the test methods.

The use of the KI method described earlier for assessing fume cupboards could be further explored. The equipment could be placed with 4 samplers spaced around the spinning disc, as in the BS 5726 : 1992, but at fixed distances relative to it and in the same positions relative to the aperture plane. If only one test was assumed at each position, then the spinning disc could be moved around the aperture in the 6 positions as for the BS 7258 test. This would be similar to the Bicen rig (1993) but using the active challenge of the KI test. If a minimum performance criteria in terms of face velocity was set above 0.5 m/s as is commonly used, then this method could prove possible. Further work would be required to compare this containment test method with those in the BS, ASHRAE and DIN fume cupboard standards. European standards, which will supersede some National Standards, are being developed. These are awaited with interest.

In all open fronted containment systems protection of the operator or the work was achieved by an "air barrier" and perhaps a comparable method for use on all systems should be focused more closely in this region. Techniques could be developed on the principle of detecting any reverse flows in the aperture plane which result in leakage out of the cupboard. Small point source and sampling probes could be deployed close to and either side of the aperture plane, which could be moved around the aperture and placed closer to the corners and the edges. The challenge would be greater than that experienced in practice so as to achieve good sensitivity, would not require complete mixing within the working volume or to challenge the weakest point which may not always be known, and be adaptable for use with particle and gas tracers. To exploit fragile situations, an external disturbance would be employed in the test strategy. The system and principle described could be further adapted for on-line monitoring, i.e. making it unobtrusive to work practices but provide early indication of turbulence and leakage from the aperture. This would be more sensitive than just a measure of velocity.

8.3 Hospital burns unit and 'Ultra Clean' Ventilation (UCV) systems

The 3 stage strategy described in 8.2 above, was applied to a complex ventilation system in a hospital burns unit (referred to as the Unit hereafter) where large burns were treated within an ultra clean ventilation system. With few additional methods the equipment used for assessing the performance of open fronted containment systems was used for assessing this Unit.

STAGE 1. Flow visualisation using smoke, was shown to be the simplest and most graphic method which characterised the performance of the Unit and UCV giving an immediate perception of the overall performance and identified the most important aspects of ventilation. This was not sufficient to show compliance with the design parameters.

STAGE 2. Air pressure, temperature, humidity and air flow measurements were made which showed whether the unit was built or being maintained to the design criteria, but did not

demonstrate the performance for contamination control. By making absolute counts of particles and airborne bacteria this demonstrated regions of personnel activity or excessive turbulence compared to regions of non-activity and stagnation where settling was considerable. This showed how good the UCV was in maintaining low numbers of particles and bacteria below the canopy and at the bed surface during activity and non-activity. However, these methods did not assess the potential for cross-infection/contamination within the unit or between regions in the intensive care room.

STAGE 3. Quantitative analysis was carried out using SF₆ gas and KI particle tracers. This provided a more exhaustive method for assessing the Unit and UCV performance in terms of contamination control. These showed how a potential contaminant may be distributed within the rooms of the Unit and how well isolated various regions were from the source of the potential contaminant; between patients or between staff and patients. The limitation of these point source and sampling methods was the relative positioning of the equipment with respect to each other, air mixing patterns, regions of entrainment and the re-circulation of air through the ventilation system. The gas tracer could not be used for assessing the isolation of the clean zone under the canopy from the rest of the room as any gas released was recycled back into the room through the canopy. This was not a problem using particle tracers because they were removed in the air supply by HEPA filtration units. There was a limitation using particle tracers for assessing cross contamination over long distances and around closed doors due to settling and impaction.

The ventilation principle of the Unit was to have a positively pressurised ultra clean zone within a negatively pressurised intensive care room relative to the unit corridor. Each bedroom in the Unit was negatively pressurised relative to the corridor and the corridor negatively pressurised relative to the hospital ward. Access to the Unit from an adjacent hospital ward was through positively pressurised airlocks relative to the corridor and the ward. This was intended to prevent cross infection/contamination between rooms in the Unit and between the Unit and the hospital ward. The UCV ventilation had a partial canopy ending 2 m above the floor so as not to limit access and an exit velocity of 0.38 m/s at 20°C (minimum) based on DHSS reports (1986) and 0.51 m/s at 40°C (maximum).

What the strategy identified was that the pressures and airflows measured within the Unit differed from the design specifications because of changed ventilation settings and operational procedures (viz. open doors). It was shown there was effective isolation of the hospital ward from the intensive care room and potential contaminants did not move from the intensive care room to the hospital ward. However, there was no effective isolation of the intensive care room from the hospital ward and potential contamination moved into the intensive care room from the hospital ward.

Within the intensive care room it was found that although the measured pressures were similar to the design specifications, the principle of having "leaky" entrance doors produced draughts which could potentially introduce contamination around the patient within the "clean" zone. It was also found within the "clean" zone that there was negligible air flow near to the bed surface at maximum and normal ventilation settings, the buoyancy of the air and the partial length canopy obviously having an effect.

The airflows in the room were shown to be asymmetrical around the canopy. This was due to the close proximity of the walls, the position of the room extracts and the draughts in the room which prevented a smooth flow of air from beneath the canopy into the room which was so important for proper function. There was little entrainment of contamination over the bed surface at the middle and head end but more contamination was found towards the foot end. It was found that draughts and airflow weakness at the foot end of the bed resulted in contamination of the bed surface from regions outside the canopy.

Contamination of the bed surface was not further affected by the movement of people in the room outside of the canopy periphery but movement in and out of the clean zone allowed contamination to be drawn over the entire bed surface.

At commissioning the only criteria for performance had been to establish the recommended exit velocity measured at the edge of the canopy at ambient temperatures and which gave a flow rate of 0.1 m/s at the bed surface, further complemented by flow visualisation. At higher supply temperatures the flow rate was increased to maintain 0.1 m/s at the bed surface. This was supported by bacterial counts under the canopy (<10 bcp/m³). Annual inspections involved flow visualisation, face velocity measurements and bacterial counts beneath the canopy to assess any deterioration in performance. There had been no attempt to use STAGE 3 tracer testing procedures to establish area protection of the ventilation system and possible cross contamination whether steady state or during environmental disturbances.

All the assessment methods were used for analysing design changes. It was found that the supply temperature and buoyancy had an enormous effect on the room airflows and the distribution of particles and tracers. The effect of room supply, draughts and extracts had a profound effect on room airflows whatever the supply temperature. It was considered that having extracts near to the floor level could eliminate the buoyant effects of the air. Preventing draughts from beneath doors exaggerated draughts from around the other gaps in the doors. This caused greater disturbance at the foot end of the bed resulting in more contamination over the bed surface from the room.

Extension of the canopy had an effect of increasing temperature and velocity at the bed surface and limited the encroachment of contamination over the bed surface. The extension of the canopy at the foot end of the bed only, had similar effects to the extension of the

complete canopy preventing gross disturbances at the foot end of the bed. The presence of the bed was shown to have an important effect on the airflow beneath the canopy. Without it there was no defined air flow from the canopy and no resistance to the mixing of room air and potential contaminants beneath it.

Thus the use of the three stage strategy and basically the same equipment used to assess open fronted containment systems was shown to be important for assessing the performance of this complex ventilated burns unit and intensive care room. This was not used at commissioning and none of the potential and actual failures in contamination control realised.

8.4 Computational Fluid Dynamics (CFD)

As an additional method for inclusion in STAGE 3 of the strategy or as a three stage strategy of its own, CFD (see chapter 6) was investigated.

STAGE 1. The simulation allowed visualisation of the whole solution domain or any particular region of interest in either the xyz plane for 3D models as vectors for airflow.

STAGE 2. The simulation could be interrogated and the value of each vector, the air pressure and temperature could be known.

STAGE 3. As a mathematical code then any model may be incorporated which described a physical phenomenon such as a secondary species which may be seeded into the airflow. This was used to monitor the dispersal of a potential contaminant throughout the solution domain.

The simulations compared well with physical measurements. In terms of flow visualisation they were very comparable. However, there was greater disparity in terms of quantitative analysis. The fume cupboard models were shown to be sensitive to the turbulence model specified, the solution grid density and its level of refinement. The program did not accurately simulate air flow around the aerodynamic features, i.e. above and below the lipfoil, but the 3D model was more representative than 2D model. In the UCV model there was some disparity in actual values of temperature, airflows and contaminant dispersal. However, the relative trends were similar and the same conclusions gained from each.

Differences between the CFD and physical measurements were due to limitations in both methods such as sensitivity, accuracy and position for physical measurements and for CFD uncertainty in boundary conditions, physical assumptions, level of detail, modelling techniques, turbulence modelling and ultimately limitations in computing power and memory. In the CFD model used, no curved boundaries were possible and these were represented as a series of straight lines, thus requiring a high level of grid refinement in these areas increasing the demand on computer power. Also in the representation of small draughts beneath doors,

a high level of grid refinement was required relative to the whole domain. Where the simulation became more detailed and complicated with more boundary conditions, more grid cells and greater variability in flow regimes and turbulence so the limits on computer memory, speed and the model code were influenced.

For the complete 3D simulations of the fume cupboard and UCV the solution time was 2 - 3 days on a PC486DX66 personal computer. This time would be expected to reduce with more powerful and faster hardware but at an expense and eventually there must be a balance between what can be achieved and the cost in achieving it.

The aerodynamic features of the fume cupboard were modelled as separate simulations, allowing more detailed analysis on a smaller scale. Simulation of airflow past the lipfoil and sash handle showed how each influenced local turbulence caused by sharp edges and how a smoothed entry profile could eliminate these. This allowed optimisation of design, limited only by the representation of curved boundaries.

The complete cupboard simulations could not show this level of detail around these features but gave a mean estimation of the flow within these regions and how it affected the whole flow field. This allowed the comparison of cupboard designs and the relative benefit of each design feature on the overall performance. The CFD model clearly distinguished between good and bad cupboard designs.

The CFD model was also used to assess the cupboard performance when a simulated operator was standing in front causing a blockage or when there was an environmental disturbance in the form of a cross draught. This clearly showed the potential of the CFD for comparing designs with reference to installation and "in-situ" conditions. A study of the effects of different room ventilation and fume cupboard containment was carried out by Flomerics and NIH which was intended to form a basis for future laboratory designs. However, this did not take into account fume cupboard design and thus a development of this study would be to take selected cases and match them to supposed good and bad cupboard designs and investigate localised effects. Also, it would be useful to develop further, simulations of "in-situ" conditions such as with an operator working or with cupboard contents. This would be able to establish minimum design criteria for fume cupboards.

The use of the 2D models for assessing microbiological safety cabinet performance clearly showed how turbulent were the airflows within a class I cabinet and in terms of modern fume cupboard design philosophy how poor it was. The model was also applied to class II cabinets which clearly showed how a delicate balance was required between the inflow and downflow of air in order to control product and operator protection. These were simple models which only took 1 hour to solve but served to indicate clearly microbiological safety cabinet performance. This could be developed further, made more complex and used as for fume

cupboard performance, i.e., to set minimum design criteria in prototype development and show how a design could perform when installed. The advantage was that class I and II cabinets had no curved boundaries making modelling much simpler.

The 3D fume cupboard model was used to simulate dispersal of tracer within the working volume according to the BS, ASHRAE and DIN injector methods. This correlated well with physical measurements showing that the tracer was not completely mixed with the working volume when released from one position. With the sources in the centre line of the aperture width, the BS and ASHRAE injectors were shown to distribute tracers in a similar manner which identified recirculation zones across the work surface from which leakage occurred in box type fume cupboards. However the DIN injector was shown to disperse tracer into the upper regions of the working volume and thus did not identify the leakage from the work surface. This compared well with earlier work (Fletcher^{Johnson}, 1992) that suggested that the DIN injector may identify leakage near to the sash handle but not near to the work surface.

From these tests of tracer dispersal the CFD model was shown to be more sensitive than the gas tracer physical measurements. The calculated concentration of tracer in the sash plane was around the maximum sensitivity for physical measurements of SF₆ tracer gas, i.e., 1 ppb. If these simulations were compared to physical measurements, then for the aerodynamic fume cupboard tested, SF₆ tracer would not be sampled in the sash plane using the physical measurement method, but for a box type cupboard it would be.

This identified another very important conclusion about the use of CFD. It could be used to identify where to release the tracer, in what manner, where the containment weak spots would be, where to sample and how efficient sampling methods could be. It could be very important in the development of new physical gas tracer methods. Further work would be needed, using a different CFD code, to simulate the motion of particle tracers and model the KI test method. CFD could be used to develop new containment tests.

Simulating the air flow and distribution of gas tracer within the intensive care room of the hospital burns Unit gave similar conclusions based on the design data, the measured data and from physical measurements. However, it did not identify problems such as unwanted draughts through drawers (section 7.7.1) and other departures from the design. It was thus relevant in predicting how a design will function in theory but not necessarily how it actually will function when built. Accordingly, it would still be necessary to carry out physical tests to validate and commission a facility.

The CFD model showed great potential in predicting what would happen when there was a departure from design criteria or when the design was altered. The simulation based on design data could be fine tuned using existing physical measurements and then used as an

analytical tool to observe the effects of proposed corrective procedures for faults or proposed improvements by changes in design.

In the intensive care room simulation predicting the effect of design changes compared well with the physical measurements. These changes were much simpler to set up using the CFD program and relatively faster to compute and make conclusions. Also, the potential number of detailed design changes that could be made using the CFD model was greater than could be practically undertaken using physical measurements and were non-intrusive. This showed that alterations which may have been thought beneficial could actually reduce performance and thus be a costly mistake if physical measurements were used.

For physical measurements the relative position of the source and the samplers could be critical to each other and to the room ventilation points. The CFD model could be used to select the most suitable positions at which to place the source and the sampler for physical tracer measurements i.e. identify regions where protection may be weak.

It was concluded from the simulations of open fronted containment and UCV system performance that the CFD program could be included as a stage 3 quantitative assessment method but also that it could be used as a strategy of its own. This had more relevance at the design stage to predict how a system would function when built. However, without physical measurements there was no way of knowing whether the system actually performed to the design criteria when built and this was still a necessary step for commissioning and routine maintenance. Using the physical measurements the CFD program could be used to study the effect of design changes and corrective procedures on the as-built case.

Further, in the design stages, the program could be used to simulate the effects of potential challenges to performance and establish certain performance criteria. It could be used to optimise the design of open fronted containment, UCV systems and hospital operating theatres. In this study, the simulations were steady state but transient simulations could also be carried out to observe the effect of time dependant disturbances.

There is a limitation to the use of CFD because of the time taken and expense of developing and solving the simulations, to test and validate them. This has to be weighed against the building of physical models and testing with physical measurements. For open fronted containment systems this may be hard to justify because of profit margins involved. For the UCV, on a much larger scale, this may be justified because it can help to avoid in the event of design errors being made, expensive alterations to buildings and the subsequent downtime for such work to take place. Further work would thus have to be done using more powerful computers to weigh up the commercial viability of such an exercise. At the end of the day, physical measurements still had to be used for the purpose of commissioning.

Bibliography

ACGIH, American Conference of Governmental Industrial Hygienists (1982). *Industrial Ventilation - A Manual of Recommended Practice. 7th edition. Cincinnati, Ohio, U.S.A.*

Akers, R.L., Walker, R.J., Sabel, F.L. & McDade, J.J. (1969). Development of a Laminar Air-Flow Biological Cabinet. *American Industrial Hygiene Association Journal* 30, 177-185.

Anderson, J.D. (1992)^a. Basic Philosophy of CFD. In: *Computational Fluid Dynamics: An Introduction. (ed Wendt, J.F.) Springer-Verlag, Berlin, Germany.*

Anderson, J.D. (1992)^b. Governing Equations of Fluid Dynamics. In: *Computational Fluid Dynamics: An Introduction. (ed Wendt, J.F.) Springer-Verlag, Berlin, Germany.*

Anderson, J.D. (1992)^c. Mathematical Properties of the Fluid Dynamic Equations. In: *Computational Fluid Dynamics: An Introduction. (ed Wendt, J.F.) Springer-Verlag, Berlin, Germany.*

Anderson, J.D. (1992)^d. Transformations and Grids. In: *Computational Fluid Dynamics: An Introduction. (ed Wendt, J.F.) Springer-Verlag, Berlin, Germany.*

Anderson, J.D. (1992)^e. Discretization of Partial Differential Equations. In: *Computational Fluid Dynamics: An Introduction. (ed Wendt, J.F.) Springer-Verlag, Berlin, Germany.*

AS1386. (1989). Clean rooms and clean work stations. *Standards Association of Australia, North Sydney, Australia.*

AS2243. (1992). Safety in laboratories : Part 8 : Fume cupboards. *Standards Association of Australia, North Sydney, Australia.*

AS2252. (1994). Part 1 : Biological safety cabinets (class I) for personnel and environmental protection. *Standards Association of Australia, North Sydney, Australia.*

AS2252. (1994). Part 2 : Biological safety cabinets (class II) for personnel, environmental and product protection. *Standards Association of Australia, North Sydney, Australia.*

ASHRAE 110. (1993). Method of Testing Performance of Laboratory Fume Cupboards. *American Society of Heating, Refrigeration and Air-Conditioning Engineers, Atlanta, Georgia, U.S.A.*

Austin, P.R. (1970). Design and Operation of Clean Rooms. *Business News Publishing Company, New York, U.S.A.*

B.O.H.S., British Occupational Hygiene Society, London (1976). A Guide to the Design and Installation of Laboratory Fume Cupboards. Hygiene Technology Guide Series No.1. *H & H Scientific Consultants Ltd. in association with Science Reviews Ltd., Northwood, Middlesex, England.*

B.O.H.S., British Occupational Hygiene Society, London (1988). Controlling Airborne Contaminants in the Workplace. Technical Guide No.7. (series ed. Ogden, T. & Hughes, D.) *H & H Scientific Consultants Ltd. in association with Science Reviews Ltd., Northwood, Middlesex, England.*

Barkley, W.E. (1972). Evaluation and Development of Controlled Air Flow Systems for Environmental Safety in Biomedical Research. *PhD Thesis, University of Minnesota, U.S.A.*

Bicen, A.F. (1991)^a A draft on - Recommendations for Containment Testing of Fume Cupboards (91/55088). *British Standards Institute, London, England.*

Bicen, A.F. (1991)^b Second Interim Report - Evaluation of DD 191 Fume Cupboard Containment Testing and Grading (91/55087). *British Standards Institute, London, England.*

Bicen, A.F. (1992). Final report - Evaluation of Fume Cupboard Containment and Face Velocity Test Methodologies (92/52326). *British Standards Institute, London, England.*

Bicen, A.F. (1993)^a Test Methodologies and Requirements for BS 7258 and Comparisons of National Standards. In: *A Short Course on Fume Cupboard Standards, Invent U.K., Imperial College, London, England.*

Bicen, A.F. (1993)^b Novel Methods for On-Site Performance Testing, Monitoring and COSHH Assessments. In: *A Short Course on Fume Cupboard Standards, Invent U.K., Imperial College, London, England.*

BS1752. (1983). Specification for laboratory scintered or frittered filters including porosity grading. *British Standards Institution, London, England.*

BS3202. (1959). Recommendations on Laboratory Furniture and Fittings. *British Standards Institution, London, England.*

BS5726. (1992). Microbiological Safety Cabinets. Parts 1,2,3 and 4. *British Standards Institution, London, England.*

BS7258. (1990). Laboratory Fume Cupboards. Parts 1,2 and 3. *British Standards Institution, London, England.*

BS7258. (1994). Laboratory Fume Cupboards. Parts 1,2,3 and 4. *British Standards Institution, London, England.*

Caplan, K.J. & Knutson, G.W. (1978). Laboratory fume hoods: A performance test. *ASHRAE Transactions* **84**, 511-521.

Caplan, K.J. & Knutson, G.W. (1982)^a A performance test for laboratory fume hoods. *American Industrial Hygiene Association Journal* **43**, 722-737.

Caplan, K.J. & Knutson, G.W. (1982)^b Influence of room air supply on laboratory hoods. *American Industrial Hygiene Association Journal* **43**, 738-746.

- Chamberlain, R.I. & Leahy, J.E. (1978). Laboratory Fume Hood Standards Recommended for the U.S. Environmental Protection Agency (EPA). *EPA Contract No. 68-01-4661*.
- Charnley, J. (1964). A sterile air operating enclosure. *British Journal of Surgery*. **51**, 195-202
- Charnley, J. (1973). Clean air in the operating room. *The Cleveland Clinical Quarterly* **40**, 99-114.
- Clark, R.P. (1973). The role of the human micro-environment in heat transfer and particle transport. *PhD Thesis, The City University, London, England*.
- Clark, R.P. & Goff, M.R. (1981). The Potassium Iodide Method for Determining Protection factors in Open-fronted Microbiological Safety Cabinets. *Journal of Applied Bacteriology* **51**, 439-460.
- Clark, R.P., Elliott, C.J. & Lister, P.A. (1981). A Comparison of Methods to Measure Operator Protection Factors in Open-fronted Microbiological Safety Cabinets. *Journal of Applied Bacteriology* **51**, 461-473.
- Clark, R.P. & Edholm, O.G. (1985). Man and His Thermal Environment. *Edward Arnold (publishers) Ltd., London, England*.
- Clark, R.P., Reed, P.J., Seal, D.V. & Stephenson, M.L. (1985). Ventilation conditions and air-borne bacteria and particles in operating theatres: proposed safe economics. *Journal of Hygiene, Cambridge*. **95**, 325-335.
- Clark, R.P., Grover, F. & Wright, I.M. (1987). Cabinet Reshuffle. *Laboratory Practice*, October.
- Clark, R.P. (1989). The Performance, Installation, Testing and Limitations of Microbiological Safety Cabinets. *Occupational Hygiene Monograph No.9., 2nd. edition. (series ed. Hughes, D.) H & H Scientific Consultants Ltd. in association with Science Reviews Ltd., Northwood, Middlesex, England*.
- Clark, R.P., Osborne, R.W., Pressey, D.C., Grover, F., Keddie, J.R. & Thomas, C. (1990). Open Fronted Safety Cabinets in Ventilated Laboratories. *Journal of Applied Bacteriology* **69**, 338-358.
- Collins, C.H. (1988). Laboratory-acquired infections. History, incidence, causes and prevention. *2nd. edition. Butterworths, London, England*.
- Cook, J.D. & Hughes, D. (1986). Fumecupboards Revisited. *Occupational Hygiene Monograph No.2. (series ed. Hughes, D.) H & H Scientific Consultants Ltd. in association with Science Reviews Ltd., Northwood, Middlesex, England*.
- COSHH. (1994). Control of Substances Hazardous to Health Regulations. *Department of Health, London, England*.
- DD191. (1990). Draft for Development : Method for Determination of the Containment Value of a Laboratory Fume cupboard. *British Standards Institution, London, England*.
- DD80. (1982). Draft for Development : Laboratory Fume cupboards. Parts 1,2 and 3. *British Standards Institution, London, England*.

DHSS, Department of Health and Social Security (1986). Requirements for Ultra-Clean Ventilation (UCV) Systems for Operating Departments - draft report No.205/J20/VB study group 10, *HBD 4, DHSS, London, Germany*.

Diberardinis, L.J., First, M.W. & Ivany, R.E. (1991). Field results of an in-place, quantitative performance test for laboratory fume hoods. *Applied Occupational Environmental Hygiene* **6**, 227-231.

Dick, E. (1992)^a Introduction to Finite Element Techniques in Computational Fluid Dynamics. In: *Computational Fluid Dynamics: An Introduction*. (ed Wendt, J.F.) Springer-Verlag, Berlin, Germany.

Dick, E. (1992)^b Introduction to Finite Volume Techniques in Computational Fluid Dynamics. In: *Computational Fluid Dynamics: An Introduction*. (ed Wendt, J.F.) Springer-Verlag, Berlin, Germany.

DIN 12 924. (1991). Part 1. Laboratory furniture; fume cupboards; general purpose fume cupboards; types, main dimensions, requirements and testing. *German Institute for Standardisation, Berlin, West Germany*.

DIN 12 950. (1991). Laboratory furniture; safety cabinets for microbiological and biotechnological work; requirements and testing. *German Institute for Standardisation, Berlin, West Germany*.

DS457. (1986). Danish Association of Engineers standard for Fume cupboards. *Danish Association of Engineers Standard, Copenhagen, Denmark*.

Everett, K. & Hughes, D. (1981). A Guide to Laboratory Design. *3rd edition*. Butterworths, London, England..

Faircliff, R. (1984). In: *The Design and Utilization of Operating Theatres* (eds. Johnston, I.D.A. & Hunter, A.R.) Edward Arnold, (publishers) Ltd., London, England.

Farquharson, G.J. (1988). Design, installation, commissioning, testing and validation of pharmaceutical clean rooms. (C510/88). *Institution of Mechanical Engineers, London, England*.

Fisher, E.H. & Rhodes, N. (1996). Uncertainty in Computational Fluid Dynamics. *Proceedings of the Institution of Mechanical Engineers, Bournemouth, England*.

Fletcher, B. & Johnson, A.E. (1992)^a Containment Testing of Fume Cupboards - Part 1: Methods. *Annals of occupational hygiene* **36**, 239-252.

Fletcher, B. & Johnson, A.E. (1992)^b Containment Testing of Fume Cupboards - Part II: Test-Room Measurements. *Annals of occupational hygiene* **36**, 395-405.

Fletcher, B. & Johnson, A.E. (1992)^c Containment Testing. *Proceedings of the American Conference of Government Industrial Hygienists, Cincinnati, Ohio, U.S.A.*

Flomerics Limited. (1994). Flovent[®] version 1.4, Reference Manual. *Flomerics Ltd., Surrey, England*.

Foord, N. & Lidwell, O.M. (1972). The control of ventilation of airborne bacterial transfer between hospital patients, and its assessment by means of a particle tracer. I. An airborne-particle tracer for cross infection. *Journal of Hygiene, Cambridge*. **70**, 279-286.

Foord, N. & Lidwell, O.M. (1975)^a. Airborne infection in a fully air conditioned hospital. I. Air transfer between rooms. *Journal of Hygiene, Cambridge*. **75**, 15-30.

Foord, N. & Lidwell, O.M. (1975)^b. Airborne infection in a fully air conditioned hospital. II. Transfer of airborne particles between rooms resulting from the movement of air from one room to another. *Journal of Hygiene, Cambridge*. **75**, 31-44.

Gasser, F. & Hunt, J.S. (1988). A class 100 clean room from concept to construction. (C502/88). *Institution of Mechanical Engineers, London, England*.

Grover, F. (1994). Safety legislation and COSHH regulations. In: *Testing Containment Systems, Thermal Biology Research Unit, King's College London, London, England*.

Hall, R.C. & Broyd, T.W. (1988). Airflow modelling in the design and operation of clean rooms. (C501/88). *Institution of Mechanical Engineers, London, England*.

Hambraeus, A. & Sanderson, H.F. (1972). The control of ventilation of airborne bacterial transfer between hospital patients, and its assessment by means of a particle tracer. III. Studies with an airborne-particle tracer in an isolation ward for burned patients. *Journal of Hygiene, Cambridge*. **70**, 299-312.

Hampl, V. & Shulman, S. (1985). Use of Tracer Gas Techniques for Industrial Exhaust Hood Efficiency Evaluation - Application of Sulfur Hexafluoride for Hood Controlling Particulate Emissions. *American Industrial Hygiene Association Journal* **46**, 7, 379-386.

Hampl, V., Johnston, O.E. & Watkins, D.S. (1988). Application of an Air Curtain-Exhaust System at a Multiple Opening Veneering Press. *Applied Industrial Hygiene* **3**, 10, 291-298.

Hesketh, H.E. (1974). Understanding & controlling air pollution. *2nd edition*. *Ann Arbor Science Publishers Inc., Michigan, U.S.A.*

Hidy, G.M. (1984). Aerosols: An Industrial and Environmental Science. *Academic Press, Inc., New York, U.S.A.*

Holton, J., Ridgeway, G.L. & Reynoldson, A.J. (1990). A Microbiologists View of Commissioning Operating Theatres. *Journal of Hospital Infection* **16**, 29-34.

Howorth, F.H. (1984). The air in the operating theatre. In: *The Design and Utilization of Operating Theatres* (eds. Johnston, I.D.A. & Hunter, A.R.) *Edward Arnold (Publishers) Ltd., London, England*.

Hughes, D. (1980). A Literature Survey and Design Study of Fume Cupboards and Fume Dispersal Systems. *Occupational Hygiene Monograph No.5*. (series ed. Hughes, D) *H & H Scientific Consultants Ltd. in association with Science Reviews Ltd., Northwood, Middlesex, England*.

Hughes, H.C., Reynolds, S. & Rodriguez, M. (1996). Designing Animal Rooms to Optimize Airflow Using Computational Fluid Dynamics. *Pharmaceutical Engineering* **16**, 44-65.

Ivany, R.E., First, M.W. & Diberardinis, L.J. (1989). A new method for quantitative, in-use testing of laboratory fume hoods. *American Industrial Hygiene Association Journal* **50**, 275-280.

Janssen, G., Lamersm, A. & Jansen, J. (1992). A Numerical Parameter Study for a Turbulent Backward Facing Step Problem. *PHOENIX Journal* **2**, 144-154.

JISK3800. (1994). Class II Biological Safety Cabinets. *Japanese Industrial Standards Committee, Tokyo, Japan*.

Jones, R.L., D.G., S., Eagleson, D., Greenier, T.J. & Eagleson, J.M. (1990). The Effects of Changing Intake and Supply Air Flow on Biological Safety Cabinet Performance. *Applied Occupational Environmental Hygiene* **5**, 370-377.

Kennedy, D.A. (1987). Water Fog as a Medium for Visualization of Airflows. *Annals of Occupational Hygiene* **31**, 255-259.

Kennedy, D.A. (1988). Studies in laboratory-acquired infection, with particular reference to the role of equipment. *PhD Thesis, University of London, London, England*.

King's College London. (1995). Internal Report - Fume Cupboard Survey. *King's College London, London, England*.

Kruse, R.H., Puckett, W.H. & Richardson, J.H. (1991). Biological Safety Cabinetry. *Clinical Microbiology Reviews* **4**, 207-241.

Lidwell, O.M. (1960). The evaluation of ventilation. *Journal of Hygiene, Cambridge*. **58**, 297-305.

Lidwell, O.M. (1972). The control of ventilation of airborne bacterial transfer between hospital patients, and its assessment by means of a particle tracer. II. Ventilation in subdivided isolation units. *Journal of Hygiene, Cambridge* **70**, 287-297.

Lidwell, O.M. (1975). Airborne infection in a fully air conditioned hospital III. Transport of gaseous and airborne particulate material along ventilated passageways. *Journal of Hygiene, Cambridge*. **75**, 45-56.

Lidwell, O.M. (1981). Airborne bacterial and surgical infection. *American Journal of Medicine* **70**, 693-697.

Lidwell, O.M., Lowbury, E., Whyte, W., Blowers, R., Stanley, R. & Lowe, D. (1982). The effect of ultraclean air in operating rooms on deep sepsis in the joint after total hip or knee replacement: a randomised study. *British Medical Journal* **285**, 10-14.

Lidwell, O.M., Lowbury, E., Whyte, W., Blowers, R., Stanley, R. & Lowe, D. (1983). Airborne contamination of wounds in joint replacement operations: the relationship to sepsis rates. *Journal of Hospital Infection* **4**, 111-131.

Lidwell, O.M. (1984). Bacterial considerations. In: *The Design and Utilization of Operating Theatres*. (eds. Johnston, I.D.A. & Hunter, A.R.) Edward Arnold (Publishers) Ltd., London, England.

Lind, A. (1957). Ventilated Cabinets in a Tuberculosis Laboratory. *Bulletin of the World Health Organisation* **16**, 448.

Ljungqvist, B., Reinmuller, B. & Nydahl, R. (1994). Microbiological Assessment in Clean Zones for Aseptic Production. *Journal of R3-Nordic* **23**, 7-10 & 27-28.

Matthews, J.A. (1985). An Evaluation of Test Methods for Microbiological Safety Cabinets. *MPhil Thesis, Cambridge College of Arts and Technology, Cambridge, England*.

McDade, J.J., Sabel, F.L., Akers, R.L. & Walker, R.J. (1968). Microbiological Studies on the Performance of a Laminar Air-Flow Biological Cabinet. *Applied Microbiology* **16**, 1086-1092.

McDevitt, J.J., Lees, S.J. & McDiarmis, M.A. (1993). Exposure of Hospital Pharmacists and Nurses to Antineoplastic Agents. *Journal of Occupational Medicine* **35**, 57-60.

Merzkirch, W. (1987). Flow Visualisation. 2nd. edition. Academic Press, New York, U.S.A.

Mosovsky, J.A. (1995). Sulfur Hexafluoride Tracer Gas Evaluations on Hood Exhaust Reductions. *American Industrial Hygiene Association Journal* **56**, 44-49.

Newsom, S.W.B. (1974). A test system for the biological safety cabinet. *Journal of Clinical Pathology* **27**, 585-589.

Newsom, S.W.B. (1976). Laboratory Infections - Their Control by Containment. *MD, Thesis, University of London, England*.

Newsom, S.W.B. (1979)^a Performance of Exhaust Protective (Class I) Biological Safety Cabinets. *Journal of Clinical Pathology* **32**, 576-583.

Newsom, S.W.B. (1979)^b Class II (Laminar Flow) Biological Safety Cabinets. *Journal of Clinical Pathology* **32**, 505-513.

Newton, G., Brown, S., Dias, J.J. & Bullock, D. (1991). "Can Conventional Theatre Clothing be as Effective as the "Space Suit"? *Meeting of the British Orthopaedic Association, April, Brighton, England*.

NFX15-203. (1987). Laboratory Equipment. Fume Cupboards. General - Classification - Dimensions - Specifications. *L'association Francaise de Normalisation (AFNOR), Paris, France*.

NFX15-206. (1987). Laboratory Equipment. Fume Cupboards. Test Methods. *L'association Francaise de Normalisation (AFNOR), Paris, France*.

NFX44-201. (1984). Microbiological Safety Cabinets. Definitions - Classifications - Characteristics - Safety Requirements - Test Methods. *L'association Francaise de Normalisation (AFNOR), Paris, France.*

Niemela, R., Lefevre, A., Muller, J.P. & Aurbertin, G. (1991). Comparison of three tracer gases for determining ventilation effectiveness and capture efficiency. *Annals of Occupational Hygiene* **35**, 405-417.

NIH. National Institutes of Health. (1996). Developing New Guidelines to Maximise Laboratory Hood Containment. *National Institutes of Health, Bethesda, Maryland, U.S.A.*

Noble, W.C., Lidwell, O.M. & Kingston, D. (1963). The size distribution of airborne particles carrying micro-organisms. *Journal of Hygiene, Cambridge.* **61**, 385-391.

NSF49. (1983). Class II (Laminar Flow) Biohazard cabinetry. *National Sanitation Foundation, Ann Arbor, Michigan, U.S.A.*

Ollair Limited (1988). Omniflow® 4th generation Ultraclean zone. *Ollair Ltd., Chorley, England.*

Palmer, G. (1988). A biotechnology research facility case study. (C504/88). *Institution of Mechanical Engineers, London, England.*

Papa, L.J. (1966). A Quantitative Approach to Proper Evaluation of Laboratory Fume Hoods. *Air Engineer* **8**, 20-30.

Patankar, S.V. (1981) Numerical Heat Transfer and Fluid Flow. (*McGraw Hill, New York, U.S.A.*).

Peck, R.C. (1982). Validation of a method to determine a protection factor for laboratory hoods. *American Industrial Hygiene Association Journal* **43**, 596-601.

Petersen, N.J. (1970). Evaluation of a Vertical Laminar Flow Biological Safety Cabinet. *W-13 062 NASA* **43**, 596-601.

Purtell, P.L. (1995). Turbulence: A Roadblock to Computational Fluid Dynamics. *Naval Research Reviews* **47**, 20-25.

R.S.C. The Royal Society of Chemistry (1989). COSHH in Laboratories. *The Royal Society of Chemistry, London, England.*

R.S.C. The Royal Society of Chemistry (1990). Guidance on Laboratory Fume Cupboards. In: *Technical Guide Series of the British Occupational Hygiene Society.* (Eds. Ogden, T.L. & Hughes, D) *H & H Scientific Consultants Ltd. in association with Science Reviews Ltd., Northwood, Middlesex, England.*

Rake, B.W. (1978). Influence of Crossdrafts on the Performance of a Biological Safety Cabinet. *Applied and Environmental Microbiology* **36**, 278-283.

Reynolds, O. (1881). An experimental investigation of the circumstances which determine whether the motion of water shall be direct or sinuous and the law of resistance in parallel channels. *Papers on Mechanical and Physical Subjects* 2, 51.

Roach. (1981). On the Role of Turbulent Diffusion in Ventilation. *Annals of Occupational Hygiene* 24, 105-132.

Robertson, P. & Bailey, P.V. (1980). Suggested improvements to prevent the escape of fume beneath the sash of a fume cupboard. *Annals of Occupational Hygiene* 23, 305-309.

Rooth, G. (1949). Aerosols. *Acta Medica Scandinavica Supplement* 6, 34.

Saunders, G.T. (1993). Laboratory Fume Cupboards - A User's Manual. *Wiley & Sons, Inc., New York*.

Schicht, H.H. (1988). Clean room technology - the concept of total environmental control for advanced industries. (C500/88). *Institution of Mechanical Engineers, London, England*.

Seal, D.V. & Clark, R.P. (1990). Electronic particle counting for evaluating the quality of air in operating theatres: a potential basis for standards? *Journal of Applied Bacteriology* 68, 225-230.

Shaw, B.H. (1972). Heat and mass transfer by natural convection and forced airflow through large rectangular openings in a vertical partition. In: *Proceedings of Heat and Mass Transfer by Combined Forced and Natural Convection, Manchester. Institution of Mechanical Engineers, London, England*.

Smith, C.T., Flynn, M.R. & Dement, J.M. (1994). A design and Performance Analysis of Laboratory Fume Hoods. *Applied Occupational Environmental Hygiene* 9, 117-124.

Vincent, J.H. (1990). The fate of inhaled aerosols: A review of observed trends and some generalizations. *Annals of Occupational Hygiene* 34, 623-637.

Wake, D. (1985). "KI-Discus" Potassium Iodide Aerosol : Size Distribution Analysis using the TSI Aerodynamic Particle Sizer. (IR/L/DF/85/07). *Health and Safety Executive, Sheffield, England*.

Walton, W.H. & Prewett, W.C. (1949). The production of sprays and mists of uniform drop size by means of spinning disc type sprayers. *Proceedings of the Physical Society* 62, pt. 6, no. 354b, 341-350.

Watson, W.H. & Liddicoat, M.I. (1985). Recent History of Atmospheric Trace Gas Concentrations Deduced from Measurements in the Deep Sea: Application to Sulphur Hexafluoride and Carbon Tetrachloride. *Atmospheric Environment* 19, 1477-1484.

Wendt, J.F. (1992). *Computational Fluid Dynamics: An Introduction*. Springer-Verlag, Berlin, Germany.

Whitelaw, J.H. (1993). Introduction to Fume Cupboards and Standards. In: *A Short Course on Fume Cupboard Standards*, Invent U.K., Imperial College, London, England.

Whitfield, W.J. (1962). A New Approach to Clean Room Design. Sandia Corp. Technical Report No. SC-4673 (RR), *Sandia Corp., Albuquerque, N.M., U.S.A.*

Whyte, S. & Shaw, B.H. (1973). Airflow through doorways. In: *Airborne Transmission and Airborne Infection*. (eds. Hers, J.F. & Winkler, K.C.) *Oosthoek Publishing Co. Ltd. Utrecht, Holland*.

Whyte, S., Shaw, B.H. & Barnes, R. (1973). A bacteriological evaluation of laminar - flow systems for orthopaedic surgery. *Journal of Hygiene, Cambridge* **71**, 559-564.

Whyte, W., Lidwell, O.M., Lowbury, E.J.L. & Blowers, R. (1983). MRC committee recommendations: Suggested bacteriological standards for air in ultra-clean operating rooms. *Journal of Hospital Infection* **4**, 133-139.

Williams, W.E.O. & Lidwell, O.M. (1957). A Protective Cabinet for Handling Infective Material. *Journal of Clinical Pathology* **10**, 400-402.

Williams, W.E.O. & Harding, L. (1969). Studies of the effectiveness of an isolation ward. *Journal of Hygiene* **67**, 649-657.

Wright, W.C. (1964). Diseases of Workers. *Hafner Publishing Company, New York, U.S.A.*

Appendix 1 A summary of the physical properties, methods of generation, dispersal and deposition of potential airborne contaminants

(Hidy 1984, Collins 1988, Kennedy, 1988)

A1.1 Definitions

A1.1.1 Gases and vapours

Gases and vapours may react chemically with other pollutants in the atmosphere to form secondary pollutants which can be either (or both) gases or aerosols, chemically irritate organic material such as living tissue and react with and destroy inanimate objects. Gas clouds will expand by diffusion until the molecules are equally distributed within a localised area. Gas can only be changed to a liquid or a solid state by the continued effect of increased pressure and/or decreased temperature. Vapour is the gaseous form of substances that also exist in the solid or liquid state at normal pressures and temperatures

A1.1.2 Dusts

These are suspensions of solid particles brought about by mechanical disintegration of material which is suspended by mixing in a gas. Generally, dusts are quite heterogeneous in composition and have poor colloidal stability with respect to gravitational settling because they are made up of large particles ($1 - > 300 \mu\text{m}$).

A1.1.3 Smokes and fumes

Smoke covers a wide variety of aerial dispersions dominated by residual material from burning, or from condensation of supersaturated vapours. Such clouds generally consist of particles of material of low volatility, in relatively high concentrations. Because of the small size of the particles, smokes may remain suspended for extended periods of time. A principle criterion defining smokes is one of particle size; the distribution in diameter is constrained from $10 \mu\text{m}$ to less than $0.1 \mu\text{m}$.

When smoke formation accompanies traces of noxious vapours, it may be called a fume is ($0.001 - 1.0 \mu\text{m}$). Fumes are often generated by condensation of materials from the gaseous state usually after volatilization from the molten or liquid state. They may be used to describe a particle cloud resulting from the mixing and chemical reactions of vapours.

A1.1.4 Mists

Suspensions of liquid droplets by atomisation or vapour condensation are called mists. These aerial suspensions often consist of particles $> 1 \mu\text{m}$ in diameter, and relatively low concentrations are involved.

A1.1.5 Aerosols

Aerosols can be defined as colloidal suspensions of particles in a gas that are larger than molecular size, yet not large enough to settle under gravity, and are often considered to be from $0.01 \mu\text{m}$ to $50 \mu\text{m}$ in size. The term aerosols has been used to describe dust, mist, smoke, fog, haze and fumes in this size range.

A1.2 Generation

The source of potential contaminants can be:

Surfaces

Cleaning processes

Work processes burning, boiling liquids
 splashing/spillages
 propulsion from pipettes/needles/syringes
 animal work
 machines

Humans skin/hair particles
 sneezing/coughing

The mechanisms of generation includes:

 supersaturation
 gas phase chemical reactions
 disintegration of liquids
 sprays by centrifugation
 atomisation by acoustic disturbance
 aerodynamic atomisation
 nebulisation

A1.3 Transport

A1.3.1 Gases and vapours

The main transport processes of gases include phoresis, molecular diffusion, absorption and adsorption. The movement of gases as a result of a gradient is due to phoretic forces. These include pressure, temperature and concentration. Diffusion of gases depends equally on the nature of the fluids as well as the physical conditions.

A1.3.2 Droplets/Particles

When particles, suspended in a fluid medium, are placed in a region where there is an energy gradient, they will travel to that part of the region where the energy level is lowest. The most familiar example is the phenomenon of gravitational settling in which particles move only vertically and down. Thus particles moving under gravitational forces will only settle on surfaces with a horizontal component.

Electrical fields can produce movement in aerosol particles. Charged particles will move in uniform electrical fields, while either charged or uncharged particles will travel in non-uniform fields. Particles in an area where a thermal gradient exists will move to the cooler part of the zone. The net result is that particles are moved in a resultant direction, giving deposition on surfaces that do not necessarily have a horizontal component.

When an airstream containing particles is forced to change direction because an obstacle is in its path, those particles which have sufficient inertia will continue on in their original trajectories until they impact on the surface of the obstacle. Smaller or lighter particles will continue to move around the obstacle. Depending upon the shape of the obstacle, some collection may occur on the downstream face as a result of turbulent eddy formation.

Diffusion, coalescence, nucleation, and other similar type processes are primarily the result of interparticle forces. They have no direct effect upon contaminant deposition. They change the particle characteristics sufficiently so that the deposition pattern will change. Diffusion produces random particle motion, resulting in translation of particles from an expected narrow trajectory to a broad path. Brownian motion of the particles may also result in coalescence and growth of particles. If growth occurs, more material will be impacted than if it had not grown. Coalescence and growth may occur as a result of electric fields, gravitational effects, and turbulence. If the particle is capable of absorbing water vapour (of initiating droplet growth by nucleation), it may grow to a size which would be collected under conditions that would not normally permit collection of the dry particle alone. In short, the interparticle forces may lead to a change in the particle characteristics that will change its normal deposition probability.

The energy gradient forces are directed toward the particles suspended in the air and are independent of any inertial forces resulting from the movement of the air. Because of this, these energy gradient forces are probably the most important in causing contamination. The removal from the air of larger particles is influenced by inertial impaction mechanisms and particles smaller than this by diffusional mechanisms. There is a point however where removal is least efficient as particles cross between influences from inertia or diffusional mechanisms (Fig. A1.1).

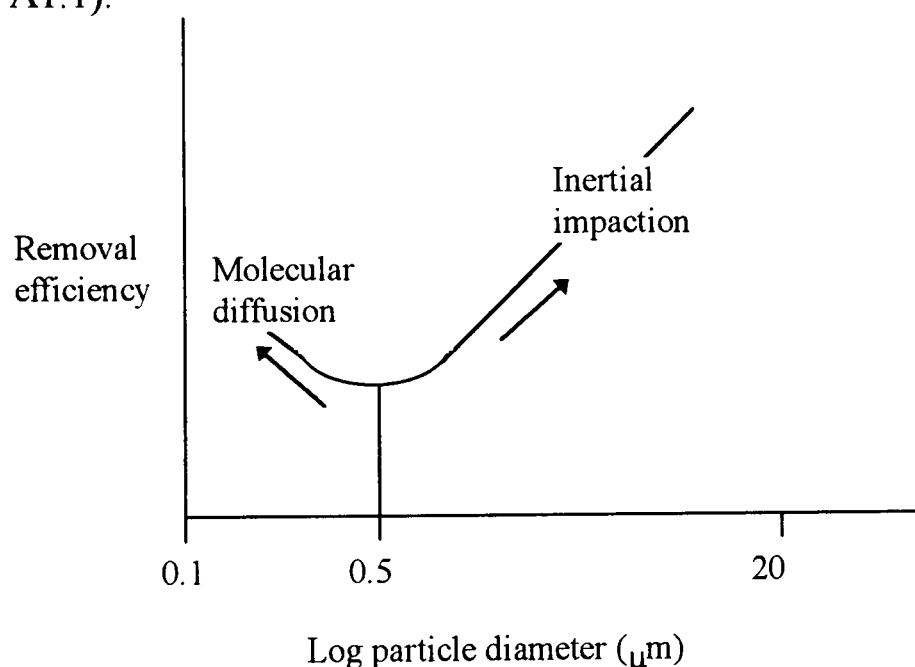


Fig. A1.1 Particle deposition efficiency as a function of particle size (Hesketh, 1974).

A1.4 Summary of size distribution

The size of droplet/particle is critical in terms of contamination. The physical size of a particle is important in terms of penetration and the settling velocity in terms of deposition. Perhaps the most important particles especially with respect to health are those that once become airborne have equivalent sizes such that they remain airborne for very long periods of time and can be transported for large distances along with air currents (Tables A1.1 & A1.2). This will depend on the velocity of movement of the ambient air but the size range of particles < 100 μm are of general interest because they have very low settling velocities even in still air and that the majority of air movement in any workplace is of the order of 0.2-0.3 m/s (B.O.H.S., 1988). Particles in the size range 0.5 - 5 μm may penetrate into the alveoli of the lungs. Below 0.5 μm the particles may enter and leave the lungs without being deposited and above 5 μm they will be filtered in the first stages of the lung. Particles of sizes >5 μm have also been found to be important in a medium by which bacteria may be suspended in on air currents.

The following are the size range of equivalent particle diameters (d_s , the diameter of an equivalent sphere of the same density and terminal velocity) and settling velocities of airborne matter (summarised from a table in Hidy (1984), reprinted from Lapple (1961) and the Stamford Research Institute).

Size (diameter) μm	Angstrom Units \AA	Reynolds Number	Settling Velocity cm/sec (sg 2.0)
0.001 - 0.01	1 - 10	1×10^{-12} - 1×10^{-10}	1×10^{-6} - 1×10^{-5}
0.01 - 0.1	10 - 100	1×10^{-10} - 1×10^{-8}	1×10^{-5} - 2×10^{-4}
0.1 - 1	100 - 1000	1×10^{-8} - 5×10^{-6}	2×10^{-4} - 7×10^{-3}
1 - 10		5×10^{-6} - 4×10^{-3}	7×10^{-3} - 6×10^{-1}
10 - 100		4×10^{-3} - 3×10^0	6×10^{-1} - 4×10^1
100 - 1000		3×10^0 - 4×10^{-2}	4×10^1 - 6×10^2
1000 - 10000		4×10^{-2} - 1×10^{-4}	6×10^2 - 2.4×10^3

Table A1.1 Physical characteristics of particles

Airborne Matter	Particle size range (μm)
Fume	0.001 - 1
Dust	1 - >300
Mist	<0.01 - 10
Spray	10 - >300
Clay	<0.1 - 2
Silt	2 - 20
Fine sand	20 - 200
Coarse sand	200 - 2000
Gravel	>2000
Common atmospheric dispersoids	
Smog	<0.01 - 200
Clouds and fog	2 - 80
Mist	80 - 200
Drizzle	200 - 500
Rain	500 - 1000
Particle type	Particle size range (μm)
Molecular diameters	<0.01
Oil smokes	0.03 - 1
Tobacco smoke	0.01 - 1
Atmospheric dust	0.01 - 2 (~0.001 - 20)
Aitken nuclei	~0.005 - 0.2
Sea salt nuclei	0.03 - 0.5
Combustion nuclei	0.01 - 0.1
Nebuliser drops	1 - 20
Hydraulic nozzle drops	55 - 5000
Pneumatic nozzle drops	10 - 100
Pollens	10 - 100
Plant spores	10 - 40
Lung damaging dust	0.5 - 5
Viruses	0.003 - 0.05
Bacteria	0.3 - 30
Human hair	30 - 200
Red blood cell of human	7.5 & 0.3

Table A1 2 Typical sizes of airborne particles and gas dispersoids

Appendix 2 Qualitative assessment methods

Air itself does not absorb light in the visible spectrum and is thus transparent as are gases, vapours and particles < 25 µm. However, the effect of air movement on light scattering matter placed in its field of flow is obvious and the majority of visualisation methods rely on this fact whereas other methods make use of the physical properties of the air itself (Merzkirch, 1987).

- 1. Techniques by which foreign material is added to the flowing fluid.
- 2. Techniques in which changes in the fluid density causing a change in the refractive index may be observed using optical methods.
- 3. Techniques in which energy is applied to the fluid and the increased energy level of particular fluid elements may be distinguished from the rest of the fluid.

METHOD	DESCRIPTION
Tuft method	Movement of tufts of thread suspended in the flow field.
Body surface Tracing	Material on the body surface varies its shape according to the flow.
Chemical reaction	Chemical reaction between the fluid and a substance spread over the body surface or between the fluid and another injected fluid.
Electric controlled	Controlled electric current causing ionisation of the air or production of smoke from oil dripped onto an electrically heated wire.
Direct injection of tracer into the flow field to either scatter or absorb light.	
Smoke	Smoke particles to scatter light
Water fog	Water droplets to scatter light
Dust or Tyndall lamp	Observing forward scattering of light from suspended particles
Shadowgraph, Schlieren photography, Mirage methods	Change in refractive index of the fluid by temperature or other density changes.
Mach-Zehnder interferometer	Observation of interference fringe patterns
Laser holographic interferometer	Observation of holographic interference from laser light source
Laser induced fluorescence	Fluid is seeded with fluorescent material which radiates when excited with laser light.
Speckle method	Scattered light from suspended particles in a laser light sheet causing interference and a speckling effect.

Table A2.1 Summary of methods used for the visualisation of fluid flow (Merzkirch, 1987)

Most of these methods provide detailed assessment over small areas. In contamination control the main visualisation media used has been smoke and water fog visualisation methods.

Appendix 3 Quantitative assessment methods

Particles used as tracer material should be small enough to assume a motion that is the same as that of the suspending fluid, in direction and magnitude of velocity. The difference between the movement of the fluid and that of the foreign material can be minimised, but not totally avoided, by using material with a density almost coinciding with that of the fluid. This also applies to gas tracers.

Qualitative measurements provide only limited data on the interaction between the source, its motion in the air and the exposure of the work, worker and the general environment. If one resolves the light scattered from single particles suspended in the fluid flow, the observation becomes quantitative and allows for measuring the velocity of the scattered, which in many cases can be taken as the fluid velocity. Other quantitative methods do not require the scatter of light from matter as means of measurement and thus may include gases, vapours and fine particles.

The material ideally should have similar physical and chemical properties to the potential contaminant or should be a compromise where several contaminants are of interest. The method of generation of the contaminant should be similar if not the same as that of interest and the conditions with which it is sampled should not interfere with the transport mechanism. The latter is of great interest and presents problems, for both absolute measurements or measurements using tracers, in deciding which method to use whether it is intrusive or non-intrusive and whether passive or active.

The use of quantitative information though also has its limitations with respect to the positions of release and sampling of the tracer. Does this reflect the real exposure. This depends on the tracer used and the sensitivity of the measuring instrument. The perfect method would be to measure the actual exposure to the contaminating species in real time and in the position which is most vulnerable to contamination. However sometimes this is not possible due to the sensitivity of the measuring instrument, the hazard of the contaminating species, and due to the fact that exposure is not steady and may fluctuate over long periods of time, and that a facility used to control contamination may use a very varied potential contaminants. It also does not allow prediction. In this case other tracers are used to substitute and be representative of the contaminating species.

The use of particle and gaseous tracers thus have their differences where each are subject to different forces which effect their transport in air and which thus affect their choice as a tracer. This has been studied in many reports where the major difference between them is the deposition of particles out of the fluid flow mainly as a result of gravitational settling but also as a result of impaction and phoretic forces. In the built environment and contamination control facilities this has been looked at, (Chamberlain, 1978; Foord, 1972; Foord, 1975; Foord, 1975; Hambræus, 1972; Hampl, 1985; Lidwell, 1972; Lidwell, 1975; Shaw, 1972; Whyte, 1973). However as tracers it is assumed that in certain circumstances the difference will be small compared to the distance between the sampling point and the generation source and the settling velocity with respect to the fluid flow.

This has been approached with respect to containment facilities.

Particle generation methods	Sampling methods
Supersaturation Particles from gas phase chemical reactions Disintegration of liquids Sprays by centrifugation Atomisation by acoustic disturbance Aerodynamic atomisation Nebulisation	Impingement separators Settling chambers Centrifugal separators Filtration Thermal precipitation Mechanical separators Electrical precipitators Optical and electronic Particle counting Particle concentration

Table A3.1 Aerosol generation and sampling techniques (Hidy, 1984)

Gas tracer generation methods	Gas Sampling methods
Jets Diffusers	Spectroscopy (e.g. Infra-red) Electron capture Gas chromatography Flame ionisation Acoustic

Table A3.2 Gas tracer generation and sampling techniques (Hidy, 1984)

Appendix 4 Fume cupboard survey at King's College London

A survey was carried out to assess the type, condition and performance of the fume cupboard stock being used presently at King's College London. The results may be indicative of the state of fume cupboards in other similar institutions.

General observations were made of the cupboard including the dimensions, physical condition and the services installed. Performance tests were based on face velocity measurements and visualisation of airflows into and within the fume cupboard. These methods of performance assessment were regarded as being of secondary importance to complete containment testing but as BS 7258 : 1994 still only recommended a containment test and due to the scale of the project and limited time, face velocity and visualisation were considered satisfactory indicators. The methods used were also part of a hierarchy of tests specified in BS 5726 : 1992 for the performance assessment of microbiological safety cabinets. The College had its own method of assessing fume cupboard performance but this required the cupboard to be empty and thus was not appropriate.

Ultimately, the cupboards were graded to give a quick reference idea of performance. In all some 221 cupboards with 309 sash faces were tested.

A4.1 Methods used in performance evaluation

The tests were performed at working sash heights of 250 and 500 mm (unless otherwise stated). This height was measured from the top edge of either the bench or lipfoil (where fitted) to the lower edge of the sash. Where a cupboard had two or three sashes, all sashes were positioned at the same working height during the tests, and each face tested.

Performance tests were carried out for each fume cupboard in the condition in which it was found (viz. with whatever equipment was present at the time). A photographic record was kept of each fume cupboard at the time of the tests. No attempt was made to alter the environmental conditions around the cupboard. This meant that people were allowed to enter and leave the laboratory as they wished. This was considered to give an indication of the cupboard performance as installed and in working conditions.

The following tests were carried out to establish the performance of the fume cupboards:

A4.1.1 Air flow visualisation

Water fog generated by an ultrasonic nebuliser (De VILBISS Co. Ltd.) (Kennedy, 1987) was used to visualise the direction of air flowing into the cupboard across the face of the working aperture and it was directed against the inflowing air to look for any regions of leakage. It was also used to;

1. Visualise the airflow within the cupboard for areas of excessive turbulence.
2. To demonstrate any scrolling movement above the sash at the top of the working volume.
3. To assess the effectiveness of scavenging of air from the work surface.
4. To visualise the airflow over the front lipfoil (if fitted) and to show how efficiently the mist was dispersed.

A4.1.2 Face velocity

The inflow face velocity was measured with a 100 mm diameter rotating vane anemometer (AIDEL OW DEVELOPMENTS Ltd.) at six points in the plane of the aperture for a working

aperture of 500 mm (Fig. A4.1) and 3 points for a working aperture of 250 mm. The anemometer calibration was covered in chapter 3, section 3.8.1.2)

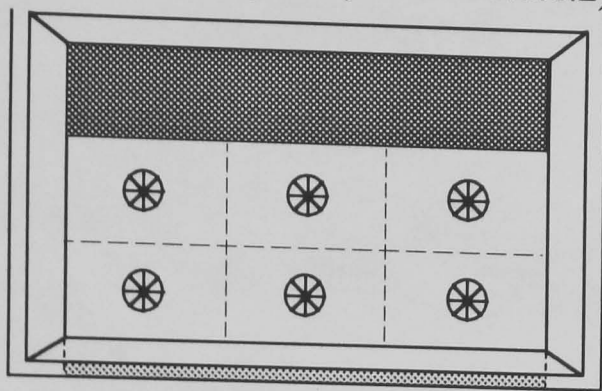


Fig. A4.1 Position of rotating vane anemometer head in the plane of the sash for an ‘aerodynamic’ fume cupboard.

The fume cupboard standard BS 7258 : 1994 specified (for maintenance purposes) a grid of minimum 9 points at the normal working aperture using a rotating vane anemometer. For commissioning and type testing of fume cupboards numerous points were required using a thermistor or hot wire anemometer, but this was a time consuming method. The mean face velocity determined from the six point grid used for this survey was shown not to be statistically different from the mean velocity determined using these other measurement grids (Fig. A4.2). The standard errors were representative of the variation in mean velocity at the individual measurement points from the overall mean face velocity which was apparent in aerodynamic fume cupboards, the flows being greater towards the faired edges. The measurement grid was considered to give a realistic number of measured points in reasonable time.

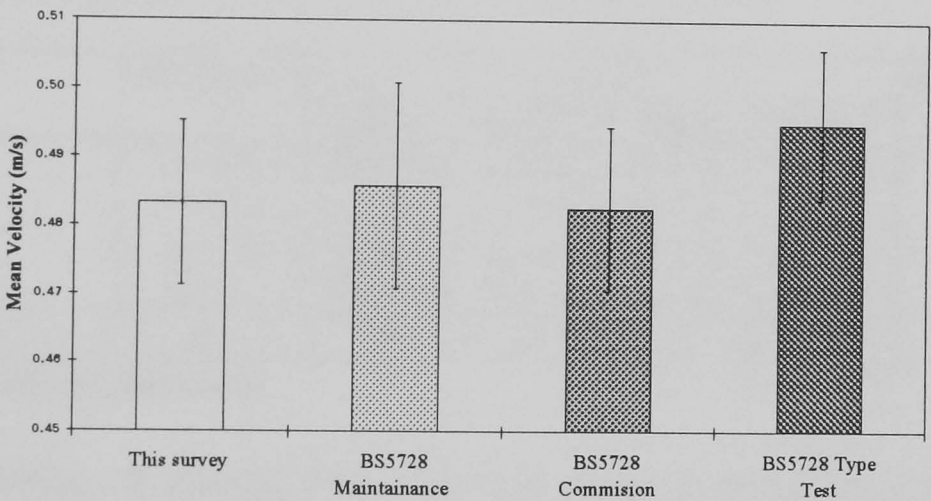


Fig.A4.2 Comparison of the mean face velocity measured at a working aperture (500 mm) of an aerodynamic fume cupboard with differing number of sample positions (error bar ± 1 SEM as an estimate of variation of mean velocities measured at a point from the overall mean face velocity)

A4.2 Number and type of fume cupboards tested at King’s College London

Number of fume cupboards tested in the survey			221
Number of tests performed (1 test per sash)			309
Fume cupboard type	Number in survey	% of total	
Aerodynamic	61	27.6 %	
Box type with single sash	89	40.3 %	
Box type with double sash	46	20.8 %	
Box type with triple sash	12	5.4 %	
Box type with opposing sashes (x2)	8	3.6 %	
Portable type with aerodynamic front	4	1.8 %	
Walk-in	1	0.5 %	

Table A4.1 Number and type of fume cupboards tested

Surprisingly there were very few aerodynamic cupboards. For analysis the cupboard types were grouped into ‘aerodynamic’ fume cupboards and those fume cupboards with no aerodynamic facias were termed ‘conventional’ cupboards.

A4.3 Fume cupboard exterior material types

Material	Aerodyn'c	Box				Aerodyn'c portable	Walk in
		Single	Double	Triple	2 sided		
Chipboard/laminate	3.3 %						
Fibreglass/GRP	50.0 %						
Glass/laminate		1.1 %					
Metal/stainless steel	35.0 %	1.1 %				25.0 %	
PVC/plastics	10.0 %	5.6 %			62.5 %		100 %
Wood/glass	1.7 %	92.2 %	100 %	100 %	37.5 %	75.0 %	
Total no. cupboards	60	89	45	12	8	4	1

Table A4.2 Fume cupboard exterior material

The materials used in the construction of the fume cupboards reflected the type, use and cost. The box types were made of reinforced glass and wood with tiled work surfaces and the relatively modern aerodynamic fume cupboards were made of composite materials. Some of the cupboards reflected the work expected to be carried out in them. The majority of the two sided cupboards were made of PVC/Plastics, being used for isotope work, the aerodynamic ones ranged from stainless steel work interiors for radioactive work to fibreglass which were for more general purpose work.

A4.4 Subjective assessment of fume cupboard cleanliness

Cleanliness	Aerodyn'c	Box				Aerodyn'c portable	Walk in
		Single	Double	Triple	2 sided		
Good	28.3 %	26.0 %	11.1 %	25.0 %		25.0 %	
Just acceptable	28.3 %	14.3 %	13.3 %	8.3 %	50.0 %		
Dirty	31.7 %	40.3 %	51.1 %	58.3 %	37.5 %	75.0 %	100.0 %
Filthy	11.7 %	19.5 %	20.0 %	8.3 %	12.5 %		
Total no. cupboards	60	77	45	12	8	4	1

Table A4.3 Fume cupboard cleanliness

From the observations, it seemed that users and departments cared little for their fume cupboards. The data may have been weighted due to the large number of fume cupboards used for teaching in which the students possibly had no real instruction, understanding or respect for the condition of the cupboard.

A4.5 Subjective assessment of fume cupboard condition

Condition	Aerodyn'c	Box				Aerodyn'c portable	Walk in
		Single	Double	Triple	2 sided		
Average & above	93.3 %	71 %	76 %	58.3 %	62.5 %	100.0 %	100.0 %
Poor	6.7 %	29 %	24 %	41.7 %	37.5 %		
Total no. cupboards	60	79	42	12	8	4	1

Table A4.4 Fume cupboard condition

The majority of cupboards which were assessed as being in poor condition, had cracked or broken tiles which lined the work surface and walls. Some had obvious fire damage, were badly corroded or the glass was cracked. That there were only a few aerodynamic cupboards assessed as being in a poor condition was considered due to the materials of construction

being more resilient. Often there was evidence that bunsen burners had melted the plastic walls.

A4.6 Subjective assessment of fume cupboard blockage

Condition	Aerodyn'c	Box				Aerodyn'c portable	Walk in
		Single	Double	Triple	2 sided		
Cluttered	24.6 %	26.4 %	44.5 %	8.3 %	42.8 %	33.3 %	
Moderate	52.4 %	32.2 %	20 0 %	41.7 %	28.6 %	66.7 %	
Minimal	19.7 %	34.5 %	13.3 %	41.7 %	14.3 %		
None	3.3 %	6.9 %	22.2 %	8.3 %	14.3 %		100.0 %
Total no. cupboards	61	87	45	12	7	3	1

Table A4.5 Fume cupboard condition

A high percentage of cupboards were cluttered with equipment, mainly bottles and glassware. Sometimes, these items obscured the rear scavenging slot eliminating any scavenging across the work surface. In other cases, large items of equipment such as gas chromatograms obscured nearly the whole of the working volume; the cupboard simply being used as a captor hood.

A4.7 Fume cupboard performance

A4.7.1 Mean face velocity

Mean face velocity was given a score using a banding system:

≥0.5m/s	1
<0.5>0.3m/s	2
<0.3>0m/s	3
=0m/s	no flow detected

The face velocity was established as being important in resisting environmental disturbances (Caplan, 1982), 0.5 m/s being recognised as the recommended minimum average face velocity. The velocity banding used in this survey was based on the literature and on the recommended face velocities in BS 7258 : 1994 which stated “In practice, with the sash set at the maximum working opening, it is unlikely that face velocities below 0.3 m/s will give satisfactory containment. In some cases, face velocities of 0.5 m/s or above may be necessary”.

Following the survey it was found that 96.6 % of the aerodynamic cupboards tested had average face velocities > 0.5 m/s at a working sash height of 250 mm dropping to 70.2 % at a working sash height of 500 mm, a decrease of only 26.4 % of the number of cupboards suggesting that the majority were in excess of 1 m/s (Fig. A4.3 & A4.4, Table A4.8 & A4.9). The total range of average face velocities was from 0.27 m/s - 1.75 m/s at a working sash height of 250 mm and 0.35 m/s - 1.10 m/s at a working sash height of 500 mm. Only 1 of these cupboard types tested was found to have been switched off, however 2 had no flow through them with the sash raised to 500 mm but on reducing this to 250 mm a draught was measurable. This was thought to be more probably due to thermal updrafts through the ducting rather than to mechanical ventilation.

86 % of conventional fume cupboards had an average measured face velocity > 0.5 m/s at a working sash height of 250 mm dropping to 38.5 % at a working sash height of 500 mm, a decrease of 47.5 % with a greater proportion of cupboards having face velocities less than 1 m/s (Fig. A4.3 & A4.4, Table A4.8 & A4.9). The total range of average face velocities was

from 0.10 m/s - 2.17 m/s at a working sash height of 250 mm and 0.07 m/s - 1.31 m/s at a working sash height of 500 mm. 35 conventional cupboard types tested had no flow through them. All the cupboards with triple sashes had face velocities > 0.5 m/s at 250 mm, and the number only reduced by 7 % when the sash was raised to 500 mm.

The effect of raising the sash from 250 mm to 500 mm working aperture height on the scored variables was analysed using the students paired t-test. There was an extremely significant difference between the average face velocity at working aperture heights of 250 mm and 500 mm ($P = 3 \times 10^{-21}$ for aerodynamic cupboards, 5.2×10^{-22} for conventional cupboards and 5.1×10^{-34} for all cupboard types) showing as expected that by raising the sash there is a subsequent reduction in face velocity (using data in which each cupboard was tested at both 250 and 500 mm heights and excluding those through which no flow was measured).

The range of velocities seemed excessive with some very high velocities. However, while this was not unusual with regard to the literature, it did suggest that not much attention was paid to the recommended face velocity of 0.5 m/s and economics - unnecessary loss of heated air.

A4.7.2 Variation of velocity across the plane of the working aperture

This was scored with respect to the mean face velocity

Variation $\leq 20\%$ & face velocity ≥ 0.5 m/s	1
Variation $\geq 20\%$ & face velocity ≥ 0.5 m/s	2
Variation $\leq 20\%$ & face velocity ≤ 0.5 m/s	3
Variation $\geq 20\%$ & face velocity ≤ 0.5 m/s	4

It was generally accepted that, with a carefully designed, aerodynamically styled fumecupboard, a velocity of 0.5 m/s, with ± 20 % variation across the opening, was adequate to provide a reasonable degree of containment. This velocity was sufficient to overcome many of the adverse effects caused by air currents resulting from movements of the operator (Caplan, 1982).

89.8 % of the aerodynamic working apertures tested at 250 mm met this minimum criteria (score 1), but on raising the sash to 500 mm, the number were reduced to 47.4 % (decrease 42.4 %) (Fig. A4.5 & A4.6, Table A4.9 & A4.10). However, the number of cupboards with variation < 20 % irrespective of face velocity only dropped from 93.2 % to 71.6 %. This was a combination of both a decrease in velocity (26.4 %) and an increase in variation on raising the sash to 500 mm. It would appear from the results that not only was the reduction in score due to a decrease in face velocity below 0.5 m/s but also due to an increase in variation of those cupboards with face velocities above 0.5 m/s. There was a significant increase in variation when the sash was raised to a working aperture of 500 mm from 250 mm (Fig. A4.7) ($P = 4.1 \times 10^{-7}$).

Conventional box cupboards were expected to have a greater degree of variation depending on the design features. The cupboards assessed were of varying design ranging from those with a single extract hole in the top to those with tapered extract ducts, those with no baffle to those with full rear baffles, and some which had retro fitted lipfoils in an attempt to smooth the airflow over the lower front lip. From the results at a working sash height of 250 mm, 74.2 % had a velocity > 0.5 m/s and a variation about this < 20 % (84.9 % < 20 % irrespective of face velocity) (Fig. A4.5 & A4.6, Table A4.9 & A4.10). As the sash was raised to 500 mm the number with a velocity > 0.5 m/s and a variation about this < 20 % dropped to 17.3 % (36.9 % with a variation of face velocity < 20 % irrespective of face

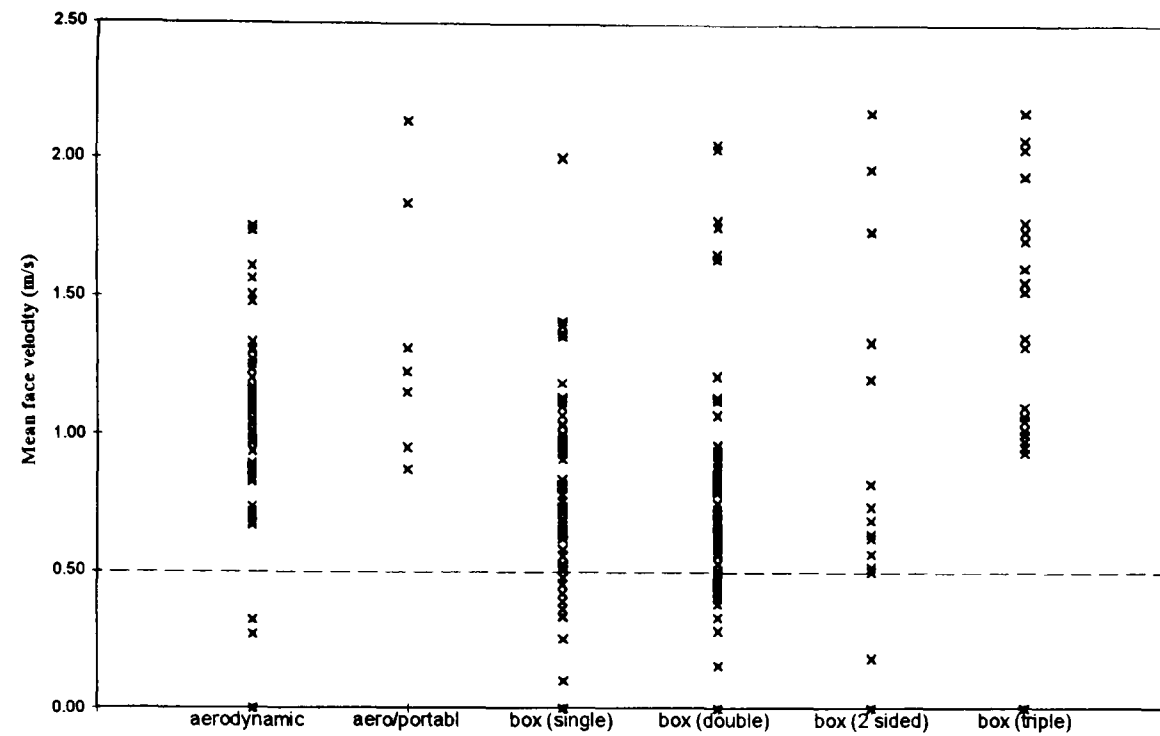


Figure A4.3 Velocity measurements at a working aperture height 250 mm

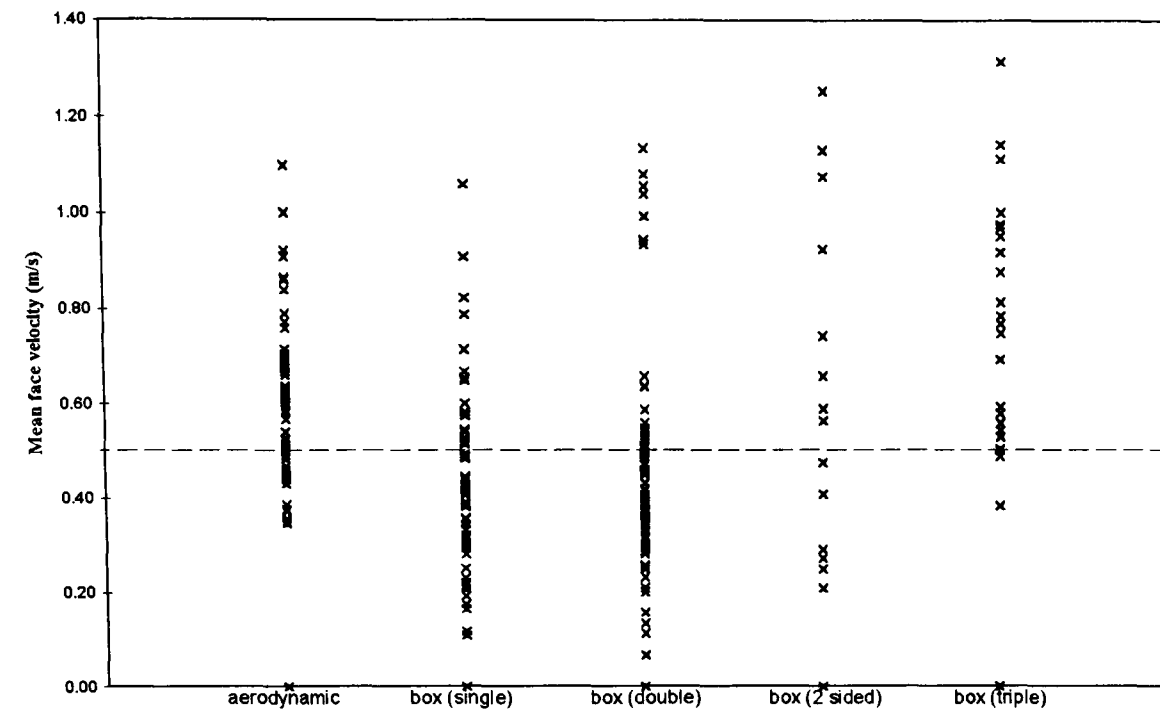


Figure A4.4 Velocity measurements at a working aperture height 500 mm

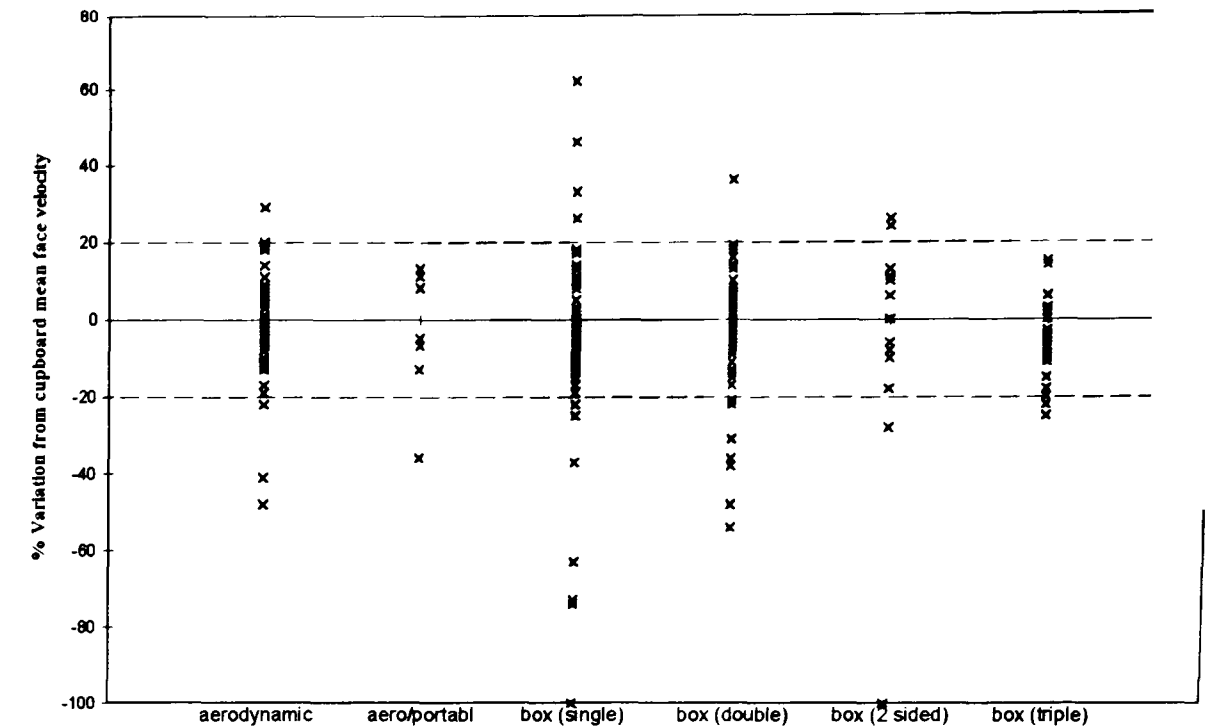


Figure A4.5 Variation in mean velocity measurements at a point from the overall mean face velocity at a working aperture height 250 mm

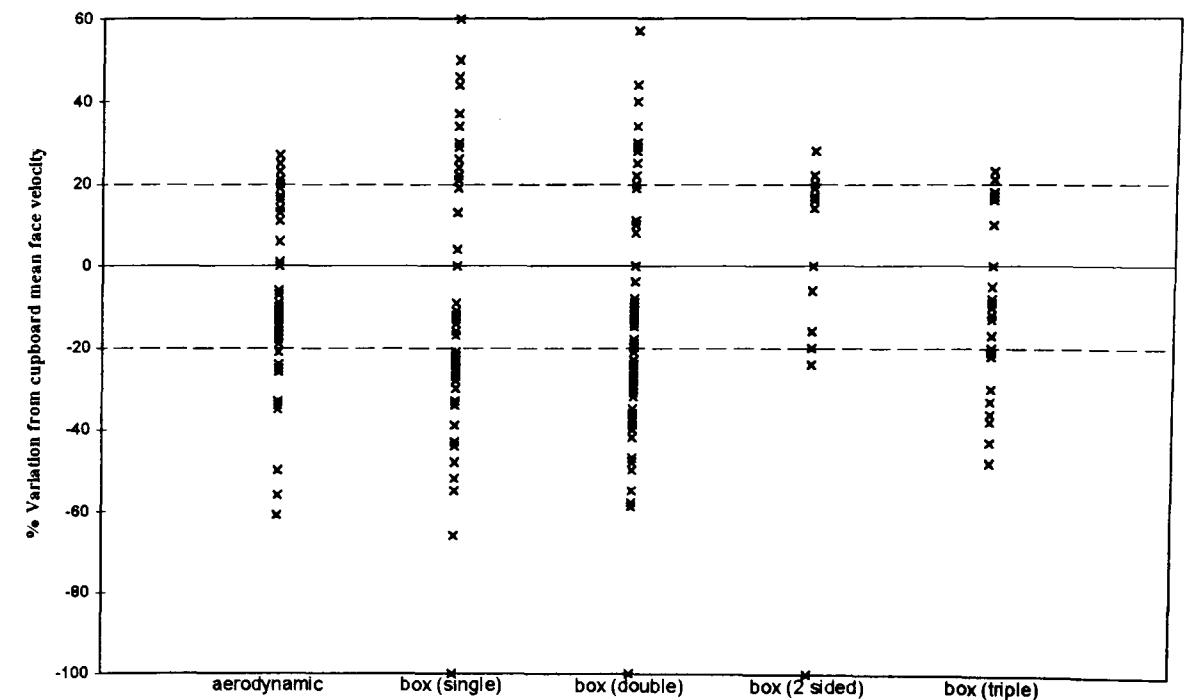


Figure A4.6 Variation in mean velocity measurements at a point from the overall mean face velocity at a working aperture height 500 mm

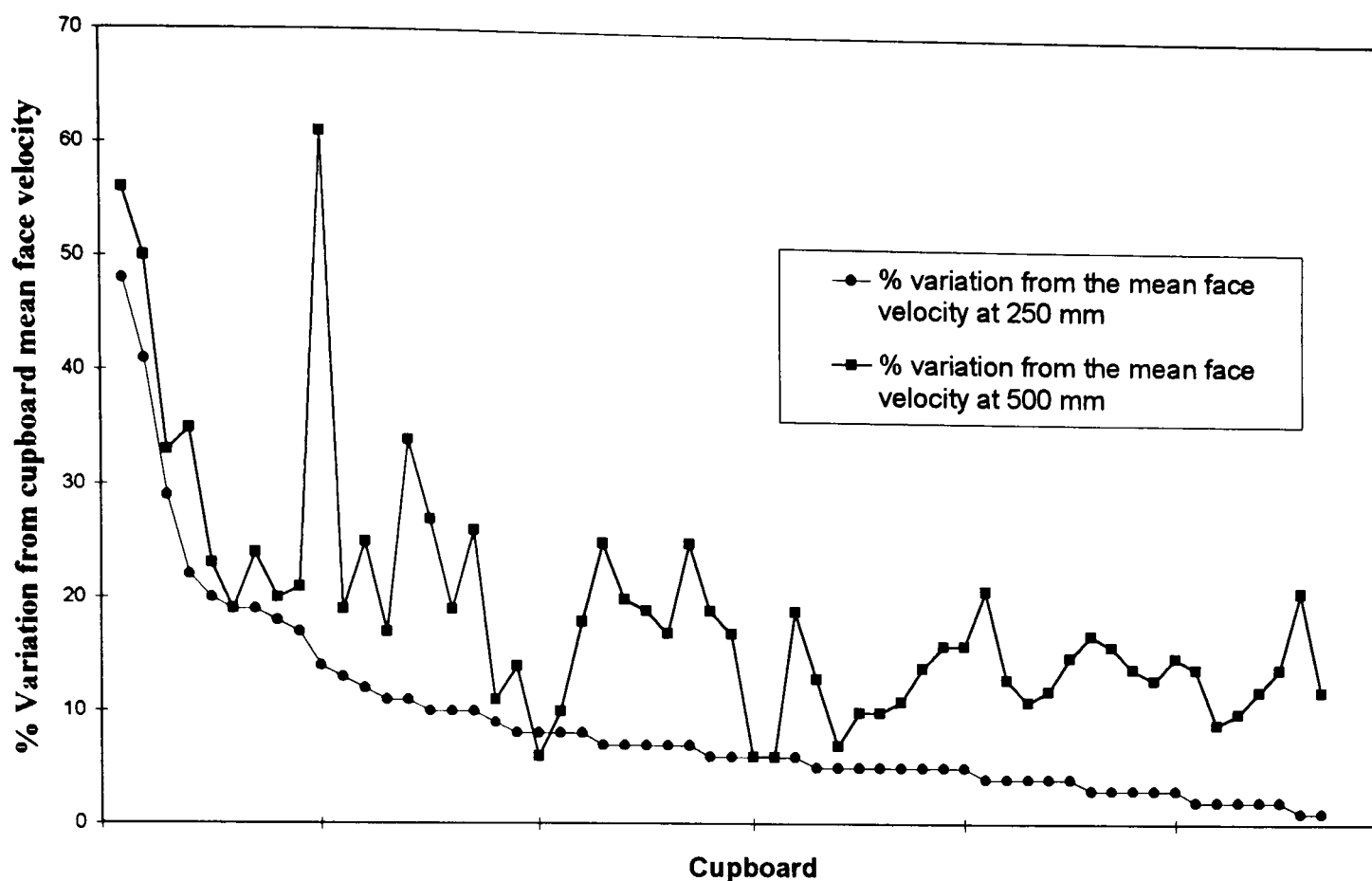


Figure A4.7 Comparison of % variation in the mean velocity measured at a point from the overall mean face velocity at working aperture heights of 250 mm and 500 mm for 'aerodynamic' fume cupboards.

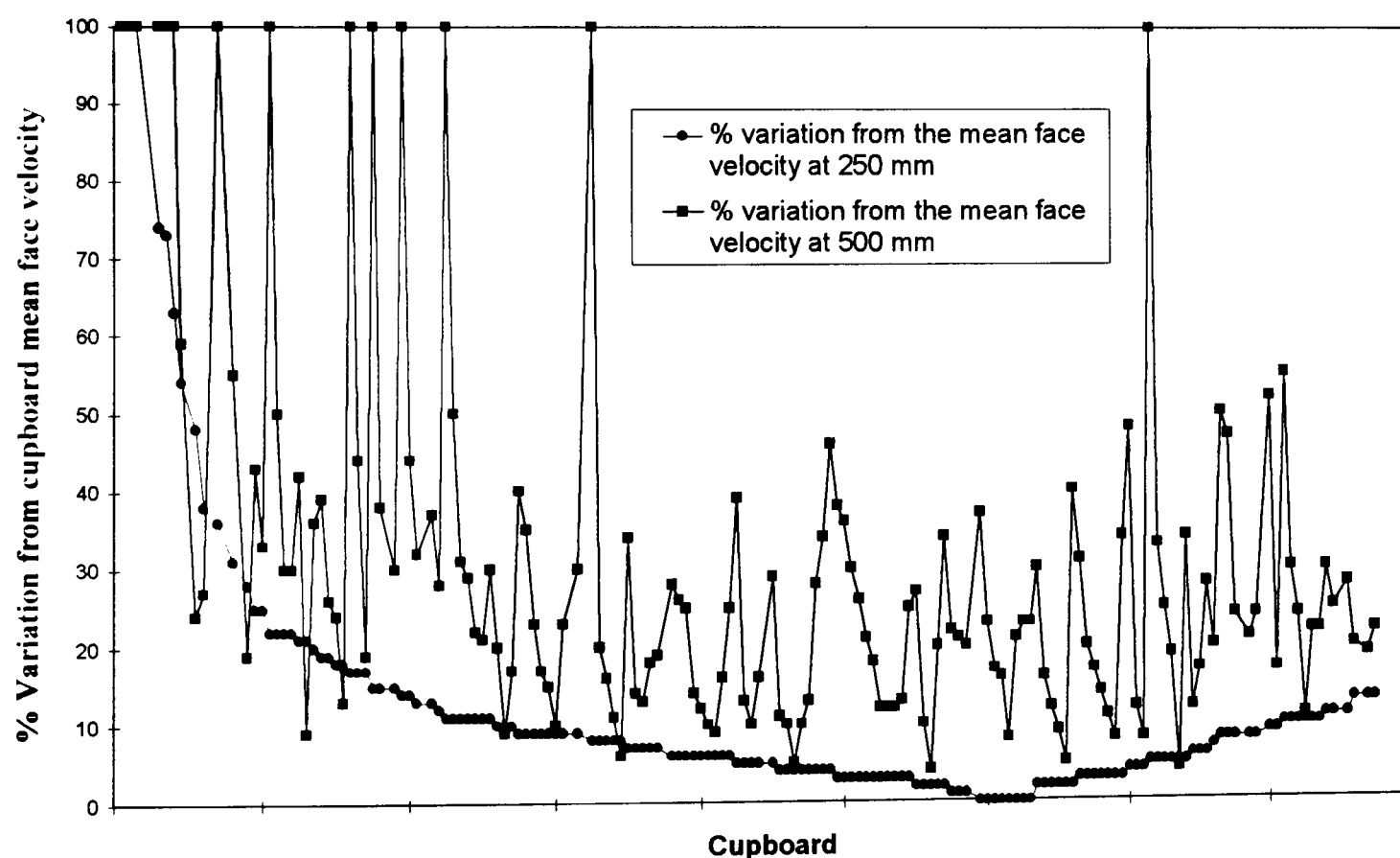


Figure A4.8 Comparison of % variation in the mean velocity measured at a point from the overall mean face velocity at working aperture heights of 250 mm and 500 mm for 'conventional' fume cupboards.

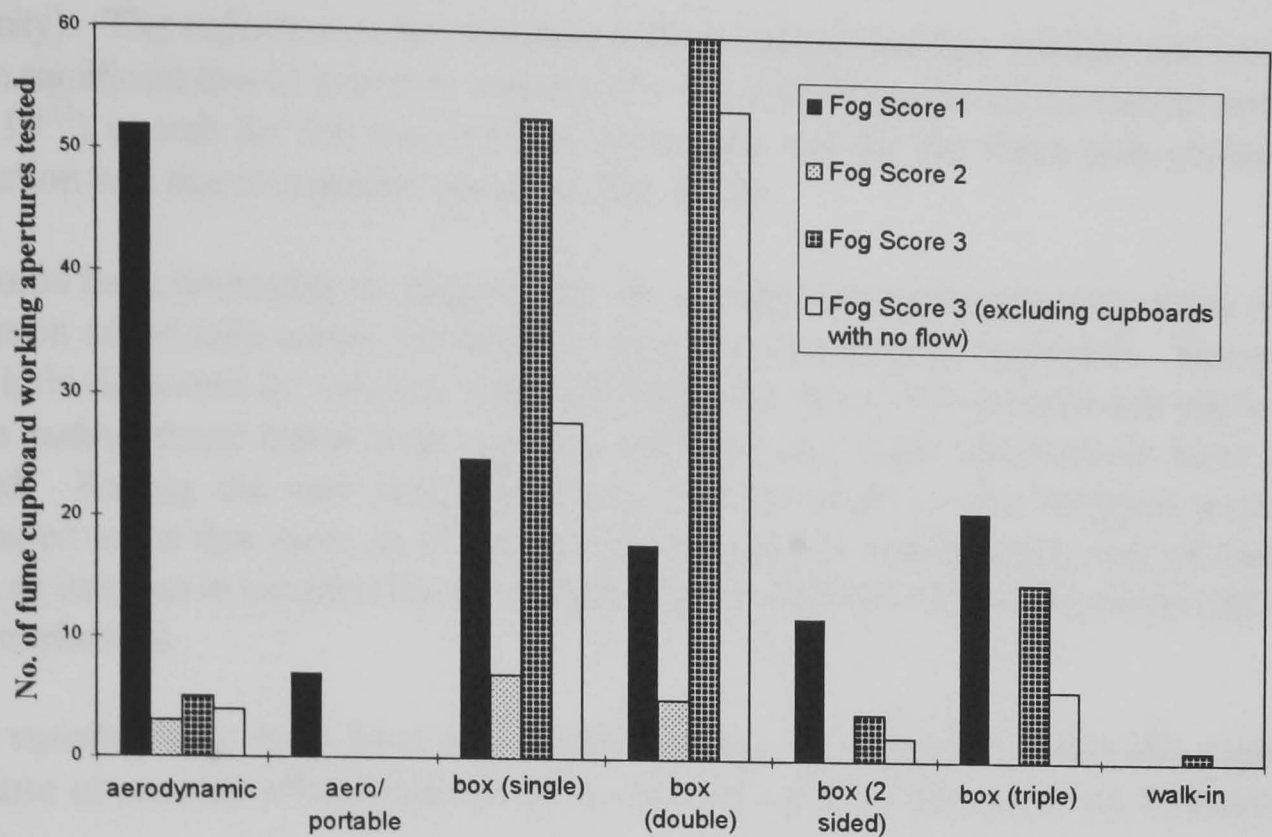


Figure A4.9 Fog scores at a working aperture of 250 mm

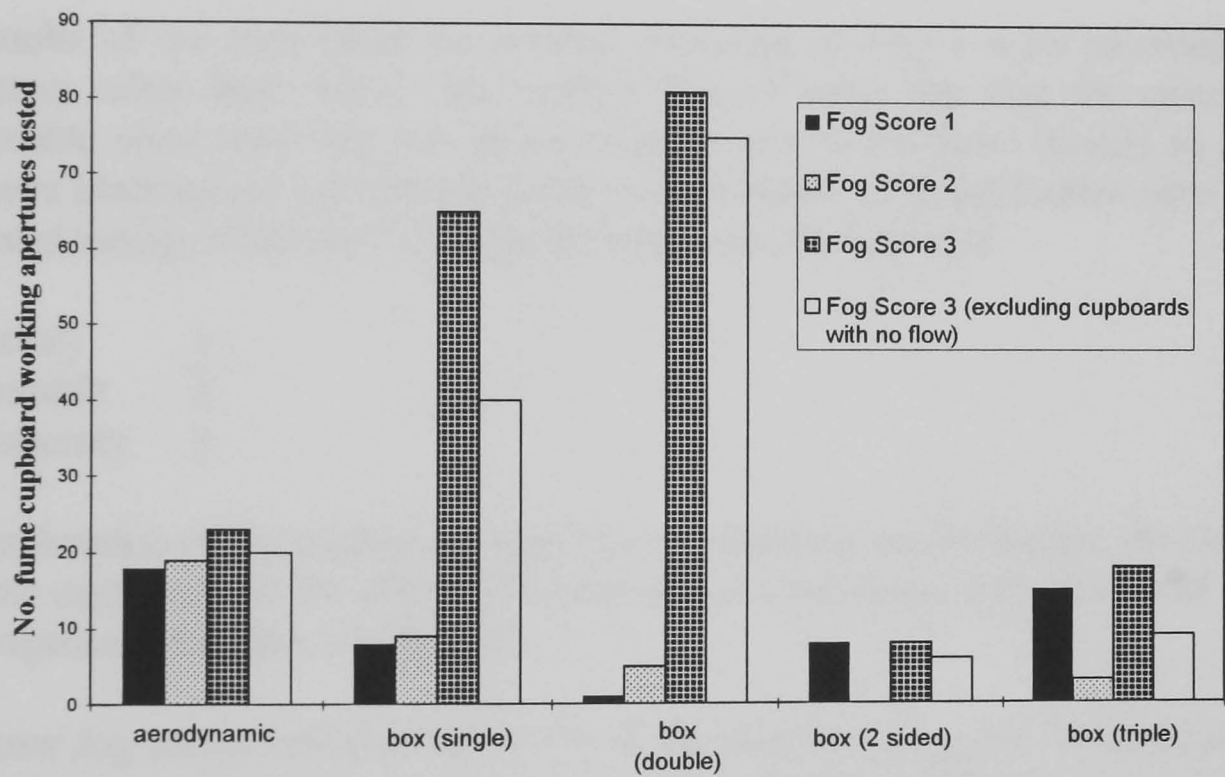


Figure A4.10 Fog scores at a working aperture of 500 mm

velocity). The reduction in the numbers with recommended face velocity and variation was more significant due to a drop in velocity ($P = 5.2 \times 10^{-22}$) than to an increase in variation ($P = 1 \times 10^{-15}$) overall for the conventional cupboards, but for the triple sash cupboards there reduction was due to a greater variation (Fig. A4.8).

It would be encouraging to suggest that the aerodynamic cupboards were more resistant to variation of velocity across the aperture than the conventional cupboards. However, there was little difference in variation with sash height for those conventional box cupboards with triple sashes, those tested with opposing apertures and those aerodynamic fume cupboards tested. Raising the sash height obviously had an effect on the variation score but this appeared to be due more to a decrease in face velocity and perhaps error of measurement than an increase in variation for all cupboard types apart from the aerodynamic and triple sash box cupboards.

The variation may have been due to the presence of equipment inside the cupboard, but because of possible effects from all the conflicting variables this could not be assessed on its own.

A4.7.3 Visualisation/Fog score

The results of the tests using the method described in A4.1.1 were recorded as either satisfactory when there was a clear inward flow of water fog over the entire aperture, questionable when water fog was shown to linger around the lipfoil (usually as a result of equipment blockage) or substantially under the sash handle or unsatisfactory when there was substantial leakage of the mist back into the room from the cupboard.

Satisfactory	1
Questionable	2
Unsatisfactory	3

The combination of the cupboard design, the face velocity, its distribution, the clutter inside the fume cupboard and the effect of environmental disturbances was considered potentially better represented by flow visualisation.

The water fog scores indicated that 87 % of the aerodynamic apertures tested at 250 mm were satisfactory (score 1) but only 30 % were satisfactory at 500 mm (a 56.5 % reduction on the number of cupboard apertures of those tested) (Tables A4.10-A4.13). This was due to 32 % of the apertures at 500 mm being scored 2 because of reverse flows around the lipfoil; where fog was seen to accumulate in eddies on the lipfoil, or because of bounce off equipment placed too near to the opening. At the lower aperture setting this did not seem to be a problem but was very noticeable at the higher sash heights.

34 % of the conventional cupboards were satisfactory but 51 % of those with a measurable flow were not satisfactory at a working sash height of 250 mm. At 500 mm, only 15 % were satisfactory, 73 % were unsatisfactory (Tables A4.10-A4.13).

The results of the water fog test were more condemning than the velocity or variation scores which was demonstrated in Figs. A4.11 - A4.24. Considering all cupboards at a working aperture height of 250 mm the decrease in the number of fume cupboards with increasing score for the variables of velocity and variation compared well. However the fog score does not reflect this and the number of cupboards decreases then increases with increasing score.

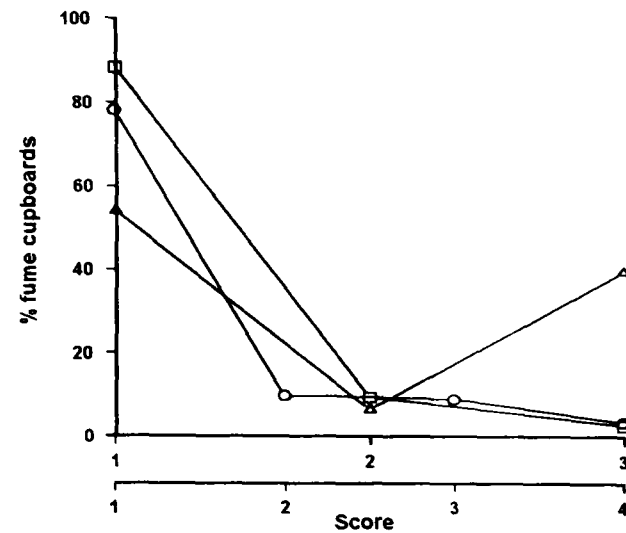


Figure A4.11 % of all cupboard faces tested at height 250 mm and their scored variables: velocity □, variation of velocity ○, and fog △.

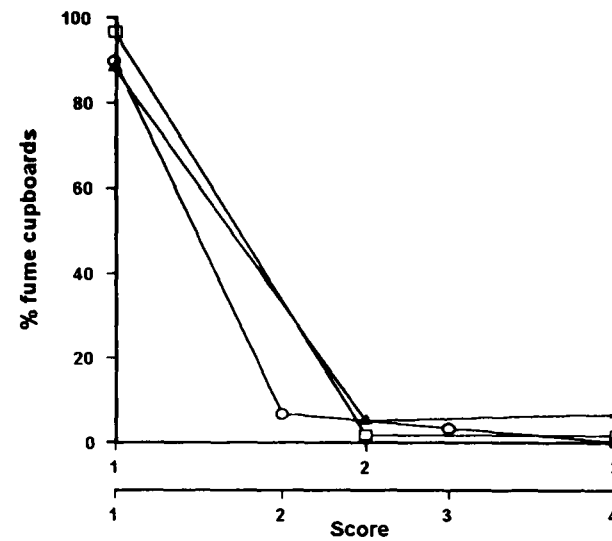


Figure A4.13 % of aerodynamic cupboard faces tested at height 250 mm and their scored variables: velocity □, variation of velocity ○, and fog △.

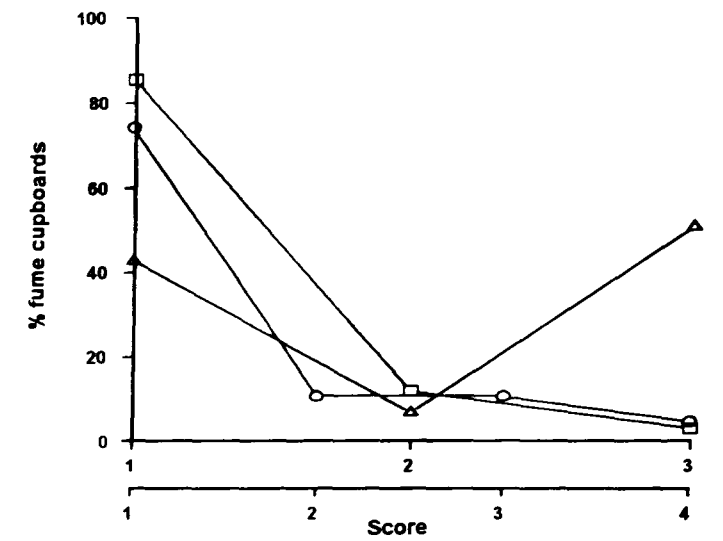


Figure A4.15 % of conventional cupboard faces tested at height 250 mm and their scored variables: velocity □, variation of velocity ○, and fog △.

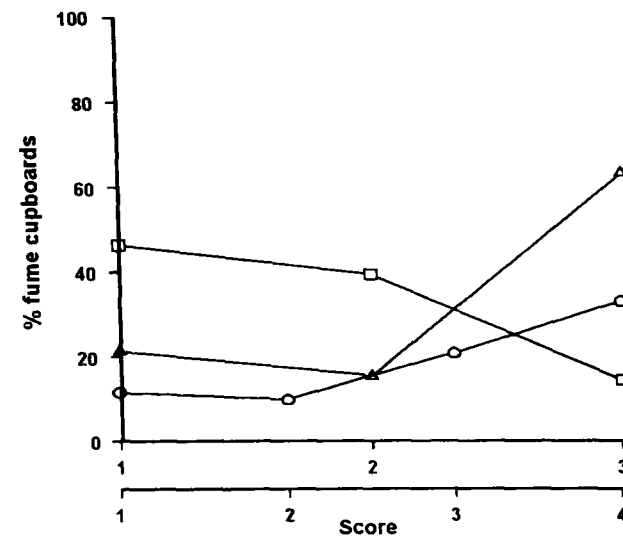


Figure A4.12 % of all cupboard faces tested at height 500 mm and their scored variables: velocity □, variation of velocity ○, and fog △.

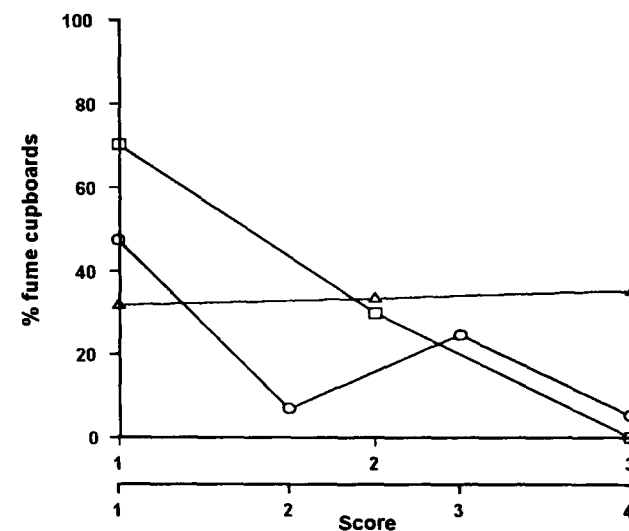


Figure A4.14 % of aerodynamic cupboard faces tested at height 500 mm and their scored variables: velocity □, variation of velocity ○, and fog △.

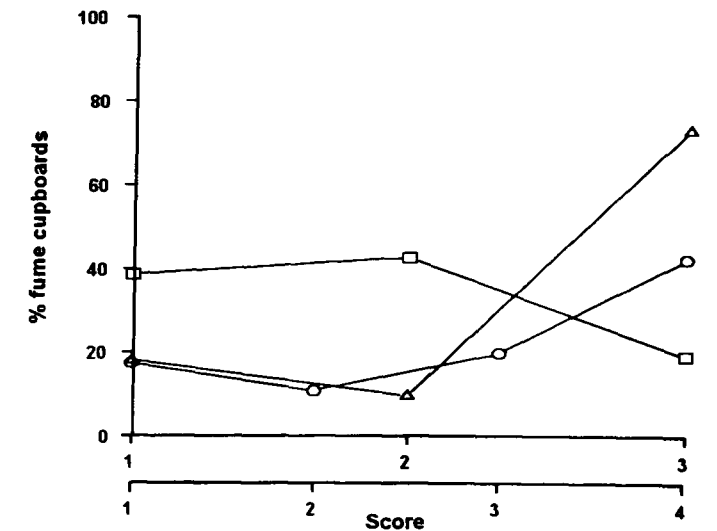


Figure A4.16 % of conventional cupboard faces tested at height 500 mm and their scored variables: velocity □, variation of velocity ○, and fog △.

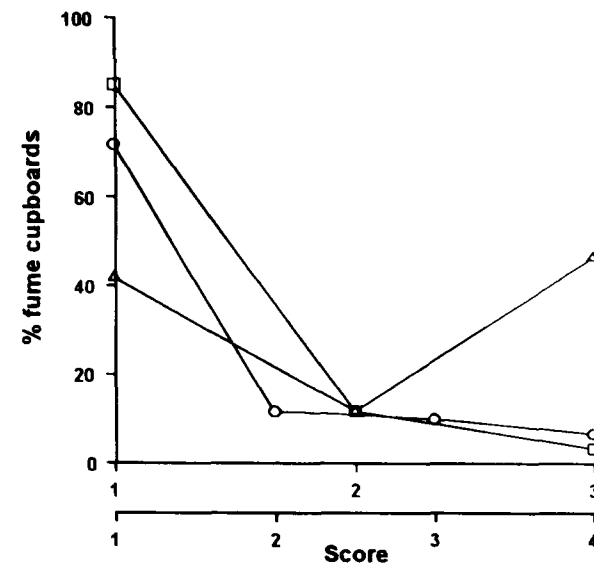


Figure A4.17 % of single sash cupboard faces tested at height 250 mm and their scored variables: velocity \square , variation of velocity \circ , and fog Δ .

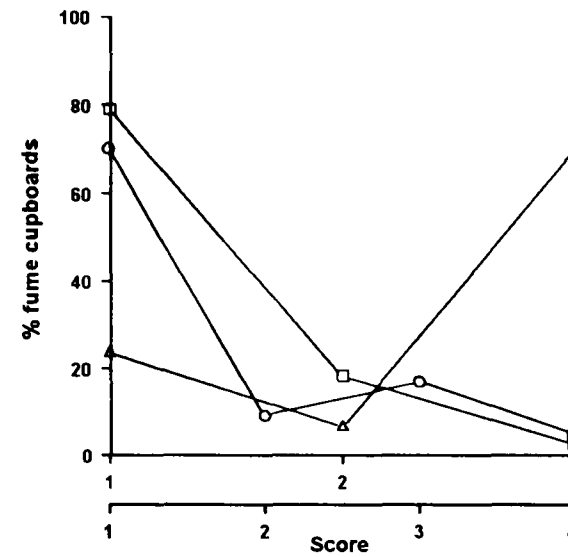


Figure A4.19 % of double sash cupboard faces tested at height 250 mm and their scored variables: velocity \square , variation of velocity \circ , and fog Δ .

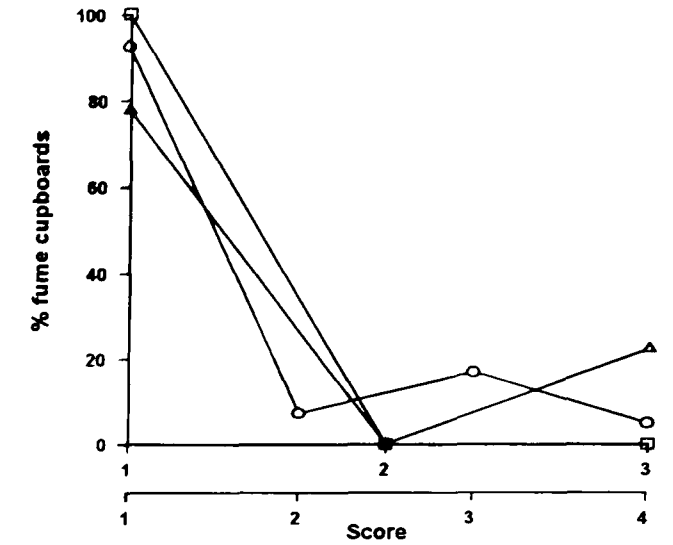


Figure A4.21 % of triple sash cupboard faces tested at height 250 mm and their scored variables: velocity \square , variation of velocity \circ , and fog Δ .

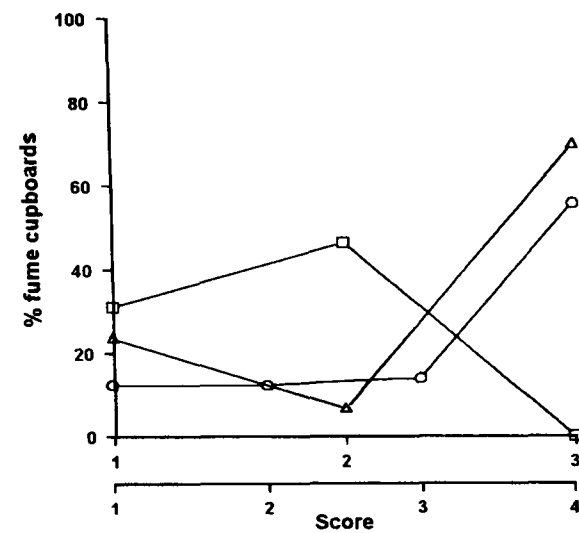


Figure A4.18 % of single sash cupboard faces tested at height 500 mm and their scored variables: velocity \square , variation of velocity \circ , and fog Δ .

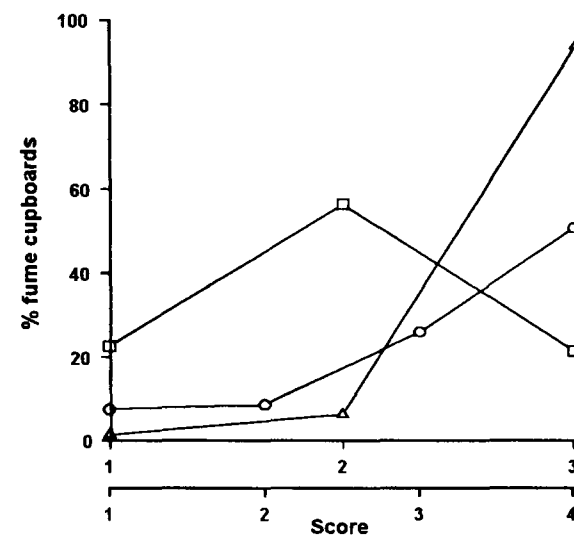


Figure A4.20 % of double sash cupboard faces tested at height 500 mm and their scored variables: velocity \square , variation of velocity \circ , and fog Δ .

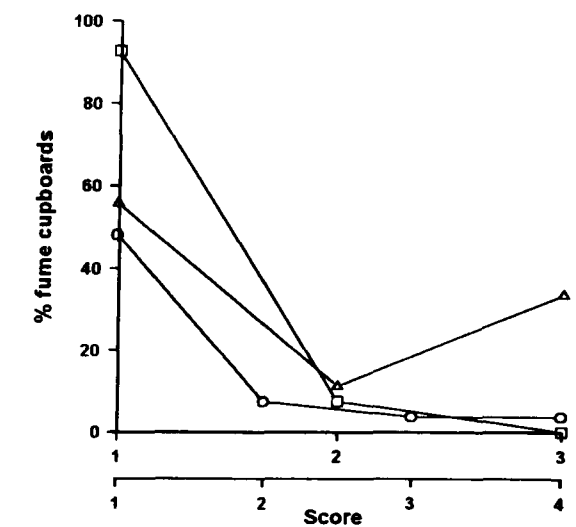


Figure A4.22 % of triple sash cupboard faces tested at height 500 mm and their scored variables: velocity \square , variation of velocity \circ , and fog Δ .

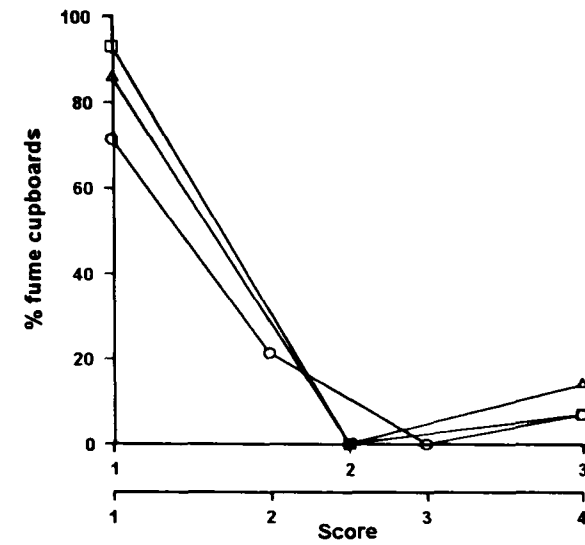


Figure A4.23 % of double sided cupboard faces tested at height 250 mm and their scored variables: velocity □, variation of velocity ○, and fog Δ.

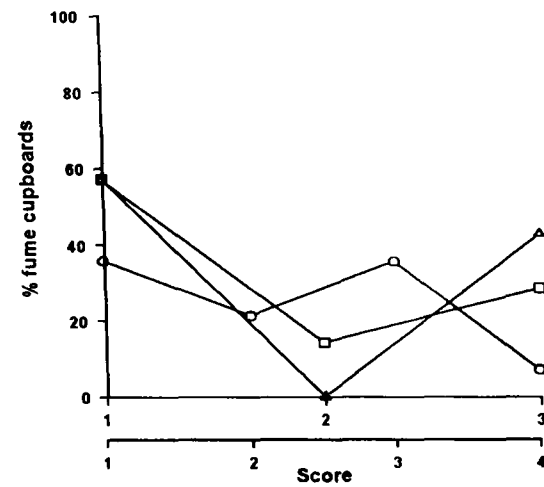


Figure A4.24 % of double sided cupboard faces tested at height 500 mm and their scored variables: velocity □, variation of velocity ○, and fog Δ.

At a working aperture height of 500 mm there is little change in the number of cupboards and velocity or variation score but the number increases with increasing water fog score.

The data for aerodynamic cupboards showed a good comparison for all three scored variables at a working aperture height of 250 mm but at 500 mm as the number of cupboards decreased with increasing velocity and variation scores, again the number increased with increasing fog score. This pattern was also reflected to large extent for all the other cupboard types which showed by the hierarchy of tests performed and the scoring system that use of water fog visualisation could identify a poor performing fume cupboard whereas the face velocity and variation were perhaps not as such good indicators of fume cupboard performance.

A4.7.4 Grading of scores

Each of the scored variables were used as indicators of fume cupboard performance whether better or poorer, each being influenced by more conflicting factors; viz. fume cupboard design, operating parameters and the external and internal environment. However, from the figures A4.11 - A4.24 it was obvious that there was little correlation between these variables and thus individually, each could not be relied upon to give an absolute assessment of overall containment efficiency by themselves. Thus in order to assess the performance of the fume cupboard a grading score was chosen which took into account all three scored variables when measured at the working aperture.

Grade = Velocity score x Variation score x (Water Fog visualisation score)²

Thus the lower the grading value the better the cupboard performance. The water fog score was squared so as to give weight to this parameter as it was considered to be a more indicative factor in the overall assessment of the fume cupboard performance.

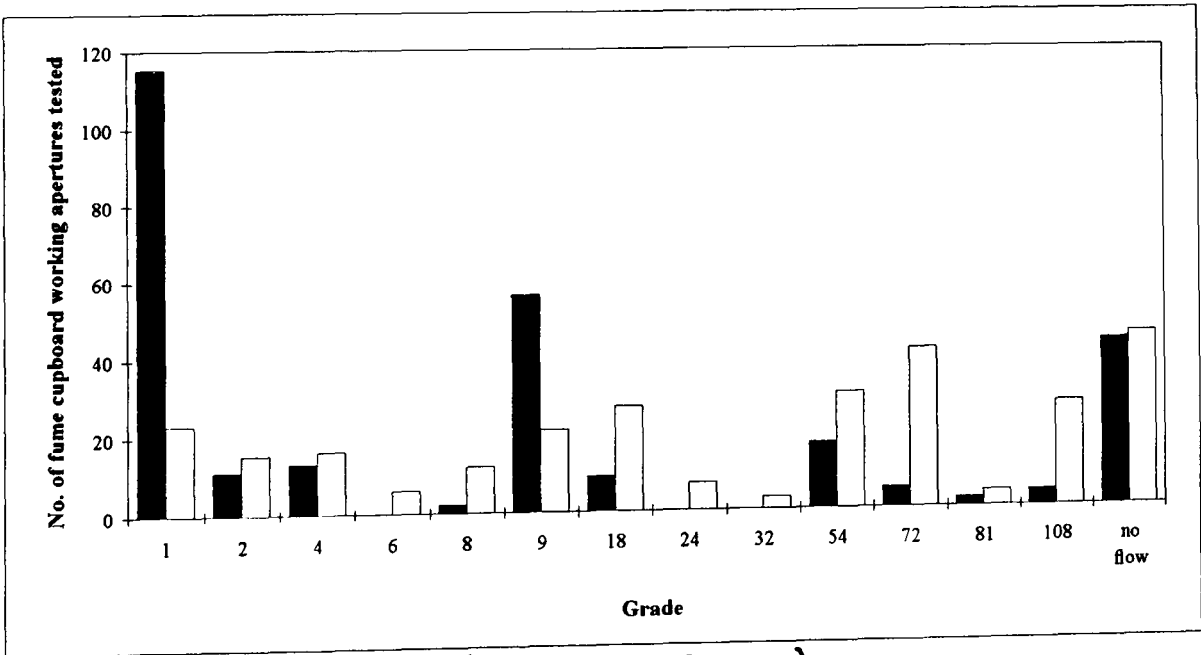


Fig. A4.25 Fume cupboard grading scores. (■ 250mm □ 500mm).

The scored variables had little correlation with each other as did the grade. The grade was influenced more by the water fog score due to the weighting in the calculation. However it did serve to group the performances of the fume cupboards.

It was clear from Fig. A4.25 that at a working sash height of 250 mm there was a large proportion of fume cupboards with low grade i.e. good performance. However, it was also obvious that on raising the sash to what may be considered the normal working height of 500 mm the number of good performers decreased and poor performers increased (Table A4.14). This was also disturbing because very few of the sashes had locking mechanisms and they could easily be raised above 500 mm (to 826 mm in some cases). Table A4.7 showed how at these heights there were few good performers. A major reason was that the face velocity decreased and the variation increased. The water fog did not necessarily follow this trend.

Aerodynamic cupboards (n = 57)	Conventional cupboards (n = 175)
2.8×10^{-7}	1.39×10^{-19}

Table A4.6 Comparison of grade with sash height (Student’s paired t-test)

Grade	Aerodynamic cupboards	Conventional cupboards
2		2
18		1
72	1	6
108		6

Table A4.7 Grading of cupboards with sashes fully open, ranging from working apertures at 682 - 826 mm for conventional cupboards and 598 mm for an aerodynamic cupboard.

Comparison between fume cupboard types was impossible due to the uncontrolled confounding variables but was used in this sense to compare ‘aerodynamic’ fume cupboards with the grouped ‘conventional’ fume cupboard.

Of the fume cupboards assessed in this institution, comparison of the trend in percentage of aerodynamic fume cupboards with grade was not that different from the more conventional type of cupboards at a working sash height of 250 mm and 500 mm (Figs. A4.26 - A4.29). The only differences were towards the higher and lower grades in that there was a higher percentage of aerodynamic cupboards with good grades and none with the lowest grades, whereas there were conventional cupboards with the lowest grade. This then suggested and agreed with the literature that even with installation of aerodynamic cupboards which were supposed to have very much improved containment performance over the conventional box cupboards, the relative improvement did not always follow and that other variables (including installation and maintenance) were just as important.

This could also be seen in the retro fit of conventional box cupboards. Some had lipfoils fitted obviously in an attempt to improve performance at the front edge and over the work surface. However the performance of these when compared to the completed survey showed no improvement (Fig. A4.30 & A4.31).

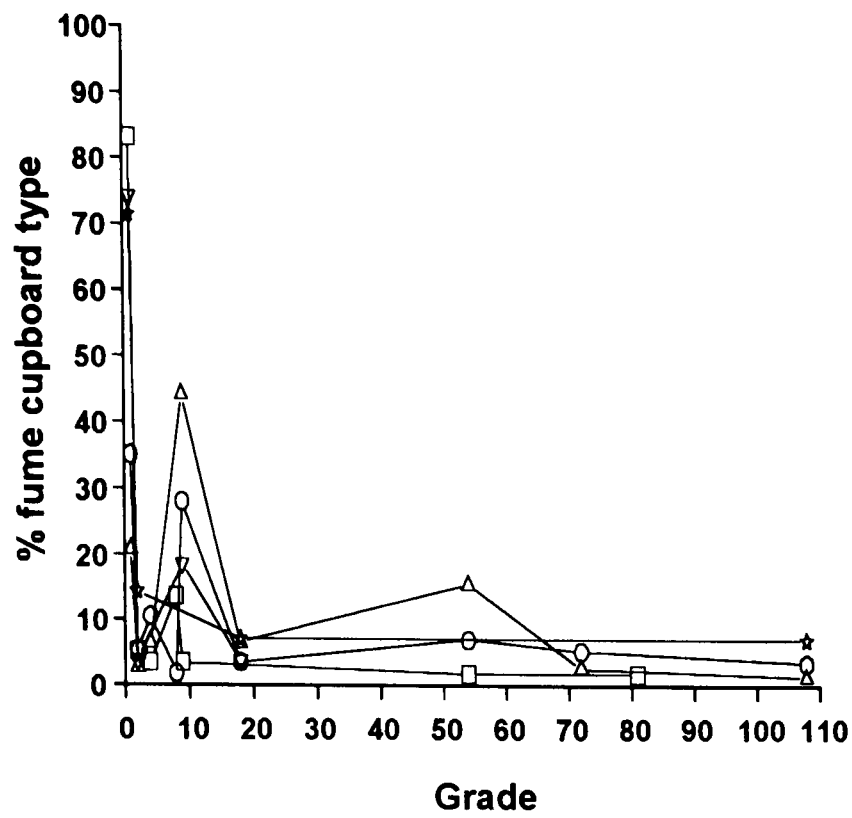


Figure A4.26 The grading of fume cupboard type at a working aperture height of 250 mm. Aerodynamic □, single sash box type ○, double sash box type △, triple sash box type ▽, and double sided box type *.

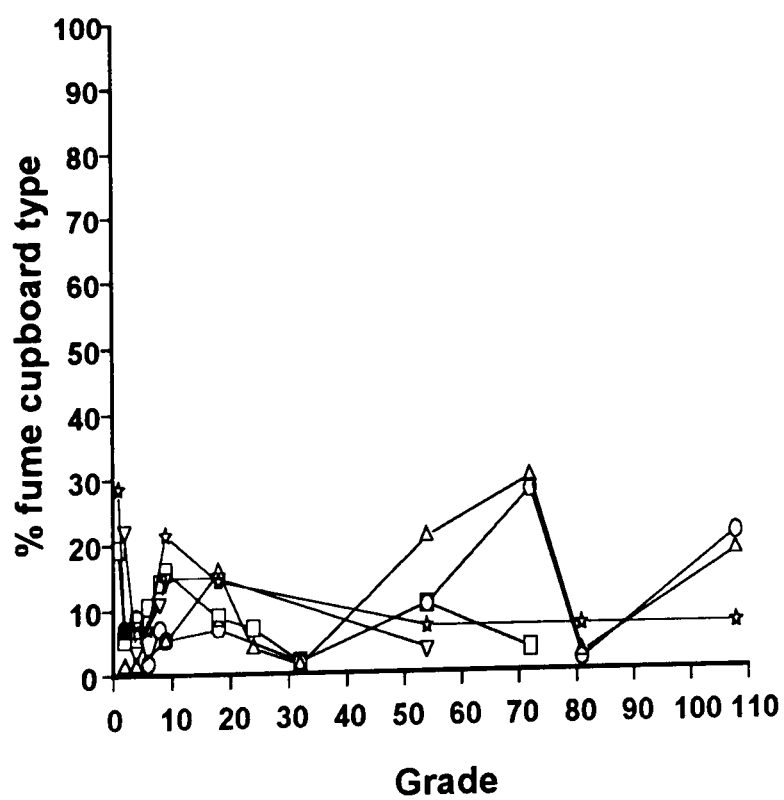


Figure A4.27 The grading of fume cupboard type at a working aperture height of 500 mm. Aerodynamic □, single sash box type ○, double sash box type △, triple sash box type ▽, and double sided box type *.

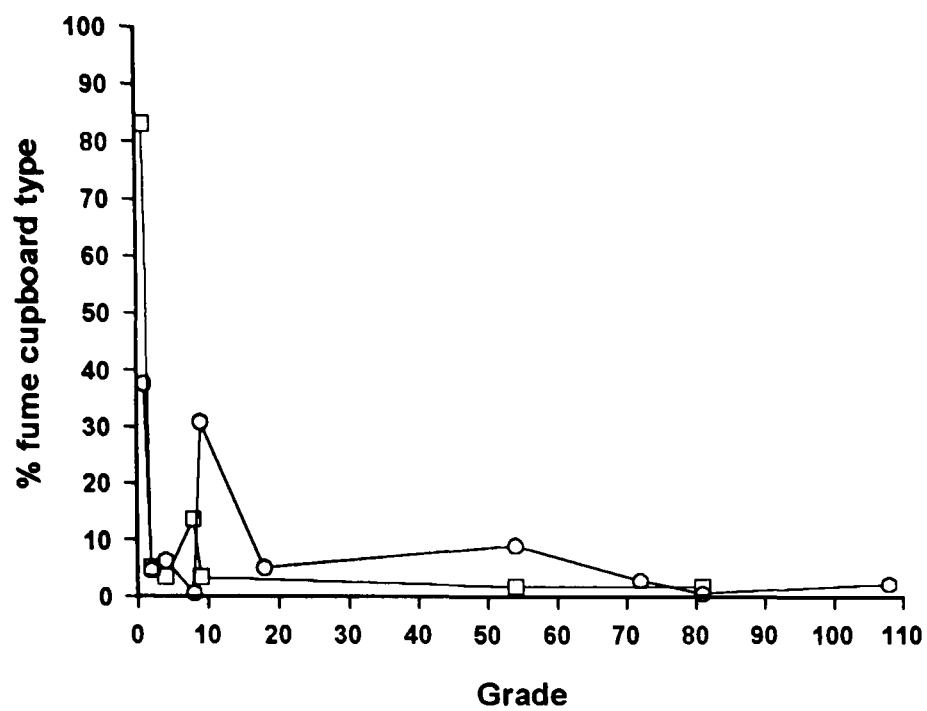


Figure A4.28 The grading of fume cupboard type at a working aperture height of 250 mm. Aerodynamic □, grouped conventional type O.

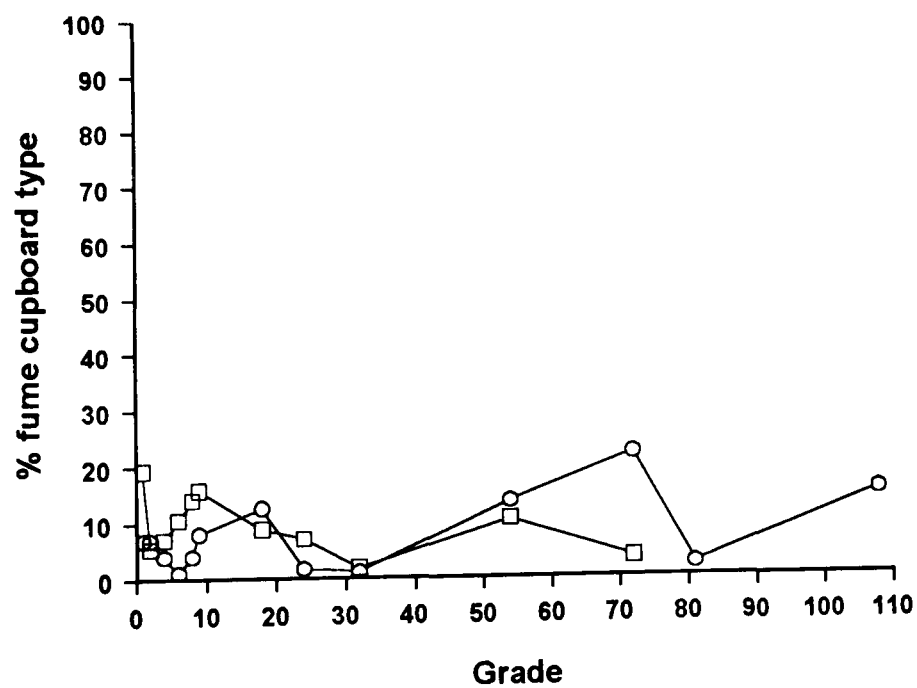


Figure A4.29 The grading of fume cupboard type at a working aperture height of 500 mm. Aerodynamic □, grouped conventional type O.

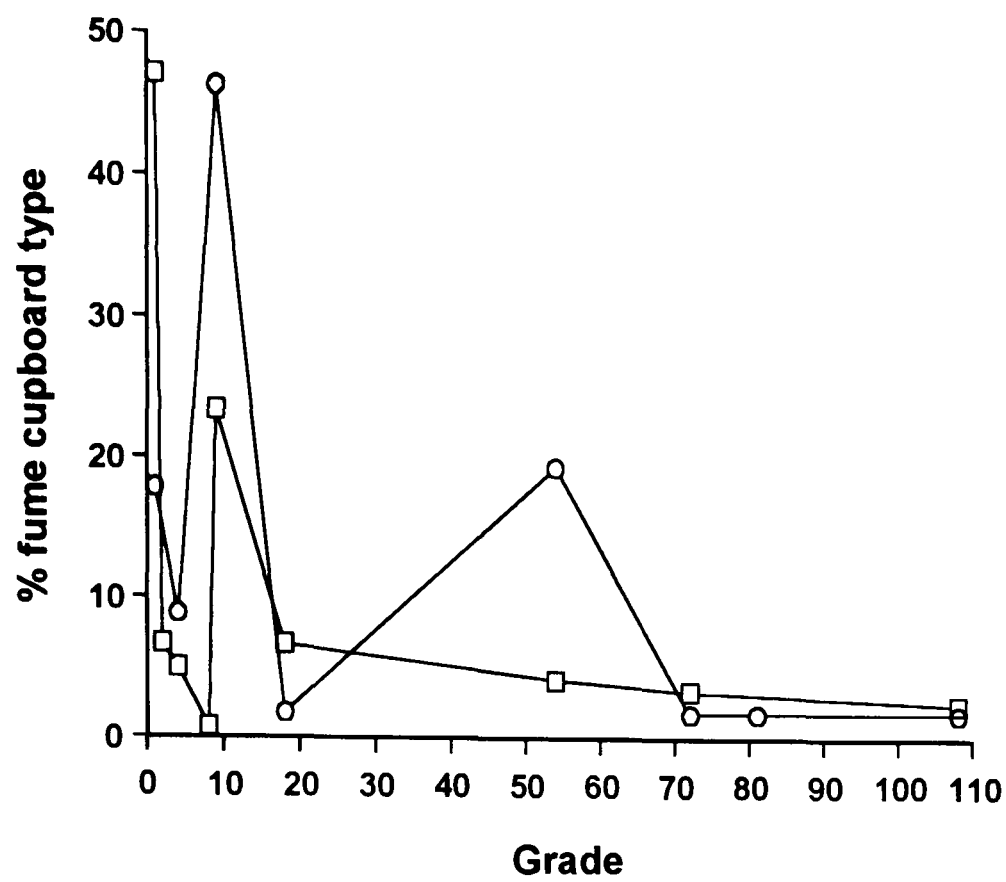


Figure A4.30 The grading of fume cupboard type at a working aperture height of 250 mm. conventional cupboards without retro fitted lipfoils \square , conventional cupboards with retro fitted lipfoils \circ .

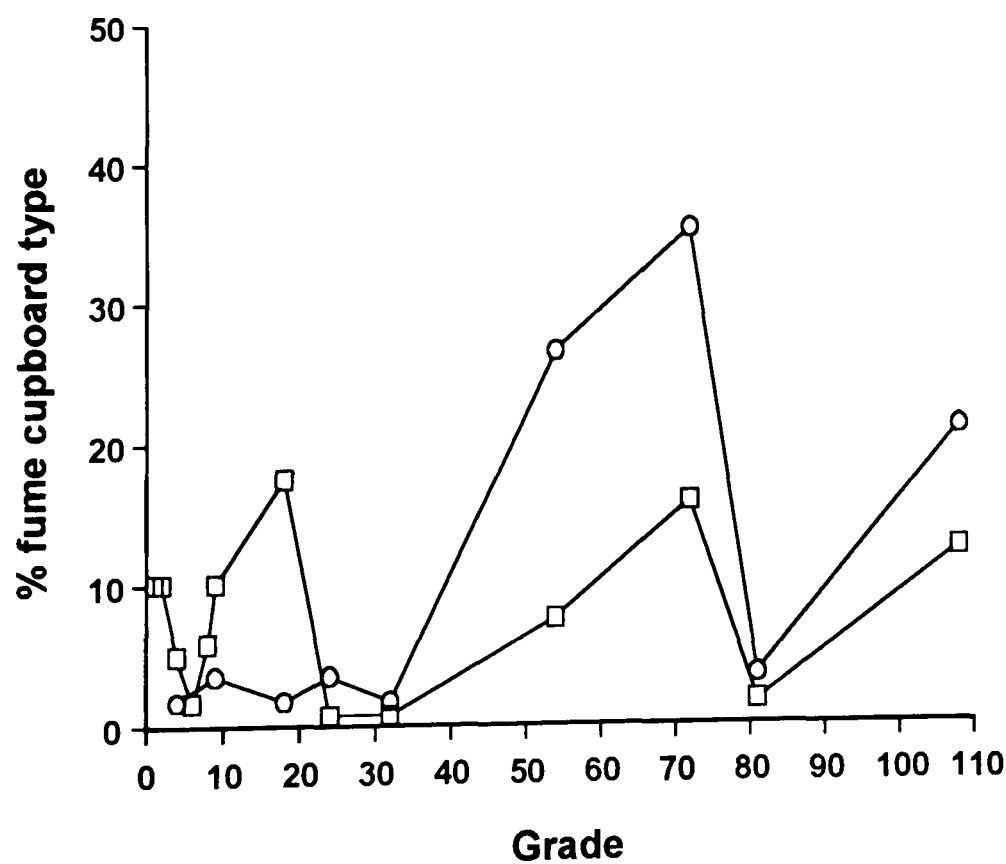


Figure A4.31 The grading of fume cupboard type at a working aperture height of 500 mm. conventional cupboards without retro fitted lipfoils \square , conventional cupboards with retro fitted lipfoils \circ .

Vel band		Aero-dynamic	Box single	Box Double	Box Triple	Box Dbsided	Aero-portable
Score 1	216 cupboard faces tested (75 % of total number)						
	Number	57	51	61	27	13	7
	% total	19.9%	17.8%	21.3%	9.4%	4.5%	2.4%
	% type*	96.6%	85%	79%	100%	93%	100%
	% band	26%	24%	28%	13%	6%	3%
	Mean vel	1.06 m/s	0.91 m/s	0.86 m/s	1.41 m/s	1.04 m/s	1.35 m/s
	Co V %	24%	31%	42%	29%	56%	34%
Score 2	22 cupboard faces tested (7.6 % of total number)						
	Number	1	7	14			
	% total	0.3%	2.4%	4.9%			
	% type*	1.7%	11.7%	18.2%			
	% band	5%	32%	64%			
	Mean vel	0.32 m/s	0.4 m/s	0.44 m/s			
	Co V %	0%	14%	10%			
Score 3	6 cupboard faces tested (2.1 % of total number)						
	Number	1	2	2		1	
	% total	0.3%	0.7%	0.7%		0.3%	
	% type*	1.7%	3.3%	2.6%		7.1%	
	% band	17%	33%	33%		17%	
	Mean vel	0.27 m/s	0.18 m/s	0.22 m/s		0.18 m/s	
no-flow	Co V %	0%	61%	41%		0%	
	43 cupboard faces tested (15.3 % of total number)						
	Number	1	25	6	9	2	
	% total	0.3%	8.7%	2.1%	3.1%	0.7%	
	% type	2%	29%	7%	56%	6%	
	% band	2%	57%	14%	20%	5%	
No. faces tested (287)		60	85	83	36	16	7
*No. with air flow		59	60	77	27	14	7

Table A4.8 Velocity measurements at a working sash height of 250 mm

Vel band		Aero-dynamic	Box single	Box Double	Box Triple	Box Dbsided
Score 1	109 cupboard faces tested (38.7 % of total number)					
	Number	40	18	18	25	8
	% total	14.2%	6.4%	6.4%	8.9%	2.9%
	% type*	70.2%	31%	22.5%	93%	57%
	% band	26%	24%	28%	13%	6%
	Mean vel	0.68 m/s	0.66 m/s	0.74 m/s	0.79 m/s	0.87 m/s
	Co V %	19%	23%	32%	29%	31%
Score 2	93 cupboard faces tested (33 % of total number)					
	Number	17	27	45	2	2
	% total	6%	9.6%	16%	0.7%	0.7%
	% type*	29.8%	46.6%	56.3%	7.4%	14.3%
	% band	18%	29%	48%	2%	2%
	Mean vel	0.42 m/s	0.4 m/s	0.39 m/s	0.44 m/s	0.44 m/s
	Co V %	11%	13%	17%	17%	11%
Score 3	34 cupboard faces tested (12.1 % of total number)					
	Number		13	17		4
	% total		4.6%	6%		1.4%
	% type*		22.4%	21.3%		28.6%
	% band		38%	50%		12%
	Mean vel		0.21 m/s	0.22 m/s		0.26 m/s
no-flow	Co V %		29%	30%		14%
	45 cupboard faces tested (16.3 % of total number)					
	Number	3	25	6	9	2
	% total	1.1%	8.9%	2.1%	3.2%	0.7%
	% type	5%	30%	7%	25%	13%
	% band	7%	54%	13%	20%	4%
No. faces tested (281)		60	83	86	36	16
*No. with air flow		57	58	80	27	14

Table A4.9 Velocity measurements at a working sash height of 500 mm

Variation % band		Aero- dynamic	Box single	Box Double	Box Triple	Box Dbsided	Aero- portable
Score 1	191 cupboard faces tested (66.3 % of total number)						
	Number	53	43	54	25	10	6
	% total	18.4%	14.9%	18.8%	8.7%	3.5%	2.1%
	% type*	89.8%	71.7%	70.1%	92.6%	71.4%	85.7%
	% band	28%	23%	28%	13%	5%	3%
Score 2	24 cupboard faces tested (8.3% of total number)						
	Number	4	7	7	2	3	1
	% total	1.4%	2.4%	2.4%	0.7%	1.0%	0.3
	% type*	6.8%	11.7%	9.1%	7.4%	21.4%	14.3%
	% band	17%	29%	29%	8%	13%	4%
Score 3	21 cupboard faces tested (7.3 % of total number)						
	Number	2	6	13			
	% total	0.7%	2.1%	4.5%			
	% type*	3.4%	10%	16.9%			
	% band	10%	29%	62%			
Score 4	8 cupboard faces tested (2.8 % of total number)						
	Number		4	3		1	
	% total		1.4%	1.0%		0.3%	
	% type*		6.7%	5%		7.1%	
	% band		50%	38%		13%	
no-flow	43 cupboard faces tested (15.3 % of total number)						
	Number	1	25	6	9	2	
	% total	0.3%	8.7%	18.4%	3.1%	0.7%	
	% type	1.7%	29.4%	7.2%	25%	12.5%	
	% band	2%	57%	120%	20%	5%	
No. faces tested (287)		60	85	83	36	16	7
*No. with air flow		59	60	77	27	14	7

Table A4.10 % variation of velocity measurements from the mean face velocity at a working sash height of 250 mm

Variation % band		Aero- dynamic	Box single	Box Double	Box Triple	Box Dbsided
Score 1	58 cupboard faces tested (20.6 % of total number)					
	Number	27	7	6	13	5
	% total	9.6%	2.5%	2.1	4.6%	1.8%
	% type*	47.4%	12.3%	7.4%	48.1%	35.7%
	% band	47%	12%	10%	22%	9%
Score 2	51 cupboard faces tested (18.1% of total number)					
	Number	4	7	7	2	3
	% total	4.6%	3.5%	4.6%	4.3%	1.1%
	% type*	7%	12.3%	8.6%	7.4%	21.4%
	% band	25%	20%	25%	24%	6%
Score 3	49 cupboard faces tested (17.4 % of total number)					
	Number	14	8	21	1	5
	% total	5%	2.81%	7.4%	0.4%	1.8%
	% type*	24.6%	14%	25.9%	3.7%	35.7%
	% band	29%	16%	43%	2%	10%
Score 4	78 cupboard faces tested (27.7 % of total number)					
	Number	3	32	41	1	1
	% total	1.1%	11.3%	14.5%	0.4%	0.4%
	% type	5.3%	56.1%	50.6%	3.7%	7.1%
	% band	4%	41%	53%	1%	1%
no-flow	45 cupboard faces tested (16.4 % of total number)					
	Number	3	25	6	9	2
	% total	1.1%	8.9%	2.1%	3.2%	0.7%
	% type	5%	31%	7%	25%	13%
	% band	7%	54%	13%	4%	2%
No. faces tested (281)		60	82	87	36	16
*No. with air flow		57	57	81	27	14

Table A4.11 % variation of velocity measurements from the mean face velocity at a working sash height of 500 mm

Fog band		Aero-dynamic	Box single	Box Double	Box Triple	Box Dbsided	Aero-portable
Score 1	135 cupboard faces tested (47 % of total number)						
	Number	52	25	18	21	12	7
	% total	18%	9%	6%	7%	4%	2%
	% type*	88.1%	41.7%	23.4%	77.8%	85.7%	100%
	% band	39%	19%	13%	16%	9%	5%
Score 2	14 cupboard faces tested (5% of total number)						
	Number	3	7	5			
	% total	1%	2%	2%			
	% type*	5.1%	11.7%	6.5%			
	% band	21%	50%	36%			
Score 3	94 cupboard faces tested (32.9 % of total number)						
	Number	4	28	54	6	2	
	% total	1.4%	9.8%	18.9%	2.1%	0.7%	
	% type*	6.8%	46.7%	70.1%	22.2%	14.3%	
	% band	4.3%	29.8%	57.4%	6.4%	2.1%	
no flow	43 cupboard faces tested (15.3 % of total number)						
	Number	1	25	6	9	2	
	% type	0.3%	8.7%	2.1%	3.1%	0.7%	
	% total	2%	29%	7%	56%	6%	
	% band	2%	57%	14%	20%	5%	
No. faces tested (286)		60	85	83	36	16	7
*No. with air flow		59	60	77	27	14	7

Table A4.12 Fog scores at a working sash height of 250 mm

Fog band		Aero-dynamic	Box single	Box Double	Box Triple	Box Dbsided
Score 1	50 cupboard faces tested (17.7 % of total number)					
	Number	18	8	1	15	8
	% total	6.4%	2.8%	0.4%	5.3%	2.8%
	% type*	31.6%	13.8%	1.3%	55.6%	57.1%
	% band	39%	16%	2%	30%	16%
Score 2	36 cupboard faces tested (12.8% of total number)					
	Number	19	9	5	3	
	% total	6.7%	3.2%	1.8%	1.1%	
	% type*	33.3%	15.5%	6.3%	11.1%	
	% band	53%	25%	14%	8%	
Score 3	150 cupboard faces tested (53.4 % of total number)					
	Number	20	40	75	9	6
	% total	7.1%	14.2%	26.7%	3.2%	2.1%
	% type*	35.1%	69%	93.8%	33.3%	42.9%
	% band	13.3%	26.7%	50%	6%	4%
no-flow	45 cupboard faces tested (16.3 % of total number)					
	Number	3	25	6	9	2
	% total	1.1%	8.9%	2.1%	3.2%	0.7%
	% type	5%	30%	7%	25%	13%
	% band	7%	54%	13%	20%	4%
No. faces tested (281)		60	83	86	36	16
*No. with air flow		57	58	80	27	14

Table A4.13 Fog scores at a working sash height of 500 mm

Possible Scores	Aerodynamic		Box							
	250	500	Single		Double		Triple		2 sided	
			250	500	250	500	250	500	250	500
1	49	11	20		16		20	8	10	4
2	3	3	3	4	2	1	1	6	2	1
4	2	9	6	5	5	1		1		
6		4		1						1
8	1	5	1	4				3		
9	2	7	16	3	33	4	5	4		3
18		5	2	4	5	12	1	4	1	2
24		4				3				
32		1		1		1				
54	1	6	4	6	12	16		1		1
72		2	3	16	2	23				
81	1			1	1	2				1
108			2	12	1	14			1	1
no flow	1	3	25	25	6	6	9	9	2	2
Total cupb'd	60	60	82	82	83	83	36	36	16	16
with flow	59	57	57	57	77	77	27	27	14	14

Table A4.14 Grading of fume cupboards at working aperture of 250 and 500 mm)

Possible Scores	Aerodynamic		Box							
	250	500	Single		Double		Triple		2 sided	
			250	500	250	500	250	500	250	500
1	83.1%	19.3%	35.1%		20.8%		74.1%	29.6%	71.4%	28.6%
2	5.1%	5.3%	5.3%	7%	2.6%	1.3%	3.7%	22.2%	14.3%	8.3%
4	3.4%	7%	10.5%	8.8%	6.5%	1.3%		3.7%		
6		10.5%		1.8%						
8	13.6%	14%	1.8%	7%				11.1%		
9	3.4%	15.8%	28.1%	5.3%	44.2%	5.2%	18.5%	14.8%		25%
12				7%						
18		8.8%	3.5%		6.5%	15.6%	3.7%	14.8%	7.1%	16.7%
24		7%				3.9%				
32		1.8%		1.8%		1.3%				
54	1.7%	10.5%	7%	10.5%	15.6%	20.8%		3.7%		
72		3.5%	5.3%	28.1%	2.6%	29.9%				
81	1.7%			1.8%		2.6%				8.3%
108			3.5%	21.1%	1.3%	18.2%			7.1%	8.3%
Total cupb'd	60	60	82	82	83	83	36	36	16	16
with flow	59	57	57	57	77	77	27	27	14	14

Table A4.15 Grading of fume cupboards at working aperture of 250 and 500 mm (% total working cupboards)